

EYEC Monograph

4th European Young Engineers Conference

April 27-29th 2015
Warsaw

Organizer:

Scientific Club of Chemical and Process Engineering
Faculty of Chemical and Process Engineering
Warsaw University of Technology

Patronage:



4th European Young Engineers Conference

www.eyec.ichip.pw.edu.pl

Copyright © 2015, Faculty of Chemical and Process Engineering,
Warsaw University of Technology

Edited by
Michał Wojasiński, MSc Eng.
Bartosz Nowak, MSc Eng.

ISBN 978-83-936575-1-3

Printed in 100 copies

The authors are responsible for the content of the papers.
All papers reviewed by Scientific Committee.

Published by:
Faculty of Chemical and Process Engineering, Warsaw University of
Technology

Printed in Poland by:
Institute for Sustainable Technologies – National Research Institute
26-600 Radom, 6/10 Pułaskiego Street,
phone (+48) 48 36-442-41, fax (+48) 48 36-447-65
<http://www.itee.radom.pl>

Contents

Introduction	14
Scientific Committee	15
Scientific Commission	16
Organizing committee	18
Invited lectures	19
Prof. Jerzy Baldyga, PhD Eng.	19
Prof. Marc-Olivier Coppens	20
Bruno Bastos Sales, PhD.....	22
Naresh Kasoju, PhD	23
Anna Zalewska, PhD	24
Monograph articles	25
Gold nanoparticles properties and recent advances	
M. Blicharska, et al.	25
The TS-1 catalyst and its utilization in the epoxidation processes	
E. Drewnowska, et al.	45
Thermocatalytic polyolefin processing system in pure synthetic oil distiller	
Ł. Grabowski, et al.	59
Application of UV spectrophotometry in the quality control of galactooligosaccharides production	
S. Koncz, et al.	70
Silica-templated three-dimensional graphene xerogels	
I. Kondratowicz, et al.	79
Transition Metal Oxides influence on phosphate and borate glasses structure	
T. Lewandowski, et al.	97
Parameters of epoxidation of vegetable oils in the presence of acidic ion-exchange resins	
K. Malarczyk, et al.	113
Natural monoterpenes: their chemical properties and applications on the example of limonene	
M. W. Malko, et al.	123
COD reduction in landfill leachate treatment by Photo Electro - Fenton process – an overview	
R. Nikpour, et al.	134
The biotechnological potential of ionic liquids	
U. Świerczek, et al.	151

Coating of stainless steel 316L with organic layer for medical purposes: problematic issue of surface pre-treatment	
P. Trzaskowska, et al.	163
Surface plasmon resonance in detection of biological threats	
M. Trzaskowski	171
Luminescence properties of Eu³⁺ and Tb³⁺ doped silica-based xerogels	
M. Walas, et al.	180
Innovative screening device for high-sensitive chemical vapors detection	
A. Zalewska	194
Scientific Articles.....	207
The utilization of the TS-1 catalyst in the epoxidation of diallyl ether	
E. Drewnowska, et al.	207
Study on conditions for formation of amino acid - zinc suspensions	
R. Dyja, et al.	220
The products of limonene oxidation on the titanium-silicate catalysts and their properties and applications	
A. Gawarecka, et al.	229
The release studies of undecylenoyl phenylalanine through cellulose based membranes	
A. Główska, et al.	241
The Industrial Heritage in nowadays Polish cities	
J. Gruszczyńska	250
Astaxanthin –the strongest natural antioxidant	
J. Igielska-Kalwat, et al.	264
Assessment of pollutant content in energy willow (<i>Salix viminalis</i>) growing in Puczniew village	
M. Janas, et al.	272
Detection of emulsion destabilisation processes on the basis of selected physicochemical parameters	
A. Kapuścińska, et al.	281
Effect of acetic acid to ethylenic unsaturation molar ratio on the course of rapeseed oil epoxidation	
K. Malarczyk, et al.	289
The epoxidation of limonene in toluene using hydrogen peroxide and over the Ti-MCM-41 catalyst	
M. W. Malko, et al.	295
Impact of loads and biofeedback to behavior of the center of gravity of the body	
M. Andryszczyk, et al.	305

Application of selected transition metals lignosulfonates as hydrogen peroxide electrochemical sensors and as electroplating baths	
K. Śron, et al.	322
Influence of kind of sugars on selenium enrichment in baker's yeast	
B. Szulc-Musioł, et al.	329
Using hydrogen to recycle neodymium magnets	
M. Szymański, et al.	338
Influence of direct crystallization process on the bioactivity of silicate-phosphate glasses from $\text{KCaPO}_4\text{-SiO}_2$ system	
A. Wajda, et al.	343
Ti-MWW catalyst – the titanium silicate catalyst with the MWW topology	
M. Walasek, et al.	352
Abstracts	360
Thermo-Optical Parameters of Amorphous a-C:N:H Layers	
E. Baraniak, et al.	360
Elimination of pollutants by adsorption onto activated carbon prepared from pistachio nut shells	
A. Bazan, et al.	361
Gold nanoparticles in catalysis	
M. Blicharska, et al.	362
Preparation and application new hybrid materials	
M. Blicharska, et al.	363
Potentiometric response of solid contact ion selective electrodes (SC-ISE's) using carbon black supporting platinum nanoparticles	
L. Cabaj, et al.	364
Electrochemical properties of solid contact ion selective electrodes modified with several nanomaterials	
L. Cabaj, et al.	365
Synthesis, microstructural studies and second-order optical nonlinearity of rare earth doped orthorhombic $\text{Bi}_2\text{ZnB}_2\text{O}_7$	
M. Chronik, et al.	366
Modification of material's surface properties by direct laser interference lithography	
K. Strzyż, et al.	367
Synthesis of periodic mesoporous organosilicas modified with Nb	
P. Dębek, et al.	368
The utilization of the TS-1 catalyst in the epoxidation of diallyl ether	
E. Drewnowska, et al.	369

Optimization of amino acid-zinc carriers	
R. Dyja, et al.	370
Dissolution profiles of optimized amino acid-zinc carriers	
R. Dyja, et al.	371
Natural stabilizers increasing survival of <i>Lactobacillus rhamnosus</i> during spray drying process	
A. Fedorowicz, et al.	372
Visible-light photochemical degradation of 2,4-dichlorophenol in aqueous solutions by singlet oxygen	
M. Fozzpańczyk, et al.	373
Synthesis and applications of the TS-1 catalyst	
A. Gawarecka, et al.	374
The release studies of undecylenoyl phenylalanine through cellulose based membranes	
A. Główska, et al.	375
Thermocatalytic polyolefin processing system in pure synthetic oil distiller	
Ł. Grabowski, et al.	376
The industrial heritage in nowadays Polish cities	
J. Gruszczyńska	377
Visible light driven photocatalytic elimination of organic- and microbial pollutions by rutile-phase titanium dioxides	
T. Gyulavári, et al.	378
Synthesis and mesomorphic properties of 2,3-difluoro-4,4''-dialkyl- and 2,2',3,3'-tetrafluoro-4,4''-dialkyl-p-terphenyl's homologous series	
P. Harmata, et al.	379
The influence of lateral substitutes on birefrigerence value of compounds based on molecular cores – tolanes and bistolanes	
P. Harmata, et al.	380
In vivo studies of cosmetic formulations with β-carotene	
J. Igielska-Kalwat, et al.	381
Manufacturing and characteristics of Al₂O₃-Al functionally graded materials for brake disc application	
J. Jakubowska, et al.	382
Assessment of pollutant content in energy willow growing in Puczniew village	
M. Janas, et al.	383
Nanoporous titanium dioxide layer as substrate for enhanced osteoblast-like cells growth	
M. Jarosz, et al.	384

Novel silver multielectrode sensor for stripping analysis	
K. Jedlińska, et al.....	385
Application of microfibrillar cellulose (mfc) obtained from agro-food byproducts for improved barrier and mechanical properties of paper	
M. Jotko, et al.	386
Assessing the applicability of 2H-1-benzopyran-2-one derivatives as a fluorescent molecular sensor for on-line monitoring photopolymerization processes	
I. Kamińska, et al.	387
Analysis of the stability of cosmetic emulsion containing jasmonates using the multiple light scattering phenomenon	
A. Kapuścińska, et al.	388
The use of diffusion phenomena in the theoretical model of active substances transdermal transport	
A. Kapuścińska, et al.	389
The crystallization pathway and photocatalytic activity of Bi₂WO₆ microflowers	
Z. Kása, et al.	3890
Sawdust pellets from coniferous species as precursors of carbonaceous adsorbents	
J. Kaźmierczak-Razna, et al.	391
Extraction methods of ranitidine isolation from natural water	
I. Kiszkiel	392
Influence of the reaction time on the epoxidation of linseed oil with performic acid	
M. Kłos, et al.	393
Rheological properties of liquid surface layer in selected commercial instant coffee	
J. Kmiecik, et al.	394
Application of UV spectrophotometry in the quality control of galactooligosaccharides production	
S. Koncz, et al.	395
Synthesis of silica-templated three-dimensional graphene xerogels	
I. Kondratowicz, et al.	396
Preparation of abrasion resistant ceramic – intermetallics composites using sintering method with the exothermic reaction	
M. Kopeć	397
Graphene oxide coating used to modified method of interference-wedge in the study of optical parameters in the nematic liquid crystal	
K. Kowiorski, et al.....	398

Tert-butanol as radical scavenger material for investigation of heterogeneous photocatalysis and other advanced oxidation processes	
Z. Kozmér, et al.	399
Research on optimally balanced bioelements rate in in vitro cultured mushroom	
A. Krakowska, et al.	400
Analysis of selected micro and macro elements in <i>in vitro</i> culture of <i>Bacopa monnieri</i>	
A. Krakowska, et al.	401
Cellulose acetate membranes for dyes removal from liquid phase	
J. Krasoń, et al.	402
Cyclodextrin production from different types of starch - kinetic characteristics	
B. Kudawska, et al.	403
Transition Metal Oxides influence on phosphate and borate glasses structure	
T. Lewandowski, et al.	404
Energetic properties of a new salt of TNBI	
R. Lewczuk, et al.	405
Effect of the electrode roughness on the electrode reaction	
A. Ładocha, et al.	406
Comparision of coffee beans and grounds as additives for <i>Macrolepota konradii</i> biomass production	
Ł. Łopusiewicz, et al.	407
Effect of acetic acid to ethylenic unsaturation molar ratio on the course of rapeseed oil epoxidation	
K. Malarczyk, et al.	408
The epoxidation of R(+)-limonene in the presence of toluene using hydrogen peroxide and over the Ti-MCM-41 catalyst	
M. W. Malko, et al.	409
Adsorption of L-histidine onto mesoporous carbons functionalized with carboxylic groups	
M. Marciniak, et al.	410
Knowledge and model-based framework for nanofiltration modelling	
A. Marecka, et al.	411
Investigation of surface leakage current for HgCdTe barrier infrared detectors	
O. Markowska, et al.	412

The effect of construction and operating conditions of medical inhaler on atomization process	
M. Matuszak	413
Chiral terphenylates – perspective materials for fast switching modes	
K. Milewska	414
New high tilted antiferroelectric liquid crystals for multimedia LCD's	
K. Milewska, et al.	415
Effects of formic acid and sodium formate on the $\cdot\text{OH}$-initiated transformation of phenol	
M. Náfrádi, et al.	416
Pollutant emission from biomass combustion	
G. Wielgościński, et al.	417
COD reduction in landfill leachate treatment by photo electro-Fenton process – an overview	
R. Nikpour, et al.	418
The use of electrochemical impedance spectroscopy to study the semiconducting properties of oxide layers on titanium alloys in a simulated body fluid	
P. Osak, et al.	419
Multi-electrode potentiometric sensor	
M. Pięk, et al.	420
All-solid-state nitrate-selective potentiometric electrode with carbon black	
M. Pięk, et al.	421
Characteristics of metallic structured catalysts for catalytic combustion of biogas	
E. Piwowarczyk, et al.	422
Synthesis and physicochemical properties of amine modified	
E. Ptaszkowska, et al.	423
High nitrogen slats of azotetrazole	
J. Rećko, et al.	424
Application of core-shell mesoporous silica nanospheres modified with titanium dioxide in cement mortars for self-cleaning and bactericidal purposes	
P. Sikora, et al.	425
The influence of nanosilica on the mechanical properties of polymer-cement composites (PCC)	
P. Sikora, et al.	426

Structural analysis and photocatalytic activity of titania photocatalysts immobilized onto ceramic paper support	
G. Simon, et al.	427
Biodegradable polymer composites with nanoparticles of silver and natural fibers to the elements of rehabilitation equipment in veterinary medicine	
N. Sitek, et al.....	428
The relation between Kirkendall porosity and Matano plane position in binary system Fe-Pd	
W. Skibiński, et al.	429
Verification of ciders origin based on voltammetric signals	
W. Sordoń, et al.	430
Freeze-dried microcapsule in bioconversion reaction of whey	
M. Stobińska, et al.	431
Influence of incubation condition on selenium enrichment in baker's yeast	
B. Szulc-Musioł, et al.	432
Using hydrogen to recycle neodymium magnets	
M. Szymański, et al.....	433
Impact of loads and biofeedback to behavior of the center of gravity of the body	
S. Śmigiel, et al.	434
Application of selected transition metals lignosulfonates as hydrogen peroxide electrochemical sensors and as electroplating baths	
K. Śron, et al.	435
Ionic liquids as interdisciplinary materials	
U. Świerczek, et al.	436
The biotechnological potential of ionic liquids	
U. Świerczek, et al.	437
Biocompatible coatings for stainless steel surfaces	
P. Trzaskowska, et al.	438
Portable system for detection of biological threats	
M. Trzaskowski, et al.....	439
Influence of direct crystallization process on the bioactivity of silicate-phosphate glasses from $\text{KCaPO}_4\text{-SiO}_2$ system	
A. Wajda, et al.	440
Luminescence properties of Eu^{3+} and Tb^{3+} doped silica-based xerogels	
M. Walas, et al.	441
Novel titanium-silicate catalysts with the MWW topology	
M. Walasek, et al.	442

Construction and application of bismuth bulk electrode for adsorptive stripping determination of cobalt(II)	
K. Węgiel, et al.	443
Phosphorothioate analogs of uridine nucleotides in wound healing	
E. Węglowska, et al.	444
The analysis of discharge coefficient for atomization of the liquid of different viscosity	
S. Włodarczak.....	445
Solution blow spinning of polyurethane nanofibers	
M. Wojasiński, et al.	446
Chemical engineer vs biology – a case study about toxicity of ZnO based nanomaterials	
A. Wojewódzka, et al.	447
Application of Ytria-stabilized Zirconia materials for heavy metals removal	
M. Wolska, et al.....	448
Innovative screening device for high-sensitive chemical vapors detection	
A. Zalewska.....	449
Nickel aluminate spinel (NiAl₂O₄) in Al₂O₃/NiO and Al₂O₃/Ni system	
J. Zygmontowicz, et al.....	450
Index	451

Introduction

The very idea of European Young Engineers Conference arrived in year 2011, during Students Scientific Club meeting. We were wondering, how we can develop our work and how to provide a new, attractive and easy way to exchange knowledge and experience between young people. People who, like us, believe, that science and engineering are the best ways to develop.

Ever since, we work very hard to make our Conference better and better. After previous three editions, we can say that event like EYEC is still highly desired. Our goal was to create a possibility for young scientists to show their work for public. For many of EYEC participants, our conference was the first step in their career. Thanks to EYEC's scope, friendly atmosphere and high level of presented research, we believe that it is the best way to start or continue your scientific career.

During the EYECs' second edition we come up with an idea to provide our participants more space to present their scientific work. Since 3rd edition of EYEC we issue the EYEC Monograph, our very first and the most important piece of written work. In this book you can find the most promising, important and reviewed papers of European Young Scientists. We hope, that this book you are holding will be the first step in career of each and every of participants of our conference.

The book, as well as conference, covers following matters:

- process engineering
- chemical engineering
- process equipment
- biomedical engineering
- nanotechnologies & nanomaterials
- bioprocess engineering
- environment protection
- material engineering
- other engineering disciplines

We hope you will find the papers within this book highly interesting and important, as we do.

Organizing Committee
Editorial Team of EYEC Monograph

Scientific Committee

Chairman

Prof. Eugeniusz Molga, PhD Eng.

Prof. Tomasz Ciach, PhD Eng.

Prof. Paweł Gierycz, PhD Eng.

Prof. Leon Gradoń, PhD Eng.

Prof. Marek Henczka, PhD Eng.

Prof. Arkadiusz Moskal, PhD Eng.

Prof. Tomasz Sosnowski, PhD Eng.

Prof. Andrzej Stankiewicz, PhD Eng.

Beata Butruk-Raszeja, PhD Eng.

Robert Cherbański, PhD Eng.

Katarzyna Dąbkowska, PhD Eng.

Jakub Gac, PhD Eng.

Anna Jackiewicz, PhD Eng.

Magdalena Jasińska, PhD Eng.

Andrzej Krasieński, PhD Eng.

Zoltan Kovacs, PhD Eng.

Łukasz Makowski, PhD Eng.

Marcin Odziomek, PhD Eng.

Wojciech Orciuch, PhD Eng.

Agata Penconek, PhD Eng.

Paweł Sobieszuk, PhD Eng.

The Editorial Team of EYEC Monograph is extremely grateful for the effort and work of Scientific Committee put on the reviewing process of all the manuscript published in this book. Right after authors, without your work this book would not be created. Thank you.

Organizing Committee

Editorial Team of EYEC Monograph

Scientific Commission

Chairman

Prof. Tomasz Sosnowski, PhD Eng.

Vice-Dean for Scientific Affairs of Faculty of Chemical and Process Engineering at Warsaw University of Technology.

He received his PhD (in 1997) and DSc title (habilitation, 2006) from Warsaw University of Technology for the research related to dynamic interfacial phenomena and their relevance for hydrodynamics and mass transfer in the human respiratory system. He was a post-doc fellow at Lovelace Respiratory Research Institute in Albuquerque, USA (1999-2000) where he worked on aerosol systems for drug delivery by inhalation. From that time problems of chemical engineering applications in biomedicine have remained his main field of scientific activity.

Prof. Sosnowski is an author of more than 60 scientific papers in JCR journals and more than 200 other scientific publications (journal papers, book chapters, conference communications). In 2010 he published a book "*Respirable aerosols and inhalers*" (in Polish; 2nd edition in 2012) which was focused on the application of engineering methods in designing of medical inhalers and analyzing aerosol flow and particle-lung interactions. He is a co-author of 3 granted patents and 6 patent applications. He is also a scientific expert of European Medicine Agency (EMA - London) and the member of Managing Committee of the European Initiative COST.

Anna Jackiewicz, PhD Eng.

She graduated from the Faculty of Chemical and Process Engineering of the Warsaw University of Technology in 2004. Her masters thesis was also appreciated by the Award of the Ignacy Łukasiewicz Grant Fund of PGNiG S.A. for the best Master's thesis. In November 2010, she received a PhD degree and her Doctoral thesis entitled "Investigation into filtration of aerosol particles in inhomogeneous fibrous filters" was distinguished by the Faculty Council and by the jury awarding the Fiat grants. Dr Anna Jackiewicz has been employed by the Warsaw University of Technology as Assistant Professor since 2011. She is the supervisor of the filtration laboratory operating within the Department of Integrated Processes Engineering.

Dr Anna Jackiewicz is co-author of 47 papers published in periodicals and conference materials. She has presented her research results at 13 international and 9 national conferences. She received scholarships for distinguished Ph.D. students in the field of science and research and scholarship for young scientists awarded by the Centre for Advanced Studies, Warsaw University of Technology, and by the Marshal of the Mazowieckie province. In

2011, she was granted an individual Award of the Rector of the Warsaw University of Technology for scientific achievements. Her profile was presented at the exhibition entitled "Maria Skłodowska-Curie in the Service of Science Yesterday and Today" at the European Parliament in Brussels. Since 2012 Dr Jackiewicz is the manager of the Leader III project from the National Centre for Research and Development. This year she was awarded first place in the project called "Internship as a success of a scientist", intended to strengthen the cooperation between researchers and enterprises.

Her scientific interests: separation processes of gas-solid and liquid particles, filtering media design, modeling of filtration in fibrous filters, techniques for aerosol generation and detection, materials science.

Zoltan Kovács, PhD

Dr Kovács holds the position of associate professor at the Department of Food Engineering at the Corvinus University of Budapest, Hungary.

He earned his Ph.D. degree on Chemical Engineering from the Institute of Process Engineering at the Johannes Kepler Universitaet Linz, Austria. Prior to his current position, he had worked as senior scientist at the Institute of Bioprocess Engineering and Pharmaceutical Technology of the University of Applied Sciences Mittelhessen, Giessen, Germany. He has been a regular reviewer for reputed scientific journals, published 3 book chapters, over 20 peer-reviewed papers in top journals, 60+ papers in conference proceedings, and filled one patent application. He has received distinctions from the European Membrane Society, the Association of German Engineers, and since 2013 he is a Marie Curie Researcher. He has participated to and is responsible for many out-of-campus projects with industrial partners in the field of bioprocess and membrane technology design and development.

Agata Penconek, PhD Eng.

PhD, assistant professor at the Faculty of Chemical and Process Engineering Warsaw University of Technology, Poland.

2008: MSc in biotechnology, 2009: BCH in biology; 2014 PhD in chemical engineering; Scientific interests: anthropogenic aerosols (e.g. diesel exhaust particles), their filtration, deposition in human respiratory system, and interaction with eukaryotic/prokaryotic cells, aerosol particle transfer through mucus layer, aerosol particle mechanics.

Author and co-author of 8 scientific papers and chapter in one book.

Recipient of 1st prize in Research Grants Competition Investin 2012 and scholarship of the Mazowieckie Voivodeship Local Government.

Organizing committee

Members of the Scientific Club of Chemical and Process Engineering

Head of Committee
Aneta Gawryszewska

Zuzanna Bojarska
Luiza Kaszubowska, BSc Eng.
Marta Kisiel, BSc Eng.
Bartosz Nowak, MSc Eng.
Joanna Witkowska, MSc Eng.
Michał Wojasiński, MSc Eng.

Invited lectures

Prof. Jerzy Bałdyga, PhD Eng.



Prof. Jerzy Bałdyga (1950), PhD; DSc, has been since 1997 a Professor of Chemical Engineering at the Warsaw University of Technology, Faculty of Chemical and Process Engineering, Division of Engineering and Dynamics of Chemical Reactors Warsaw Poland.

He has received his MSc in Chemical Engineering in 1974, PhD in Chemical Engineering in 1981, and DSc (habilitation) in Chemical Engineering in 1989, all from Warsaw University of Technology. In 1997 he has got the Chair of Mechanical Engineering and Process Dynamics at the Chemical Engineering Faculty, Warsaw University of Technology. Since 2005 till 2012 he has been a Dean of the Faculty . He has been a visiting professor in: ETH Zurich and University of Saskatchewan. He co-operates with many industrial companies including: DSM, Groningen, The Netherlands; BASF, Ludwigshafen, Germany; Bayer, Germany, Merck, Germany, BPD, Bradford, UK; AUSIMONT, Italy, Solvay, France. He is a Member of Institution of Chemical Engineers, Delegate of Poland to Working Party on Mixing of European Federation of Chemical Engineering and Chair of Working Party on Mixing of European Federation of Chemical Engineering, Member of Committee of Chemical & Process Engineering PAN (Chairman of Mixing Section), and member of North American Mixing Forum.

Research of Professor Bałdyga can be characterized as application of fluid mechanics to problems of chemical engineering and chemical reaction engineering.

Prof. Bałdyga will present a lecture about **“Mixing and agitation effects in product engineering.”**

Prof. Marc-Olivier Coppens



Marc-Olivier Coppens is the Ramsay Memorial Professor and Head of Department of Chemical Engineering at University College London (UCL), since 2012.

He holds MSc (1993) and PhD (1996) degrees in chemical engineering from Ghent University in Belgium; was postdoctoral fellow at Yale and UC Berkeley; was at TU Delft from 1998-2006, where he became van Leeuwenhoek Professor in Reactor & Catalysis Engineering in 2001 and Chair of Physical Chemistry and Molecular Thermodynamics in 2003. He was a Professor at Rensselaer Polytechnic Institute (RPI) from 2006-2012.

Professor Coppens' research centers on Nature-Inspired Chemical Engineering (NICE), that is, to design and realize efficient chemical reaction processes, porous catalysts, and separation systems, guided by the fundamental mechanism underlying desirable properties, like scalability and robustness, in biological systems, from molecular to macroscopic scales. Applications are in the areas of resource efficiency (energy, water and materials), sustainable chemical production, and health.

As of 2013, he is also Director of UCL's new Centre for Nature Inspired Engineering – one of five, 5M£ “Frontier Engineering” Awards given by the UK's National Science Foundation, EPSRC. Other awards include Young Chemist and PIONIER Awards from the Dutch National Science Foundation (NWO), an RSC Catalysis Science and Technology Lecture Award (Zürich, 2012) and several invited named lectureships, including the Somer Lectures at METU (Ankara, 2014), and visiting professorships (Norwegian Academy of Science and Letters, Beijing University of Chemical Technology; East China University of Science and Technology). He has published over 100 peer-reviewed journal publications to date, and presented more than 50 keynote and plenary lectures at international conferences.

In 2014, he became a Fellow of the Institution of Chemical Engineers (IChemE). In 2015, he was also appointed as the first International Director of the American Institute of Chemical Engineers (AIChE) Catalysis and Reaction Engineering (CRE) Division, and is active on AIChE's International Committee and for the Particle Technology Forum (PTF).

A passionate educator, he won the Rensselaer School of Engineering Innovation in Teaching Award in 2012.

He serves on the Advisory or Editorial Boards of Chemical Engineering Science, Powder Technology and KONA, amongst other journals. He consults for various companies, and is or has been advisor to the Chemical Engineering Departments of Hong Kong University of Science and Technology (HKUST), Universidad de los Andes in Colombia, and ETH Zürich.

Prof. Coppens will present a lecture about **"Nature-Inspired Chemical Engineering – Pathways to Innovation and Sustainability"**

Bruno Bastos Sales, PhD



Bruno Bastos Sales was born in Fortaleza, Brazil. There he lived till graduating with a B.Sc. in Physics at the Federal University of Ceara. He subsequently moved to Recife, Brazil to pursue a M.Sc. in Energetic and Nuclear Technologies at the Federal University of Pernambuco. His interest in sustainability led to his move to Leeuwarden, the Netherlands, where he worked on the topic of Blue Energy: Renewable Energy from Mixing River and

Sea water as his PhD project at Wetsus and Wageningen University. Finally he kept involved in sustainable water technology and green energy production at VITO in Belgium as a Postdoctoral Researcher.

Dr. Bastos is an experienced researcher in the field of Renewable Energy, more specifically developing the Capacitive Blue Energy technology. This technique uses the adsorption capacity of activated carbon to alternately store and release ions. The physical chemical process is particularly interesting when applied to regions where rivers meet the sea, and the difference in salinity allows the generation of electricity (Blue Energy).

He has more than 17 publications on the topic, with more than 200 citations and several invited talks. His current interests range also from Water Technologies to Electrochemistry Techniques.

Dr. Bastos will present a lecture about "**Bringing the Blue into Green's Energy Palette**"

Naresh Kasoju, PhD



He obtained his B.Sc. in Biotechnology (2004, gold medalist) from the Kakatiya University, Warangal, India, M.Sc. in Biotechnology (2006) from the Osmania University, Hyderabad, India, and, Ph.D. in Biotechnology (2012) from the Indian Institute of Technology, Guwahati, India. He is currently affiliated with the Institute of Macromolecular Chemistry, Prague, Czech Republic. Recently, he visited the University of Oxford, Oxfordshire, United Kingdom. He is a young researcher in the field of Biomedical Engineering, more specifically in Biomaterials, Extracellular Matrix Engineering and Cell-based Therapies. So far, he has co-authored 25 peer-reviewed publications with more than 900 citations and participated in 20 conferences. He received 4 best presentation awards, and as part of Student and Young Investigator Section programme he was selected as a session chair at TERMI-EU 2013 in Istanbul. He is acting as a member of editorial board of 2 journals and as a reviewer for 12 journals. He is currently working on the bioinspired engineering of an artificial microenvironment for potential islet transplantation applications.

Dr. Kasoju will present about **“Bioengineered pre-vascularized beds for islet transplantation: a materials perspective”**.

Anna Zalewska, PhD



PhD. Eng. Anna Zalewska – She is a specialist in the field of Explosives and has a well-established expertise in the detection of explosives vapors. Master thesis made at the Central Police Headquarters Forensic Laboratory. The aim of this study was to develop the effective methods of the extraction of the trace amounts of explosives from clothes. Doctoral studies, carried out in the Department of Energetic Materials at the Department of Chemistry, Warsaw University of Technology.

She defended doctoral thesis on "New possibilities of the screening mobile devices in the detection of the explosives" and she is an assistant professor at the Military Institute of Chemistry and Radiometry, where she is a specialist in the field of trace analysis especially by ion mobility spectrometry and differential ion mobility spectrometry. She participated and giving a speech in international trade fairs and many conferences.

Dr Zalewska will present a speech about: **“Innovative screening device for high-sensitive chemical vapors detection”**

Monograph articles

Gold nanoparticles properties and recent advances

*Magdalena Blicharska¹, Sylwia Żołądek¹, Anna Dobrzeniecka¹, Paweł Kulesza¹

¹Faculty of Chemistry, Warsaw University, Warsaw, POLAND

e-mail: mblicharska@chem.uw.edu.pl

Keywords: gold nanoparticles, catalysis, nanomedicine, nanotechnology

ABSTRACT

Gold is commonly known as a yellow noble metal which is chemically inert. However after reducing to the nano-size it exhibits rich chemistry, possess distinct physical and chemical attributes which make this metal unique. Gold nanoparticles (AuNPs) have continued to receive considerable attention due to their fascinating size-related electronic, magnetic and optical properties.

The present review deals with the synthesis methods and physicochemical properties of gold nanoparticles. Finally, some aspects of the recent advances in the biomedical and electrocatalytic applications of nanostructural gold are considered too.

INTRODUCTION

Nanotechnology had already been unconsciously used for thousands of years and gold nanostructures have been synthesized for over 2000 years in a whole range of media including glasses, polymers and water. From a scientific point of view the development of the chemical synthesis of gold nanoparticles dates from the middle of the nineteenth century, when Michael Faraday reduced tetrachloroaurate using white phosphorus to yield deep-red gold sols. Since then, many methods based on the reduction of gold salts have been developed by various researchers. The Turkevich employed a mild reducing agent, sodium citrate, to form spherical gold nanoparticles suspended in water of around 10–20 nm in diameter [1,2]. Brust–Schiffrin was to report synthesis of the alkanethiolate-protected gold nanoparticles. The approach uses thiol ligands and is carried out in a two-phase system [3]. The gold precursor (AuCl_4^-) salt was transferred from an aqueous solution to an organic phase using tetraoctylammonium bromide as the phase transfer agent and then is reduced by sodium borohydride in the presence of an alkanethiol stabilizing agent. Chemical composition and properties of the passivating, highly ordered monolayers of thiol ligands can be manipulated through the ligand-exchange reaction [4]. The concept allowed to convert alkanethiolate-modified gold nanoparticles via ligand exchange to Au nanoparticle systems stabilized through the adsorption of anionic phosphomolybdate (PMo_{12}) on their surfaces. Such particles were

spontaneously immobilized on glassy carbon, by linking via ultra-thin polymer (PANI or PPy) structures to form network films with polyoxometalate-modified gold nanoparticles [4].

Gold is one of the most desirable among metals and generate a lot of interest since ancient times. The most famous example of ancient nanotechnology is the Lycurgus Cup, a dichroic glass cup with a mythological scene. Moreover the **Medieval Stained Glass** containing tiny amounts of colloidal gold and silver, is an example of the practise of the early forms of nanotechnology [5,6,7,8].

Gold nanoparticles play an important role in several applications from industrial to medical, where the fundamental goal of the colloidal gold synthesis is to obtain nanoparticles with tailored shape and size [8]. In this review we summarize some of the applications of nanostructural gold in the fields of biomedicine, environmental monitoring and electrocatalysis.

DISCUSSION SECTIONS

Gold nanoparticles properties

Miniaturization of macroscopic size to the nano-scale is associated with the induction of significant structural and surface changes due to the strong development of surface area. Surface/volume ratio of nanomaterials increases with decreasing diameter of these structures generating an increase in surface energy. This is the cause of the differences in the properties of nanomaterials and their equivalents in the form of bulk matter, for example: the melting point of 2.5 nm gold particles was reported to be about 930 K, much lower than its bulk value of 1336 K. Bulk gold is shiny and yellow but the color of the nanoparticles depends on the shape, size of the nanoparticle and dielectric constant of the surrounding medium [6,9]. Gold spheres dispersed in water solutions are purple-red in color which is associated with the surface plasmon band (SPB) in the visible region around 520 nm. The SPB is due to the collective oscillations of the free conduction electrons induced by an interacting electromagnetic field (6s electrons of the conduction band for AuNPs)[6,8]. Formation of large aggregates causes a reversible change in color of the AuNPs suspension from red to violet due to coupling to surface plasmons in aggregated colloids [6,10].

Because of very high surface/volume ratio resulting in high reactivity nanoparticles exhibit tendency to merge into larger aggregates. For this reason AuNPs need to be stabilized. Generally, two main strategies appear in the literature, regarding either the steric or kinetic stabilization. The steric stabilization can be achieved by the use of chemically attached organic ligands including polymers, amines or peptides. The electrostatic (kinetic) stabilization

is based on the coulombic repulsion between negatively charged layers protecting nanoparticles [11,12,13,14]. Alternative strategy to stabilize nanoparticles against agglomeration is to support nanoparticles on a solid surfaces, including single and multi-walled carbon nanotubes, graphene, Norit, TiO₂, ZrO₂, Fe₃O₄ and silica particles [15,16,17,18]. The approach is based on the van der Waals, hydrogen bonding and electrostatic forces between gold and support, reducing the mobility and aggregation of the gold catalyst [17,18].

Preparation of gold nanoparticles

There has been tremendous progress over the past decade in the synthesis of gold nanoparticles with a good monodispersity. In particular, AuNPs of various sizes and shapes can be obtained by so-called “top-down” methods, in which nanoparticles are directly generated from bulk gold via atoms by various distribution techniques [19]. Another words „top-down” involves the mechanical grinding of the macroscopic metal and subsequent stabilization of the resulting nanosized particles by the addition of the interfacial protecting agents. In this field metal vapor techniques, including laser ablation methods have become commonly used for the production of a wide range of gold nanostructures [20,21,22]. Nevertheless “top-down” approach is limited because the size distribution of the resulting AuNPs is usually rather broad [23]. The “bottom-up” methods are defined as those by which gold nanoparticles are directly generated according to chemical routes using gold precursors as starting materials, linked with reduction steps. Moreover the “bottom-up” methods involve the electrochemical pathways of the controlled nanoparticle preparation in which the metal cations are transferred to the cathode, where reduction, nucleation and finally stabilization occur [24, 25, 26]

A large variety of stabilizers, including water-soluble polymers, surfactants or capping agents are used to avoid coalescence between the gold nanoclusters, preventing them against agglomeration. Series of reducing agents have been utilized for the preparation of gold nanoparticles, including: H₂, NaBH₄, N₂H₂, NH₂OH, ethanol, ethylene glycol, formamide, citric and ascorbic acid [19]. The size- and shape-selected synthesis of the resulting gold nanoparticles can be achieved by altering the relative growth rates of different facets by the selective localization of surface-modifying or capping agents, but also by the modulation of nucleation and reaction parameters such as time, temperature, reagent concentration and pH [27].

Some research concerned the synthesis of gold nanostructures stabilized with polyoxometalates acting as both reducing and capping agents. Two main strategies appear in the literature: the reduced polyoxometalates, necessary for

carrying out the process, can be obtained by photochemical reduction or be synthesized directly with reducing capabilities [28,29,30].

Also the green synthesis of metallic nanoparticles is being investigated to protect the environment by decreasing the use of toxic chemical substances and eliminating biological risks in pharmaceutical and biomedical applications. Many natural products including pure compounds from plants [31] or plant extracts [32] represent excellent scaffolds for this purpose. In the case of green synthesis the natural substances act as reducing and stabilizers agents or serve dual roles for the production of AuNPs [33,34,35]. For synthesis the gold nanoparticles also living organism are involved for example alfalfa plant [36] and microorganisms such as fungus [37], alga [38], yeast [39] and bacteria [40]. This type of synthesis involved microbes occurring intracellularly [41] or extracellularly [42] using cells extracts.

Application of gold nanoparticles in electrocatalysis

A tremendous amount of research has been carried out in the field of the application of gold nanoparticles in electrocatalysis, particularly with respect to sensors and fuel cells. It has been found that gold as a bulk metal is fairly unreactive due to the qualities of low adsorption energy and high dissociation barriers [43] while in the form of nanostructures Au exhibits an unusually high electrocatalytic activity, assigned to the quantum size effects [44], charging of the gold particles [45] and presence of low coordinated sites [46]. There are still many disagreements concerning the nature of the mechanism and effects that contribute to the overall process. Probably the catalytic activity of gold nanoparticles is not the result of a single contribution, but arises from a combination of different effects [47].

In this field the role of the gold structure and oxide support have not yet been resolved. Some studies have demonstrated that efficiency of the gold catalyst can be further improved by the modification of the electrocatalytic interface by utilizing reducible metaloxides of variable stoichiometry such as MnO_x , TiO_x , FeO_x and CoO_x whereas the oxides of fixed stoichiometry, including Al_2O_3 are not capable to contribute to the catalytic activity of the AuNPs [48]. It has been established that the catalytic properties of the gold nanoparticles can be dramatically influenced by their size [49]. The gold nanostructures less than 5 nm in diameter are known to be the most catalytically active for several chemical reactions. This phenomenon might be attributed to the high fraction of the low-coordinated Au atoms located at the corners and edges of Au nanoparticles being the active sites and to the quantum-size behavior [44].

The Au nanoparticles have been shown to act as effective catalysts towards low-temperature oxidation of CO [47] and reduction of O_2 . The most

likely explanation of this phenomenon is associated with the decrease of the binding energy of O₂ or CO approximately linearly with decreasing coordination number of Au following decline of the nanoparticle diameter [47,50]. Moreover the possible mechanism may involve electronic interactions between the perimeter atoms of the gold cluster and appropriate oxide substrate that control the reaction of O₂ and CO along the perimeter [51].

Recently, studies have shown that phosphomolybdate-protected gold nanoparticles (PMo₁₂/AuNP_s) seem to be particularly attractive for various electrocatalytic applications both as supports (carriers) or as the metal active sites [29]. It was found that well-defined spherical polyoxometallate-modified Au nanoclusters of 30-40 nm are good candidates for application as supports (carriers) for platinum catalyst. The combination of PMo₁₂-modified Au nanoparticles with Pt black has yielded an efficient electrocatalytic system for electrooxidation of ethanol in acidic medium [29]. It has been established that impregnation of TiO₂ with phosphomolybdate-protected gold nanoparticles followed by deposition of conventional platinum black nanoparticles (ca. 7–9 nm), led to the enhancement effect promoting efficient ethanol electrooxidation [28]. This phenomenon was attributed to the improvement of overall conductivity (due to the presence of nanostructured gold) at the electrocatalytic interface (including TiO₂-support), as well as and possibility of specific Pt–TiO₂ or Pt–Au electronic interactions and existence of active hydroxyl groups (on titanium dioxide or polyoxometallate surfaces) in the vicinity of catalytic Pt sites [28].

In recent years, great efforts have been devoted to catalysts based on platinum-free materials for oxygen reduction, particularly with respect to potential applications in sensors and fuel cells. Some of the literature studies elucidate the influence of the electrodeposition of Au nanoparticle onto a polycrystalline Au electrode on the electrocatalytic reduction of molecular oxygen acidic media. It was shown that increase of the gold particle size to the micron scale resulted in a loss of the catalytic activity towards oxygen reaction [52].

Moreover nanostructural-gold based catalysts may potentially act as promising alternatives for the Pt active towards the electro-oxidation of methanol in fuel cells. It has been established that the high oxidation activity of gold in alkaline medium is related to the high resistance of Au toward the “poisoning effects” due to generation of the reaction intermediates like CO [53]. Even more promising results were provided by the multifunctional hybrid system composed of gold nanoparticles homogeneously dispersed on the multi-walled carbon nanotube- support. The overall enhancement effect was attributed to the combination of mediating capabilities of surface oxygen complexes

created at the sidewall of carbon nanotubes and redox transition of the interfacial mediator species created by hydrous oxide/adatom mediator (IHOAM) which takes place at a potential within the double layer region [54].

Biomedical applications of gold nanoparticles

Because of the unique properties gold nanoparticles are already at a point where even commercial applications in medical fields are known, including: diagnostics, therapy, prevention and hygiene [55,56]. Another developing field of biomedical applications of AuNPs is the targeted delivery of drugs. It can be assumed that gold nanoparticles may act as drug carriers especially for antibiotics and antitumor agents [55,57]. In the literature there are described many examples of the applications of gold nanoparticles as carriers for antitumor substances for example: platinum complexes [58], doxorubicin [59], paclitaxel [60], 6-mercaptopurine [61] and antibiotics such as vancomycin [62] and ciprofloxacin [63]. Not all antibiotics -ampicillin, streptomycin, gatifloxacin, norfloxacin- form stable complexes with gold nanoparticles, nevertheless, their activity when mixed with AuNPs was higher than that of the antibiotic when used alone [64,65]. The conjugation was carried out either by simple physical adsorption of the drugs onto AuNPs or via the use of linkers such as: alkanethiol, polymer and amines. The organic monolayers protecting nanoparticles are fundamentally important for modeling the interactions between the AuNPs and its environment, moreover they can be readily modified to incorporate a diverse array of functionalized ligand [14,66,67]. Linker molecules can be arranged to contain a thiol group on one terminal end and an amine ($-NH_2$) or carboxylic acid ($-COOH$) functional group on the other end. This type of modification of introducing free functional group allows for drug coupling to the nanoparticle through many different ways [68]. The use of Au nanoparticles as delivery systems for therapeutics has manifold benefits allowing to modify the existing drugs, improve their pharmacokinetics and the stability against decomposition and solubility. Incorporation of drug molecules in nanoparticles causes that nanosystems are often accumulated at higher concentrations when compared to normal drugs, thereby enabling higher dose delivery to target tissues reducing non-specific side effects leading to reduced systemic toxicity [57,67,68]. It was also reported to use nanomultifunctional delivery systems, in which the gold nanoparticles were loaded with specific therapeutic agents exhibiting medicinal and diagnostic properties, to create a combined therapy [69]. In addition to the drug delivering into the body provided by gold nanomaterials, current applications may include the detection, diagnosis of early stage cancer, therapy and monitoring the effectiveness of treatment. Thermal methods have been used in tumor therapy since the 18th century, which

based on their operation is cell death as a consequence of necrosis processes, but the effect of temperature is operative not only in cancer cells but also in the healthy ones. These treatments are considered to be highly efficient but on the other hand they are concerned to be drastic, non-reversible and non-selective [70,71]. Gold nanoparticles are currently providing alternative techniques for remote and localized heating because AuNPs absorb light millions of times stronger than the organic dye molecules and nearly 100% of absorbed light is converted to heat. Moreover, they are very photostable, biocompatible and they can be easily injected into organisms and effectively incorporated into the cells [55,71]. In 2003 AuNPs were applied as agents for photothermal therapy (PTT). Pitsillides et al. described gold nanoparticles coupled with a nanosecond Nd:YAG pulsed laser for in vitro photothermal therapy of lymphocytes [72]. The photothermal efficiency of AuNPs is depending on many factors including their shape. The gold nanospheres[73], nanoshells[74], nanorods[75] and nanocages[76] have already been reported in the literature to be used in PTT, demonstrating effective photothermal destruction of cancer cells. The gold nanorods enable effective treatment at three times lower laser intensity, when compared to nanoshells. This is because nanorods exhibit higher absorption efficiency than nanoshells with the SPR at the same wavelength [77].

The gold nanoparticles have also been used in photodynamic therapy (PDT). This type of oncological therapy is based on the use of light-sensitive agents for examples dyes and visible light of a certain wavelength corresponding to the absorption maximum of the dye. Radiation with laser light causes the heat release and in addition photochemical generation of singlet oxygen and others highly active radicals inducing necrosis and apoptosis of tumor cells. Because of the PDT low efficacy, the light-sensitive agents have to remain in the organism for a long time which may result in the fact that patient's tissues remain highly sensitive to light. Gold nanoparticles are used to improve the efficacy of PDT through enhanced the efficacy of photosensitiser [55,78].

Khaing Oo et al used gold nanoparticles as a vehicle to deliver 5-aminolevulinic acid in fibrosarcoma tumor cells, yielding significantly more reactive oxygen species, causing more cytotoxicity to tumor cells than 5-aminolevulinic acid alone [79]. Stuschiskaya et al. reported that the anti-HER2 antibodies-phtalocyanine-polyethylene glycol-gold nanoparticle conjugate leads to the enhancement of drug targeting to the breast cancer cells followed by photodynamic treating. The above-mentioned 4-component gold nanoparticle conjugates are very promising photodynamic therapy agents [80]. Lkhagvadulam et al demonstrated that gold nanoparticles conjugate purpurin-18-N-methyl-D-glucamine (Pu-18-NMGA) resulted in higher photodynamic activity than that of the free Pu-18-NMGA. Moreover the size-dependent

photodynamic activity had also been investigated. It was concluded that the highest photodynamic activity was corresponding to the bigger sizes of the AuNPs conjugate which could efficiently transport the Pu-18-NMGA into the cells when compared to smaller size of the AuNPs conjugate [81]. There are also conducted research of the use of the gold nanoparticles for combined photothermal and photodynamic therapy. Kuo and coworkers have presented the example of using gold nanomaterials simultaneously serving as photodynamic and photothermal agents to destroy malignant cells [82]. Hari and colleagues described acridine orange tethered chitosan reduced gold nanoparticles as an effective photosensitizer carrier system as well as photothermal agent for enhanced PDT and PTT targeting of breast cancer cells [83].

Gold nanoparticles are also widely used not only for cancer therapy. The positive results achieved upon intra-articular and subcutaneous introduction of colloidal gold into rats with collagen- and pristan- induced arthritis were described [84,85]. Bowman et al. reported the first application of a derivative of the potent HIV inhibitor coated with AuNPs [86]. Mahmoud et al. has suggested the possibility of electrochemical detection of HIV type-1 protease (HIV-1 PR) using traditional electroanalytical techniques such as cyclic voltametry and electrochemical spectroscopy. The sensing electrode modified with ferrocene-peptide conjugate/AuNPs/thiolated single walled carbon nanotubes showed remarkable detection and high sensitivity with an estimated detection limit of 0.8 picomolar (pM) [87].

Another applications of gold nanoparticles

Gold nanoparticles have a growing importance in the field of forensic science. Gold proved to be an effective metal in fingerprint detection. The interest on AuNPs is due to their high stability towards oxidation and the stability of developed fingerprints over time [88]. Hussain et al. reported the use of AuNPs to develop a bio-ink on paper and polymer. Latent fingerprints are made visible in a single step by in situ growth of gold nanoparticles on ridge patterns at room temperature. The components of human sweat are responsible for the reduction of ionic gold to form gold nanoparticles [89]. One step to detect the latent fingermarks with gold nanoparticles presented also Gao et al. who prepared AuNPs using sodium borohydride as reducing agent in the presence of glucose. This single-metal nanoparticles deposition method (SND) has been performed in a wide pH range (2.5–5.0) on several non-porous items and the color of fingermarks detected by the SND was reddish [90]. The use of gold nanoparticles might be an attractive alternative to the methods suffering from restrictive experimental conditions, high cost preparation and some harmful solvents involved.

AuNPs play also an increasingly important role in environmental monitoring. Colloidal gold is used especially in the detection of pollutants and is applied in environmental sensing. AuNPs are used to enhance the performance of electrochemical sensors which have been widely investigated in the field of environmental pollutants screens. Gooding et al. proposed an electrochemical sensor for the detection of copper ions that has a limit of detection below 1 pM. Gold nanoparticles were attached to the terminus of the self assembled monolayer (SAM) modified electrode. Then the gold nanoparticles were modified with cysteine to allow copper accumulation, thus a higher percentage of copper from the solution was collected at the electrode giving the enhanced detection limits [91]. Wang et al. described the colloidal gold immunoassay as a rapid visual qualitative assay that produced a simple presence/absence test for ochratoxin A (another type of naturally occurring toxins is ochratoxin A in foods) which had a visual detection limit of 1.0 ng mL⁻¹ [92]. The changes associated with AuNPs aggregation were exploited by Dasary's group for the detection of 2,4,6-trinitrotoluene (TNT). They describe cysteine modified gold nanoparticle based on label-free surface enhanced Raman spectroscopy (SERS) probe for detection of trace amounts of TNT from environmental samples (recognition in 2 pico molar level in aqueous solution) [93].

Spherical nano-sized gold is not inherently toxic to human skin cell [94,95], therefore it is used in many cosmetics for example in gold facial masks which improve the skin elasticity, revitalizes the skin and thereby reduces the formation of wrinkles [96,97]. Taufikurohmah et al. presented synthesis of gold nanoparticles by use of glycerin as matrix and sodium citric as reduction agent. Glycerin is an ingredient of many cosmetics due to gold nanoparticles prepared in glycerin matrix *can be safe component in creams* [98]. *Many reports have described also bactericidal properties of nanostructural gold* [99], for this reason they are important component of hygiene products such as toothpaste.

Gold nanoparticles can be also alternative for organic colourants. Johnston et al. presented an innovative approach to the synthesis and use of gold nanoparticles as novel stable colourants utilising the surface plasmon resonance colouring effect. The resulting gold nanoparticles were chemically bound to the sulfur in the cystine amino acids in the keratin protein to form a stable nanogold wool fibre. Compare to traditional organic dyes gold colourant is stable in sunlight, UV light and it does not wash or rub out. Gold nanoparticles exhibit different colours depend on particle size or shape and hence colours in a nanogold wool composite fibre can be varied [100].

CONCLUSION

Bulk gold is well known for being chemically inert, but reduction of its size to the nano-scale changes the metal properties and possess distinct physico-chemical attributes which make the nanostructures of gold unique. Due to specific properties AuNPs are the subject of increasing number of reports and publications. Moreover they play an important role in nanoscience and nanotechnology. Nanostructural gold has grown significantly modes of preparation, described is more and more synthesis approaches including: mechanical, chemical and bio methods. The stabilization of AuNPs by various functional ligands create new possibilities and rich molecular chemistry. In conclusion, the reactivity of the gold nanoparticles is fully promising for optical, sensing, environmental monitoring, catalytic and biomedical applications.

REFERENCES

- 1 Turkevich J., Stevenson P.C., Hillier J., A study of the nucleation and growth processes in the synthesis of colloidal gold, *Discussions of the Faraday Society*, 1951, 11, 55-75
DOI: 10.1039/DF9511100055
- 2 Kimling J., Maier M., Okenve B., Kotaidis V., Ballot H., Plech A., Turkevich Method for Gold Nanoparticle Synthesis Revisited, *The Journal of Physical Chemistry B*, 2006, 110, 15700-15707
DOI: 10.1021/jp061667w
- 3 Brust M., Walker M., Bethell D., Schiffrin D.J., Whyman R., Synthesis of thiol-derivatised gold nanoparticles in a two-phase Liquid–Liquid system, *Journal of the Chemical Society, Chemical Communications*, 1994, 7, 801-802
DOI: 10.1039/C39940000801
- 4 Ernst A.Z., Zoladek S., Wiaderek K., Cox J.A., Kolary-Zurowska A., Miecznikowski K., Kulesza P.J., Network films of conducting polymer-linked polyoxometalate-modified gold nanoparticles: Preparation and electrochemical characterization, *Electrochimica Acta*, 2008, 53, 3924-3931
DOI: 10.1016/j.electacta.2007.12.053
- 5 Edwards P.P., Thomas J.M., Gold in a Metallic Divided State – from Faraday to Present-Day Nanoscience, *Angewandte Chemie International Edition*, 2007, 46, 5480–5486
DOI: 10.1002/anie.200700428
- 6 Daniel M.C., Astruc D., Gold Nanoparticles: Assembly, Supramolecular Chemistry, Quantum-Size-Related Properties, and Applications toward Biology, Catalysis, and Nanotechnology, *Chemical Review*, 2004, 104, 293-346
DOI 10.1021/cr030698

- 7 Freestone I., Meeks N., Sax M., Higgitt C., The Lycurgus Cup – A Roman Nanotechnology, *Gold Bulletin*, 2007, 40, 270-277
- 8 Eustis S., El-Sayed M.A., Why gold nanoparticles are more precious than pretty gold: Noble metal surface plasmon resonance and its enhancement of the radiative and nonradiative properties of nanocrystals of different shapes, *Chemical Society Reviews*, 2006, 35, 209–217
DOI: 10.1039/b514191e
- 9 Roduner E., Size matters: why nanomaterials are different, *Chemical Society Reviews*, 2006, 35, 583–592
DOI: 10.1039/b502142c
- 10 Apyari V.V., Arkhipova V.V., Dmitrienko S.G., Zolotov Y.A., Using Gold Nanoparticles in Spectrophotometry, *Journal of Analytical Chemistry*, 2014, 69, 1–11
DOI: 10.1134/S1061934814010031
- 11 Toma H.E., Zamarion V.M., Toma S.H., Araki K., The Coordination Chemistry at Gold Nanoparticles, *Journal of the Brazilian Chemical Society*, 2010, 21, 1158-1176
DOI: <http://dx.doi.org/10.1590/S0103-50532010000700003>
- 12 Benkovičová M., Végso K., Šiffalovič P., Jergel M., Majková E., Luby S., Šatka A., Preparation of sterically stabilized gold nanoparticles for plasmonic applications, *Chemical Papers*, 2013, 67, 1225–1230
DOI: 10.2478/s11696-013-0315-y
- 13 DeLong R.K., Reynolds C.M., Malcolm Y., Schaeffer A., Severs T., Wanekaya A., Functionalized gold nanoparticles for the binding, stabilization, and delivery of therapeutic DNA, RNA, and other biological macromolecules, *Nanotechnology, Science and Applications*, 2010, 3, 53–63
DOI: 10.2147/NSA.S8984
- 14 Sperling R., Parak W.J., Surface modification, functionalization and bioconjugation of colloidal inorganic nanoparticles, *Philosophical Transactions of the Royal Society A*, 2010, 368, 1333–1383
DOI: 10.1098/rsta.2009.0273
- 15 Carabineiro S.A.C., Martins L.M.D.R.S., Avalos-Borja M., Buijnsters J.G., Pombeiro A.J.L., Figueiredo J.L., Gold nanoparticles supported on carbon materials for cyclohexane oxidation with hydrogen peroxide, *Applied Catalysis A: General*, 2013, 467, 279–290
- 16 Mahyari M., Shaabani A., Bide Y., Gold nanoparticles supported on supramolecular ionic liquid grafted graphene: a bifunctional catalyst for the selective aerobic oxidation of alcohols, *RSC Advances- The Royal Society of Chemistry*, 2013, 3, 22509–22517
DOI: 10.1039/c3ra44696d

- 17 Zheng N., Stucky G.D., A General Synthetic Strategy for Oxide-Supported Metal Nanoparticle Catalysts, *Journal of the American Chemical Society*, 2006, 128, 14278-14280
DOI: 10.1021/ja0659929
- 18 Haruta M., Catalysis of gold nanoparticles deposited on metal oxides, *Feature*, 2002, 6, 102-115
- 19 Merza K.S., Al-Attabi H.D., Abbas Z.M., Yusr H.A., Comparative Study on Methods for Preparation of Gold Nanoparticles, *Scientific Research Green and Sustainable Chemistry*, 2012, 2, 26-28
DOI:org/10.4236/gsc.2012.21005
- 20 Matsuo N., Muto H., Miyajima K., Mafune F., Single laser pulse induced aggregation of gold nanoparticles, *Physical Chemistry Chemical Physics*, 2007, 9, 6027-6031
DOI: 10.1039/B709982G
- 21 Geohegan D.B., Time-resolved imaging of gas phase nanoparticle synthesis by laser ablation, *Applied Physics Letters*, 1998, 72, 2987-2989,
DOI: 10.1063/1.121516
- 22 Amendola V., Rizzi G.A., Polizzi S., Meneghetti M., Synthesis of Gold Nanoparticles by Laser Ablation in Toluene: Quenching and Recovery of the Surface Plasmon Absorption, *The Journal of Physical Chemistry B*, 2005, 109, 23125–23128
DOI: 10.1021/jp055783v
- 23 Bradley J.S., Schmid G., Clusters and Colloids, VCH, Weinheim, 1994.
- 24 Gaffet E., Tachikart M., ElKedim O., Rahouadj R., Nanostructural Materials Formation by Mechanical Alloying: Morphologic Analysis Based on Transmission and Scanning Electron Microscopic Observations, *Materials Characterization*, 1996, 36, 185-190
- 25 Etesami M., Salehi Karoonian F., Mohamed N., Electrochemical Deposition of Gold Nanoparticles on Pencil Graphite by Fast Scan Cyclic Voltammetry, *Journal of the Chinese Chemical Society*, 2011, 58, 688-693
- 26 Germana N., Ramanavicius A., Ramanaviciene A., Electrochemical deposition of gold nanoparticles on graphite rod for glucose biosensing, *Sensors and Actuators B: Chemical*, 2014, 203, 25-34
DOI:10.1016/j.snb.2014.06.021
- 27 Sohn K., Kim F., Pradel K.C., Wu J.S., Peng Y., Zhou F.M., Huang J.X., Construction of evolutionary tree for morphological engineering of nanoparticles, *ACS Nano*, 2009, 3, 2191-2198
DOI: 10.1021/nn900521u
- 28 Zoladek S., Rutkowska I.A., Kulesza P.J. ,Enhancement of activity of platinum towards oxidation of ethanol by supportingon titanium dioxide

- containing phosphomolybdate-modified gold nanoparticles, *Applied Surface Science*, 2011, 257, 8205-8210
DOI: 10.1016/j.apsusc.2011.04.080
- 29 Zoladek S., Rutkowska I.A., Skorupska K., Palys B., Kulesza P.J., Fabrication of polyoxometallate-modified gold nanoparticles and their utilization as supports for dispersed platinum in electrocatalysis, *Electrochimica Acta*, 2011, 56, 10744-10750
DOI: 10.1016/j.electacta.2011.04.020
- 30 Keita B., Liu T., Nadjro L., „Synthesis of remarkably stabilized metal nanostructures using polyoxometalates, *Journal of Materials Chemistry*, 2009, 19, 19-33
DOI: 10.1039/b813303d
- 31 Sanna V., Pala N., Dessì G., Manconi P., Mariani A., Dedola S., Rassu M., Crosio C., Laccarino C., Sechi M., Single-step green synthesis and characterization of gold-conjugated polyphenol nanoparticles with antioxidant and biological activities, 2014, 9, 4935–4951
DOI: 10.2147/IJN.S70648
- 32 Parida U.K., Bindhani B.K., Nayak P., Green Synthesis and Characterization of Gold Nanoparticles Using Onion (*Allium cepa*) Extract, *World Journal of Nano Science and Engineering*, 2011, 1, 93-98
DOI:10.4236/wjnse.2011.14015
- 33 Bhau B.S., Ghosh S., Puri S., Borah B., Sarmah D.K., Khan R., Green synthesis of gold nanoparticles from the leaf extract of *Nepenthes khasiana* and antimicrobial assay, *Advanced Materials Letters*, 2015, 6, 55-58
DOI: 10.5185/amlett.2015.5609
- 34 Sujitha M.V., Kannan S., Green synthesis of gold nanoparticles using Citrus fruits (*Citrus limon*, *Citrus reticulata* and *Citrus sinensis*) aqueous extract and its characterization, *Spectrochimica Acta Part A: Molecular and Biomolecular Spectroscopy*, 2013, 102, 15–23
DOI:10.1016/j.saa.2012.09.042
- 35 Elia P., Zach R., Hazan S., Kolusheva S., Porat Z., Zeiri Y., Green synthesis of gold nanoparticles using plant extracts as reducing agents, *International Journal of Nanomedicine*, 2014, 9, 4007–4021
DOI: 10.2147/IJN.S57343
- 36 Gardea-Torresdey J.L., Parsons J.G., Gomez E., Peralta-Videa J., Troiani H.E., Santiago P., Yacaman M.J., Formation and Growth of Au Nanoparticles inside Live Alfalfa Plants, *Nano Letters*, 2002, 4, 397–401
DOI: 10.1021/nl015673

- 37 Kitching M., Ramani M., Marsili E., Fungal biosynthesis of gold nanoparticles: mechanism and scale up, *Microbial Biotechnology*, 2014, DOI:10.1111/1751-7915.12151
- 38 Arockiya Aarthi Rajathi F., Parthiban C., Ganesh Kumar V., Anantharaman P., Biosynthesis of antibacterial gold nanoparticles using brown alga, *Stoechospermum marginatum* (kützing), *Spectrochimica Acta Part A: Molecular and Biomolecular Spectroscopy*, 2012, 99, 166–173
DOI:10.1016/j.saa.2012.08.081
- 39 Mourato A., Gadanho M., Lino A.R., Tenreiro R., Biosynthesis of Crystalline Silver and Gold Nanoparticles by Extremophilic Yeasts, *Bioinorganic Chemistry and Applications*, 2011, 1–8
DOI:10.1155/2011/546074
- 40 Iravani S., Bacteria in Nanoparticle Synthesis: Current Status and Future Prospects, *International Scholarly Research Notices*, 2014, 1–18
DOI:10.1155/2014/359316
- 41 Ahmad A., Senapati S., Khan M.I., Kumar R., Ramani R., Srinivas V., Sastry M., Intracellular synthesis of gold nanoparticles by a novel alkalotolerant actinomycete, *Rhodococcus* species, *Nanotechnology*, 2003, 14, 824–828
- 42 Gupta S., Bector S., Biosynthesis of extracellular and intracellular gold nanoparticles by *Aspergillus fumigatus* and *A. flavus*, *Antonie van Leeuwenhoek*, 2013, 103, 1113–1123
DOI 10.1007/s10482-013-9892-6
- 43 Hammer B., Norskov J. K., Why gold is the noblest of all the metals, *Nature*, 2002, 376, 238-240
DOI:10.1038/376238a0
- 44 Valden M., Lai X., Goodman D. W., Onset of catalytic activity of gold clusters on titania with the appearance of nonmetallic properties, *Science*, 1998, 281, 1647-1650
- 45 Sanchez A., Abbet S., Heiz U., Schneider W. D., Häkkinen H., Barnett R. N., Landman U., When Gold Is Not Noble: Nanoscale Gold Catalysts, *The Journal of Physical Chemistry A*, 1999, 103, 9573-9578
DOI: 10.1021/jp9935992
- 46 Mavrikakis M., Stoltze P., Nørskov, J. K., Making gold less noble, *Catalysis Letters*, 2000, 64, 101-106 (doi –brak)
- 47 Arenz M., Landman U., Heiz U., CO Combustion on Supported Gold Clusters, *ChemPhysChem*, 2006, 7, 1871-1879
DOI: 10.1002/cphc.200600029
- 48 Schubert M.M., Hackenberg S., van Veen A.C., Muhler M., Plzak V., Behm R.J., CO Oxidation over Supported Gold Catalysts-“Inert” and “Active” Support

- Materials and Their Role for the Oxygen Supply during Reaction, *Journal of Catalysis*, 2001, 197, 113–122
DOI: 10.1006/jcat.2000.3069
- 49 Haruta M., Size - and support-dependency in the catalysis of gold, *Catalysis Today*, 1997, 36, 153-166 (doi –brak)
- 50 Molina L.M., Hammer B., Theoretical study of CO oxidation on Au nanoparticles supported by MgO(100), *Physical Review B*, 2004, 69, 155424-21
DOI: doi. 10.1103/PhysRevB.69.155424
- 51 Wolf A.; Schuth F., A systematic study of the synthesis conditions for the preparation of highly active gold catalysts, *Applied Catalysis A: General* 2002, 226, 1-13
DOI: 10.1016/S0926-860X(01)00772-4
- 52 El- Deab M.S., Ohsaka T., An extraordinary electrocatalytic reduction of oxygen on gold nanoparticles-electrodeposited gold electrodes, *Electrochemistry Communications* 4, 2002, 288-292
DOI:10.1016/j.elecom.2004.10.010
- 53 Assiongbon K.A., Roy D. ,Electro-oxidation of methanol on gold in alkaline media: Adsorption characteristics of reaction intermediates studied using time resolved electro-chemical impedance and surface plasmon resonance techniques, *Surface Science*, 2005, 594, 99 -119
DOI:10.1016/j.susc.2005.07.015
- 54 Zoladek S., Rutkowska I.A., Magdalena Blicharska M., Gierwatowska M., P. J. Kulesza, Multifunctional Nanostructured Materials for Oxidation of Methanol, *ECS Transactions* 2013, 53, 1-10 DOI:10.1149/05328.0001ecst
- 55 Dykman L.A., Khlebtsov N.G., Gold Nanoparticles in Biology and Medicine: Recent Advances and Prospects, *Chemical Society Reviews*, 2012, 41, 2256-2282
DOI: 10.1039/c1cs15166e
- 56 Giasuddin A.S.M., Jhuma K.A., Mujibul Haq A.M., Use of Gold Nanoparticles in Diagnostics, Surgery and Medicine: A Review, *Bangladesh journal of medical biochemistry*, 2012, 5, 56-60 DOI:10.3329/bjmb.v5i2.13346
- 57 Khan A.K., Rashid R., Murtaza G., Zahra A., Gold Nanoparticles: Synthesis and Applications in Drug Delivery, *Tropical Journal of Pharmaceutical Research*, 2014, 13, 1169-1177
DOI:10.4314/tjpr.v13i7.23
- 58 Dhar S., Daniel W.L., Giljohann D.A., Mirkin C.A., Lippard S.J., Polyvalent Oligonucleotide Gold Nanoparticle Conjugates as Delivery Vehicles for Platinum(IV) Warheads, *Journal of the American Chemical Society*, 2009, 131, 14652-14653
DOI: 10.1021/ja9071282

59 Asadishad B., Vossoughi M., Alemzadeh I., Folate-Receptor-Targeted Delivery of Doxorubicin Using Polyethylene Glycol-Functionalized Gold Nanoparticles, *Industrial and Engineering Chemistry Research*, 2010, 49, 1958-1963

DOI: 10.1021/ie9011479

60 Paciotti G.F., Kingston D.G.I., Tamarkin L., Colloidal gold nanoparticles: a novel nanoparticle platform for developing multifunctional tumor-targeted drug delivery vectors, *Drug Development Research*, 2006, 67, 47-54

DOI: 10.1002/ddr.20066

61 Podsiadlo P., Sinani V.A., Bahng J.H., Kam N.W., Lee J., Kotov N.A., Gold nanoparticles enhance the anti-leukemia action of a 6-mercaptopurine chemotherapeutic agent, *Langmuir*, 2008, 24, 568-574

62 Gu H., Ho P.L., Tong E., Wang L., Xu B., Presenting Vancomycin on Nanoparticles to Enhance Antimicrobial Activities, *Nano Letters*, 2003, 3, 1261-1263

DOI: 10.1021/nl034396z

63 Rosemary M.J., MacLaren I., Pradeep T., Investigations of the antibacterial properties of ciprofloxacin@SiO₂, *Langmuir*, 2006, 22, 10125-10129

DOI: 10.1021/la061411h

64 Saha B., Bhattacharya J., Mukherjee A., Ghosh A.K., Santra C.R., Dasgupta A.K., Karmakar P., In Vitro Structural and Functional Evaluation of Gold Nanoparticles Conjugated Antibiotics, *Nanoscale Research Letters*, 2007, 2, 614-622

DOI:10.1007/s11671-007-9104-2

65 Grace A.N., Pandian K., Quinolone Antibiotic-Capped Gold Nanoparticles and Their Antibacterial Efficacy Against Gram Positive and Gram Negative Organisms, *Journal of Bionanoscience*, 2007, 1, 96-105

DOI:10.1166/jbns.2007.018

66 Boccalon M., Bidoggia S., Romano F., Gualandi L., Franchi P., Lucarini M., Pengo P., Pasquato L., Gold nanoparticles as drug carriers: a contribution to the quest for basic principles for monolayer design, *Journal of Materials Chemistry B*, 2015, 3, 432-439

DOI: 10.1039/c4tb01536c

67 Vigderman L., Zubarev E. R., Therapeutic platforms based on gold nanoparticles and their covalent conjugates with drug molecules, *Advanced Drug Delivery Reviews*, 2013, 65, 663-676

DOI:10.1016/j.addr.2012.05.004

- 68 Dreaden E.C., Austin L.A., Mackey M.A., El-Sayed M.A., Size matters: gold nanoparticles in targeted cancer drug delivery, *Therapeutic Delivery*, 2012, 3, 457–478
DOI:10.4155/tde.12.21
- 69 Larson T.A., Bankson J., Aaron J., Sokolov K., Hybrid plasmonic magnetic nanoparticles as molecular specific agents for MRI/optical imaging and photothermal therapy of cancer cells, *Nanotechnology*, 2007, 18, 1–8
DOI:10.1088/0957-4484/18/32/325101
- 70 Jaque D., Martinez Maestro L., del Rosal B., Haro-Gonzalez P., Benayas A., Plaza J.L., Martin Rodriguez E., Garcia Sole J., Nanoparticles for photothermal therapies, *Nanoscale*, 2014, 6, 9494–9530
DOI: 10.1039/c4nr00708e
- 71 Huang X., El-Sayed M.A., Gold nanoparticles: Optical properties and implementations in cancer diagnosis and photothermal therapy, *Journal of Advanced Research*, 2010, 1, 13–28
DOI:10.1016/j.jare.2010.02.002
- 72 Pitsillides C.M., Joe E.K., Wei X., Anderson R.R., Lin C.P., Selective Cell Targeting with Light-Absorbing Microparticles and Nanoparticles, *Biophysical Journal*, 2003, 84, 4023–4032
DOI: 10.1016/S0006-3495(03)75128-5
- 73 Pissuwan D., Cortie C.H., Valenzuela S.M., Cortie M.B., Gold nanosphere-antibody conjugates for hyperthermal therapeutic applications, *Gold Bulletin*, 2007, 40, 121–9
- 74 Hirsch L.R., Stafford R.J., Bankson J.A., Sershen S.R., Rivera B., Price R.E., Nanoshell-mediated near-infrared thermal therapy of tumors under magnetic resonance guidance, *Proceedings of the National Academy of Science of the USA*, 2003, 100, 13549–13554
DOI: 10.1073/pnas.2232479100
- 75 Huang X., El-Sayed I.H., Qian W., El-Sayed M.A., Cancer cell imaging and photothermal therapy in the near-infrared region by using gold nanorods, *Journal of the American Chemical Society*, 2006, 128, 2115–2120
DOI: 10.1021/ja057254a
- 76 Chen J., Wang D., Xi J., Au L., Siekkinen A., Warsen A., Immuno gold nanocages with tailored optical properties for targeted photothermal destruction of cancer cells, *Nano Letters*, 2007, 7, 1318–1322
DOI:10.7150/thno.7064

77 Jain P.K., Lee K.S., El-Sayed I.H., El-Sayed M.A., Calculated absorption and scattering properties of gold nanoparticles of different size, shape, and composition: applications in biological imaging and biomedicine, *The Journal of Physical Chemistry B*, 2006, 110, 7238–7248

DOI: 10.1021/jp057170o

78 Hone D.C., Walker P.I., Evans-Gowing R., FitzGerald S., Beeby A., Chambrier I., Cook M.J., Russell D.A., Generation of Cytotoxic Singlet Oxygen via Phthalocyanine-Stabilized Gold Nanoparticles: A Potential Delivery Vehicle for Photodynamic Therapy, *Langmuir*, 2002, 18, 2985-2987

79 Oo M.K.K., Yang X., Du H., Wang H., 5-aminolevulinic acid-conjugated gold nanoparticles for photodynamic therapy of cancer, *Nanomedicine*, 3, 777-786

DOI 10.2217/17435889.3.6.777

80 Stuchinskaya T., Moreno M., Cook M.J., Edwards D.R., Russell D.A., Targeted photodynamic therapy of breast cancer cells using antibody phthalocyanine-gold nanoparticle conjugates, *Photochemical and Photobiological Sciences*, 2011, 10, 822–831

DOI: 10.1039/c1pp05014a

81 Lkhagvadulam B., Kim J.H., Yoon I., Shim Y.K., Size-Dependent Photodynamic Activity of Gold Nanoparticles Conjugate of Water Soluble Purpurin-18-*N*-Methyl-*D*-Glucamine, *BioMed Research International*, 2013, 1–10

DOI:10.1155/2013/720579

82 Kuo W.S., Chang Y.T., Cho K.C., Chiu K.C., Lien C.H., Yeh C.S., Chen S.J., Gold nanomaterials conjugated with indocyanine green for dual-modality photodynamic and photothermal therapy, *Biomaterials*, 2012, 33, 3270–3278

DOI:10.1016/j.biomaterials.2012.01.035

83 Hari K., Pichaimani A., Kumpati P., Acridine orange tethered chitosan reduced gold nanoparticles: a dual functional probe for combined photodynamic and photothermal therapy, *RSC Advances*, 2013, 3, 20471–20479

DOI: 10.1039/c3ra44224a

84 Tsai C.Y., Shiau A.L., Chen S.Y., Chen Y.C., Cheng P.C., Chang M.Y., Chen D.H., Chou C.H., Wang C.R., Wu C.L., Amelioration of Collagen-Induced Arthritis in Rats by Nanogold, *Arthritis and Rheumatism*, 2007, 56, 544–554

DOI: 10.1002/art.22401

85 Brown C.L., Whitehouse M.W., Tiekink E.R.T., Bushell G.R., Colloidal metallic gold is not bio-inert, *Inflammopharmacology*, 2008, 16, 133–137

DOI: 10.1007/s10787-007-0017-6

- 86 Bowman M.C., Ballard T.E., Ackerson C.J., Feldheim D.L., Margolis D.M., Melander C., Inhibition of HIV Fusion with Multivalent Gold Nanoparticles, *Journal of the American Chemical Society*, 2008, 130, 6896–6897
- 87 Mahmoud K.A., Luong J.H.T., Impedance Method for Detecting HIV-1 Protease and Screening For Its Inhibitors Using Ferrocene-Peptide Conjugate/Au Nanoparticle/Single-Walled Carbon Nanotube Modified Electrode, *Analytical Chemistry*, 2008, 80, 7056–7062
- 88 Mohamed A.A., Gold is going forensic, *Gold Bulletin*, 2011, 44, 71–77
DOI 10.1007/s13404-011-0013-x
- 89 Hussain I., Hussain S.Z., Rehman H., Ihsan A., Rehman A., Khalid Z.M., Brustc M., Cooper A.I., In situ growth of gold nanoparticles on latent fingerprints—from forensic applications to inkjet printed nanoparticle patterns, *Nanoscale*, 2010, 2, 2575–2578
DOI: 10.1039/c0nr00593b
- 90 Gao D., Li F., Songa J., Xua X., Zhanga Q., Niua L., One step to detect the latent fingerprints with gold nanoparticles, *Talanta*, 2009, 80, 479–483
DOI:10.1016/j.talanta.2009.07.007
- 91 Gooding J.J., Shein J., Lai L.M.H., Using nanoparticle aggregation to give an ultrasensitive amperometric metal ion sensor, *Electrochemistry Communications*, 2009, 11, 2015–2018
DOI:10.1016/j.elecom.2009.08.043
- 92 Wang X.H., Liu T., Xu N., Zhang Y., Wang S., Enzyme-linked immunosorbent assay and colloidal gold immunoassay for ochratoxin A: investigation of analytical conditions and sample matrix on assay performance, *Analytical and Bioanalytical Chemistry*, 2007, 389, 903–911
DOI: 10.1007/s00216-007-1506-6
- 93 Dasary S.R., Singh A.K., Senapati D., Yu H., Ray P.C., Gold Nanoparticle Based Label-Free SERS Probe for Ultrasensitive and Selective Detection of Trinitrotoluene, *Journal of the American Chemical Society*, 2009, 131, 13806–13812
DOI: 10.1021/ja905134d
- 94 Sonavane G., Tomoda K., Sano A., Ohshima H., Terada H., Makino K., In vitro permeation of gold nanoparticles through rat skin and rat intestine: Effect of particle size, *Colloids and Surfaces B: Biointerfaces*, 2008, 65, 1–10
DOI:10.1016/j.colsurfb.2008.02.013
- 95 Menon G.K., Brandsma J.L., Schwartz P.M., Particle-mediated gene delivery and human skin: Ultrastructural observations on stratum corneum barrier structures, *Skin Pharmacology and Physiology*, 2007, 20, 141–7
DOI:10.1159/000098165

96 Azarbayjani A.F., Qun L., Chan Y.W., Chan S.Y., Novel Vitamin and Gold Loaded Nanofiber Facial Mask for Topical Delivery, *American Association of Pharmaceutical Scientists*, 2010, 11, 1164–1170

DOI: 10.1208/s12249-010-9475-z

97 Bangale M.S., Mitkare S.S., Gattani S.G., Sakarkar D.M., Recent nanotechnological aspects in cosmetics and dermatological preparations, *International Journal of Pharmacy and Pharmaceutical Sciences*, 2012, 4, 88-97

98 Taufikurohmah T., Sanjaya I.G.M., Baktir A., Syahrani A., TEM Analysis of Gold Nanoparticles Synthesis in Glycerin: Novel Safety Materials in Cosmetic to Recovery Mercury Damage, *Research Journal of Pharmaceutical, Biological and Chemical Sciences*, 2014, 5, 397-407

99 Ravishankar R. V., Jamuna B. A., Nanoparticles and their potential application as antimicrobials, *Science against microbial pathogens: communicating current research and technological advances*, 197-209

100 Johnston J.H., Lucas K.A., Nanogold synthesis in wool fibres: novel colourants, *Gold Bulletin*, 2011, 44, 85-89

DOI 10.1007/s13404-011-0012-y

The TS-1 catalyst and its utilization in the epoxidation processes

*Ewa Drewnowska¹, Agnieszka Wróblewska¹

¹Institute of Organic Chemical Technology, West Pomeranian University of Technology, Szczecin, POLAND

e-mail: ewa.sokalska@zut.edu.pl

Keywords: epoxidation, TS-1 catalyst, diallyl ether, allyl-glycidyl ether

ABSTRACT

The description of the history of the studies on the synthesis of the TS-1 catalyst, its structure and structure of the active species of Ti in the TS-1 was presented. In this work the main apparatus used in the hydrothermal synthesis of the zeolite type materials was shown. Also the main methods of the synthesis of this catalyst were presented. Moreover, the utilization of this catalyst in the epoxidation processes was described, especially in the epoxidation of allyl alcohol (AA) and diallyl ether (DAE). The main ways of these two epoxidation processes were shown. The applications of the products of allyl alcohol and allyl ether epoxidation were presented (allyl-glycidol ether, glycidol, glycerol, diglycidyl ether, acrolein).

INTRODUCTION

In the epoxidation process, epoxides are obtained as the main products. The epoxides are cyclic compounds with the 3-membered ring which is composed of an oxygen atom and two carbon atoms [1]. The epoxidation process relies on the reaction of alkenes with oxidizing agents. In the organic technology there are four main methods of the epoxide obtaining from olefinic compounds:

- a) chlorine method (hydrochloric acid (I) or its salts) [2],
- b) epoxidation with peracids [3],
- c) epoxidation with organic and non-organic hydroperoxides (hydrogen peroxide in the presence of titanium silicate catalysts) [4], t-butyl hydroperoxide also in the presence of titanium silicate catalysts),
- d) epoxidation with molecular oxygen [5].

In the epoxidation the following oxidizing agents can be used: hydrogen peroxide, peracids, peroxides and hydroperoxides. The oxidizing agents are not active without of an appropriate catalyst which can activate the epoxidation reaction. For example, in the epoxidation of allyl alcohol (AA) and diallyl ether (DAE) the system of hydrogen peroxide/titanium silicate catalyst is very often used.

A considerable development in the studies on the titanium silicate catalysts syntheses was observed in XX century, mainly in years 1980-1995. It was connected with the discovery of the TS-1 catalyst. This material was very active catalyst for the oxidation processes used 30 wt% hydrogen peroxide as the oxidizing agent. Also the catalyst such as Ti(IV)/SiO₂ was studied in the epoxidation process but it was inactive in the studied conditions and it needed very high concentration of hydrogen peroxide >95 wt%. The active species of Ti were different for these two catalyst, for Ti(IV)/SiO₂ the active species were in the form of Ti $\frac{1}{4}$ O, and for TS-1 a tetrahedrally coordinated Ti in the silica lattice was the active species of the catalyst [6].

The TS-1 catalyst belongs to the group of synthetic zeolites and it is one of the most known titanium silicate catalysts. Its precursor is the ZSM-5 material. The TS-1 catalyst is obtained in the reaction of the sources of Si and Ti (TEOS – tetraethyl o-silicalite and TBOT – tetrabutyl o-tytaniate). The synthesis is performed in the presence of tetrapropylammonium hydroxide (TPAOH) as a template (compound which allows to obtain the structure with the appropriate order and size of the pores) [7].

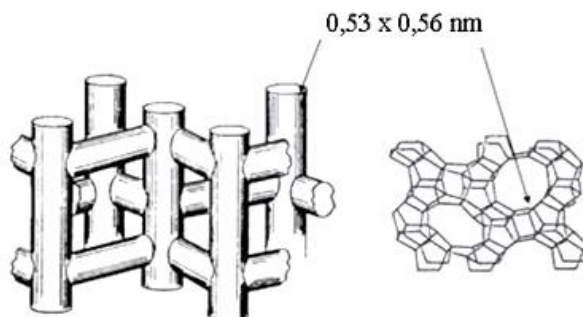


Fig. 1 The system of channel in the TS-1 catalyst [8]

The structure of the TS-1 catalyst is denoted as the MFI. It is characterized by three dimensional channel system which is linear and zigzag. The TS-1 crystallizes in the orthorhombic system and its crystals have the size from 0.1 to 5 μm. The size of the channel amounts to 0.54 x 0.56 nm. The entrances to the channels are restricted by 10 edges [6-12]. The size of the channels is appropriate to adsorb molecules with the size to 6Å. The size of the pores of the TS-1 causes that this catalyst can be used only for the epoxidation of unsaturated compounds having small molecules [6]. The TS-1 catalyst can selectively oxidized the most of organic compounds such as: olefines, alkanes, alcohols and phenols with help of hydrogen peroxide and at mild conditions.

The discovery in 1980 the titanium silicalite TS-1 material containing in the structure tetrehydrally coordinated Ti atoms enabled to design new industrial

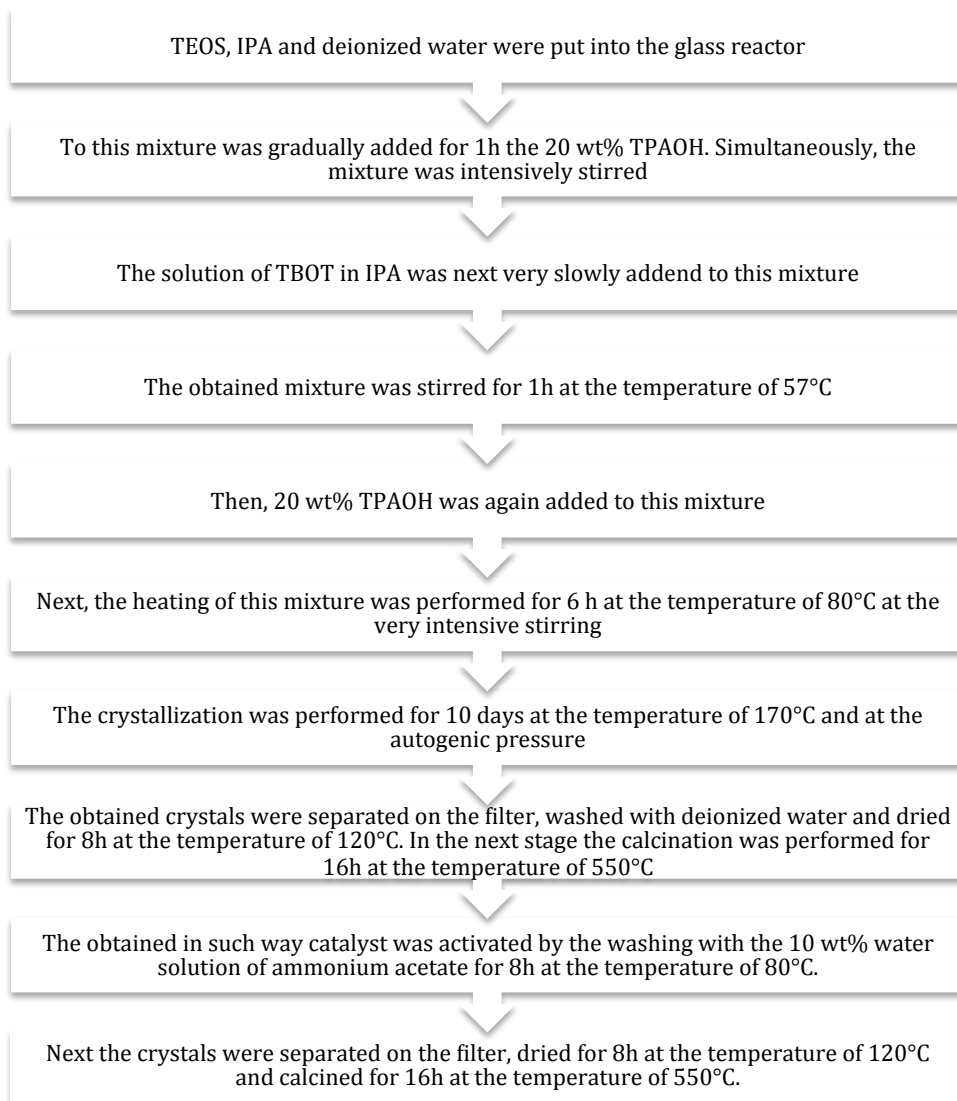
processes fulfill the green chemistry requirements [2]. The TS-1 catalyst has been industrially utilized in some organic processes: the epoxidation of propylene, the hydroxylation of phenol, and the ammoxidation of cyclohexanone [3-5].

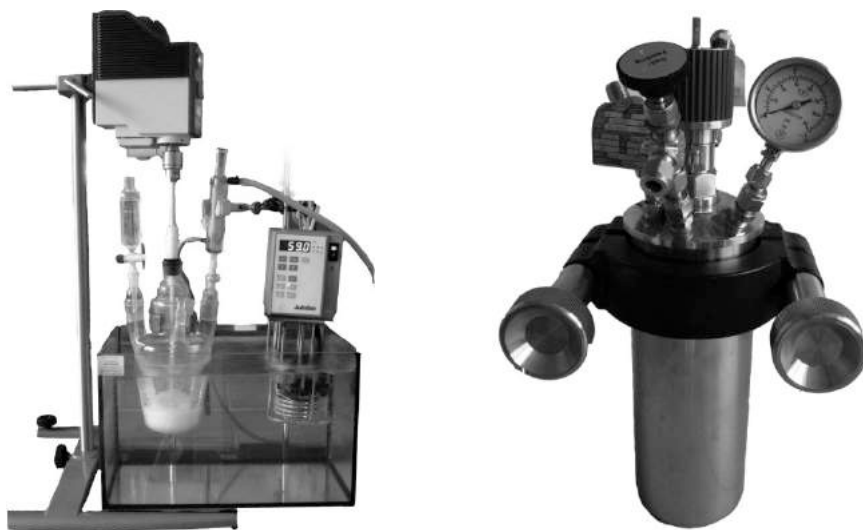
The TS-1 catalyst can be used in the epoxidation of AA to glycidol (2,3-epoxy-1-propanol), which is a very valuable intermediate for the organic syntheses. Glycidol, which can undergo the partial hydration to glycerol in the reaction conditions, is the main product of the epoxidation of allyl alcohol. Depending on the conditions of the epoxidation a small amount of ethers (diallyl ether (DAE) and allyl-glycidol ether (AGE)) is formed in this process. Glycidol is utilized in the syntheses of the surface active compounds (cosmetics for skin cleaning and the moisturize preparations, toothpastes, mouthwashes, bath fluids, shampoos, and agent for disinfection) [13]. The surface-active agents are also used as food emulgators in the production of margarines, ice-creams, and vegetable butters [14, 15]. For other applications of glycidol belong plasticizers, fabric dyes, photochemical compounds, rubbers, varnishes, and plastics [15]. Block copolymers swelling in water and methanol are obtained in the reaction of glycidol with ethylene oxide. Glycidol is used for the synthesis of many biologically active compounds, primarily obtained from living organisms (algae and fungus). One of the most important applications of glycidol is the synthesis of antiviral and analgesic drugs. During the antiviral drugs obtained on the basis of glycidol are drugs which can fight with HIV virus. A very important application of glycidol is the production cardiac drugs that lower blood pressure and restore heart rhythm [16, 17].

AGE is obtained as the main product during the process of DAE epoxidation over the TS-1 catalyst. AGE is a very valuable intermediate which is used in the synthesis of epoxy resins, epoxy adhesives, powder coatings, and epoxy paints. AGE is also used for production of explosive materials and cryptands [18, 19]. AGE together with the carbon dioxide and in the presence of an ionic liquid as a catalyst forms a carbonates [19], which are used as: aprotic polar solvents, electrolytes for batteries and raw materials for the synthesis of the reactive polymers. AGE takes part in the synthesis of linear, branched and cyclic oligoglycerol standards, which are used as: polymer additives, emulgators, stabilizers, dispersants, and components of paints and pesticides [20]. AGE is also used for the obtaining of the anti-arrhythmia agents [21]. Moreover, in the epoxidation of DAE also by-products are formed: AA, glycidol, 3-allyloxy-1,2-propanediol, diglycidyl ether and glycerol. These compounds also have a lot of applications.

The methods of TS-1 synthesis

The general method of the TS-1 synthesis relies on the mixing of the source of Si and Ti in the appropriate amount and on the addition of the template – tetrapropylammonium hydroxide (TPAOH). During the studies on the synthesis of the TS-1 the mixtures of the TPOH with tetraethylammonium hydroxide also were used. The main method of the TS-1 synthesis is the hydrothermal method. In this method the hydrothermal crystallization of the TS-1 gel containing TPAOH and the hydrolyzed sources of Ti and Si at the temperature of about 170°C for some days is performed. The general scheme of this hydrothermal method is presented below [22]:





a) b)
Fig. 2 The apparatus for the synthesis of the TS-1 catalyst: the glass reactor (a) and the Berghof autoclave (b)



Fig. 3 The obtained TS-1 catalyst in the form of the white powder

The characteristic of the obtained TS-1 catalyst was performed with help of the following instrumental methods: XRD (X'Pert PRO Philips diffractometer, Cu K α radiation), IR (Nicolet FT/IR-380 Thermo Electron Corporation) – the sample for studies was prepared as the pills in KBr, UV-Vis (SPECORD M40 type V-530) and SEM (JOEL JSM-6100 instrument) and X-ray microanalysis.

The XRD pattern of the TS-1 catalyst is usually made in the range of 2θ angle 6° to 60° . For the measurements the Cu K α radiation is used. An example of the XRD pattern for the TS-1 catalyst is presented below (Fig. 4) [23].

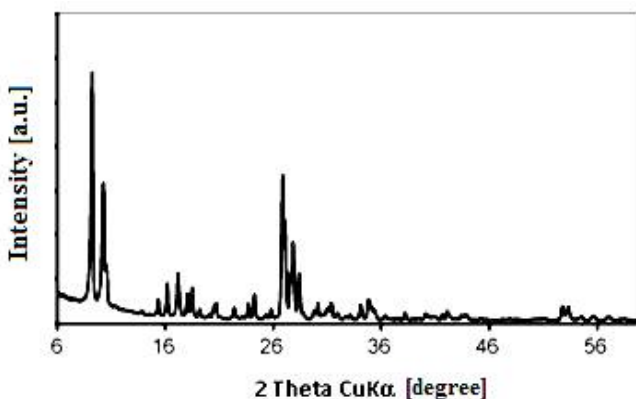
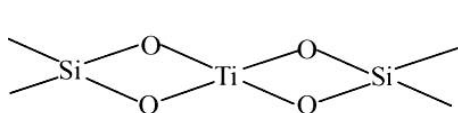


Fig. 4 The literature XRD pattern of the TS-1 catalyst [24]

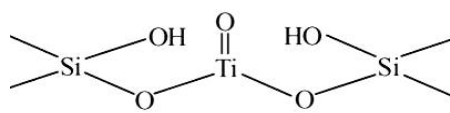
In the XRD pattern of the obtained TS-1 catalyst there are present the following characteristic bands for the 2 Theta angle: 9.22; 10.22; 26.87; 27.87 and 28, which confirm the obtaining of the MFI structure.

In order to confirm the introduction of the Ti atoms into the structure of the obtained catalyst the studies by the IR method were performed – Fig. 5. In the IR spectrum of TS-1 catalyst there was visible the band at 960 cm^{-1} which is connected with the tetrahedrally coordinated Ti in the silica structure. This band is connected with the hindrance of the polar bonds Si-O-Ti or with the presence of titanyl group (T=O). In the region of the zeolite framework vibration, the bands showing a cut off at $1000\text{--}1300\text{ cm}^{-1}$ are observed (Si-O-Si stretching vibration) [24].

The way of the binding of Ti atoms in the structure of the TS-1 catalyst can be presented as follows [25]:



tetrahedrally coordinated Ti



Ti in the form of the titanyl group

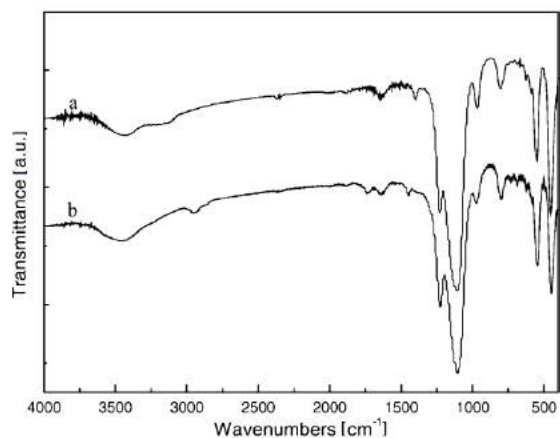


Fig. 5 The literature IR spectrum of the TS-1 catalyst: the fresh (a) and the recycled (b) [26]

The TS-1 is also investigated by the UV-Vis method.

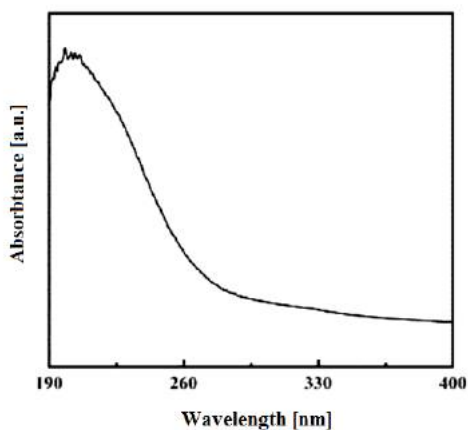


Fig. 6 The literature UV-Vis spectrum of the TS-1 catalyst [27]

The UV-Vis spectrum shows an intense band at 210 nm, which is assigned to the Ti atoms included into the structure of the catalysts (Ti^{+4} ions) and two weak bands at 260 and 290 nm which are described to the titanium in the coordination of +5 or +6 (the presence of titanium at this coordination numbers is connected with the adsorption of water molecules (or solvent molecules) at the titanium active centers) or to the dimeric species of Ti in the structure of the catalyst – Figure 7. The lack of the band at 330 nm is a proof of the absence of anatase in the studied sample.

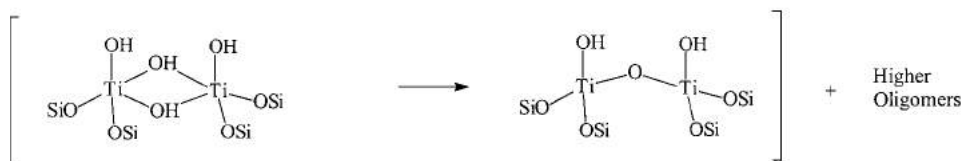
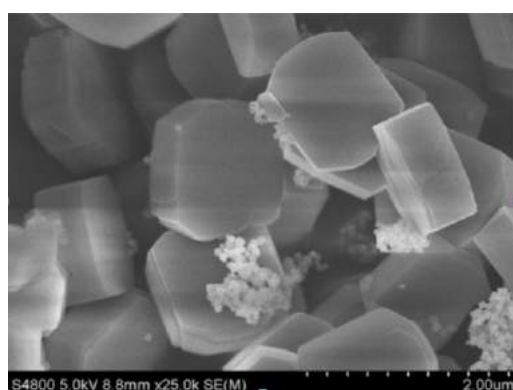
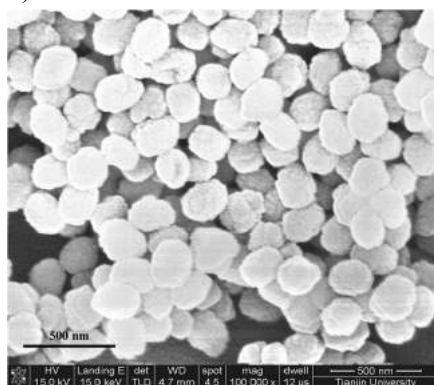


Fig. 7 Dimeric species of Ti in the structure of the TS-1 catalyst [28]

The morphology of the TS-1 crystals is described with help of SEM method. Figure 8 shows that the TS-1 catalyst is composed from the hexagonal, homogeneous crystals with the size of $0.1\mu\text{m} \times 2.0\mu\text{m}$. The crystals can form bigger structures [29, 30].



a)



b)

Fig. 8 The literature SEM micrographs of the TS-1 catalyst: (a) [30] and (b) [31]

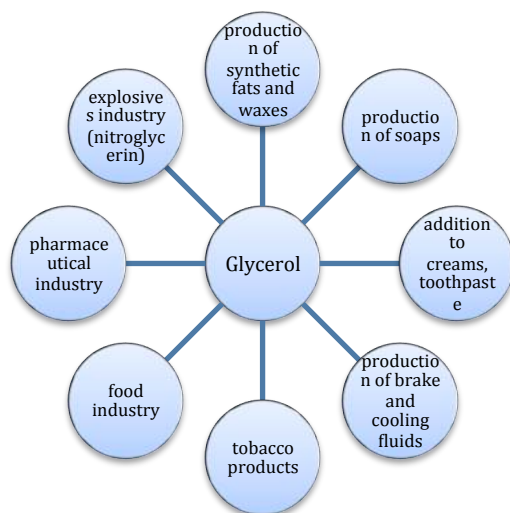


Fig. 11 The application of glycerol

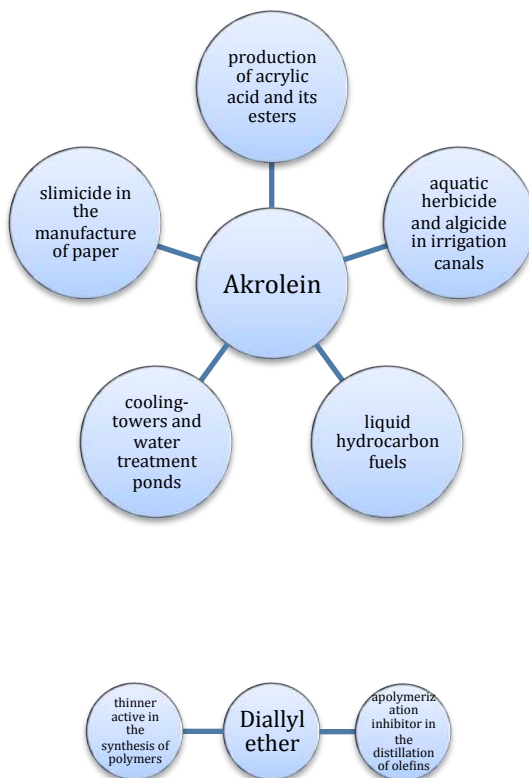


Fig. 12 The application of acrolein and diallyl ether

In the process of DAE epoxidation as the main product AGE is obtained. In this process also other very valuable compounds are formed. The main reactions of this process are presented below – Figure 13.

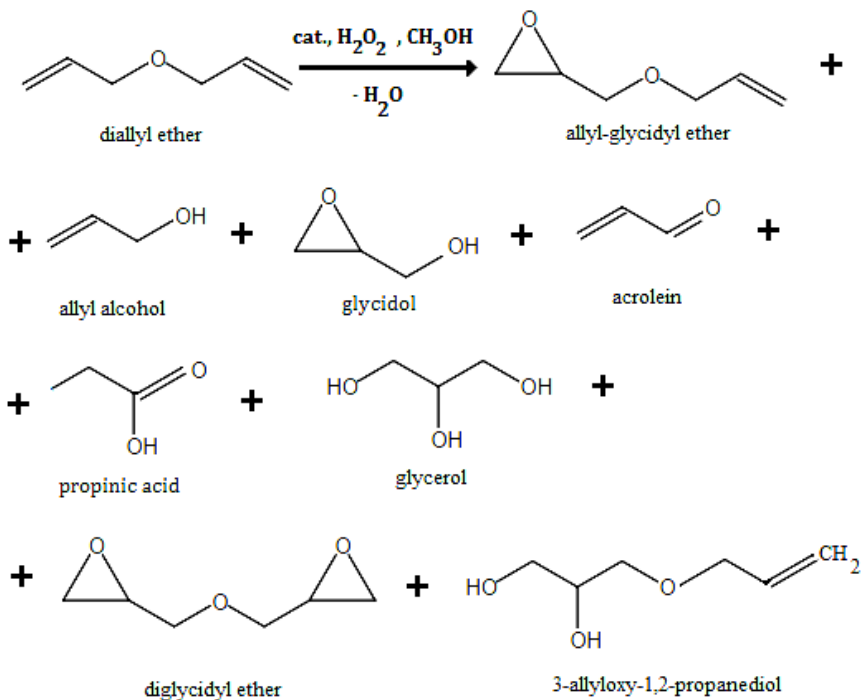


Fig. 13 The main reactions of the process of DAE epoxidation

AGE and other products of this process have a lot of applications. These applications are presented below – Figures 14-15.

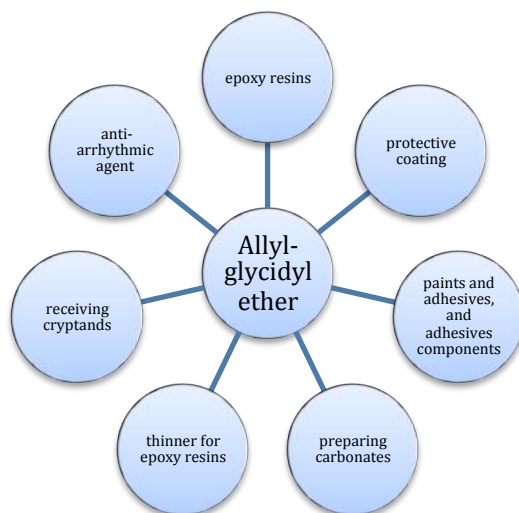


Fig. 14 The application of allyl-glycidyl ether

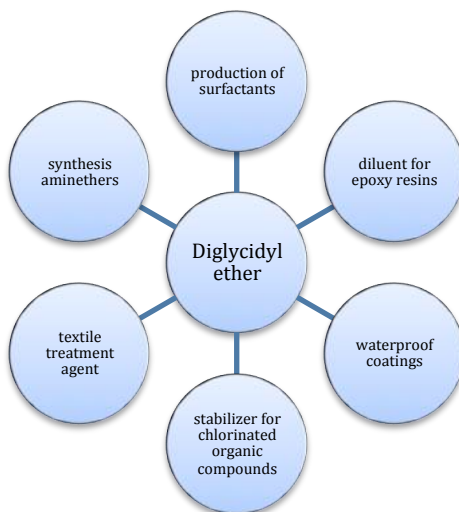


Fig. 15 The application of diglycidyl ether

CONCLUSIONS

The TS-1 catalyst is the very valuable catalyst for the organic syntheses. The reactions which proceed in the presence of the TS-1 material are very selective reactions because some of the products can be obtained with the selectivity of 100 mol%. To the main processes which proceed in the presence of the TS-1 catalyst belong the epoxidation of AA and DAE. These processes provide very valuable main products (glycidol, AGE) and very valuable by-products (glycerol, acrolein, and diglycidyl ether). The large number of the applications of the mentioned above compounds cause that these processes are

now very intensively studied and new catalysts are applied for these processes, for example: TS-1, Ti-MCM-41, Ti-MWW or Ti-SBA-15.

REFERENCES

1. Mc Murry J. 2003. *Chemia organiczna tom 3*. PWN. Warszawa.
2. Cai C., Dai H., Chen R., Su C., Xu X., Zhang S., Yang L. 2008. Studies on the kinetics of in situ epoxidation of vegetable oils. *Eur. J. Lipid Sci. Technol.* 110: 341-346.
3. Mungroo R., Pradhan N.C., Goung V.V., Dalai A.K. 2008. Epoxidation of canola oil with hydrogen peroxide catalyzed by acidic ion exchange resin. *J. Am. Oil Chem. Soc.* 85: 887-896.
4. Goud V.V., Pradhan N.C., Patwardhan A.V. 2006. Epoxidation of karanja (*Pongamia glabra*) oil by H₂O₂. *J. Am. Oil Chem. Soc.* 83: 635-640.
5. Goud V.V., Patwardhan A.V., Pradhan N.C. 2006. Studies on the epoxidation of mahua oil (*Madhumica indica*) by hydrogen peroxide. *Bioresource technol.* 97: 1365-1371.
6. Oyama S. T. *Mechanisms in homogeneous and heterogeneous epoxidation Catalysis*, Elsevier, Amsterdam 2008.
7. Wróblewska A., Milchert E., Ławro E. 2006. Epoksydacja 2-buten-1-olu na katalizatorze TS-1, *Przem. Chem.* 85/8-9, 687.
8. Bartkowiak M., Milchert E., Lewandowski G. 2011. Kierunki w rozwoju technologii przemysłu chemicznego, Wydawnictwo ZUT w Szczecinie, Szczecin.
9. Łukasiewicz M., Pielichowski J. 2002. Nadtlenek wodoru w nowoczesnych procesach technologii organicznej, *Przem. Chem.* 81/8, 509-512.
10. Ziółek M., Nowak J. 1999. *Kataliza Heterogeniczna*, Wydawnictwo Uniwersytetu im. A. Mickiewicza Poznań.
11. Pruchnik F. *Kataliza homogeniczna*, PWN Warszawa, 1993.
12. Pruchnik F. *Chemia metaloorganiczna*, PWN Warszawa 1991.
13. Kłopotek A., Kłopotek B. 1990. 2,3-Epoxypropanol-1 jako substrat do syntezy środków powierzchniowo-czynnych, *Przem. Chem.* 69, 248– 251.
14. M. Von Wolfgang, A. Klemann, G. Schreyer, 1975. Glycid-herstellung und eigenschften, *Chem.* 1, 19–25.
15. Wróblewska A., Milchert E. 2003. Bezodpadowe epoksydowanie alkoholu allilowego w obecności katalizatorów tytanowo-silikalitowych, *Przem. Chem.* 82, 1063–1065.
16. Milchert E., Wróblewska A. 1996. Otrzymywanie glicydołu, *Przem. Chem.* 75/10, 367-368.
17. Wróblewska A., Monografia habilitacyjna, Epoksydowanie związków allilowych nadtlaniem wodoru w obecności katalizatorów tytanowo-silikalitowych, Wydawnictwo Politechniki szczecińskiej, Szczecin, 2008.

18. Lukyanenko N., Reder A. 1988. Macroheterocycles. Part 42.A facile synthesis of dihydroxy cryptands and their dehydroxylation, *J. Chem. Soc. Perkin Trans. I*, 2533-2536.
19. Park Dae-Won, Mun Na-Young, Kim Kyung-Hon, Kim Il, Park Sang-Wook. 2006. Addition of carbon dioxide to allyl glycidyl ether using ionic liquids catalysts, *Catalysis Today* 115: 130-133.
20. Cassel S., Cebaig C., Benvegno T., Chaimbault P., Lafosse M., Plusquellec D., Rollin P. 2001. Original synthesis of linear, branched and cyclic oligoglycerol standars, *Eur. J. Org. Chem.* 875-896.
21. Hauck F., Glenn J., Anti-arrhythmia agents, US Patent. 4,279,902 (1981).
22. Thangaraj A., Kumar R., Ratnasamy P. 1990. Direct catalytic hydroxylation of benzene with hydrogen peroxide over titanium-silicalite zeolites. *Appl. Catal.*, 57: L1-L3.
23. Wróblewska A., Fajdek A. 2010. Epoxidation od allyl alcohol to glycidol over the microporous TS-1 catalyst, *J. Hazard. Materials.* 179, 258-265.
24. Wu, P., Tatsumi, T., Komatsu, T. & Yashima, T. 2001. A novel titano-silicalite with MWW structure: I. Hydrothermal synthesis, elimination of extraframework titanium, and characterizations. *J. Phys. Chem. B* 105(15), 2897 – 2905. DOI: 10.1021/jp002816s.
25. Wróblewska A., Milchert E. 2005. Charakterystyka katalizatorów tytanowo-silikalitowych, *Przem. Chem.* 84/10, 723-727.
26. Wang Q., Mi Z., Wang L. 2005. Epoxidation of allyl choride with molecular oxygen and 2-ethyl-anthrahydroquinone catalyzed by TS-1, *J. Mol. Catal. A: Chemical.* 229, 71-75.
27. Wu G., Wang Y., Feng W., Shi H., Lin Y., Zhang T., Jin X., Wang S., Wu X., Yao P., Epoxidation of propylene with H₂O₂ catalyzed by supported TS-1
28. Marchese L., Gianotti E., Dellarocca V., Maschmeyer T., Rey F., Coluccia S., Thomas J. M. 1999. Structure.functionality relationships of grafted Ti-MCM41 silicas. Spectroscopic and catalytic studies. *Phys. Chem. Chem. Phys.* 1, 585-592.
29. Lin J., Xin F., Yang L., Zhuang Z. 2014. Synthesis, characterization of hierarchical TS-1 and its catalytic performance for cyclohexanone ammoximation, *Catalysis Communication.* 45, 104-108.
30. Guoqiang Wu, Yaquan Wang, Lina Wang, Wenping Feng, Hainan Shi, Yi Lin, Teng Zhang, Xing Jin, Shuhai Wang, Xiaoxue Wu, Pengxu Yao. 2013. Epoxidation of propylene with H₂O₂ catalyzed by supported TS-1 catalyst in a fixed-bed reactor: Experiments and kinetics. *Chem. Engineering. J.* 215-216, 306-314.

Thermocatalytic polyolefin processing system in pure synthetic oil distiller

* Łukasz Grabowski¹, Marta Wołosiewicz-Głąb²

¹AGH Faculty of Mining and Geoengineering, Department of Economics and Management in Industry

²AGH Faculty of Mining and Geoengineering, Department of Environmental Engineering and Mineral Processing

e-mail: lukgrabo@agh.edu.pl

Keywords: *polyolefins, plastics, synthetic oil, distiller, alternative fuel*

ABSTRACT

Polyolefins (polyethylene PE and polypropylene PP) are a major group of synthetic plastics. Due to the distinctive uniform chemical composition and high availability, they are interesting raw material for further processing and, consequently, to reduce the amount of waste.

The paper reviews properties of polyolefins. The treatment and management of this type of waste have been presented. The process of obtaining a pure synthetic oil in distilleries and the possibilities to use thermocatalytic polyolefin processing system have been described.

The paper outlines the prospects for using this type of technology. The analysis of the technology was carried out taking into account the various stages of the recovery process, economics and environmental impact.

Plastics are widely used in all industries. The plastics industry plays an important role in the economic growth through innovation in many sectors of the European economy, including the automotive, electrical and electronics industry, construction and food and beverage production [1].

With its diverse, unique chemical and physical properties as also the ability to modify any of them using a variety of plastic additives have almost unlimited possibilities of use. Unfortunately the variety of material properties, requires a specific technology depending on type of waste polyolefin when the reuse is considered [7].

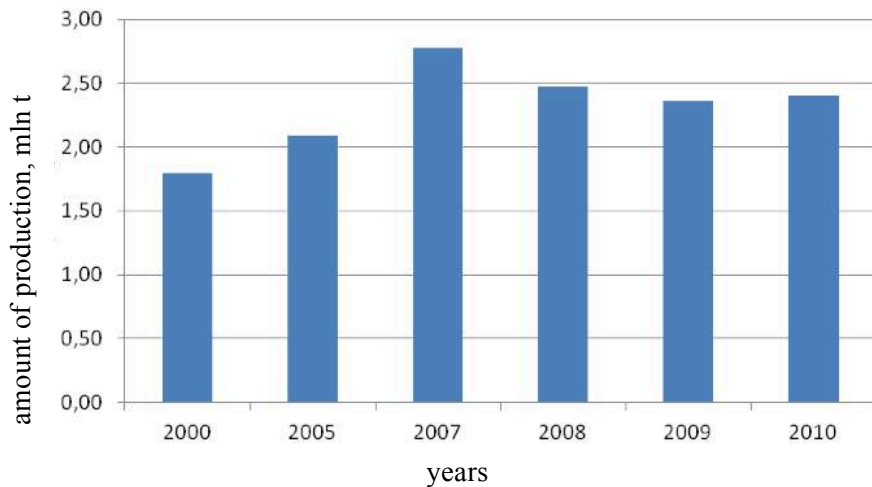


Fig. 1 Manufacture of plastics in Poland [6].

Most recent recycling technologies require homogeneous polymer as a secondary raw material. Plastic waste fraction due to dirt and heterogeneity are not suitable for recycling and is so far mainly deposited on municipal landfills. However, high calorific values of waste plastics make them suitable for energy production, where they can be for example used as a permanent secondary fuel [1].

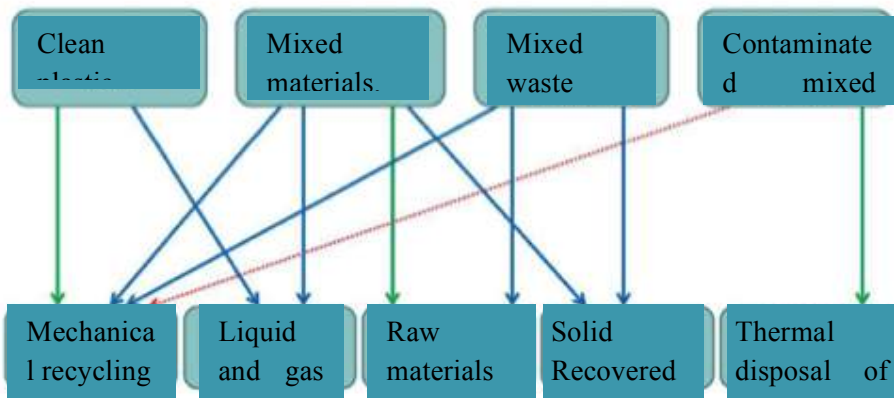


Fig. 2 Methods of recycling and recovery of different fractions of waste plastics [14].

The "top five" plastics, which have a major market shares, are as follows: polyethylene (PE), polypropylene (PP), polyvinyl chloride (PVC), polystyrene (PS), polyethylene terephthalate (PET) [14].

The polyolefins are thermoplastic polymers manufactured from crude oil. They contain in their structure mainly carbon and hydrogen, in which there are long chains of carbon -CCC-, constituting the basic skeleton of the polymer chains themselves. In this group, the basic plastics are polyethylene (PE) and polypropylene (PP) [1]. Among the plastics they occupy a prominent place in the world in terms of production volume. In 2006, in Poland, polyolefins consumption was approx. 22 kg per person in 2008, the value is increased by 4 kg per person, and in 2010 the level was already approx. 33 kg per person [7] (see Fig. 3).

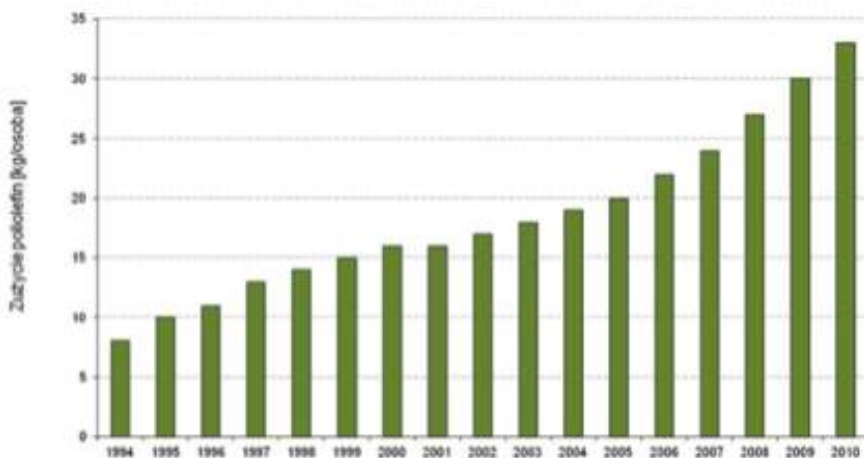


Fig. 3 Consumption of polyolefins in Poland

Lifetime of plastic products is short or very short (e.g. packaging films). The lack of a waste incineration plants in the country, determines that the storage is the main method of their utilization.

Polyolefins are readily biodegradable and will back up their storage in the tens or even hundreds of years.

Generally, reducing the amount of waste being stored by recycling, preceded by selective collection, seems to be a reasonable way of limiting their amount collected on landfills [14].

Methods of polyolefin waste management

Polyethylene and polypropylene are approx. 7% of total municipal waste.

In Poland, in 2014 approx. 860 thousand tons polyolefins were landfilled. The European Union claimed that all member countries were committed to limit the amount of wastes deposited on landfills by 50% in 2013, threatening heavy fines. Waste segregation alone will not solve the problem of their vast and

growing quantities. It is necessary to develop effective solutions for waste management and processing technology [14].

There are many different concepts of recycling plastics [11,12]:

Chemical recycling - includes processes in which the all waste materials with different composition and properties are processed together (e.g. the production of fuel oils of plastics, production of thermal insulation materials, packages etc.).

Recycling energy - waste incineration and the generation of one of solid, liquid and gas.

Feedstock recycling - processing of waste materials and products to a raw material, from which these materials were produced.

Material recycling - plastics are processed by melting or dissolving.

Organic recycling - biological decomposition of waste in controlled conditions by using microorganisms.

PE waste have a high calorific value (Tab. 1) and can be used as fuel to produce electricity and heat [10].

Table 1 Comparison of the calorific value of different fuels.

Fuel	The calorific value
Coal	25-28 MJ/kg
Wood	7-14 MJ/kg
Oil	40-48 MJ/kg
Polyethylene	44 MJ/kg

Incineration of PE, however, faces some technical difficulties. New EU recommendations postulate reducing waste incineration to chemical or material recycling.

Mechanical impurities, as well as presence of other types of polymers, which results in heterogeneity of the raw material and phase change are serious difficulties in performing combustion of polymers [14].

All of these disposal methods use polyolefins in various degrees, depending on the instantaneous and local economic conditions as well as on the access of technology and raw materials. The applicability of the method depends on the following characteristics of the waste: the homogeneity of raw materials, the type of additives, color, degree of degradation, etc. Generally, the recycling of polyolefins in Poland is not implemented on a large scale [1].

The methods of processing waste plastics polyolefin to components of solid and liquid fuels.

An interesting feature of polyolefins is their relatively easy disintegration (cracking) at elevated temperature. The molten plastic material in the range 4000°C (4500°C) - 8000°C cracking takes place in chemical bonds and the low molecular weight products are formed, which are subsequently distilled off [1]. Typically four product fractions can be achieved from this process [9]:

- a. The gaseous products which are not condensed,
- b. The liquid hydrocarbons, made of condensable hydrocarbons C₆-C₂₀ saturated and unsaturated, aliphatic and cyclic,
- c. Solid products of C₂₀-C₄₀ paraffin (C₆₀); they are distilled from the reaction environment together with the lower-boiling components and crystallize from the condensed mixture at low temperature
- d. Coke that is solid and non-distilled residue of the reaction.

Apparatus for converting waste plastic packaging into liquid hydrocarbons and structured paraffin oil may have different design. In particular, they may be liquid metal reactors to ensure the desired uniform distribution of temperature in the reaction chamber [9].

Production of liquid hydrocarbon mixtures of waste plastic packaging is economically viable project, because making this type of plastic is involved in obtaining revenue from product sales and also associated with taking recycling fees for accepting this type of waste to transform [9].

Thermal processes

Polyolefins exposed to high temperature undergo chemical degradation. Long carbon chains break and create products with lower molecular weight. Depending on the chosen technology, different proportions of gaseous, liquid and solid (paraffins and coke) products can be achieved [6].

Thermal cracking

Heating the polyolefins at temperatures of 380-480°C leads to progressive cracking of the polymer chains (reaction thermal cracking). The higher the temperature used, the process faster is. Moreover, the temperature affects the proportions of components of the cracking product. Polyolefins (PE) waste cracking is carried out under anaerobic conditions [3].

Catalytic cracking

The process of cracking enhanced by using reasonable catalysts provides additional benefits. The cracking temperature is lowered and the quality of reaction products is improved (they are characterized by more consistent composition). These catalysts are usually various zeolites dispersed directly in the reaction mixture in the reactor [3].

Liquid-metal reactors

An interesting method of providing heat to the waste PE is the use of molten metals as energy carriers (lead, zinc) [9].

An additional mechanical agitation strongly enhances heat transfer. The volatile pyrolysis products leaving the reactor are condensed in an external condenser. The gaseous fraction is used to heat the reactor [9].

Fluidized bed reactors

Molten PE is fed onto a bed of sand grains with a diameter of around 0.2 mm and kept in a fluidized state by inert gas (nitrogen). The temperature of the fluidized bed is kept at 500°C using an external heat source [1].

Cracking in water

PE shredded waste is initially mixed with water, and then heated up to 300-500°C at elevated pressure in the range 560 to 840 atm. A thermal cracking of waste polyethylene occurs under these conditions [1].

Hydrocracking

Thermal cracking process can also be carried out in the presence of hydrogen. Hydrocracking is carried out at elevated pressure and because of the use of hydrogen, the associated hazards and required measures of process safety are more demanding with regards to equipment used (e.g. ATEX certification) [5].

Radiant heating

In this process the heat for pyrolysis is supplied to the reactor by means of infrared. Wastes are moving on a conveyor belt in the reactor chamber, which located below the system providing radiant energy to melt and carry out cracking [4].

Pyrolysis in plasma

Radical destruction of the carbon chain may be performed at a very high temperature plasma reactor reaching up to 8000°C [2].

Preliminary irradiation of waste

A potential preliminary irradiation by gamma radiation of polyethylene waste to cause the chemical degradation to monomers. Such prepared polyethylene is much easier to proceed with thermal degradation [1].

Production of synthesis gas

The waste polyolefin consisting of carbon and hydrogen are suitable for the processing of synthesis gas. The waste is first subjected to hydrocracking in a hydrogen atmosphere in a batch reactor for 30 min at 70 atm and 430°C, and then liquid products are contacted with the oxygen-containing gas at the temperature of 1315°C at the pressure of 3.5 MPa in the presence of steam as temperature moderator [1].

Distillery machine - an installation for thermal processing of crystalline polyolefin plastic waste

Production of raw materials for distillers are two types of waste polyolefins: PE (polyethylene) and PP (polypropylene) [15].

These materials must be segregated from other waste type groups or / and other plastic type groups.

The polymers are fed into the process in their original form. Soft plastic waste are mainly in form of films, bags, etc. For the waste plastics are mostly hard pack. Technology of processing of the waste from packaging made of plastic is designed for ecological and safe management of this group of municipal waste. Raw materials for the conversion process are, for example: destroyed agricultural films, used packages, containers, cans, boxes, etc. A good resource to the transformation process are different polyolefin raw materials, which cannot be recycled, i.e. fast reforming due to irreversible changes that have taken place in them, and because of the difficulty of unsegregation of the individual ranges (e.g. polyethylene of high and low density, atactic and isotactic polypropylene, polystyrene, methyl methacrylate and polymethyl methacrylate) [15]. For the purpose of the transformation described these materials (waste) can be mixed in any proportion, that is, as indeed in deposits on municipal landfills.

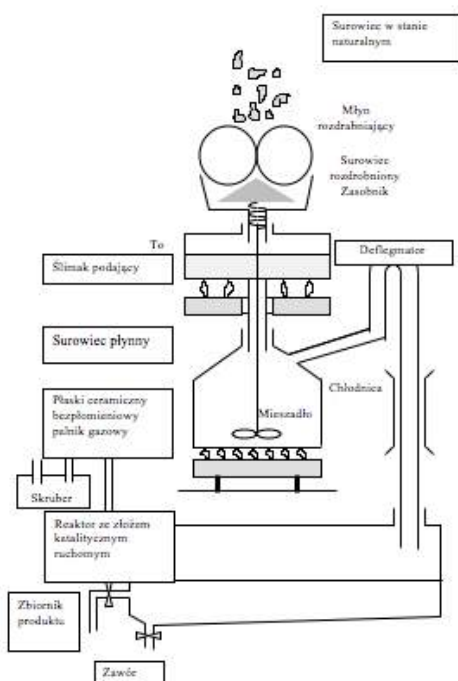


Fig. 4 Concept diagram of plastics transforming installation [15]

The main sources of supply in raw materials to production plant are [15]:

- Plant waste segregation, usually erected at the landfill,
- Companies engaged in the trading and only pre-processing of waste plastics,
- Manufacturers of plastic products subject to compulsory recycling of used products,
- Import,
- Recovery Organizations.

In Europe, in each country separately, waste plastics are processed in the amount of tens of thousands tons of rolling manner, which means only a few percent of such waste produced on an annual basis. Thus, the project development opportunities are not limited in this case, the possibility of raising the production of raw materials are very promising [15].

In addition, one can expect that, with increasing the amount of sorted waste in the market, their price will be systematically reduced. Besides, the recyclers will receive money for accepting the waste for recycling, which will be for them a second stream of income, except for revenues generated from the sale of the product [15].



Fig. 5 Plastic waste in terms of energy efficiency

Distillery machine of the 9th-generation produced by Generator-HHO has a modular structure, wherein the single module has a capacity of 100 l / h. Module dimensions: 25m x 1m, h = 2.5 m, Weight - 1t [13]. Each module is partially powered by electricity, and partially with heat energy recovered from the process gas. The distribution of this energy has been designed that the heat supplied to bottom heaters of the distillers is fully covered by energy coming

from incineration of the gaseous fraction coming off the process. Therefore, in this case, it is autonomous installation.

The distillery machine can also cooperate with generator equipped with a petrol engine [13].

Reducing distillery operating costs of energy costs makes them very economically attractive. Examples of test results are shown in Table number 2 and 3:

Table 2. Number of paraffin test result obtained from a soft polyethylene PE-LD [13].

Distillation range [°C]	Density in 20°C [g/cm ³]	Contents of sulfur [%]	Flash point [°C]	Temperature melt flow [°C]	Viscosity in 20°C [cSt]	Performance [% m/m]
up to 140	0,724	0,012	+2	-	0,6310	6,9
140-240	0,767	0,022	34	<-50	1,3671	17,0
240-350	0,791	0,004	99	-16	3,4638	14,2
rest	-	0,0083	176	+32	-	60,6

Table 3. The results of the converted car motor oil in comparison to the parameters used oil and standard values for light fuel oil [13].

Parameters specifying	Units	Used oil	Converted used oil	Light fuel oil
Density in 20°C	g/cm ³	0,891	0,840	0,850
Density in 15°C	g/cm ³	0,897	0,843	-
Viscosity in 40°C	0E	13,7= 101 mm ² /s	1,34= 4,53 mm ² /s	-
Viscosity in 20°C	0E	-	1,66= 7,9 mm ² /s	5,8 mm ² /s
Water content	%	1,6	-	0,01
Freezing point	0C	>-40	- 30	
Flash-point	0C	-	60	
Acid Number	mg KOH/g	17,4	3,8	
Sulfur content	%	0,68	0,41	0,28
Carbon residue	%	2,8	0,06	0,02
Carbon	%	-	86,7	86,0
Hydrogen	%	-	12,1	13,4
Oxygen	%	-	0,50	0,53

Parameters specifying	Units	Used oil	Converted used oil	Light fuel oil
Nitrogen	%	-	0,02	0,02
Heat of combustion	kJ/kg	-	45 250	45 850
The calorific value	kJ/kg	-	42 150	42 800
(CO ₂)max	%	-	15,80	15,34

The machine in addition to plastic processing capability has other application objectives, with all of them having a positive impact on the environment. The installation consists of two distillers for processing waste plastics, synthetic fuel and synthetic paraffin, which were used for further technological purposes. Such fuel is cheap - the approx. cost of producing is 0.8 to 1.0 zł / kg. Production of synthetic oil from waste plastic packaging is economically viable project, because making this type of plastic is involved in obtaining revenue from product sales and also associated with taking recycling fees for accepting this type of waste to be converted. Oil itself has very good parameters [13].

In principle, the process of transformation thermocatalytic waste plastics to a synthetic fuel is low pressure operation, which significantly reduces cost of equipment and makes it easy to control.. However, if the waste is moist, steam is being produced. During the process,. with temperature of approx. 400⁰C, the steam is capable to create pressure of several tens atm inside the reactor [15].

SUMMARY

Polyolefin waste due to mass manufacture and due to its chemical composition is very attractive resource for oil production and energetics. Studies on the recycling of this waste is carried out for years.

Practical implementations in this area in large-scale exist only for several recent years. Only profitable technologies can be implemented in practical application. Undoubtedly, one of the technologies are distillers. The profitability of technology, in addition to the operational and capital costs including energy costs, arises mainly from the availability of cheap raw materials . In times of difficulties and rising energy oil prices, favorable circumstances occurs for processing of polyolefin waste to fuel and synthetic oils.

For the production of synthetic liquid fuel components are only used waste polyolefin plastic, because only one, among many other types of plastic

are made from monomers containing only carbon and hydrogen atoms, as well as monomers of a standard liquid fuels.

REFERENCES

1. Grzybowski P., Przetwarzanie odpadów poliolefinowych na produkty paliwowe, Chemik, 2012, Vol. 66, nr 7, p. 725-734
2. Pilawski M., Pabjan Z., Ziętek M., Bartczak M.: BiLokalne zespoły paliwowoenergetyczne wytwarzanie wodoru z odpadów organicznych. Paliwa z Odpadów 2003 vol. IV Helion Gliwice, p. 181-186.
3. Nolte M. J., Zięba A.: Sposób i układ do prowadzenia krakingu odpadów poliolefinowych. Patent PL 351703 (2002).
4. Tokarz Z.: Układ doprowadzania i rozdzielania ciepła, zwłaszcza do linii produkcyjnej ciągłego przetwarzania odpadów z tworzyw sztucznych. Patent PL 352342 (2002).
5. Tokarz Z.: Zespół reaktora, zwłaszcza do ciągłej transformacji termokatalitycznej odpadów z tworzyw sztucznych. Patent PL 352344 (2002).
6. Bogacka M., Gan K., Sadowska K., Archiwum Gospodarki Odpadami i Ochrony Środowiska vol.16, nr 1(2014) p. 59-68.
7. <http://topgran.utp.edu.pl/pdfy/Recykulacja%20tworzyw%20sztucznych%20w%20Polsce.pdf>
8. Marek Pilawski, Zbigniew Pabjan, Michał Ziętek: „Proces i urządzenie do przetwarzania odpadowych opakowań z tworzyw sztucznych”, II Międzynarodowe Seminarium Naukowo-Techniczne : „WYBRANE PROBLEMY W BUDOWIE I EKSPLOATA CJI MASZYN” i II Ogólnopolskie Forum : „MASZYNY I URZĄDZENIA DO UTYLIZACJI ODPADÓW”, Politechnika Białostocka, AGH, KBN - Sekcja Budowy Maszyn, Białystok-Białowieża, 28-31 sierpień 2002 r., materiały w: Zeszyty Naukowe Politechniki Białostockiej 2002, Nauki Techniczne Nr XXX, Budowa i Eksploatacja Maszyn Z.XX
9. Pilawski M., Pabjan Z., Bartczak M., System OPO- odpady pracujące na odpady, Archiwum Gospodarki Odpadami, nr 4 (2006), p. 69-78.
10. http://ros.edu.pl/text/pp_2008_037.pdf
11. Zieliński T., Kaczmarek M.: Tworzywa Sztuczne i Chemia, nr.1, styczeń/luty 2008 r.
12. PlasticsEurope: The Compelling Facts About Plastics - Analysis of plastics production demand and recovery for 2006 in Europe, January 2008.
13. <http://www.slideshare.net/filipsz/destylatki-generatorhho>
14. Czop M., Archiwum Gospodarki Odpadami i Ochrony Środowiska, nr 15 (2013), p. 71-80
15. <http://vivasto.pl/technologie.php>

Application of UV spectrophotometry in the quality control of galactooligosaccharides production

Sára Koncz¹, Ferenc Firtha², *Zoltán Kovács¹

¹Department of Food Engineering, Corvinus University of Budapest, Hungary

²Department of Physics and Control, Corvinus University of Budapest, Hungary

e-mail: zoltan.kovacs5@uni-corvinus.hu

Keywords: *galactooligosaccharides, online monitoring, UV spectrophotometry, partial least square regression, prebiotics, chemical analytics, chemometrics*

ABSTRACT

Galactooligosaccharides (GOS), hence they have a positive effect on the microbial composition of the gut, are considered as prebiotics. From lactose as substrate, GOS are produced by enzymatic synthesis with β -galactosidases. In the industrial practice of GOS production, batch reactors are widely used. In order to make the process more effective and to reduce costs, other configurations, like enzyme membrane reactors or immobilized enzyme reactors operating in continuous fashion, can be considered. The implementation of such processes requires the online monitoring of the quality of the product stream.

The enzymatic reaction results in a saccharide mixture consisting of non-reacting lactose, GOS of various degree of polymerization, and glucose as by-product. The standard chemical analysis of such multi-component products involves High Performance Liquid Chromatography (HPLC). Although HPLC is reliable and accurate, it is generally considered as a time-consuming, expensive, and offline method.

This research deals with the development of an online technique that allows the real-time monitoring of carbohydrate composition during the production of GOS. For that purpose, we considered ultraviolet-visible (UV) spectrophotometry combined with partial least squares regression (PLSR).

Eighty-one samples, containing various amounts of mono-, di-, and oligosaccharides, were generated in our lab by using an enzyme membrane reactor. UV spectral data of the samples were used together with the respective concentration data quantified by HPLC, in order to develop a PLSR model. Our results show that UV spectral data combined with PLSR data processing can be used in quality control of continuous GOS production.

INTRODUCTION

Galactooligosaccharides (GOS), hence they have a positive effect on the microbial composition of the gut, are considered as prebiotics. GOS are reported to enhance health related physiological activities, decrease the number of

potentially pathogenic bacteria, stimulate absorption of some minerals and decrease blood lipids content [1]. Their stability under acidic conditions and good solubility make GOS appropriate for functional ingredients in various food products such as yoghurts, bakery products, beverages, and infant food. They can be considered as sweeteners with low caloric value and do not affect blood sugar level. The annual production of GOS is estimated to 20'000 tons, and the quantity produced rises with 3-5% a year [2].

GOS are carbohydrates, generally described by the formula $\text{Gal}_n\text{-Glu}$, where $n=2-20$ [3]. They are synthesized from lactose by the enzymatic activity of β -galactosidase. The enzyme is capable to hydrolyze the substrate to glucose and galactose. Hydrolysis increases sweetness and lowers lactose level, which is beneficial for lactose intolerant consumers. The competing transgalactosylation reaction, and thus the formation of GOS results oligosaccharides of various degree of polymerization (DP) [4].

In industrial practice, GOS is produced in stirred-tank reactors operating in batch mode. The enzyme catalysis takes place in a reactor using soluble enzymes. The reaction results in a saccharide mixture consisting of non-reacting lactose, GOS of various degrees of polymerization (typically DP3-DP6), and glucose as by-product. After the catalytic performance the solution is heated up in the reactor to inactivate the enzyme. This is a simple and easily controlled configuration.

There are also alternative routes to overcome some of the drawbacks associated with the production in conventional batch reactors. Using enzymatic membrane reactors (EMR) or immobilized packed-bed reactors enables us the reuse of enzymes, and results in an enzyme-free product [5]. Although these configurations make the process more effective and reduce costs, the implementation of such processes requires the online monitoring of the quality of the product stream.

The standard chemical analysis of such multi-component products consisting of carbohydrates involves High Performance Liquid Chromatography (HPLC). HPLC is generally considered as a reliable, accurate and well-established method. However, it is time-consuming, laborious, requires the dilution of the samples and expensive instrumentation.

Since HPLC is an off-line technique, there is a considerable long delay between sampling from the production line at the facility and receiving information on the actual carbohydrates composition from the analytics lab. In order to quantify the substrate level and the product yield in real time, a novel, online monitoring concept is to be developed.

Molecular spectroscopy represents a potential candidate for the rapid detection of carbohydrates. Dias et al. [6] have first shown that UV-spectroscopy

combined with chemometrics methods, such as partial least-squares regression (PLSR) and artificial neural networks (ANN), could serve as a fast alternative method for monitoring GOS production. They have successfully implemented UV-PLSR and UV-ANN to predict the concentration of two compounds (lactose and total GOS) in samples taken from fermentation broth. The proposed method involved the filtration and dilution of the samples prior to UV analysis.

The aim of this paper is to investigate the applicability of UV-spectroscopy for determining the carbohydrate composition of enzyme-free process streams. In this study, we employ EMR, that allows the continuous production of enzyme-free GOS, to generate samples. We then use HPLC as a reference method for carbohydrate analysis and apply UV&PLSR to estimate the concentration of individual fractions in the GOS-containing saccharides mixtures.

Materials and methods

In this section we introduce the reader to the chemicals, equipments and relevant operational conditions we used to obtain a big number of samples that serves as basis for further chemical and mathematical analysis.

Chemicals

Pharmaceutical grade α -lactose monohydrate (commercial name: Lactochem® Pharma Fine Powder) and β -galactosidase enzyme (commercial name: Biolacta N5 by Daiwa Kasei K.K., Japan) derived from *Bacillus circulans*, were provided by Friesland Campina DOMO (Amersfoort, the Netherlands).

Laboratory set-up of enzymatic membrane reactor (EMR)

The P&ID drawing of the lab-scale EMR is shown in Fig.1. The EMR consists of a stirred-tank reactor and an external ultrafiltration (UF) module. The enzymatic catalysis takes place in the stirred-tank reactor (TK-1) using soluble enzymes. The feed pump (P-1) circulates the enzyme-containing reaction liquid through the UF module (M-1). The desired cross-flow rate of the pump can be adjusted with the frequency drive of the pump. The temperature of the reactor is monitored with a thermometer and controlled by an external bath thermostat.

The UF membrane completely rejects the enzymes but allows the passage of carbohydrates. The driving force of the filtration is the pressure difference between the retentate (PIT-102) and the permeate side (PIT-103) of the membrane. The retentate-side pressure is adjusted manually with the control-valve (V-1).

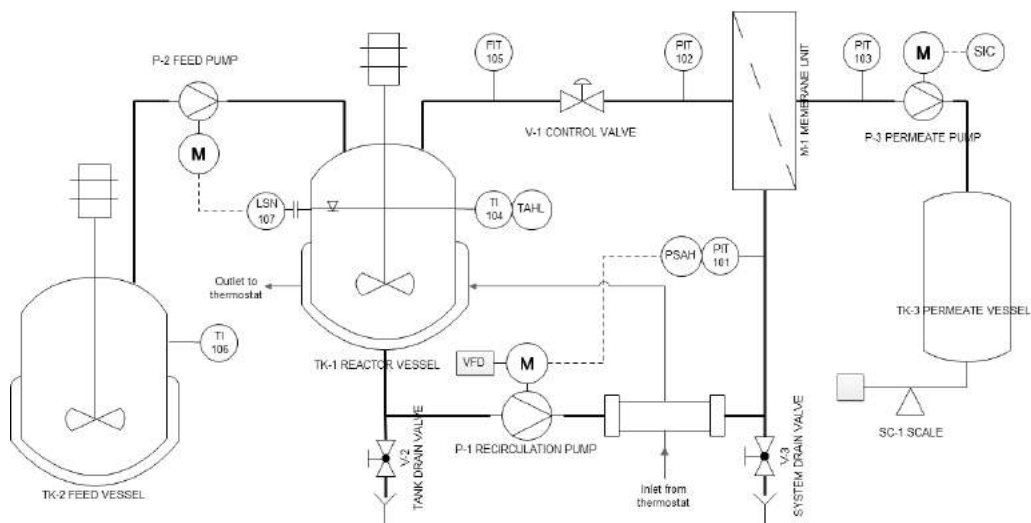


Fig. 1 Piping and instrumentation diagram of continuous ultrafiltration-assisted enzymatic reactor (EMR)

In continuous operation mode, fresh substrate solution is continuously supplied to the reactor from the feed vessel (TK-2), and the enzyme-free product is collected in TK-3. In order to ensure a stable catalytic performance, the residence time (i.e. the ratio of reactor volume to product flow-rate) has to be kept constant. This can be achieved by ensuring that the volumetric flow-rate of the permeate (i.e. product stream) is equal to the feed (i.e. fresh lactose-solution).

For controlling the permeate flow-rate, a pump (P-3) on the permeate-line was employed. The rotation of the peristaltic pump (P-3) was adjusted to the desired value ensuring a constant flow-rate. The volume of the reaction liquid in the EMR kept constant by employing a conductive level switch that switches on and off the feed pump (P-2). Thus, fresh substrate-solution is pumped from the thermostated feed tank (TK-2) into the reactor.

Sample preparation

Samples containing mono-, di-, and oligomers in various concentrations were obtained from two experiments (Run No.1 and Run No.2) using the EMR. Operational and reaction conditions of these two experimental runs are described below.

Run No.1: A 30 w/w% lactose solution was prepared and its pH was set to 6.0 using NaOH. Two litres of the lactose solution was introduced to the reactor. The reactor was thermostated at 50°C, and 2 g of Biolacta N5 was dosed into the vessel, i.e. the enzyme concentration in the reactor was set to 0.1 w/w%. After

enzyme dosage, the circulation pump was put into operation using a cross flow-rate of 0.15 m³/h. The retentate pressure was set to 1.0 bar with the pressure adjusting valve. Then, the permeate pump was set to generate a constant flow-rate of 0.90 L/h. The volume of the reactor was kept constant by dosing fresh lactose solution into the reactor at the same rate as permeate collected, resulting the constant residence time of 1.8 h. The EMR was operated in continuous fashion for 7 hours. After 3 hours of operation, 18 g of fresh enzyme was dosed into the reactor, i.e. the enzyme concentration in the reactor was adjusted to 1.0 w/w%. Temperature, retentate- and permeate-side pressures, permeate flow-rate, and total mass of collected permeate were monitored during the process run. Samples were periodically taken from the permeate stream (i.e. from the enzyme-free product stream) for carbohydrate analysis.

Run No.2: The EMR was operated in the so called total-recycle mode, i.e. both permeate and retentate streams were recirculated into the reactor. Six kg of reaction liquid consisting of 30 w/w% lactose was prepared, and its pH was set to 6.0 using NaOH. The process liquid was introduced into the reactor and thermostated to 50°C. The circulation pump was put into operation using a cross flow-rate of 0.15 m³/h. Then, enzyme was dosed into the reactor resulting an enzyme concentration of 0.3 w/w%. After enzyme dosage, the retentate pressure was set to 1.0 bar with the pressure adjusting valve. The EMR was operated in batch fashion for 6 hours. Temperature, retentate-side pressure, and permeate flow rate were monitored during the process run. Samples were collected periodically taken from the permeate stream (i.e. from the enzyme-free product stream) for carbohydrate analysis.

Chemical analysis

A High-performance liquid chromatography (HPLC) system by Thermo Separations was used as reference method for carbohydrate analysis. The HPLC set-up includes an Intersciences SCM1000 degasser, a gradient pump P200, an Autosampler AS100, and a built-in Column Oven. A Melz LCD 312 differential refractive index (RI) detector by VDS optilab Chromatographetechnik GmbH (Berlin, Germany), a N2000 Chromatography Data System from Science Technology (Hangzhou, China), and a N2000 Photographic Data Workstation software package from Science Technology (Hangzhou) Inc. (Hangzhou, China) were employed for peak detection and integration. An RNM Carbohydrate 8% Na⁺ 300x7.8 (Phenomenex, Torrance, USA) analytical column together with guard column was used at 50°C at 0.4 mL/min with pre-filtered (2 µm) DI water as mobile phase. Samples taken from the permeate of the 10 kDa membrane were not subject to heat treatment.

The UV spectrophotometry analysis was carried out with a Spectronic GENESYS 5 UV-Visible Spectrophotometer manufactured by Thermo Electron Corporation (Waltham, Massachusetts, USA). Absorbance of samples from 201 to 300 nm at intervals of 3 nm was measured without dilution at room temperature.

Partial Least Squares Regression (PLS)

The *plsregress* function of Matlab (Mathworks Inc., US) was used to calculate the principal component scores of the independent data (**X** matrix of the UV spectra data) and the dependent data (**Y** matrix of the carbohydrate composition determined by HPLC) and to set up a regression model between the scores.

RESULTS AND DISCUSSION

Eighty-one samples consisting of various amount of mono-, di-, and oligosaccharides were generated using an enzyme membrane reactor (EMR). All samples were collected from the enzyme-free permeate (i.e. the product) stream of the EMR. The samples obtained during Run No.1 and Run No.2 were first analyzed by HPLC in order to quantify concentrations of glucose, galactose, DP2, DP3, DP4 and DP5 fractions. The composition determined by HPLC serves as reference data. Then, the UV spectra of the collected samples were recorded according to the method described in the section of Material and Methods.

Note that this study does not aim at investigating optimal operational conditions for EMR. Our primer goal is to obtain a dataset in which the saccharides composition varies in a wide spectrum. We attempt to cover a broad range of carbohydrates composition in order to simulate possible scenarios that may occur in real-life applications operating under both optimal and suboptimal conditions. It is to be noted that other technologies, such as packed bed reactors, in which an enzyme-free product is released, are also suitable to generate such a dataset. In this sense, the choice of EMR is arbitrary.

The saccharides composition determined by the RI-HPLC method of three, randomly selected samples, which were collected from the enzyme-free product stream of the EMR, are shown in Fig.2. The figure serves as an illustrative example of how the quality of the product may be altered during GOS production.

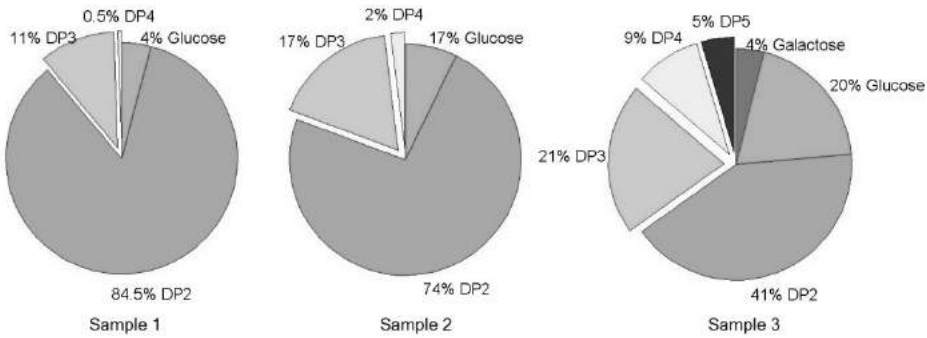


Fig. 2 High-performance liquid chromatography analysis of the carbohydrate composition of three selected samples taken from the product stream of enzyme membrane reactor.

Fig.3. shows the UV spectra in the range of 200 to 300 nm of the three, randomly selected samples. The large deviation observed in the absorption features is attributed to the relative ratio of mono-, di-, and polysaccharides present in the products. This figure serves as an illustrative example for demonstrating that UV spectroscopy has the potential of being used as a rapid analytical tool and is worth of in-depth investigation.

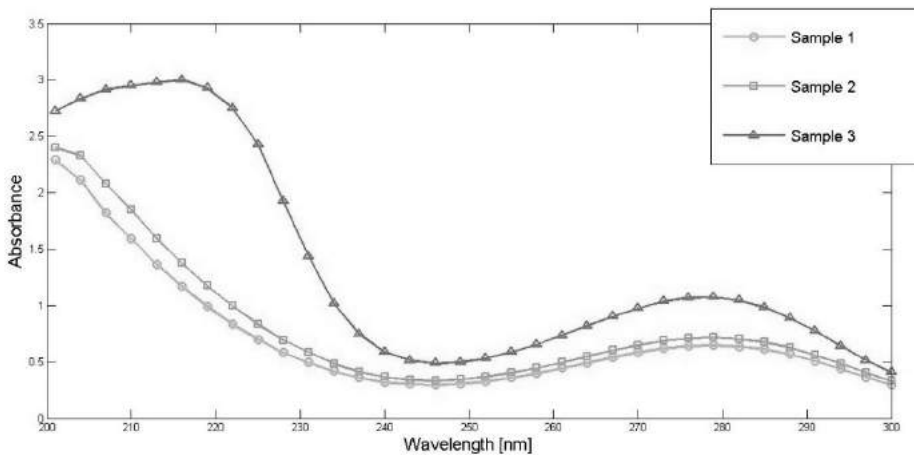


Fig. 3 UV spectra (absorbance versus wavelength) of the three selected samples.

For the establishment of an empirical relationship between the UV spectra and reference data, PLSR was used. In general, PLS regression is a bilinear technique that extracts the most relevant information as a mathematical model of linear combinations of the spectral bands to predict a property of interest (chemical, physical or sensory attributes) of different samples.

The experimental dataset containing 81 observations was divided into two subsets: the training set consisting of 61 randomly chosen observations and 76

the external validation set (or also called, test set) consisting of the remaining 20 observations. Then, the *plsregress* function of Matlab (Mathworks Inc., US) was used to fit a PLSR model to the seven responses (Glu, Gal, DP2, DP3, DP4, DP5, DP3-5) using 10-fold cross-validation. Some preliminary diagnostics were performed to find the optimal number of PLSR components. Based on the variance explained in the response variable as function of the number of components (data not shown here), eight PLSR components were selected for further analysis.

Fig.4. shows the concentration of the saccharides fractions measured with the reference method (HPLC) and that of estimated by UV spectroscopy combined with PLSR using 8 PLSR components.

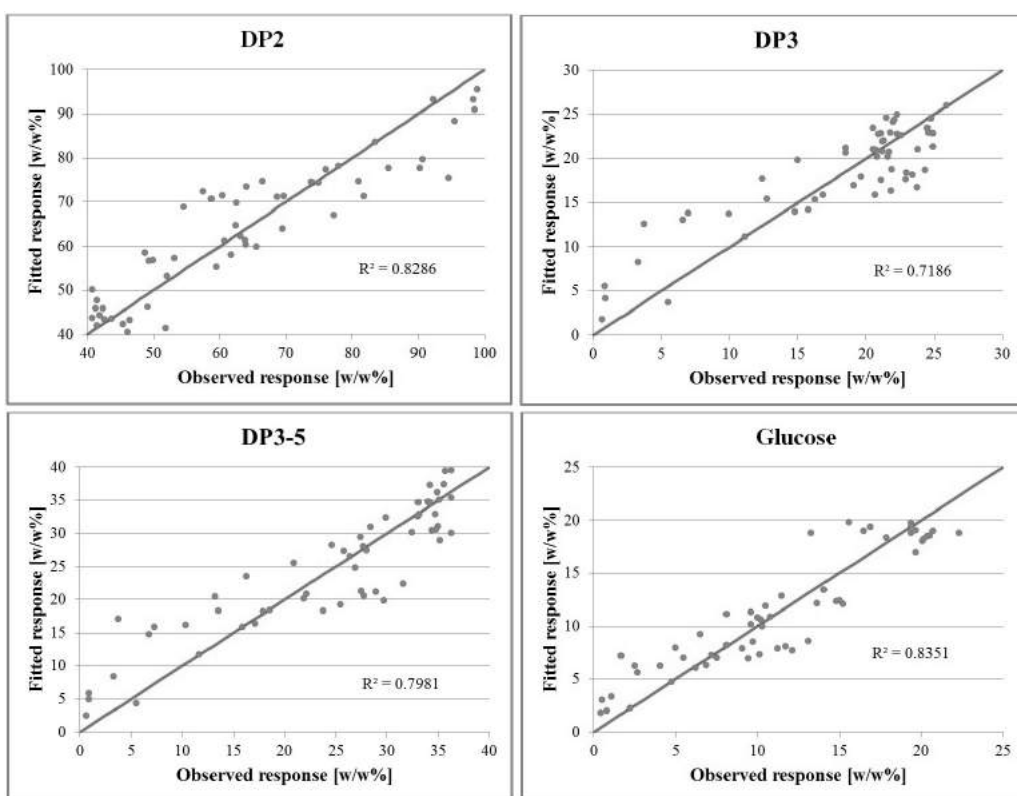


Fig. 4 Fitted response (UV&PLSR estimates) versus observed response (HPLC reference data) for some of the individual carbohydrate fractions.

As shown in Fig.4., the estimated values agree well with the measured data. Obviously, the UV&PLSR method under-performs HPLC technique in terms of accuracy and sensitivity, and thus, it will not completely substitute the standard HPLC procedure. However, it could be applied as a robust method in

the quality control of GOS production to detect possible failures of GOS synthesis in real time.

Based on our results we can conclude that UV spectroscopy combined with PLSR analysis allows the quantitative, real-time analysis of the relative amount of the individual carbohydrate fractions in the process solution at certain critical points of the GOS production line. Our further research aims at investigating the performance of artificial neural networks as an alternative to PLSR.

REFERENCES

[1] Macfarlane, G.T., Steed, H. and Macfarlane, S. (2008), Bacterial metabolism and health-related effects of galacto-oligosaccharides and other prebiotics. *Journal of Applied Microbiology*, 104: 305–344. doi: 10.1111/j.1365-2672.2007.03520.x

[2] Affertsholt-Allen T. 2007. *Market developments and industry challenges for lactose and lactose derivatives*. IDF Symposium “Lactose and its Derivatives.” Moscow. Available from: http://lactose.ru/present/1Tage_Affertsholt-Allen.pdf. Accessed Sept 30, 2009.

[3] Eric Benjamins (2014). Galacto-oligosaccharide synthesis using immobilized β -galactosidase, PhD thesis, University of Groningen, Groningen, Netherlands. ISBN: 978-94-6108-802-4

[4] Aaron Gosling, Geoff W. Stevens, Andrew R. Barber, Sandra E. Kentish, Sally L. Gras, Recent advances refining galactooligosaccharide production from lactose, *Food Chemistry*, Volume 121, Issue 2, 15 July 2010, Pages 307-318, ISSN 0308-8146, <http://dx.doi.org/10.1016/j.foodchem.2009.12.063>.

[5] Z Kovács, E Benjamins, K Grau, A U Rehman, M Ebrahimi, P Czermak (2013) Recent developments in manufacturing oligosaccharides with prebiotic function In: *Adv Biochemical Engineering/Biotechnology - Biotechnology of Food and Feed Additives* Edited by: P. Czermak and H. Zorn. Springer-Verlag Berlin Heidelberg, pp. 1-39. DOI:10.1007/10_2013_237

[6] Luís G. Dias, Ana C.A. Veloso, Daniela M. Correia, Orlando Rocha, Duarte Torres, Isabel Rocha, Lúgia R. Rodrigues, António M. Peres, UV spectrophotometry method for the monitoring of galacto-oligosaccharides production, *Food Chemistry*, Volume 113, Issue 1, 1 March 2009, Pages 246-252, ISSN 0308-8146, <http://dx.doi.org/10.1016/j.foodchem.2008.06.072>.

Silica-templated three-dimensional graphene xerogels

*Izabela Kondratowicz, Kamila Żelechowska, Wojciech Sadowski

Department of Solid State Physics, Faculty of Applied Physics and Mathematics,
Technical University of Gdańsk, Narutowicza 11/12, 80-823 Gdańsk, POLAND

*e-mail: ikondratowicz@mif.pg.gda.pl

Keywords: porous materials, graphene oxide, graphene xerogels, silica particles,

ABSTRACT

Most porous carbons require the uniform pore size distribution therefore many approaches have been applied to template the carbon scaffolds and among them the use of silica particles is the easiest and the most effective. After discovering of graphene, the whole family of new carbon nanomaterials arose and one of the promising materials is graphene xerogel (GX) with a three-dimensional, highly porous structure. This monograph reviews different carbonaceous materials and the methods used to template them as well as presents the preliminary experiments in templating the microporous structure of GX using silica particles.

INTRODUCTION

Carbon xero- and aerogels are the examples of non-oxide porous materials that are of great industrial and academic interest due to their high surface area, low density, good electrical conductivity, chemical inertness and low cost of fabrication. The process of their synthesis is usually based on creating a gel that is in the next step dried. During the drying process at room temperature the evaporation of the solvent occurs which leads to the collapse of the pore structure due to the capillary stress and the so-called xerogels are created [1]. Aerogels are formed after the supercritical drying when the liquid solvent is transformed into gas beyond its critical point (by increasing the pressure and temperature) so in the absence of surface tension that destroys the pore network. The same results can be obtained when drying under ambient atmosphere which is a less energy-consumed and less dangerous method [2,3]. The prevention of a gel shrinkage can be also ensured by decreasing the pressure and temperature (freeze-drying) and the materials produced this way are called cryogels.

Porous carbons are characterized in terms of their specific surface area and porosity. The proper size of pores as well as their morphology are of great significance as they determine the ability of carbons to adsorb different kinds of molecules, from liquid to gas, such as hydrogen, catalysts molecules as well as

biomolecules e.g. proteins. According to the IUPAC (International Union of Pure and Applied Chemists) nomenclature [4], the porous materials are divided in respect of their pore size thereby micro-, meso- and macroporous materials are classified with the range of dimensions depicted on the picture below. Figure 1 shows the graph with the IUPAC nomenclature.

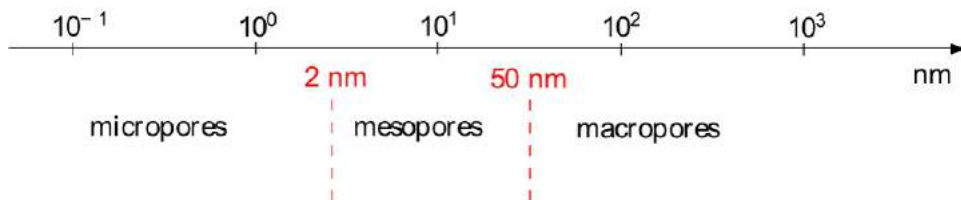


Fig. 1 IUPAC nomenclature for porous materials

The presence of pores of different dimensions has an influence on the surface area of the material and results in the ability of carbons to adsorb molecules of various sizes. The typical microporous materials with pore diameters below 2 nm are zeolites and metal-organic frameworks which are used for small gas molecules adsorption [5]. The examples of mesoporous materials (with the diameter between 2 and 50 nm) can be mesoporous silicates (SBA or M41S). The pores above 50 nm are called macropores and the representatives of this class are porous glasses and amorphous aluminosilicates [6, 7]. The applications of porous carbons are widespread and include the liquid separation [8], molecule adsorption [9, 10], hydrogen storage [11], catalysts supports [12], as well as electrode materials for fuel and biofuel cells [13, 14], ultracapacitors [15] or batteries [16]. Pores in carbon materials have been identified by different techniques. The morphology, pore parameters and their distribution can be determined using X-ray photoelectron spectroscopy (XPS), X-ray diffraction (XRD), scanning electron microscopy (SEM), BET (Braunauer-Emmett-Teller) surface analysis [6,7].

The next part of the manuscript is organized as follows: in the first subsection the synthesis of different porous carbon materials is described. The second subsection consists of a description of the two methods of templating the carbon scaffold, namely the soft and hard templating. Then the porous, 3D structures of graphene are presented with the possible applications for these materials. The second section describes the attempts that were done to template the graphene xerogel scaffold using silica particles in order to enlarge the surface area. In the third and fourth section the results and conclusions are presented.

Synthesis of porous carbons

The fabrication of carbonaceous xero(aero)- gels focuses mainly on creating gels that are then subjected to a suitable drying process. Many approaches to optimize the methods of the synthesis have been taken [17-19]. All the works show that the composition of carbon precursors as well as the conditions of the process (temperature, pressure etc.) are significant for tailoring the properties of the resulting material. The most common way of producing carbon aerogels is the polycondensation of resorcinol-formaldehyde (R-F) mixture established by Pekala [20,21]. Figure 2 shows the steps in the fabrication of carbon aerogels. Typically, this polymer resin is first dissolved in a solvent (usually water) with catalyst that helps to cross-link the polymer network. The solvent is then removed by other solvent (e.g. acetone) and dried. At the end the pyrolysis is performed in order to “burn” the polymer at the elevated temperature under the nitrogen flow, leaving the material rich in carbon.

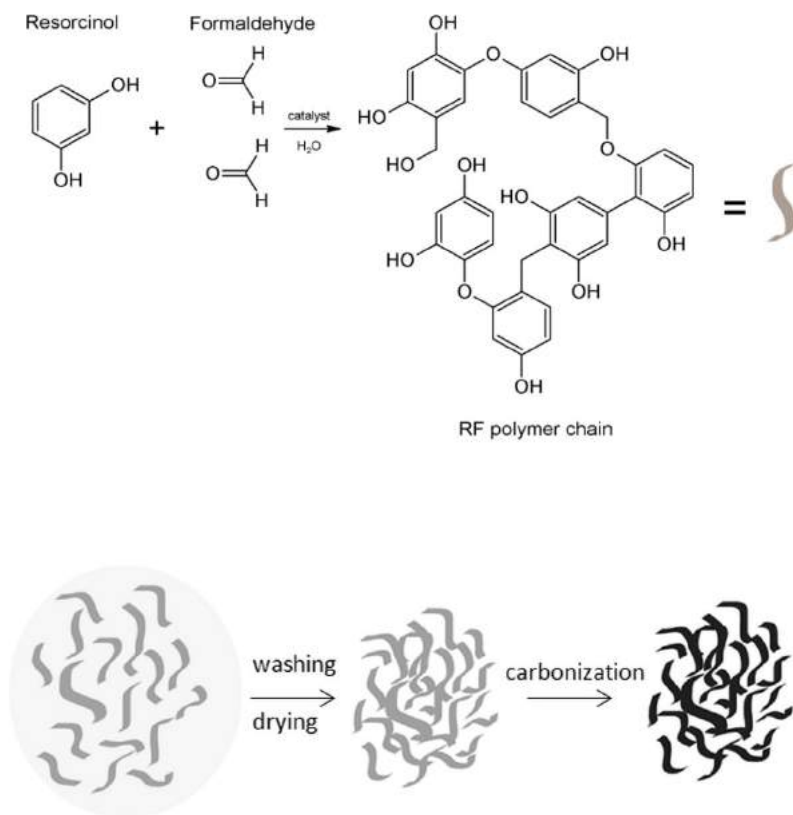


Fig. 2 Top: Polycondensation of formaldehyde and resorcinol, bottom: Process of carbon aerogel formation

Feng [22] et al. dissolved 99% resorcinol (1,3-dihydroxybenzene) with 37% formaldehyde (methanal) in water in different molar ratios (R/F=2/2, 2/3, 2/4). The sodium carbonate was used as a catalyst and its concentration was also changed (R/C ratio= 400, 200, 100) to verify its effect on the gelation time. The authors conclude that the gelation time increases with the increasing R/F ratio while decreases when the amount of catalyst is lower. Due to the high cost of resorcinol and time-consuming supercritical drying, there is a need to look for cheaper precursors and other methods of drying. Scherdel [23] studied the alternative route of synthesis using phenol and formaldehyde as a carbon source, n-propanol as a solvent and hydrochloric acid (37%) as a catalyst along with the drying at ambient conditions (65°C, atmospheric pressure). The as-obtained carbon materials possess high specific surface area (572 m²/g), micropore volumes up to 0.24 cm³/g, external surface areas (150 m²/g) and mesopore volumes up to 0.69 cm³/g with the medial pore size of 17 nm. The porous carbons can be further activated by means of physical and chemical methods [24]. Activation means that the pores (mainly micropores) are created. This leads to the increase in pore volume, change of their shape or generation of new pores. Physical methods include the use of different gases (O₂, CO₂, steam) while chemical ones use KOH, NaOH, H₂SO₄ or H₃PO₄ that can penetrate into the carbon bulk and react with it. Due to this procedures the performance of carbon aerogels may be enhanced and can provide materials with tailored electrochemical or mechanical properties.

Controlling the pore size distribution with templates

After the carbonization of carbon precursors the pores of various diameters are created thus the precise control of pore size in carbon materials is crucial for many applications. The importance of developing the new techniques of templating has been pointed out in many previous studies [25, 26]. Generally the two main methods of controlling the carbon frameworks have been known so far. The hard-templating method uses a porous template and the carbon scaffold is created in the pores of the template. Afterwards, the template is removed, leaving the carbon structure that is an inverse replica of the template architecture [27]. Many inorganic templates are used for this purpose such as zeolites (aluminosilicates), ordered mesoporous silicas, silica particles, polymer beads. The templates should be stable in the synthesis conditions, should not react with carbon and be easy to dissolve after the process is done. Sakintuna et al. [28] studied the nanoporous carbon materials with zeolite templates. They added 1 g of a commercially available zeolite to a solution containing 1.25 g of sucrose, 0.07 ml of H₂SO₄ and 5 ml of water in order to impregnate the template with carbon precursor. The mixture was then dried for 6 h at 100°C and another 6 h at

160°C. The carbonization was carried out at different temperatures. This resulted in materials with BET surface around 50 m²/g with uniform pore diameter of 4 nm. Kruk et al. [29] used the ordered mesoporous silica (SBA-15) and polyacrylonitrile as a carbon source that were mixed together and subjected to the carbonization process. They applied the heat treatment at 2480 K under argon atmosphere that helped to eliminate the microporosity in the carbon material.

The soft-templating methods are based on the self-assembly of the template and the carbon precursor together in a solution. The templates used widely are block copolymers. At the temperatures up to 400°C the carbon precursor (polymer) cross-linked while the higher temperatures enable to remove the block copolymers with the carbonization of a precursor at the same time [30]. Balach et al. [31] used a cationic polyelectrolyte as a template and RF gels as a carbon source. Polydiallyldimethylammonium chloride (PDADMAC) helped avoiding the pore collapse during the air drying of the gel and the resulting materials exhibit high surface areas (675 m²/g) with micro- and mesopores. Górka et al. [32] synthesized porous carbons using a dual templating- by means of resorcinol/formaldehyde as a carbon precursor and poly(ethylene oxide)–poly(propylene oxide)–poly(ethylene oxide) triblock copolymer as soft template and TEOS-generated silica particles as hard templates. The resulting material possessed cylindrical pores after thermal decomposition of copolymer and spherical pores after dissolving of silica particles. The hierarchical carbons obtained this way have a surface area and pore volume of 2800 m²/g and 6.0 cm³/g, respectively. The template-free methods to create ordered structures may be also applied for instance by the use of spherical polystyrene chains that crosslink with each other through carbonyl (-CO-) bridges [33].

Graphene aero- and xerogels

After the isolation of graphene- a single two-dimensional sheet of graphite- in 2004, there has been an enormous interest in utilizing this new material as an electrode in devices such as (bio)fuel cells, batteries or supercapacitors. A single- and multilayer graphene can be produced using a chemical vapor deposition (CVD) method which is also suitable for molding a three-dimensional graphene structures. Chen et al. [34] prepared 3D graphene using a nickel foam as the growth substrate and ethanol as a carbon source. The nickel foam was soaked with ethanol and then etched away in HCl at 60°C revealing a 3D graphene electrode. One of the methods for the easy fabrication of graphene is the use of graphene oxide as a precursor [35]. Graphene oxide is a single sheet of graphene that was treated with strong oxidizers resulting in the

introduction of oxygen-containing groups on the edges and basal plane of graphene layer. This operation causes the disruption in a hexagonal network of carbon atoms and thus affects the electrical conductivity of graphene oxide which is an insulator. For this reason, the GO needs to be reduced and to do that different methods are applied including chemical, electrochemical, thermal or photo reduction [36]. The resulting material is a derivative of graphene and should be called reduced graphene oxide as the studies show that it is not possible to remove all of the oxygen-containing groups [37]. In this manuscript we keep the nomenclature 'graphene' for simplicity being aware that the obtained material properties are different from the pure graphene. The recent studies [38-40] show that the self-assembly of graphene oxide upon reduction leads to the creation of free-standing reduced graphene oxide hydrogels. They can be formed during the hydrothermal reduction in an autoclave when the properties of graphene oxide change from hydrophilic to hydrophobic. This causes the reaggregation of graphene sheets through π - π stacking and the encapsulation of water molecules between the sheets still possessing residual functional groups [41]. Shi et al. [42] prepared the hydrogel by heating up the GO solution up to 180°C for 12 h. The hydrogel possessed good mechanical properties as well as good electrical conductivity ($5 \cdot 10^3$ S/cm). The easiest, one-pot synthesis of graphene gels may involve the use of hydrothermal reduction along with chemical treatment using a weak reducing agent. Ascorbic acid is a good candidate for this purpose [43]. The porosity of such aero- or xerogels is not uniform and the wide range of pore sizes is observed in such materials. To the best of our knowledge there is still no researches regarding the methods of templating graphene xerogels made of graphene oxide precursor and thus the efforts need to be taken to ensure the suitable pore dimensions of this promising material that could lead to the high specific surface area for the adsorption of different molecules.

EXPERIMENTAL

Reagents and apparatus

For the synthesis of silica particles, tetraethyl orthosilicate (TEOS) (99.99%, Aldrich), ethanol (EtOH, POCh) and ammonium hydroxide (25%, Aldrich) were used without any further purification. For the synthesis of graphene xerogels, the graphene flakes were used as a carbon precursor (Sigma Aldrich), potassium permanganate, sulfuric acid (99%) and phosphoric acid (85%), hydrochloric acid (HCl, 36%), L-ascorbic acid and hydrogen peroxide were used were purchased from POCh and used without any further purification.. Hydrofluoric acid (HF, 49%, POCh) was used as an etchant. Distilled water was utilized throughout the experiments.

For microscopy analysis the Scanning electron microscope FEI Quanta FEG 250 was used and the BET surface analysis was performed using AreameterII, Strohlein Instruments.

Synthesis of silica particles

To begin with, the silica particles were synthesized using the traditional sol-gel method found in the literature [44, 45]. We prepared three samples with different amount of a precursor (TEOS) in order to obtain particles of different sizes. Briefly, 4.2 ml of ammonium hydroxide was mixed with 75 ml of ethanol and 10 ml of distilled water. It was stirred magnetically for 15 minutes. Afterwards, 1 ml and 10 ml of TEOS was added to the solution and kept stirred at 30°C for 6 h to let the solution form a gel. Then, the gel was centrifuged and washed with ethanol and water (3x 5minutes, 10000 rpm). The smallest particles were prepared using the modified method [46] in which 5 ml of TEOS was dissolved in 30 ml of EtOH and was ultrasonicated at room temperature for 10 min. Then 1 ml of water was added dropwise. After 1.5 h the ammonia was dropped to the solution and sonication was continued for 3 h. The gel was centrifuged and washed with ethanol and distilled water, dried in the oven at 90°C. In this way the particles of sizes 300, 150 and 50 nm, respectively, were fabricated.

In order to create graphene xerogels, graphene oxide (GO) was used as a precursor. The synthesis of GO was based on modified Hummers method described in [46]. First 0.2 g of graphite flakes was mixed with 0.6 g of KMnO_4 . Then the mixture of $\text{H}_2\text{SO}_4/\text{H}_3\text{PO}_4$ (12 ml:3 ml) was slowly added to the solids. We used an ice bath to keep the temperature below 20°C and provide the safety of the experiment. The suspension was left for 24 h with the magnetic stirring. 3% of hydrogen peroxide was added in order to stop the reaction. It resulted in a color change of suspension to dark yellow and a production of graphite oxide (GrO). The suspension was centrifuged at 15000 rpm for 10 min and washed several times with deionized water and 3% of HCl. To obtain graphene oxide (GO), the suspension of GrO powder in water (0.1 mg/ml) was ultrasonicated for 4 h.

The next step was to template the architecture of graphene xerogels. Graphene oxide suspension was mixed with silica particle water dispersions in two different mass ratio- 1:1 and 10:1. Figure 3 presents the general scheme of the GX synthesis.

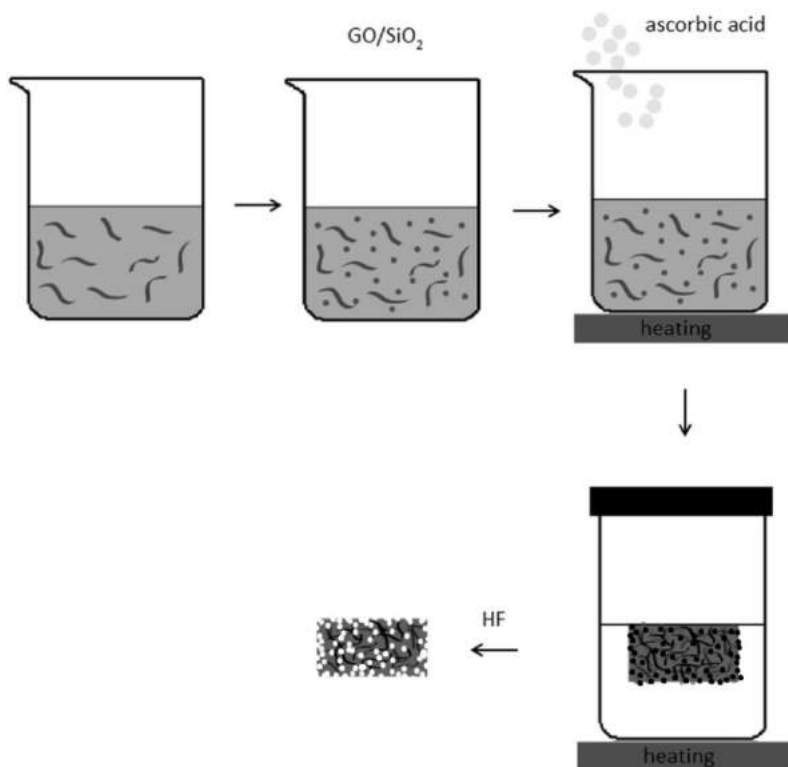


Fig. 3 The synthesis of silica-templated graphene xerogels.

First, 12 mg of GO powder was dispersed in 6 ml of distilled water (2 mg/ml of GO) and sonicated for 1 h. Then 12 mg (ratio 1:1) or 1.2 mg (ratio 10:1) of SiO_2 particles (300 nm) was added and the whole was ultrasonicated for another 2 h to ensure the uniform dispersion of particles and graphene oxide sheets. This was done to compare the influence of different particles sizes on the surface area of xerogels. For the synthesis of xerogels with particles of 150 and 50 nm the reverse order of the synthesis was applied. First 1.2 mg of silica particles (150 or 50 nm) was dispersed in water for 1 h and then 12 mg of GO (giving a ratio 10:1) was added and the whole was sonicated for another 2 h.

For the creation of graphene xerogels, the hydrothermal method of reduction through self-assembly of reduced graphene oxide sheets was used for all samples. Ascorbic acid (AA) was chosen as a reducing agent. 24 mg of AA was added to the vials with GO/ SiO_2 dispersions. The vials were sealed and heated up in an oil bath up to 90°C . After 2-3 hours, the reduced graphene oxide hydrogels started to shape which can be seen in Figure 4.



Fig. 4 Graphene hydrogel after complete formation.

After their complete formation, the hydrogels were cool down and washed with water and ethanol many times for to remove any residual acid and were dried at room temperature. The next step was to etch silica nanoparticles by soaking in the concentrated HF for 24 h. Afterwards the xerogels were rinsed with water for 2 days to remove the acid and obtain a neutral pH. They were left to dry at room temperature. The samples that were prepared in these experiments were denoted as **GX300-1:1**, **GX300-10:1**, **GX150-10:1** and **GX50-10:1** whereas the the first number indicates the diameter of the silica particles used and the second the mass ratio of GO:SiO₂. For a comparison, the graphene xerogel without silica nanoparticles was also prepared and denoted as **GX**.

RESULTS AND DISCUSSION

After the synthesis of silica particles the SEM images were taken. They confirmed that the created particles possess diameters of approximately 300, 150 and 50 nm and are quite uniform in dimension and shape which can be seen on Figure 5 (for 300 nm).

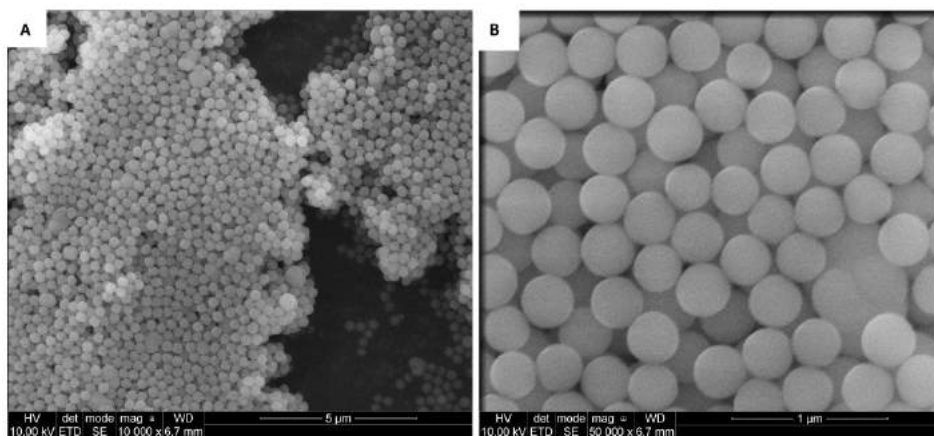


Fig. 5 SEM images of the obtained silica particles of a diameter around 300 nm.

Graphene xerogels were imaged using SEM. Figure 6 shows the overall picture of a xerogel **GX300-1:1** after etching, showing a highly developed external surface area.

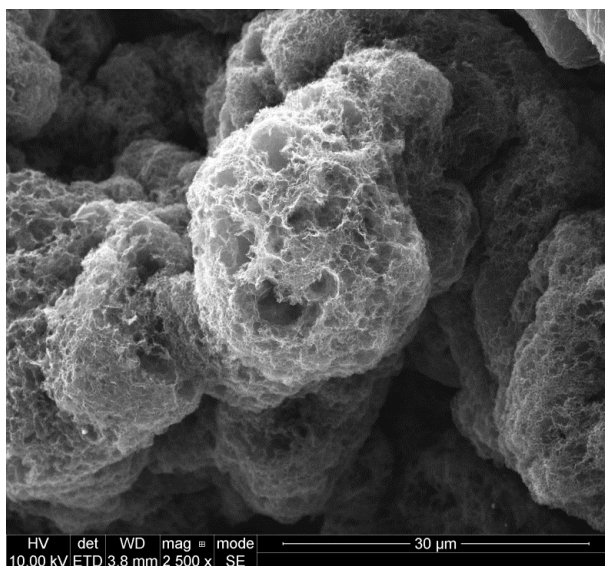


Fig. 6 SEM image of a xerogel (magnification 2500x).

To optimize the methods of the xerogel synthesis the different conditions of experiments need to be compared. Figure 7 shows a non-templated graphene structure (**GX**) that possesses a non-uniform surface structure with pores of a dimension ranging from a few to hundreds of nanometers. SEM images of template xerogels were then taken before and after etching silica nanoparticles. The comparison of **GX300-1:1** before and after etching is depicted in Figure 8 and the comparison of **GX300-10:1** is shown in Figure 9.

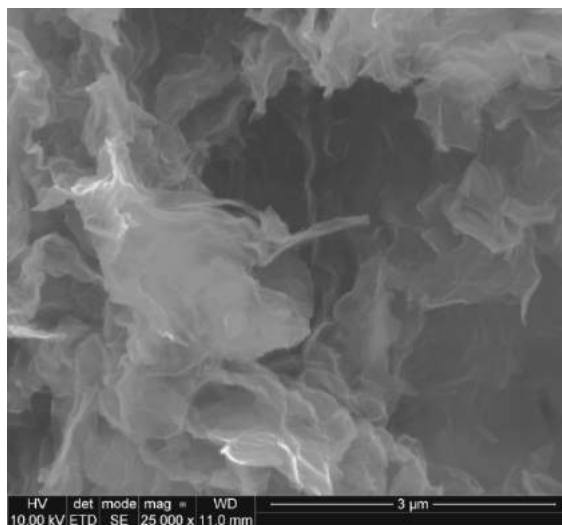


Fig. 7 SEM image of the non-templated graphene xerogel (GX).

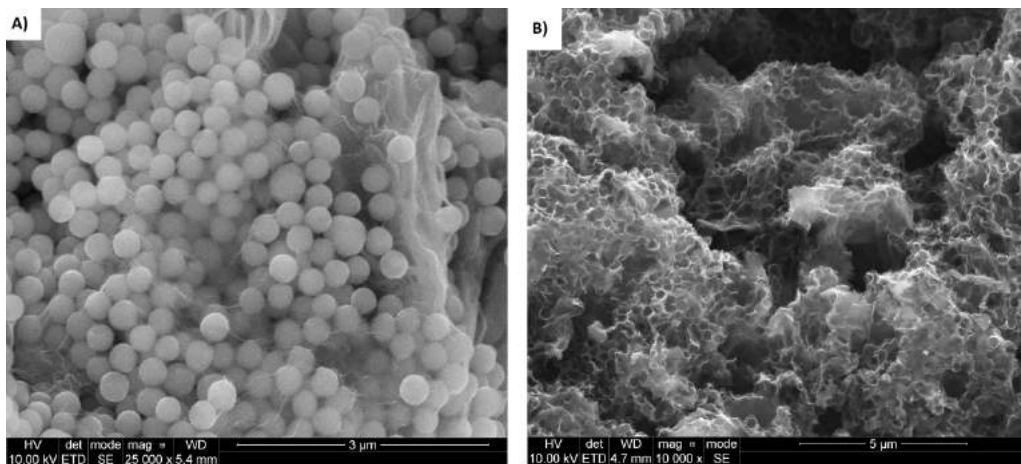


Fig. 8 A) GX300-1:1 before and B) after etching of silica particles.

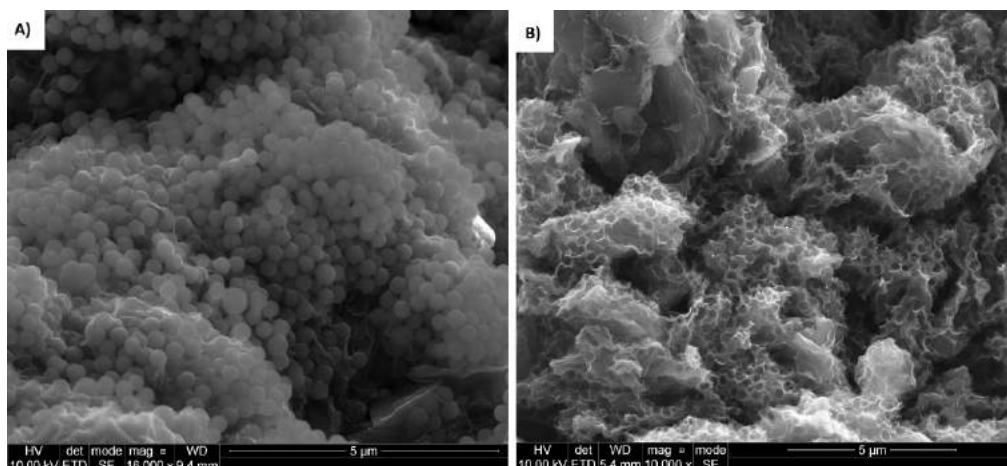


Fig. 9 GX-10:1 before A) and after B) etching of silica particles.

It can be seen from the images on the left that the silica particles are concentrated on a surface of xerogels and are covered with thin layers of graphene. After silica etching, the pockets where silica particles were placed are empty with well visible edges and shapes. Figure 10 shows the zoomed image of GX300-1:1. The estimated cavity sizes after the silica removal were measured to be the same as a silica diameter (approximately 300 nm). Thus the pores after etching and subsequent drying at room temperature did not undergo any collapse.

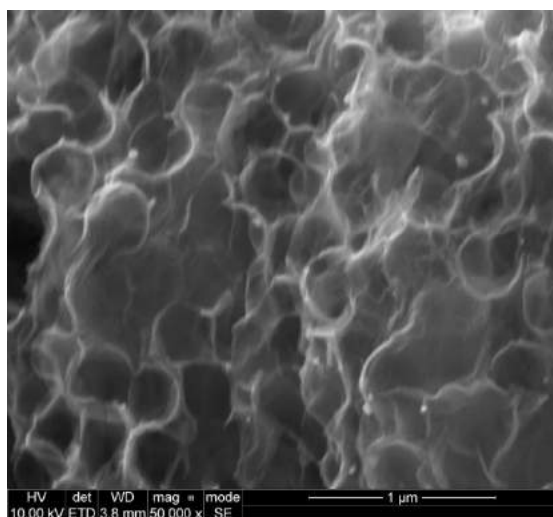


Fig. 10 SEM image of a surface of GX300-1:1 (scale 1 μm).

Comparing the morphology of materials with different GO to SiO₂ mass ratio, no differences can be observed. Silica particles tend to accumulate on a surface of a structure causing the external surface to be well developed in both

cases. The BET surface area was estimated to be around 50 m²/g and did not vary much for both samples. Figure 11 shows the SEM images of **GX150-10:1** and **GX50-10:1**. In both cases the silica particles agglomerate on the surface and the order of adding the substrates has no influence on the resulting materials.

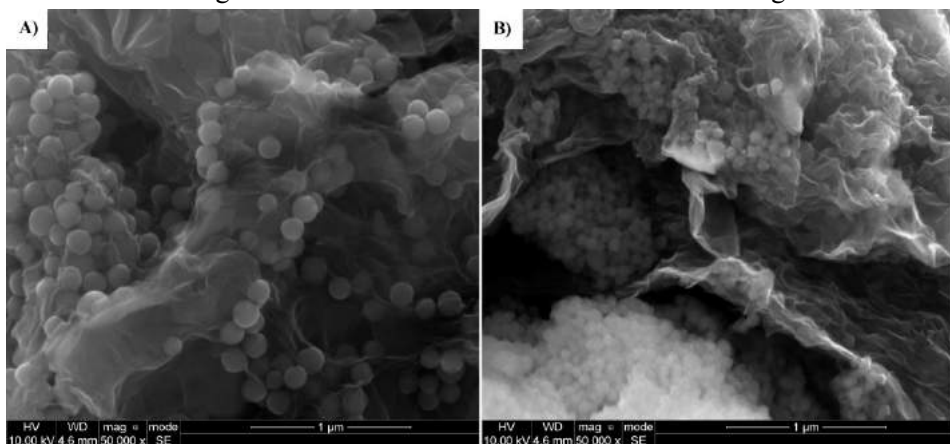


Fig. 11 A) **GX150-10:1** and B) **GX50-10:1** with silica particles

This mechanism can be explained owing to the negative charge both on graphene oxide sheets and silica particles in water. These two repel each other electrostatically when put together and can be uniformly distributed during the sonication. After the reduction of graphene oxide the negatively-charged oxygen-containing groups are mostly removed. Thereby the van der Waals and π - π interactions come into play and they cause the reduced graphene oxide sheets to re-stack. During this process the negatively-charged silica particles are being arranged on the outer surface of the created hydrogel (repelling from each other) with the graphene sheets trapped mainly inside the structure. The schematic picture of this mechanism is presented in Figure 12.

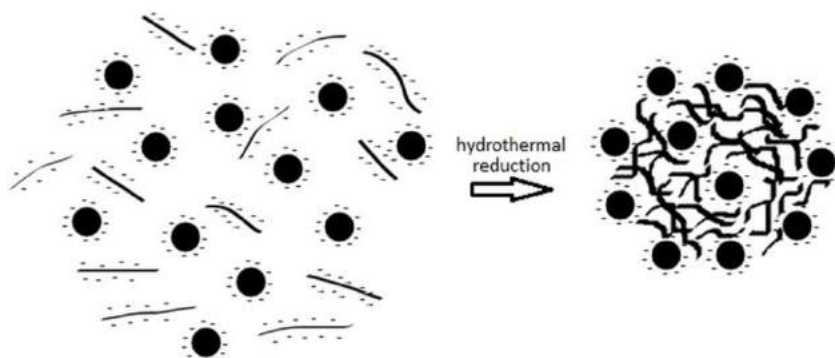


Fig. 12 The schematic drawing of the formation mechanism of silica-templated graphene xerogels (“minus” signs around particles and sheets indicate the negative charge).

CONCLUSIONS

We prepared graphene xerogels with well-defined surface morphology by the use of 300, 150 and 50 nm silica particles. In comparison to the non-templated graphene surface, such xerogels exhibit highly developed specific surface area with the ordered structure. After etching of SiO₂ followed by drying at room temperature, the pores remained their size and shape without significant collapse. The silica particles tend to agglomerate on the outer surface of the structures due to the electrostatic repulsion with graphene oxide sheets and between single particles. This method of templating graphene xerogels using silica particles as hard templates seems to be promising and need further investigations. Such porous materials could be used as the complete electrodes for the adsorption of bigger molecules such as enzymes for biosensor and biofuel cells applications.

ACKNOWLEDGEMENT

The authors would like to thank Jakub Karczewski for providing the SEM images.

REFERENCES

- [1] Job N., They A., Pirard E., Marien J., Kocon L., Rouzaud J.-N., Beguin F., Pirard J.-P., Carbon aerogels, cryogels and xerogels: Influence of the drying method on the textural properties of porous carbon materials, *Carbon*, 2005, 43, 2481–2494, DOI:10.1016/j.carbon.2005.04.031
- [2] Wu D., Fu R., Zhang S., Dresselhaus M. S., Dresselhaus G., Preparation of low-density carbon aerogels by ambient pressure drying, *Carbon*, 2004, 42, 2033–2039, DOI:10.1016/j.carbon.2004.04.003
- [3] Li L., Guo X., Zhong B., Chen Y., Li L., Tang Y., Fang W., Preparation of carbon aerogel by ambient pressure drying and its application in lithium/sulfur battery, *Journal of Applied Electrochemistry*, 2013, 43, 65-72, DOI: 10.1007/s10800-012-0505-2
- [4] Rouquerol J., Avnir D., Fairbridge C. W., Everett D. H., Haynes J. M., Recommendations for the characterization of porous solids (Technical REPORT), *Pure and Applied Chemistry*, 1994, 66, 1739-1758 DOI:10.1351/pac199466081739
- [5] Takashi K., Control of pore structure in carbon, *Carbon*, 2000, 38, 269-286, DOI:10.1016/S0008-6223(99)00142-6
- [6] Kou L., Wang Y.H., Dong Y., Han D.Z., Ni B., Yan Z.F., One-step synthesis of three-dimensionally ordered macro-mesoporous silica-alumina composites, *Materials Letters*, 2014, 121, 212–214, DOI:10.1016/j.matlet.2014.01.144

- [7] Sakintuna B., Yurum Y., Templated Porous Carbons: A Review Article, *Industrial and Engineering Chemistry Research*, 2005, 44, 2893-2902 DOI:10.1021/ie049080w
- [8] Yang Y., Tong Z., Ngai T., Wang C., Nitrogen-Rich and Fire-Resistant Carbon Aerogels for the Removal of Oil Contaminants from Water, *ACS Applied Materials & Interfaces*, 2014, 6, 6351–6360, DOI: 10.1021/am5016342
- [9] Zuo L., Song W., Shi T., Lv C., Yao J., Liu J. F., Weng Y., Adsorption of aniline on template-synthesized porous carbons, *Microporous and Mesoporous Materials*, 2014, 200, 174–181, DOI: 10.1016/j.micromeso.2014.08.036
- [10] Kanga K.Y., Leea B.I., Leea J.S., Hydrogen adsorption on nitrogen-doped carbon xerogels, *Carbon*, 2009, 47, 1171-1180, DOI:10.1016/j.carbon.2009.01.001
- [11] Tiana H.Y., Buckleya C.E., Wangc S.B., Zhou M.F., Enhanced hydrogen storage capacity in carbon aerogels treated with KOH, *Carbon*, 2009, 47, 2112–2142, DOI: 10.1016/j.carbon.2009.03.063
- [12] Marie J., Berthon-Fabry S., Achard P., Job N., Lambert S., Carbon xerogels as catalyst supports for PEM fuel cell cathode, *Energy Conversion and Management*, 2008, 49, 2461–2470, DOI:10.1016/j.enconman.2008.03.025
- [13] Glora M., Wiener M., Petričević R., Pröbstle H., Fricke J., Integration of carbon aerogels in PEM fuel cells, *Journal of Non-crystalline solids*, 2001, 285, 283-287, DOI:10.1016/S0022-3093(01)00468-9.
- [14] Servat K., Tingry S., Brunel I., Querelle S., Cretin M., Innocent C., Jolivalt C., Rolland M., Modification of porous carbon tubes with enzymes: application for biofuel cells, *Journal of Applied Electrochemistry*, 2007, 37, 121–127, DOI: 10.1007/s10800-006-9221-0
- [15] Qie L., Chen W., Xu H., Xiong X., Synthesis of functionalized 3D hierarchical porous carbon for high-performance supercapacitors, *Energy Environmental Science*, 2013, 6, 2497-2504, DOI: 10.1039/C3EE41638K
- [16] Wang L., Schütz C., Salazar-Alvarez G., Titirici M.-M., Carbon aerogels from bacterial nanocellulose as anodes for lithium ion batteries, *RSC Advances*, 2014, 4, 17549-17554, DOI: 10.1039/C3RA47853J
- [17] Marie J., Berthon-Fabry S., Achard P., Chatanet M., Pradourat A., Chainet E., Highly dispersed platinum on carbon aerogels as supported catalysts for PEM fuel cell-electrodes: comparison of two different synthesis paths, *Journal of Non-Crystalline Solids*, 2004, 350, 88–96, DOI:10.1016/j.jnoncrysol.2004.06.038
- [18] Schwan M., Ratke L., Flexibilisation of resorcinol–formaldehyde aerogels, *Journal of Materials Chemistry A*, 2013, 1, 13462-13468, DOI: 10.1039/C3TA13172F

- [19] Li W., Reichenauer G., Fricke J., Carbon aerogels derived from cresol–resorcinol–formaldehyde for supercapacitors, *Carbon*, 2002, 40, 2955–2959, DOI:10.1016/S0008-6223(02)00243-9
- [20] Pekala R.W., Organic aerogels from the polycondensation of resorcinol with formaldehyde, *Journal of Material Science*, 1989, 24, 3221–3227, DOI: 10.1007/BF01139044
- [21] Pekala R.W., Alviso C.T., Kong F.M., Hulsey S.S., Aerogels derived from multifunctional organic monomers, *Journal of Non-Crystalline Solids*, 1992, 145, 90–98, DOI: 10.1016/S0022-3093(05)80436-3
- [22] Feng Y.N., Miao L., Cao Y.G., Nishi T., Tanemura S., Tanemura M., K. Suzuki K., Fabrication of Carbon Aerogels, *Advanced Materials Research*, 2006, 11-12, 19-22, Asian International Conference on Advanced Materials, ISBN: 9780878499793
- [23] Scherdel C., Reichenauer G., Carbon xerogels synthesized via phenol–formaldehyde gels, *Microporous and Mesoporous Materials*, 2009, 126, 133–142, DOI:10.1016/j.micromeso.2009.05.033
- [24] Kwon S.H., Lee E., Kim B.S., Kim S.G., Lee B.J., Kim M.S., Jung J.C., Activated carbon aerogel as electrode material for coin-type EDLC cell in organic electrolyte, *Current Applied Physics*, 2014, 14, 603-607, DOI:10.1016/j.cap.2014.02.010
- [25] Inagaki M., Pores in carbon materials-importance of their control, *New Carbon Materials*, 2009, 24, 193–232, DOI:10.1016/S1872-5805(08)60048-7
- [26] Zhao X. S., Su F., Yan Q., Guo W., Bao X.Y., Lv L., Zhou Z., Templating methods for preparation of porous structures, *Journal of Material Chemistry*, 2006, 16, 637–648, DOI: 10.1039/b513060c
- [27] Xia Y., Yang Z. and Mokaya R., Templated nanoscale porous carbons, *Nanoscale*, 2010, 2, 639–659, DOI: 10.1039/b9nr00207c,
- [28] Sakintuna B., Aktaş Z., Yürüm Y., Synthesis of porous carbon materials by carbonization in natural zeolite nanochannels, *Prepr. Pap.-Am. Chem. Soc., Div. Fuel Chem*, 2003, 226, 614-615, 226th National Meeting of the American-Chemical-Society, ISSN: 00657727
- [29] Kohlaas K.M., Ruoff R.S., Celer E.B., Jaroniec M., Kruk M., Dufour B., Matyjaszewski K., Kowalewski T., Partially graphitic, high-surface-area mesoporous carbons from polyacrylonitril, *Microporous and Mesoporous Materials*, 2007, 102, 178–187, DOI:10.1016/j.micromeso.2006.12.027
- [30] Sterk L., Gorka J., Jaroniec M., Polymer-templated mesoporous carbons with nickel nanoparticles, *Colloids and Surfaces A: Physicochem. Eng. Aspects*, 2010, 362, 20–27, DOI:10.1016/j.colsurfa.2010.03.028
- [31] Balach J., Tamborini L., Sapag K., Facile preparation of hierarchical porous carbons with tailored pore size obtained using a cationic polyelectrolyte as a soft

- template, *Colloids and Surfaces A: Physicochem. Eng. Aspects*, 2012, 415, 343–348, DOI:10.1016/j.colsurfa.2012.10.016
- [32] Gorka J., Jaroniec M., Hierarchically porous phenolic resin-based carbons obtained by block copolymer-colloidal silica templating and post-synthesis activation with carbon dioxide and water vapor, *Carbon*, 2011, 49, 154-160 DOI:10.1016/j.carbon.2010.08.055
- [33] Dutta S., Bhaumik A., Wu K. C.-W., Hierarchically porous carbon derived from polymers and biomass: effect of interconnected pores on energy applications, *Energy Environmental Science*, 2014, 7, 3574–3592, DOI: 10.1039/c4ee01075b
- [34] Prasad K. P., Chen Y., Chen P., Three dimensional Graphene-Carbon Nanotube Hybrid for High- Performance Enzymatic Biofuel Cells, *ACS Applied Materials & Interfaces*, 2014, 6, 3387–3393, DOI: 10.1021/am405432b
- [35] Park S., Ruoff R.S., Chemical methods for the production of graphenes, *Nature Nanotechnology*, 2009, 4, 217-224, DOI:10.1038/nnano.2009.58
- [36] Pei S., Cheng H. M., The reduction of graphene oxide, *Carbon*, 2012, 50, 3210 – 3228, DOI:10.1016/j.carbon.2011.11.010
- [37] Xu C., Yuan R.S., Wang X., Selective reduction of graphene oxide, *New Carbon Materials*, 2014, 29, 61–66, DOI:10.1016/S1872-5805(14)60126-8
- [38] Zhong Y. et al., Effect of graphene aerogel on thermal behavior of phase change materials for thermal management, *Solar Energy Materials & Solar Cells*, 2013, 113, 195–200, DOI:10.1016/j.solmat.2013.01.046
- [39] Ellsworth M.W., Wang J., Graphene Aerogels, *ECS Transactions*, 2009, 19, 241-247, DOI: 10.1149/1.3119548
- [40] Nguyen H.T., Nguyen S.T., Nguyen Pam PV., Fan Z., Duong H.M., Rinaldi A., Morphology control and thermal stability of binderless-graphene aerogels from graphite for energy storage applications, *Colloids and Surfaces A: Physicochem. Eng. Aspects*, 2012, 414, 352–358, DOI:10.1016/j.colsurfa.2012.08.048
- [41] Dreyer D., Park S., Bielawski C.W., Ruoff R.S., The chemistry of graphene oxide, *Chemical Society Reviews*, 2010, 39, 228-240, DOI: 10.1039/B917103G
- [42] Xu Y., Sheng K., Li C., and Shi G., Self-Assembled Graphene Hydrogel via a One-Step Hydrothermal Process, *ACS Nanotechnology*, 2010, 4, 4324-4330, DOI: 10.1021/nm101187z
- [43] Marconnet A., Fan Z., Tng D.Z.Y., Lim C.X.T., Liu P., Nguyen S.T., Xiao P., Lim C.Y.H., Duong H.M., Thermal and electrical properties of graphene/carbon nanotube aerogels, *Colloids and Surfaces A: Physicochem. Eng. Aspects*, 2014, 445, 48– 53, DOI:10.1016/j.colsurfa.2013.12.083

- [44] Stober W., Fink A., Bohn E., Controlled growth of monodisperse silica spheres in the micron size range, *Journal of Colloid Interface Science*, 1968, 26, 62-69, DOI: 10.1016/0021-9797(68)90272-5
- [45] Sreenivasa R. K., El-Hami K., Kodaki T., Matsushige K., Makino K., Novel method for synthesis of silica nanoparticles, *Journal of Colloid and Interface Science*, 2005, 289, 125–131, DOI:10.1016/j.jcis.2005.02.019
- [46] Jafarzadeh M., Rahman I. A., Sipaut C. S., Synthesis of silica nanoparticles by modified sol-gel process: the effect of mixing modes of the reactants and drying techniques, *Journal of Sol-Gel Science and Technology*, 2009, 50, 328-336, DOI: 10.1007/s10971-009-1958-6

Transition Metal Oxides influence on phosphate and borate glasses structure

*Tomasz Lewandowski, Marta Przeźniak-Welenc, Leszek Wicikowski
Faculty of Applied Physics and Mathematics, Gdansk University of Technology,
Gdansk, POLAND
Email: tlewandowski@mif.pg.gda.pl

Keywords: *Transition metals, FTIR, glass materials, DSC*

ABSTRACT

Borate and phosphate glasses possess many potential luminescence and optical applications. With their low melting point, they are one of the most often studied amorphous materials. In recent years these glasses, doped with transition metal oxides (TMO), gained much attention due to their tunable structural and thermal properties. Review of systems containing TMOs was presented. Additionally synthesis of binary MnO-P₂O₅ and MnO-B₂O₃ systems was presented. In this work xMnO-(100-x)P₂O₅ and xMnO-(100-x)B₂O₃ (where x = 40, 50 and 60 mol%) glasses have been synthesized and compared. Conventional melt-quenching technique has been used in both cases. Amorphous material has been obtained in two series of samples. Infrared spectroscopy studies (FTIR) shown some structural modifications in function of MnO content. It is proposed that MnO causes degradation of structural units of both phosphate and borate glasses. DSC studies presented different effect on T_g and melting temperature change in case of considered systems. Further, TMO affects differently the thermal stability of synthesized glasses.

INTRODUCTION

Even though glass materials are known for centuries they are still important part of everyday life. Glass is of great importance in industry, electronic devices, chemicals detection etc. Nowadays compositions based on borate and phosphate glasses play major role in industry connected with sensor technology, catalysis, illumination, sealing, or radiation waste storage [1,2,3]. Additionally, this systems are promising for laser hosts and data storage materials. Phosphate and borate glasses are considered to be good converting layer in solar cells and promising sealants or proton conducting materials in low temperature fuel cells [4,5,6]. In the last few decades glasses doped with transition metal oxides and rare earth oxides started to play a key role in development of novel glass materials. Many of newly synthesized amorphous systems exhibit dramatic change of hardness, viscosity and luminescence properties. That change can lead to a new potential applications. However,

knowledge about the nature of structural changes of glass material doped with transition metal oxides is often limited due many problems in characterization of structural changes and these problems are still a subject of intense research. Additionally, doping with considerable amount of metal oxides such as iron, lead, zinc, manganese oxides results in difficulties with obtaining the amorphous state in product due crystallization of transition metal phase. This fact greatly influences costs of material synthesis. To avoid this it is necessary to perform intense research on TMO influence on glass structure in systems of great industrial and technical importance.

Examination of amorphous material structure requires employment of such techniques as infrared spectroscopy, X-Ray photon spectroscopy or electron paramagnetic resonance. Here FTIR (Fourier transform infrared spectroscopy) technique will be reviewed. This technique usually employed in polymer and drug analysis can often be used in determination of glass internal structure. In fact FTIR is used to detect and describe alterations of doped glass structure quantitatively and qualitatively. Infrared measurements with Fourier transform offer fast and low-cost measurement procedure and results with high signal/noise ratio. Thus, spectroscopic results in infrared range in case of borate and phosphate systems are abundant and widely available in literature. This work is dedicated to review the spectroscopic studies on the most interesting and promising borate and phosphate systems.

PHOSPHATE GLASS STRUCTURE

Phosphate glasses are especially interesting because of their low melting point and wide compositional glass forming range. This advantages are the reason that their utilization is considered in many technological aspects. Phosphate glasses, first synthesized in the beginning of XX century, found applications in laser technology as laser hosts (in high energy- high power HEHP and high average power HAP lasers), light emitting diodes, and proton conducting materials as well as catalysts. However, major drawback of phosphate glass is its limited durability in atmospheric conditions and low resistance to water present in the air. This disadvantages forced the researchers to find some ways to improve physical and chemical properties of this material. Functionalization of glass material could not take place without profound knowledge about glass matrix structure. Even though glass materials are amorphous, one has to know that although there is no long range order in glass matrices, short range order is present. This is what is called “glass structure” – basic building blocks of glass ordered in short range regime and connected to each other to form, from macroscopic point of view, true, amorphous glass matrix. In case of phosphate glass PO_4 tetrahedrons can be found that connect

with other tetrahedrons to finally form long 1D chains. These chains through bending and entanglement form 3D structure of phosphate glass. Every tetrahedron possesses three oxygen atoms able to form oxygen bridges that connect the building blocks. Because of that entangled structure of phosphate chains these glasses exhibit low melting point, high thermal expansion coefficient and low resistance to water. Such structure permits compositional modifications through use of dopants such as transition metal oxides. In description of phosphate glass structure one can find helpful parameters that allow to characterize phosphate glass compositions. It is possible to define material using so called O/P ratio (oxygen to phosphorus ratio) that helps to quantitatively illustrate relation of oxygen and phosphorus atoms number. Characterization of phosphate glass requires to define basic building block (PO_4 tetrahedron) with notation Q similar to silicate glass case. One can distinguish Q^3 , Q^2 , Q^1 , and Q^0 tetrahedrons. There are several types of phosphate glass that can be identified depending on glass composition. One can distinguish ultra-, meta-, poly-, pyro- and orthophosphate glasses that can be described as follows:

- *Ultraposphate glasses* with more than 50% of P_2O_5 with O/P ratio in 2.5-3 range. Most of the structure is composed of Q^3 and Q^2 tetrahedrons. The more dopants present in material the more of Q^2 tetrahedrons in the structure which is caused by the appearance of P-O-P bond breaking process.
- *Metaphosphate glasses* in which exactly 50% of P_2O_5 can be found. Glass matrix consists of chains and rings of Q^2 tetrahedrons. However such composition is in practice hard to obtain.
- *Polyphosphate glasses* with less than 50% of P_2O_5 in its composition. In such glasses Q^1 tetrahedrons start to appear. Degradation of phosphate matrix and chains proceeds.
- *Pyrophosphate glass* - composition of O/P ratio equal to 3.5. Dimers of Q^1 tetrahedrons connected with each other are present in material.
- *Orthophosphate glass* with O/P ratio higher than 3.5 and depolymerized structure of Q^0 tetrahedrons without bridging oxygen atoms.

REVIEW OF STRUCTURAL STUDIES ON PHOSPHATE SYSTEMS

In this review focus will be put on phosphate glasses doped with TMOs but mainly with high amount of transition metal oxides. Moreover, their structural characterization with FTIR technique will be reviewed. Influence of TMOs on material properties strongly depend on introduced structural

modifications. Knowledge about structural changes induced by addition of TMOs is therefore important.

Likelihood of phase separation in sample volume or high probability of inhomogeneities occurrence make the synthesis of TMO-doped glass problematic. This is the reason that there is relatively small number of publications concerning this type of glass systems. However, some studies about two and three component glass materials based on phosphate and borate glasses are listed and described in review below.

ZnO-P₂O₅ systems

Zinc addition to phosphate glass matrix influences properties such as glass melting temperature and chemical durability. Way of how zinc atoms impact phosphate glass structure has been a subject of many papers. Weng et al. [7] performed doping of ZnO-P₂O₅ system with ZnCl₂ to improve the chemical durability of the glass through elongation of mean phosphate chain length. FTIR studies revealed internal structure of binary ZnO-P₂O₅ glass. Results are presented in Fig. 1.

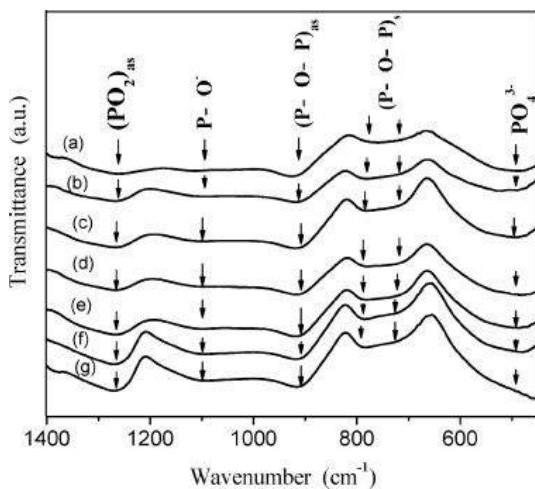


Fig. 1 FTIR spectra of the $x\text{ZnCl}_2-(50-x)\text{ZnO}-50\text{P}_2\text{O}_5$ glasses (a) $x = 0$, (b) $x = 1$, (c) $x = 3$, (d) $x = 5$, (e) $x = 10$, (f) $x = 15$, and (g) $x = 20$ mol%. Reprinted from Materials Chemistry and Physics, Volume 115, Issues 2009, Pages 628-631 with permission from Elsevier.

Main features of ZnO doped phosphate glass spectra are similar to that of materials doped with other transition metal oxides. In fact the absorption near 1240–1280 cm^{-1} assigned to the O–P–O asymmetric stretching modes is visible, furthermore at about 1100 cm^{-1} P–O– (Q₁) groups vibration mode is observable. Bands near 880–910 cm^{-1} and 740–780 cm^{-1} are due to the asymmetric and the symmetric stretching modes of the P–O–P bonds.

Fe₂O₃-P₂O₅ system

Iron oxide-phosphate glass possess wide spectrum of potential applications in sealing, laser hosts, electrolytes and nuclear waste containing materials. This glasses possess increased chemical durability compared to pure phosphate glass with low glass transition and melting points which in result leads to low cost manufacturing. Such systems are especially interesting due to their semiconducting properties and small polaron hopping conduction mechanism because of presence of iron cations in two valance states Fe²⁺ and Fe³⁺. This is the reason that some works [8,9] dealt with determination and description of Fe₂O₃ containing systems based on phosphate glass. Moustafa and others [10] performed FTIR measurements on binary Fe₂O₃-P₂O₅ glass samples. The aim of his work was to determine that there any correlation between conduction character and glass structure is visible. Results of the infrared spectroscopy measurement is presented in Fig. 2.

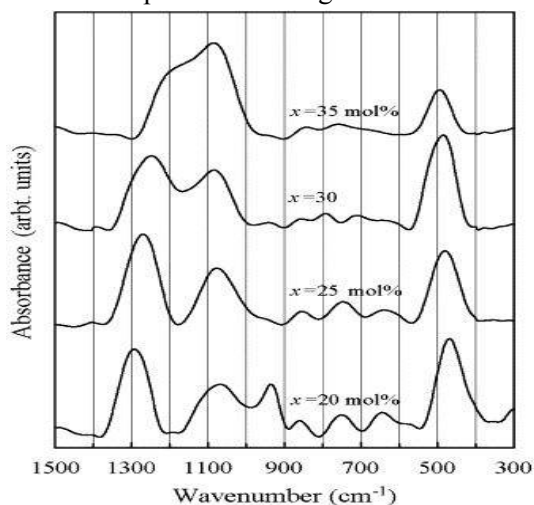


Fig. 2 FTIR spectra of xFe₂O₃-(100-x)P₂O₅ glass samples where x=20, 25, 30, 35 mol% of Fe₂O₃. Reprinted from *Physica B: Condensed Matter*, Volume 353, Issues 1–2, 2004, Pages 82-91 with permission from Elsevier.

Authors explain that spectra possess characteristic bands attributed to vibrations of various bonds in superstructural units of phosphate glass. Beginning with the band of P=O asymmetric stretching vibration at approximately 1300 cm⁻¹, then P-O(-) vibration band at about 1050 cm⁻¹. There are visible P-O-P symmetric and asymmetric stretching vibration at 860 cm⁻¹ and 750 cm⁻¹ respectively. However no Fe-O-P or Fe-O vibration band has been detected. It has been predicted that either no such bonds exist in glasses of considered compositional range, or this band has been masked by P-O-P vibration band.

BORATE GLASS STRUCTURE.

Borate glasses containing TMOs are very promising materials and possess variety of potential applications in electronic and optoelectronic devices. Employing such materials requires knowledge about their internal structure and genesis of structure related property modifications. Such modifications can be induced by, for example, doping of the borate glass with dopants such as alkali metal oxides or transition metal oxides. Glasses like silicate or phosphate glasses will change their properties in ordinary manner: viscosity will fall, melting and glass transition temperatures will drop with increasing dopant concentration. In borate glasses this is not the case. Borate glass matrix composed mainly of BO_3 so called “triangles” connected in ring-like superstructural units namely boroxol rings will react differently on same dopant level. Change of the boron coordination number is interesting phenomenon occurring in borate glass. Although in crystal phases based on boron oxide only three-coordinated boron atoms are present this is not the case in borate oxide glasses. One can find evidence of existence of three-fold and four-fold coordinated boron atoms. This is the reason that so called “borate anomaly” actually happens. Boron atoms change their coordination number in specific compositional range depending on dopant used. This process is competing with breaking of B-O-B bridges and in some compositional range it dominates. This leads to “anomalous” changes in viscosity and other physical and thermal properties comparing to behavior of other oxide glasses.

REVIEW OF BORATE SYSTEMS. STRUCTURAL STUDIES

Ag_2O doped borate glass

Interesting borate system doped with silver oxide has been a subject of a number of papers [11,12,13]. Many researchers see a potential way to increase luminescent properties in silver addition to glass matrix. One of the works [11] presented FTIR studies on $20\text{Ag}_2\text{O}-80\text{B}_2\text{O}_3$ composition. Band at 1050 cm^{-1} is observed and assigned to the vibration of BO_4 tetrahedrons. Chryssikos and Kamitsos interpretate [14] the band at 1340 cm^{-1} to the asymmetric stretching of BO_3 triangles. Intense adsorption bands at about 1050 and 930 cm^{-1} were assigned to the vibration of BO_4 groups, of the pentaborate superstructural units.

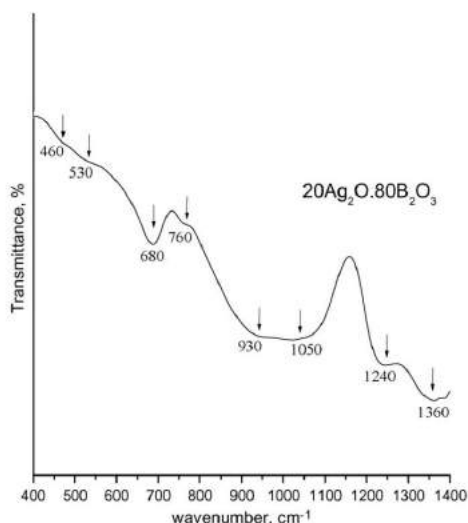


Fig. 3 IR spectrum of silver-borate glass. Reprinted from Materials Research Bulletin, Volume 43, Issue 7, 2008, Pages 1905-1910 with permission of Elsevier.

Another promising application of $\text{Ag}_2\text{O}-\text{B}_2\text{O}_3$ glass is superionic materials with relatively high conductivities at room temperatures. Superionic character of these glasses is introduced through doping it with metal halides for example AgI. This is done in work of Hudgens and Martin.[13] Authors claim through infrared studies it can be concluded that AgI addition does not change the BO_3/BO_4 ratio however this dopant causes the structure of glass to be more ordered. This can be concluded after measuring the FWHM of bands due to B-O vibrations in aforementioned superstructural units. Reduction of FWHM can be due to contraction of angle distribution in glass material.

ZnO and Fe_2O_3 doped borate glass systems

Some of the TMOs can act as a network modifier and network former depending on the metal cation coordination. One of these oxides is zinc oxide. It can exist in four-fold coordination when it is network former and in six-fold coordination when it acts as a network modifier. Such behavior opens a wide spectrum of potential glass modification strategies - and in effect, can lead to interesting final properties of obtained glass samples. Additionally aforementioned borate glass tendency to form many kinds of superstructural units that allow one to obtain different glass structures depending on composition and synthesis conditions. Recently scientific community paid more attention on such systems due to their possible applications as hosts for luminescent materials. Ehrt [15] reports that it was possible to obtain

50ZnO-50B₂O₃ homogenous composition. Glass ceramics originated from that composition shown good luminescent properties. Knowledge about internal structure of such systems can be obtained with help of infrared spectroscopy. There are some works that were dedicated to characterize structure modifications in function of dopant concentration. Pascuta et al. [16] worked on ZnO-Fe₂O₃-B₂O₃ glass system.

First of all FTIR spectra of Fe₂O₃-B₂O₃-ZnO system possess characteristic band at 680-685 cm⁻¹ corresponding to the band due to B–O–B bending vibrations. Authors observed it shifts to lower wavenumbers with increasing content of Fe₂O₃ which is probably due structure modification and breaking of B-O-B bridges. Bands of B-O bonds stretching vibrations in BO₄ superstructural units from diborate (875 cm⁻¹) and other groups (about 1000 cm⁻¹) were also detected. Additionally boron-oxygen bond vibrations in various BO₃ based units were observed at 1400cm⁻¹. Moreover, evidence for crystalline phase namely ZnFe₂O₄ has been detected.

SYNTHESIS OF BINARY MnO-P₂O₅ AND MnO-B₂O₃ glass samples.

This work was focused on binary manganese-phosphate and manganese-borate glass synthesis. Authors are not aware of any previous works dealing with glasses containing more than 60 mol% of MnO.

Experimental

To achieve that samples containing 40, 50 and 60 mol % of MnO have been prepared. Such compositions were acquired by mixing (NH₄)₂HPO₄ and MnO powders in correct proportions. In case of borate glass H₃BO₃ was used. Ingredients were crushed until fine grain size has been achieved. Samples were melted in porcelain crucibles at approximately 1000 °C. Glass samples were kept at this temperature for 20 minutes. Whole process took place in atmospheric conditions. Afterwards, glasses were quenched on preheated metal plate by melt-quenching technique.

Characterization methods

Fourier Transform Infrared measurements were performed on Perkin-Elmer Frontier MIR/FIR spectrometer. Crushed glass material has been mixed in agate mortar with spectroscopic KBr to acquire 2% concentration of glass in every sample. Each one weighed approximately 200 mg. Glass-potassium bromide pellets have been pressed on hand-press to obtain almost transparent pallets. The spectra were taken in the range of 550-4000 cm⁻¹ with a 2 cm⁻¹ resolution. Differential Scanning Calorimetry measurements has been performed

on Netzsch STA 449F1. Fine crushed 5 mg samples were heated in Pt/Rh crucibles with heating rate of 15 °C/min to 1100°C in argon atmosphere.

CHARACTERIZATION OF MnO-P₂O₅ SYSTEM

Fourier Transform Infrared results

Spectra are presented in Fig. 4. Firstly, O-P-O vibration band at approximately 575 cm⁻¹ is present. Then band of P-O-P symmetrical stretching vibration is visible. Asymmetric stretching vibration of P-O-P can be observed at 910 cm⁻¹. Further, one can find (PO₃)²⁻ (PO₄)³⁻ and (PO₂)⁻ stretching vibrations bands. Finally band of P=O asymmetric stretching is observable.[17] Detailed results are presented in Tab. 1. With increase of MnO concentration O-P-O bending and P-O-P stretching bands centers are shifting to higher wavenumbers. This phenomenon may be due to manganese atoms influence on these bonds like band shortening or weakening. Similarly, observable shift of P=O stretching band towards lower wavenumbers is probably caused by weakening of these bonds caused by Mn atoms influence. No band attributed to vibration of Mn-O bonds has been detected. However shifts of phosphate related bands point out that some influence of Mn atoms on glass structure actually exist. Manganese atoms act destructively on connectivity of phosphate glass matrix creating more Q₀ units in place of other units. This should happen due to high amount of MnO added to phosphate glass samples.

Table 1 Manganese-phosphate absorption bands positions [17]

Vibration	60MnO-40P ₂ O ₅ 50MnO-50P ₂ O ₅ 40MnO-60P ₂ O ₅		
	C [cm ⁻¹]		
O-P-O bending vibration	576	573	571
P-O-P symmetric str. vibration	748	732	737
		790	788
P-O-P asym.str.vibration	913	904	911
P-O- in Q1 str. vibration	-	988	992
P-O- in Q0 str. vibration	1081	1088	1082
P-O- in Q2 str. vibration	-	-	1156
P=O stretching band	1252	1275	1276

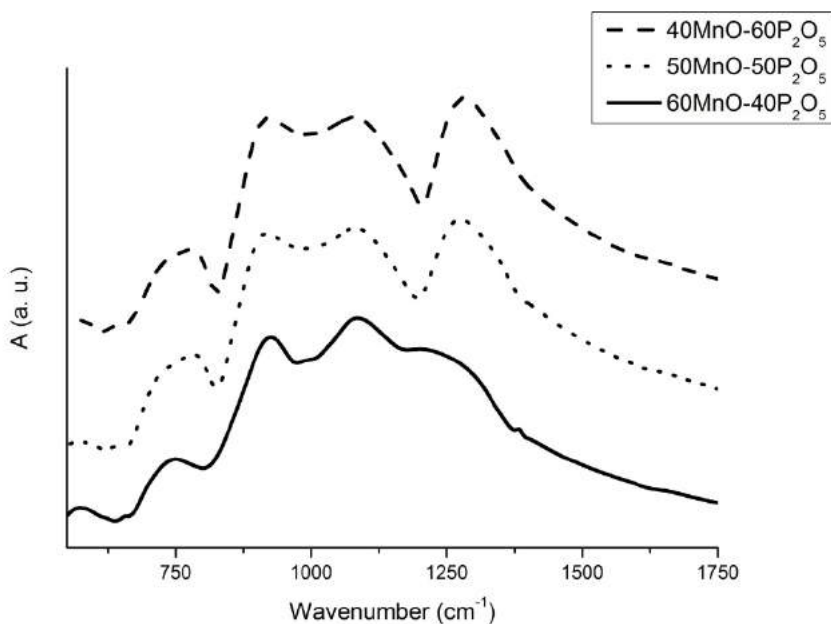


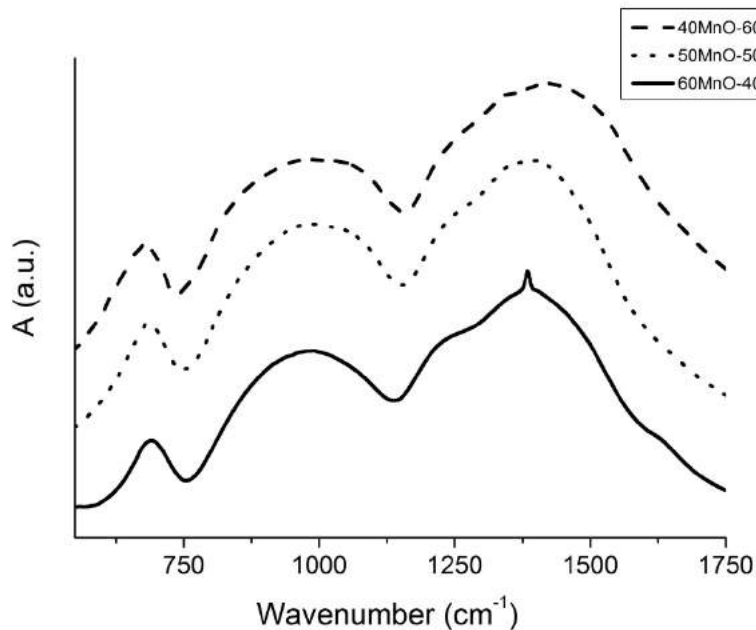
Fig. 4 FTIR spectra of phosphate glasses

CHARACTERIZATION OF MnO-B₂O₃ SYSTEM

Measurement procedure described above has been also performed in case of MnO-B₂O₃ glass samples. Some changes in spectra are visible with increasing MnO content. FTIR spectra of binary manganese-borate glasses possess three main bands. Beginning with low wavenumber values, narrow band at approximately 680 cm⁻¹ is observable. It is due to stretching vibrations of B-O-B bonds. Band in 730-1100 cm⁻¹ range is attributed to stretching of B-O bonds in BO₄ tetrahedrons from various borate groups. Additionally band at 1200-1500 cm⁻¹ range is due to B-O bond stretching in BO₃ triangle like elements in borate groups. Shift of B-O-B bending and BO₄ stretching modes to higher wavenumber values can be due shortening of this bands [18].

Table 2 Manganese-borate absorption bands positions [18]

Vibration	60MnO-40B ₂ O ₃	50MnO-50B ₂ O ₃	40MnO-60B ₂ O ₃
	C [cm ⁻¹]	C [cm ⁻¹]	C [cm ⁻¹]
B-O-B bending	686	675	665
B-O stretching in BO ₄ in diborate groups	895	879	866
B-O stretching in BO ₄ of tri tetra- and pentaborate groups	1045	1041	1039
B-O stretching in BO ₃ of orthoborate groups	1219	1230	1249
B-O stretching in BO ₃ form other borate groups	1382	1389	1423

**Fig. 5** Manganese-borate glass FTIR spectra**DSC results**

On the basis of DSC spectra it can be noticed that the same addition of MnO leads to different change in thermal parameters in phosphate and borate glass matrices. In case of phosphate glass as presented in Fig. 6 glass transition

temperature shifts to lower temperature values. On the other hand T_g increases in case of 60MnO-40P₂O₅ composition is achieved. It is also clearly visible that drastic drop of thermal stability parameter takes place when 60 mol% of MnO is achieved. On the other hand increase of TS parameter is observable between 40 mol% and 50 mol% of MnO in sample. In case of borate glass samples (Fig. 7) glass transition temperature and thermal stability parameter decrease with increasing amount of MnO in glass matrix. Thermal stability has been calculated according to equation [19]:

$$TS = T_{conset} - T_g \quad (1)$$

where T_{conset} is the onset of first crystallization peak and T_g is glass transition temperature.

Table 3 Thermal parameters of manganese-phosphate glass samples

Compositions	T_g [°C]	T_c [°C]	TS [°C]
60MnO-40P ₂ O ₅	510	607	79
50MnO-50P ₂ O ₅	492	825	286
40MnO-60P ₂ O ₅	494	805	262

Table 4 Thermal properties of manganese-borate glass samples

Compositions	T_g [°C]	T_{cl} [°C]	TS [°C]
60MnO-40B ₂ O ₃	543	668	112
50MnO-50B ₂ O ₃	556	696	129
40MnO-60B ₂ O ₃	564	741	130

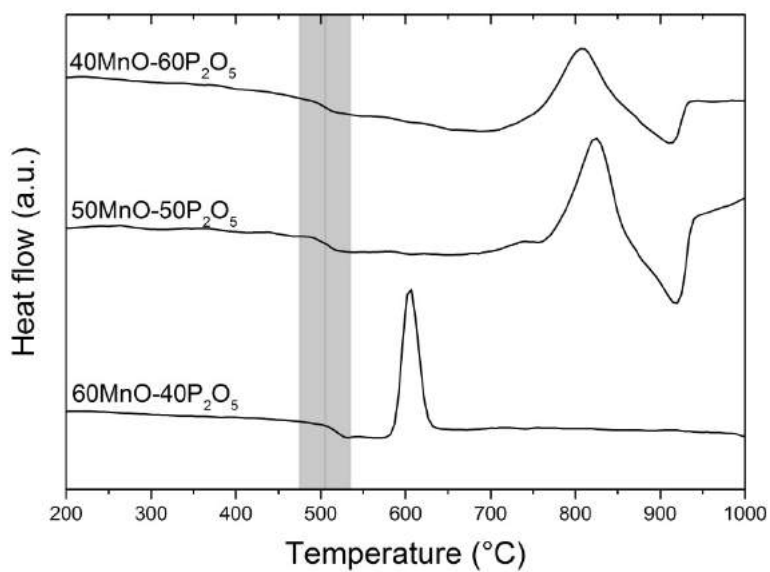


Fig. 6 DSC spectra of manganese-phosphate glass samples

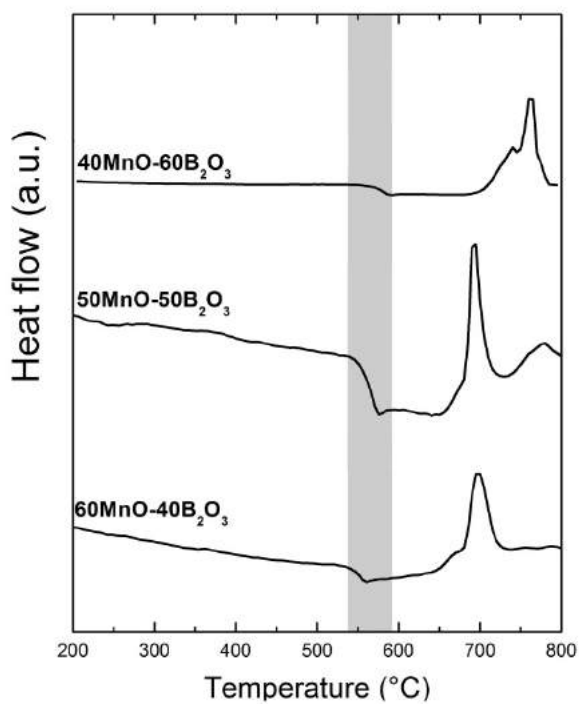


Fig. 7 DSC spectra of manganese-borate glass samples

DISCUSSION

Review of FTIR spectroscopy studies on phosphate and borate glass materials doped with transition metal oxides has been presented. It can be concluded that FTIR spectroscopy is useful tool in characterization of amorphous material structure changes. It is possible to measure quantitatively and qualitatively changes of position of the bands and band intensities. With a correct structural model of considered glass one can conclude about bond length and strength changes induced by dopant.

Review presented in this work shown that phosphate and borate glasses possess characteristic IR absorption bands. This is in fact useful for material identification. Bands due to bending and stretching of various bonds such as O-P-O and P-O-P and P=O bonds occurred. Similarly, borate glass FTIR spectra possess specific features characteristic for this material.

Structural modifications caused by TMOs such as zinc, iron and manganese are similar. Addition of these oxides leads to gradual destruction of P-O-P and B-O-B bonds. Additionally transition metal influence can lead to shifts of absorption bands. Finally, at some point some of TMO's are able to form its own amorphous phase and create TM-O (Transition Metal-Oxygen) bonds which can be detected with infrared spectroscopy technique.

Concluding on the basis of performed FTIR measurements manganese oxide addition to phosphate and borate glasses led to change of absorption bands positions. In case of borate glass it is possible that Mn-O bonds exists but band due vibration of that bond can be masked by other bands (B-O-B bond vibration band). This shifts can be due shortening of P-O and B-O bonds in glass matrix. One can notice that borate glass absorption bands width decrease with increasing amount of MnO which can indicate decrease in bond angle distribution. No such behavior is clearly visible in case of phosphate glass samples spectra.

DSC measurements shown different influence on thermal stability of glasses. In case of borate glass samples one can notice stable shift of T_g to lower temperature values. Same trend is observable for thermal stability parameter. Situation for phosphate glass samples is different. First, with increase of MnO content one can observe decrease of T_g and TS, however the highest T_g and lowest TS values are achieved for 60MnO-40P₂O₅ composition. This may be due structure degradation or appearance of Mn containing amorphous phase.

REFERENCES

[1] Elisa, M., Sava, B. a., Vasiliu, I. C., Monteiro, R. C. C., Veiga, J. P., Ghervase, L., ... Iordanescu, R. (2013). Optical and structural characterization of samarium and europium-doped phosphate glasses. *Journal of Non-Crystalline Solids*, 369, 55–60. doi:10.1016/j.jnoncrysol.2013.03.024

- [2] Baccaro, S., Catallo, N., Cemmi, a., & Sharma, G. (2011). Radiation damage of alkali borate glasses for application in safe nuclear waste disposal. *Nuclear Instruments and Methods in Physics Research, Section B: Beam Interactions with Materials and Atoms*, 269(2), 167–173. doi:10.1016/j.nimb.2010.10.019
- [3] Sengupta, P. (2012). A review on immobilization of phosphate containing high level nuclear wastes within glass matrix - Present status and future challenges. *Journal of Hazardous Materials*, 235-236, 17–28. doi:10.1016/j.jhazmat.2012.07.039
- [4] Boccolini, a., Marques-Hueso, J., Chen, D., Wang, Y., & Richards, B. S. (2014). Physical performance limitations of luminescent down-conversion layers for photovoltaic applications. *Solar Energy Materials and Solar Cells*, 122, 8–14. doi:10.1016/j.solmat.2013.11.005
- [5] Kim, J. E., Park, S. B., & Park, Y. Il. (2012). Proton-conducting zirconium phosphate glass thin films. *Solid State Ionics*, 216, 15–18. doi:10.1016/j.ssi.2011.12.004
- [6] Ishiyama, T., Suzuki, S., Nishii, J., Yamashita, T., Kawazoe, H., & Omata, T. (2014). Proton conducting tungsten phosphate glass and its application in intermediate temperature fuel cells. *Solid State Ionics*, 262, 856–859. doi:10.1016/j.ssi.2013.10.055
- [7] Weng, C. Z., Chen, J. H., & Shih, P. Y. (2009). Effect of dehydroxylation on the structure and properties of ZnCl₂-ZnO-P₂O₅ glasses. *Materials Chemistry and Physics*, 115, 628–631. doi:10.1016/j.matchemphys.2009.01.022
- [8] Doweidar, H., Moustafa, Y. M., El-Egili, K., & Abbas, I. (2005). Infrared spectra of Fe₂O₃-PbO-P₂O₅ glasses. *Vibrational Spectroscopy*, 37, 91–96. doi:10.1016/j.vibspec.2004.07.002
- [9] Moguš-Milanković, a, Šantić, a, Gajović, a, & Day, D. . (2003). Spectroscopic investigation of MoO₃-Fe₂O₃-P₂O₅ and SrO-Fe₂O₃-P₂O₅ glasses. Part I. *Journal of Non-Crystalline Solids*, 325, 76–84. doi:10.1016/S0022-3093(03)00362-4
- [10] Moustafa, Y. M., El-Egili, K., Doweidar, H., & Abbas, I. (2004). Structure and electric conduction of Fe₂O₃-P₂O₅ glasses. *Physica B: Condensed Matter*, 353, 82–91. doi:10.1016/j.physb.2004.09.004
- [11] Dimitriev, Y., Bachvarova-Nedelcheva, A., & Iordanova, R. (2008). Glass formation tendency in the system SeO₂-Ag₂O-B₂O₃. *Materials Research Bulletin*, 43, 1905–1910. doi:10.1016/j.materresbull.2007.06.054
- [12] Belharouak, I., Weill, F., Parent, C., Le Flem, G., & Moine, B. (2001). Silver particles in glasses of the “Ag₂O-ZnO-P₂O₅” system. *Journal of Non-Crystalline Solids*, 293-295, 649–656. doi:10.1016/S0022-3093(01)00843-2

- [13] Foltyn, M., Wasiucioneck, M., Garbarczyk, J., & Nowiński, J. L. (2005). Effect of nanocrystallization on electrical conductivity of glasses and composites of the AgI-Ag₂O-B₂O₃ system. *Solid State Ionics*, 176, 2137–2140. doi:10.1016/j.ssi.2004.08.049
- [14] Chryssikos, G. I. Kamitsos A. Wright, S. Feller, C. Hannon (Eds.), Proceedings of the Second International Conference on Borate Glasses Crystals and Melts, Society of Glass Technology, Sheffield, UK (1997)
- [15] Ehrt, D., Jena, F., & Jena, F. D.-. (2013). Zinc and manganese borate glasses – phase separation , crystallisation , photoluminescence and structure, 54(2), 65–75.
- [16] Pascuta, P., Bosca, M., Borodi, G., & Culea, E. (2011). Thermal, structural and magnetic properties of some zinc phosphate glasses doped with manganese ions. *Journal of Alloys and Compounds*, 509(11), 4314–4319. doi:10.1016/j.jallcom.2011.01.056
- [17] Pascuta, P., Borodi, G., Jumate, N., Vida-Simiti, I., Viorel, D., & Culea, E. (2010). The structural role of manganese ions in some zinc phosphate glasses and glass ceramics. *Journal of Alloys and Compounds*, 504(2), 479–483. doi:10.1016/j.jallcom.2010.05.147
- [18] Ardelean, I., Cora, S., Ciceo Lucacel, R., & Hulpus, O. (2005). EPR and FT-IR spectroscopic studies of B₂O₃Bi₂O₃MnO glasses. *Solid State Sciences*, 7, 1438–1442. doi:10.1016/j.solidstatesciences.2005.08.017
- [19] A. Dietzel *Glasstech. Berl.*, 22 (1968), p. 41

Parameters of epoxidation of vegetable oils in the presence of acidic ion-exchange resins

*Kornelia Malarczyk, Eugeniusz Milchert

Faculty of Chemical Technology and Engineering, West Pomeranian University of Technology in Szczecin

e-mail: kornelia.malarczyk@zut.edu.pl

Key words: epoxidation, epoxidation of vegetable oils, *acidic ion exchange resins*, review

ABSTRACT

The paper gives a survey of literature on the processes of epoxidation of vegetable oils by peroxyacids in the presence of acidic ion exchange resins as catalysts. The impact of the type of carboxyl acid, temperature, rate of stirring, amount of catalyst and molar ratios of acetic acid/unsaturated bond and hydrogen peroxide/unsaturated bond on the relative percentage of conversion to oxirane and iodine number, is discussed. The optimum parameters of the processes are given.

INTRODUCTION

Vegetable oils are water-insoluble, hydrophobic substances of plant origin that are made up of one mole of glycerol and three moles of fatty acids and are commonly referred to as triacylglycerols [1]. The fatty acids are monocarboxylic acids of the chain hydrocarbon made of a different number of carbon atoms from 4 to more than 30. The chemical formula of an exemplary triacylglycerol is presented in Fig. 1.

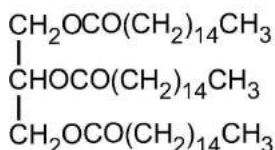


Fig. 1 Glycerol tripalmitate

Vegetable oils contain mainly fatty acids with 16, 18 and 20 carbon atoms. The composition of fatty acids depends on many factors, but mainly on the species and variety of the source plant. Fatty acids are described by a proportion of the number of carbon atoms to the number of double bonds, e.g. the notation 20:0 means that the acid contains 20 carbon atoms and it lacks double bonds, while 20:1 described the acid with 20 carbon atoms and one

double bond [2]. The composition of fatty acids in selected vegetable oils is given in Table 1.

Table 1 The composition of fatty acids (wt. %) in selected vegetable oils [3,4]

Fatty acid	A ^a B ^b	Acid content [wt.%]			
		Rapeseed oil	Palm oil	Sunflower oil	Soybean oil
Myristic	14:0	trace amounts	0 - 2	trace amounts	trace amounts
Palmitic	16:0	2 - 6	36 - 48	3 - 10	7 - 20
Palmitoleic	16:1	0 - 1	-	0 - 1	trace amounts
Stearic	18:0	1 - 3	3 - 6	1 - 10	3 - 6
Oleic	18:1	50 - 66	38 - 44	20 - 40	22 - 34
Linoleic	18:2	18 - 30	9 - 12	50 - 70	48 - 58
Linolenic	18:3	6 - 12	-	0 - 1	4 - 10
Arachidic	20:0	0 - 3	0 - 1	0 - 1	0 - 3
Gadoleic	20:1	0 - 4	-	trace amounts	0 - 1
Erucic	22:1	0 - 5	-	trace amounts	-

^a Number of carbon atoms

^b Number of unsaturated bonds

Vegetable oils contain other components besides esters of glycerol fatty acids. Triacylglycerols make 98-99% of the content of commercially available rapeseed oil, the other components are the so-called unsaponifiables, among them biologically active compounds, phenol compounds, sterols and tocopherols [5]. Vegetable oils are rather chemically inactive. In order to be used for the production of e.g. polymers, they must be endowed with functional groups. One of the modification methods of fatty acid triglycerides is the epoxidation process in which epoxy groups are formed. Recently, much progress has been made in the methods of conversion of unsaturated bonds in triacylglycerols to epoxide functional groups. As the criterion for assessing the technological parameters is the degree of conversion of unsaturated bonds calculated on the basis of the iodine numbers and the degree of relative conversion to oxirane according to the equation:

$$RCO = O_{ex}/O_{th}$$

where:

O_{ex} – experimentally determined content of oxirane oxygen (%/100g of oil),

O_{th} – theoretical content of oxirane oxygen (%/100g of oil).

$$O_{th} = (IV_o/2A_i)/[100 + (IV_o/2A_i)A_o] \times A_o \times 100,$$

IV_o – the iodine number before epoxidation (g/100g of oil),
 A_o and A_i – atomic masses of oxygen and iodine.

APPLICATION OF EPOXIDIZED VEGETABLE OILS

A general aim of new technologies is to obtain epoxidized vegetable oils of the highest possible content of epoxide groups, which is equivalent to obtaining products of the lowest possible number of unsaturated bonds. The compounds containing a low number of unsaturated bonds show higher quality and are valuable substrates for industrial applications [6]. They are used as plastifiers and stabilisers of plastics, e.g. polyvinyl chloride. Their increasing application in the production of polyurethanes, surfactants, resins and glues, lubricants and paints has been observed [7-10]. Thanks to the high reactivity of the oxirane ring, they can be used in the production of e.g. alcohols, glycols, polyols, glycol monoesters and diesters and carbonyl compounds [6,11].

METHODS AND MECHANISMS OF VEGETABLE OIL EPOXIDATION

Epoxidation of vegetable oils can be carried out by the conventional methods, chemical-enzymatic methods, the processes with employment of acidic ion-exchange resins and those with the use of high valence metals [12-14,6].

Of industrial significance is the process performed with the use of peroxycarboxylic acid, which is either introduced into the reaction system or is generated *in situ* in the reaction medium. In the process of epoxidation with the use of peroxyacids obtained *in situ*, two reactions run simultaneously: generation of peroxyacid (1) and its use in the epoxidation (2), in the reaction with the unsaturated bond of the oil (Fig. 2).

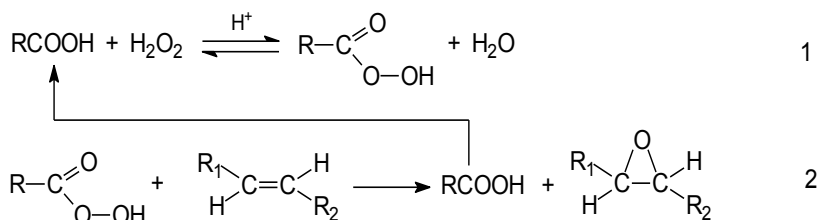


Fig. 2 Reaction of epoxidation with peroxyacids

In industrial processes, peroxycarboxylic acid is obtained in the reaction of acetic acid or formic acid with hydrogen peroxide, in the presence of a strong mineral acid, usually sulphuric(VI) acid. Other catalysts, although less effective, used in the process of obtaining peroxycarboxylic acids are nitrogen(V) acid, orthophosphoric(V) acid and hydrochloric acid [15,16]. The use of a strong mineral acid enhances the rate of peroxyacid formation, which hinders its decomposition and permits production of epoxidized oil in high yields. On the

other hand, the use of mineral acid limits the selectivity and intensifies the side reaction of the epoxy ring opening. Finally it leads to reduced selectivity and conversion of epoxy-compounds and formation of glycols and hydroxyacylic compounds.

EPOXIDATION OF VEGETABLE OILS IN THE PRESENCE OF ACIDIC ION EXCHANGE RESINS AS CATALYSTS

The use of the resins makes the process more friendly for the environment because of much easier separation of the catalyst and carboxylic acid. Besides, their use permits achievement of higher (than when using mineral acids) selectivity of transformation to the epoxy-compound by decreasing the rate of oxirane ring opening, mainly to glycols and glycol monoesters. The epoxidation of vegetable oils in the presence of the resins can be performed in benzene, toluene, hexane or heptane as a solvent, used in the amount of about 20 wt % relative to oil. The catalysts are acidic ion exchange resins, mainly Amberlite IR-120, Amberlite IR-122, Amberlyst - 15 and Dowex 50Wx2 [12-14,17-20]. They are introduced in the form of granules. The resin matrix contains acidic functional groups. Chemically, the resins are sulphonated copolymers of styrene and divinylbenzene, differing in the content of the cross-linking agent, acidity and form (Fig. 3).

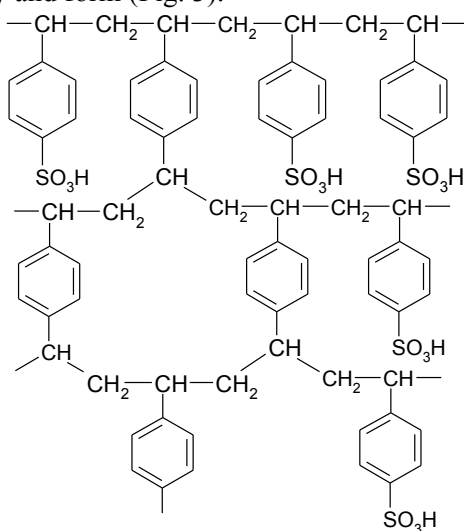


Fig. 3 Structure of ion-exchange resins used in the process of vegetable oil epoxidation.

Physicochemical properties of selected ion exchange resins used for epoxidation of vegetable oils are characterised in Table 2.

Table 2 Physicochemical properties of acidic resins [20]

Type of ion exchange resin	Composition	Acidity (meq H ⁺ /g)	Surface area (m ² /g)	Pore size (nm)
Amberlyst 15	Copolymer styrene + 20% divinylbenzene	4,72	51	40-80
Amberlite IR-120	Copolymer styrene + 8% divinylbenzene	4,5	Non measurable	Non measurable
Dowex 50Wx2	Copolymer styrene + 2% divinylbenzene	4,3	Non measurable	Non measurable

The character of the process of vegetable oil epoxidation depends on temperature, rate of stirring, type and amount of the catalyst used and the molar ratios of carboxylic acid/ unsaturated bond and hydrogen peroxide/ unsaturated bond. The type of carboxylic acid use is also important. Meshram et al. [14] have proved that it is more effective to use acetic acid than formic acid for production of epoxidized saffron oil. After eight hours of the process in the same conditions, the conversion to oxirane was by 20% higher when acetic acid was used than with formic acid. Acetic acid was also a more effective oxygen carrier than formic acid in the process of epoxidation of rapeseed oil. Mungroo et al. [6] have reported by about 10% higher relative conversion of double bonds to oxirane when carrying out epoxidation of rapeseed oil with the use of peroxyacetic acid than with formic acid. The use of peroxyacetic acid is also more economically beneficial because of lower cost of recovery of acetic than formic acid. The problem are the close boiling points of formic acid and water, which hinder the separation by distillation. Moreover, work with formic acid is hazardous as it can decompose by explosion, especially above the concentration of 50% wt. According to the kinetic measurements, the reaction with acetic acid are slower than those with formic acid [21].

According to literature, the molar ratio of carboxylic acid to double bond varies from 0.2 to 1 mol. Carboxylic acid acts as a carrier of oxygen and is recovered after the reaction. Unfortunately, it can cause the opening of epoxy ring. It has been shown that too low amount of carboxylic acid slows down the reaction, while its too high amount decreases the selectivity of conversion to epoxide. Therefore, an optimum level of carboxylic acid is desired to speed up the conversion to oxirane ring with minimal epoxy ring breaking [14]. The optimum molar ratio of carboxylic acid to double bond generally recommended is 0.5 : 1. [6,18,19,21-24].

The type of vegetable oils subjected to epoxidation is essential for the outcome of the process. A comparison of the epoxidation processes of different

oils has been made by e.g.. Kim & Sharma [25]. They used the acidic ion exchange resin Amberlite IR-120 as a catalyst and in the same conditions performed epoxidation of the following oils: cotton, canola, linseed, coconut, soybean oil and radish seed oil. A carefully weighted portion of oil was placed in a flask with acetic acid and a catalyst in the amount of 25 wt % with respect to oil. The mixture was stirred for 5 hours at 60°C and then a 30% solution of hydrogen peroxide was dosed in drops. In total, 1 mole of CH₃COOH and 2 moles of H₂O₂ were introduced per one double bond in the oil. After some time, the reaction mixture was filtered off. The organic layer was washed with a solution of sodium carbonate and dried on anhydrous magnesium sulphate. When applying oils with fatty acids of a large number of unsaturated bonds, the epoxidized product was obtained with high selectivity, the products were characterised by the highest content of epoxide groups (the highest epoxide number) and the hydroxyl number higher than obtained when using oils of a lower iodine number. The best results were obtained for linseed oil, which contains over 50% of α -linolenic acid whose molecule has 3 unsaturated bonds.

An important parameter influencing the course of epoxidation is temperature. The effect of this parameter has been usually studied in the range from about 30 to 70 or 90°C [16,23,26]. The optimum temperature is recommended to be 65-70°C, as in this temperature range a minimum degradation of epoxy rings and good stability of resins were observed. A smaller number of epoxide groups formation above this range of temperatures can follow from two reasons. Firstly, an increase in the temperature has increased the rate of oxirane hydrolysis to α -glycol. Secondly, at high temperatures the catalyst might have lost its functionality [18].

An interesting method for the epoxidation of linseed oil and soybean oil is based on the use of a thin-film reactor. The process is run with the *in situ* obtained acetic or formic peroxyacids. In the continuous process, the reaction takes place in a thin layer kept on the heated surface of the reactor. Water is distilled off and the product is collected at the bottom of the reactor. By changing the flow rate of the substrates or the molar ratio of hydrogen peroxide to oil, it is possible to regulate the degree of epoxidation. The process was the fastest at the thin film temperature from the range 38-55°C under pressure of 25 - 400 mm Hg [27].

In general, with increasing amount of the catalyst, the epoxidation rate increases, which is related to the increasing number of active groups and increasing total area of the catalyst. The recommended optimum amount of ion exchange resin in the processes of epoxidation of vegetable oils is 15 - 22 wt% with respect to oil, depending on the substrates used (mainly the type of oil) and

on the other parameters of the process. Above this content the stability of the epoxide ring decreased [13,14,18].

The ion exchange resins used as catalysts in the vegetable oils epoxidation can be used more than once. After the reaction, the resin is separated from the post-reaction mixture through filtration, washed with water and diethyl ether and dried at first at the ambient temperature and then at 100°C to remove moisture. This procedure permits the use of the same portion of the catalyst for four times, but the catalyst activity gradually decreases [18]. According to literature data, the hydrogen peroxide solutions in the processes of epoxidation of vegetable oils have concentrations of 30%, 35% or rarely, 50%. The molar ratio of hydrogen peroxide to the double bond number should be at least 1:1, while the optimum ratio for the majority of oils is 1.5:1 [6,18,19,21,23,24]. The effect of the rate of stirring was performed changing this parameter in the range 500 - 2500 rpm. For the epoxidation of mahua oil, the optimum stirring speed was 2500 rpm, for the epoxidation of karanja oil, the optimum stirring speed was 1500 rpm, while for cottonseed oil the optimum stirring speed was 1800 rpm [16,18,26].

CONCLUSIONS

Analysis of the above presented data taken from the survey of literature in the field has illustrated the benefits of applying peroxyacetic acid and strongly acidic ion exchange resins in the process of epoxidation of vegetable oils. The optimum conditions of epoxidation depend on the type of oil and technological parameters used. Therefore, for each type of oil and for each method the studies must be performed to establish the optimum parameters of the process.

REFERENCES

1. Ma F., Hanna M. A., Biodiesel production: a review, *Bioresource Technology*, 1999, 70, 1, 1-15
DOI: 10.1016/S0960-8524(99)00025-5
2. Żak I., Szoltysek-Boldys I., Chapter in the book: Kwasy tłuszczowe i ikozanoidy, *Chemia medyczna*, Śląska Akademia Medyczna, 2001
3. Walisiewicz-Niedbalska W., Kijeński J., Lipkowski A. W., Różycki K. Postępy w rozwoju badań nad otrzymywaniem biodiesla. *Przemysł Chemiczny*, 2006, 85, 12, 1586-1591
4. Chowdhury K., Banu L. A., Khan S., Latif A. Studies on the Fatty Acid Composition of Edible Oil. *Bangladesh, Journal of Scientific and Industrial Research* 2007, 42, 3, 311-316
5. Żbikowska A., Oleiste dobro narodowe, *Przegląd gastronomiczny*, 2010, 3, 10-11

6. Mungroo R., Pradhan N. C., Goud V. V., Dalai A. K., Epoxidation of canola oil with hydrogen peroxide catalyzed by acidic ion exchange resin, *Journal of the American Oil Chemists' Society*, 2008, 85, 9, 887-896
DOI: 10.1007/s11746-008-1277-z
7. Monteavaro L. L., Da Silva E. O., Costa A. P. O., Samios D., Gerbase A. E., Petzhold C. L., Polyurethane networks from formiated soy polyols: synthesis and mechanical characterization, *Journal of the American Oil Chemists' Society* 2005 82, 5, 365-371.
DOI: 10.1007/s11746-005-1079-0
8. Burkart K., Guth J., Letzelter T., Schweinzer J., Strzel H. J., Pat. Preparation of orthoesters, US 6281392, 1999
9. Penczek P., Abramowicz D., Rokicki G., Ostrysz R., Nienasycone żywice poliestrowe modyfikowane olejem roślinnym i dicyklopentadienem, *Polimery*, 2004, 49, 11-12, 767-773.
10. Viček T., Petrović Z. S., Optimization of the Chemoenzymatic Epoxidation of Soybean Oil, *Journal of the American Oil Chemists' Society*, 2006, 83, 3, 247-252
DOI: 10.1007/s11746-006-1200-4
11. Chlebicki J., Matyschok H., Synteza i epoksydowanie estrów etylowych nienasyconych kwasów tłuszczowych oraz ich wykorzystanie w produkcji związków powierzchniowo czynnych, *Przemysł Chemiczny*, 2005, 84, 12, 933-938
12. Malarczyk K., Milchert E., Kłos M., Vegetable oils epoxidation methods, *Dokonania Młodych Naukowców*, 2014, 3, 4, 114-116
13. Goud V. V., Patwardhan A. V., Dinda S., Pradhan N. C. Epoxidation of karanja (*Pongamia glabra*) oil catalysed by acidic ion exchange resin, *European Journal of Lipid Science and Technology*, 2007, 109, 6, 575-584
DOI: 10.1002/ejlt.200600298
14. Meshram P. D., Puri R. G., Patil H. V., Epoxidation of Wild Safflower (*Carthamus oxyacantha*) Oil with Peroxy acid in presence of strongly Acidic Cation Exchange Resin IR- 122 as Catalyst, *International Journal of ChemTech Research*, 2011, 3, 3, 1152-1163
15. Dinda S., Patwardhan A. V., Goud V. V., Pradhan N. C., Epoxidation of cottonseed oil by aqueous hydrogen peroxide catalysed by liquid inorganic acids *Bioresource Technology* 2008, 99, 9, 3737-3744
DOI: 10.1016/j.biortech.2007.07.015
16. Goud V. V., Patwardhan A. V., Pradhan N. C., Studies on the Epoxidation of Mahua Oil (*Modhumica Indica*) by Hydrogen Peroxide, *Bioresource Technology* 2006, 97, 12, 1365-1371
DOI: 10.1016/j.biortech.2005.07.004

17. Fiszer S., Szałajko U., Szeja W., Niemiec P. Epoksydowane oleje roślinne jako środki smarowe, *Przemysł Chemiczny*, 2003, 82, 8-9, 1016-1019
18. Dinda S., Goud V. V., Patwardhan A. V., Pradhan N. C. Selective epoxidation of natural triglycerides using acidic ion exchange resin as catalyst, *Asia-Pacific Journal Of Chemical Engineering*, 2011, 6, 6, 870-878
DOI:10.1002/apj.466
19. Sinadinovic-Fiser S., Jankovic M., Petrovic Z. S. Kinetics of *in situ* Epoxidation of Soybean Oil in Bulk Catalyzed by Ion Exchange Resin, *Journal of the American Oil Chemists' Society*, 2001, 78, 7, 725-731
DOI: 10.1007/s11746-001-0333-9
20. Rios L. A., Echeverri D. A., Franco A. Epoxidation of jatropfa oil using heterogeneous catalysts suitable for the Prileschajew reaction: Acidic resins and immobilized lipase. *Applied Catalysis A: General*, 2011, 394, 1-2, 132-137
DOI:10.1016/j.apcata.2010.12.033
21. Goud V. V., Patwardhan A. V., Dinda S., Pradhan N. C., Kinetics of epoxidation of jatropha oil with peroxyacetic and peroxyformic acid catalysed by acidic ion exchange resin, *Chemical Engineering Science*, 2007, 62, 15, 4065-4076
DOI: 10.1016/j.ces.2007.04.038
22. Sinadinović-Fišer S., Janković M., Borota O., Epoxidation of castor oil with peracetic acid formed *in situ* in the present of an ion exchange resin, *Chemical Engineering and Processing* 2012, 62, 106-113
DOI: 10.1016/j.cep.2012.08.005
23. Petrović Z. S., Zlatanić A., Lava Ch. C., Sinadinović-Fišer S., Epoxidation of soybean oil in toluene with peroxyacetic and peroxyformic acids — kinetics and side reactions, *European Journal of Lipid Science and Technology*, 2002, 104, 5, 293-299
DOI: 10.1002/1438-9312(200205)104:5<293::AID-EJLT293>3.0.CO;2-W
24. Metzger J. O., Bornscheuer U., Lipids as renewable resources: current state of chemical and biotechnological conversion and diversification, *Applied Microbiology and Biotechnology*, 2006, 71, 1, 13-22
DOI 10.1007/s00253-006-0335-4
25. Kim. J. R., Sharma S., The development and comparison of bio-thermoset plastics from epoxidized plant oils, *Industrial Crops and Products*, 2012, 36, 1, 485-499
DOI: 10.1016/j.indcrop.2011.10.036

26. Goud V. V., Patwardhan A. V., Pradhan N. C., Kinetics of in situ Epoxidation of Natural Unsaturated Triglycerides Catalyzed by Acidic Ion Exchange Resin, *Industrial & Engineering Chemistry Research*, 2007, 46, 10, 3078-3085

DOI: 10.1021/ie060146s

27. Nowak J. A., Zillner T. A., Mullin L. P., Pat. Oxidation with hydrogen peroxide, acetaldehyde monoperoxide, or organic hydroperoxide; cyclization, etherification, US 6734315 B1, 2004

Natural monoterpenes: their chemical properties and applications on the example of limonene

*Mariusz Władysław Malko, Agnieszka Wróblewska, Marika Walasek
Institute of Organic Chemical Technology, Faculty of Chemical Technology and Engineering, West Pomeranian University of Technology, Szczecin, Pułaskiego 10, 70-322 Szczecin, Poland
e-mail address: mariuszmalko@gmail.com, agnieszkawroblewska@zut.edu.pl

Keywords: *terpenes, isoprenoids, limonene*

ABSTRACT

The present paper reviews the latest progress in the chemistry of natural isoprenoids on the example of limonene, the methods of its obtaining, characteristics, properties and possible applications in various sectors of the industry.

INTRODUCTION

According to the definition, terpenes (sometimes named as isoprenoids) are organic compounds with general formula of $(C_5H_8)_n$. They are defined as materials whose structure is built up of isoprene (2-methyl-1,3-butadiene) units. This group of compounds includes acyclic and cyclic hydrocarbons and their oxygenated derivatives, such as ketones, aldehydes and alcohols. These compounds exhibit often stereoisomerism. In order to obtain terpenes very often plants have to be cut, for example during the production of incense and of myrrh balsam trees. Terpenes are mainly obtained by extraction or steam distillation. They are used in the preparation of valuable oils from fragrant floral species. Extracts and distillates, known as essential oils are used in the manufacture of perfumes, food flavors and herbal medicines [1].

Biochemical and biological functions of terpenes have not been fully understood. Many plants produce volatile terpenes to lure specific pollinators of these plants, or vice versa, to chase away the animals for which these plants are food. Less volatile and more bitter or poisonous terpenes can be used in the protection of plants against animals. Terpenes can also play a role of fitohormones in plants. Terpenes are considered as the most common natural compounds [2]. Their name comes from turpentine.

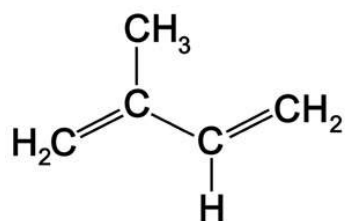


Fig. 1 The structural formula of isoprene

Turpentine is an oleoresin, which is a mixture of essential oils and resins obtained from soft coniferous trees. It is a viscous, pleasantly scented lotion which proceed out of the cut or scratch the bark or wood. Turpentine consists of more than 4000 of terpenes, mainly these are the monoterpenes alpha-pinene and beta-pinene, and also carene, camphene, dipentene, and terpinolene. However, the chemical composition of turpentine is variable and depends on the source and methods of its preparation. It is widely used in organic syntheses as a substrate for the production of camphor and menthol, as a solvent for varnishes paints, resins and waxes, polishes and cleaners, in perfumery and in veterinary practice as an expectorant and antiseptic [3].

Depending on the number of isoprene units, which are present in the main molecular skeleton, terpenes can be divided as follows:

- a) Monoterpenes are lipophilic, liquid compounds composed of isoprene hydrocarbons (2-methyl-1,3-butadiene) and originated by the attachment of two or more isoprene molecules. They are generally characterized by a distinctive, intense aroma, which give the essential oils. This group of compounds includes: monocyclic monoterpenes as hydrocarbons (limonene, felandren, p-cymene), alcohols (menthol, thymol, carvacrol, terpineol), ketones (menthone, carvone, pulegone), oxides (eucalyptol, ascaridol), dicyclic (α -, β -pinene, borneol, tujol, thujone, camphor, fenchon) and acyclic (myrcene, ocymen, linalool, geraniol, citronellol, citral A, B citral, citronellal). In addition to the essential oils, monoterpenes can be components of resins and balsams. They are of plant origin and may find a broad applications in many different areas of industry, from food chemistry and chemical ecology to pharmacology and pharmaceuticals [4].

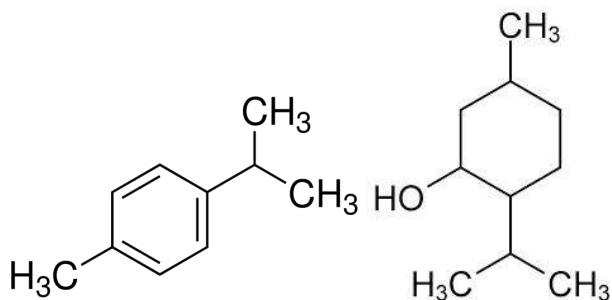


Fig. 2 The structural formulas of p-cymene and menthol

- b) Sesquiterpenes consist of three isoprene units and have the molecular formula of $C_{15}H_{24}$. Like monoterpenes, sesquiterpenes may be acyclic or contain rings, including many unique combinations. They base on hydrocarbons (eg. chamazulene, bisabolene, kadifene, caryophyllene), alcohols (eg. α -, β -bisabololene) or ketones (eg. akorone, waleranon). Sesquiterpene lactones are present in some plants: eudesmanu type (eg. alantolaktone, tetrahydridentyne B), garmacrane (eg. parthenolide) and fungi (eg. tremulane). They are characterized by their ability to precipitate proteins and may cause allergic contact reactions [5-6].

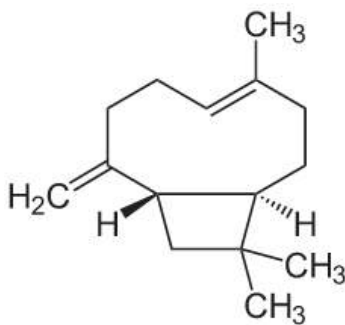


Fig. 3 The structural formula of caryophyllene

- c) Diterpenes are composed of four groups of isoprene. They may be hydrocarbons, alcohols, acids, lactones, esters or glycosides. To diterpenes also belong diterpene alkaloids, such as aconitine or taxol. Diterpene structure may be either acyclic (eg. forming chlorophyll, vitamin C and tocopherols phytol) and cyclic. The compounds of cyclic structure are divided into five different types: labdane (eg. forskolin), furanolabdane (eg. Marrubiin), klerodane, abietane (eg. Carnosic acid), kurane (eg. Stevioside) and gibberellins (eg. Gibberellic acid). They can

be found mainly in plant resins. They are characterized by a high boiling point. These compounds can find numerous applications in medicine [7].

- d) Triterpenes are compounds consisting of six isoprenoid residues, usually of an acid. This group includes acids such as oleanolic acid, ursolic or glycyrrhetic. They have antioxidant properties. Ursolic acid has a very strong antiproliferative activity and induces apoptosis (self-destruction, programmed cell death) in tumor cell lines. Triterpenes may also be in the form of alcohols, for example betulin or taraksasterol. The structure of triterpenes can be steroid, tetracyclic or pentacyclic. These compounds are ingredients of resins, juices, milk, and tissues. Sometimes triterpenes present in plants are connected with the sugars (saponosides triterpene).

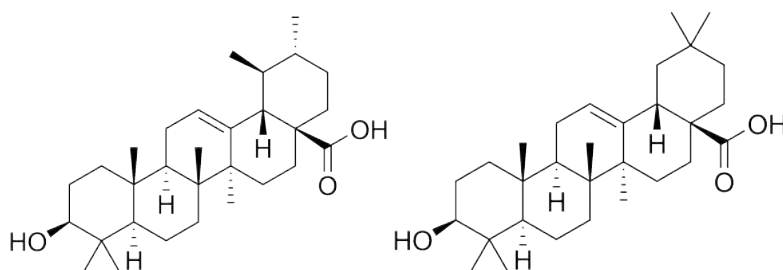


Fig. 4 The structural formula of ursolic acid and oleanolic acid

- e) Carotenoids are organic pigments (yellow, orange or red) that are found in the chloroplasts and chromoplasts of plants and some other photosynthetic organisms, including some bacteria and fungi. They are composed of eight isoprene units. They are generally found in the form of hydrocarbons. They are so-called tetraterpenes. There are over 600 known carotenoids; they can be divided into two classes, xanthophylls (which contain oxygen) and carotenes (which are purely hydrocarbons, and contain no oxygen). Carotenoids such as lycopene and β -carotene have plenty of scientific and commercial value. Currently, carotenoids are used commercially as natural food colorants, nutrient supplement, feed additives, animal feed supplements and, more recently, as nutraceuticals for cosmetic and pharmaceutical purposes [8].

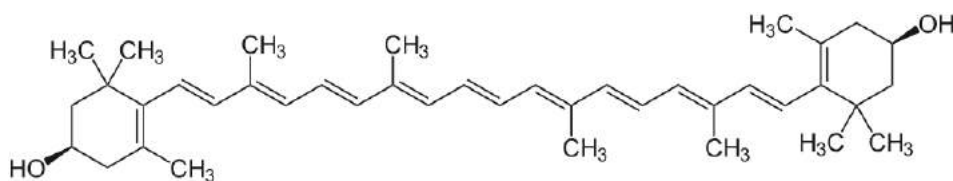


Fig. 5 The structural formula of β -carotene

- f) Polyterpenes are complex macromolecular compounds, even with more than 1000 groups of isoprene. As an example of isoprene polymer, natural rubber can be given [9]. Important for the rubber industry are two materials: rubber and gutta-percha polyterpenes. Gutta-percha is a product of the coagulation of the latex. Its main chemical component is trans - 1,4 - polyisoprene - isomer of the main component of natural rubber. Gutta-percha is hard plastic, crystal, color from dirty white to brown. Even at temperatures in the range 50-70°C it has the properties of thermoplastic melts with decomposition at approx. 130°C with density 0,95-1,02 g/cm³. It is resistant to weather conditions, natural environment, and rather chemically resistant. It can undergo aging under the influence of oxygen and ozone. However, it is possible to prevent this process with using suitable additives. This material is soluble in aromatic and chlorinated hydrocarbons. It is a good electrical insulator [10].

Natural rubber is a substance derived from the milk juice (latex) gum plants - trees, bushes or plants. From chemical point of view, the main constituent of natural rubber is polyisoprene and specifically one of it is cis -poly (1,4- isoprene) weighing molecular to 450 thousand [11].

LIMONENE AS A REPRESENTATIVE OF THE GROUP OF MONOTERPENES

Among the well-known terpene compounds best known and most widely used is limonene. Limonene is a naturally occurring compound belonging to cyclic monoterpenes. It has one chiral center, and thus, it can form two different enantiomers (Fig.5).

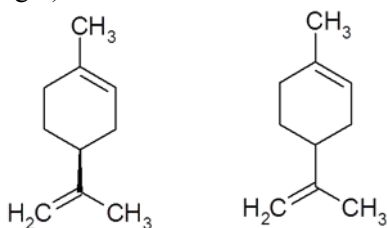


Fig. 6 The enantiomers of limonene

The most widespread in nature is R-(+)-limonene. It is the main component of essential oils obtained from the peels of citrus fruits, which are by-products in the production of fruit juices. Limonene is characterized by a fresh citrus scent. It has different properties, than S-(-)-limonene. It occurs in small amounts in the carrot root or in the caraway. It is characterized by pine

aroma. Limonene chemical structure is similar to many monoterpenoic oxygen derivatives, such as perillyl alcohol, carveol, carvone, menthol with a pleasant smell. Therefore, it may be a precursor in the process of the smelling compounds synthesis. Recently, research on the biotransformation of R-(+)-limonene to the α -terpineol has been performed. This compound is a commercially important product used in soaps, cosmetics and fragrance formulations, and it is characterized by a floral scent.

METHODS OF LIMONENE OBTAINING

The most flourishing of the citrus juice production was observed in the 40s of the twentieth century and it is still growing. The demand seeks to obtain as much as possible juices with minimizing waste products at the same time. Production of citrus fruit juices are determined by the type of fruit and its structure. Types of fruit can be classified as following:

- fruits of the orange: The sweet orange, bitter orange, mandarin,
- fruits of yellow: lemon, lime, limetta, and grapefruit.

Oranges are the basic raw material in the production of juices including citrus oil containing 95% limonene. Below is presented the list of the main types of oranges grown in different countries citrus fruit:

- Brazil: Hamlin and Pera,
- US: Navel, Valencia, Jaffa and Pineapple,
- Italy: Biondo Commune, Ovale,
- Spain / Morocco: Navel, Valencia, Jaffa.

As the citrus fruits grow throughout the year, and their aging period can take a total of five months, the fruit obtained vary depending on the time of harvest, in particular as regards the acid content of fruit sugar content and pigment. Different time of puberty significantly affects the final product. There are two main production fields in industrial citrus processing, and the differences between these two are related to the geographical area where the fruits are processed. In the Americas (Brazil, USA), large quantities of fruit are processed into standard products in a relatively small number of very large companies. In other countries with a more favorable climate (Israel, Italy, Morocco, etc.), production concentrates on a wide range of special products.

These products are made in medium-sized and small companies. The technology used for processing raw products in the production of juice is virtually identical throughout the world. The freshly harvested, healthy and intact fruits are stored in silos after they are delivered to the processing plant. They are then washed, sorted according to size and processed into juice. One method of preparing R-(+)-limonene is shown in Figure 6. Where: 1 - Extractor, 2 - Vibrating screen, 3 - Pump, 4 - Tank, 5 - Pump, 6 - Hydrocyclone, 7 -

Separator (first stage), 8 - Buffer tank, 9 - Mohno pump, 10 - Separator (second stage), 11 - Pure oil tank, 12 - Automatic filter, 13 - Treatment tank, 14 - Pump, F - Fruits, J - Juice, O - Essential oil, T - Emulsion, U - Solids, sand, W - Water.

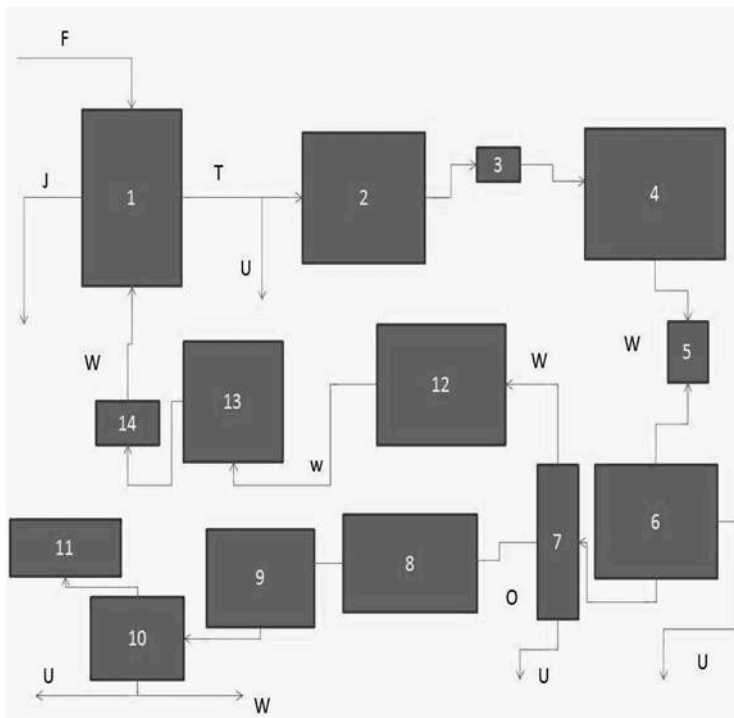


Fig. 7 Industrial installation for production of essential oils

The Fig. 6 shows a part of the flowsheet production of citrus juice because of major interest in the production of orange oil instead of orange juice. The peel contains the valuable peel oils. These peel oils are the principal factors which affect the taste of the juice. The proportion of the oil in the juice should be between 0.01 and 0.03% if the juice. These oils are stored in fatty vesicles on the surface of an orange peel. Essential oils have many applications, such as the compounds of the flavor and aroma. Several methods are available to recover essential oil. Fruits and juice (for recovery of oils) are extracted in a single step where the extractors are used in the processing of citrus fruits. Peel fruits are cut and compressed. To give crude oil is then washed with water and using a pump fed to the tank. The resulting oil/water emulsion contains from 70-90 % essential oil from the peel. In subsequent steps the crude orange oil is separated from the aqueous layer with separators and then purified of solids (sand, seeds). Skin wash water recycled in the process contains between 2 to 5 kg of oil per 100 kg of raw material to be treated is subject to the type of fruit and processing. Ready pure product is stored in tanks.

Other method of obtaining limonene used on a laboratory scale is steam distillation. Orange peels are grounded, and then placed in a reactor equipped with a magnetic stirrer. Reactor is heated to a temperature of 80°C. To the heated reactor the steam is introduced and essential oils are separated from the orange peels and distilled with water steam. After distillation, the aqueous layer was obtained and also lighter, water-insoluble layer of oil is visible.



Fig. 8 Scheme of apparatus for steam distillation

Another laboratory method of obtaining of limonene is the extraction with help of volatile solvents. The extracted liquid is separated from the aqueous layer, filtered, and then the solvent is evaporated at ordinary pressure and subsequently under reduced pressure. Waxes and resins which are also present in the liquid are separated by dissolving in hot alcohol and then then these compounds are crystallized and filtered. The yield of this process is approx. 0.9 - 3.5%. The disadvantage of this method is the need to use solvents that do not leave after evaporation of the fragrance. The solvents are volatile and of course, chemically inert.

APPLICATIONS OF LIMONENE

R-(+)-limonene is mainly used in the aromatherapy and in the food industry. It is the main component of citrus oils, which are used as food flavors. A number of properties of the compounds showing effect of fragrance or which are biologically active (applicable to medicine) is similar to the R-(+)-limonene carbon skeleton. Thus the compound was applied to their preparation, often by simple one- or two-stage transformations [12]. These compounds include α -terpineol, carveol, carvone, perillyl alcohol, menthol and 1,2-epoxylimonene

(oxidized derivatives of limonene). All of these compounds are much more valuable than limonene and are used in perfumery and food, as constituents of perfumes for flavoring cosmetics, beverages and food. In addition, p-cymene is used for the production of p-cresol [13]. R-(+)-limonene is also present in carbonated drinks produced by large corporations like Coca-Cola Company, in fruit juices, ice cream and sweets [14]. Left-handed isomer of limonene is present in the oils of bergamot and eucalyptus. However, unlike the R-(+)-limonene it is less active and has a pine scent. It is used in air fresheners in admixture with ozone and it effectively removes the smell of cigarette smoke. In the textile industry limonene can be encapsulated in polyurethane-urea coatings as a fragrance compound. In agriculture it is used as a feed ingredient for poultry Herbromix® [15]. R-(+)-limonene toxicology is well known. For example, oral lethal oral dose of the R-(+)-limonene rats is 4400 mg / kg. What is more, its properties are considered environmentally friendly. Basically, it is a biodegradable compound having exceptionally good affinity for fat thus it was used as a cleaning agent, and as alternative solvent and chlorinated oil. Today the products containing the composition of the R-(+)-limonene are used in the aerospace, automotive, electronics as solvents [16].

Limonene can be conveniently formulated with surfactants to create environmentally friendly water cleaning preparations with low flammability, suitable for the treatment of contaminated surfaces in many industrial environments (cleaning concrete, marine vessels, to remove inks and adhesives [17]. As a solvent, R-(+)-limonene was also used instead of n-hexane in extraction processes of olive oil and other fats produced by Milestone group [18].

Very interesting application of limonene used on an industrial scale is its use as relationship-enhancing process of extraction and purification of crude oil from oil sand (bitumen) [19].

From a medical point of view, R-(+)-limonene is very good solvent of cholesterol [20]. It is used in clinical removing gallstones. It also can neutralize stomach acid and promotes normal peristalsis. R-(+)-limonene are also active against certain types of cancer [21]. Limonene stops the progression of breast cancer and colon cancer.

Due to the presence of two double bonds in the structure and a six-membered ring, R-(+)-limonene is a good starting material for the production of valuable products. It can easily undergo the processes of isomerization, hydrogenation and epoxidation. Very valuable is the utilization of R-(+)-limonene for the production of high polymers which have special applications for example biological active polyesters of R-(+)-limonene and 5-hydroxymethylfurfural which act as coatings of the window panes exhibiting

good permeability and stability to light and forming an effective barrier to oxygen and water [19-20]. In the food industry a major role play polymers of R-(+)-limonene and poly(lactic acid) or poly(hydroxybutyrate). The resulting films are biodegradable and biocompatible in contact with food [22].

REFERENCES

1. Breitmaier E., Terpenes. Flavors, Fragrances, Pharmaca, Pheromones. *WILEY-VCH*. p. 1-3. 2006.
2. INCHEM – Turpentine, classification, hazard and property table. Website: <http://www.inchem.org/documents/icsc/icsc/eics1063.htm>. Date of use: 9.02.2014.
3. Kent, A. Riegel's Handbook of Industrial Chemistry (Eighth Edition). *Van Nostrand Reinhold Company*. p. 569. 1983.
4. Turina A. del V., Nolan M.V., Zygadlo J.A., Perillo M.A. Natural terpenes: Self-assembly and membrane portioning. *Biophysical Chemistry*. 122. 2006 p. 101-113.
5. Suchý M., Herout V., Šorm F. On terpenes. CLIII. The proof of existence and structure of hydroxycostunolide, a sesquiterpenic lactone of germacrane type in *Artemisia balchanorum*. *Collect. Czech. Chem. Commun.* 12. 1963 p. 1618-1620.
6. Yin R.H., Zhao Z.Z., Chen H.P., Yin X., Ji X., Dong Z.J., Li Z.H., Feng T, Liu J.K. Tremulane sesquiterpenes from cultures of the fungus *Phellinus igniarius* and their vascular-relaxing activities. *Phytochemistry Letters*. 10. 2014. p. 300-303.
7. Lanzotti V. Diterpenes for Therapeutic Use. *Natural Products*. 2013. p. 3173-3191.
8. Jaswir I., Noviendri D., Hasrini R.F., Octavianti F. Carotenoids: Sources, medicinal properties and their application in food and nutraceutical industry. *Journal of Medicinal Plants Research*. 5 (33). 2011. p. 7119-7131.
9. Kang H., Kang M.Y., Han K.H. Identification of natural rubber and characterization of rubber biosynthetic activity in fig tree. *Plant Physiol*. 123 (3). 2000. p. 1133-42.
10. Marroquín B.B., Wolf T.G., Schürger D., Willershausen B. Thermoplastic Properties of Endodontic Gutta-percha: A Thermographic In Vitro Study. *Journal of Endodontics*. 41. 1. 2015. p. 79-82.
11. Rubber Greve H.H., 2. Natural in Ullmann's Encyclopedia of Industrial Chemistry. 2000. *Wiley-VCH, Weinheim*. DOI:10.1002/14356007.a23_225.
12. Trytek M., Paduch R., Fiedurek J., Kandefer-Szerszeń M. Monoterpeny – stare związki, nowe zastosowania i biotechnologiczne metody ich otrzymywania, *Biotechnologia*. 1. 76. 2007. p. 135-155.

13. Virota M., Tomao V., Ginies C., Visinoni F., Chemata F., Green procedure with a green solvent for fats and oils' determination: Microwave-integrated Soxhlet using limonene followed by microwave Clevenger distillation *Journal of Chromatography A* . V1196–1197, 2008, p. 147–152.
14. Uemura M., Hata G., Toda T., Weine F. S., Effectiveness of eucalyptol and d-limonene as gutta-percha solvents 23, 12,1997. p. 739–74.
15. . Ciriminna, M. Lomeli-Rodriguez, P. D. Cara, J. A. Lopez-Sanchez, M. Pagliaro Limonene: a versatile chemical of the bioeconomy DOI: 10.1039/c4cc06147k.
16. Toplisek T., Gustafson R., *Precis. Clean.*, 3, 1995, 17–22.
17. Cortez M. J., Rowe H. G., *Alternative Response Technologies: Progressing Learnings*, Interspill 2012, Houston, Texas, February 15, 2012.
18. Lazenby H. US Oil Sands' biosolvent extraction patent approved. *Mining Weekly*, 22 April 2014.
19. Faure K., Bouju E., Suchet P., Berthod A., *Anal. Chem.*, 85, 2013, p. 4644–4650.
20. Chemat S., Tomao V. and Chemat F., Limonene as Green Solvent for Extraction of Natural Products, in *Green Solvents I: Properties and Applications in Chemistry*, ed. A. Mohammad and Inamuddin. *Springer Science + Business Media*. 2012. p. 175–186.
21. Shah U., Shah R., Acharya S., Acharya N. Novel anticancer agents from plant sources. *Chinese Journal of Natural Medicines*.. 11 (1). 2013, p. 16-23.
22. Chemat F., Tomao V., Visinoni F., EP pat.1 955 748 A1. 2008.

COD reduction in landfill leachate treatment by Photo Electro - Fenton process – an overview

*Ramin Nikpour¹, Maciej Szwał¹, Wojciech Piątkiewicz¹, Michał Zalewski¹

¹Faculty of Chemical and Process Engineering, Warsaw University of Technology, Warsaw, POLAND

e-mail: r.nikpour@ichip.pw.edu.pl

Keywords: *Electrochemical Advanced Oxidation Processes, Photo Electro - Fenton, COD removal, Free Radical Technology, landfill leachate*

ABSTRACT

Nowadays, human activities produce large quantities of waste and sewage and therefore, are causing some environmental risks towards public health and ecosystems.

Landfill leachate treatment is one of the important issue among the waste management systems, because untreated leachate can impact both surface and groundwater sources.

Advanced oxidation processes such as electro-Fenton and photo electro-Fenton are promising alternatives to other biological and classic physicochemical methods and have been applied effectively in leachate treatments. These advanced methods create a large amount of free radicals such as “hydroxyl” ($\bullet\text{OH}$) which can remove both organic and oxidizable inorganic components due to their ability to change in the chemical structure of the pollutants.

This study is an overview about chemical oxygen demand (COD) reduction from leachate by using the continuous photo electro-Fenton method due to the increasing importance of its application. This reaction is a catalytic reaction that iron ion from a ferrous salt is its catalyst and simultaneously, hydrogen peroxide is added to leachate. Main advantages of these technology such as environmental friendly and good economic situation are reviewed. And also some influencing factors and parameters in this process including reaction time, electrical current density and voltage, size and distance between the electrodes particularly their materials, the optimum pH, initial concentration of ferrous ion, H_2O_2 to Fe(II) molar ratio and etc. are investigated by using the other authors reports and their available experimental results. Also applying the electrodes made of suitable materials such as graphite cathode and titanium with the platinum coating anode are discussed in this work.

Reflection on the perspective in the future is providing an improved mathematical model that can better explain the operating conditions of this process. In this path, suitable experimental results are needed therefore, an

installation of photo electro-Fenton system will prepare and new desired results will report in the next related works in future.

INTRODUCTION

More recently, both municipal and industrial solid waste generations have been increased due to the “urban development”, *increasing the commercial activities* and industrial growth in many countries, which should be considered as the environmental important issues of the day [1,2]. Essence of the wastes are different from one region to another region according to the features of population and socio-economics, life style, attitudes of society, periodicity of their collection and the governing laws [3]. Although there are some alternative methods such as recycling, composting and incineration [4], but sanitary landfilling method is still the most popular technique used to manage the waste due to its technical and economic benefits [2,4,5,6,7] such that over 95% of total municipal solid wastes (MSWs) are disposed by this method around the world [1,2,3]. However, the leachate generation from landfill is the main secondary problem in this technology for the public health and ecosystems and therefore requires more treatment [2,6,7]. Leachate is highly contaminated wastewater that is produced from solid wastes undergoes a series of physicochemical and biological interactions in combination with percolating rainwater and moisture through the body of landfill treatment [1,2,5,8]. Indeed, landfill leachate is a complex mixture of very concentrated organic materials which may be very toxic and therefore untreated leachate seepage can be an environmental serious concern for surface water, soil and groundwater resources [3,7,9,10,11].

There are many different materials (mostly biodegradable organics) in composition of leachate. Also, large amounts of ammonia-nitrogen, chlorinated organic compounds, some heavy metals and inorganic salts can be found in leachate [1,2,3]. Constituents of landfill leachate are affected by many factors, including age of landfill, quality and quantity of solid waste, hydrogeology of the site (soil properties), site climate, season, rainfall patterns, percolation of rainwater, biological and chemical processes occurring in the landfill, morphology of landfill, operation conditions and facilities, cover design, waste depth and interaction of leachate with environment [2,5,3,7]. Based on the age of landfill, leachate can be classified into three categories: young, middle-aged and old. In general, young leachates (< 2 years) are commonly characterized by high biochemical oxygen demand (BOD=4000–13,000 mg/L) and chemical oxygen demand (COD=30,000–60,000 mg/L), high biodegradability (BOD₅/COD > 0.4), almost high TOC, low pH values (< 4.0) and high organic fraction with relatively low molecular weight which are mainly volatile fatty acids (VFA). With increasing the age of leachate, a series of long-term anaerobic reaction

occurs between 2 to 10 years and thereby, old leachate (> 10 years) have a relatively low COD (<4000 mg/L), low biodegradability (BOD5/COD < 0.3), lower TOC, pH (7.5-8.5), and high molecular weight compounds such as humic and fulvic acids which are in contrast of VFA [1,2,7,9].

However, the topic of waste landfill and risks of leachate production is an important issue in Europe and other parts of the world, and landfill leachate should be appropriately treated before discharge into the environment and even requires pre-treatment before blending it with the sewer [4]. There are various types of municipal, industrial, hazardous, toxic and even biomedical pollution among the wastes [8]. Consequently, there are wide variety of biological, physical and chemical methods to treat leachate. However, a final universal solution has not been found yet [4].

Methods of leachate treatment

Variety of prevalent technologies which are used to treat leachate for different purposes (recirculating it to landfill and or discharging it into the sewer or surface water) are classified into the following two main groups: [2,4,5,6,7,8]:

1. biological methods in both aerobic and anaerobic systems (examples of aerobic systems include aerated lagoons, rotating biological contactors (RBC), aerobic activated sludge, attached growth aerobic system, moving-bed biofilm reactor (MBBR), biofilters, trickling filter, sequential batch reactor (SBR) and co-treatment with sewage, and examples of anaerobic systems are upflow anaerobic sludge blanket (UASB), nitrification/denitrification and anammox)
2. Physical and chemical methods (such as air stripping, coagulation–flocculation, adsorption through activated carbon, membrane technologies including reverse osmosis (RO) and nanofiltration (NF), chemical oxidation and eventually advanced oxidation processes (AOPs).

Since the early 1970s many studies have been investigated about above various processes in landfill leachate treatment [2]. Based on other reports, the biological treatment (including aerobic and anaerobic processes and nitrification/denitrification method) are effective and cheap for young leachate with high BOD5/COD but they generally are not considered suitable for treating old leachate with lower BOD5/COD due to presence of bio-refractory compounds (such as humic substance or surfactants), or high concentration of toxic metals [2,4,7]. Hence, physical and chemical methods are mostly useful for this type of landfill leachate [2] and can successfully remove the refractory substances from stabilized old leachate and also can be used as the final treatment of the leachate which is passed from biological pre-treatment [5]. But on the other side most of physico-chemical conventional methods have high costs in term of initial investment of main equipment, need to high energy and

chemicals & consumables (such as coagulant) [12]. Also other available technologies such as RO membrane separation process or adsorption via activated carbon just separate streams and involve the phase transfer of pollutants and thereby environmental concerns will continue [4]. Lately, advanced oxidation processes (AOPs) have attracted much attention as the promising alternative methods to enhance the treatment of leachate [2,11]. AOPs can produce highly reactive free radicals such as hydroxyl radical ($\bullet\text{OH}$) as a main oxidizing agent [2,3,7]. Free radicals are unstable molecules, atoms or ions which have an unpaired electron in their outer orbit. Therefore, they are capable to degrade a wide range of refractory compounds and oxidizable inorganic components [12,13] in waste water and landfill leachate [4,5]. Indeed, free radicals make some changes in the chemical structure of the pollutants. This process is often done by hydrogen abstraction according to eq. (1) or sometimes organic free radicals ($\text{R}\bullet$) are produced by electrophilic addition. In the latter process double bonds will help and therefore radicals will be able to react with oxygen molecules and create peroxy radicals and also will begin some oxidation by chain reaction. Organic free radicals may be mineralized completely during this process [12,14].



Thus AOPs are often known as the free radical technology (FRT) too by production the free radicals and are environmentally friendly emerging technologies and effective to reduce the BOD and COD pollutants from the wastewater and also landfill leachate [12,15]. AOPs can be appropriate methods when the kinetics of processes are too slow in older conventional methods due to their above mentioned drawbacks. Table 1. presents the various of AOPs that are categorized [2,4,5]:

Table 1 The various of proposed (AOPs) for landfill leachate treatment [2,4,5].

AOPs (FRT)	Homogenous system	Non-photochemical methods (without irradiation)	O ₃ /H ₂ O ₂ O ₃ /OH O ₃ /catalyst H ₂ O ₂ /Fe ²⁺ (Fenton's process)
		Photochemical methods (with irradiation)	O ₃ /UV H ₂ O ₂ /UV O ₃ /H ₂ O ₂ /UV electron beam H ₂ O ₂ /US H ₂ O ₂ /Fe ²⁺ /UV (photo- Fenton)
	Hetrogeneous system	Non-photochemical methods (without irradiation)	Electro-Fenton (EF)
		Photochemical methods (with irradiation)	UV/TiO ₂ Photocatalysis TiO ₂ /O ₂ /UV TiO ₂ /H ₂ O ₂ /UV Photo electro-Fenton

In recent years, electro-Fenton and photo electro-Fenton processes have been considered in order to improve the efficiency of landfill leachate treatment among the AOPs [5]. But it should be noted that maybe precise and desirable standards cannot be achieved by a single procedure in a leachate treatment plant and it usually requires a combination of two or more processes including chemical, physical and biological steps [4,16]. By contrast, advanced electro oxidation such as electro-Fenton and photo electro-Fenton processes have high costs of operation compared with other conventional technologies, therefore their single implementation are not cost-effective as a full treatment for landfill leachate. In general it is better to use FRT to improve the quality of leachate or as the final step in a combined leachate system [1]. Another advantage of AOPs is their high degree of flexibility. Because generation of free radicals under oxidation processes in these technologies can be used individually or in combination with O₃, H₂O₂, TiO₂, UV radiation, electron-beam irradiation and ultrasound and eventually Fenton reagent (see Table 1.) in order to increase the (OH•) generation [12].

Chemical oxygen demand (COD) is the main important indicator of wastewater quality and in landfill leachate treatment issues. This study is an overview on COD reduction and also color and odor [5] removal in landfill leachate treatment by electro-Fenton and particularly photo electro-Fenton processes.

Electro-Fenton and photo electro-Fenton processes

One of the promising AOPs is Fenton process which is diagnosed as an effective method in leachate treating today [4]. In particular, Fenton oxidation is very powerful in combination with electrochemistry and UV- radiation (Photo electro-Fenton) [3,7].

About 120 years ago, Henry John Horstman Fenton (born 1854) observed for the first time the oxidation of tartaric acid as one of the organic compounds by hydrogen peroxide in the presence of iron(II) ion ($\text{H}_2\text{O}_2 + \text{Fe}^{2+}$). This oxidation process was known as “Fenton reaction”, and sometimes alternatively, the Fenton reagent [17]. Although Fenton reaction maybe is recognized as an undesirable factor in bio-molecules and damaging of cells and thus causes the aging and many diseases in some biological issues, but this reaction is *suitable* for environmental protection *particularly* in wastewater and landfill leachate treatments and groundwater remediation [12,17]. By the mid-nineteenth century, with the introduction of AOPs in various industries including waste water treatment plants, Fenton reaction subsequently found an important role in this context. In particular, by understanding the performance of electro-chemical oxidation in environmental protection and waste water treatment topics in the 70’s to 90’s (see table 2), combining these two together (Fenton reaction + electrochemistry) were presented as the modern electro-Fenton [18,19].

Table 2 Historical trends in the most important research works for organic compound degradation by electro-oxidation that have been reported by the related authors.

Date	Researcher(s)	The main compound decomposition	Ref.
Since 1936	Matsuda R., Nishimori T. et al.	sol gel - cyanide	[19,20]
1951,1953	Heard R. D. H. et al., & Jones A. R. et al.	cyanide	[21]
1973	Nilsson et al. & Mieluch et al.	phenol	[19,22]
1975	Dabrowski et al.	phenol-containing wastes	[19]
1975	Papouchado et al. I	phenolic compounds	[19]
1979	Koile and Jonhson	phenolic films from platinum anodes	[19]
1979,1980s	Smith de Sucre	Phenol	[19]
1980s	Kirk, Stucki, Kotz, Chettiar and Watkinson	cyanide and phenolic and some other organic compounds	[19]
Since 1990s	Comninellis	different organic compounds	[19]
1993	Do and Chen	formaldehyde	[5]
1995	Brillas et al.	aniline	[5]
1999	Alvarez-Gallegos and Pletcher	Phenol	[5]

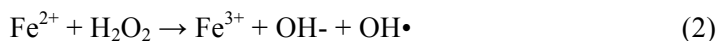
Over the *past two decades*, especially after 2000 not only many proper investigations have been done in case of decomposition of various types of organic compounds in waste water and landfill leachate treatments, but also some of them have focused in effective parameters in operation conditions, electrodes materials, mechanisms and kinetic model description. In the recent

years kinetic models in first and second orders for humic acid [23] and 2,4-dichlorophenoxyacetic acid, 1.1 order for aniline by only Fenton reaction and 0.46 order for aniline by electro-Fenton method are presented during these studies by several researchers. However most of them still applied first order model for electro-Fenton reaction [19,24]. A good new model which recently has been provided solely to describe phenol degradation is the inverted “S” shape curve model [24].

Although the ultraviolet (UV) technology was discovered more than one-hundred years ago, but its usage in wastewater treatment plants is about 35 years. Eventually by entering UV radiation in this field in the last two decades, especially in the last 10 years the modern advanced method of photo electro-Fenton (electro-Fenton + UV) is suggested for COD reduction in waste water and landfill leachate treatment by several researchers [5,7,10,11,16,24,25].

In general, AOPs consist of two stages: the first stage is the formation of free radicals such as hydroxyl as the strong oxidant, and the second stage is the reaction of these oxidants with organic compounds in the aqueous phase according to reaction (1).

Overall form of a classical Fenton reaction is as follows:



According to “Haber and Wiess” mechanism of Fenton reaction [17,30] hydroxyl radicals are produced via electron transferring between hydrogen peroxide (H_2O_2) and ferrous(II) ion (Fe^{2+}) [4,7,10]. This means that one electron reduction in H_2O_2 is occurred by Fe^{2+} [17] which there is in a salt of iron such as FeSO_4 and called the same Fenton reagent in this process [3]. It should be noted that H_2O_2 concentration decreases in the conventional Fenton reaction after adding a chemical over time. Reports indicate that most of oxidants are removed by adding H_2O_2 in a closed reactor due to radicals attack. This disadvantage can be corrected by taking advantage of electricity application according to electrochemical oxidation technology. In other words, electro-Fenton is a kind of electro advanced oxidation processes (EAOPs) that has advantages of both two electrochemical process and conventional Fenton reaction [5,20,31]. In general electrochemical oxidation is divided into two major categories: 1) Direct electro-oxidation at the anode or anodic oxidation, 2) Indirect electro-oxidation by using suitable oxidants that are formed on the anode [19]. In direct electro-oxidation process, hydroxyl radicals are produced by oxidation of water directly in anode (reaction 3), therefore it is known as anodic oxidation. Hydroxyl radical is produced in various high-voltage anodes (platinum, lead dioxide, tin dioxide, boron-rich diamond from boron (BDD), etc). Based on Aturan & Varias studies

(2007), most of used anodes in environmental issues are Platinum and BDD [20,31].



Indirect electro-oxidation methods are the reactions of homogeneous organic pollutants with generated strong oxidants which are performed during the electrolysis process and are including two applied methods: a) Electro-oxidation with activated chlorine where is a direct anodic oxidation. The chloride ions in wastewater lead to the formation of free chlorine and species of oxygenated chlorinated oxidants that can oxidize the organic pollutants to their mineralization. b) Electro-Fenton (EF) and photo electro-Fenton (PEF) processes. In this processes hydrogen peroxide (H_2O_2) is produced continuously by two regenerated electrons from dissolved oxygen molecules (O_2) in the carbon cathode under acidic condition and in a continuous mode which has been decomposed by ferrous ion (Fe^{2+}) as a catalyst. The accumulation of H_2O_2 concentration in aqueous solution depends on rates of its generation and consumption [24]. This electrochemical reaction is as follows (cathodic reaction) [12,19,29]:

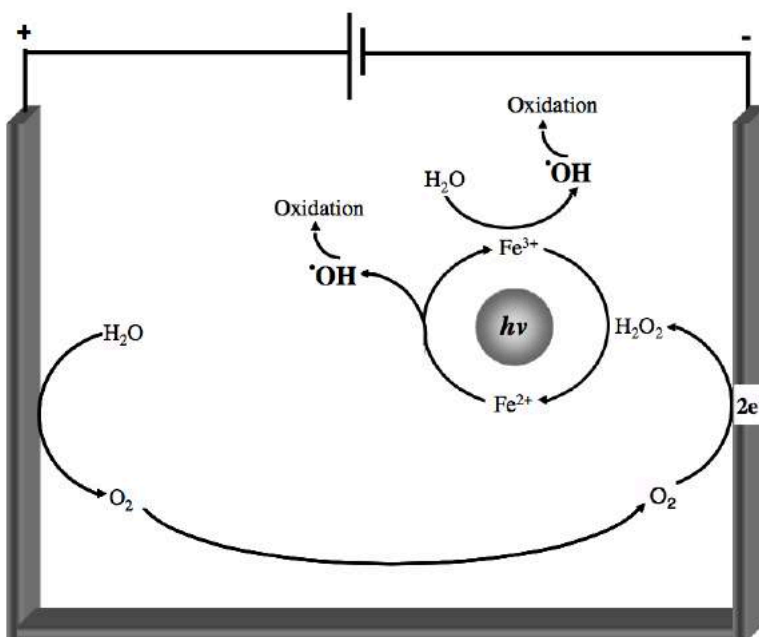


Fig. 1 Generation of free hydroxyl radicals ($\cdot\text{OH}$) by

means of EF and PEF processes. [33]

Usually there are two types of EF system. In the first type, Fenton reagent (Fe^{2+}) and H_2O_2 are added from outside and the electrodes are inside. Anode also has the function of catalyst too in this type of EF. Whilst in the second type, H_2O_2 is added from outside too but Fe^{2+} is generated via immolation of cast iron anode [3].

The proliferation the main Fenton's reagent (2) can also be done by electrochemical regeneration of Fe^{2+} via cathodic reduction of Fe^{3+} (5). Therefore, this mode allows a higher generation of H_2O_2 via reaction (4) [15,28,30].



The production of $\bullet\text{OH}$ radicals accelerates in a electro-Fenton process as a result according to reaction (6):



Carbon in various forms, including graphite, flat carbon and carbon fibers is widely used as a cathode material for hydrogen peroxide generation because it exhibits a range of electrochemical activities towards oxygen reduction, high potential for hydrogen evolution and low catalytic activity for hydrogen peroxide decomposition [5,31]:



Other parasitic adverse reactions that arise from very active hydroxyl radicals attack, include [17,32]:



These reactions can be controlled by optimization the design and operating parameters such as electricity current and pH. As it was mentioned before, the procedures of free radicals production in this technology can be photochemical (by utilizing the UV radiation or combination the EF+ UV) and non-photochemical [12,14,15]. In the absence of UV light, ferric ions (Fe^{3+}) accumulate in the solution and the reaction will stop when all of ferrous ion (Fe^{2+}) are used. In the presence of light or in other word, in the same photo electro-Fenton process new ferrous ions (Fe^{2+}) regenerate from photo reduction

of Ferric ions (Fe^{3+}) or the photolysis of $\text{Fe}(\text{OH})^{2+}$ according to following reaction and the cycle will continue [27,28,30,32,33,36]:



Usage of EF and PEF in wastewater and landfill treatments in order to decompose pollutants and thus COD reduction have the following advantages [19,24,26,28,30,34]:

- Converting the organic compounds to carbon dioxide (CO_2), water and inorganic materials
- High efficiency
- Environmentally friendly
- Sufficient safety
- Facility and volubility
- Automation capabilities (sensor technology)
- Cost-effective than conventional chemical dosing methods

Here is tried to collect and present the range of values of the design criteria, parameters and system specifications based on other reports that are used for their experimental works in EF and PEF methods in order to reduce COD from wastewater and landfill leachate (Table 3).

Table 3 Design criteria and operating parameters and EF/PEF systems specifications

Parameters	Range of values	Ref.
volumetric flows	0.5 – 100 l/h	[1][16][28]
COD	600 – 26000 mg/l	[1][5][16][28]
Reaction time	6 – 420 min	[1][5][11][16][19][37][38]
electricity current density	0.5 – 20 A (0.85 – 250 mA/cm ²)	[3][10][11][15][26][33][37][38]
applied potentials (voltages)	2 – 30 V (0.5 – 1.5 V/SCE)	[11][22][28]
initial pH	2 – 13 (mostly acidic solution)	[3][7][26][32][37][38]

H ₂ O ₂ concentration	2.2 – 50 m.mol/l	[3][7][32][39]
Fe ²⁺ concentration	0.5 – 10 g/l	[3][7][39]
[H ₂ O ₂]/[Fe ²⁺]	1 – 12 (1.5 was the best)	[5][7][23]
COD removal efficiency	15 - 99 %	[3][5][7][11][16]
Color removal	90 – 99 %	[10][16]
Distance between the electrodes	1.5– 5 cm	[5][10]
temperature	20 – 50 C (should be higher than 8 C)	[5][7][23][28]
UV lamp power	125 W (80 – 160 kW/m ²)	[5][7][10][11][39]
UV Wavelength	200 – 400 nm	[10][11][26][28][33][37][39]

DISCUSSION

All reports confirm that electro-Fenton and photo electro-Fenton methods can be utilized to reject COD from wastewater and landfill leachate. There are various factors which affect the efficiency. Some of the most important parameters are briefly mentioned here:

Effect of electricity current density- The reported experimental results show that COD removal efficiency will be increased with the increasing of electricity current density, but further increase of current will reduce the removal efficiency from a specified point.

Effect of Fenton reagent dosage- The COD reduction efficiency is increased when H₂O₂ concentration and Fe²⁺ concentration are increasing.

Effect of pH- pH is one of the most important and very sensitive factor because the efficiency of COD reduction in a short range of pH is too high, but before or after of this range of pH, COD reduction is low and remains constant with more changes. Therefore pH is one the limiter parameter in this process.

Effect of temperature- Changes in temperature often has not tangible impact on COD reduction. Very small amount of COD directly increases with increasing the temperature. But it should not be forgotten that at the higher

temperature than 50°C, H₂O₂ decomposes into oxygen and water. Also reactions will be impaired in very cold temperatures (<8°C) [5].

Effect of time- Usually can be observed a sharp increasing in COD reduction within a short time period (4 hours maximum), but after all that there isn't any significant changes on COD removal.

Effect of distance between electrodes- Some researchers found that changing the distance between electrodes will affect the system efficiency. And the best and optimum distance should be obtained individually for each material of electrodes and pollutant compounds.

It is felt that more works are needed on the optimization of parameters particularly influence of cathode potential, [H₂O₂]/[Fe²⁺] ratio, material of electrodes and maybe some other effective factors.

CONCLUSION

Electro-Fenton and photo electro-Fenton processes have appropriate performance in wastewater and landfill leachate treatments in terms of COD reduction and color and also odor removal. These technologies can be used to improve the quality of leachate or be utilized as a polishing stage in a landfill leachate treatment [5].

Related reports indicate that Photo electro-Fenton has higher decomposition efficiency of refractory compounds than other conventional AOPs such as conventional electro-Fenton, photo Fenton and classical Fenton processes [35].

A rough estimation of operating costs of a landfill leachate treatment plant by EF technology is about 0.008 US\$ (2003) per m³ leachate and per ppm removed COD [5] and a little more maybe by PEF method. In conclusion, therefore they are economical methods in this case.

Reported results have indicated that the rate of oxidation and COD removal efficiency are strongly dependent on initial pH, initial concentration of Fenton reagents, initial COD concentration and reaction temperature.

In this regard, further studies are needed to obtain better response models that could explain all the mechanism characteristics and effective parameters such as pH, concentration of Ferrous ion, electric current density, etc. in electro-Fenton and photo electro-Fenton processes [24].

Recommendation

Suggestions for future research of this work is a new response model providing based on kinetic of COD reduction reaction which includes all effective parameters in both electro oxidation (EF) and photolysis reactions. It is

suggested to install a system consisting graphite cathode and titanium with coated platinum anode in order to obtain the experimental results.

Since the major contaminant composition in the stabilized leachate is humic acid, therefore it can be used in laboratory research works instead of real landfill leachate with a good approximation.

ACKNOWLEDGEMENTS

Scope of this work is based on Prof. W. Piątkiewicz's investigations related to wastewater treatment plants for laboratories and workshops in Warsaw University of Technology (WUT), the faculty of Chemical and Process Engineering and also for Polymemtech co. projects under the guidance of Dr. Maciej Szwałt. This work is a part of PhD thesis under supervision of Prof. Piątkiewicz too.

REFERENCES

- [1] Wei L., Qixing Z., Tao H., Removal of Organic Matter from Landfill Leachate by Advanced Oxidation Processes: A Review, *International Journal of Chemical Engineering*, 2010, 1-10.
- [2] Ozcan A., Sahin Y., Oturan M.A., Complete removal of the insecticide azinphos-methyl from water by the electro-Fenton method - A kinetic and mechanistic study, *Water Research*, 2013, 47, 1470 – 1479.
[doi:10.1016/j.watres.2012.12.016](https://doi.org/10.1016/j.watres.2012.12.016)
- [3] Daud Z., Fatimah N., Hanafi M., Awang H., Optimization of COD and Colour removal From Landfill Leachate by Electro-Fenton Method, *Australian Journal of Basic and Applied Sciences*, 2013, 7, 8, 263-268.
- [4] Wiszniewski J., Robert D., Surmacz-Gorska J., Landfill leachate treatment methods: A review, *Environ Chem Lett*, 2006, 4, 51–61.
- [5] Umar M., Hamidi A., Aziz, M., Suffian Y., Trends in the use of Fenton, electro-Fenton and photo-Fenton for the treatment, *Waste Management*, 2010, 30, 2113–2121.
[doi:10.1016/j.wasman.2010.07.003](https://doi.org/10.1016/j.wasman.2010.07.003)
- [6] Abbas A., Jingsong G., Review on Landfill Leachate Treatments, *American Journal of Applied Sciences*, 2009, 6, 672-684.
- [7] Hermosilla D., Cortijo M., Pao Huang C., Optimizing the treatment of landfill leachate by conventional Fenton and photo-Fenton processes, *Science of the Total Environment*, 2009, 407, 11, 3473–3481.
[doi:10.1016/j.scitotenv.2009.02.009](https://doi.org/10.1016/j.scitotenv.2009.02.009)
- [8] Kumar S., Katoria D., Singh G., Leachate Treatment Technologies, *International Journal of Environmental Engineering and Management*, 2013, 4, 5, 439-444.

- [9] Baig S., Thiéblin E., Chapter in book: Landfill Leachate Treatment: Case studies, *Degremont*, 1940
- [10] Wu X., Zhang H., Li Y., Zhang D., Li X., Factorial design analysis for COD removal from landfill leachate by photo assisted Fered-Fenton process, *Environ Sci Pollut Res*, 2014, 21, 8595–8602.
- [11] Zhao X., Qu J., Liu H., Wang C., Xiao S., Liu R., Liu P., Lan H., Hu C., Photoelectrochemical treatment of landfill leachate in a continuous flow reactor, *Bioresource Technology*, 2010, 101, 3, 865–869.
doi:10.1016/j.biortech.2009.08.098
- [12] Nikpour Khoshgrudi R., Piątkiewicz W., Zalewski M., Szwaś M., Free radical technology usage dor COD removal in wastewater treatment, Warsaw University of Technology, 2013
- [13] Glaze, William, Kang, Joon-Wun, Chapin, Douglas, The Chemistry of Water Treatment Processes Involving Ozone, Hydrogen Peroxide and Ultraviolet Radiation, *Ozone Science Engineering: The Journal of the International Ozone*, 1987, 9, 4, 335 - 352.
- [14] Quiroz M.A., Bandala E.R., Martínez-Huitle, Chapter in book: Advanced Oxidation Processes (AOPs) for Removal of Pesticides from Aqueous Media, *Agricultural and Biological Sciences - Pesticides – Formulations, Effects, Fate*, 2011, ISBN 978-953-307-532-7.
- [15] Wang C., Chou W., Chung M., Kuo Y., COD removal from real dyeing wastewater by electro-Fenton technology using an activated carbon fiber cathode, *Desalination*, 2010, 253, 1-3, 129–134.
doi:10.1016/j.desal.2009.11.020
- [16] Tauchert E., Schneider S., Lopes de Morais J., Peralta-Zamora P., Photochemically assisted electrochemical degradation of landfill leachate, *Chemosphere*, 2006, 64, 9, 1458–1463.
doi:10.1016/j.chemosphere.2005.12.064
- [17] Barbusinski K., Fenton reaction - controversy concerning the chemistry, *Ecological Chemistry and Engineering*, 2009, 16, 3, 347-358.
- [18] Huitle C.A.M., Direct and indirect electrochemical oxidation of organic pollutants, *Ph.D. Thesis*, University of Ferrara, Italy, 2004.
- [19] Martinez-Huitle C., Ferro S., Electrochemical oxidation of organic pollutants for the wastewater treatment: direct and indirect processes, *Chem. Soc. Rev.*, 2006, 35, 1324–1340.
- [20] Rossa M., Navarro F., Wai Lin S., Violante Delgadillo V., Cyanide Degradation by Direct and Indirect Electrochemical Oxidation, *J. Mex. Chem. Soc.*, 2011, 55, 1, 51-56.

- [21] Fedurco M., Jorand C., Augustynski J., Electrochemical Conversion of Cyanide into Methylamine and C1–C2 Hydrocarbo, *J. Am. Chem. Soc.*, 1999, 121, 4, 888–889.
- [22] Xiong Y., He C., T.Karlsson H., Zhu X., Performance of three-phase three - dimensional electrode reactor for the reduction of COD In simulated wastewater-containing phenol, *Chemosphere*, 2003, 50, 1, 131-136.
doi:10.1016/S0045-6535(02)00609-4
- [23] Wu Y., Zhou S., Qin F., Zheng K., Yea X., Modeling the oxidation kinetics of Fenton’s process on the degradation of humic acid, *Hazardous Materials*, 2010, 179, 1-3, 533 – 539.
doi:10.1016/j.jhazmat.2010.03.036
- [24] Liu X., LI X. Z., Leng Y.L., Wang C., Kinetic modeling of electro-Fenton reaction in aqueous solution, *Water Res.*, 2007, 41, 5, 1161-1167.
doi:10.1016/j.watres.2006.12.006
- [25] Mohajeri S., Abdul Aziz H., Hasnain Isa M., Ali Zahed M., Nordin Adlan M., Statistical optimization of process parameters for landfill leachate treatment using electro-Fenton technique, *Journal of Hazardous Materials*, 2010, 176, 1-3, 749 – 758. doi:10.1016/j.jhazmat.2009.11.099
- [26] Khataee A., Fathinia M., Seyyednajafi F., Ranjbar H., Combination of anophotocatalysis with electro-Fenton-like process in the removal of phenol from aqueous solution: GC analysis and response surface approach, *International Journal of Industrial Chemistry*, 2012, 1-11.
- [27] Musaviyan M., Reza'ee A., Contaminated wastewater treatment containing industrial dyes by consolidated method of electro chemical - Gamma radiation, *Forth Congress of Occupational Health in Iran*, 2004, 355 – 361.
- [28] El-Ghenymy A., Antonio Garrido J., Centellas F., Arias C., Lluís Cabot P., Rodríguez R., Brillas E., Electro-Fenton and Photoelectro-Fenton Degradation of Sulfanilic Acid Using a Boron-Doped Diamond Anode and an Air Diffusion Cathode, *J. Phys. Chem.*, 2012, 116, 3404 – 3412.
- [29] Zhang H., Zhang D., Zhou J., Removal of COD from landfill leachate by electro-Fenton method, *Journal of Hazardous Materials*, 2006, 135, 1-3, 106-111. doi:10.1016/j.jhazmat.2005.11.025
- [30] Isarain-Chavez E., Antonio Garrido J., Rodríguez R., Centellas F., Arias C., Cabot P., Brillas E., Mineralization of Metoprolol by Electro-Fenton and Photoelectro-Fenton Processes, *J. Phys. Chem.*, 2011, 115, 1234–1242.
- [31] Brillas E., Sire’s I., A. Oturan M., Electro-Fenton Process and Related Electrochemical Technologies Based on Fenton’s Reaction Chemistry, *Chem. Rev.*, 2009, 109, 6570 – 6631.
- [32] Bagheri A., Musavi Gh. and Khanin A., Evaluation efficacy of Electro-Fenton process in industrial wastewater treatment contain high concentrations of

formaldehyde, *Iranian Journal of Health and Environmental*, 2012, 2, 143-156 (in Persian language).

[33] Peralta-Hernández J.M., Martínez Huitle C., Recent Advances in the Application of Electro-Fenton and Photoelectro-Fenton process for removal of Synthetic Dyes in wastewater treatment, *J. Environ. Eng. Manage.*, 2009, 19, 5, 257-265.

[34] Rosales E., Pazos M., Ángeles Sanromán M., Advances in the Electro-Fenton Process for Remediation of Recalcitrant Organic Compounds, *Chemistry Engineering Technology*, 2011, 609 – 617.

[35] Ratanatamskul C, Masomboon N., Ming-Chun L., Application of Fenton Processes for Degradation of Aniline, *Agricultural and Biological Sciences*, 2011, 463 – 474.

[36] Mahmoodi N.M., Rayat-Tari K.H., Borhany S., Arami M., Nourmohammadian F., Decolorization of Colored Wastewater Containing Azo Acid Dye Using Photo-Fenton Process: Operational Parameters and a Comparative Study, *Iranian Journal of color science and technology*, 2008, 31-40 (in Persian language).

[37] Ricky P., Yu-Jen Sh., Yu-Jen H., Yao-Hui H., Treatment of real wastewater using semi batch (Photo)-Electro-Fenton method, *Sustain. Environ. Res.*, 2011, 21, 389-393.

[38] Haiqing Xu., Aiping Li., Liangdong F., Xiaochun Ch., Shijie D., Destruction of Cyanide in Aqueous Solution by Electrochemical, *Int. J. Electrochem. Sci.*, 2012, 7, 7516-7525.

[39] Jeyong Y., Yoonki K., Roles of Oxidation and Coagulation in Fenton Process for the removal of Organics in Landfill Leachate, *J. Ind. Eng. Chem.* 2002, 8, 5, 410-418.

The biotechnological potential of ionic liquids

*Urszula Świerczek, Joanna Feder-Kubis

Faculty of Chemistry, Wrocław University of Technology, Wrocław, POLAND

e-mail: urszula.swierczek@pwr.edu.pl

Keywords: *organic salts, biotransformation, biocatalysis, biofuel*

ABSTRACT

For thousands of years, biotechnology has been an important part of human life. In the beginning, this technology have been used without understanding: how does it work? Today, thanks to science, biotechnology can help us in medicine, agriculture and in almost every branch of industry (as an example: chemical, petrochemical, food industry).

Biotechnology is promising for producers and consumers. The growing demand for high quality bio-products (such as: enzymes, antibodies, drugs) show that this technology is necessary and should be developed.

Examples of ionic liquid used in biotechnological processes are described in a significant part of literature. These compounds are considered to be an alternative to unfriendly organic solvents for biocatalysis and biotransformations. Ionic Liquids (ILs) are defined as organic salts with melting point below 100°C, but sometimes they remain liquid at room temperature (RTILs - Room Temperature Ionic Liquids). Due to possibility of tuning physicochemical and biological properties, they are known as “designer solvents”. The advantages of ILs are low vapour pressure, nonflammability, biocompatibility, high conversion rates, solubility of many of organic and inorganic substances etc. Therefore, these salts might be excellent enzymatic reaction media, in terms of enhanced activity, stability or selectivity of proteins.

In recent years, ionic liquids have been widely used in processes: biodiesel or biomass production, synthesis of enormous number of useful intermediates and active pharmaceutical ingredients. Furthermore, ILs can be applied in sewage treatment plant as co-solvent in enzyme-based purification of water.

Ionic liquids are often related to as the “green compounds”. They can go well with enzymes in many biotechnological processes. These low-melting salts are more eco-friendly media for biocatalysis and biotransformations than other organic substitutes. Ionic liquids tend to be a perfect solution for biotechnology.

INTRODUCTION

Ionic liquids (ILs) are not a new discovery (the first example was published in 1914) but they are still investigated by the great interest of

scientists. They have very typical chemical structure. These compounds consist only of ions: generally organic cations and optionally organic or inorganic anions (Figure 1). Even though they belong to the group of very popular salts in chemistry, ILs are characterized by very low melting point (below 100°C). In theory, the synthesis of millions of new ionic liquids is still possible [1-2].

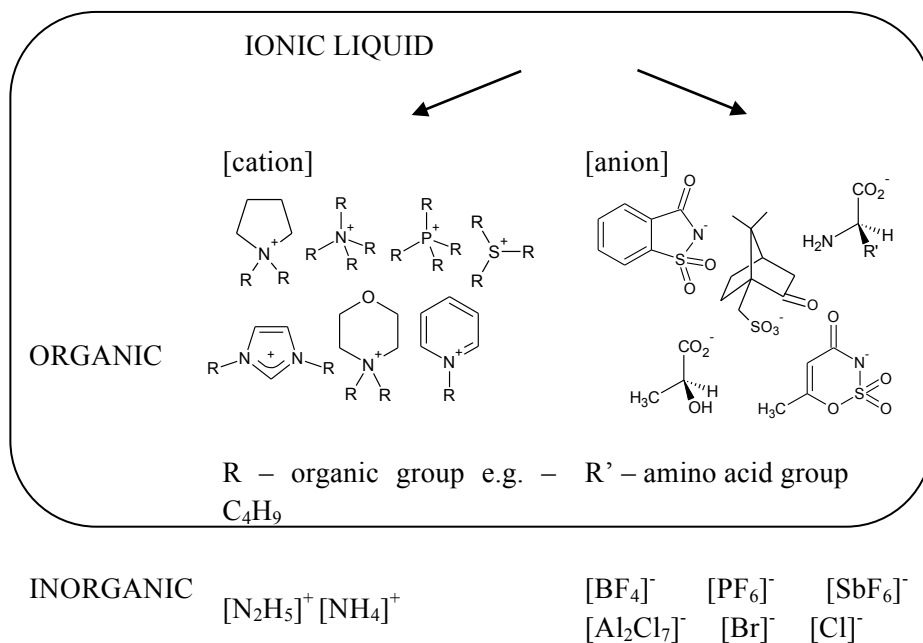


Fig. 1 Examples of common cations and anions pairs [1-4].

What's more some ionic liquids remain liquid at room temperature, which is defined as Room Temperature Ionic Liquids (RTILs) [3][4]. The respective selection of ions is the main factor that influences the melting points of the salts (Table 1). Generally, the growth of anion size results in lower melting temperature and similarly in cation: larger cations tend to reduce melting point [5].

Table 1 Changes in melting points for salts with increasing size of ions [5].

IONIC LIQUIDS		
[cation] ⁺	[anion] ⁻	melting point (m.p.) (°C)
[EtMeIm] ⁺	[Cl] ⁻	87
	[PF ₆] ⁻	60
	[AlCl ₄] ⁻	7
[Me ₄ Am] ⁺	[Br] ⁻	>300
[Bu ₄ Am] ⁺		124-128
[Oc ₄ Am] ⁺		95-98

cation: [EtMeIm]⁺ - ethylmethylimidazolium; [Me₄Am]⁺ - tetramethylamonium; [Bu₄Am]⁺ - tetrabutylamonium; [Oc₄Am]⁺ - tetraoctylamonium.

Properties of ionic liquids as a reaction medium

Thus, the cation-anion structure influences the properties of particular ILs. By the change of one of the ions, the physicochemical properties of these salts can be finely tuned, which makes them a perfect medium for many chemical reactions [3]. Ionic liquids are generally non-flammable and chemothermostable therefore, they might be used in hazardous and strongly exothermic processes. ILs have a wide range of solubilities and miscibilities with water and other solvents (some are hydrophilic while others are hydrophobic). Low temperature salts are characterized by negligible vapor pressure, so they are regarded as safer reaction medium. Their tunable properties make them “designer solvents”. It should be emphasized that these features cannot be reached with conventional organic solvents [2].

The first publication describing successful application of ionic liquids as catalysts in Friedel-Crafts synthesis appeared in the 80's. Since that time ILs have been used in almost every field of chemistry: catalysis, extraction, separation, as surfactants, battery fill or termofluids and lubricants [6]. But in the last decades ionic liquids appeared also the biotechnological industry interest [3].

IONIC LIQUIDS IN BIOTECHNOLOGY

Biotechnological processes such as: fermentation and biotransformation can deliver many compounds: vitamins, amino acids, antibiotics (penicillin and cephalosporin) and useful chemicals of high quality (alcohols, chiral amines) [3][6]. They are promising alternative for the environmental-friendly production. Thanks to application of enzymes or whole cells of microorganisms we can obtain higher enantio-, regio- and chemoselectivities of the reaction, which might reduce the level of potential pollution and costs of the mentioned process [5].

For a long time it was thought that enzymes as versatile catalysts should be used only in their natural aqueous environment, which was limited to water-soluble substrates. It turned out that lipases, proteases and many other enzymes can be efficient as well in organic solvents, but each enzyme requires at that time an optimal degree of hydration.

The introduction of green chemistry rules forces the industry to cut down on toxic solvents. RTILs seem to be an ideal solution [7].

Ionic liquids and enzymes

The first documented application of enzymes and ILs dates back to the 1984. The article showed unexpectedly the activity of alkaline phosphatase in aqueous mixture of etylamonium nitrate $[\text{EtNH}_3][\text{NO}_3]$ [5].

Nowadays, the literature describes lots of examples of higher activity and stability of these natural catalysts in presence of ionic liquids. It can be said that ILs may take place of traditional organic substances as: toluene, hexane, acetonitrile, which cannot be applied in clean "green" technologies. In some cases only incubation is sufficient to improve catalytic properties of an enzyme. The best example is thermolysin, that retained its activity at 37°C for 144 hours in $[\text{BuMeIm}][\text{PF}_6]$ – 1-butyl-3-methylimidazolium hexafluorophosphate (Figure 2) environment which was still active, whereas the same treatment in ethyl acetate resulted in the loss of elementary activity [7]. Ionic liquids cooperate well with enzymes.

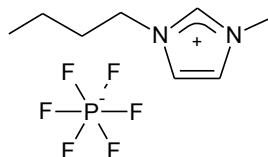


Fig. 2 $[\text{BuMeIm}][\text{PF}_6]$

They may be able to stabilize and protect thermally the working proteins. 350% growth of activity of *C. antarctica* lipase B after contact with IL is promising because it may play a vital role in biotechnological industry i.e. alcoholysis, transesterification, kinetic resolution of chiral alcohols, esterification of carbohydrates and synthesis of polyesters [8]. Numerous researches

have shown that enzymes exhibit greater stability in pure ILs than in traditional organic solvents. Hydrophobic ionic liquids (including long chains in the cation) present less tendency to take away the essential water molecules from the protein and thereby, they are better for enzyme activity [9].

In the case of the other enzymes used in multiphase system (Figure 3), the structure of specific cation-anion pair is also important [3][10].

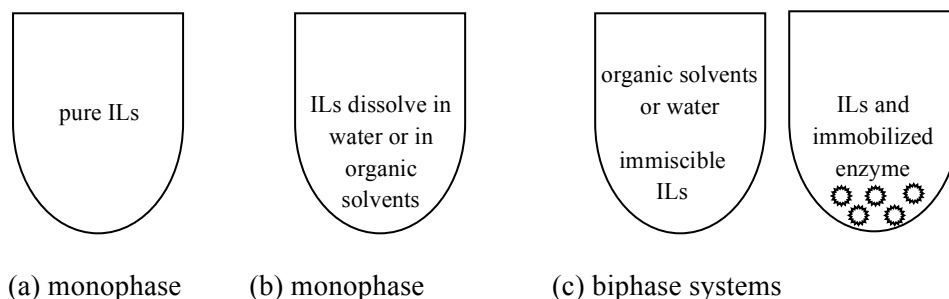
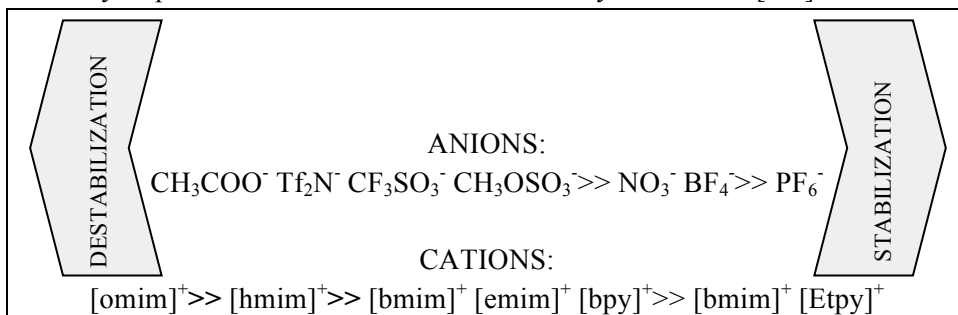


Fig. 3 Example of phase system in biocatalytic process [2-3][10]

Ionic liquids in the presence of H₂O dissociate into independent ions, which influence the stability of the protein. Due to tunable properties of discussed salts we can generate suitable compounds to preferable bioreaction. The Hofmaister series was established (Figure 4) [10] but the relationship between activity or stability of protein and structure of ILs is not fully understood [7-9].



[OcMeIm]⁺ - cation 1-octyl-3-methylimidazolium; [HeMeIm]⁺ - cation 1-hexyl-3-methylimidazolium; [EtMeIm]⁺ - 1-ethyl-3-methylimidazolium; [BuPy]⁺ - cation butylpyridinium; [EtPy]⁺ - cation ethylpyridium.

Fig. 4 The Hofmaister series for ILs components [9]

BIOTECHNOLOGICAL APPLICATIONS OF IONIC LIQUIDS

With a green vision of the overall process it is necessary to use more favorable (eco-safer, biocompatible and efficient) solvents like ionic liquids. In the scientific literature many examples of using these salts in enzymatic reactions are described (Table 2) [7].

The stability and activity of proteins is one of the requirements of useful industrial processes. In the perfect vision, only expected (selective) product should be obtained. However, it often involves using the specialist catalyst. Ionic liquids can be a “green” alternative to enantio-/stereospecific reactions [12-13].

Table 2 Short review of application ILs in different kinds of reactions
[3][5][7][11]

Biocatalyst	Ionic liquid	Reaction
<i>Rodococcus</i> R312	[BuMeIm][PF ₆]	extraction of erythromycin
bakers' yeast		reduction of ketones
α -chymotrypsin	[OcMeIm][PF ₆] [EtMeIm][(CF ₃ SO ₂) ₂ N] [MeOc ₃ Am][(CF ₃ SO ₂) ₂ N]	transesterification
termolysine	[BuMeIm][PF ₆]	synthesis of <i>Z</i> -aspartame
β -galactosidase (<i>Bacillus circulans</i>)	[MeMeIm][MeSO ₄]	synthesis of lactose by reverse hydrolysis
horseradish peroxidase (HRP)	[BuMeIm][PF ₆]	synthesis of polyaniline
D-amino acid oxidase (DAAO)	[BuMeIm][BF ₄] [BuMeIm][PF ₆] [MeMeIm][MeMePO ₄] [BuMeIm][(CF ₃ SO ₂) ₂ N]	production of 7-aminocephalosporanic acid
chloroperoxidase (CPO)	[BuMeIm][MeSO ₄] [MeMeIm][MeSO ₄] [BuMeIm][Cl] [BuMeIm][BF ₄] [BuMeIm][PF ₆]	hydrolysis of epoxide
Aldolase	[BuMeIm][PF ₆]	aldol addition
subtilisine	[BuMeIm][PF ₆]	Peptide synthesis
laccase	[BuMeIm][PF ₆]	Oxidation of anthracene

cations: [MeOc₄Am] – methyltriocetylammmonium;

anions: [(CF₃SO₂)₂N] - bis(trifluoromethanesulfone)-imide; [MeMePO₄] – dimethylphosphate; [MeSO₄] –methylsulfate;

Examples of enzymatic reactions

Lipase as the most popular enzyme in chemical industry has become a model-enzyme for reaction with ILs. Several reactions are catalyzed by this enzyme:

- Esterification
- Transesterification (alcoholysis)
- Perhydrolysis
- Aminolysis (amide synthesis) [13]

The research shows that lipase, in environment of numerous ionic liquids, maintain the high substrate specificity and conversion rates [3][13]. An ideal example is reaction of glucose (Figure 5).

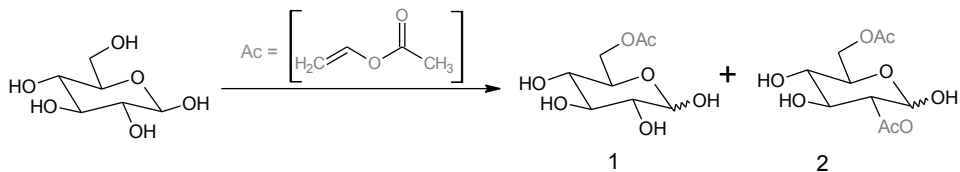


Fig. 5 Acylation of glucose [12].

Applied lipase B (CaL B) demonstrated very high activity (more than 99 % conversion) in ILs and in traditional solvents (THF) – tetrahydrofuran. Thanks to ionic liquid [MeOBuIm][BF₄] – methoxybutylimidazolium tetrafluoro-borates the reaction proceeded in low temperature (55°C instead of >200°C) and more selective product was obtained (Table 3).

Table 3 Products of acylation reaction of glucose [13]

medium	structure	concentration of product [%]	
		1	2
organic solvent		53	47
ionic liquid		93	6

The similar relationship was observed during acylation of different glycosides catalysed by *Candida rugosa* lipase in CHCl₃ and compared with [BuMeIm][PF₆]. In case of ionic liquid, higher yields (25% vs. 82%) and better regioselective (e.g. 77% vs. 90%) was obtained [14].

The recent reports give an example application of ionic liquids with very long chains (about 16 atoms of carbon) in the ammonium cation – [C₁₆Me₃Am][NTf₂] – in synthesis of flavor substances by lipase (Figure 6).

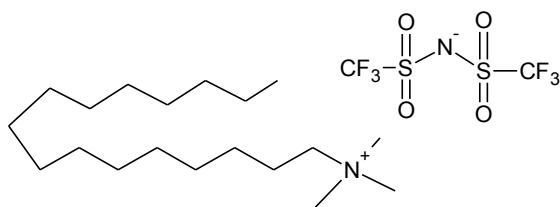


Fig. 6 Structure of [C₁₆Me₃Am][NTf₂]

among the most important fragrance compounds used in the food, cosmetic and pharmaceutical industries. Using ILs may replace difficult extraction and allow to obtain nearly pure synthetic compounds [15].

Lipases and ionic liquids are very useful in production of medicines, for example: ibuprofen. As only (*S*)-ibuprofen is characterized by anti-inflammatory and painkilling properties, the enantioselective medium and/or enzyme is necessary [16]. Another example of industrial use of ILs and catalytic protein refers to *Z*-aspartame where thermolysine retain the same activity in [BuMeIm][PF₆] just like in an organic solvent [2][12]. It is expected that in the near future ionic liquids will improve sewage treatment processes. Oxygenase (particular laccase from *Cerrena unicolor*) due to the high stability and activity in an environment of many ILs might be used in water purification of phenolic compounds [17][18].

Biomass conversion

A petroleum and fossil fuels resources are not inexhaustible. New technologies of energy and chemicals production are needed [19]. Lignocellulosic materials, also known as plant biomass (agricultural waste, wood or energy crops [20]) are an abundant renewable resource on Earth. The conversion of this raw material can deliver a great number of important industrial compounds. The components of lignocellulose are:

- Cellulose (long chains of glucose monomers)
- Hemicellulose (polysaccharides consisting of a range of monosaccharide monomers – especially xylose)
- Lignin (complex crosslinked polymer with phenolic components) [2].

All above-mentioned carbohydrates can be hydrolyzed to monosaccharide sugars, which can ferment to ethanol [19], acetone or butanol. It is worth mentioning that the alcohol – C₂H₅OH is crucial chemical for potential biofuel production [21].

In the beginning ionic liquids were used for extractive separation after fermentation process, but presence of [BuMeIm][PF₆], [OcMeIm][PF₆] or other salts did not enhance the efficiency. Recent research has shown that

This method is a simple example of bioesteryfication, whereby esters from natural compounds (geraniol, cytro-nellol, nerol and anisyl alcohol) can be produced. Flavour geranyl acetate and other esters are

lignocellulosic materials dissolve in an imidazolium ILs into glucose, xylose and other monomers [2]. Certain ionic liquids are a promising class of compounds for biomass pretreatment, because they reduce resistance to enzymatic hydrolysis. However, a large number of ILs may inhibit commercially available enzymes such as: cellulases. On the other hand, due to tunable properties it is possible to formulate tolerant-system, containing for example [EtMeIm][OAc] – 1-ethyl-3-methylimidazolium acetate [22].

Nowadays, depletion of fossil fuels is major environmental and energy security issue. Biomass can be competitive, natural and renewable alternative for the production of biofuels and chemicals [23]. Therefore, the application of ionic liquids in the production of biofuel can contribute to environment protection.

CONCLUSION

The structure of ionic liquids influence their physicochemical properties. Depending on the cation and anion, the character of whole ILs is changing. It means that the properties of these salts can be finely tuned, which makes them a perfect medium for many chemical reactions.

In the last decade, ionic liquids have found application in biotechnology. Their major advantages are: high conversion rate, high yield of process, stability and unusual activity of catalytic protein. A huge number of studies demonstrate the utility of ionic liquids in enzymatic reactions (for example: production of drugs, vitamins, amino acids and many useful chemicals). Biotransformation and biocatalysis with ILs is promising alternative for toxic organic synthesis. They don't generate a pollution and avoid using harmful catalytic agents. Ionic liquids are very chemically- and thermostable. These salts can work in every kind of phase system (alone, with water or an enzyme immobilized on a support). Although, the Hofmeister series was developed, the relationship between enzyme-IL is still not fully understood.

Scientists predict that ionic liquids will improve sewage treatment processes and biofuel production from plants – natural, renewable resources.

Undoubtedly, ILs are compounds with very high potential for biotechnology.

Acknowledgment. This research was financed by the National Science Centre (Poland) grant no. 2013/09/D/ST5/03904

REFERENCES

[1] Wasserscheid P., Keim W., Ionic liquids – New “Solution” for transition metal catalysis, *Angewandete Chemie – International Edition*, 2000, 39, 21, 3773-3789.

- [2] Freemantle M.: An introduction to ionic liquids, *The Royal Society of Chemistry*, 2010.
- [3] Dominquez de Maria P.: Ionic liquids in biotransformations and organocatalysis, *Wiley-VCH*, 2012.
- [4] Cull S.G., Holbrey J.D., Vargas-Mora V., Seddon K.R., Lye G.J., Room-Temperature Ionic Liquids as Replacements for Organic Solvents in Multiphase Bioprocess Operations, *BIOTECHNOLOGY AND BIOENGINEERING*, 2000, 69, 2, 227 – 233
DOI: 10.1002/(SICI)1097-0290(20000720)69:2
- [5] Wasserscheid P., Welton T., Ionic Liquids in Synthesis, *Wiley-VCH*, 2002.
- [6] Torimoto T., Tsuda T., Okazaki K., and Kuwabata S., New Frontiers in Materials Science Opened by Ionic Liquids, *Advanced Materials*, 2010, 22, 1196–1221
DOI: 10.1002/adma.200902184
- [7] Cantone S., Hanefeld U., Basso A. Biocatalysis in non-conventional media—ionic liquids, supercritical fluids and the gas phase. *Green Chemistry*, 2007, 9, 954–971
DOI: 10.1039/b618893a
- [8] Yang Z., Pan W., Ionic liquids: Green solvents for nonaqueous biocatalysis, *Enzyme and Microbial Technology*, 2005, 37, 19-28.
doi:10.1016/j.enzmictec.2005.02.014
- [9] Tavares A.P.M., Rodríguez O., Macedo E.A., Chapter 20: New Generations of Ionic Liquids Applied to Enzymatic Biocatalysis, *Ionic Liquids - New Aspects for the Future*, *InTech* 2013, 537-556.
- [10] Galonde N., Nott K., Debuigne A., Deleu M., Jerome C., Paquot M., Wathelet J-P., Use of ionic liquids for biocatalytic synthesis of sugar derivatives, *Journal of Chemical Technology and Biotechnology*, 2012, 87, 451–471
DOI: 10.1002/jctb.3745
- [11] Quijano G., Couvert A., Amrane A., Ionic liquids: Applications and future trends in bioreactor technology, *Bioresource Technology*, 2010, 101, 8923–8930
DOI: 10.1016/j.biortech.2010.06.161
- [12] van Rantwijk F., Sheldon R., Biocatalysis in Ionic Liquids, *Chemical Review*, 2007, 107, 2757-2785
DOI: 10.1021/cr050946x
- [13] van Rantwijk F., Lau R., Sheldon R., Biocatalytic transformations in ionic liquids, *TRENDS in Biotechnology*, 2003, 21, 3, 131-136
DOI: 10.1016/S0167-7799(03)00008-8

- [14] Roosen C., Müller P., Greiner L., Ionic liquids in biotechnology: applications and perspectives for biotransformations, *Applied Microbiology and Biotechnology*, 2008, 81, 607–614
DOI 10.1007/s00253-008-1730-9
- [15] Lozano P., Bernal J.M., Gómez C., García-Verdugo E., Burguete M.I., Sánchez G., Vaultier M., Luis S.V., Green bioprocesses in sponge-like ionic liquids, *Catalysis Today*, 2014, article in press
DOI: 10.1016/j.cattod.2014.08.025
- [16] Proszowska A., Siódmiak T., Marszał M., Ciecze jonowe – nowe możliwości w syntezie substancji leczniczych, *Annales Academiae Medicae Silesiensis*, 2012, 66, 2, 59–65
- [17] Bryjak J., Koźlecki T., Stabilność lakazy w obecności cieczy jonowych, *Inżynieria i Aparatura Chemiczna*, 3, 2009, 30-31
- [18] Bryjak J., Feder-Kubis J., Laccase activity and stability in the presence of menthol-based ionic liquids, *Acta Biochimica Biologica*, 2013, 60, 4, 741–745
- [19] Gräsvik J., Winstrand S., Normark M., Jönsson L.J., Mikkola J-P., Evaluation of four ionic liquids for pretreatment of lignocellulosic biomass, *BMC Biotechnology*, 2014, 14, 34
DOI:10.1186/1472-6750-14-34
- [20] Mora-Pale M., Meli L., Doherty T.V., Linhardt R.J., Dordick J.S., Room Temperature Ionic Liquids as Emerging Solvents for the Pretreatment of Lignocellulosic Biomass, *Biotechnology and Bioengineering*, 2011, 108, 6, 1229-1245
DOI: 10.1002/bit.23108
- [21] Lonzano P., García-Verdugo E., Bernal J.M., Izquierdo D.F., Burguete M.I., Sánchez-Gómez G., Luis S.V., Immobilised Lipase on Structured Supports Containing Covalently Attached Ionic Liquids for the Continuous Synthesis of Biodiesel in scCO₂. *Chemistry and sustainability energy and materials*, 2012, 5, 4, 790–798
DOI: 10.1002/cssc.201100692
- [22] Gladden J.M, Park J.P., Bergmann J., Reyes-Ortiz V., D’haeseleer P., Quirino B.F., Sale K.L., Simmons B.A., Singer S.W., Discovery and characterization of ionic liquid-tolerant thermophilic cellulases from a switchgrass-adapted microbial community, *Biotechnology for Biofuels*, 2014, 7, 15, 1-12
DOI: doi:10.1186/1754-6834-7-15

[23] Datta S., Holmes B., Park J.I., Chen Z., Dibble D.C., Hadi M., Blanch H.W., Simmons B.A., Sapro R., Ionic liquid tolerant hyperthermophilic cellulases for biomass pretreatment and hydrolysis, *Green Chemistry*, 2010, 12, 338–345

DOI: 10.1039/b916564a

Coating of stainless steel 316L with organic layer for medical purposes: problematic issue of surface pre-treatment

*Paulina Trzaskowska¹, Tomasz Ciach¹

¹Faculty of Chemical and Process Engineering, Warsaw University of Technology, Warsaw, POLAND

e-mail: p.trzaskowska@ichip.pw.edu.pl

Keywords: stainless steel 316L, biomaterials, cardiovascular implants

ABSTRACT

In present paper we summarize problems concerning pre-treatment of stainless steel (SS) 316L that is an initial step in every procedure of SS coating with organic layer. SS 316L naturally presents a passive layer of oxides that should be removed before introducing an organic film. In general, there are two main methods of such: electropolishing and mechanical polishing. It comes from the literature that electropolishing enables complete oxides layer removal, but it is controversial whether there is a need of further smoothing the surface with aggressive acids. Mechanical polishing leaves the surface standardized, yet still rough, and there is no evidence that the layer of oxides is completely cleared off after that. There is a lack of detailed data considering the influence of both pre-treatment methods on subsequent organic coating. Basing on our own experience we claim that mechanical polishing guarantees better adhesion of organic film, whereas there is practically no adhesion on electropolished surface, which does not clearly follow from the literature review.

INTRODUCTION

In modern history, metals have been used as implants for more than 100 years ago [1]. From now on metals have been applied in medicine due to their superior features overcoming ones provided by polymers and ceramics: an excellent combination of strength and ductility. Metallic implantable devices are present in cardiosurgery (stents, artificial valves), in orthopedic (total joint replacement, plates enabling reparation of bones) and in dentistry (restoration of teeth).

Stainless steel 316L (SS 316L) is among three most commonly used metallic implantable materials. Due to high chromium, nickel and molybdenum content (17%, 11,5% and 2,3%, respectively [2]) it exhibits valuable corrosion resistance. The reason of it is that steel develops chromium oxide layer on its surface. If the protective film is broken and exposes the metal underneath, a new oxide film begins to form for further protection [3]. High corrosion resistance predestinates SS 316L to be applied in medicine. However, it does not possess

biofunctionalities like blood compatibility, bone conductivity and bioactivity [1]. Hence, surface modifications are required. A deep understanding of processes that occur on the surface of implanted SS 316L device is essential to undertake research focusing on improving SS 316L properties.

Figure 1 presents a simplified chart of blood - biomaterial interactions. As for SS 316L implants that are assigned to contact blood (like stents or artificial valves) the process of body - biomaterials interaction goes as follows [4-7]. All blood components adsorbed on the surface produce biochemical signals that can trigger the activation of blood clots forming process (thrombosis). Clots forming on the surface of an implant is considered to be extremely dangerous to patients. A clot is likely to detach and occlude a vessel, thus causing a life-threatening condition such as heart attack or stroke [4].

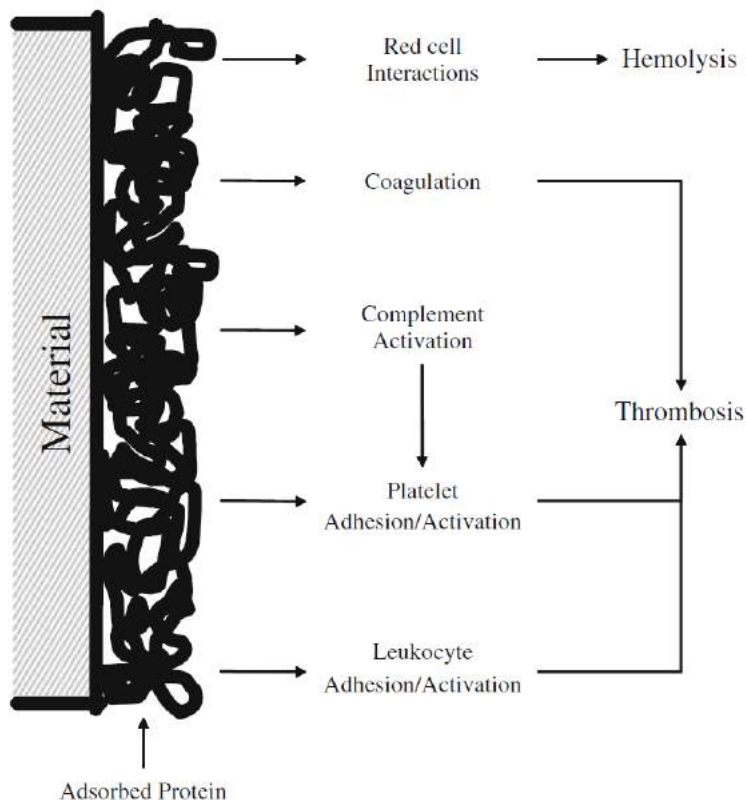


Fig. 1 A simplified chart of blood - implanted biomaterial interaction resulting in e.g. inflammation and blood clotting [6]

On the other hand, SS 316L releases toxic chromium and nickel ions [8] that can cause a necrosis or apoptosis of blood cells and cells from surrounding tissues due to their ability of cell membrane damaging [9]. The isolation of the

surface from tissues seems to be a reasonable way to prevent the intoxication of organs. Moreover, in case of stents made from SS 316L there is also a problem of restenosis [10,11]. This is a phenomenon of reclosing the lumen of the vessel occluded with arteriosclerosis plaque, that has been previously widened by a stent. The reclosing is a result of a vessel tissue (mainly endothelium) damage. The common statement is that coating a stent with a biocompatible layer could be a solution for this problem.

Since all the unwanted effects occur at the interface between a material surface and blood, the most suitable approach is to coat the surface with a biocompatible layer isolating it from tissues and thus improving its cooperation with blood components. Introducing an organic layer on metallic surface is not a trivial matter, mainly because of problems with adhesion between polymer and metal. Thus, stability of obtained “hybrid” materials is not certain. Metal surface that is going to be coated needs to undergo a pre-treatment process in order to improve the attachment of organic layer. Although in existing body of literature there are many works concerning the issue of initial treatment, we feel that provided data and conclusions are not sufficient. In this paper we attempt to summarize major issues that have to be taken into consideration during the initial step of SS 316L surface modification.

DISCUSSION

As it was mentioned above, SS 316L is naturally covered with a layer of metal oxides and hydroxides with adsorbed hydrocarbons [8,11]. This passive layer provides anti-corrosion properties, nevertheless its properties differ strongly from the properties of steel. Oxides layer could be classified as ceramics layer rather than metallic layer [8,11]. It appears clearly from the literature that for proper and durable coating of SS surface the oxides layer has to be removed. There are two general methods of oxides layer removal: electrochemical polishing and mechanical polishing.

Electrochemical polishing

This method utilizes dipping a piece of metal (in this case SS 316L) into a solution containing a mixture of acids and/or organic solvents and then force the current flow in order to dissolve of metal ions and removal of non-metallic inclusions which are responsible in promoting corrosion process and formation of new, smooth and chemically homogenous layers on different metal substrates. There are many studies focusing on selection of parameters that are most suitable to apply during electropolishing of SS 316L. Authors usually take acid mixture composition, temperature, current density and type organic additives

into consideration. What is distinguishable, all authors undertaking this issue aim at obtaining the most smooth surface as possible.

Lyczkowska et al. [12] indicated that the smoothest surface is obtained when electropolishing bath consists of a) sulphuric acid 96% , ortophosphoric acid 85% and triethanolamine 99% in 1: 1,70:0,10 ratio by weight or b) sulphuric acid 96% and ortophosphoric acid 85% in 1:1,50 ratio by weight with addition of glycerol 99%, oxalic acid and acetanilide (200 g/dm³ of each). For both baths a significant decrease of surface roughness was indicated at relatively low current density: 20 A/dm² and relatively low temperature: 55°C (roughness parameter - R_a - decreased from 200nm to 80-60nm). Organic additives slow down the process of ions dissolving by complexing iron atoms and thus protecting the surface from breaches. Authors indeed obtained a smooth surface, however they did not attempt to cover such surface with any organic layers. Other authors [8,11] applied slightly different method parameters (respectively: current density value at 75 A/dm² and 25 A/dm², with and without organic additives, 90°C and 50°C, 3min and 20min) but reported completely unlike observations. According to them, the surface of electropolished SS 316L exhibits macroscopic irregularities (figure 2), and also the presence of phosphate layer was determined. This contamination has to be removed since it would impair corrosion resistance in vivo. Haidapoulos et al. [11] applied acidic dipping in the mixture of nitric acid at 70% (10% v/v), hydrofluoric acid at 50% (2% v/v) and deionized water (88% v/v), during 30s at 50°C. After that, the surface was very clean and smooth (figure 2). Latifi et al. [8] proposed the dipping of SS 316L surface in an optimized mixture of hydrofluoric acid (2% v/v), nitric acid (10% v/v) and deionized water in 3:9:88 ratio by weight. The highest corrosion resistance was confirmed for 20 min of dipping in 45°C. Acidic mixture of the same composition is also applied for SS 316L surface treatment by other authors, but they state that after that a thermal annealing of the surface in 1000°C is obligatory [13]. Moreover, they report that dipping in acids and thermal annealing should be performed before electropolishing to get better results.

Electrochemical polishing of metals including SS 316L has been deeply studied by different groups of researchers. This method is widely known in industry as a method of improvement of metal surface appearance and increase of corrosion resistance and certainly it leads to a complete removal of oxides layer. However, we claim that this type of polishing is not dedicated for biomedical application. Although it has been determined that electropolished SS 316L does not exhibit in vitro cytotoxicity [8], its influence on tissues in vivo is still very unclear [14]. Moreover, steps involving acid dipping and/or annealing seem to be unavoidable, nevertheless the usage of such harsh conditions is not

safe nor cheap. Hydrofluoric acid is extremely dangerous to use even in form of diluted solutions [15]. As we discuss fabrication of materials that are going to be further studied for non-toxicity and biocompatibility, it should be remembered that selection of mild parameters and substrates is valuable. What is more, in our opinion very smooth surfaces (“mirror-like”) obtained as described above preclude adhesion of organic layers that are to be introduced in the next step. It has been proven during our laboratory trials. Nevertheless, authors who apply electropolishing before organic layer deposition on metals [16] do not mention any problems with adhesion.

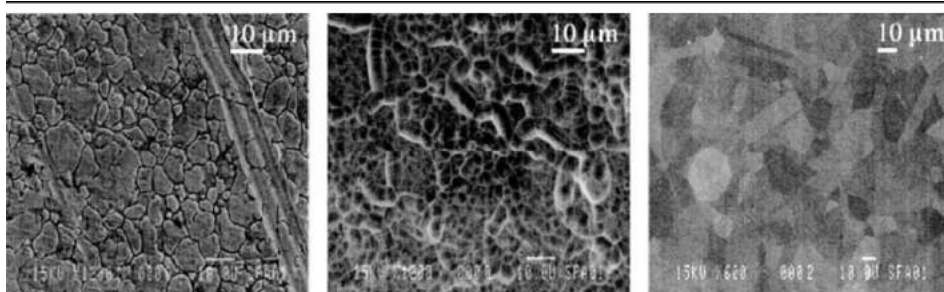


Fig. 2 SEM images of SS 316L surfaces: untreated, electropolished and acid-dipped in order to remove large irregularities. One can notice that after electropolishing the surface is unacceptably rough, with was not reported [12] by other authors [11].

Mechanical polishing

Mechanical polishing is the most commonly applied method of metallic surface pre-treatment before organic layer deposition. All authors use very similar procedure of successive polishing the surface of metal object with grit sandpaper of increasing gradation, for instance for 600 to 1200 [17], from 600 to 4000 [18] or from 120 to 4000 [19]. Some researchers prefer more precise polishing, e.g. with diamond paper and then by Al_2O_3 powder [20] or with polishing paste grid size $0.05 \mu\text{m}$ [21]). Samples are then cleaned to remove debris from the polishing steps and degrease the surface. It has to be emphasized that in every reported case of mechanical polishing authors aim at obtaining “mirror-like” metal surface (e.g. “mirror - like” titanium surface [21]). Despite that mechanical polishing is used very often, it is hard to find works considering polished surface roughness evaluation. Shahryani et al. [19] determined the roughness of SS 316L surface polished with the use of emery papers of various grids: from 120 to 4000. The surfaces were characterized using optical profilometry. For a sample polished with paper with the grit number of 120 and 4000 R_a value were $585 \pm 35\text{nm}$ and $14 \pm 1 \text{ nm}$, respectively. This work however

does not concern introduction of organic coating onto polished surface. The study in which authors determined the surface roughness of titanium samples and then coated them with organic layer does not link calculated R_a values with organic layer stability [21].

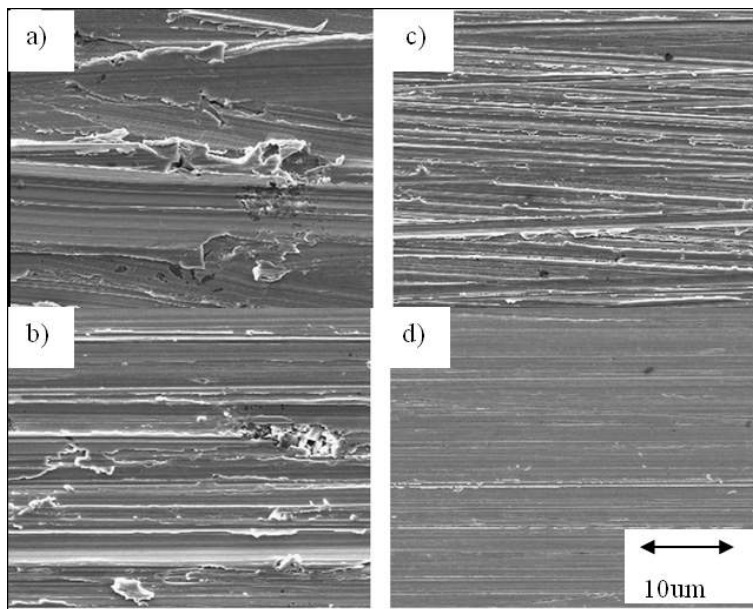


Fig. 3 Examples of SEM images of SS 316L polished with emery papers of various grits: a) 120, b) 320, c) 600, d) 2400. [19]

The vast majority of authors do not take into consideration the influence of polished surface roughness on organic coating efficiency. Nevertheless, as it comes from our laboratory experiments, mechanical polishing is crucial to guarantee a proper adhesion of organic layer to metallic surface (including SS 316L). It is surprising that there are no works clearly claiming this. Also, it is not certain whether mechanical polishing in fact removes oxides layer from the surface of SS 316L. We assume that the goal of mechanical polishing is to eliminate bigger irregularities and thus standardize samples' surface rather than to clear away oxides layer. Also, it could be suspected that decreasing R_a value to some level is beneficial for organic layer adhesion, however too low R_a value results in deterioration of adhesion efficiency. We feel that more detailed research in this field is needed.

CONCLUSIONS

The stage of metallic surface pre-treatment is very important to obtain stable and resistant superficial organic layers. We find surprising that in existing body of literature there is no clear statement concerning the effect of SS 316L

surface pre-treatment on subsequent stage of coating. On one hand, it is advised to remove oxides layer because of its unstable character and electropolishing is a recommended way to do it. However, it follows from experimental trials that this method could be inefficient, likely to worsen organic film adhesion and hazardous to use. As for mechanical polishing, it probably does not remove oxides layer as thoroughly as electropolishing. Nevertheless, because it standardizes roughness on the whole surface of a sample, it increases the level of organic film adhesion. Still, it has to be emphasized that these conclusions come from our personal experience rather than from a literature review since reported works do not clearly concern the effect of surface pre-treatment on organic film introducing. Finally, mechanical polishing cannot be applied to stents since these are delicate objects of complex geometry that are likely to be squeezed. In this case there should be other methods of pre-treatment developed, such like acid etching or hydroxide treatment [21].

REFERENCES

- [1] Hermawan H., Ramdan D., Djuansjah J.R.P., Chapter in the book: Metals for Biomedical Applications, *Biomedical Engineering - From Theory to Applications, InTech*, 2011
- [2] <http://www.stalenierdzewne.pl>, 2015
- [3] www.aperam.com, Stainless steel and corrosion, 2015
- [4] Williams D.F., Tissue-biomaterial interactions, *Journal of Materials Science*, 1987, 22, 10, 3421-3445
- [5] Berg J.M., Tymoczko J.L., Stryer L., Strategie regulacyjne - enzymy i hemoglobina, *Biochemia, Wydawnictwo Naukowe PWN*, 2005
- [6] Gavalas V.G., Berrocal M.J., Bachas L.G., Enhancing the blood compatibility of ion-selective electrodes, *Analytical and Bioanalytical Chemistry*, 2006, 384, 1, 65-72
- [7] Ratner B.D., Bryant S.J., Biomaterials: Where we have been and where we are going, *Annual Review of Biomedical Engineering*, 2004, 641-75
- [8] Latifi A., Imani M., Khorasani M.T., Joupari M.D., Electrochemical and chemical methods for improving surface characteristics of 316L stainless steel for biomedical applications, *Surface and Coatings Technology*, 2013, 2211-12
- [9] Świczko-Żurek B., Biologiczna ocena biogodności, *Biomateriały, Wydawnictwo Politechniki Gdańskiej*, 2009
- [10] Milleret V., Ziogas A., Buzzi S., Heuberger R., Zucker A., Ehrbar M., Effect of oxide layer modification of CoCr stent alloys on blood activation and endothelial behavior, *Journal of Biomedical Materials Research - Part B Applied Biomaterials*, 2014

- [11] Haïdopoulos M., Turgeon S., Sarra-Bournet C., Laroche G., Mantovani D., Development of an optimized electrochemical process for subsequent coating of 316 stainless steel for stent applications, *Journal of Materials Science: Materials in Medicine*, 2006, 17, 7, 647-657
- [12] Łyczkowska E., Lochyński P., Chlebus E., Electropolishing of a stainless steel, *Przemysł Chemiczny*, 2013, 92, 7, 1364-1366
- [13] Zhao H., Humbeeck J.V., Sohier J., Scheerder I.D., Electrochemical polishing of 316L stainless steel slotted tube coronary stents, *Journal of Materials Science: Materials in Medicine*, 2002, 13, 10, 911-916
- [14] De Scheerder I., Verbeken E., Van Humbeeck J., Metallic surface modification, *Seminars in interventional cardiology : SIIC*, 1998, 3, 3-4, 139-144
- [15] www.sigmaaldrich.com, 2015
- [16] Zammarelli N., Luksin M., Raschke H., Hergenröder R., Weberskirch R., "Grafting-from" Polymerization of PMMA from stainless steel surfaces by a raft-mediated polymerization process, *Langmuir*, 2013, 29, 41, 12834-12843
- [17] Dadafarin H., Konkov E., Omanovic S., Electrochemical functionalization of a 316L stainless steel surface with a 11-mercaptopundecanoic acid monolayer: Stability studies, *International Journal of Electrochemical Science*, 2013, 8, 1, 369-389
- [18] Harvey J., Bergdahl A., Dadafarin H., Ling L., Davis E.C., Omanovic S., An electrochemical method for functionalization of a 316L stainless steel surface being used as a stent in coronary surgery: Irreversible immobilization of fibronectin for the enhancement of endothelial cell attachment, *Biotechnology Letters*, 2012, 34, 6, 1159-1165
- [19] Shahryari A., Kamal W., Omanovic S., The effect of surface roughness on the efficiency of the cyclic potentiodynamic passivation (CPP) method in the improvement of general and pitting corrosion resistance of 316LVM stainless steel, *Materials Letters*, 2008, 62, 23, 3906-3909
- [20] De Giglio E., Cometa S., Satriano C., Sabbatini L., Zambonin P.G., Electrosynthesis of hydrogel films on metal substrates for the development of coatings with tunable drug delivery performances, *Journal of Biomedical Materials Research - Part A*, 2009, 88, 4, 1048-1057
- [21] Willumeit R., Schuster A., Iliev P., Linser S., Feyerabend F., Phospholipids as implant coatings, *Journal of Materials Science: Materials in Medicine*, 2007, 18, 2, 367-380

Surface plasmon resonance in detection of biological threats

*Maciej Trzaskowski¹

¹Faculty of Chemical and Process Engineering, Warsaw University of Technology, Warsaw, POLAND

e-mail: m.trzaskowski@ichip.pw.edu.pl

Keywords: *surface plasmon resonance, portable analytical devices, bacteria detection*

ABSTRACT

Surface plasmon resonance phenomenon (SPR) is becoming one of the mostly used effect in detection of interactions between analytes and immobilized biomolecules. The main reason is that it enables fast, accurate and marker-free analysis. Many types of SPR chips are already developed and designed for different uses. From miniature chips capable of being installed in portable devices to complex SPRi matrixes, together with variety of surface modification strategies the analytical technique of SPR offers great range of applications.

In this review the main focus has been put on use of SPR for detection of harmful microorganisms. Most frequently used SPR chips and methods of their modification have been described. The paper also presents recent achievements in field of miniaturization of SPR technique and applying it in portable detection systems dedicated for bacteria identification.

INTRODUCTION

Surface plasmon resonance (SPR) phenomenon has been firstly observed in 1902 by an American scientist R.M. Wood who discovered abnormalities in spectrum of light reflected in metal diffraction grating [1]. It has been proven, that these abnormalities are caused by excitation of surface electromagnetic waves. In 1968 Otto proved that the decrease of intensity of light reflected in attenuated total reflectance method (ATR) is caused by excitation of surface plasmons [2]. Observations of plasmons in other ATR configurations were also conducted by Kretschmann and Reather [3]. In the 80s Liedberg built a first SPR sensor which enabled examinations of interactions between compounds by observing changes of surface refractive index measured with the use of surface plasmons. A few years later commercial SPR sensors (SPR chips) have been introduced.

SPR is a phenomenon that is observed mainly on nanolayers of noble metals (gold in most cases). It can be applied in studies of all types of interactions between analyte present in examined liquid sample and ligand immobilized on the surface of metal, that exhibits affinity to the analyte. The

SPR effect depends on the change of mass that occurs when analyte attaches to the surface what causes the change of refractive index in the proximity of the gold surface (Fig. 1). This change can be noticed by precise observation of monochromatic light beam reflected from the gold. The shift of minimum of intensity of reflected light is understood as shift of resonance angle which can be further calculated as change of mass attached to surface of metal.

In contrast to other methods used to examine interactions between biologically active compounds, SPR does not require use of any additional developing reagents and enables real-time analysis. SPR chips combined with modern surface modification techniques, micro fluidic systems and appropriate software give an unique opportunity to study reaction mechanisms, specificity of ligands and even process kinetics [4]. In this work the focus is put on techniques applied in studies concerning the use of SPR in detection of harmful microorganisms for environmental monitoring and food safety control purposes.

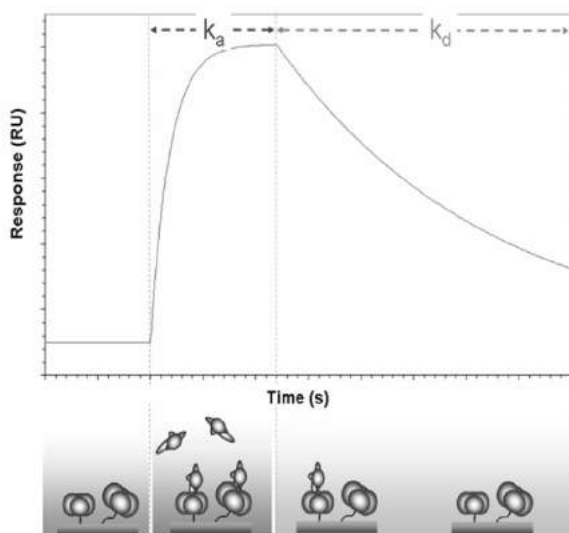


Fig. 1 An example diagram of SPR sensor response changing in time (sensogram). It represents processes of attachment (k_a) and detachment (k_d) of an analyte molecule to ligand bound to the surface of gold [5].

The use of SPR technique in detection of bacteria has been reported frequently. The main advantage of use of SPR method for identification of bacteria species when compared to other methods is speed of analysis. Single SPR experiment utilizing specific antibodies can be performed as fast as in several minutes when traditional standard culture-based identification can take even weeks [6]. More convenient, nucleic acid identification-based methods, utilizing polymerase chain reaction or enzyme linked immunoassays based on

antigen-antibody affinity may take less than an hour but are also slower and require more stages of sample preparation and development to acquire measurable results [7].

SPR TECHNOLOGIES APPLIED IN BACTERIA DETECTION

SPR chips

Standard commercially available planar SPR chips have been successfully used in many cases in detection of bacteria. An important work concerning control of food-borne salmonellosis disease has been done by group of Keusgen, who demonstrated a successful detection of *Salmonella typhimurium* bacteria in milk with the use of standard Kretschmann - Reather type chip offered by Plasmonics [8]. These bacteria have been also detected by means of SPR method in chicken meat by group of Lan, who used Spreeta SPR chip [9]. The same type of chip was also used for detection of milk contamination by *Staphylococcus aureus*. Group of Furlong developed SPR experiment in which *S. aureus* toxin was detected at femtomolar levels [10]. Often chosen chips for bacteria detection (Biacore chips manufactured by GE Healthcare) have been used in detection of *B. Anthracis* [11], *S. typhimurium* [12], *E. Coli* and many other harmful bacteria species [3].

In order to enhance detection level and sensitivity of analyses of bacterial samples some special types of SPR chips have been introduced.

Long range SPR (LRSPR) sensors have been developed to enlarge the distance of possible detection of mass change from around 200 nm from sensor surface to over 1000 nm [13]. This approach helps not only to detect bacteria more precisely what was shown by Vala et al. on example of *E. coli* [14], but also enables observations of larger living cells of higher organisms, as did group of Chabot who demonstrated SPR study of cell toxicity [15].

SPR chips can be modified by introducing nanostructures of noble metals on their surfaces in order to enhance plasmon resonance phenomenon with a phenomenon of localized plasmon resonance [16]. This approach resulted in design of new type of SPR chips - LSPR that were used by Fu et al. in detection of *Salmonella* contamination of food [17].

In the latest trend of SPR research standard SPR chips have been replaced with SPR matrixes that can be considered as chips with many measuring spots on their surfaces. Every spot of such matrix is treated as a single sensing channel and is usually modified by attachment of a different sensing compound. This approach is referred to as SPR Imaging or SPRi and enables to do very fast screening analyses for detection of many different bacteria species at the same time. Such design have been used to screen for 3 popular food poisoning bacteria species by Pilarik et al. [18]. It has been also used for precise

detection of *E. coli* strains by Mondani et al. [19] and to monitor biofilm growth by Abadian et al. [20].

Methods of modification of SPR chips

There are many reported methods of immobilization of ligands used for identification of bacteria species. Ligands are in most cases antibodies against specific bacteria. Fragments of bacterial DNA chains are also used as ligands in order to find bacteria in samples that undergo lysis procedure prior to detection experiments.

Physical adsorption to the surface of SPR chips is applied in case of ligands that easily adhere to surface of gold [6]. It is rarely used because of the low stability of surface modified this way and poor repeatability of experiments. In most cases covalent binding of ligands directly to the surface or via spacing molecule is preferred. This strategy of immobilization is applied in order to attach ligands for bacteria detection - nucleic acids and antibodies [6,7].

Direct stable immobilization on the metallic surface of a chip can be performed through the process of molecular self assembly when the ligand particle possesses free active thiol group [23]. Thiol group of selected compound creates semi-covalent bond with gold. By means of this process a highly organized monolayer of thiol containing particles can be created [21]. The process of binding via thiol affinity to gold is used in most cases to bind a spacer molecule to which a final ligand is attached in further modification steps. As spacer molecules there are often used natural or artificial polymers containing (apart from thiol residue) free functional groups such as carboxyl or amine group, and they are usually modified poly(ethylene glycols) or polysaccharides [23]. The advantage of such way of immobilization is, apart from better selection of chemical routes, an improvement of accessibility of ligand to bacterial analyte.

Spacer molecules containing carboxyl groups are very convenient as they can be used in amine coupling reaction in order to bind virtually any ligand containing amine groups. In this popular reaction carboxyl groups are firstly activated with 1-Ethyl-3-(3-dimethylaminopropyl) carbodiimide (EDC) and N-hydroxysuccinimide (NHS) to form active succinimide esters attached to the surface [24]. These groups very easily react with amine groups of proteins and can be substituted with amine bond. The main limitation of this reaction is that it cannot be performed in environment of buffer containing any amines or other reactive species of nitrogen as they will react and bind with the surface instead of the protein that is intended to be attached. The often problem is the need of washing out sodium azide that is used as a preservative in commercially

available antibodies of the protein solution prior to immobilization as it reacts more effectively with succinimide esters than amine groups of the antibody [21].

Another popular method of linking ligand molecules with surface is the use of biotin-avidin chemistry. As this interaction is very strong it is considered one of the most efficient and reliable means of attachment of ligands to the surface. This approach is mostly used in binding of DNA fragments as sensing molecules. An advantage of this modification technique is a possibility of reversing of the binding what results in easy regeneration of the chip [22].

Use of SPR in portable detection systems

Thanks to great simplicity and short time of detection process SPR can be a good detection method in situations when time of analysis is the key factor or when access to well equipped laboratories and qualified personnel is hard to obtain. There are reports of implementation of SPR technique in portable systems for detection of harmful microorganisms in environmental samples directly on site of suspected contamination. In portable SPR sensing systems the Texas Instruments Spreeta chips are used most frequently. They contain all the components necessary for performance of SPR experiment and have been proven useful in detection of bacteria and bacterial toxins with good sensitivities [25]. The follower of Spreeta - TI Spreeta 2000 chip (Fig. 2) is an even further step in terms of miniaturization and functionality. It contains three measurement channels, out of which one or two can be used as reference channels, and other can be modified by attachment of antibodies, DNA chains etc.

Naimushin et al. developed a portable system able to detect up to 24 analytes including *F. tularensis*, *B. anthracis* and other dangerous bacteria species. The design was called SPIRIT system and was a complete analytical system closed in a suitcase-shaped casing weighting about 3 kg. The sensing principle of SPR was provided by application of 8 Spreeta 2000 - miniature 3-channel sensing chips modified with different antibodies specific against selected bacteria species and viruses [26]. Similar system utilizing Spreeta chips was also designed by Chinowsky for examination of air samples and was installed on board of an aircraft [27]. Duman and Piskin developed a portable SPR detection system utilizing Spreeta chips with attached ssDNA fragments as sensing ligands. It was designed for detection of *M. tuberculosis* and *M. gordonae* DNA chains in clinical samples [28]. Usachev et al. studied bacteria detection in aerosol. Their design was based on planar SPR chips and was demonstrated to successfully detect *E. coli* bacteria in aerosol samples [29]. Finally a portable detection system containing a temperature control module for outdoor environmental analyses has been demonstrated by Naimushin et al. [30].

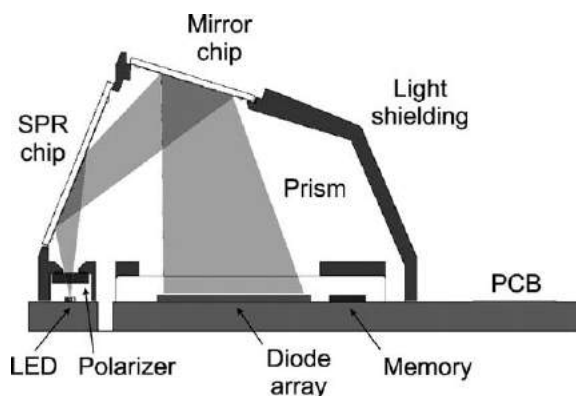


Fig. 2 Schematic illustration of Spreeta 2000 SPR chip [31].

CONCLUSIONS

The modern technique of SPR becomes a very popular method of analytical chemistry in studies of specificity of interactions of biologically active compounds, especially bacteria species and antigens against them. The main reason is the speed of the direct analysis without need to use additional markers. Biological sensors that use SPR are also characterized by low detection limits and high specificity provided by use of specific ligands immobilized on their surfaces. Application of the SPR technique for advanced biological analyses gains popularity because of its constant development and possibilities of implementation in new systems.

REFERENCES

- [1] Wood R.W., On a Remarkable Case of Uneven Distribution of Light in a Diffraction Grating Spectrum, *Proceedings of the Physical Society of London*, 1902, 18, 1, 269–275, DOI:10.1088/1478-7814/18/1/325
- [2] Otto A., Excitation of nonradiative surface plasma waves in silver by the method of frustrated total reflection, *Zeitschrift Für Physik*, 1968, 216, 4, 398–410, DOI:10.1007/BF01391532
- [3] Homola J., Surface plasmon resonance sensors for detection of chemical and biological species, *Chemical Reviews*, 2008, 108, 2, 462–93, DOI:10.1021/cr068107d
- [4] Wijaya E., Lenaerts C., Maricot S., et al., Surface plasmon resonance-based biosensors: From the development of different SPR structures to novel surface functionalization strategies, *Current Opinion in Solid State and Materials Science*, 2011, 15, 5, 208–224, DOI:10.1016/j.cossms.2011.05.001
- [5] ICx Nomadics Inc., Sensiq Explorer Chemistry Manual, 2010

- [6] Starodub N.F., Ogorodniichuk J., Lebedeva T., Shpylovyy P., Immune biosensors based on the SPR and TIRE : efficiency of their application for bacteria determination, 2013, 9032, 2013–2016, DOI:10.1117/12.2044648
- [7] Mauriz E., Calle a., Lechuga L.M., Quintana J., Montoya a., Manclús J.J., Real-time detection of chlorpyrifos at part per trillion levels in ground, surface and drinking water samples by a portable surface plasmon resonance immunosensor, *Analytica Chimica Acta*, 2006, 561, 1-2, 40–47, DOI:10.1016/j.aca.2005.12.069
- [8] Barlen B., Mazumdar S.D., Lezrich O., Kämpfer P., Keusgen M., Detection of Salmonella by Surface Plasmon Resonance, *Sensors*, 2007, 7, 8, 1427–1446, DOI:10.3390/s7081427
- [9] Lan Y., Wang S., Yin Y., Hoffmann W.C., Zheng X., Using a Surface Plasmon Resonance Biosensor for Rapid Detection of Salmonella Typhimurium in Chicken Carcass, *Journal of Bionic Engineering*, 2008, 5, 239–246, DOI:10.1016/S1672-6529(08)60030-X
- [10] Naimushin A.N., Soelberg S.D., Nguyen D.K., et al., Detection of Staphylococcus aureus enterotoxin B at femtomolar levels with a miniature integrated two-channel surface plasmon resonance (SPR) sensor, *Biosensors & Bioelectronics*, 2002, 17, 6-7, 573–84
- [11] Wang D.-B., Bi L.-J., Zhang Z.-P., et al., Label-free detection of B. anthracis spores using a surface plasmon resonance biosensor, *The Analyst*, 2009, 134, 4, 738–42, DOI:10.1039/b813038h
- [12] Medina M.B., Binding interaction studies of the immobilized Salmonella typhimurium with extracellular matrix and muscle proteins, and polysaccharides, *International Journal of Food Microbiology*, 2004, 93, 1, 63–72, DOI:10.1016/j.ijfoodmicro.2003.10.008
- [13] Yanase Y., Hiragun T., Ishii K., et al., Surface plasmon resonance for cell-based clinical diagnosis, *Sensors (Basel, Switzerland)*, 2014, 14, 3, 4948–59, DOI:10.3390/s140304948
- [14] Vala M., Etheridge S., Roach J. a., Homola J., Long-range surface plasmons for sensitive detection of bacterial analytes, *Sensors and Actuators, B: Chemical*, 2009, 139, 59–63, DOI:10.1016/j.snb.2008.08.029
- [15] Chabot V., Miron Y., Grandbois M., Charette P.G., Long range surface plasmon resonance for increased sensitivity in living cell biosensing through greater probing depth, *Sensors and Actuators, B: Chemical*, 2012, 174, 94–101, DOI:10.1016/j.snb.2012.08.028
- [16] Cinel N. a., Bütün S., Özbay E., Silver nano-cylinders designed by EBL used as label free LSPR nano-biosensors, *Plasmonics in Biology and Medicine*, 2011, 7911, 791111I–791111I–7, DOI:10.1117/12.879139

- [17] Fu J., Park B., Zhao Y., Limitation of a localized surface plasmon resonance sensor for Salmonella detection, *Sensors and Actuators, B: Chemical*, 2009, 141, 1, 276–283, DOI:10.1016/j.snb.2009.06.020
- [18] Piliarik M., Párová L., Homola J., High-throughput SPR sensor for food safety, *Biosensors and Bioelectronics*, 2009, 24, 1399–1404, DOI:10.1016/j.bios.2008.08.012
- [19] Mondani L., Roupioz Y., Delannoy S., Fach P., Livache T., Simultaneous enrichment and optical detection of low levels of stressed Escherichia coli O157:H7 in food matrices, *Journal of Applied Microbiology*, 2014, 117, 537–546, DOI:10.1111/jam.12522
- [20] Abadian P.N., Tandogan N., Webster T.A., Goluch E.D., Real-time detection of bacterial biofilm growth using surface plasmon resonance imaging, Proc. 16th Int. Conf. Miniaturized Syst. Chem. Life Sci. MicroTAS 2012, Chemical and Biological Microsystems Society, 2012
- [21] Rusmini F., Zhong Z., Feijen J., Protein immobilization strategies for protein biochips, *Biomacromolecules*, 2007, 8, 6, 1775–89, DOI:10.1021/bm061197b
- [22] Torun O., Hakkı Boyacı I., Temür E., Tamer U., Comparison of sensing strategies in SPR biosensor for rapid and sensitive enumeration of bacteria, *Biosensors & Bioelectronics*, 2012, 37, 1, 53–60, DOI:10.1016/j.bios.2012.04.034
- [23] Lahiri J., Isaacs L., Tien J., Whitesides G.M., A Strategy for the Generation of Surfaces Presenting Ligands for Studies of Binding Based on an Active Ester as a Common Reactive Intermediate: A Surface Plasmon Resonance Study, *Analytical Chemistry*, 1999, 71, 4, 777–790, DOI:10.1021/ac980959t
- [24] Walker J.M., Surface Plasmon Resonance: Methods and protocols
- [25] Dudak F.C., Boyacı I.H., Rapid and label-free bacteria detection by surface plasmon resonance (SPR) biosensors, *Biotechnology Journal*, 2009, 4, 7, 1003–11, DOI:10.1002/biot.200800316
- [26] Chinowsky T.M., Soelberg S.D., Baker P., et al., Portable 24-analyte surface plasmon resonance instruments for rapid, versatile biodetection., *Biosensors & Bioelectronics*, 2007, 22, 9-10, 2268–75, DOI:10.1016/j.bios.2006.11.026
- [27] Naimushin A.N., Spinelli C.B., Soelberg S.D., et al., Airborne analyte detection with an aircraft-adapted surface plasmon resonance sensor system, *Sensors and Actuators B: Chemical*, 2005, 104, 2, 237–248, DOI:10.1016/j.snb.2004.05.020
- [28] Duman M., Piskin E., Detection of Mycobacterium tuberculosis complex and Mycobacterium gordonae on the same portable surface plasmon

resonance sensor, *Biosensors and Bioelectronics*, 2010, 26, 2, 908–912, DOI:10.1016/j.bios.2010.06.071

[29] Usachev E.V., Usacheva O.V., Agranovski I.E., Surface plasmon resonance-based bacterial aerosol detection, *Journal of Applied Microbiology*, 2014, 117, 1655–1662, DOI:10.1111/jam.12638

[30] Naimushin A.N., Soelberg S.D., Bartholomew D.U., Elkind J.L., Furlong C.E., A portable surface plasmon resonance (SPR) sensor system with temperature regulation, *Sensors and Actuators B: Chemical*, 2003, 96, 1-2, 253–260, DOI:10.1016/S0925-4005(03)00533-1

[31] Chinowsky T., Quinn J., Bartholomew D., Kaiser R., Elkind J., Performance of the Spreeta 2000 integrated surface plasmon resonance affinity sensor, *Sensors and Actuators B: Chemical*, 2003, 91, 1-3, 266–274, DOI:10.1016/S0925-4005(03)00113-8

Luminescence properties of Eu^{3+} and Tb^{3+} doped silica-based xerogels

*Michalina Walas¹, Barbara Kościelska¹, Tomasz Lewandowski¹, Marcin Łapiński¹, Wojciech Sadowski¹, Andrzej M. Kłonkowski¹, Wiesław Wiczak², Irena Bylińska²

¹Faculty of Applied Physics and Mathematics, Solid State Department, Gdansk University of Technology, Gabriela Narutowicza 11/12, 80-233 Gdansk, POLAND

²Faculty of Chemistry, Gdansk University, Wita Stwosza 63, 80-308 Gdansk, POLAND

e-mail: mwalas@mif.pg.gda.pl

Keywords: luminescence, lanthanide ions, LED, energy transfer, sol-gel method

ABSTRACT

Pure SiO_2 xerogels and SiO_2 xerogels containing $\text{SrF}_2: \text{Eu}^{3+}/: \text{Tb}^{3+}$ crystals were prepared using sol-gel method. Luminescent spectra showed excitation and emission peaks characteristic to Eu^{3+} and Tb^{3+} $4f - 4f$ transitions. ET $\text{Tb}^{3+} \rightarrow \text{Eu}^{3+}$ has been observed. XRD pattern of SiO_2 matrix confirmed lack of long range order. Patterns of $\text{SiO}_2\text{-SrF}_2\text{:Eu}^{3+}$ and $\text{SiO}_2\text{-SrF}_2\text{:Tb}^{3+}$ showed peaks corresponding to SrF_2 . SEM images have shown agglomerates of particles and presence of pores. FTIR spectra showed bands related to Si-O vibrations and vibrations associated with the OH groups. Thus, $\text{SiO}_2\text{-SrF}_2$ system doped with Eu^{3+} and Tb^{3+} could be a potential candidate for LEDs applications. Review of other materials for LED applications is also presented.

REVIEW - INTRODUCTION

Luminescent properties of rare-earth ions have been widely investigated during last decades because of their possible application for optical sources and amplifiers operating at wavelengths compatible with fiber communications technology. One of the most important materials used in optoelectronics is silica and silicon and in this case rare-earth doping of both, silica and silicon have been areas of major importance [1].

DISCUSSION

Rare-earth doped materials (so called phosphors) play a significant role in light-emitting diodes (LED) technology. LEDs are regarded as the next generation devices in the lighting industry as well as in display systems due to their energy saving character, environment friendliness, small size and long persistence [2]. Generally, phosphor consists of both an activator and a host. The

activator plays major role in obtaining efficient emission and rare-earth ions are widely used as activators due to their unique spectral properties. These properties of RE³⁺ ions arise from the *f–f* transitions within 4*f* orbitals, which are partially shielded by the 5*s* and 5*p* orbitals [3]. The intra-4*f* transitions are parity forbidden; however they are made partially allowed by crystal field interactions mixing opposite parity wavefunctions [1]. Therefore, the influence of the host matrix on the optical transitions within the 4*f* configuration is small, but essential [4].

The emission of Eu³⁺ ion consists of lines in the red spectral area. This lines correspond to transitions from the excited ⁵D₀ level to the ⁷F_J (J=0, 1, 2, 3, 4, 5, 6) of the 4*f*⁶ configuration [4]. The emission of Tb³⁺ is due to transition ⁵D₄–⁷F_J, which is mainly in the green range area. There is also a considerable contribution to the emission from the higher-level emission ⁵D₃ – ⁷F_J, mainly in the blue range area. Luminescence properties of materials doped with both Eu³⁺ and Tb³⁺ ions have been widely investigated for many decades resulting in application of these materials as phosphors in many applications. The most important advantage of those ions is fact that they emit narrow lines and their emission lifetime is long in a wide variety of hosts [1, 5]. These phenomena create the possibility as effective luminescent centers in different hosts, for example [6] and [7].

The influence of various compounds as well as ions co-doped samples containing RE³⁺ ions for luminescent properties of RE³⁺ ions has been largely investigated. For example, presence of Al₂O₃ co-doped silica glass fibers and telluride based glasses has been confirmed to improve the dispersion of rare earth ions in the glass network to limit the concentration quenching of photoluminescence [8, 9]. Another way to increase luminescence properties of RE³⁺ ions is trough co-doping with Bi³⁺ ions. Bi³⁺ ions can function as both an activator and a sensitizer for luminescent materials though the energy transfers between Bi³⁺ and RE³⁺ ions in different host materials [10, 11]. *Yang et al.* [10] have reported red emission enhancement of Ca₂Al₂SiO₇:Eu³⁺ by adding Bi³⁺ ions into the phosphor instead of increasing Eu³⁺ ions concentration. This is effective method for achieving improved luminescence efficiency of phosphors at much lower cost.

Energy (ET) transfer is one of the nonradiative processes in which the excitation energy of donor is transferred to a nearby acceptor via long-range dipole-dipole interactions. Energy transfer between RE ions has been widely examined due to its possible application in various technologies. For example, [12] and [13] were investigating energy transfer from Gd³⁺ to Eu³⁺ ions in silica xerogels that find application in phosphors and in fluorescent lamps to convert the ultraviolet light to visible light. The electronic energy absorbed as UV

photon by donor Gd^{3+} ion migrates within the material and finally the energy is transferred to a visible-luminescent acceptor Eu^{3+} ion. Energy transfer between Eu^{3+} and Tb^{3+} entrapped in different host matrices has been also largely investigated, e.g. in the aluminoborosilicate glasses systems [14] or in the Y_2O_3 nanosheets and nanorods [15]. In both situations results showed that Eu^{3+} and Tb^{3+} doped systems may be promising luminescence materials for the development of LEDs.

One of the most widely used techniques of fabrication luminescent materials is sol-gel method. This technique is very flexible route for the fabrication of a large variety of photonic materials in various configurations, such as monoliths, coatings, fibers, films etc. It is a convenient way to produce at low temperatures, high purity and chemical homogeneity optical materials [12]. Sol-gel method uses metal alkoxides as precursors for the synthesis and production of glasses, ceramics and composites through a series of chemical-physical processes, including hydrolysis, condensation and thermal treatment [16]. In case of host material, it should have excellent physical, mechanical and chemical stability. For example, silica glasses have been of particular interest due to their advantages such as small thermal expansion coefficient, good thermal and chemical stability in comparison with conventional luminescence glasses prepared using melt-quenching method. Unfortunately, luminescence intensities of silica glasses are relatively low due to their high phonon vibrational energy which quenches luminescence of rare earth ions [17]. In order to improve luminescence properties of systems based on silica matrices (e.g. glasses, xerogels) one can dope them with low phonon energy nanoparticles. For example, *S. Georgescu et al.* [18] have investigated Er^{3+}/Yb^{3+} co-doped CaF_2 nanocrystals in sol-gel derived glass-ceramics. Similar nanomaterials have been investigated as a host for luminescence ions such as fluorides (e.g. $NaYF_4$ [19]), the III-nitrides (e.g. GaN [20]) or silver nanoparticles [21]. One of the most investigated nanomaterials for luminescence application is strontium fluoride SrF_2 . For example, [22] presents glass-ceramics with embedded SrF_2 nanophase enriched into the rare earth ions. The properties of SrF_2 such as much smaller size of nanocrystals than the visible wavelength and very similar refractive index between nanocrystals and glassy host are considered. Therefore, glass-ceramics combine excellent luminescent properties connected with presence of the nanophase with the mechanical, chemical and physical properties of glasses.

EXPERIMENTAL - INTRODUCTION

Oxyfluoride glass-ceramics have been extensively studied due to their potential applications as host matrices for optical active rare-earth (RE) ions

because they combine the low-phonon energy ascribed to the fluoride nanocrystals with the thermal, chemical and mechanical stability of oxide glasses [23].

Sol-gel technique is one of the most widely used methods for optical materials fabrication because of the simplicity of this method, as well as low cost and in contrast to conventional melt-quenching technique, ability to perform it at room temperatures. Finally, glass-ceramics are obtained by heat treatment of precursor glasses, obtained by the sol-gel method. Unfortunately, hydroxyl groups (OH) present in samples made by the sol-gel technique are responsible for quenching the luminescence of the RE³⁺ ions, but during the heat treatment process they are partially eliminated [12].

In the present work, the lanthanide ions have been embedded in two silica-based matrices: SiO₂ and SiO₂-SrF₂. The matrices were prepared by the sol-gel method and then heat-treated. Their structural characteristics and luminescence properties were investigated and compared. Preliminary results suggest that SiO₂ based phosphors are potential candidates for LED applications [2].

EXPERIMENTAL METHODS

Silica gels have been prepared by sol-gel method. Tetraethylorthosilicate (TEOS) has been dissolved in the ethyl alcohol and in the next step water was added. Rare earth nitrates RE (NO₃)₃ (RE=Eu³⁺, Tb³⁺) have been dissolved into ethyl alcohol and added to the solution. The molar ratio of TEOS: CH₃COOH: H₂O was 1:8:4. The ammonia was used as catalyst and the solution has been stirred for 1 hour to form a homogeneous mixture. Obtained sol was allowed to form gel at room temperature and then has been dried in 120°C for 3 hours. Finally, xerogels were heat treated in different temperatures to partially eliminate presence of OH groups in samples. In result, samples SiO₂:RE³⁺ were obtained.

The preparation process of mixed RE³⁺ containing silica/strontium fluoride solution involved introduction of SrF₂: RE³⁺ crystal phase obtained by precipitation method into the silica solution. The drying process was identical as described for the previous sample. Resulting xerogels were heat treated in order to obtain glass-ceramics samples SiO₂:SrF₂:RE³⁺.

XRD measurements were performed on Philips XPERT PLUS diffractometer with Cu-K α radiation ($\lambda=0.154$ nm). The size of crystallites in SiO₂:SrF₂:RE³⁺ was estimated based on Scherrer's equation. FTIR measurements were carried out on Perkin-Elmer Frontier MIR/FIR spectrometer with TGS detector. The measurements were performed on pellet samples mixed with potassium bromide KBr in weight ratio ([Sample]: [KBr]) 1:100. The spectra

were taken in the mid-infrared range. SEM images were performed on FEI QUANTA FEG 250 for powdered samples. Luminescent emission and excitation spectra were investigated on HORIBA JOBIN YVON FluoroMax-4 spectrofluorometer. Luminescence measurements required pellet samples with weight ratio [Sample]: [KBr] 1: 1. All results are presented below.

RESULTS AND DISCUSSION

XRD measurements

Fig.1. presents X-Ray spectrum of xerogel matrix SiO_2 doped directly with Eu^{3+} ions heated to 1000°C . Characteristic amorphous halos with no peaks corresponding to crystalline phase indicate lack of long range periodicity in the sample. Spectra do not show any indication of silica crystallization as well.

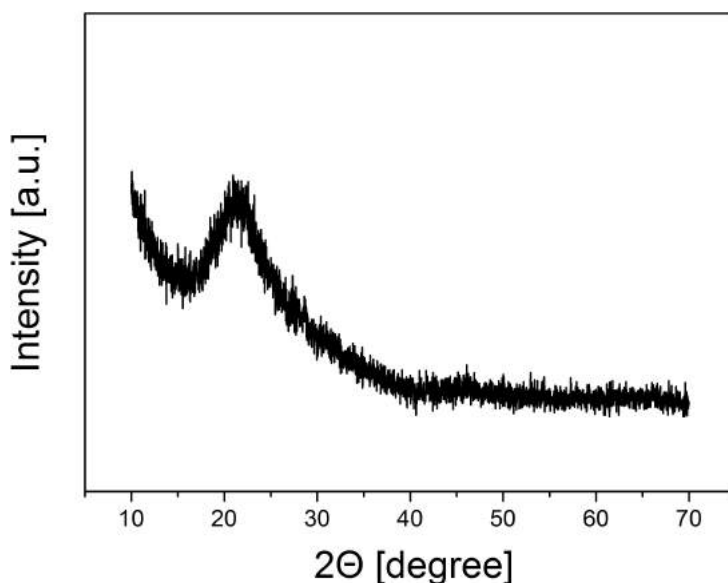


Fig. 1 X-ray spectrum of $\text{SiO}_2:\text{Eu}^{3+}$ (1000°C) sample.

The X-Ray diffraction spectra of $\text{SiO}_2\text{-SrF}_2:\text{Eu}^{3+}$ (a) and $\text{SiO}_2\text{-SrF}_2:\text{Tb}^{3+}$ (b) samples dried at 120°C are presented in Fig.2. Structural differences are clearly observable as a result of loading silica matrix with strontium fluoride crystalline phase. One can observe peaks corresponding to SrF_2 phase in both silica-strontium fluoride systems: doped with Eu^{3+} and Tb^{3+} ions. An amorphous halo is seen in those X-Ray diffraction spectra, however the intensity is low. Again, there are no peaks corresponding to crystalline silica.

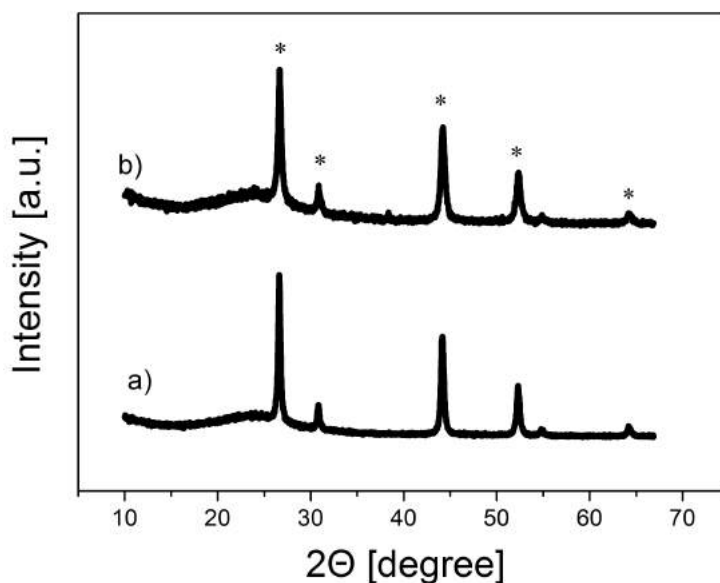


Fig. 2 X-ray spectrum of: (a) $\text{SiO}_2\text{-SrF}_2\text{:Eu}^{3+}$ (120°C) and (b) $\text{SiO}_2\text{-SrF}_2\text{:Eu}^{3+}$ (120°C) samples.

The average diameter of crystallites D was estimated based on Scherrer's equation (1) using data collected during XRD measurements:

$$D = \frac{k\lambda}{\beta \cos\theta} \quad (1)$$

where k is the shape factor, $\lambda(=0.154\text{nm})$ represents the wavelength of $\text{Cu K}\alpha$ radiation, θ is the Bragg angle of X-Ray diffraction peak and β represents corrected half width of the diffraction peak. The mean size of SrF_2 diameter in case of sample $\text{SiO}_2\text{-SrF}_2\text{:Eu}^{3+}$ was evaluated to be 48nm while for $\text{SiO}_2\text{-SrF}_2\text{:Tb}^{3+}$ the estimated size is 87nm . It was consistent with the aim of preparing silica matrices loaded with nanocrystallites that are preferred due to their enhancing of luminescent properties of RE^{3+} ions [18].

FTIR measurements

Fourier transform infrared (FTIR) spectroscopy was used to analyze the structural composition of silica matrix SiO_2 doped directly by Eu^{3+} ions as well as SiO_2 loaded with SrF_2 crystals doped with Eu^{3+} ions. FTIR spectrum of $\text{SiO}_2\text{:Eu}^{3+}$ sample heat-treated at 1000°C is shown on Fig.3. Bands present on this spectrum correspond to several types of vibrations. In the spectral region of

400-1200 cm^{-1} observed bands are due to the vibrations of silica network. The band at 474 cm^{-1} is attributed to Si-O-Si bond bending vibrations, similar to band at approximately 808 cm^{-1} which is associated with symmetric stretching vibrations of Si-O-Si groups. At 1116 cm^{-1} one can observe band corresponding to asymmetric stretching vibrations of Si-O-Si groups.

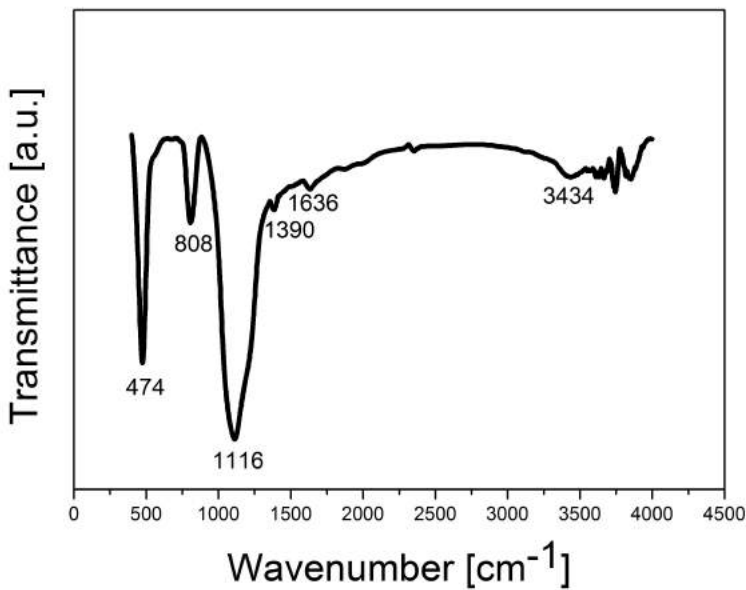


Fig. 3 FTIR spectrum of $\text{SiO}_2:\text{Eu}^{3+}$ (1000°C) sample.

Next, spectral region consist bands attributed to the OH groups and molecular water in the sample. Weak band observed at approximately 1390 cm^{-1} corresponds to the vibrations of H-O-H groups. At 1636 cm^{-1} one observes another weak band attributed to the bending vibrations of silanol Si-OH groups. The last band at app. 3434 cm^{-1} corresponds to stretching vibrations of OH groups.

Fig.4. presents FTIR spectrum of the SiO_2 sample loaded with SrF_2 nanocrystals doped with Eu^{3+} ions (dried at 120°C). One can observe several bands attributed to the presence of water in the samples prepared by sol-gel method. The broad band of high intensity is observed at around 3440 cm^{-1} corresponds to the vibrations of OH groups. The band at 1632 cm^{-1} corresponds to bending vibration of silanol Si-OH groups.

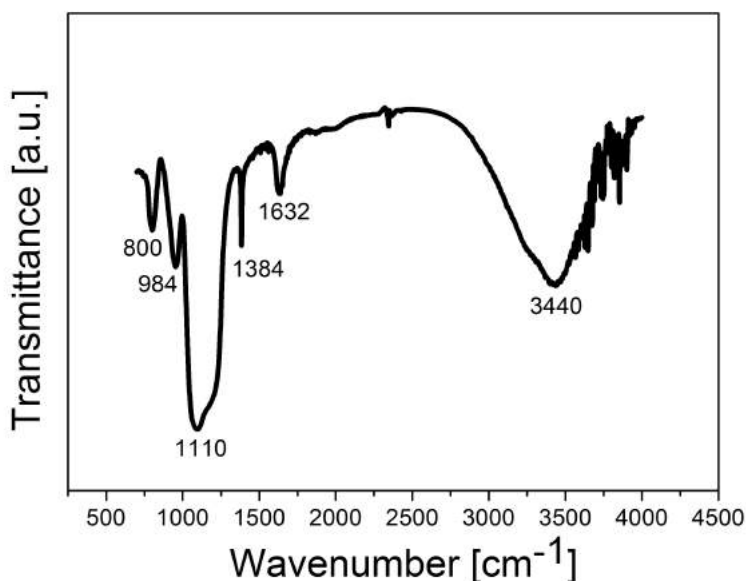


Fig. 4. FTIR spectrum of $\text{SiO}_2\text{-SrF}_2\text{:Eu}^{3+}$ (120°C) sample.

The band at 1110 cm^{-1} is assigned to asymmetric stretching vibrations of Si-O-Si bridging bonds. The bands at 984 cm^{-1} and 800 cm^{-1} are attributed to stretching vibrations of Si-OH groups [16, 24].

SEM measurements

SEM images have been taken in order to investigate the structure of the prepared samples. Fig.5. presents SEM image of $\text{SiO}_2\text{:Eu}^{3+}$ heat-treated in 1000°C sample. Image has been taken at 20000x magnification. Amorphous character of silica matrix is confirmed which corresponds to the X-Ray diffraction spectrum of sample, although in this case the structure appears to be dense due to removal of water molecules during the heat-treatment procedure [16].

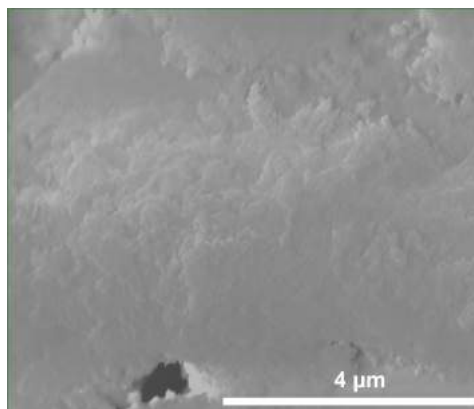


Fig. 5 SEM image of SiO₂:Eu³⁺ (1000°C) sample

Fig.6. shows SEM image of SiO₂-SrF₂:Eu³⁺ (a) and SiO₂-SrF₂:Tb³⁺ (b) dried in 120°C samples. Images have been taken at 20000x magnification. The structure of samples presented on (a) and (b) images has similar character – no significant morphological differences are observed between samples.

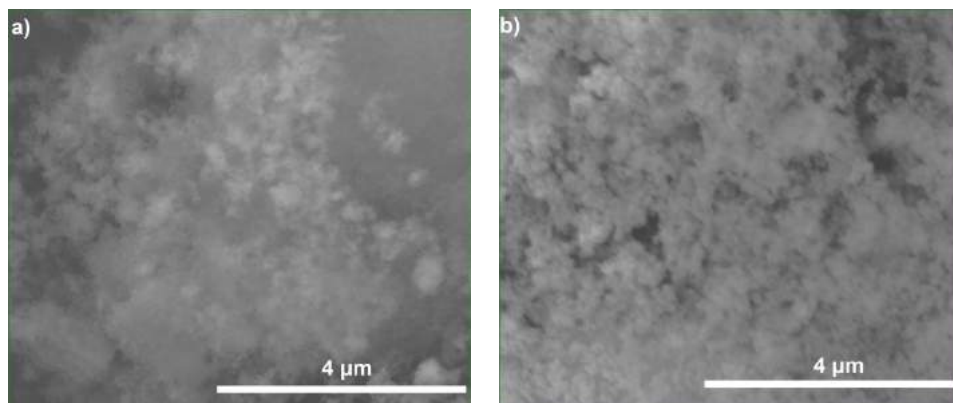


Fig. 6 SEM images of: (a) SiO₂-SrF₂:Eu³⁺ (120°C) and (b) SiO₂-SrF₂:Tb³⁺ (120°C) samples.

One can observe agglomerates of particles and presence of pores confirming amorphous character of these samples. Unfortunately, presence of crystalline phase is not confirmed due to insufficient magnification achieved during measurements of these samples. Therefore, both images (a) and (b) reflect structure of amorphous silica matrices, confirmed with the XRD spectra. For sample SiO₂-SrF₂:Eu³⁺ the EDX spectrum has been made to investigate the elemental analysis (Fig.7.).

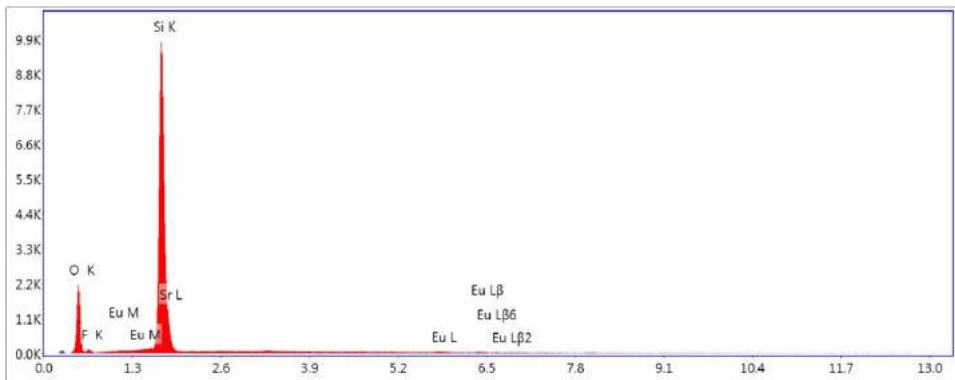


Fig. 7 EDX spectrum of $\text{SiO}_2\text{-SrF}_2\text{:Eu}^{3+}$ sample. Intensity of signal is presented in function of X-Ray radiation energy in keV.

Representative peaks correspond to O, Si, Sr, F and Eu are clearly identify. Although, results obtained for light elements, e.g. F could not be accurate due to the equipment limitations. In case of Eu results, the difference between theoretical and measured amount of this element could be due to low mole percent of RE^{3+} ions applied in prepared samples.

Luminescence measurements

Fig.8. presents luminescence spectra of sample $\text{SiO}_2\text{-SrF}_2\text{:Tb}^{3+}$ dried in 120°C . Excitation spectrum (a) achieved when sample was irradiated by $\lambda_{\text{em}}=543\text{nm}$ light wavelength consists several peaks corresponding to $4f - 4f$ transitions into Tb^{3+} ions: ${}^7\text{F}_6 \rightarrow {}^5\text{D}_0$ (317nm), ${}^7\text{F}_6 \rightarrow {}^5\text{L}_9$ (351nm), ${}^7\text{F}_6 \rightarrow {}^5\text{D}_3$ (378nm), ${}^7\text{F}_6 \rightarrow {}^5\text{D}_4$ (486nm). Peaks observed in emission spectrum (b): 478nm, 543nm and 583nm are attributed to the ${}^5\text{D}_4 \rightarrow {}^7\text{F}_6$, ${}^5\text{D}_4 \rightarrow {}^7\text{F}_5$, ${}^5\text{D}_4 \rightarrow {}^7\text{F}_4$ transitions, respectively [25].

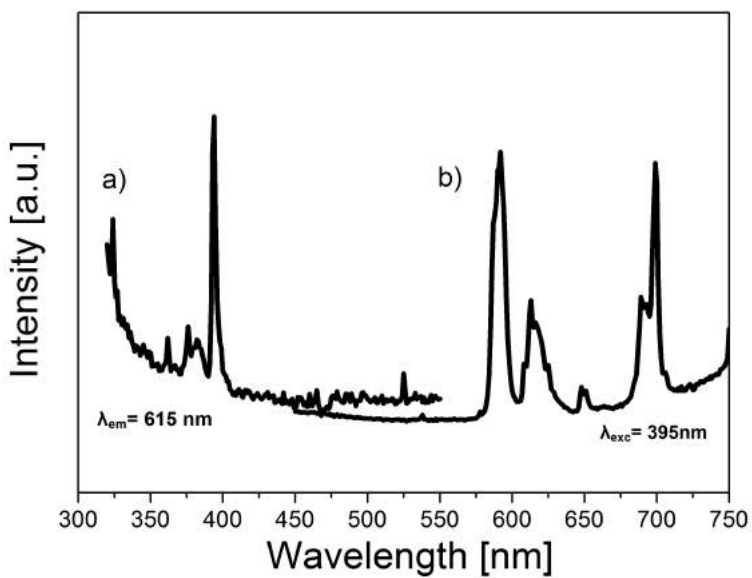


Fig. 8 Luminescence spectra of $\text{SiO}_2\text{-SrF}_2\text{:Tb}^{3+}$ (120°C) sample.

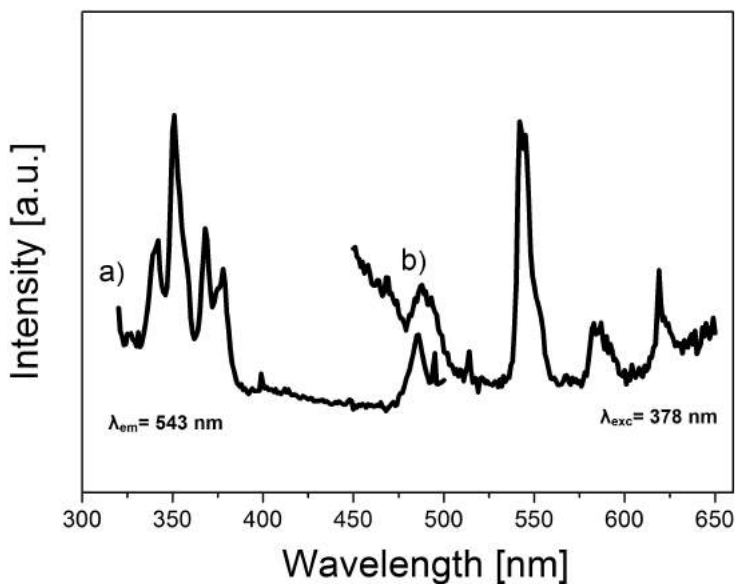


Fig. 9 Luminescence spectra of $\text{SiO}_2\text{-SrF}_2\text{:Eu}^{3+}$ (120°C) sample.

Excitation (a) and emission (b) spectra of $\text{SiO}_2\text{-SrF}_2\text{:Eu}^{3+}$ dried in 120°C are presented on Fig.9. The main excitation peaks for both samples ($\lambda_{\text{em}}=615\text{nm}$)

can be assigned to $^5D_4 \rightarrow ^7F_0$ (362nm), $^5L_7 \rightarrow ^7F_0$ (383nm), $^5L_6 \rightarrow ^7F_0$ (394nm) and $^5D_2 \rightarrow ^7F_0$ (465nm) transitions, respectively. Emission spectra achieved with $\lambda_{exc}=395\text{nm}$ wavelength show peaks corresponding to $4f - 4f$ of Eu^{3+} ions: 578nm ($^5D_0 \rightarrow ^7F_0$), 592nm ($^5D_0 \rightarrow ^7F_1$), 613nm ($^5D_0 \rightarrow ^7F_2$), 651nm ($^5D_0 \rightarrow ^7F_3$) and 700nm ($^5D_0 \rightarrow ^7F_0$), respectively [25].

Luminescence spectra of silica xerogel doped with Eu^{3+} and Tb^{3+} ions dried at 120°C are demonstrated in Fig.10.

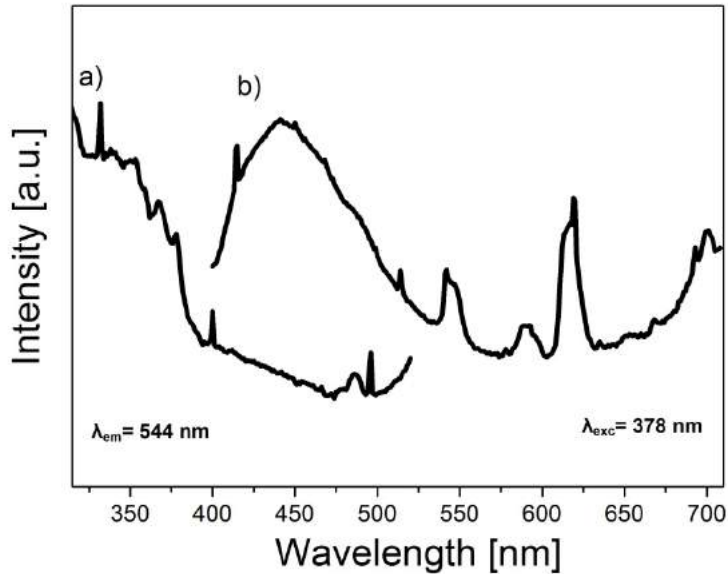


Fig. 10 Luminescence spectra of $\text{SiO}_2: \text{Eu}^{3+}: \text{Tb}^{3+}$ (120°C) sample.

Significant bands in the excitation spectrum (a) have been achieved when sample was irradiated by $\lambda_{em}=544\text{nm}$ wavelength. They can be found at 378, 485 and 400nm which correspond to the $4f - 4f$ transitions $^7F_6 \rightarrow ^5D_3$, $^7F_6 \rightarrow ^5D_4$ of Tb^{3+} and $^7F_0 \rightarrow ^5L_6$ of Eu^{3+} ions, respectively. Emission spectrum (b) ($\lambda_{exc}=378\text{nm}$) consist several peaks corresponding to characteristic transitions in Tb^{3+} : 542nm ($^5D_4 \rightarrow ^7F_5$) and Eu^{3+} : 592nm ($^5D_0 \rightarrow ^7F_1$), 619nm ($^5D_0 \rightarrow ^7F_2$) and 701 ($^5D_0 \rightarrow ^7F_4$). There is also a broad band present ($\lambda_{max}=441\text{nm}$) arising from the excitation of the silica matrix. Presence of bands corresponding to $4f - 4f$ transitions of Eu^{3+} ions in the emission spectrum achieved for the λ_{exc} characteristic to the Tb^{3+} excitation suggest energy transfer (ET) between Tb^{3+} and Eu^{3+} ions. As a result, sample doped with Eu^{3+} and Tb^{3+} ions emits in bluish-green, green and greenish-yellow range. Additionally, radiating in blue range takes place as a result of silica excitation [24].

CONCLUSIONS

Samples containing silica matrices doped directly by RE³⁺ (RE=Tb, Eu) ions and loaded with SrF₂ ions doped with RE³⁺ ions were synthesized by sol-gel technique. Their structure and luminescence properties were investigated. Preliminary results confirm amorphous character of silica matrices and in case of samples loaded with SrF₂ presence of the nanocrystalline phase. The emission and excitation spectra of all samples exhibit peaks corresponding to the 4*f* – 4*f* transition in RE³⁺ ions. Additionally, when sample of silica doped with both, Eu³⁺ and Tb³⁺ ions was irradiated by the wavelength $\lambda_{exc}=378\text{nm}$ (characteristic for the Tb³⁺ excitation) peaks corresponding to Eu³⁺ and Tb³⁺ emission occur indicating that energy transfer Tb³⁺→Eu³⁺ takes place. In the next step of research samples of silica matrix loaded with SrF₂ nanocrystals doped with both Eu³⁺ and Tb³⁺ ions need to be prepared and their structural and luminescence properties should be investigated to determinate possibility of using the material as a potential candidate for LED phosphors [24].

REFERENCES

- [1] A.J. Kenyon / *Progress in Quantum Electronics* 26 (2002) p. 225-284 doi:10.1016/S0079-6727(02)00014-9
- [2] Fuwang Mo, Peican Chen, Anxiang Guan, Xinguo Zhang, Chengyi Xu, Liya Zhou / *Ceramics International* (Received 09.07.2014, accepted 28.08.2014)
- [3] Corneliu S. Stan, Nathalie Marcotte, Marius S. Secula, Marcel Popa / *Optical Materials* 35 (2013) 1741-1747 doi:10.1016/j.optmat.2013.05.025
- [4] B. Szpikowska-Sroka, M. Żądło, R. Czoik, L. Żur, W.A. Pisarski / *Journal of luminescence* 154 (2014) p.290-293 doi:10.1016/j.jlumin.2014.05.004
- [5] Y. Kondo, K. Tanaka, R. Ota, T. Fujii, Y. Ishikawa / *Opt. Mat.* 27, (2005) 1438-1444 doi:10.1016/j.optmat.2004.10.007
- [6] S. Zhao, F. Xin, S. Xu, D. Deng, L. Huang, H. Wang, Y. Hua / *Journal of Non-Crystalline Solids* 357, p. 2424-2427 doi:10.1016/j.jnoncrysol.2010.11.092
- [7] I. Cho, J-G. Kang, Y. Sohn / *Journal of Luminescence* 157 (2015) p. 264-274 doi:10.1016/j.jlumin.2014.09.006
- [8] Sinaa Ibrahim, Harth Ibrahim / *International Journal of Application or Innovation in Engineering & Management* 2 (2013), p.111-116
- [9] G. Blasse, B.C. Grabmaier: *Luminescent Materials* (Springer, Berlin 1994)
- [10] A.M. Klonkowski, B. Grobelna, S. Lis, S. But / *Journal of Alloys and Compounds* 380 (2004) p. 205-210 doi:10.1016/j.jallcom.2004.03.045
- [11] J.-C.G. Bünzli, G.R. Choppin (Eds.), *Lanthanide Probes in Life Chemical and Earths Sciences: Theory and Practice* Elsevier Amsterdam (1989) (Chapter 7)

- [12] R. Guo, S. Tang, F. Zheng, Z. Yang, D. Tan / *Journal of Alloys and Compounds* 550 (2013) p. 459-462 doi:10.1016/j.jallcom.2012.10.077
- [13] S. Balaji, K. Biswas, A.D. Sontakke, G. Gupta, D. Ghosh, K. Annapurna / *Spectrochimica Acta Part A: Molecular and Biomolecular Spectroscopy* 133 (2014) p. 318-325 doi:10.1016/j.saa.2014.04.113
- [14] A. Monteil, S. Chaussedent, G. Alombert-Goget, M.J. Gaumer Obriot, S.L.J. Ribeiro, Y. Messaddeq, A. Chiasera, M. Ferrari / *J. Non-Cryst. Solids* 353 (2007) 2150-2156 doi:10.1016/j.saa.2014.04.113
- [15] P. Yang, X. Yu, H. Yu, T. Jiang, X. Xu, Z. Yang, D. Zhou, Z. Song, Y. Yang, Z. Zhao, J. Qiu / *Journal of Luminescence* 135 (213) p. 206-210 doi:10.1016/j.saa.2014.04.113
- [16] H. Zhu, Z. Xia, H. Liu, R. Mi, Z. Hui / *Materials Research Bulletin* 48 (2013) 3513-3517 doi:10.1016/j.materresbull.2013.05.045
- [17] L. Jin, X. Lei, X. Du, W. Chen, L. Ren / *Optik* 125 (2014), p. 4035-4038 doi:10.1016/j.ijleo.2014.03.003
- [18] S. Georgescu, A.M. Voiculescu, C. Matei, C.E. Secu, R.F. Negrea, M. Secu / *Journal of Luminescence* 143 (2013) 150–156 doi:10.1016/j.jlumin.2013.04.002
- [19] A. Santana-Alonso, A.C. Yanes, J. Méndez-Ramos, J. del-Castillo, V.D. Rodríguez / *Journal of Non-Crystalline Solids* 356 (2010) 933–936 doi:10.1016/j.jnoncrysol.2009.12.023
- [20] M. Bouguerra, M.A. Belkhir, D. Chateigner, M. Samah, L. Gerbous, G. Nouet / *Physica E* 41 (2008) 292–298 doi:10.1016/j.physe.2008.07.010
- [21] Arun Kumar K V, Revathy K P, Prathibha Vasudevan, Sunil Thomas, Biju P R, Unnikrishnan N V / *Journal of Rare Earths*, Vol. 31, No. 5, May 2013 doi:10.1016/S1002-0721(12)60301-9
- [22] X. Qiao et al. / *Journal of Luminescence* 131 (2011) 2036–2041 doi:10.1016/j.jlumin.2011.05.012
- [23] Jing Huang, Yantang Huang n , Tianjiao Wu, Yu Huang, Peijin Zhang / *Journal of Luminescence* 157 (2015) 215-219
- [24] M. Zalewska, A.M. Klonkowski / *Optical Materials* 30 (2008) 725–729 doi:10.1016/j.optmat.2007.02.021
- [25] Y.I. Choi et al. / *Journal of Luminescence* 158 (2015) 27–31 doi:10.1016/j.jlumin.2014.09.030

Innovative screening device for high-sensitive chemical vapors detection

*Anna Zalewska¹

¹ Military Institute of Chemistry and Radiometry, Warsaw, POLAND

e-mail: a.zalewska@wichir.waw.pl

Keywords: *Differential ion mobility spectrometry, DMS, chemical warfare agents, explosives*

ABSTRACT

In Military Institute of Chemistry and Radiometry was made portable contamination signaling device (PRS-1) used for detection and identification wide range of chemical substances. PRS-1 was constructed based on the differential ion mobility spectrometry (DMS). DMS belongs to the group of methods based on an ion mobility effect and it can be used in screening mobile devices for high-sensitive detection of chemical warfare agents, explosives and drugs. Detection possibilities of apparatus using the DMS method are based on the occurrence of different mobility of ions (K) in the alternating electric field.

Our device is designed for the detection of chemical warfare agents, and initial testing of the detection explosives yielded positive results and form the basis for the concept of further research. Innovative solutions applied to the device PRS-1 cause that its technical parameters are very high – one of the best in the world. Its high detection parameters allow for take a chance to select biomarkers in exhaled air. Based on the collected spectra will be determined the differences in position and amplitude of received signals, what can be used to find correlation between the occurrence of pathogenic changes and particular volatile organic compound (VOC) to define biomarkers. Obtained results will provide a basis for further research to develop applications leading to early diagnosis of asymptomatic diseases.

In summary it can be concluded that the DMS method allow for detection of chemical vapors up to ppb-ppt level using ion mobility determinate on the experimental way (K) for different voltages of the electric field (E).

INTRODUCTION

Currently one of the most important civilization problems is to ensure the safety of civilians. Appearing terrorist threats associated with attempts of bringing explosive materials (EM) or their components to the public transport (planes, trains, ships, subways, buses, etc.) determine the need for their rapid and efficient detection, thereby justify the implementation of the analytical instruments which use the latest achievements of technical ideas. As a result of

continuous development of science is creation of new and more sophisticated technological solutions which may find diverse and more widely applications. One of the areas which, due to its specificity must be open to innovative products is forensics. The need to respond to the changing methods and tools of crime cause its continuous development. There are many analytical methods used throughout the country in forensic laboratories, with the modern equipment often require the development of appropriate, additional procedures and methods of sampling and analysis, particularly in-situ. The most preferred would be the use of rapid screening methods for detection at the scene, and in the next step to collect and securing samples for laboratory tests.

Screening methods are characterized by a short analysis time, high sensitivity and the ability to develop a non-destructive method of collecting evidence, which is important in forensic studies. There are many known techniques used for explosives or chemical warfare agents detection but diverse places and ways of their use as well as requirement of really low detection limit allowing for detection on the “dog's nose” level are reason for their continues improvement. One of the methods used for detection of traces amount is differential ion mobility spectrometry (DMS) which allows for detection of very low concentration analyzed substances.

MATERIALS AND METHODS

The detection systems which are most commonly used are the current methods using the ion mobility effect i.e. IMS (Ion Mobility Spectrometry), ITMS (Ion Track Mobility Spectrometry), IIMS (Ion Inverse Mobility Spectrometry), FAIMS (Field Asymmetric Ion Mobility Spectrometry). ECD - electron capture detection is the primary technique used as a base to the modern ones. The advantages of these techniques include mobility of detectors, their ease of use, relatively low cost, short-time analysis, the detection of a large number of key explosives materials (EM) and high sensitivity particularly in the case of the FAIMS [1].

Ion mobility spectrometer (IMS) as an analytical tool was first presented at the turn of the year 1960-1970 by M.J. Cohen and F.W. Karasek. In the 90s of the last century was a major development in the work on ion mobility spectrometry technology and IMS-based devices, which reduced the size of spectrometers. IMS technique was used to detect trace amounts of many compounds, such as chemical warfare agents, drugs, explosives and pollutants. Also, some other advantages of ion mobility spectrometer may include, analytical flexibility and the ability to monitor compounds in the real time [2]. The obtained sample is introduced into the spectrometer then is heated to obtain vapours of analyte which leads to the ionisation and reaction region by passing

clean dry carrier gas (air) (Fig. 1). The ionization region is a source of ionizing radiation - β -emitter ^{63}Ni . The electrons react with the flowing particles and allow the formation of negative ions for molecules with a *high electron affinity*, such as explosives. In the ionization region can be also chloride anions which react with molecules EM to form charged ions. They are formed due to the presence of additional gas (dopant) which is usually organic chlorine compound such hexachloroethane or methylene chloride [2]. Across the length of the ion mobility spectrometer is generated an electrical field. The polarity of this field is positive or negative, depending on the substance. Ions with the proper charge can move through the reaction region to the drift region due to an instantaneous opening and closing of the shutter grid. Drift of ions takes place at atmospheric pressure and the time needed for traveling the drift region and reach to the electrodes (Faraday - Plate) is called the drift time (t).

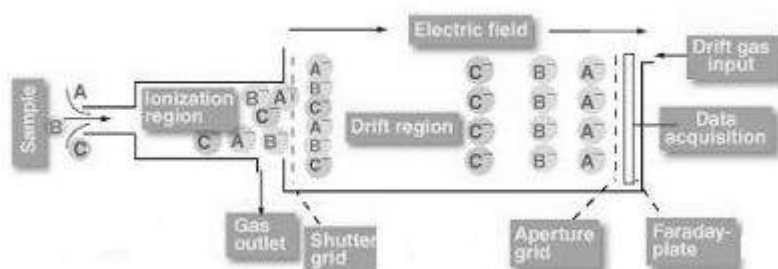


Fig. 1 Ion drift trajectory in IMS [3]

Drift time is a function of the charge, mass, size of the ion and is related to the ion velocity (v), mobility (K) and the drift voltage (V), as shown by the following formulas:

$$v = \frac{d}{t} \quad (1)$$

$$K = \frac{v}{E} = \frac{d^2}{Vt} \quad (2)$$

where:

v – ion velocity [$\text{cm} \cdot \text{s}^{-1}$],

d – drift length [cm],

t – drift time [s],

K – ions mobility [$\text{cm}^2 \cdot \text{V}^{-1} \text{s}^{-1}$],

V – drift voltage (V),

E – electric field strength [$\text{V} \cdot \text{cm}^{-1}$].

Type of generated ions and their mobility are characteristic for the substance, and allows the identification of analyte. Reactions that occur between the ions in the classic IMS have been the subject of many experimental work and research that consist in determining their effect on the shape and arrangement of the peaks in the spectrograms [4-7]. The literature describes two methods based on ion mobility which are a variation of the classical IMS. One of them is the ion trap mobility spectrometry (ITMS), and the second the ion inverse mobility spectrometry (IIMS). Both ITMS as IMS separates the ionized substances then measures the mobility of ions in an electric field. Subsequently vapour samples are ionized in the ionization chamber through the semipermeable membrane. In contrast to the IMS, the ionization process allows to equilibrate outside the electric field. The ions pass into the drift region where are accelerated by an electric field and directed to the collector. The ITMS detector has no the shutter grid allowing more of the ions penetrate into the drift region. Improving the IMS analysis system by ITMS technology allows for significant improvement in the efficiency of ionization and also the sensitivity of the detector. The inverted impulse, applied to the shutter grid is used in the IIMS which in contrast to the IMS remains open most of the time. This allows increasing the resolution to 60%. This recent method is in the area of research and not yet available in any IIMS detector [8].

Nonlinear ion mobility depending on the intensity of the electric field are defined in various ways, including as follows:

- DMS (Differential Ion Mobility Spectrometry), which examines the growth of ion mobility caused by changes in the electric field (E) and is also known as IMIS (Ion Mobility Increment Spectrometry) or SIMI (Spectrometry of Ion Mobility Increment);
- FAIMS (High Field Asymmetric Waveform IMS) – technique based on the presence of a strong electric field as a time dependent periodic asymmetric wave, also referred to as (RF)IMS (Radio-frequency).

It follows that the concept of DMS can be a general term and include other names introduced in order to determine the characteristics of the specific methods. While the IMIS (SIMI) and INLDS are generally reserved for Russian literature, in which the phenomenon of non-linearity, as characteristic of this phenomenon is also defined as NZPI (rus. Nelinejnaja Zavisimost 'Podvizhnosti Ionov), and the main (most common) differential IMS takes the name of FAIMS due to the asymmetry in the result of superposition of applied waves [9].

One of the new methods, which might be used in screening mobile devices to high-sensitive detection of chemical warfare agents, explosives and drugs is differential ion mobility spectrometry (DMS), which belongs to the group based on an ion mobility effect. Existing mobile detectors based of this method are

characterized by the nominally high sensitivity and enable the detection of multiple chemical compounds such as explosives, chemical warfare agents or drugs. Detection possibilities of apparatus using the DMS method are based on the occurrence of different mobility of ions (K) in the alternating electric field. High and asymmetric voltage (RF, HSV) is applied perpendicularly to the direction of the gas flow thus providing a separation field. Under its influence, ion mobility become dependent on the intensity of the electric field which does not determine the analyte detection (Fig. 2).

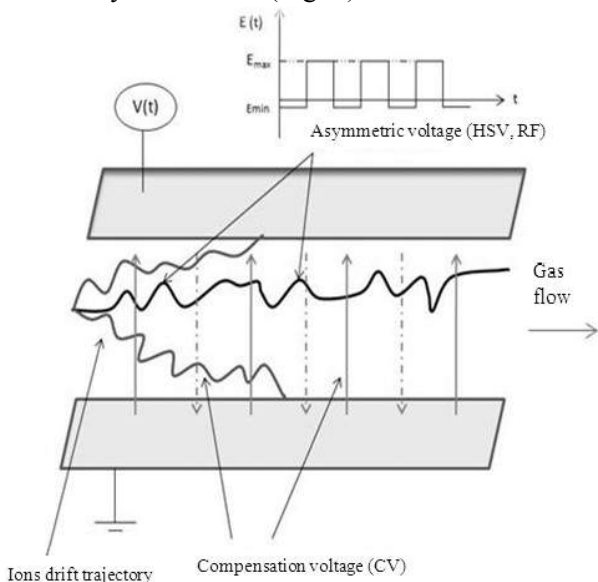


Fig. 2 Ion drift trajectory in DMS

The high voltage causes a change in the ion drift trajectory what cause collision with ancillary electrode and are neutralized. In this case, their detection is not possible (Figure 3).

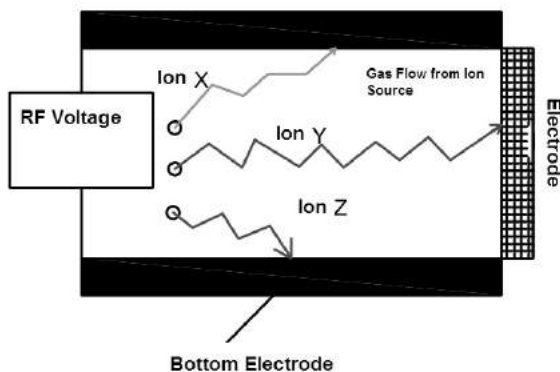


Fig. 3 Drift of ions in alternating electric field

Analyzing Figure 3 you can see that applying the same voltage RF does not allow the capture ion X and Z by the collecting electrode. Therefore, it was necessary to impose additional compensation voltage (CV), which will allow the ion drift through the entire length of the measuring chamber (Fig. 4).

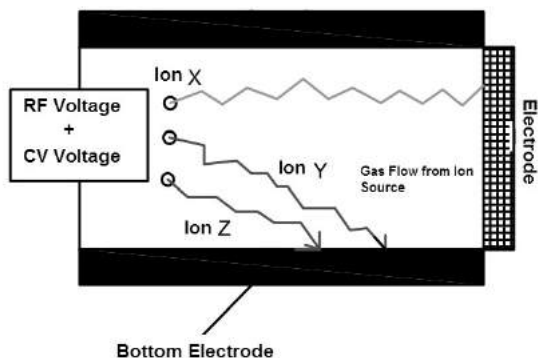


Fig. 4 Drift of ions in the alternating electric field and the applied voltage compensating CV

Under the influence of an applied compensating voltage ion X, which previously was not detected (Fig. 3) reaches the working electrode and is recorded for an applied voltage CV (Fig. 4). In practice this is reflected in the number and position of peaks on the alarm signal scale of the device. It should be noted that in a very specific range of the compensating voltage on the working electrode may be recorded signal to a specific ion or few for different ions with the corresponding characteristic values of the voltage CV [9-12].

In these methods separation of ions takes place according to their differences in mobility in the gas under the influence of high and low electric field [2]. In the case of weak electric fields – several hundred V/cm – ion mobilities are independent of electric field (IMS). Increasing the electric field (DMS) to several kV/cm leads to nonlinearities, where ion mobilities are dependent on the electric field. The nature of these changes is dependent on the type of ions and their mass, shape and the effective temperature.

In Figure 5 is shown an example of the dependence of ion mobility (K) and electric field for several gaseous substances.

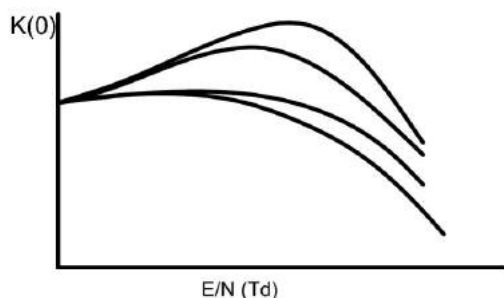


Fig. 5 The dependence of ion mobility on the electric field for a few selected gaseous substances [13]

Mobility of ions in this case is dependent on the E and the number of gas molecules (N) and can be represented as a function of $K(E/N)$, according to the relationship which is described by the formula 3.

$$K(E/N) = K_0 \cdot [1 + \alpha(E/N)] \quad (3)$$

where:

K – ion mobility, $\text{cm}^2/\text{V}\cdot\text{s}$,

E – intensity of the electric field, V/cm ,

K_0 – reduced ion mobility for weak electric field, $\text{cm}^2/\text{V}\cdot\text{s}$,

N – number of gas molecules in a volume of 1 cm^3 ,

E/N – Towends number called Td, and expresses the size of the field strength to the quantity of gas molecules in a volume of 1 cm^3 ($1 \text{ Td} = 1 \cdot 10^{-17} \text{ Vcm}^2$),

$\alpha(E/N)$ – dependence of the changes of reduced mobility in function of electric field strength and the molecular density,

$K(E/N)$ – ion mobility depending on the Towends number.

Thus, in the case of IMS the intensity of the electric field is constant and low ($250\text{-}300 \text{ V}\cdot\text{cm}^{-1}$), but in DMS (FAIMS) is variable and asymmetric ($16\text{-}18 \text{ kV}\cdot\text{cm}^{-1}$). Whilst the drift of ions is linear in IMS, in DMS the ions are oscillating and high and asymmetric voltage (RF, HSV) is applied perpendicularly to the direction of the gas flow providing a separation field. Under its influence, ion mobility become dependent on the intensity of the electric field in contrast to the classical IMS. A second electric field produced by a weak compensating voltage is superimposed on the high voltage RF and allow ions to traverse the drift region and register at a collector (Fig. 3 and 4).

Must be assumed that factors such as electrostatic interactions arising from the dipole moments and charge distribution, hydraulic resistance ensuing from the construction of molecules and molecular weight and shape of the

particles will have an impact on the separation of ions in a high RF field. Depending on the distribution of positive and negative charges ions are repelled or attracted by the electric field of appropriate polarity, resulting in slowing down or speeding up their drift towards the electrode - update the drift trajectory. Ion mobility in this method is thus determined by a hypothetical equation indicative of complex non-linear relationships:

$$K = K_0 + (K_1E^2 + K_2E^4 + \dots) \quad (4)$$

In the above equation in addition to K_0 (K_0 - reduced ion mobility) are included adjustments (K_1, K_2, \dots, K_i), which represent non-linear nature. The additional to K_0 members mainly depends on the nature of the ion. DMS (FAIMS) technology depends on many molecular factors, not only on the difference of K (mobility), this is why it can be increased as compared to the IMS. Moreover, it can be varied with E , because of very different K_1, K_2, K_i for the molecules, when even K_0 is similar [14].

Therefore, the method using experimentally marked characteristics enables detection of vapour at very low concentrations.

The spectrometer built based on this technique allows the simultaneous operation in negative ion mode and positive, which greatly improves the possibility of detection devices, and offers a greater resolving power than the IMS (Ion mobility spectrometry) device.

In this work we used traces of chemical warfare agents like: soman, tabun, mustard gas, Vx and explosives like: TNT, DNT, PiCl, RDX, PETN. We detect them using spectrometer PRS-1 designed in Military Institute of Chemistry and Radiometry.

RESULTS AND DISCUSSION

We obtained very interesting results which were used in the next steps of our research works. Examples of spectrograms obtained for examined chemicals shows following figures (Fig. 6-9)

The following figures (Fig. 6-9) shows some examples of spectrograms which are obtained for examined chemicals:

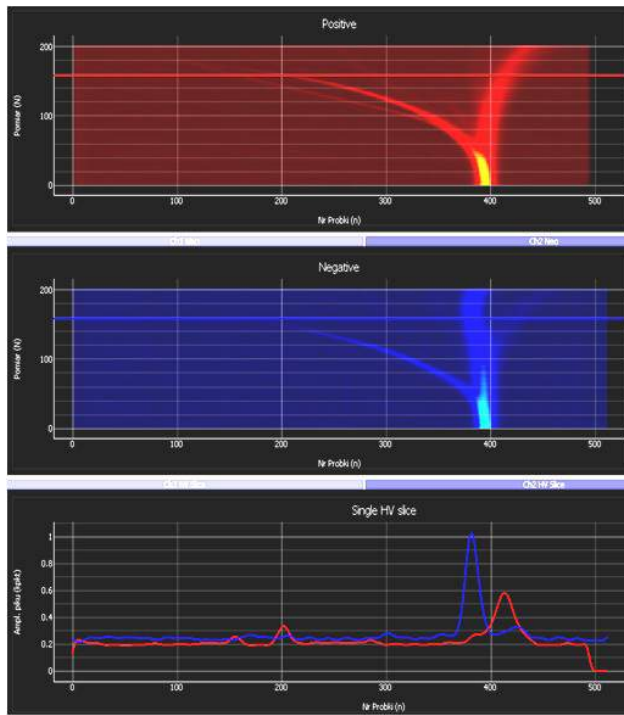


Fig. 6 Spectrogram for trinitrotoluene (TNT)

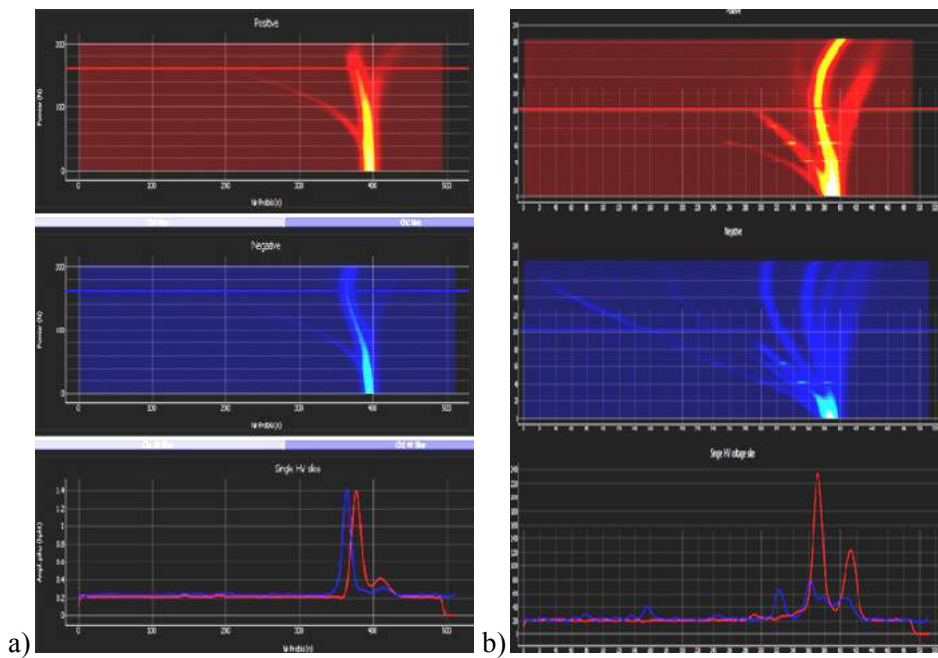


Fig. 7 Spectrogram for: a) dinitrotoluene (DNT), b) picryl chloride (PicCl)

Spectrogram consist of 3 parts. The first one (red color) is spectrum for positive ions for the whole range of the asymmetric voltage. The second one (blue color) corresponds to negative ions and the third one shows negative and positive peaks for selected asymmetric voltage. For TNT it can be observed characteristic peaks in negative and positive ion mode, where one of them (in both mode) is RIP (“Reactant Ion Peak”).

In fig.7 we can observe different signals for each substance. In case of DNT, we received a very characteristic peak with high amplitude in positive and also negative ion mode. For PiCl we received many peaks in negative ion mode and a bit less in positive but one of them with a very high amplitude. These obtained results allow the analysis of registered differences in spectrograms which further enables the identification of the measuring substance.

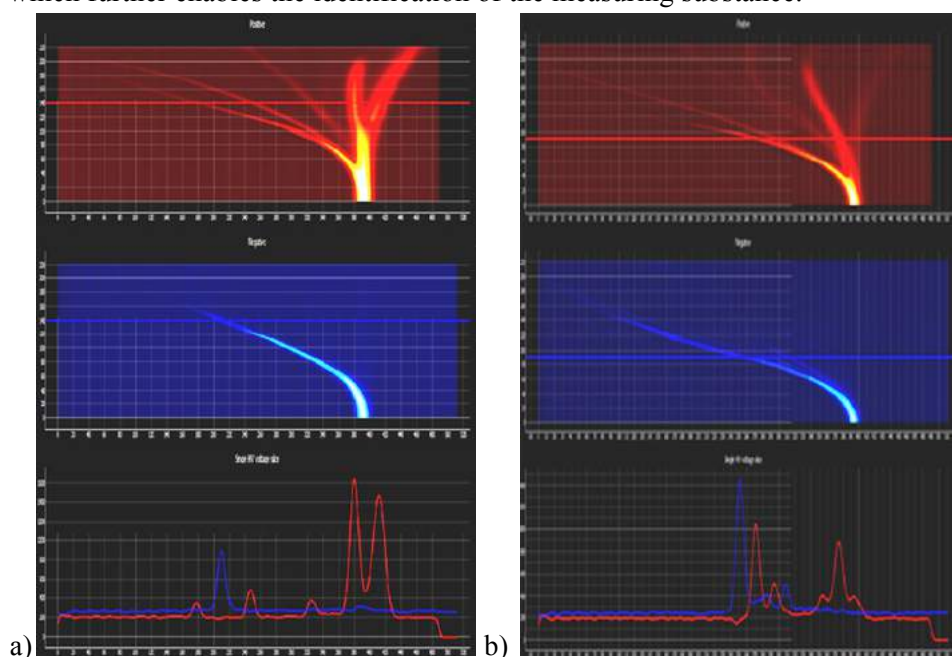


Fig. 8 Spectrogram for: a) soman, b) tabun

In case of chemical warfare agents we received mainly characteristic peaks in positive ion mode (Fig. 8).

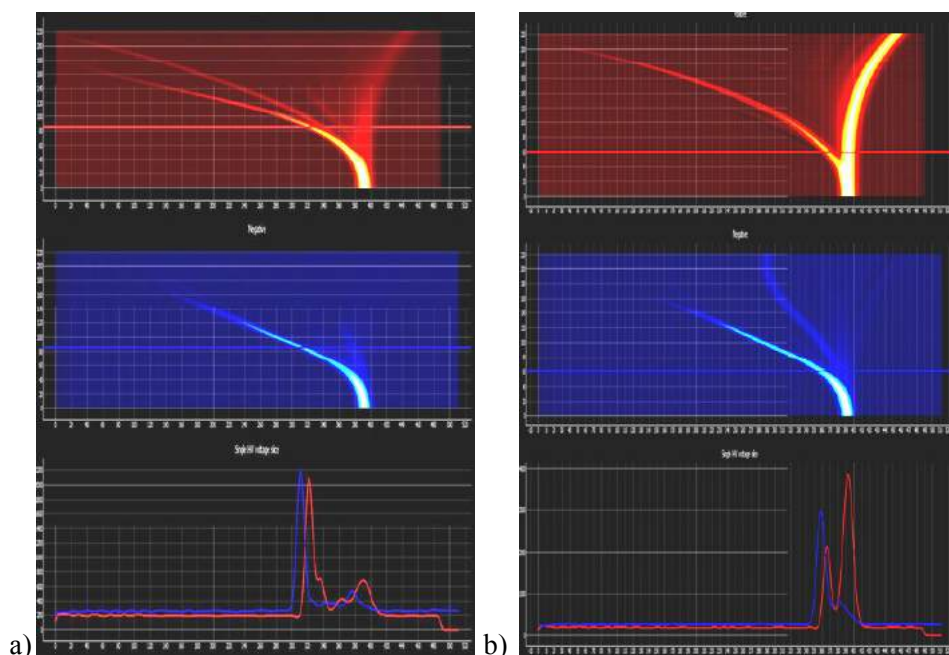


Fig. 9 Spectrogram for: a) mustard gas, b) VX

By analyzing the above spectrograms (Fig.9) we can observe the clear characteristic peak in positive and also in negative ion mode in case of VX, but it allows the identification of this analyte.

PRS-1 device correctly identifies soman from $20 \mu\text{g}\cdot\text{m}^{-3}$ level and mustard gas from $100 \mu\text{g}\cdot\text{m}^{-3}$. The device sensitivity in case of chemical warfare agents detection is on ppb level.

SUMMARY

Spectrometer PRS-1, based on DMS technology, was designed for the detection of chemical warfare agents but initial testing of the detection of explosives yielded positive results and forms the basis for the concept of further research. Received spectrograms show wide device detection possibilities and open a new way to make some new experiments about effective identification. High detection parameters of PRS-1 allow to take a chance to detect very little differences between CWA and EM and also volatile substances especially volatile organic compounds (VOCs). Obtained results can provide a basis for further research to develop applications leading to early diagnosis of asymptomatic diseases.

In summary it can be concluded that the DMS method used in mobile devices allows for detection of chemical vapors up to ppb-ppt level.

REFERENCES

- [1] Rhykerd Ch. L., Hannum D. W., Murray D. W., Parmeter J. E., Guide for the Selection of Commercial Explosives Detection Systems for Law Enforcement Applications, Sandia National Laboratories, 1999
- [2] Li F., Xie Z., Schmidt H., Sielemann S., Baumbach J.I., Ion mobility spectrometer for online monitoring of trace compounds, *Spectrochimica Acta Part B*, 2002, 57, 1563-1574
- [3] Sheble N., Ion mobility spectroscopy, *InTech*, 2002
- [4] Tabrizchi M., Khezri E., The effect of ion molecule reactions on peaks in ion mobility spectrometry, *International Journal for Ion Mobility Spectrometry*, 2008,11, 19-25, DOI 10.1007/s12127-008-0002-9
- [5] Borsdorf H., Influence of structural features of isomeric hydrocarbons on ion formation at atmospheric pressure, *International Journal for Ion Mobility Spectrometry*, 2008,11, 27-33, DOI 10.1007/s12127-008-0003-8
- [6] Bell A.J., Hayhurst C.J., Mayhew C.A., Watts P., On the reactions of perfluoroisobutene with some anions in the gas phase: studies in an ion mobility spectrometer, *International Journal of Mass Spectrometry and Ion Processes*, 1994,140, 133-147, DOI 10.1016/0168-1176(94)04082-6
- [7] Giles K., Grimsrud E.P., The kinetic ion mobility mass spectrometer: measurements of ion-molecule reaction rate constants at atmospheric pressure, *Journal of Physical Chemistry*, 1992, 96, 6680-6687, DOI 10.1021/j100195a030
- [8] Tabrizchi M., Jazan E., Inverse ion mobility spectrometry, *Analytical Chemistry*, 2010, 82, 746–750
- [9] Shvartsburg A.A., Differential Ion Mobility Spectrometry: Nonlinear Ion Transport and Fundamentals of FAIMS, *CRC Press*, 2008
- [10] Buryakov I.A., Krylov E.V., Nazarov E.G., Rasulev U.K., A new method of separation of multi-atomic ions by mobility at atmospheric pressure using a high-frequency amplitude-asymmetric strong electric field, *International Journal of Mass Spectrometry and Ion Processes*, 1993, 128, 3, 143–148, DOI 10.1016/0168-1176(93)87062-W
- [11] Borsdorf H., Mater T., Electric field dependence of ion mobilities of aromatic compounds with different ionic mass and different functional groups, *International Journal for Ion Mobility Spectrometry*, 2010, 13, 103–108, DOI 10.1007/s12127-010-0047-4
- [12] Eiceman G.A., Karpas Z., Ion Mobility Spectrometry, Second Edition, *Taylor & Francis Group*, 2005
- [13] Buczkowska A., Zalewska A., Sikora T., Maziejuk M., DMS as a tool for rapid detection of trace amounts of chlorine and ammonia, *Wybrane problemy naukowo-badawcze chemii i technologii chemicznej*, Politechnika

Warszawska Wydział Budownictwa Mechaniki i Petrochemii, 2013, 183-190

[14] Zalewska A., New possibilities of the screening mobile devices in the detection of the explosives, *Doctoral thesis*, Warsaw, 2013

Scientific Articles

The utilization of the TS-1 catalyst in the epoxidation of diallyl ether
*Ewa Drewnowska¹, Agnieszka Wróblewska¹, Alicja Gawarecka¹, Marika Walasek¹

¹Institute of Organic Chemical Technology, West Pomeranian University of Technology, Szczecin, POLAND, ul. Pulaskiego 10, 70-322 Szczecin
e-mail: ewa.sokalska@zut.edu.pl, agnieszka.wroblewska@zut.edu.pl

Keywords: *epoxidation, TS-1 catalyst, diallyl ether, allyl-glycidyl ether*

ABSTRACT

In this work the studies on the utilization of the microporous TS-1 catalyst in the epoxidation of diallyl ether (DAE) with the 30 wt% aqueous solution of hydrogen peroxide and in the presence of methanol as the solvent were presented. In the reaction of diallyl ether epoxidation - allyl-glycidyl ether (AGE) was formed as the main product. AGE is very important raw materials having a lot of applications. During the studies on the DAE epoxidation the influence of the following parameters was investigated: the temperature and the molar ratio of DAE/hydrogen peroxide.

INTRODUCTION

The first catalyst, from the family of titanium silicate catalysts, was the titanium silicalite TS-1 catalyst. It was mainly used in the oxidation processes which were performed in the presence of a dilute solution of hydrogen peroxide (a 30 wt% water solution). The Ti(IV)/SiO₂ catalyst which was also tested in the epoxidation in the presence of hydrogen peroxide was not active in this process. The main cause of this was the presence of water in the reaction medium. Moreover, the utilization of this catalyst needed a high concentration of hydrogen peroxide (above >95%) in order to obtain the high selectivity of the epoxide compound. The structures of both catalysts are different, probably the Ti(IV)/SiO₂ includes (Ti $\frac{1}{4}$ O) species and the TS-1 includes the tetrahedral Ti atoms in the silica structure [1].

The TS-1 catalyst belongs to the group of synthetic zeolites and is one of the most known titanium silicate catalysts. Its precursor is the ZSM-5 material. The TS-1 catalyst is obtained in the reaction of the source of Si and Ti (TEOS – tetraethyl o-silicalite and TBOT – tetrabutyl o-tytaniat). The synthesis is performed in the presence of tetrapropylammonium hydroxide (TPAOH) as a template (compound which allows to obtain the structure with the appropriate order and pore size) [2].

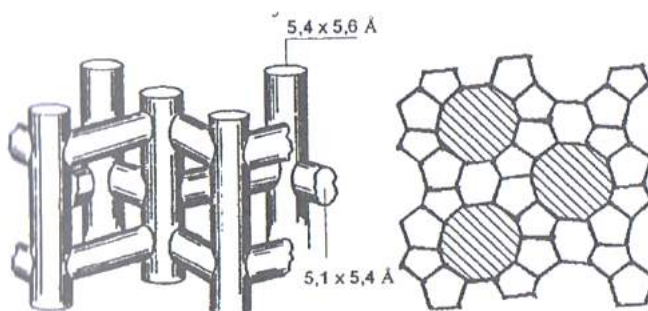


Fig.1 The system of channel in the TS-1 catalyst [3]

The structure of the TS-1 catalyst is denoted as the MFI. It is characterized by three dimensional channel system which is linear and zigzag. The TS-1 crystallizes in the orthorhombic system and its crystals have the size from 0.1 to 5 μm . The size of the channel amounts to 0.54 x 0.56 nm. The entrances to the channels are restricted by 10 edges [2-7]. The size of the channels is appropriate to adsorb molecules with the size to 6 \AA . The size of the pores of the TS-1 causes that this catalyst can be used for the epoxidation of unsaturated compounds with small molecules [2]. The TS-1/ H_2O_2 system selectively oxidizes the most of organic compounds such as: alkenes, alkanes, alcohols and phenols. The TS-1 catalyst has been industrially utilized in the following organic processes: in the epoxidation of propylene, in the hydroxylation of phenol and in the ammoxidation of cyclohexanone [8,9,10]. These processes fulfill the green chemistry principles [11].

During the process of DAE epoxidation over the TS-1 catalyst as the main product AGE is obtained. AGE is a very valuable intermediate which is used in the synthesis of: epoxy resins, epoxy adhesives, powder coatings, and epoxy paints. AGE is also used for production of explosive materials and cryptands [12]. During the epoxidation of DAE also the following by-products are formed: allyl alcohol, glycidol, 3-allyloxy-1,2-propanediol, diglycidyl ether and glycerol. These compounds also have a lot of applications.

MATERIALS AND METHODS

The TS-1 catalyst was synthesized by the method of Thangaraj et al. [13]. For the TS-1 synthesis the following raw materials were used: tetraethyl o-silicalite as the source of Si (98%, Aldrich), tetrabutyl o-tytaniatate as the source of Ti (97%, Fluka), the 20 wt% water solution of tetrapropylammonium hydroxide as the template - TPAOH (1M, Sigma-Aldrich) and isopropyl alcohol as the solvent – IPA (a.g., Chempur).

The synthesis of the TS-1 catalyst can be described as follows: TEOS, IPA and deionized water were put into the glass reactor (Fig.2a). To this mixture

was gradually added for 1h the 20 wt% TPAOH. Simultaneously, the mixture was intensively stirred. Next, the solution of TBOT in IPA was very slowly added to this mixture. The obtained mixture was stirred for 1h at the temperature of 57°C. Then, to this mixture was again added the 20 wt% solution of TPAOH. Next, this mixture was heated for 6 h at the temperature of 80°C and at the very intensive stirring. At the next stage, the obtained gel was hydrothermally crystallized in the autoclave (BERGHOF autoclave) (Fig.1b) with the capacity of 500 ml, equipped with the PTFE insert. The crystallization was performed for 10 days at the temperature of 170°C and at the autogenic pressure. The obtained crystals were separated on the filter, washed with deionized water and dried for 8h at the temperature of 120°C. In the next stage the calcination of the catalyst was performed for 16h and at the temperature of 550°C. The obtained catalyst was activated by the washing with the 10 wt% water solution of ammonium acetate for 8h at the temperature of 80°C. Next, the crystals of the TS-1 were separated on the filter, dried for 8h at the temperature of 120°C and calcined for 16h at the temperature of 550°C. The finally obtained product was in a form of a white powder (Fig.3).



a)



b)

Fig. 2 The apparatus for the synthesis of the TS-1 catalyst: the glass reactor (a) and the Berghof autoclave (b)



Fig. 3 The obtained TS-1 catalyst in the form of the white powder

The characteristic of the obtained TS-1 catalyst was performed with help of the following instrumental methods: XRD (X'Pert PRO Philips diffractometer, Cu $K\alpha$ radiation), IR (Nicolet FT/IR-380 Thermo Electron Corporation) – the sample for studies was prepared as the pill in KBr, UV-Vis (SPECORD M40 type V-530) and SEM (JOEL JSM-6100 instrument).

With the utilization of the obtained TS-1 catalyst the studies on the influence of temperature and molar ratio of DAE/hydrogen peroxide on the course of DAE epoxidation were performed. In the epoxidation methanol was used as the solvent. For the epoxidation the following raw materials were used: DAE (98%, Sigma-Aldrich), methanol (>98.9%, Chempur), hydrogen peroxide (30 wt% water solution, Chempur) and the obtained for these studies the TS-1 catalyst. The studied parameters were changed in the following ranges: temperature from 20°C to 80°C, and molar ratio of EDA/H₂O₂ from 0.25:1 to 5:1. The intensity of stirring was constant - 500 rpm.

The post-reaction mixtures were analyzed by the GC method. In the GC method FOCUS apparatus was used. It was equipped with a FID detector and the capillary column Quadrex 30m x 250 μ m x 0.25 μ m and the autosampler. The conditions of the analyses are presented below: pressure of helium 45 kPa, the sample chamber temperature of 200°C, the detector temperature of 250°C, the temperature of the thermostat increased according to the following program: 60°C for 1 min., increase of the temperature 15°C/min, isothermally 200°C for 3 min., cooling to 60°C, sensitivity 100 and the value of the sample 4 μ l.

For quantitative analyses also were used: iodometric titration method [14] and potentiometric titration method [15].

After quantitative analyses the mass balance for each synthesis was calculated and main functions describing the process were determined: the selectivity of AGE, the conversion of DAE and the selectivity of transformation to organic

compounds in relation to hydrogen peroxide consumed. These functions were calculated in the following way:

$$S_{\text{AGE/DAE}} = \frac{\text{amount of moles of AGE}}{\text{amount of moles of DAE consumed}} \cdot 100 \text{ [mol\%]}$$

$$C_{\text{DAE}} = \frac{\text{amount of moles of DAE consumed}}{\text{amount of moles of DAE introduced into reactor}} \cdot 100 \text{ [mol\%]}$$

$$S_{\text{org. comp.}} = \frac{\text{amount of moles of formed organic compounds}}{\text{amount of moles of H}_2\text{O}_2 \text{ consumed}} \cdot 100 \text{ [mol\%]}$$

RESULTS

The XRD pattern of the obtained TS-1 catalyst was made in the range of 2θ angle from 6° to 60° , with help of Cu $K\alpha$ radiation – Fig. 4. This XRD pattern is similar to the literature data [16] (Fig. 4).

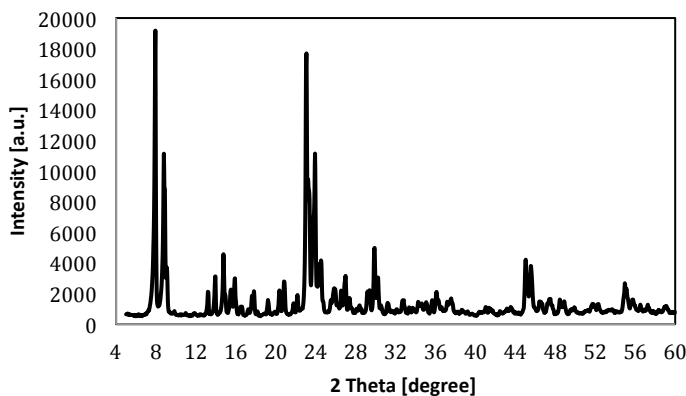


Fig. 4 The XRD pattern of the obtained TS-1 catalyst

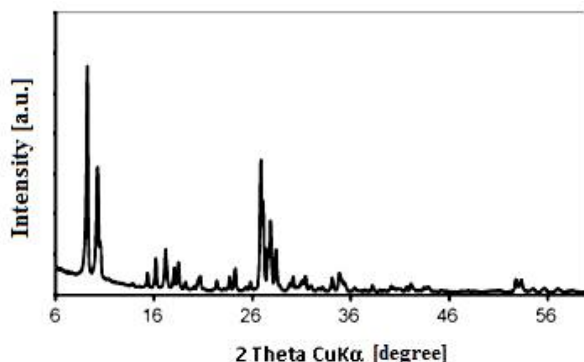


Fig. 5 The literature XRD pattern of the TS-1catalyst [16]

In the XRD pattern of the obtained TS-1 catalyst there are present the following characteristic bands for 2 Theta angle: 7-10; 22-25; 44-46, which confirm the obtaining of the MFI structure.

The studies using the IR method were made (Fig. 6) in order to confirm the introduction of the Ti atoms into the structure of the obtained catalyst. There is visible the band at 960 cm^{-1} in the IR spectrum of TS-1 which is connected with the tetrahedral coordinated Ti in the silica structure. This band is connected with the hindrance of the polar bonds Si-O-Ti or with the presence of titanyl group (T=O).

The studies using the UV-Vis method were also performed for confirmation the introduction of Ti into the silica structure (Fig. 8). The obtained spectrum was similar to the literature data [17] (Fig. 9).

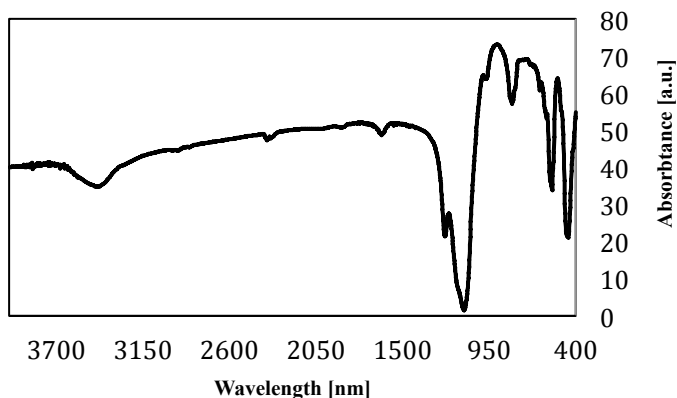


Fig. 6 The IR spectrum of the obtained TS-1catalyst

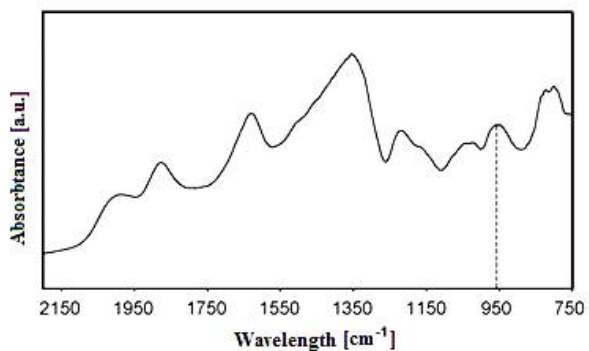


Fig. 7 The literature IR spectrum of the TS-1 catalyst [16]

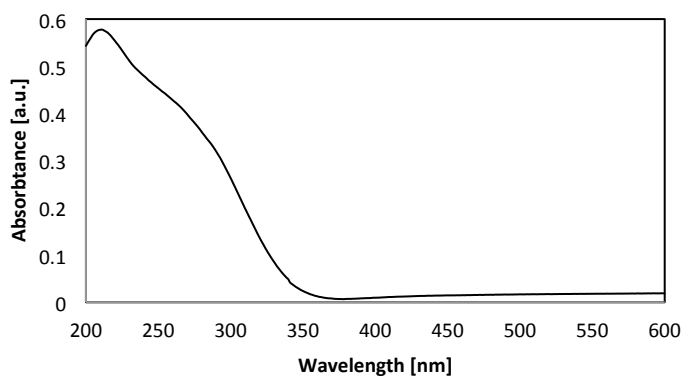
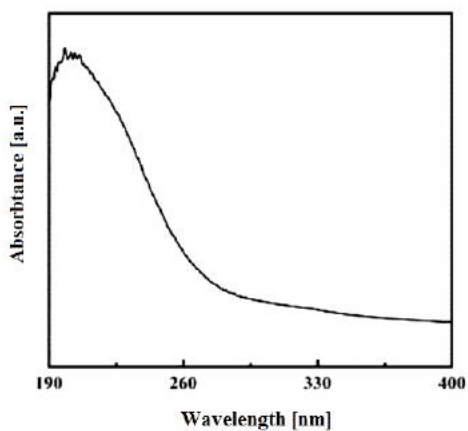


Fig. 8 The UV-Vis spectrum of the obtained TS-1 catalyst



The literature UV-Vis spectrum of the TS-1 catalyst [17]

The UV-Vis shows an intense band at 210 nm, which is assigned to the Ti atoms included into the structure of the catalysts (Ti^{+4} ions) and two weak bands at 260 and 290 nm which are described to the titanium in the +5 or +6 coordination. The presence of titanium at this coordination numbers is connected with the adsorption of water molecules (or solvent molecules) at the titanium active centers. The lack of the band at 330 nm is a proof of the absence of anatase in the studied sample.

The morphology of the obtained TS-1 catalyst is presented on Fig. 10.

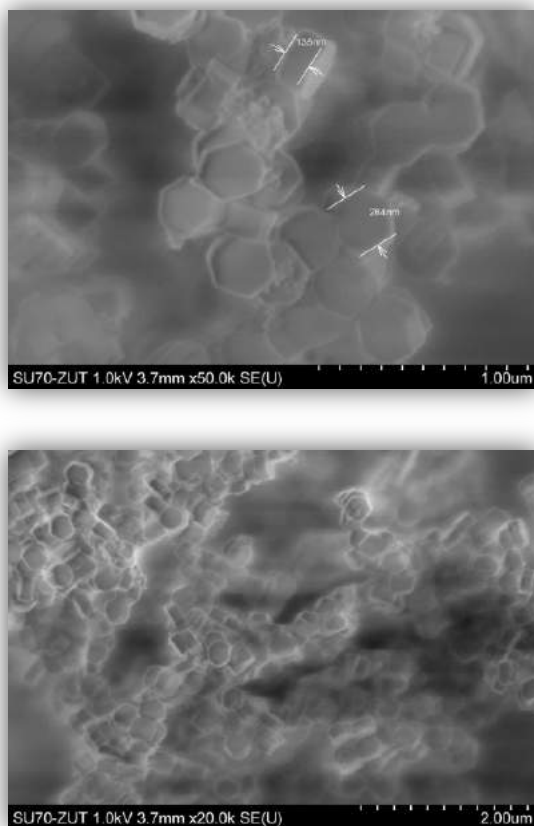


Fig. 10 The SEM micrographs of the obtained TS-1 catalyst

The SEM micrographs show that the catalyst is composed of the hexagonal, homogeneous crystals with the size of $0.3\mu\text{m} \times 0.4\mu\text{m}$. These crystals formed larger structures. The obtained material is characterized by crystals similar to the crystals of TS-1 catalyst presented in the literature [16] – Fig. 11.

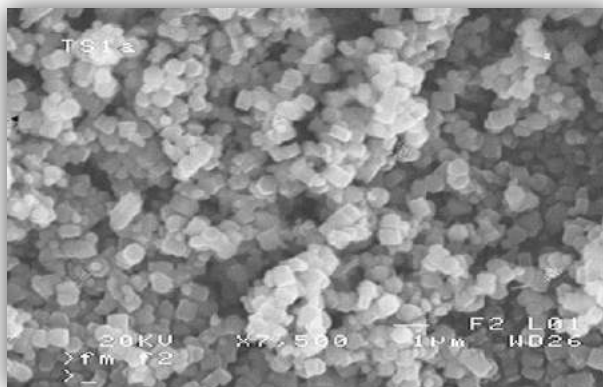


Fig. 11 The literature SEM micrograph of the TS-1 catalyst [16]

RESULTS

The results of the studies on the influence of two technological parameters on the course of DAE epoxidation with 30 wt% hydrogen peroxide over the TS-1 catalyst and in methanol as the solvent are presented in Tables 1-2 and on Fig. 12-13.

The influence of the temperature in the range of 20°C to 80°C was studied in the first stage. During these studies 7 syntheses were performed at the following parameters: the molar ratio of EDA/H₂O₂ = 1:1, the methanol concentration 50 wt%, the content of the catalyst 4 wt%, the reaction time of 3h and the intensity of stirring 500 rpm. The main function which was taken into account during establishing the best parameters of the process of DAE epoxidation was the selectivity of AGE. This product has a lot of applications in organic chemistry thus this direction of epoxidation is justified.

Table 1 The influence of temperature on the values of the main functions describing the epoxidation process: the selectivity of AGE (S_{AGE}), the conversion of DAE (C_{DAE}) and the selectivity of transformation to organic compounds in relation to hydrogen peroxide consumed ($S_{org. comp.}$).

Temperature [°C]	S_{AGE}	C_{DAE}	$S_{org. comp.}$
0	0.0	0.0	0.0
25	36.8	16.7	15.2
30	18.9	16.6	14.9
40	31.6	18.2	16.4
50	41.5	18.8	17.2
60	46.5	16.6	17.3
70	57.1	12.4	11.3
80	54.3	12.4	11.6

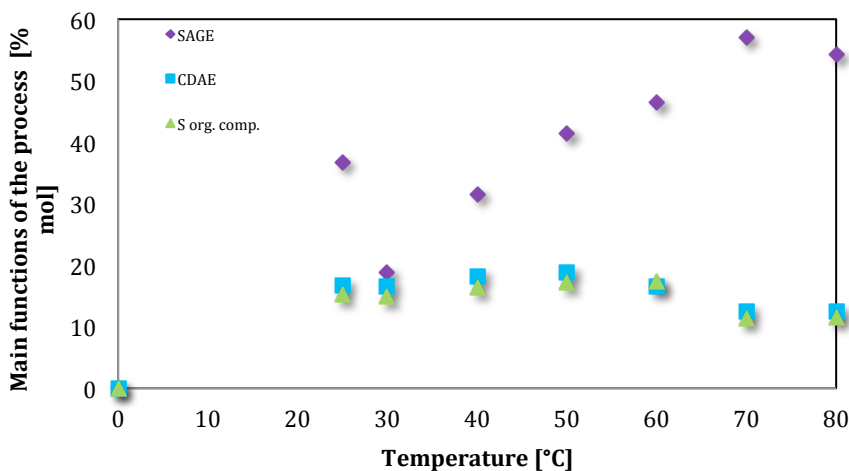


Fig. 12 The influence of temperature on the values of: S_{AGE} , C_{DAE} and $S_{org. comp.}$.

Figure 12 shows that the selectivity of AGE raises during increasing of temperature of the process performing in the range of 0-80°C from 0.0 mol% to 54.3 mol%. The conversion of DAE and the selectivity of transformation to organic compounds in relation to hydrogen peroxide consumed first increase from 0.0 mol% (the temperature of 0°C) to about 17 mol% (the temperature of 60°C) and next decrease to about 12 mol% (the temperature of 80°C). The decrease in values of these two functions is connected with the phenomenon of ineffective decomposition of hydrogen peroxide. This phenomenon is intensified at raised temperatures and it causes that lower amount of hydrogen peroxide takes part in epoxidation process. It results from Fig. 12 that at the temperature of 70°C the epoxidation of DAE undergoes the most effectively. At this temperature the most beneficial results of the epoxidation of DAE were obtained: S_{AGE} amounted to 57.1 mol%, C_{DAE} reached 12.4 mol%, and $S_{org. comp.}$ had the value of 11.3 mol%. For the next studies the temperature of 70°C was chosen as the most beneficial.

During the studies on the influence of the molar ratio of DAE/hydrogen peroxide (in the range of 0.25:1 to 5:1) 7 syntheses were performed. These syntheses were made at the following parameters: temperature of 70°C, methanol concentration of 50 wt%, the catalyst content of 4 wt%, the reaction time of 3h and the intensity of stirring 500 rpm.

Table 2 The influence of the molar ratio of DAE/hydrogen peroxide on the values of the main functions describing the epoxidation process: the selectivity of AGE (S_{AGE}), the conversion of DAE (C_{DAE}) and the selectivity of transformation to organic compounds in relation to hydrogen peroxide consumed (S_{org. comp.}).

Molar ratio DAE/H ₂ O ₂	S_{AGE}	C_{DAE}	$S_{org. comp.}$
0.25	51.8	18.3	13.2
0.5	43.9	25.4	15.4
1	57.1	12.4	11.3
2	68.9	7.2	13.9
3	54.6	7.1	20.9
4	55.3	6.5	27.5
5	47.6	6.8	38.8

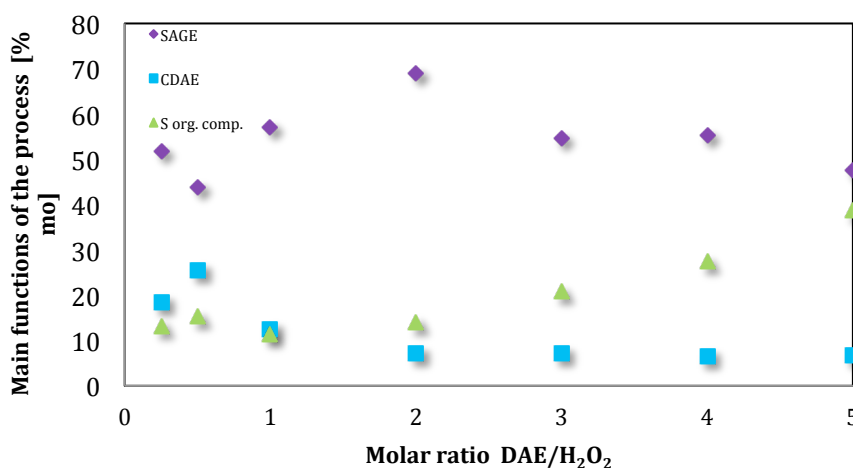


Fig. 13 The influence of the molar ratio of DAE/hydrogen peroxide on the values of: S_{AGE} , C_{DAE} and $S_{org. comp.}$.

The studies on the influence of molar ratio of reactants on the course of DAE epoxidation showed that during increasing the molar ratio of reactants from 0.25 to 5 the selectivity of AGE changed a little from 51.8 mol% to 68.9 mol% (the molar ratio of DAE/hydrogen peroxide = 2) and next decreased to 47.6 mol%. The conversion of DAE was the highest for the molar ratio of DAE/hydrogen peroxide = 0.5, and next decreased to 6.8 mol% (the molar ratio DAE/hydrogen peroxide = 5). The most beneficial results were obtained at the molar ratio of DEA/hydrogen peroxide 2:1 (Fig. 13). At this molar ratio of

reactants S_{AGE} amounted to 68.9 mol%, the conversion of DAE reached 7.2% mol, and the selectivity of transformation to organic compounds in relation to hydrogen peroxide consumed had the value of 13.9 mol%.

CONCLUSIONS

The instrumental methods which were used for the studies on the structure of the obtained TS-1 catalyst confirmed the obtaining of the MFI structure and also confirmed the absence of anatase in the obtained sample of the TS-1 catalyst. The TS-1 catalyst was very active in the epoxidation process of DAE. During the studies on the epoxidation of DAE the following parameters were taken as the most beneficial: the temperature of 70°C and the molar ratio of DAE/hydrogen peroxide amounted to 2:1.

REFERENCES

1. Oyama S. T., Mechanisms in homogeneous and heterogeneous epoxidation Catalysis, Elsevier, Amsterdam 2008.
2. Wróblewska A., Milchert E., Ławro E., Epoksydacja 2-buten-1-olu na katalizatorze TS-1, *Przem. Chem.*, 2006, 85/8-9, 687.
3. Bartkowiak M., Milchert E., Lewandowski G., Kierunki w rozwoju technologii przemysłu chemicznego, Wydawnictwo ZUT w Szczecinie, Szczecin, 2011.
4. Łukasiewicz M., Pielichowski J., Nadtlenek wodoru w nowoczesnych procesach technologii organicznej, *Przem. Chem.*, 2002, 81/8, 509-512.
5. Ziółek M., Nowak J., Kataliza Heterogeniczna, Wydawnictwo Uniwersytetu im. A. Mickiewicza Poznań, 1999.
6. Pruchnik F., Kataliza homogeniczna, PWN Warszawa, 1993.
7. Pruchnik F., Chemia metaloorganiczna, PWN Warszawa 1991.
8. Zieliński R., Wybrane zagadnienia optymalizacji statycznej, PWN Warszawa, 1982.
9. Mańczak K., Technika planowania eksperymentu, WNT Warszawa, 1976.
10. pl.wikipedia.org/wiki/epoksydacja z dnia 28.04.2012r.
11. Polański Z., Planowanie doświadczeń w technice, PWN Warszawa, 1984.
12. Lukyanenko N., Reder A., Macroheterocycles. Part 42. A facile synthesis of dihydroxy cryptands and their dehydroxylation, *J. Chem. Soc. Perkin Trans. I* 1988: 2533-2536.
13. Thangaraj A., Kumar R., Ratnasamy P., Direct catalytic hydroxylation of benzene with hydrogen peroxide over titanium-silicalite zeolites. *Appl. Catal.* 1990, 57: L1-L3.
14. Brill. W. F., Barone. B. J., The liquidphase oxidation of the lower olefins. *J. Org. Chem.* 1964, 29(1): 140-143.

15. Golowa. B M., Motowiljak W., Politanskij. S. F., Stjepanowa. M. W., Czeljadin. W. T., Opredelenie osnovnykh komponentov processa poluczenija gliceryna putem gidroksilirovanija allilovego spirta. *Zawod. Lab.* 1974, 40:1192-1194.
16. Milchert E., Wróblewska A., Otrzymywanie monoallilowych eterów gliceryny i eteru allilowo-glicydolowego. *Przem. Chem.* 1998, 77(3): 92-95.
17. Wu G., Wang Y., Feng W., Shi H., Lin Y., Zhang T., Jin X., Wang S., Wu X., Yao P., Epoxidation of propylene with H₂O₂ catalyzed by supported TS-1 catalyst in a fixed-bed reactor: Experiments and kinetics. *Chem. Engineer. J.* 2013, 215-216: 306-314.

Study on conditions for formation of amino acid - zinc suspensions

*Renata Dyja¹, Barbara Dolińska^{1,2}, Florian Ryszka²

¹Department of Applied Pharmacy and Drug Technology, Medical University of Silesia, Sosnowiec, POLAND

²Pharmaceutical Research and Product Plant "Biochefa", Sosnowiec, POLAND

e-mail: rdyja@sum.edu.pl

Keywords: *suspensions, zinc, amino acids, intercalation, model studies*

ABSTRACT

Conditions for formation of amino acid - zinc suspensions were studied. Optimal pH values providing the highest amino acid precipitation yield (the highest supporting dose) were determined. Basis on the amount of zinc and amino acid in the dispersed phase, the explanation of the mechanism formation was proposed- amino acids undergo intercalation into layered zinc hydroxide chloride.

INTRODUCTION

Combination of protein, peptides or low molecular weight substances with zinc in drug formulations provides prolonged action of these substances [1-6]. Intercalation of drug molecules into layered zinc hydroxide salts, layered hydroxides or layered double hydroxides is one of the methods of preparing sustained release drug delivery systems [4-6]. Intercalation involves incorporation of drug molecules into sparingly soluble zinc compounds forming a matrix. Co-precipitation is the simplest method of preparing this type of carriers. In this method, an alkaline solution is slowly added to the mixed organic substance and metal salt solution [6-10]. Obtained organic-inorganic hybrids are biocompatible, they improve permeation of complex through biological membranes and provide sustained release of drug [6].

Amino acids (AA) are used as model substances in studies on carriers based on the layered hydroxide salts or layered double hydroxides [7,8].

In the present study the conditions for formation of His, Trp and Tyr suspensions were tested. The methodology included the preparation of suspensions with different Zn(II):AA molar ratios and pH values. The amount of AA and Zn(II) in the dispersed phase and optimal pH values (pH_{opt}) (yielding the optimal AA-Zn(II) precipitation) were determined.

The choice of the AA was dictated by their biological role as they are a part of active sites of enzymes. Selected AA are hormone precursors- His for histamine, Tyr for catecholamines and Trp for serotonin. Moreover, the tested

AA could be easily determined by spectrophotometric method because of their aromatic structure.

MATERIALS AND METHODS

Amino acids

L-Histidine (His, $C_6H_9N_3O_2$, $\geq 99\%$ pure; MM = 155.15, pI = 7.59); L-tryptophan (Trp $C_{11}H_{12}N_2O_2$, $\geq 98\%$ pure; MM = 204.23, pI = 5.89) and L-tyrosine (Tyr $C_9H_{11}NO_3$, $\geq 98\%$ pure; MM = 181.19, pI = 5.66) were purchased from Sigma Chemical Corp., St. Louis Mo, USA. The physical and chemical properties of these compounds were tested to ensure their suitability for this study.

Reagents

Analytical grade ammonia (25%), sodium and zinc chlorides, eriochrome black T, hydrochloric acid (36%) and sodium hydroxide were purchased from Avantor Performance Materials Poland S.A., Gliwice, Poland (formerly POCH, Gliwice, Poland). The reagents satisfy the requirements of the standards.

Preparation of the suspensions

AA (His, Trp or Tyr) was dissolved in 5 ml of 0.015 M HCl and mixed with 0.75 ml of 0.1 M $ZnCl_2$ in 0.003 M HCl. Then, 0.75 – 1.45 ml of 0.2 M NaOH was added. Due to the limited solubility of Tyr in 0.015 M HCl, 0.75:1 Zn(II):Tyr molar ratio was not obtained. The total volume was adjusted to 10.0 ml with distilled water yielding suspensions with 15:1; 3:1; 1.5:1 and 0.75:1 Zn(II):AA molar ratios. The suspensions were stirred using a magnetic stirrer at 500 rpm for 25 min and then were left at room temperature for 1 h. The suspensions were then centrifuged during 10 minutes at 4000 rpm. The pH values, amounts of AA and of Zn(II) ions were then determined in the supernatant.

Determination of pH values

pH values were measured using Microcomputer pH-meter CP-315 (Poland). Electrode was calibrated using 0.05 M sodium phosphate buffer solution purchased in Chempur, Poland.

Spectrophotometric determination of AA concentration

AA concentration was measured using spectrophotometric method. The absorbance was measured in 1 cm quartz cuvettes on a CE 3021 UV-Vis spectrometer (Cecil, UK). The photometric accuracy of the spectrophotometer was ± 0.005 . The wavelengths at which maximum absorbance was observed, linear regression equations describing the relationships between AA concentration ($\mu\text{g/ml}$) and absorbance and the R^2 correlation coefficients of these equations are summarized in Table 1.

Table 1 Spectrophotometric determination of AA concentration

AA	Analytical wavelength λ (nm)	Regression equation x-absorbance y- AA concentration ($\mu\text{g/ml}$)	R^2
His	211	$y = 0.0387x + 0.0053$	0.9999
Trp	218.5	$y = 0.1758x + 0.0087$	0.9997
Tyr	222.5	$y = 0.0466x + 0.0256$	0.9998

Determination of Zn(II) ions

Zn(II) ions were determined by complexometric titration using 0.05 M EDTA in the presence of eriochrome black T in pH 10 ammonia buffer until the initially violet solution turned blue [11].

Data analysis

The results are presented as the mean value ($x \pm \text{SD}$) of 5 experiments. The results were analyzed using Microsoft's Excel computer program. The measured parameters were:

- Amount of AA or Zn(II) in the dispersed phase (μmol), calculated as the difference between their initial concentration and that in the supernatant,
- Binding efficiency of AA or Zn(II) in the dispersed phase (%), calculated as the ratio between AA or Zn(II) content in the dispersed phase and its initial content,
- Optimal for AA-Zn(II) binding in the dispersed phase pH values (pH_{opt}).

RESULTS AND DISCUSSION

Figure 1 shows the influence of pH on the amount of Zn(II) bound to AA in the dispersed phase for suspensions at all Zn(II):AA molar ratios. Basis on the regression equation pH_{opt} values were established and depicted in Figure 1.

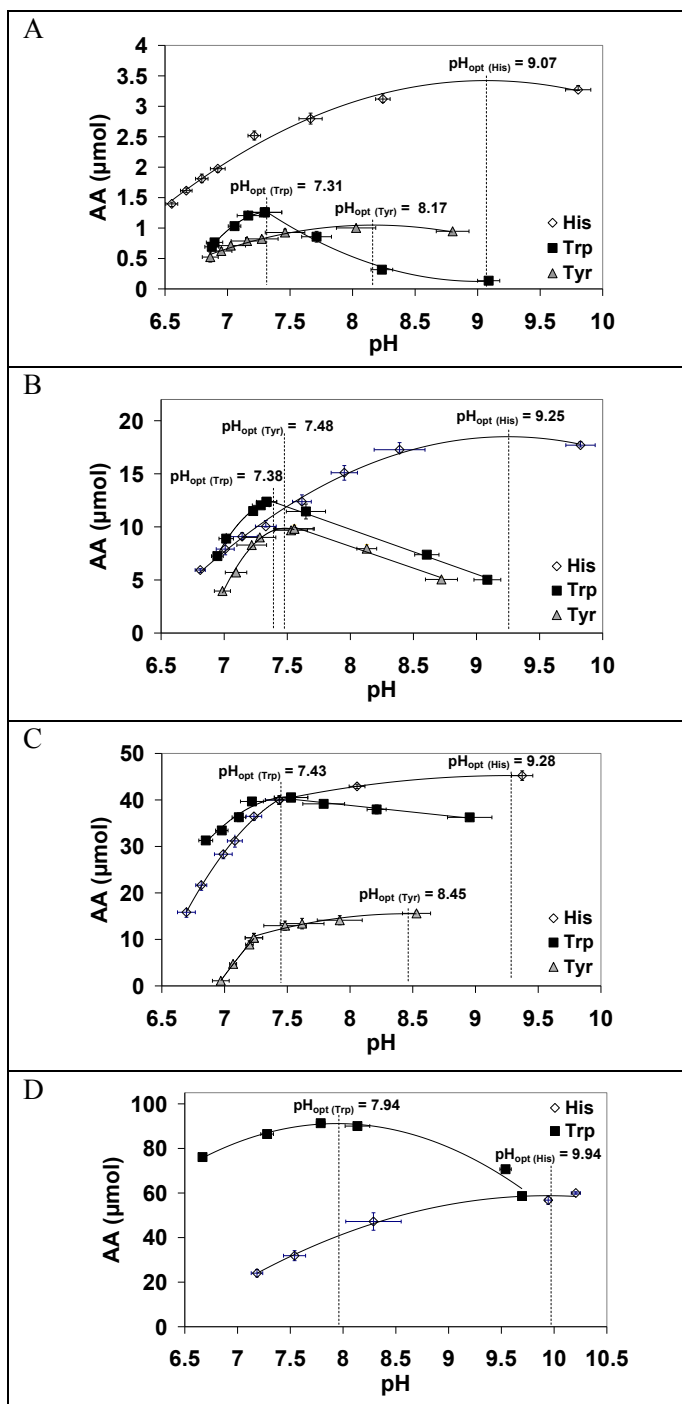


Fig. 1 The effect of pH value on the the amount of AA bound in the dispersed phase (AA (μmol)) at different Zn(II):AA molar ratios: Zn(II):AA - 15:1 (A), Zn(II):AA - 3:1 (B), Zn(II):AA - 1.5:1 (C), Zn(II):AA - 0.75:1 (D)

The pH_{opt} for His binding was 1.48-1.69 pH units above His pI ($\text{pI}=7.59$) at 15:1, 3:1 and 1.5:1 Zn(II):AA molar ratios. At 0.75:1 Zn(II):His molar ratio the pH_{opt} was 9.94 (2.35 pH units above pI). In the case of Trp ($\text{pI} = 5.89$) the pH_{opt} was 1.42 – 1.54 pH units above Trp pI ($\text{pI} = 5.89$) at 15:1, 3:1 and 1.5:1 Zn(II):AA molar ratios and at 0.75:1 Zn(II):AA molar ratio the pH_{opt} was 7.94 (2.05 pH units above pI). Tyr ($\text{pI} = 5.66$) had a pH_{opt} higher than its pI by 2.51, 1.82 and 2.79 at 15:1, 3:1 and 1.5:1 Zn(II):AA molar ratios, respectively. The higher pH_{opt} for His suspensions compared to those of Trp or Tyr can be attributed to the basic character of His.

The values of pH_{opt} higher than pI by 1.4-2.8 units may indicate the intercalation of AA molecules into layered zinc hydroxide chloride. Layers of zinc hydroxide chloride are positively charged and require stabilizing anions [7,10]. At pH values 1.4-2.8 higher than the pI , almost all of the AA molecules are negatively charged and further increase in pH value doesn't increase AA binding efficiency in the dispersed phase any further. The percent maximal theoretical binding efficiencies of AA in the dispersed phase were 90.5% for His at the 1.5:1 Zn(II):AA molar ratio; 91.1% for Trp at the 0.75:1 Zn(II):AA molar ratio and only 39.6% for Tyr at the 1.5:1 Zn(II):AA molar ratio. The higher binding efficiencies of His and Trp in the dispersed phase may be attributed to the stronger binding of Zn(II) due to the presence of the nitrogen in the aromatic ring of these AA. Decrease in the Trp and Tyr binding efficiencies above the pH_{opt} may be due to the fact that excess of hydroxide may lead to hydrolysis of the layered hydroxide salt and formation of the oxide or to the solubilization of the precipitate as a complex (zincates) [10].

The relation between pH and the amount of Zn(II) bound in the dispersed phase was also described (Figure 2).

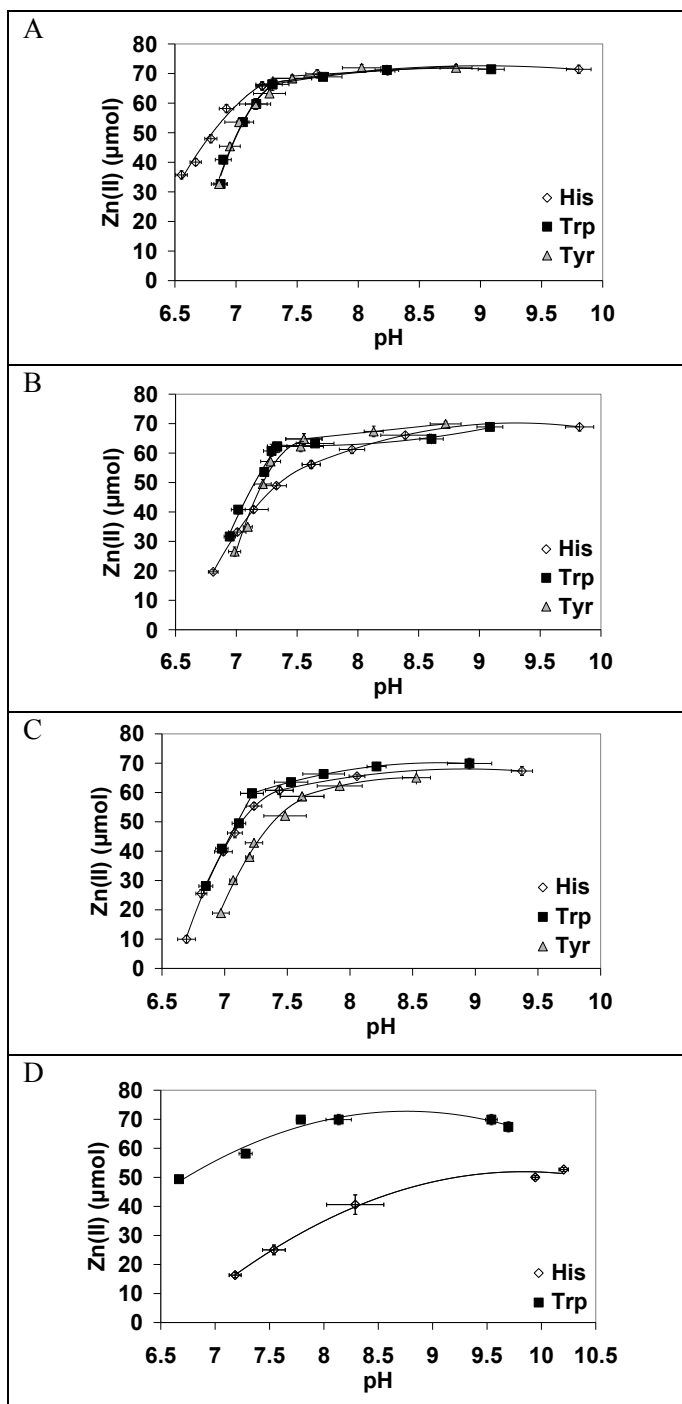


Fig. 2 The effect of pH value on the the amount of Zn(II) bound in the dispersed phase (Zn(II) (μmol)) at different Zn(II):AA molar ratios: Zn(II):AA - 15:1 (A), Zn(II):AA - 3:1 (B), Zn(II):AA - 1.5:1 (C), Zn(II):AA - 0.75:1 (D)

The percent of Zn(II) binding in the dispersed phase increased with increasing pH values- at pH = 8.0 it was already >60 μmol (> 80%) and at higher pH values it was almost complete. At higher pH values, Zn(II) binding in the dispersed phase reached 89.8 – 95.2 % (His suspensions, pH = 9.37 – 9.80), 91.8 – 95.2 % (Trp suspensions, pH = 8.95 – 9.09) and 86.4 – 95.9 % (Tyr suspensions, pH= 8.51 – 8.80) (Figure 2 A-C). At 0.75:1 Zn(II):AA molar ratio the pH dependence of Zn(II) binding in the dispersed phase is different (Figure 2 D). Binding of Zn(II) at 10 mM His was incomplete, reaching its maximum (69.3%) at pH = 9.84. It is known that His is the second most powerful chelator of Zn(II) (after Cys) [12]. This behavior allows the potential use of His-Zn(II) complexes as Zn(II) sources with enhanced solubility in alkaline media. AA-Zn(II) complexes are regarded as potential sources of easily absorbable Zn(II) [13]. Binding of Zn(II) in the dispersed phase at 10 mM Trp was almost complete (Figure 2 D).

The carboxyl and amino groups present in the tested AA are capable of forming complexes with Zn(II) [12]. In the case of His-Zn(II), Zn(II) is bound to the amino group and to the nitrogen of the imidazole ring forming the $\text{Zn}(\text{His})_2^{2+}$ complex [12-14]. In the literature there are reports of AA-Zn(II) complexes of the following types: $\text{Zn}(\text{AA})_2$, [12-15]; $\text{Zn}(\text{AA})$, [16] or $\text{Zn}_2(\text{AA})$ [17,18]. This means that Zn(II):AA molar ratios in AA-Zn(II) complexes are in the range 0.5-2.0.

The values of Zn(II):AA molar ratios in the dispersed phase are summarized in Table 2.

Table 2 Bound Zn(II): bound AA molar ratios in the dispersed phase for the suspension of the highest AA binding efficiency

Zn(II):AA molar ratio	Bound Zn(II): bound AA molar ratio in the dispersed phase		
	His	Trp	Tyr
15:1	21.8 \pm 0.6	52.8 \pm 3.2	71.9 \pm 2.8
3:1	3.9 \pm 0.1	5.1 \pm 0.1	6.6 \pm 0.4
1,5:1	1.5 \pm 0.0	1.5 \pm 0.1	4.2 \pm 0.2
0,75:1	0.9 \pm 0.0	0.8 \pm 0.0	-

The values of Zn(II):AA molar ratios in the dispersed phase were in the range 0.5-2.0 in the case of His and Trp suspensions at Zn(II):AA 0.75:1 and 1.5:1 molar ratio but were higher than 2.0 in the case of His and Trp suspensions at Zn(II):AA 3:1 and 15:1 molar ratio and all of the Tyr suspensions (Table 2). Moreover, there was a correlation between Zn(II):AA molar ratio and Zn(II) bound: AA bound molar ratio in the dispersed phase ($r > 0.99$). That facts allowed

to conclude that Zn(II) precipitates in other forms (zinc hydroxide, zinc hydroxide chloride) than sparingly soluble Zn(II)-AA complexes reported in the literature [12-18].

CONCLUSION

Conditions for formation of sparingly soluble Zn(II) matrix forming the dispersed phase of His, Trp or Tyr- Zn(II) suspensions were studied. The high correlation between Zn(II):AA molar ratio and bound Zn(II): bound AA molar ratio in the dispersed phase, the values of Zn(II):AA molar ratio in the dispersed phase greater than 2.0 and pH_{opt} values higher than pI by 1.4-2.8 units indicate AA intercalation into zinc layered hydroxide chloride. The tested method of simply co-precipitation with zinc chloride may be applied for preparing sustained release suspensions with low molecular weight substances (e.g. peptide hormones).

REFERENCES

1. Gietz U., Arvinte T., Häner M., Aebi U., Merkle H.P., Formulation of sustained release aqueous Zn–hirudin suspensions, *Eur. J. Pharm. Sci.*, 2000, 11, 33-41 DOI: 10.1016/S0928-0987(00)00072-5
2. Shi K., Cui F., Bi H., Jang Y., Shi K., Song T. Metal ions guided self-assembly of therapeutic proteins for controllable release: from random to ordered aggregation, *Pharm. Res.*, 2013, 30, 269-279 DOI: 10.1007/s11095-012-0871-9
3. Dolińska B., Ryszka F., Pulsatile and moderated release of dalareline from Zn(II) complexes in the form of suspension, *Boll. Chim. Farmac.*, 2003, 142, 10-13
4. Biswick T., Park D.H., Shul Y. G., Choy J.H., P-coumaric acid-zinc basic salt nanohybrid for controlled release and sustained antioxidant activity, *J. Phys. Chem. Solid.*, 2010, 71, 647-649 DOI: 10.1016/j.jpcs.2009.12.058
5. Saifullah B., Hussein M.Z., Hussein-Al-Ali S.H., Arulselvan P., Fakurazi S., Sustained release formulation of an anti-tuberculosis drug based on para-aminosalicylic acid-zinc layered hydroxide nanocomposite, *Chem. Centr. J.*, 2013, 7, 72 DOI: 10.1186/1752-153X-7-72
6. Kura A.U., Hussein Al-Ali S.H., Hussein M.Z., Fakurazi S., Arulselvan P. Development of a controlled release anti-parkinsonian nanodelivery system using levodopa as the active agent, *Int. J. Nanomed.*, 2013, 8, 1103-1110 DOI: 10.2147/IJN.S39740
7. Carbajal Arízaga C.G., Intercalation studies of zinc hydroxide chloride: ammonia and amino acids, *J Solid State Chem.*, 2012, 185, 150-155 DOI: 10.1016/j.jssc.2011.11.016

8. Fudala Á., Pálinkó I., Kiricsi I., Preparation and characterization of hybrid organic-inorganic composite materials using the amphoteric property of amino acids: amino acid intercalated layered double hydroxide and montmorillonite, *Inorg. Chem.*, 1999, 38, 4653-4658 DOI: 10.1021/ic981176t
9. Yasutake A., Aisawa S., Takahashi S., Hirahara H., Narita E., Synthesis of biopolymer intercalated inorganic-layered materials: intercalation of collagen peptide and soybean peptide into Zn-Al layered double hydroxide and layered zinc hydroxide, *J. Phys. Chem. Solid*, 2008, 69, 1542-1546 DOI: 10.1016/j.jpcs.2007.10.077
10. Carbajal Arizaga C.G., Satyanarayana K.G., Wypych F., Layered hydroxide salts: synthesis, properties and potential applications, *Sol. State Ion.*, 2007, 178, 1143-1162 DOI: 10.1016/j.ssi.2007.04.016
11. Polish Pharmacopeia VI, 2002, p. 692
12. Trzaskowski B., Adamowicz L., Deymier P.A., A theoretical study of zinc(II) interactions with amino acid models and peptide fragments, *J. Biol. Inorg. Chem.*, 2008, 13, 133-137 DOI: 10.1007/s00775-007-0306-y
13. Ghasemi S, Khoshgoftarmanesh AH, Hadazadeh H, Afyuni M., Synthesis, characterization, and theoretical and experimental investigations of zinc(II)-amino acid complexes as ecofriendly plant growth promoters and highly bioavailable sources of zinc, *J Plant Growth Regul.*, 2013, 32, 315-323 DOI: 10.1007/s00344-012-9300-x
14. Zhou L., Li S., Su Y., Yi X., Zheng A., Deng F., Interaction between histidine and Zn(II) metal ions over a wide pH as revealed by solid-state NMR spectroscopy and DFT calculations, *J. Phys. Chem. B*, 2013, 117, 8954-8965 DOI: 10.1021/jp4041937
15. Shindo H., Brown T.L., Infrared spectra of complexes of L-cysteine and related compounds with zinc (II), cadmium (II), mercury (II) and lead (II), *J. Am. Chem. Soc.*, 1965, 87, 1905-1909 DOI: 10.1021/ja01087a013
16. Yamauchi O., Odani A., Stability constants of metal complexes of amino acids with charged side chains. Part 1: positively charged chains, *Pure & Appl. Chem.*, 1996, 68, 469-496 DOI: 10.1351/pac199668020469
17. Aliyu H.N., Na'aliya J., Potentiometric studies on essential metal (II) amino acid complexes, *Int. Res. J. Pharm. Pharm.*, 2012; 2, 076-080
18. Dolińska B., The properties of solid Zn(II)-amino acid complexes in the form of suspensions, *Il Farmaco*, 2001, 56, 737-740 DOI: 10.1016/S0014-827X(01)01129-6

The products of limonene oxidation on the titanium-silicate catalysts and their properties and applications

*A. Gawarecka, A. Wróblewska

Faculty of Chemical Technology and Engineering, West Pomeranian University of Technology, Szczecin, ul. Pułaskiego 10, 70-322 Szczecin, POLAND

e-mail: alicja.gawarecka@zut.edu.pl

Keywords: *limonene obtaining, limonene oxidation, 1,2-epoxylimonene, perillyl alcohol*

ABSTRACT

This work presents the ways of limonene obtaining from the waste orange and lemon peels in the laboratory and in the industrial scale. Moreover, the applications of the products of limonene oxidation over the titanium silicate catalysts (TS-1 and Ti-MCM-41) are presented. Also natural sources of these products are described. Nowadays, the attention of scientist is focused on green technologies; this work presents the possibility of an effective reusing of the waste orange peels which are obtained in large amount during fruit juices process performing in factories.

INTRODUCTION

The titanium-silicate catalysts TS-1 and Ti-MCM-41 are the most frequently used in the oxidation of limonene. Limonene can be oxidized by hydrogen peroxide and the following products can be in this way obtained: 1,2-epoxylimonene and its diol, perillyl alcohol, menthol, carvone, carveol, α -terpineol, perillyl aldehyde and p-cymene.

The presented above products have a lot of applications, thus the technology of these products obtaining – by oxidation of limonene with hydrogen peroxide or t-butyl hydroperoxide is very interesting. Moreover, limonene can be very cheap and easy obtained by simply distillation or cold pressing of the waste peels of oranges.

THE METHODS OF THE NATURAL R(+)-LIMONENE OBTAINING

In nature, limonene is present in the form of two enantiomers: D- and L-limonene. These enantiomers have a different smell. L-limonene rarely occurs in nature and has a smell similar to the smell of trees and shrubs, and it can be found in the pine and fir essential oils. D-limonene is present in the orange peels and it is a component of the orange essential oil.

On an industrial scale D-limonene is produced from the peels of oranges, which are the waste material from the industry of the fruit juices. The

content of limonene in the orange essential oil obtained from the peels of oranges is very high and it amounts to about 97%. The main methods of the obtaining of limonene from orange peels are: the simply distillation (Fig. 2), the water steam distillation (Fig. 3), and the cold pressing.



Fig. 1 The simply distillation of limonene from orange peels

Figure 1 present the laboratory apparatus for the limonene separation by the simply distillation. For this method orange peels should be prepared properly - peels are first fragmented and mixed with water.



Fig. 2 The water steam distillation limonene in the laboratory scale

The orange oil can be also obtained by cold pressing of the ripe orange peels. This oil has a pleasant aroma and a mild flavor. It is mainly consisted of D-limonene (97%). The other components of this oil are: citral, n-decylaldehyde, citronellol, terpineol, anthranilic acid methyl ester and coumarine. This oil has the antibacterial properties and can be also applied as the relaxing and soothing

agent for the nervous system. Due to the large presence of monoterpenes it may also act as contact allergen [1].

Limonene can be also obtained from the orange peels by the cold pressing method during the production of the orange juice (Fig. 3). The juice extractor contains the components necessary to rupture the oil glands and extract the oil into emulsion. This process minimizes the space and energy for high yields of oil from the peels, at the same time extracting the juice. Oil extraction occurs in sequence after fruit is placed on lower extractor cup and lower cutter, the upper cup descends pressing the fruit against the lower cup and plugs are cut in the fruit. The upper cup descends, forcing the juice and inner fruit contents down through the lower cutter for juice recovery. At the same time, the peel is shredded, being forced through opening in the upper cup, which ruptures the oil glands. The upper cup assembly contains a spray ring, which applies pressurized water to the peel during and after the shredding step, emulsifying the oil as it is released. This emulsion and small particles of peels and soluble and insoluble solids flow from the extractor, are collected and sent to a finisher for initial separation of the larger practices. The finished emulsion is sent to a centrifugation process for concentration and recovery of the final cold-pressed oil [2].

The frit – (small particle of peel that are produced when the peel is removed from the rest of the fruit in the extraction cycle) is separated from the emulsion by either a screw or a paddle finisher, also may by use vibrating or gravity-flow screen in place of the finisher. Regardless of the separation method used, it must be gentle enough to prevent the extraction of naturally occurring pectin and hesperidin from the frit particles along with the emulsion. Excessive amount of pectin and/or hesperidin will interfere with the centrifuge process efficiency due to the emulsion viscosity increase [2].

Juice and oil are extracted in one process step where extractors are used for processing citrus fruit. The peel of the fruit is cut and squeezed during the processing procedure. This releases the oil which is contained in treatment. The oil is obtained from the flavedo during this mechanical washed out and separately collected during this process step [2].

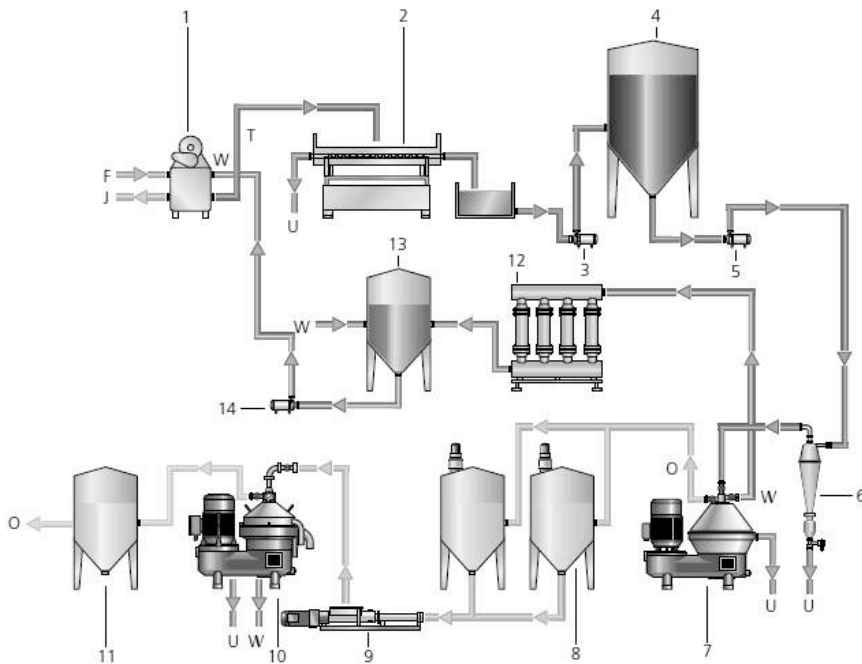


Fig. 3 Process for recovery of essential oils : 1- extractor, 2- vibrating screen, 3- pump, 4- tank, 5- pump, 6- hydrocyclone, 7- separator, 8- buffer tank, 9- Moho pump, 10- separator, 11- pure oil tank, 12- automatic filter, 13- treatment tank, 14- pump, F- fruits, J- juice, O- oil, T- emulsion, S- sand, solid, W-water [3]

To recover the oil from the emulsion, a two-stage centrifuging system typically is required. The first stage centrifuge separates most of the water and solids from the emulsion, producing an oil-rich emulsion commonly called cream. The second stage centrifuge is the polishing stage where the remaining water and fine peel particles are removed from the cream, producing purified oil [2].

De-waxing/winterizing – additional operation which is usually required before citrus peel oils are solid. All citrus oils contain a small amount of naturally occurring wax. This wax will precipitate out of the oil during storage at cold temperature and is considered by buyers to be a contaminant. If the oil is used without winterizing in clear beverage formulation that will be stored and distributed under cold conditions, the wax will cause the beverage to appear cloudy and spoiled. Winterizing is accomplished by storing the oil in cone-bottom tanks at cold temperature for a period sufficient enough to allow the wax precipitate out the oil to the bottom of tanks. This process usually takes a minimum of four weeks at storage temperatures of around 0°C. Winterizing can also be done by rapidly chilling the oil to very low temperatures with a chiller followed by a fine filtering to remove wax [2].

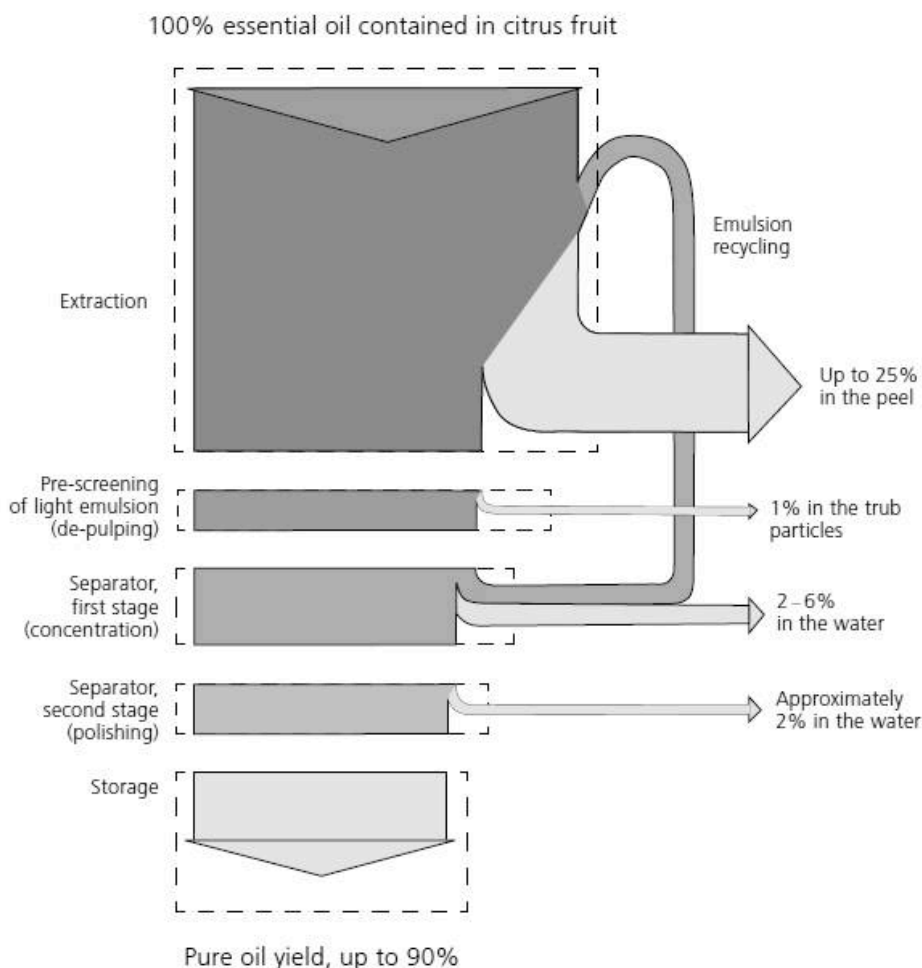


Fig. 4 Mass balance of essential oil recovery during processing [3]

Limonene is widely used in the industry as the component of: foods additives, perfumes, cosmetics and cleaning agents. It also replaced the toxic solvents in many organic reactions.

THE OXYGENATED PRODUCTS OBTAINED DURING LIMONENE OXIDATION

There are many reports showing the biotransformation of limonene in the more valuable compounds [4-18]

Currently, limonene has been intensively studied by researchers. Its oxygenated derivative - 1,2-epoxylimonene was used in the polymerization of carbon dioxide in the presence of the appropriate catalyst. The product of this polymerization (polilimonene carbonate) has similar properties as polystyrene, which is obtained from crude oil [19].

Limonene may be obtained in large amount from renewable sources – from the biomass. Therefore, researchers are interested in limonene as a substrate for syntheses of other, much more valuable compounds having the same carbon skeleton. For those oxygenated derivatives belong: 1,2-epoxylimonene, menthol, carvone, carveol, α -terpineol, perillyl alcohol and p-cymene - formed by the dehydrogenation of limonene [20].

1,2-Epoxy limonene (1,2-epoxy-p-menth-8-ene; IUPAC name: 1-methyl-4-(prop-1-en-2-yl)-7-oxabicyclo[4.1.0]heptanes, $C_{10}H_{16}O$) is isolated from oil of Cymbopogon species, orange (*Citrus sinensis*), Japanese pepper tree (*Zanthoxylum piperitum*) and others. 1,2-Epoxy-p-menth-8-ene belongs to the family of monoterpenes, containing a chain of two isoprene units. Molecular weight of 1,2-epoxylimonene amounts to 152,23 g/mol. It is used for production of nutrients, stabilizers, surfactants and emulsifiers [21].

Other interesting compound is 1,2-epoxylimonene diol (8,9-p-menthen 1,2-diol, d-limonene 1,2-diol, limonene glycol), $C_{10}H_{18}O_2$). Its molar weight amounts to 170,25 g/mol. It is a colorless to slightly yellow liquid. 1,2-Epoxy limonene diol is slightly soluble in water, soluble in ethanol. Its boiling point amounts to 54-57°C, and melting point 74°C. 1,2-Epoxy limonene diol is used as a cool minty aroma odor or flavor [22].

Perillyl alcohol is a monoterpene compound which is isolated from the following essential oils: mint, cherries (Fig. 5) or celery. In a pure form perillyl alcohol is a light brown liquid with a molecular weight of 152.23 g/mol, its density at the temperature of 25°C amounts to 0.96 g/cm³ and its boiling point is 119-121°C at the pressure of 15 mbar. Animal studies have shown that perillyl alcohol caused regression of pancreas, breast, and liver cancer. It also exhibited good results as a precautionary measure at lung tumors, colon cancer, skin cancer and as a chemotherapeutic agent at neuroblastoma, prostate cancer and colon cancer. Perillyl alcohol is an active ingredient for inducing apoptosis in tumor cells, does not adversely affect healthy cells and have the capacity to differentiate cancer cells. Its mechanism of action is not fully understood because it shows effects on many different cellular substances that regulate the growth and differentiation of cells [23]. Perillyl alcohol is also used as a fragrance component in the manufacture of perfumes and cosmetics for example: shampoos, toilet soaps and as a component of detergents and cleaners [24].



Fig 5 Cherries – the source of perillyl alcohol [25].

Menthol is one of the cyclic terpenic alcohol. It is the main component of the peppermint and the dirt essential oils. Menthol with menthon and isomenthone (two stereoisomers – menthone and isomenthone, each stereoisomer occurs in the form of a pair of enantiomers due to the two asymmetric centers in the molecule) give flavor and cooling effect of mint plants of the genus *Mentha*, especially. After the vanilla and citrus aroma (-)-menthol is the most popular component of flavoring foods and tobacco products. Moreover, menthol is the component of many products including pharmaceuticals, cosmetics, pesticides, candies, chewing gums, liqueurs, shampoos and soaps. Menthol is biologically active thus it is used as a repellent and a fungicide. Additionally, it has got antibacterial, antitumor, and anti-inflammatory properties.



Fig. 6 The menthol crystals[26]

As in the case of other unsaturated alcohols, menthol is a reactive compound and may be oxidized to the menthone. Menthol at the room temperature is a white or colorless peeling crystalline solid having a density of 0.890 kg/dm^3 and a melting point of between $41\text{-}44^\circ\text{C}$, depending on its purity (Fig. 6). Menthol is not completely soluble in water, but freely soluble in alcohols and diethyl ether or chloroform. Menthol as other terpenic alcohols do not absorb well the UV light in the range of $290\text{-}320 \text{ nm}$, while it absorbs below 290 nm , giving a peak at a wavelength of 220 nm [27]. L-menthol is an important terpenic alcohol in the flavor industry. It is obtained by the crystallization of the peppermint.

Carvone is one of the by-products of limonene epoxidation – Fig. 7. It exists in the form of two enantiomers: (-)-carvone, (+)-carvone and as the racemic mixture. (+)-Carvone is the primary constituent of the caraway and dill oil, (-)-carvone is present in the spearmint oil. Carvone is a colorless or a slightly yellow liquid. (+)-Carvone has a herbal smell which reminiscent of cumin and fennel seeds, and (-)-carvone smells like mint. Depending on the reaction conditions, during hydrogenation of carvone carveols or dihydrocarvone are obtained, which are also used as the flavor compounds. Carvone reacted also with strong acids and isomerized to the carvacrol [28].



Fig. 7 The sources of D-carvone [29]

Carveol (IUPAC 2-methyl-5-(prop-1-en-2-yl)cyclohex-2-en-1-ol) has the molar weight of $152,23 \text{ g/mol}$. It was found in caraway. Carveol is present in oil of grapefruit (*Citrus paradisi*), mandarin (*Citrus reticulata*), blackcurrant berries, celery, black tea, dill, caraway seeds and lamb's lettuce. Carveol is a flavouring agent [20]. In plants, carvone is formed in a biosynthetic pathway from limonene via hydroxylation at the C6 position, forming carveol, and subsequent oxidation of carveol to carvone [21, 22]

α -Terpineol is a colorless, a crystalline solid, having the odor of the lilac. Although terpineol is present in many essential oils, only a small amount of it is isolated, for example by the fractional distillation of the pine oil. A common method of the industrial production of α -terpineol is a synthesis involving hydration of the α -pinen or turpentine in mineral acids to crystalline cis-terpine hydrate (mp 117°C), next by partial dehydration of cis-terpine the α -terpineol is received. It is also used a selective conversion of 3-carene and limonene or dipentene to terpineol, without terpine hydrate formation. The commercial grade of terpineol mixture is composed of a liquid mixture of isomers, that contains generally α -terpineol and a considerable amount of γ -terpineol. This mixture has a stronger lilac odor than the pure, crystalline α -terpineol. Terpineol with its typical lilac odor is one of the most frequently used fragrance substances. It is stable and inexpensive, and it is usually used in soaps and cosmetics [29].

Perilla aldehyde (perillaldehyde, dihydrocuminy aldehyde; p-mentha-1,8-dien-7-al; 4-isopropenylcyclohex-1-enecarbaldehyde) is a colorless to pale yellow liquid. It has character of odors of purple perilla, cinnamic aldehyde and cuminaldehyde scent. Perilla aldehyde can be used in production of fragrances, cosmetics and food.

p-Cymene is a naturally occurring aromatic organic compound, component of many essential oils commonly the oil of cuminal and thyme. It has a weak citrus odor [29]. It is widely used as the intermediate in the synthesis of fine chemicals for flavorings, fragrances, perfumes, fungicides, pesticides etc. Moreover, it is used as the starting material for the synthesis of p-cresol and non-nitrated musks [31]. Its structure consists of a benzene ring para-substituted with a methyl group and an isopropyl group. There are two less common geometric isomers of p-cymene. o-Cymene, in which the alkyl groups are ortho-substituted, and m-cymene, in which they are meta-substituted. p-Cymene is the only natural isomer. p-Cymene is insoluble in water, but miscible with ethanol and diethyl ether.

CONCLUSIONS

The presented work shows that limonene is the very interesting raw material for the process of oxidation. The products of its oxidation are: 1,2-epoxylimonene, carvon, carveol, perillyl alcohol, α -terpineol, and menthol. The utilization of the natural limonene in oxidation process is the example of the application of biomass for synthesis of very valuable compounds [32]. The ways of limonene obtaining from biomass are cheap thus limonene is very easy available intermediate for organic syntheses.

REFERENCES

1. Karabela M. 2007, *Pancea*, 1 (18) 2007 s. 26-27
2. Citrus Peel Oil Recovery System, a manual describing the operations of JBT FoodTech's, Cold-Pressed Citrus oil Recovering system 2008, JBT FoodTech 400 Fairway Ave Lekeland Florida 33801 USA
3. Separators, Decanters and Process Line from GEA Westfalia Separator for Citrus Processing, GEA Mechanical Equipment
4. Abraham, W.-R., B. Stumpf, and K. Kieslich. 1986. Microbial transformation of terpenoids with 1-p-menthene skeleton. *Appl. Microbiol. Biotechnol.* 24: 24–30
5. Bowen, E. R. 1975. Potential by-products from microbial transformation of D-limonene, p. 304–308. Florida State Horticultural Society 4
6. Cadwallader, K. R., R. J. Braddock, M. E. Parish, and D. P. Higgins. 1989. Bioconversion of (+)-limonene by *Pseudomonas gladioli*. *J. Food Sci.* 54: 1241–1245
7. van Rensburg, E., N. Moleleki, J. P. van der Walt, P. J. Botes, and M. S. van Dyk. 1997. Biotransformation of (1)-limonene and (2)-piperitone by yeasts and yeast-like fungi. *Biotechnol. Lett.* 19:779–782
8. Rama Devi, J., and P. K. Bhattacharyya. 1977. Microbiological transformations of terpenes. Part XXII. Fermentation of geraniol, nerol & limonene by a soil pseudomonad, *Pseudomonas incognita* (Linalool strain). *Indian J. Biochem. Biophys.* 14:288–291.
9. Tan, Q., and D. F. Day. 1998. Bioconversion of limonene to α -terpineol by immobilized *Penicillium digitatum*. *Appl. Microbiol. Biotechnol.* 49:96–101.
10. Dhere, S. G., and R. S. Dhavlikar. 1970. Microbial transformations of terpenoids: limonene. *Sci. Cult.* 7:292.
11. Kraidman, G., B. B. Mukherjee, and I. D. Hill. 1969. Conversion of Dlimonene into an optically active isomer of α -terpineol by a *Cladosporium* species. *Bacteriol. Proc.* 1969:63
12. Draczyn'ska-Lusiak, B., and A. Siewin'ski. 1989. Enantioselectivity of the metabolism of some monoterpenic components of coniferous tree resin by *Armillariella mellea* (honey fungus). *J. Basic Microbiol.* 29:269–275
13. Dhavalikar, R. S., and P. K. Bhattacharyya. 1966. Microbiological transformations of terpenes. Part VIII. Fermentation of limonene by a soil pseudomonad. *Indian J. Biochem.* 3:144–157
14. Mattison, J. E., L. L. McDowell, and R. H. Baum. 1971. Cometabolism of selected monoterpenoids by fungi associated with monoterpenoid containing plants. *Bacteriol. Proc.* 1971:141

15. Chang, H. C., and P. Oriel. 1994. Bioproduction of perillyl alcohol and related monoterpenes by isolates of *Bacillus stearothermophilus*. *J. Food Sci.* 59:660–662, 686.
16. Teunissen, M. J., and J. A. M. de Bont. 1995. Will terpenes be of any significance in future biotechnology?, p. 329–337. In P. E'tie'vant and P. Schreier (ed.), *Bioflavour 95*. INRA, Paris, France
17. van Dyk, M. S., E. van Rensburg, and N. Moleleki. 1998. Hydroxylation of (+)limonene, (-) α -pinene and (-) β -pinene by a *Hormonema* sp. *Biotechnol. Lett.* 20:431–436.
18. Coates G., Byrne C., Allen S., Lobkovsky E., *J. AM. CHEM. SOC.* 2004, 126, 11404-11405.
19. Szczepanik A., Sobkowiak A , *Wiadomości Chemiczne* 63(7-8) (2009) 601-634
20. Yannai, Shmuel. (2004) Dictionary of food compounds with CD-ROM: Additives, flavors, and ingredients. Boca Raton: Chapman & Hall/CRC
21. van der Werf M.J, Boot A. M. Metabolism of carveol and dihydrocarveol in *Rhodococcus erythropolis* DCL14, *Microbiology* (2000), 146, 1129–1141
22. McCaskill, D. & Croteau, R. (1997). Prospects for the bioengineering of isoprenoid biosynthesis. *Adv Biochem Eng Biotechnol* 55, 107–146
23. Burdock George A. Fenaroli's handbook of flavour ingredients (CRC Press, Boca Raton, Fla), 6th ed 2010
24. Belanger J.T., Perillyl alcohol applications in oncology, *Alternative Medicine Review* Vol.3, Issue 6, 1998, Pages 448-457
25. Bhatia S.P., McGinty C., Letizia C.S., Api A.M. *Food and Chemical Toxicology* 46 (2008) S197–S200
26. <http://micronano.info/cherries-are-natures-healing-food/>
27. <http://www.chem.ucla.edu/harding/IGOC/M/menthol.html>
28. Kamatou G.P., Vermaak I., Viljoen A.M., Lawrence B.M. *Phytochemistry* 96 (2013) 15–25
29. Sourburg H., Panten J., *Common Fragrance and Flavor Materials* 5th edition, 2006 WILEY-VCH Verlag GmbH & Co. KGaA, Weinheim
30. <http://www.indiamart.com/shyamjittradingcompany/medical-chemical.html>
31. Maria Kamitsoua, George D. Panagiotoua, Kostas S. Triantafyllidis, Kyriakos Bourikasb, Alexis Lycourghiotisa, Christos Kordulisa, Transformation of α -limonene into p-cymene over oxide catalysts: A green chemistry approach, *Applied Catalysis A: General* 474 (2014) 224–229

32. Wróblewska A., The epoxidation of limonene over the TS-1 and Ti-SBA-15 catalyst., *Molecules* 2014, *19*, 19907-19922;
doi:10.3390/molecules191219907

The release studies of undecylenoyl phenylalanine through cellulose based membranes

*Aleksandra Głównka¹, Anna Olejnik¹, Izabela Nowak¹

¹Adam Mickiewicz University in Poznan, Faculty of Chemistry, Poznan, POLAND

e-mail: ola.glowka@gmail.com

Keywords: *release, amino acid derivative, porous membrane, active substance, undecylenoyl phenylalanine*

ABSTRACT

The release tests of active compounds from semisolids formulations are significant factor in estimating their efficiency. The tremendous progress in science has created a great variety of innovative active compounds such as amino acids derivatives like undecylenoyl phenylalanine. This compound is applied in cosmetics as skin-lightening agent to prevent skin cells from producing melanin pigmentation. The aim of this study was to monitor the release kinetics of undecylenoyl phenylalanine from hydrogels and emulsions through cellulose membranes.

INTRODUCTION

The method of the release of active substances from the semisolid dosage forms is an important step for determination of their efficacy. Therefore, the release test is adopted for assessing the quality of new formulations at their preparation stage and it is used to prove the reproducibility of the production process for each formulation batch [1]. On the basis of the data obtained in this experiment it is possible to determine the amount of drug substance released in time and create a release profile of the active substance. The release profiles are considered as an important element in development and characterization of formulations that allow also to specify the rate and extent of release of the active substance. The main apparatus used for these studies is a Franz cell. However, comparable results can be obtained by conducting research on an USP Apparatus 2 connected with UV spectrophotometer [2]. In addition, this apparatus is equipped with Teflon enhancer cells in which a formulation covered by a membrane, imitating the skin barrier, is placed. Membranes maintain the formulation in the right place and allow the active substance to diffuse through pores to receptor medium. Previously, the release studies were performed using various natural membranes for example fuzzy rat skin, hairless mouse skin, human skin [3]. However, the European Union has recently introduced ban on animal testing for cosmetic purposes (Amendment of the Cosmetics Directive -

76/768/EEC). Therefore, there is a need to find a semipermeable, synthetic and non-animal based membrane, which would have a similar release profile to natural skin and therefore it would enable to identify the proper efficiency of a topical formulation. There is a wide range of synthetic membranes available on the market such as a silicon gel sheet [4], polymethylsiloxane (PDMS) silicone, polysulfone membranes, glass fiber, PTFE-polyethylene or cellulose based membranes [5]. So far different molecules have been used as active substances in pharmacy and cosmetics. Among them are amino acids and their derivatives. They are used in cosmetics because of their multifunctionality. The amino acids-based substances not only act as natural moisturizing factors, but they also have the ability to retain water, soften and improve skin elasticity. Strengthening of the protective barrier of epidermis from the loss of moisture is a very important element to prevent aging of the skin. Phenylalanine derivative such as undecylenoyl phenylalanine (Fig.1) is used to treat skin problems associated with hyperpigmentation. This substance inhibits skin cells to produce melanin pigments by inhibiting melanin stimulating hormone MSH [6]. The aim of this study was to monitor the release kinetics of undecylenoyl phenylalanine from hydrogels and emulsions through cellulose based membranes.

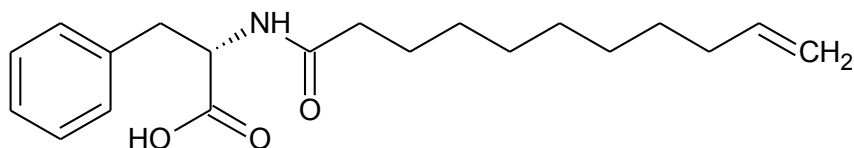


Fig.1. Chemical structure of undecylenoyl phenylalanine.

MATERIALS AND METHODS

Materials

The study was conducted on three different formulations constituted by emulsion and hydrogels containing undecylenoyl phenylalanine. They were prepared according to the composition summarized in Table 1. Potassium phosphate buffer was purchased from J.T. Baker[®]. Synthetic membranes such as regenerated cellulose (Cuprophane, Ref. 12-1370) and nitrocellulose (Protran BA 85, Ref. 10401116) were obtained from Agilent Technologies (USA) and GE Whatman (USA), respectively.

Table 1 Chemical compositions of the formulations.

		Trade name	Ingredient	Company	% weight
Emulsion	1	Tego Care 450	Polyglyceryl-3 methylglucose distearate	Evonik	4.5
	2	Tego Alkanol 1618	Cetearyl alcohol	Evonik	3.5
	3	Tegin 4100 Pellets	Glyceryl stearate	Evonik	3.5
	4	Cetiol 868	Ethylhexyl stearate	Cognis	10.0
	5	-	Deminerlized water	-	72.5
	6	Anhydrous glycerin	Glycerin	Chempur	5.0
	7	Sepiwhite	N-undecylenoyl phenylalanine	Seppic	0.5

Gel 1	1	Tego Carbomer 134	Carbomer	Evonik	0.5
	2	-	10% NaOH	Chempur	1.0
	3	-	2-propanol	Sigma Aldrich	25.0
	4	-	Deminerlized water	-	73.0
	5	Sepiwhite	N-undecylenoyl phenylalanine	Seppic	0.5
Gel 2	1	-	Hydroxyethyl cellulose (HEC)	Sigma Aldrich	2.5
	2	-	Glycerin	Chempur	10.0
	3	-	Distilled water	-	86.5
	4	-			
	5	Sepiwhite	N-undecylenoyl phenylalanine	Seppic	0.5

Semisolids preparation

Emulsion

Ingredients 1 – 4 were introduced into the beaker and heated to 70°C. In another beaker distilled water and undecylenoyl phenylalanine were placed and heated to 75°C. Both beakers were stirred. When the oil phase components were dissolved water phase was added. The mixture of both phases was cooled down to 50°C and was homogenized using a homogenizer (Yellow Line DI 25 Basic). After cooling to 30°C <http://pl.pons.com/t%C5%82umaczenie/angielski-polski/submittedglycerin> was added and homogenized.

Gel 1 – Carbomer

Carbomer was dispersed in water for 1.5 h using a magnetic stirrer. Undecylenoyl phenylalanine was dissolved in 2-propanol <http://pl.pons.com/t%C5%82umaczenie/angielski-polski/OLand> added to the beaker with carbomer. Then a solution of sodium hydroxide was added until pH of 6.5 was achieved.

Gel 2 – HEC

Water, glycerin and undecylenoyl phenylalanine were placed into the beaker and heated to 80°C. Then <http://pl.pons.com/t%C5%82umaczenie/angielski-polski/hydroksyetyloceluloz%C4%99> hydroxyethyl cellulose was added and stirred to obtain a preparation of gel consistency.

Determination of Viscosity

All viscosity measurements were performed three times at room temperature by using a rotational viscometer equipped with temperature sensor (RC02 Viscometer, Rheotec, Germany) and different spindles (R2-R7).

Release studies

The release studies of undecylenoyl phenylalanine were performed with the use of an USP Apparatus 2 (Agilent Technologies DS 708) connected with UV-Vis spectrophotometer (Fig.2). This apparatus consists of vessels with a capacity of 200 ml, placed in a water bath and paddles, which are set in rotation. Samples were placed into the enhancer cells with surface area 4 cm² and covered with the selected membrane. In this research Cuprophan membrane made of pure cellulose with the thickness of 10 µm and nitrocellulose membrane with the thickness of 125 µm, pore size 0.45 µm and binding capacity from 80 µg/cm² to 150 µg/cm² were used. The study was conducted for 24 hours at 32.3°C with stirring speed of 100 rpm. As the medium mixture of phosphate buffer and ethanol in the ratio of 65:35 was used. The concentration of the released amino acid was spectrometrically monitored at 258 nm. The release tests were performed five times.

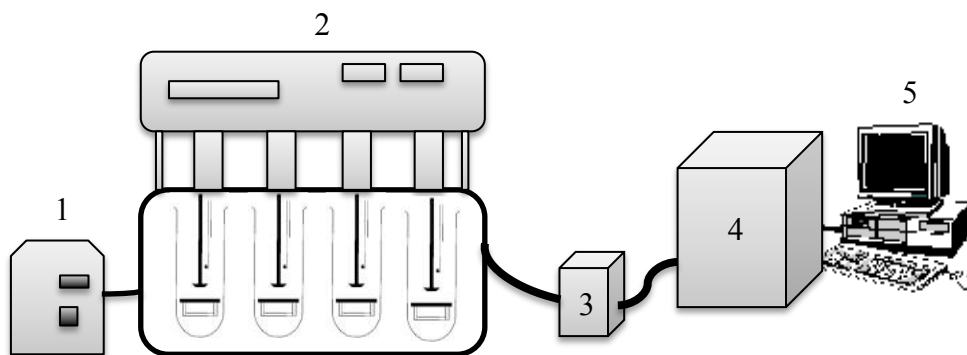


Fig. 2 Schematic representation of the USP Apparatus 2; 1-heated bath, 2-module where the active substance is released, 3 - peristaltic pump, 4 - UV-Vis spectrophotometer, 5-computer.

Membrane characterization by Atomic Force Microscopy

All measurements were performed on the NanoWizard 3-AFM (JKP Instruments, Germany) on Zeiss (AxioObserver) inverted optical microscope with epi-fluorescence at room temperature.

RESULTS AND DISCUSSION

In order to determine the release kinetics of the undecylenoyl phenylalanine the standard solution of the active substance was prepared and its characteristic analytical wavelength was distinguished. UV spectra were prepared in a mixture of phosphate buffer and ethanol in ratio 65:35. In the absorption spectrum an intense band in the range of 240-280 nm with maximum absorption (λ_{\max}) at 258 nm can be distinguished (Fig. 3). This band is formed as a result of the allowed transitions within the aromatic ring of phenylalanine. The application of UV-Vis spectroscopy enabled to estimate the release kinetics of the undecylenoyl phenylalanine from various semisolid formulations.

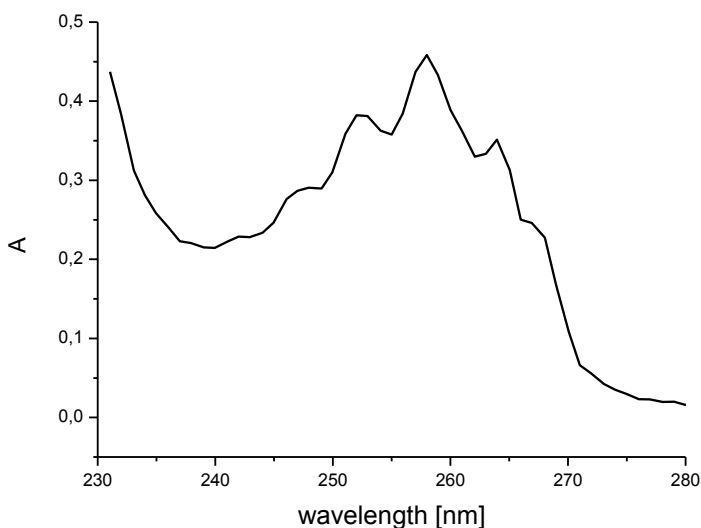


Fig. 3 UV spectrum of undecylenoyl phenylalanine.

Fig. 4 shows the percentage of undecylenoyl phenylalanine released from three semisolid formulations after 24 h. The highest diffusion rate of the active compound was observed in the case of Gel 1 based on Carbomer. After 3 h up to a half of the total mass of active substance was released and then the percentage of undecylenoyl phenylalanine in the receptor medium increased constantly in order to reach around 89% after 24 h. In the case of Gel 2 based on hydroxyethyl cellulose 50% of total mass of active substance was released after 14 h to achieve around 63% after 24 h. On the other hand, it was observed that

the lowest amount (ca. 18%) of undecylenoyl phenylalanine was diffused from emulsion. Various release rates of active compound from semisolids could be explained by their different rheological properties. The results of the viscosity measurements of obtained formulations were gathered in Table 2. Considering the results in the range 70-80% in a Brookfield scale, viscosity of formulations are as follows: Emulsion >> Gel 1 >> Gel 2. Additionally, it was shown that the obtained formulations belong to the group of non-Newtonian fluids because their viscosity changes with increasing speed of the spindle. The results proved that the release rate of active substance is highly dependent on the viscosity. Rheological analysis of the obtained formulations showed that Emulsion 1 exhibited the highest viscosity that can determine the release process of the undecylenoyl phenylalanine. This emulsion consisted of oil phase ingredients such as polyglyceryl-3 methylglucose distearate, cetearyl alcohol, glyceryl stearate, ethylhexyl stearate and glycerin that could inhibit the diffusion process of the phenylalanine derivative. On the other hand Gel 1 based on Carbomer showed the lowest viscosity that can have an influence on the release rate of undecylenoyl phenylalanine. The results proved that the specific components of the formulation could significantly affect the release process.

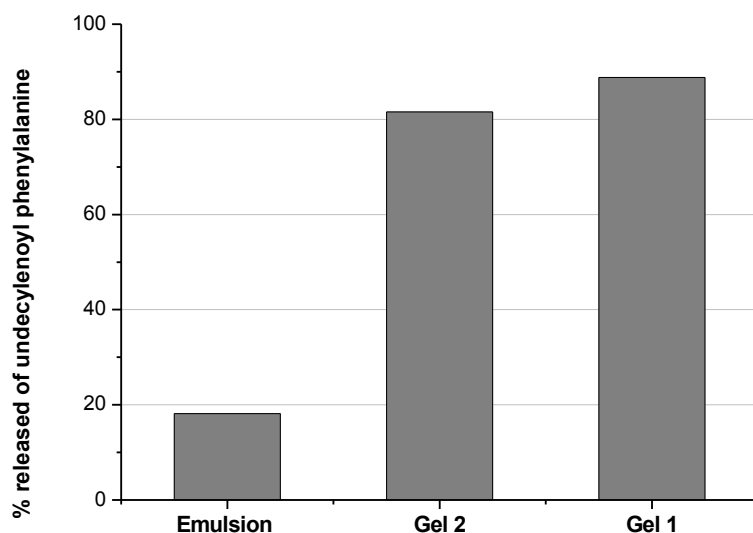


Fig.4 Percentage of undecylenoyl phenylalanine released from various formulations after 24 h through Cuprophan membrane.

Table 2. Viscosity of formulations.

Formulation	Viscosity [mPas] R5	Viscosity [mPas] R4
Emulsion 1	58 127 ± 57 (5 rpm)	-
Gel 1 - Carbomer	-	770 ± 10 (200 rpm)
Gel 2 - HEC	-	37 673 ± 99 (4 rpm)

Not only has the formulation type influence on the release rate of active substance but also the membrane type. The selection of the appropriate membrane is the critical step for the development of the methodology of release experiment. Depending on the applied membrane the kinetics of the active compound released from Gel 2 based on HEC can be described by different models (Fig. 5). The data obtained from the release of undecylenoyl phenylalanine through Cuprophan membrane can be fitted with Higuchi equation, $F = k_H t^{0.5}$ where F is the fractional release of drug, k is the Higuchi constant and t is time [7, 8] with correlation coefficient R of 0.999. On the other hand when the active substance diffused through nitrocellulose membrane the release results can be described by using Korsmeyer-Peppas model: $F = kt^n$ where k is the kinetic constant and n is the release constant (correlation coefficient, R of 0.990)

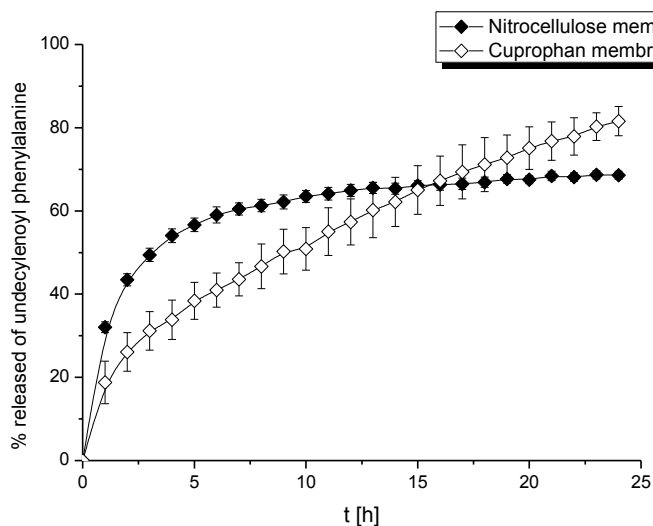


Fig.5 Release profiles of undecylenoyl phenylalanine from Gel 2 based on HEC through cellulose membranes.

The obtained results suggest that the structure of synthetic membranes can influence the release rate of undecylenoyl phenylalanine. In Fig. 5 the

atomic force microscopy images of both synthetic membranes are shown. The Cuprophan membrane (Fig. 6A) consists of longitudinal cellulose fibers separated by irregular and inhomogeneous pores. It is thought that this kind of structure resembles the disordered structure of stratum corneum [9]. It could be seen in the Fig.6 B that the structure of nitrocellulose membrane is completely different than in the case of Cuprophan membrane. The pores of this membrane varied in shape and size. Additionally they are distributed inhomogeneously that can also have an influence on the release rate of the phenylalanine derivative.

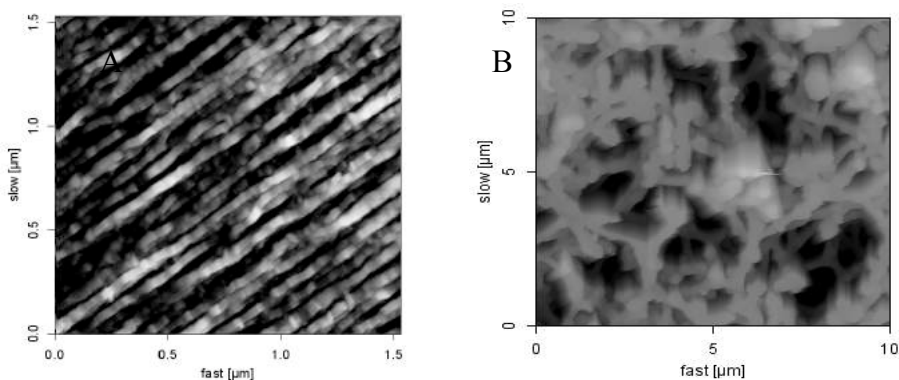


Fig.6 AFM images of Cuprophan membrane (A) and nitrocellulose membrane (B).

CONCLUSIONS

The obtained results showed that the membrane structure has the influence on the release rate of undecylenoyl phenylalanine. Depending on the applied membrane the kinetics of the active compound release from hydrogels can be described by the Korsmeyer-Peppas model or by the Higuchi model. Additionally, it was proved that the rheological properties of semisolid formulations strongly determine the release rate of active compound. The higher viscosity of the semisolid the slower is the permeation through the membrane. Therefore, hydrogels presented the fastest release rate of undecylenoyl phenylalanine and could be recommended as a vehicle for this substance.

REFERENCES

- [1] Siewert M., Dressman J., Brown C.K., Shah V.P., FIP/AAPS Guidelines to Dissolution/in Vitro Release Testing of Novel/Special Dosage Forms, *AAPS PharmSciTech*, 2013, 4 (1) Article 7
- [2] Nowak I., Olejnik A., Gościańska J., Chapter in the book: Porównanie szybkości uwalniania ibuprofenu z komercyjnie dostępnych środków o działaniu pielęgnacyjno-leczniczym, *Analityka środków kosmetycznych, Cursiva*, 2012

- [3] Shah V., Raval S., Peer S., Upadhyay U.M., A comparative evaluation of different membranes for their diffusion efficiency: an *in vitro* study, *Pharma science monitor*, 2010, Vol-1, Issue-2
- [4] Shioh-Fern N., Rouse J., Sanderson D., Eccleston G., A Comparative Study of Transmembrane Diffusion and Permeation of Ibuprofen across Synthetic Membranes Using Franz Diffusion Cells, *Pharmaceutics*, 2010, 2, 209-223
DOI: 10.3390/pharmaceutics2020209
- [5] Olejnik A., Gościańska J., Nowak I., Active Compounds Release from Semisolid Dosage Forms, *Journal of Pharmaceutical Sciences*, 2012 Vol. 101, No. 11
DOI: 10.1002/jps.23289
- [6] Katoulis A., Alevizou A., Soura E., Mantas N., Bozi E., Gregoriou S., Makris M., Rigopoulos D., A double-blind vehicle-controlled study of a preparation containing undecylenoyl phenylalanine 2% in the treatment of melasma in females, *Journal of Cosmetic Dermatology*, 2014, 13, 86-90
- [7] Higuchi T., Rate of release of medicaments from ointment bases containing drugs in suspension, *Journal of Pharmaceutical Sciences*, 1961, 50, 874-875
- [8] Higuchi T., Mechanism of sustained-action medication. Theoretical analysis of solid drugs dispersed in solid matrices, *Journal of Pharmaceutical Sciences*, 1963, 52, 1145-1149
- [9] Donnelly R.F., McCarron P.A., Zawislak A.A., Woolfson A.D., Design and physicochemical characterization of a bioadhesive patch for dose-controlled topical delivery of imiquimod. *International Journal of Pharmaceutics*, 2006, 307, 318–325.

The Industrial Heritage in nowadays Polish cities

*Joanna Gruszczyńska

Faculty of Architecture, Warsaw University of Technology, Warsaw, POLAND

e-mail: j.byszewska@gmail.com

Keywords: *industrial areas, heritage, identity*

ABSTRACT

One of the basic functions of the city is to provide a sense of security and the identity to its inhabitants. The progress of urbanization and globalization sparked fear that this values and cultural significance might be blurred. Modern city too often is build in a way which ignores ties to its history. There are examples showing that if we traced or uncovered the history and values that constitute the city image and use them in present development, it will be beneficial long term and on many levels.

INTRODUCTION

Year 2015 was announced the European Industrial and Technical Heritage Year. Considering that, it is a good time to discuss this topic. Nowadays city is rapidly developing and constantly changing. It is highly developed organism [1] in technology, communication and social point. The progress of urbanization and globalization sparked that if cultural differences were blurred the city might not fulfill the basic function: to provide inhabitants a sense of security and opportunities to develop [2]. Modern city too often is built in a way that ignores ties to its history. There are examples showing that traced, uncovered history and values that constitute the city image, used in present development, can be beneficial in long period, on many levels.

THE CITY

Since the begging of phenomenon such as 'city' was fascinating and terrifying at the same time. Men dream of city - here they see new opportunities, career sessions, enrichment and self-realization. However, living in cities he felt overwhelmed by their enormity. The city [3] is not only bustling streets, seats of government, buildings, art and cultural centers. The city is a composition that not only fascinates scientists and researchers, but also writers and travelers.

To this day, there is no single, clear definition. The term 'the city' is very complex and ambiguous concept, on whose consists of many factors. My research focuses on specific aspects of the city, such as residents, people and buildings, or sociological and architectural aspects.

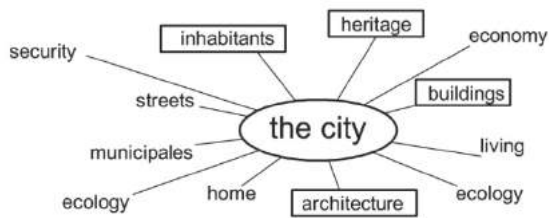


Fig 1 The diagram illustrating the question: what is the city and elements which have an impact on the city

The city is a space of our daily activities, the space in which we live, work and learn. It is a place connected to our memories and identity. As a citizens we identify ourselves with the city, it stimulates us and cause afterthought. Therefore, it such influence is a crucial element of the identity of the city [4]. The identity of the city gives a unique and symbolic meaning [5]. That ‘the specific character’ can create buildings that carry on the heritage. From a sociological point of view of spatial identity it is the emotional evaluation of the reality he sees as part of himself and feels tower with a given space.

INDUSTRIAL ARCHITECTURE AND INDUSTRIAL HERITAGE

The industrial areas can be understood in two ways. In narrow term ‘brownfields’ are as a ‘*degraded land not used or not fully used, areas intended primarily for economic activity, which has been completed*’ [6]. Wider recognition includes also areas degraded, due to industrial activities, such as mining.

According to Borsi (1975), the industrial landscape may be defined as ‘*the landscape resultant from a thoughtful and systematic activity of man in the natural or agricultural landscape with the aim of developing industrial activities*’ [7]. This definition enabled the recognition of an entire landscape as a single ‘element’.

Industrial buildings had their own architectural character. Most of industrial buildings from the late nineteenth and early twentieth-century were not plastered, due to lowering costs, were build with a facing brick. An important and characteristic element of industrial buildings was tall chimney, towering over the rest of the buildings, often higher than the church towers.

This makes the architectural and urban heritage an important part of our European history. Described objects hold/carry the history and tradition of the place where they were built. The industrial era formed the industrial heritage [8].

Industrial building had no doubt the significant part in that process, creating the cultural heritage [9].

The heritage includes not only 'monuments of high culture' such as a medieval castle or a Renaissance church, but also 'sites of every-day life', that create an industrial architecture. 'Cultural landscapes [including industrial ones] tell us who we are, far more effectively than most architecture or exhibitions in museums ever can' [10].

THE IMAGE OF INDUSTRIAL HERITAGE IN THE VIEW OF CURRENT CITIES

Every big Polish city, including cities like Warsaw, Krakow have had become the industrial centers by the end of the twentieth century. In the twenties century polish cities were dynamically developing, it was also the time of industrialization. Most of the brownfields (industrial area) are now located in the city center and most of them have become isolated, forgotten and unwanted areas, due to many reasons (e.g. economical, political and social). They are often boundaries to the natural growth of the city, what leads to multiples problems.

When, in the early 19th Century, a more intensive discussion of possible strategies to protect and restore our architectural and urban heritage began, the attention focused nearly exclusively on 'monuments of high culture'. Only more recently, in the second half of the 20th century, the attention has been extended to the Industrial Revolution and its 'sites of the everyday live'. Though now a greater understanding can be in countered how important this specific past is for our cultural community.

Brownfield sites are perceived as a threat, an obstacle to the harmonious and open-ended development of cities. They are creating a 'no man's land' described by Jan Gehl. Neglected areas are not space in which inhabitants want to reside, nor are the places that we want to take care of. Rolling industrial areas become non-places [11]. It's no one's space, not due to the lack of the owner, but the lack of human emotional ties with the place. What is important, as the old Scandinavian adage say – 'people come to, where the people are' [12].



Fig. 2 A diagram illustrating the method of operation of the industrial areas.

In Poland era of Industry was much longer then in the other parts of Europe. Considering that one might suppose we should have much more well preserved objects, but industrial architecture has been neglected for years? For

many years, in opinion of art historians and conservators, old factories and production halls were considered as not deserving protection. To this day, there are no efficient, implemented procedures for categorizing and assessing the value of industrial objects. Often fail to protect objects of unique or representative of important history in historical cities.

Up to this day, the register of monuments has been included over two thousand objects. Many objects have significant values (scientific, historical, artistic) [13], still many of them have not been entered into the register of monuments. We should be aware that many of the industrial buildings have not survived to this day. The problem of conservation protection is determined to a large extent the economic and social realities. Decisions on the protection of cultural values of these objects imply the question of the economic and social benefits of the project.

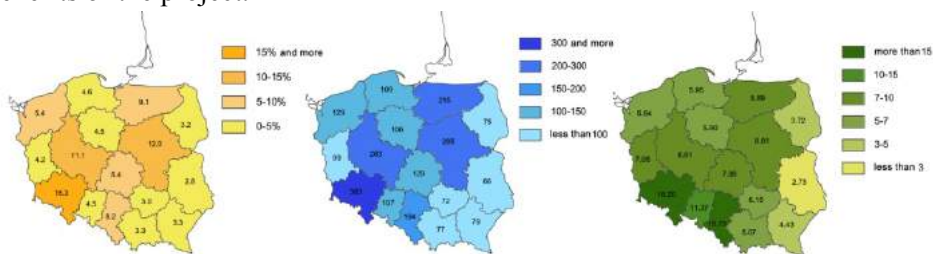


Fig.3 Diagram presents from left to right :

- the percentage of industrial facilities that are registered as monuments per province,
- the number of industrial facilities that are registered as monuments of the division into provinces,

Analysis of industrial facilities national monuments in the areas of Polish regions, where many of this objects are shown. The largest intensity of the industrials objects is in Silesia and central part of Poland. Analysis of current land within the borders of Poland when was the industrialization period and Polish territories against annexations and 1830, showed that the most intense of brownfields, which for many years was not within Polish borders. In that fact, for many years that heritage was not taken into consideration as a polish heritage of humanity.

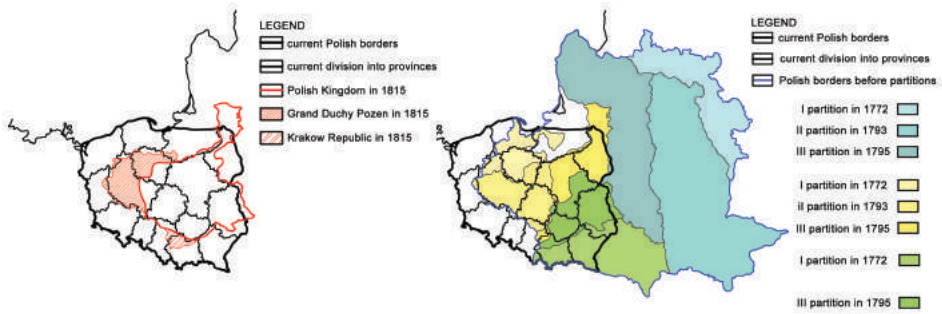


Fig.4 Analysis of the area of the current Polish boundaries:
 - left picture: current boundaries compared to 1815 boundaries
 - right picture: current boundaries compare to the time of the Polish division into Partitions

New urbanization processes in several cases contributed to dereliction of industrial areas and to the disappearance of numerous industrial values, commonly known as industrial heritage. It was forgotten that once industrial buildings were creating focal points of the city life and society’s culture. We achieved a point in development, when cities can no longer spread outside its boundaries. Areas described in the article could no longer be blank spots or ruins on the city maps. It became necessary to reuse abandoned industrial landscapes.



Fig.5 On the left: A part of Scheibler lofts redeveloped and in contrast the decaying parts

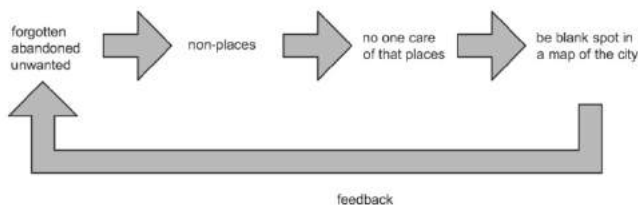


Fig.6 A diagram of this procedure from the industrial area of the city

As a result the symbol of independent Poland became the closing down Industrial Center. The negative effects of free market economy are certainly urban confusion, lack of planning and design often without context, the detachment from the history of the place, its traditions and identity. Every city has a different story, most of them used to be gray, homogeneous industrial agglomerations. Nowadays they are more lively and colorful, filled with wide range of functions. One of the basic functions of the city is to provide a sense of security and the identity to its inhabitants.

The problem with the image of industrial heritage in the view of current city is that many times the local municipality does not really understand what these areas mean for people and cities. The changing of the place or building or his function can modify the spirit of the place.

Table 1 Summary table of the advantages and problems of brownfields in the image of today's city

PROBLEMS	ADVANTAGES
<ul style="list-style-type: none"> -brownfield sites are treated as if there were no -non- places and forgotten -inhibit the growth of the city -neglected -isolated -often form complexes, which as a whole are difficult to adapt - covered an attractive areas nearby city center 	<ul style="list-style-type: none"> - create the history of the city and places - create an identity of the city - covered an attractive areas nearby city center - the memory of the city and the people (residents) - heritage - are testimony of history - traditions and culture media

RE-USE OF THE INDUSTRIAL BUILDINGS IN POLAND

The analysis of society and understanding of an area lead to gaining knowledge of the place that people wish to live in, to identify the social perception of the place. It is important to realize that the whole city is our heritage. Cultural landscapes are integral part of our society, which reveals our relationship with the land over time.

Before starting to develop a reclamation or revitalization project for a postindustrial landscape it is important to know ‘why’ and ‘how’ to reclaim and protect the industrial landscape. We should also consider why post-industrial objects after adaptation to the new functions so often are no longer associated with the industry? By entering modern function into the old building, peeled it with characteristic smell of industrial object (such as grease and coal, the characteristic sounds of the era of coal and the steam engine. On the other hand, the technology goes forward and should not pretend that these objects are able to operate today in an unchanged form.

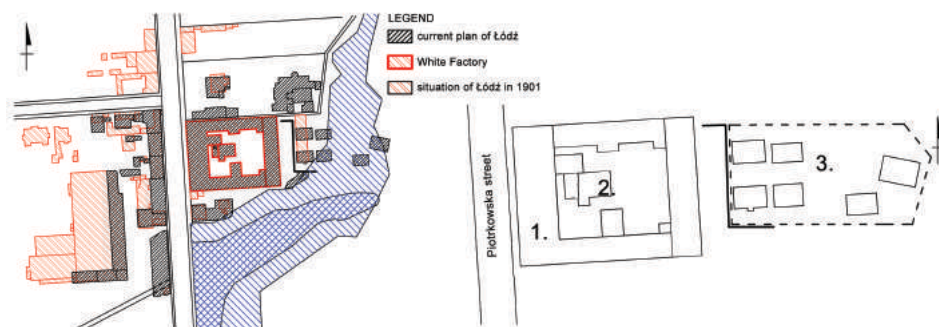
It is worth mentioning that sociological studies point out that most of the complexes and industrial objects does not exist in the public consciousness until it has been subjected to revitalization or adaptation [14]. Closed assumption, which often contain whole factory and the workers houses, make regardless of the values they carry, are ‘absent’ on the city landscape for inhabitants. Adaptation of the historic building to the new function can decide on its effective protection in the fabric of the city. *‘The potential of the monument is, however, the larger, the more value can be distinguished, find and offer potential customers.’* [15] A notable examples of revitalization may be found in Germany, Kronenberg wrote *‘basic premise was to present the hitherto inaccessible places and gain social acceptance for their the preservation and restoration’* [16]. From this point of view, each adaptation should be emphasized in the slightest element the nature of old industrial buildings, so that creates public awareness of the history of the place, and hence the need to preserve and exposure.

One of the first in Poland and first in the world adaptation of the post-industrial architecture to the museum function (preserved museum)- the Geyer’s Factory, which preserved as much as it was possible the original design and appearance of the building and could be reconciled with the new feature. When in the ‘50s began adaptation ‘postindustrial walls’ for the purposes of historical – artistic – technical museum nobody else – neither in Poland nor in the world – did not think of re-using of industrial buildings, as a precedent theoretical and practical problem. It is worth noticing, that the revitalization preserved as much of the historical substance as possible, what was outstanding in those years. Vicissitudes, periods of prosperity, have left their marks on the buildings' appearance, but never substantially changed its former plans.

On the basis of analyzing the objects listed in the register of monuments for analysis were selected examples, which are closely related to industrial pedigree.

Lodz is a city associated with the textile industry. These objects are the basis for the city's identity. In the period of the greatest development of production factory in Lodz area occupied about 20% of the city.

Geyer's factory is located in a center of Lodz nearby Piotrkowska Street (the most important street in Lodz). Today, the White Factory [17] is the seat of the Central Museum of Textiles, built by the family of the Saxon immigrant, Ludwig Geyer, in the years 1835-1886. It is a wonderful example of industrial architecture, which real beauty was appreciated in the twenty- first century. The four wings factory with the building of the Old Boiler with high chimney [18] in the middle of a big yard, two extraction towers, two pressure towers is a unique create a unique industrial architecture, unparalleled in the other factories. Factory rebuilding had already began after the Second War World, in the year 1955, when it was decided to allocate the objects for the museum purpose.



1. The first renovation and construction work began in 1958 and was limited to the western and the south wing. They consisted in adapting the factory halls to the needs of museum, so the creation the exhibition space, warehouse, office, organize internal communication (it must appear new staircases).
2. The following years it was the restoration in the west and the north wing. In 1981 began work in the Old Boiler, in which was placed the engine steam. In 2006-2008 European Union funds and investment Municipal Boat carried out investment, thanks to which the museum increase a usable space in the east wing, which houses a library and technical room, hall of working weaving and knitting machines, renovated facades internal courtyard, 'iron' courtyard and it was renovated building placed the postindustrial factory bath, which now fits the café.

Fig. 7 Analysis of areas of the White Factory - Geyer's Factory in 1901 and the current plan of Łódź

Over the years, more and more industrial objects were adapted to the new features. This is one of the ways that these objects could begin again to be a 'teeming with life' and have been revived in the city landscape. Of course there are many factors that affect whether the adaptation is correct and proper. One of them is the inhabitants' memory of the functioning of these facilities at the time of luminosity. *'The memory of the place can survive in the people comprising the community, even if the physical image of the space will be destroyed or substantially processed. The subject of the memories often is long-abandoned places. They live in the memories, stories [...].'* [19]



Fig. 8. The current state of the object The Geyer Factory, after revitalization
White Factory

Areas which are the most associated with the industry in Poland, are the Upper and Lower Silesia. In these areas, there are still many mines that work but also many, which ended its activities. The industrialized areas are associated with the mining of coal, glassworks, rolling mill and many other industrial facilities.

By theorists Silesian lands are comparable to the Ruhr area. Upper Silesia has much in common with the Ruhr in historical and demographical terms. Both territories are tight spaces developed by the industry in the nineteenth century. Silesia occupies a smaller area, but is struggling with the same problems. Production in most factories ended, as well as coal mining is no longer on this scale.

The Tradition Park In Siemianowice Śląskie was build in the site of the old mine named ‘Michał’ [20], which history dates back to the mid-nineteenth century. *In 2008, the city Siemianowice Śląskie took over the decaying engine building and the shaft ‘Cristin’, which were then in private hands. In the same year renovations and refurbishment of the object was started. The building of the museum has very important exhibition, not only for tourist but also for habitants. It preserves the memory of the past of the city Siemianowice and this parts of*

Silesia region. This is a very important stop on the trail of ‘technology monuments’ [21] on Silesian’s earth.

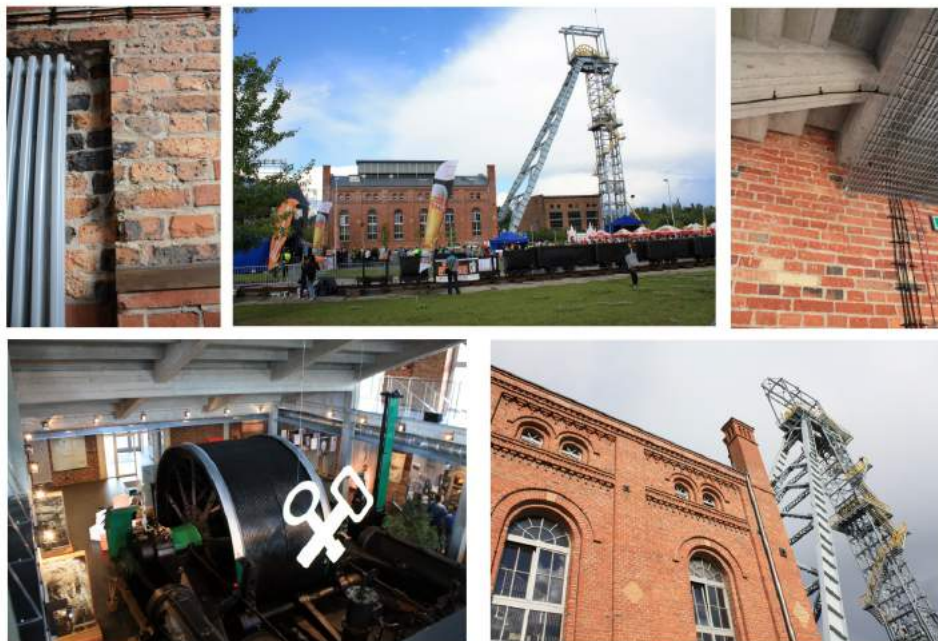


Fig. 9 The current state of the object KWK ‘Michał’, after revitalization Tradition

The current object – the *decaying* engine building has four floors which are located inter alia: modern conference room as well as steam hoisting engine (machine) from 1905 [22], model of the furnace and one of the biggest collection of mining lamps, as well as exhibits related to the Silesian industry. In the basement was arranged mining sidewalk, where with the help of multimedia, visitors can feel the atmosphere of an old mine. The landscape is complemented by a 56-meter tall exhaust tower shaft called ‘Cristin’ [23].

Adaptation of industrial facilities is often treated as a candy image so causing that boundaries between what is authentic and what is artificial are often blurred. A fine line between artificial space and historical truth - is very easy to seizure by a malfunction on historic buildings by too faithful reproduction of the historic stage of the building, or no material differences in the historical substance and new one - supplemented. A special form of mystification are spaces where authenticity is staged [24].

Table 2 Statement of adapting two assumptions analyzed. Rating .

ISSUE	WHITE FACTORY IN ŁÓDŹ	TRADITIONAL PARK IN SIEMIANOWICE ŚLĄSKIE
Adaptation all the elements of the assumption	✓	✗
Differentiated function of the object	✗	✓
New function highlights the value of buildings	✓	✓
New architectural elements	✓	✓
Visited by tourists	✓	✓
Visited by inhabitants	✗	✓
Educational function	✓	✓
Proper revitalization	✓	✓
Kept the authenticity of buildings	✗/✓	✓
Kept character of the place	✓	✓
Kept relict of history - technique monument	✓	✓
Easy to distinguish old and new elements	✓	✓
Recover the object to the city landscape	✗/✓	✓

DISCUSSION AND CONCLUSION

Nowadays city is rapidly developing it loses its relationship with history, becomes bland. That is why it is so important to re-feed and re-integrate into the city landscape the objects that create the city's identity, which should survived. Opening buildings to the public and the inhabitants (educational function [25]), causes the formation of a common awareness of space. This process of shaping public awareness and identification is often used as a part of the revitalization process.

'Now' the post industrial landscapes and as a catalyst for urban redevelopment by being a relevant element of the 'genetic code' of the city [26]. Those areas are considerate as a asset in the view if current city, what is very important for the society. The answer to question, how to re-use the abounded, forgotten industrial area, should be formulated in order to maximize benefits that may rise from its (re)development.

'(...) the longer I look at landscapes and seek to understand them, the more convinced I am that their beauty is not simply an aspect but their very essence and that, that beauty derives from the human presence. (...) The beauty that we see in the vernacular landscape is the image of our common humanity (...)'

[27]. It is important to preserve traces of the old industrial culture in city, and emphasizing the presence of this heritage, especially in the old industrial regions such as Silesia or in Lodz. While planning a development and transformation of the cities we should bear in mind their '*past, now and future*' and take in consideration long term results, results for the future generations. Robert

Archibald wrote: *'those who forget the past, and those who ignore it or try to erase, behave as if there were no future'* [28]. It is worth remembering his words.

REFERENCES

- [1] Rykwert J., Pokusa miejsca. Przeszłość i przyszłość miast. Międzynarodowe Centrum Kultury, *Kraków* 2013, p.7
- [2] The New Charter of Athens, Alinea, Firenze 2003.
- [3] One of the definitions of the term was written by Dziewoński, who understood the city as a *'historically shaped the type of housing, there is a specific set of partial community, focused on an area with a separate organization, recognized by law and producing in its operations team durable material with a specific device physiognomy, which reflects a distinct type of landscape.'*, in: Dziewoński K., for Kiełczewska-Zalewska M., *Geografia osadnictwa*, PWN, Warszawa 1972.
- [4] The identity of the city by Glińska it is *'a collection of historical conditions for the city characteristics that distinguish them from others and express themselves all the actions that are taken in the city in order to create its unique character'*. Glińska E., *Socjologiczna i marketingowa koncepcja tożsamości miasta*, [in:] *Obywatelstwo i tożsamość społeczeństwach zróżnicowanych kulturowo i na pograniczach*, tom 1, Wydawnictwo Uniwersytetu w Białymstoku, Białystok 2006, p. 33.
- [5] Glińska E., *Socjologiczna i marketingowa koncepcja tożsamości miasta*, [w:] *Obywatelstwo i tożsamość społeczeństwach zróżnicowanych kulturowo i na pograniczach*, tom 1, Wydawnictwo Uniwersytetu w Białymstoku, Białystok 2006, p. 33.
- [6] The government program for brownfields , adopted by the Council of Ministers on April 27, 2004
- [7] Borsi, F., *Le paysage de l'industrie*. Bruxelles: Archives d'Architecture Moderne, 1975
- [8] According to the Nizhny Tagil Charter the *'industrial heritage consists of the remains of industrial culture which are of historical, technological, social, architectural or scientific value'* and *'the historical period of principal interest extends forward from the beginning of the Industrial Revolution in the second half of the eighteenth century up to and including the present day, while also examining its earlier pre-industrial and proto-industrial roots'*, [in]: *The International Committee for the Conservation of Industrial Heritage (TICCIH-The Nizhny Tagil Charter for the Industrial Heritage)*, July 2003.
- [9] The Cultural Heritage based on Council of Europe Framework Convention on the Value of Cultural Heritage for Society is *'a group of resources inherited*

from the past which people identify, independently of ownership, as a reflection and expression of their constantly evolving values, beliefs, knowledge and traditions. It includes all aspects of the environment resulting from the interaction between people and places through time'. Council of Europe Framework Convention on the Value of Cultural Heritage for Society, 27.IX. 2005 in Faro, <http://conventions.coe.int/Treaty/EN/Treaties/Html/199.htm>.

[10] Hayden, D., Forward: In Search of the American Cultural Landscape, in: Alanen A. and Melnick, R., [eds.] Preserving Cultural Landscapes. Baltimore: Johns Hopkins University Press, 2000.

[11] The term 'non-place' was created by the French ethnologist and cultural anthropologist Marc Aug.

[12] Gehl J., *Życie między budynkami*, przekład Marta A. Urbańska, Wydawnictwo RAM, Kraków 2013.

[13] The Act of 23 July 2003 *on the conservation and protection of monuments*, *Dz.U. 2003 no 162 poz. 1568*.

[14] A number of studies at University in Łódź carried out relating to the public perception of industrial heritage, in: Kronenberg M., *Wpływ zasobów dziedzictwa przemysłowego na atrakcyjność turystyczna miasta. Przykład Łodzi*, wyd. uniwersytetu Łódzkiego, Łódź 2012, p 26-28, 55-56.

[15] Rouba B. J., Dlaczego adaptacje niszczą zabytki i czy tak być musi?, [in:] *Adaptacja obiektów zabytkowych do współczesnych funkcji użytkowych*, Lubelskie Towarzystwo Naukowe Międzynarodowa Rada Ochrony Zabytków ICOMOS, Politechnika Lubelska, Warszawa – Lublin 2009.

[16] Kronenberg M., *Wpływ zasobów dziedzictwa przemysłowego na atrakcyjność turystyczna miasta. Przykład Łodzi*, wyd. uniwersytetu Łódzkiego, Łódź 2012, p. 57.

[17] White Factory name comes from the color of plastered. It was one of the few industrial factories that were plastered.

[18] It was the first in Lodz octagonal factory chimney, it was build in 1827. Just in 2002 was renovated – the renovation was called as 'difficult restoration'.

[19] M. Żmudzińska-Nowak, *Miejsce tożsamość i zmiana*, Wydawnictwo Politechniki Śląskiej, Gliwice 2010, p. 96.

[20] The activities started a family Rheinbabens, which of that time was the owner of Michałowice – in 1856 was a grant mining (extended to addition areas in 1867) and the construction of wells began in 1881, two years later mined the coal. Another breakthrough from the point of view of the fate of the company was the year 1892, in which Prince Hohenlohe - Oehringen Hugo acquired a good of Michałowice and the mine. The name, under which the majority of habitants of Siemianowice city knew mine, the 'Michael', was given in 1936. Mine 'Michał' was not only heir, but also a direct continuation of more than half

a century, 'Max'. In 1905, at the mine consisted of five wells have many buildings and mining. From that year until the thirties mine managed, constantly modernizing and expanding resources Hohenlohe is plants created by Christian Kraft.

[21] Monuments trail - Tourist route connecting 36 facilities in the province of Silesia, includes museums, heritage parks, and even inhabited colonies workers, closed and still acting workshops.

[22] The museum has a very important exhibition, exciting and interesting telling of the history of the place. One of the most important exhibits is the steam engine as sources from 1905 - technical monument - funniest mine equipment.

[23] The shaft was changed in the year 1936 'Christian Kraft', which become from name the son of Prince Hohenlohe-Oehringe changed on 'Cristin'. In 1975, the exhaust tower was replaced by a new one, that was a Tradition Park visitors can admire- thanks to the renovation – seen in all its glory. This tower is one of the most important element identifying this city and create the point of local landscape.

[24] MacCannell D, *Turysta-nowa teoria klasy podróźniczej*, MUZA, Warszawa 2005, p 143-166.

[25] 'Through the didactic functions is understood as a using in the historical buildings any media knowledge of their scientific value, historical and artistic (eg. primary role, structure, operation, historical events associated with the object of their background, significance in the process of the development of civilization, etc .)', in: P. Kozarski, P. Molski, *Zagospodarowanie i konserwacja zabytkowych budowli. Poradnik*, Fortyfikacja t. XIV, Towarzystwo Przyjaciół Fortyfikacji, Warszawa 2001, p. 34-35.

[26] Bielecki C., *Gra w miasto*, Fundacja Dom Dostępnny, Warszawa 1996

[27] Jackson J., *Discovering the Vernacular Landscape*. New Haven: Yale University Press, 1984.

[28] Archibald R., *The New Town Square: Museums and Communities in Transition*, Walnut Creek, California 2004.

Astaxanthin –the strongest natural antioxidant

Joanna Igielska-Kalwat*, Izabela Nowak

Uniwersytet im. Adama Mickiewicza w Poznaniu, Wydział Chemii, Pracownia Chemii Stosowanej, Umultowska 89b, 61-614 Poznań.

e-mail: joanna.igielska@amu.edu.pl

Keywords: *astaxanthin, carotenoids, antioxidants, free radicals*

ABSTRACT

Many health problems are related to unhygienic lifestyle, wrong diet, formation of free radicals and increasing pollution of the natural environment. One of the methods that can protect our organisms against the negative effect of the above factors is through the use of antioxidants. These compounds, even at very low concentration, can delay or prevent oxidation of the substrate. Carotenoids belong to the strongest natural antioxidants. They are dyes built of 8 isoprene units. The strongest among them is astaxanthin, which is the subject of this paper.

INTRODUCTION

Many health problems are related to the degradation of the natural environment, pollution of food, wrong diet, stress provoked by increasing pace of living and the generation of free radicals. Free radicals are species that have unpaired valence electron or an open electron shell necessary for stable molecular structure. For these reasons they are highly reactive. To compensate for the lack of electrons, they take electrons from other molecules, e.g. fatty acids or proteins, and in this way generate other radicals ready to attack other molecules. Free radicals are generated in living organisms by endogenous as well as exogenous factors and are responsible for changes in the redox processes. To some of these factors we cannot respond at the level of individual. Modern medicine can cope with various diseases. Most using the therapy that use synthetic specifics, called drugs. Very often, these drugs do not cure the underlying causes of disease and its symptoms only. In addition, their use, especially in chronic diseases is related to the risk of a variety of side effects. There is one prophylactic measure everyone can take, which is a healthy diet based on natural products [1]. In particular, a diet rich in antioxidants can protect us against the harmful effect of free radicals. These compounds either hinder the formation of free radicals or are conducive to their transformation towards inactive derivatives. Strong natural antioxidants are carotenoids, of which the strongest is astaxanthin.

DISCUSSION

Human organism can produce the harmful oxygen species as a result of physiological stress or in everyday activity of the immunological system. These oxygen species, known as Reactive Oxygen Species or ROS are formed in mitochondria with participation of complexes I and III of the respiratory chain (redox reaction). These species are the singlet oxygen and hydrogen peroxide [2-5]. Singlet oxygen is molecular oxygen in the excited state and it is generated during normal biological processes in the organism. It shows a long lifetime and high reactivity. To return to the ground state it must transmit its energy to another molecule, e.g. antioxidant, and this process is known as quenching [6,7]. Free radicals are molecules with unpaired electron. Similarly as singlet oxygen, they show high reactivity, ability to join other radicals and to dismutation [4,8]. The most aggressive free radicals are peroxide anion radical, nitrogen oxide and dioxide, hydroxyl radical and alkoxy radical. To make up for the missing electron, free radicals draw electrons from neighbouring molecules and as a result they become stable but generate new radicals. The cascade of reactions can lead to damage to the main cell components [3,5]. The list of conditions related to the effect of free radicals is presented in Table 1.

Table 1 Conditions related to the effect of free radicals [9-11]

Carcinogenic processes
Diabetes and its consequences, disturbed metabolism of fats
Neurodegenerative conditions (Alzheimer's disease, Parkinson's disease, sclerosis multiplex, brain insufficiency, failing memory and ability to concentrate, state of exhaustion)
Rheumatoidarthritis, arthrosis
Alimentary tract conditions (chronic inflammation of pancreas, toxic conditions of the liver, inflammations of the liver, gastritis, stomach and duodenum ulcers, Crohn's disease, ulcerative inflammation of large intestine)
Infections (virus, fungal, AIDS, malaria,) and inflammations
Allergies
Autoimmunological conditions
Conditions of the respiratory system (chronic bronchitis, fibrosis, asthma)
Premature ageing (lupus erythematosus, cataract, dementia), premature ageing of the skin (dry skin, flabby skin, reduced firmness and elasticity)
Damage to muscles related to intense physical exercise
Macular degeneration
Skin conditions (psoriasis, eczema, damage to collagen and elastin fibres)
Damage to proteins and DNA (changes in the structure of genetic code, cell mutation)

Human organism has a few mechanisms that neutralise the harmful effects of the reactive oxygen species and free radicals. An important role among them play the mechanism based on the use of antioxidants. These compounds, even when at a low concentration with respect to the substrate, are able to delay or prevent its oxidation [12]. The antioxidants can be divided into two groups. One of them act through transfer of electrons or hydrogen atoms to free radicals, which would transform them into stable species. This group comprises phenols, quinines (e.g. galusan propylu, butylhydroxyanisole (BHA), butylhydroxytoluene (BHT), tert-butylhydroquinone), trihydroxy butyrophenons (e.g. THBP - 2,4,5- trihydroxy butyrophenon) and tocopherols. The second group comprises the compounds whose activity is based on synergism. They are capable of scavenging of the reactive oxygen species and chelating the ions taking part in formation of free radicals. These antioxidants transfer hydrogen to phenoxy radicals, leading to restoration of their original antioxidant status. The antioxidants scavenging oxygen are ascorbic acid and its derivatives (e.g. ascorbyl palmitate), amino acids, flavonoids, vitamin A, carotenoids and many other compounds [13].

Carotenoids are the yellow, orange, red or violet dyes occurring in all photosynthesising plants [14]. They are built of 8 isoprene units linked in such a way that the isoprene radicals are arranged at 180° with respect to one another. They can make acyclic, monocyclic or bicyclic compounds. These are polyene compounds in which the double bond occurs in the coupled system. At present, nearly 600 carotenoids have been identified, the majority of them occur in plants [15]. The carotenoids are divided into :

- Carotenes –the carotenoids without oxygen,
- Xanthophylls –the carotenoids containing oxygen in hydroxyl, epoxide or carbonyl groups [16].

The best known carotenoids are α, β, γ - carotene, lycopene, zeaxanthin, lutein and astaxanthin [17].

Astaxanthin, the queen of carotenoids, is a xanthophyll, contains two hydroxyl groups and two carbonyl groups (Fig.1). Thanks to this structure it show a very strong antioxidative activity and is very effective in human organisms. Thanks to the content of oxygen groups, astaxanthin is not reactive towards vitamin A. It is a natural red dye in plants and animals, e.g. in the plumage of flamingos, meat of salmons and other fish species, lobsters and shrimps. In the highest concentration it occurs in algae and they are the main source of this dye [18]. The greatest amounts (up to 3.8% dry mass) of astaxanthin are found in chlorophyceae from the genus *Haematococcus pluvialis*. Astaxanthin occurs in stereoisomers. The most often met in nature are geometric isomers (3S, 3'S) and (3R 3'R), for instance the algae from the genus

Haematococcus biosynthesise(3S, 3'S)-isomers, while the yeast Xanthophyllo myces dendrorhous synthesise(3R, 3'R) isomer. Synthetic astaxanthin occurs in form of diastereoisomers (3S, 3'S), (3R, 3'S) and (3R, 3'R)[19,20].

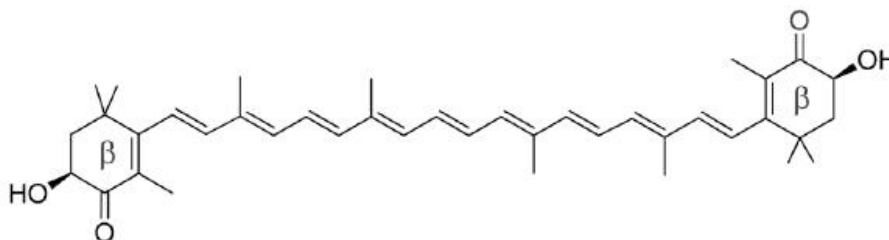


Fig. 1 Chemical formula of astaxanthin

Natural astaxanthin is a stronger antioxidant than vitamin E, β -carotene and other antioxidants (Fig. 2). It has been demonstrated in the study on rats that astaxanthin shows about 100 times greater ability to quench peroxide fatty radicals than vitamin E [21]. It shows the rare ability to pass the blood/ brain and blood/ retina barriers and thus is able to scavenge free radicals from these organs, protecting them from damage. Astaxanthin has beneficial effect on many tissues: it protects the heart against infarct and against cancer as it is conducive to generation of anticoagulants. It protects the liver and other organs against cancer and inflammations, protects the joints, sinews and muscles, reduces the risk of arthritis. On intensive physical exercise the muscles need more oxygen which can lead to cramps, while astaxanthin alleviates the process[18].

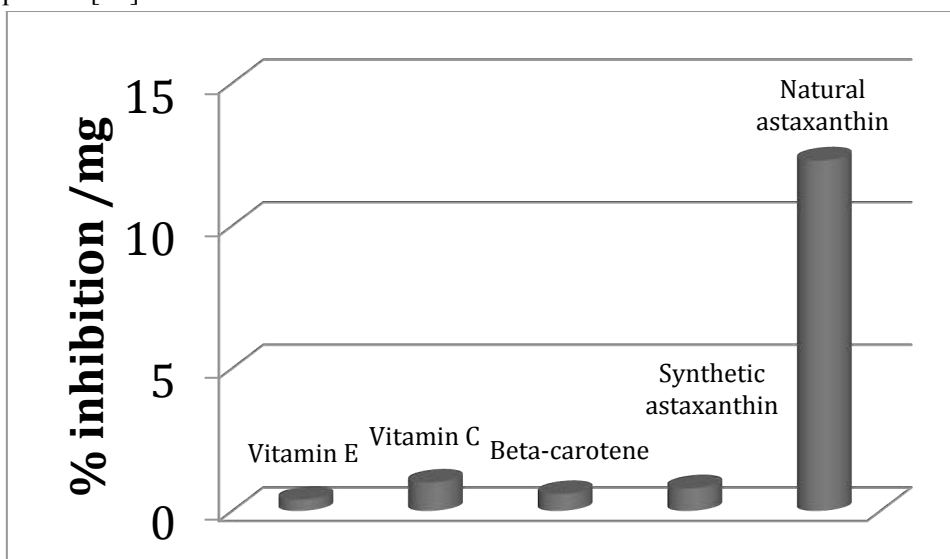


Fig. 2 The ability to deactivate free radicals in % per 1 mg of the antioxidant, taken after [18].

Astaxanthin shows better antioxidant properties than the most popular carotenoid β -carotene[21]. This latter compound is pro-oxidative towards polyunsaturated fatty acids (>85% increase in the content of hydrogen peroxide fatty acid (LOOH), the product of peroxidation of lipid). Astaxanthin gives the contrary effect, 40% decrease in the level of LOOH) [6,22]. It should be added that astaxanthin shows the highest photostability of all carotenoids, which is related to the unique position astaxanthin takes across the double lipid layer of the cell membrane, see Fig. 3 [23].

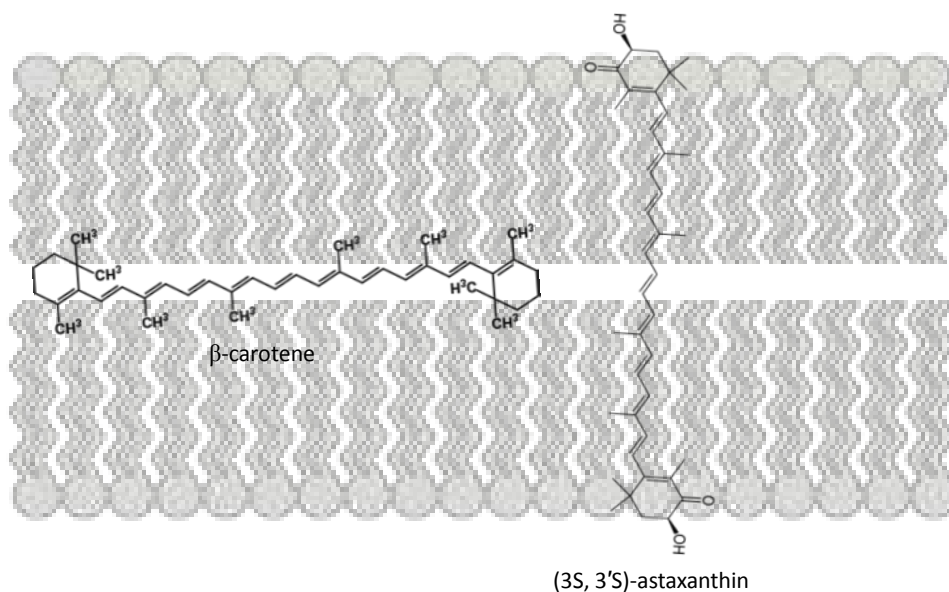


Fig. 3 Position of astaxanthin and β -carotene in the lipid membrane.

The effectiveness of antioxidants is evaluated on the basis of their ability to deactivate free radicals. One of the frequently used methods is that based on the use of DPPH (1,1-diphenyl-2-picrylhydrazyl) which is a stable free radical with an unpaired electron in the valence shell of the nitrogen atom involved in the formation of nitrogen bridge [24]. DPPH in the form of stable free radical is violet, while as a result of e reaction with a substance that can donate a hydrogen atom it forms a reduced DPPH in the form of colourless liquid. The decrease in absorbance is proportional to the amount of the oxidized form of DPPH left in the solution. Products of peroxidation of lipids are also determined by the spectrophotometric method, measuring the amount of compounds reacting with thiobarbituric acid (TBARS). Another method uses ABTS [2,2'-azobis(3-ethylbenzothiazolin-6-sulphonate)] as a free radical, as its use permits

measurements of total antioxidising activity in a sample. The radicals generated in the reaction are blue-green, antioxidants reduce the cationradicals to a degree depending on the time of the reaction, concentration and strength of the antioxidant, leading to the loss of colour.

Natural astaxanthin has been proved to be much more effective than its synthetic counterpart [25]. Synthetic astaxanthin is produced from the side products of petrochemical industry. Both, natural and synthetic astaxanthin have the same formula, but differ in the shape, natural astaxanthin occurs in the form of a single stereoisomer, while the synthetic one is a diastereoisomer, moreover, the natural one always has fatty acids at the end of its molecules. As a result of this connection the esterified molecules are obtained, which are stronger antioxidants [25].

CONCLUDING REMARKS

Astaxanthin is one of the strongest antioxidants, it is capable of binding and removing free radicals whose presence is connected with a number of diseases and also with premature skin ageing. This carotenoid hinders the processes of premature aging and related skin changes, (wrinkles, excessive drying, freckles, age-related skin discolouration, degradation of collagen), enhances protection against UV radiation. So found its application in creams with UV protection. Alleviates inflammations, strengthens muscles and helps their regeneration, protects against cancer development, protects many organs such as the liver, heart, eyes, joints, prostate and reduces the incidence of DNA damage. It slows down the oxidation processes that destroy fat cells and membrane phospholipids, therefore, can be used in creams for the face and body. Reduces the amount of melanin in the skin, which reduces the risk of discoloration, gives it a nice and uniform color. It is used in creams and nutrient regeneration. The use of astaxanthin is very beneficial for the skin, maintains a normal density and firmness [20,21].

REFERENCES

- [1] Bartosz G., *Druga twarz tlenu*, Wydawnictwo naukowe PWN, 2003
- [2] Badarinath AV., Mallikarjuna K., MadhuSudhanaChetty C., Ramkanth S., Rajan TVS., Gnanaprakash K., A review on In-vitro antioxidant methods: comparisons, correlations and considerations, *Pharm. Tech.*, 2010, 2, 1276-1285
- [3] Carocho M., Ferreira ICFR., A review on antioxidants, prooxidants and related controversy: Natural and synthetic compounds, screening and analysis methodologies and future perspectives, *Food Chem. Toxicol.*, 2013, 51, 15-25

- [4] Kisała J., Antyutleniacze pochodzenia roślinnego i syntetycznego – ich rola i właściwości, *Zeszyt Naukowy*, 2009, 11, 109-114
- [5] Lorenz R.T., Astaxanthinnature's super carotenoid, *Bio. Astin. Technical Bulletin*, 2000, 62, 1-19
- [6] Blokhina O., Virolainen E., Fagerstedt K.V., Antioxidants, oxidative damage and oxygen deprivation stress: a review, *Annals. of Botany*, 2003, 91, 179-194
- [7] NaguibYousry MA. Antioxidantactivities of astaxanthin and relatedcarotenoids, *J. Agric. Food Chem.*, 2000, 48, 1150-1154
- [8] Geens A., Dauwe T., Eens M., Application of Microbialcarotenoids as a source of colouration and growth of ornamental fish Xiphophorushelleri. *World Journal of Fish and marineSciences*, 2011, 2, 137-144
- [9] Liang J., Tian YX., Yang F., Zhang JP, Skibsted LH., Antioxidant synergism between carotenoids in membranes, Astaxanthin as a radical transfer bridge, *Food Chem.*, 2009, 115, 1437-1442
- [10] Thiel J., Elsner P., Oxidants and Antioxidants in CutaneousBiology. *Current Problem in Dermatology*, Zurich, 2001
- [11] Ziemiański Ś., Wartanowicz M., Rola wolnych rodników w procesie starzenia się ustroju, *Pol. Tyg. Lek.*, 1982, 37, 1453-1456
- [12] Grajek W., Rola przeciwutleniaczy w zmniejszeniu ryzyka wystąpienia nowotworów i chorób układu krążenia, *Żywn. Nauk. Technol.*, 2004, 38:,2-11
- [13] Moise AR., Al-Babili S., Wurtzel ET., Mechanistic Aspects of Carotenoid Biosynthesis., *Chem. Rev.*, 2014, w druku; x.doi.org/10.1021/cr400106y
- [14] Ziemiański Ś., Normy żywienia człowieka, *PZWL*, 2001
- [15] Beutner S., Bloedorn B., Frixel S., Hernandez B., Hoffmann T., Martin H., Mayer B., Noack P., Ruck Ch., Schmidt M., Schulke I., Sell S., Ernst H., Haremza S., Seybold G., Sies H., Stahl W., Walsh T., Quantitative assessment of antioxidant properties of natural colotene in antioxidant functions, *J. Sci Food Agric.*, 2001, 81, 559-568
- [16] Sikorski Z. *Chemia żywności*, *Wydawnictwo Naukowo- Techniczne*, 2007
- [17] Wilska- Jeszka J., Barwniki. Chemiczne i funkcjonalne właściwości składników żywności, *WNT*, 1994
- [18] Capelli B., Astaksantyna. Naturalna astaksantyna- królowa karotenoidów, *Copyright by Cyanotech Corporation*, 2007
- [19] Ambati R.R., Phang S.M., Ravi S, Aswathanarayana R.G., Astaxanthin: sources, extraction, stability, biological activities and its commercial applications-areview, *Mar. Drugs*, 2014, 12, 128-152
- [20] Müller L., Frohlich K., Bohm V., Comparativeantioxidantactivities of carotenoids measured by ferricreducing antioxidant power (FRAP), ABTS bleachingassay (α TEAC), DPPH assay and peroxy radical scavenging assay, *Food Chem.*, 20011, 129, 139-148

- [21] Yamashita E., Astaxanthin as a Medical Food, *FFHD*, 2013, 7, 254-258.
- [22] Tominaga K., Hongo N., Karato M., Yamashita E., Cosmetic benefits of astaxanthin on humans subjects, *Acta Biol. Chem.*, 2012, 59, 43-47
- [23] Goto S., Kogure K., Abe K., Kimata K., Kitahama K., Yamashita E., Terada H., Efficient radical trapping at the surface and inside the phospholipid membrane is responsible for highly potent antiperoxidative activity of the carotenoid astaxanthin, *Biochim. Biophys. Acta*, 2001, 1515, 251-258
- [24] Jabłońska S., Majewski S., Choroby skóry, *Wydawnictwo Lekarskiej PZWL*, 2013
- [25] Igielska-Kalwat J., Gościańska J., Nowak I., Antyoksydacyjne właściwości karotenoidów, *Kosmetyka i Kosmetologia*, 2013, 6, 3-4

Assessment of pollutant content in energy willow (*Salix viminalis*) growing in Puczniew village

Alicja Zawadzka, *Monika Janas

Faculty of Process and Environmental Engineering,
Lodz University of Technology, 90-924 Lodz, Wolczanska 215, POLAND

*e-mail: monika.janas@dokt.p.lodz.pl

Keywords: *energy willow, heavy metals, mineralization*

ABSTRACT

Recent years show a marked increase in the urbanization of greater and greater areas. A consequence of this process is the development of industry and expansion of communication routes, which is accompanied by increasing emissions of heavy metals that remain in the air and settle in the soil.

The main objective of the research was to evaluate the content of heavy metals in energy willow grown in Puczniew. Additionally, heavy metal content of soil the plantation was studied. The analysis was conducted in terms of applicability in of this type of wood from the experimental plantation as an ecological source of energy generated in the combustion process.

The content of heavy metals is important from the point of view of environmental protection because of a possibility of treating this fuel as a renewable and ecological source of energy. The applicability of ash obtained from biomass is determined by its chemical composition, especially the heavy metal content.

Based on the results obtained it has been found that energy willow (*Salix viminalis*) has a natural ability to accumulate heavy metals, so it can be used in the process of removing heavy metals and toxic substances from the environment. Moreover, due to good adaptability and strong growth potential energy willow has found many applications. Energy willow is used mainly as a cheap and renewable biofuel with low pollutant emissions to the atmosphere. However, one should be aware of the wide potential and applicability of energy willow in environmental protection, including land reclamation, removal of heavy metals from soil, land erosion prevention and flood control. Such wide applicability makes energy willow cultivation very promising.

INTRODUCTION

Currently, we witness the progressive urbanization on a growing range of areas. As a result, industry is developing and communication routes are extended. This development is accompanied by increasing emissions of heavy metals which persist in the atmosphere and are deposited in the soil, thus

contributing to the increase of agricultural wasteland. Production of plants for consumption in these areas becomes impossible due to the degree of contamination or because of unprofitability. These areas include, among others, infertile soil of lower quality class, polluted arable land in the vicinity of industrial plants, brownfield land (mining dumps) or reclaimed areas [1,2].

In view of the growing problems possibly quick and inexpensive solutions have been searched for. Currently, studies are being conducted on the usefulness of plants for the reclamation and management of contaminated soils. It has been observed that some plant species have a natural ability of accumulating heavy metals, i.e. of phytoremediation, so that they can be used in the process of purification of the environment. This group of plants with phytoremediation potential includes most plants grown for energy purposes. Special place is occupied here by energy willow as a species with wide adaptation possibilities and high production potential [3, 4, 5].

Energy willow is not very demanding in terms of soil conditions. It can be grown both in the depression areas of Żuławy and on the foothills of the height from 350 to 550 m above sea level. For planting most useful are mineral and sandy soils, as well as clay and organic soils of quality classes III, IV and V. Additionally, this plant has great tolerance to pH of the soil (pH 4.5 to 7.6) [6,7,8].

Studies were carried out to determine heavy metal content in both energy willow wood and in the soil of the experimental plantation. For this purpose the content of six selected heavy metals, i.e. lead, cadmium, nickel, chromium, copper and zinc was determined. The analysis of the results, includes additionally the permissible content of particular metals in the soil, in accordance with the Regulation of the Minister of Environment of 9 September 2002 on soil quality standards (Dz. U. 02.165.1359 of 4 October 2002). The results will be used to determine the environmental impact.

ESPERIMENTAL MATERIAL

The experimental energy willow plantation is located in a small village Puczniew, Lutomiersk municipality, Pabianice district in the Łódź region. The village is located in the Ner river valley at Łaska Upland.

The energy willow plantation was established at the initiative of the International Centre for Ecology, Polish Academy of Sciences and the University of Lodz. Within the plantation research is conducted on the use of phytoremediation for detoxification of aromatic compounds and for bioaccumulation of phosphorus compounds by the vegetation of ecotone zones.

Energy willow shrubs at the plantation were relatively young, about five years old only. The experimental material consisted of both energy willow bark

and twigs of various diameters. From each shrub 8 to 12 samples were collected, depending on the shrub size and possibility of separation of individual samples. The samples were milled and averaged and then new, small samples weighing about 1 gram were formed to be mineralized. As part of the experiments performed each sample was tested in triplicate. The samples were stored in sealed plastic bags in the laboratory.

In the plantation four different energy willow varieties with different properties were grown, namely I – RAPP, II – ORM, III – JORRUN and IV – ULV. Energy willow varieties have different growth abilities which is related to different climatic and soil requirements. The factor that determines the energy willow growth rate is a sufficient amount of moisture accumulated in the soil, especially at the early stage of cultivation, and humus content. The first two willow species are characterized by higher resistance and faster growth.

The first energy willow variety – RAPP is located in the immediate vicinity of the irrigation ditch. Another variety is grown about 15 m away from the ditch. The third variety – JORRUN is cultivated at a distance of 30 m, and the last variety IV – ULV is grown farthest away from the irrigation ditch at a distance of 50 meters. Due to these differences in the properties of individual energy willow varieties, wood samples of all varieties were used in the study. In addition, soil samples from each variety location were taken for testing.

The plantation is located on soils with worse quality classes. Specific brown soils, leached and acid soils as well as podzolic and pseudopodzolic soils prevail. In order to fertilize barren soils this area is irrigated with river waters carrying wastewater purified in the Combined Wastewater Treatment Plant.

Due to the varying distance of individual tree stands from the irrigation ditch and varying inclination of the surface, there are different arrangements of groundwater table along the slope. The level of water table is 0.8 m below the ground surface at a distance of 1 meter from the irrigation ditch and 0.2 meters below the ground surface at a distance of 50 meters.

In connection with such diverse habitat conditions, soil samples were collected as a complementary research material which was analyzed for various man-made substances in the environment. Specific soil samples were collected at a depth of 30 cm at various distances from the irrigation ditch. Soil samples were appropriately labeled with Arabic numerals: 1 – soil samples taken in the immediate vicinity of the irrigation ditch, 2 – soil collected at 15 meters from the ditch, 3 – soil samples taken in the plantation center, 4 – soil samples taken 50 m from the irrigation ditch.

From each place mentioned above three samples were taken. In total, 12 soil samples were taken and analyzed. The samples were stored in plastic sealed containers in the laboratory. After collection the samples were dried in a drying

oven at 60°C for a week. The dried soil samples weighing about 1 gram were mineralized.

EXPERIMENTAL METHODS

The content of lead, cadmium, zinc, copper, nickel and chromium in the biomass and soil samples was determined using one of the oldest methods of chemical analysis – flameless Atomic Absorption Spectrometry (AAS). This is an instrumental technique which is used for the determination of even trace amounts of various elements in various materials and media. The method consists in absorbing radiation of a characteristic wavelength by free atoms of a given element. The Atomic Absorption Spectrophotometry is based on the measurement of absorption of electromagnetic radiation by substances in a quite broad range from 180 to 900 nm [9, 10].

In this method, in order to obtain atomic gas the electronic atomization in graphite furnace atomizers was used. The device is electrically heated in four stages. In the first stage water is evaporated from the sample at the temperature 100-200°C at the time up to several tens of seconds. In the second stage the sample is mineralized. The temperature and time of this stage depend on the sample material. In the third stage, when the temperature reaches 1000 to 3000°C the evaporation and atomization of the sample take place. The process lasts for several seconds. In the last stage the sample is removed from the furnace before the next measurement cycle [10].

Wood and soil samples were mineralized in a Milestone microwave mineralizer. Digestion time was 25 min. Triple samples of wood and soil were mineralized. Each of these samples was subjected to an independent analysis and the results which are shown in the graph are the arithmetic means of the results. The results differed by up to 15%.

RESULTS

The content of selected heavy metals in energy willow wood of individual samples along with acceptable concentrations of these elements in the soil are shown in the graphs. Additionally, the graphs illustrate concentrations of particular metals in the soil.

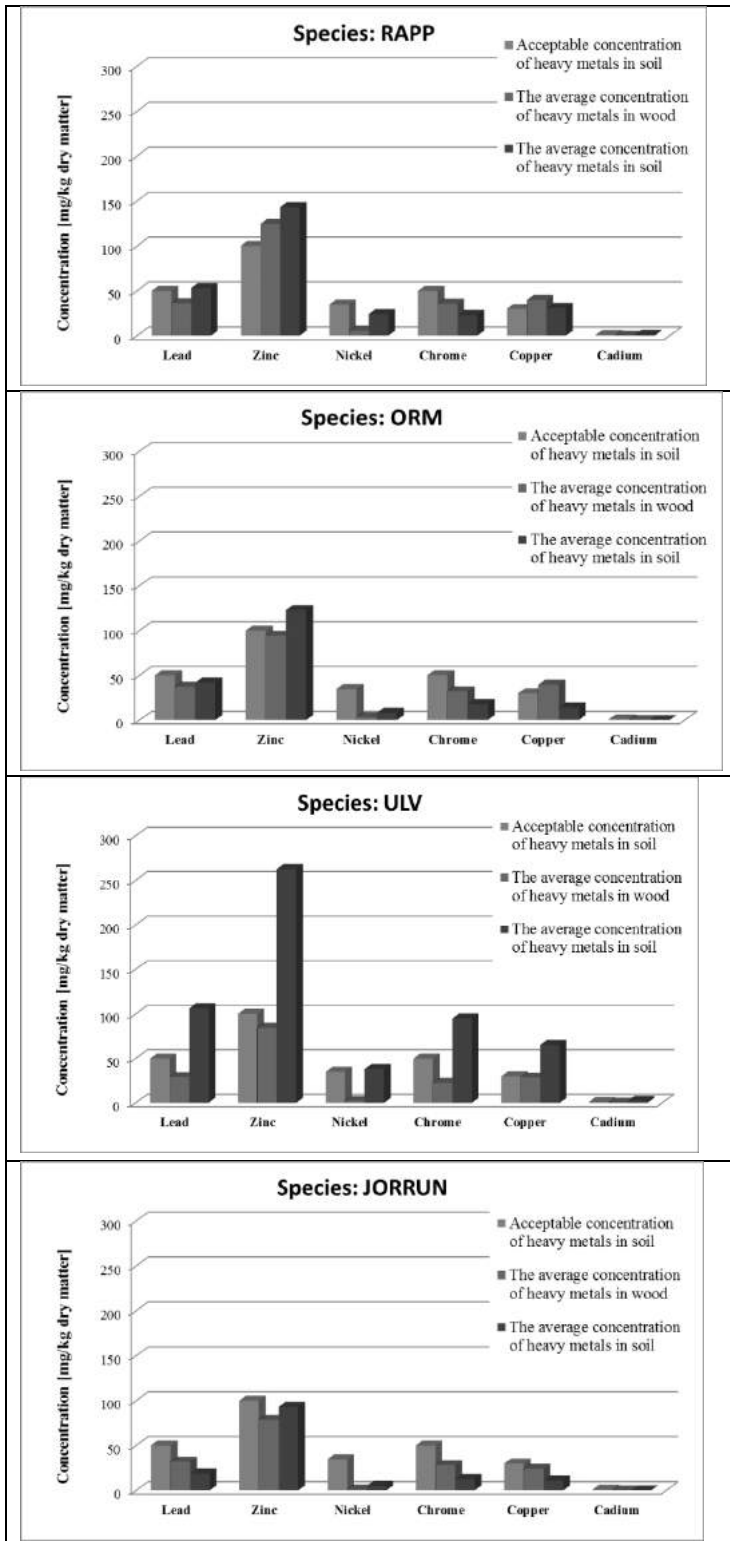


Fig. 1 Results of heavy metal analysis

Based on the results, it was found that in the energy willow wood zinc quantity was the largest among all heavy metals analyzed. Its content ranged from 78 mg/kg dry matter (JORRUN) to about 124 mg/kg dry matter (RAPP). In the soil, zinc concentration was much higher reaching 93 mg/kg dry matter (soil samples taken from the JORRUN variety plantation) and 263 mg/kg dry matter (soil samples from the ULV variety plantation).

In both wood and soil samples the content of cadmium and nickel was small, being 1 and 5 mg/kg dry matter, respectively. The deviation from the trend was observed in the RAPP and ULV varieties for which an increased nickel concentration in the soil was 24 and 38 mg/kg dry matter, respectively. The content of lead in the wood of various energy willow varieties was similar, amounting to 35 mg/kg dry matter. Quite different changes were observed in the case of lead in the soil. This concentration was diverse and ranged from 19 mg/kg dry matter for the JORRUN variety to 106 mg/kg dry matter for ULV.

The content of copper in the wood of the RAPP and ORM varieties was the same amounting to 40 mg/kg dry matter. Further on, this content decreased gradually and reached 28 mg/kg dry matter for ULV and 24 mg/kg dry matter for JORRUN. The content of this metal in soil samples was very variable. In the soil sample from the RAPP plantation it was 31 mg/kg dry matter, for ORM it was 14 mg/kg dry matter, for ULV 65 mg/kg dry matter and for JORRUN 11 mg/kg dry matter. Chromium content in both wood and soil samples was also very variable, like in the case of copper. In the wood samples this content ranged from 22 mg/kg dry matter for ULV to 36 mg/kg dry matter for RAPP, while in the soil samples it was from 13 mg/kg dry matter for JORRUN to 95 mg/kg dry matter for ULV.

DISCUSSION

The results confirm very large differences in the heavy metal content in both wood and soil samples from the energy willow plantation. The diversity and variable content of heavy metals depends primarily on the energy willow variety grown on particular areas of the experimental plantation. In addition, the concentration of heavy metals is determined by soil conditions, especially by groundwater table.

It should also be noted that only in the soil samples taken from the area where the JORRUN variety was grown the permissible heavy metal content of the soil was not exceeded. In the case of the RAPP variety the permissible zinc content was exceeded by nearly 50%. The content of zinc in the soil was 143 mg/kg dry matter, while the permissible content is 100 mg/kg dry matter. In the same variety a slightly exceeded level (by 1 mg/kg dry matter) of lead and copper was observed. The heavy metal content was slightly higher in the ORM

variety. In this case only zinc content was exceeded in the soil sample. The worst results were obtained for soil samples taken from the ULV plantation. The content of each of the analyzed metals was higher than the permissible levels determined in the Regulations on Soil Quality Standards of the Minister of Environment dated 9 September 2002.

CONCLUSIONS

The content of heavy metals is significant from the point of view of environmental protection because of a possibility of treating this fuel as a renewable and ecological source of energy.

In the process of burning the wood of this species, metals contained in it may either be oxidized or remain in the ash. As a result, due to a possible use of the ash as a fertilizer, for soil improvement and remediation, it gets to the natural environment. Chemical composition of the ash produced from biomass, especially heavy metal content, determines its use as a fertilizer [11].

In order to determine the environmental impact, the results were compared with the limit values of these metals in the soil determined in the Regulation of the Minister of Environment of 9 September 2002 on soil quality standards (Dz.U. 02.165.1359 of 4 October 2002). It was found that the wood of energy willow grown in the described conditions contained a certain amount of heavy metals. Concentration of these metals in the wood depends on their content in the habitat soil [12, 13].

Additionally the occurrence of heavy metals in the ash from combustion of energy willow will be an obstacle to its agricultural use. Among trace elements, the ash from energy willow contains more zinc and lead, while the content of cadmium and nickel is several times lower. At the same time this may suggest that willow cultivation reduces the content of heavy metals in the ecosystem [14].

Based on the results and analysis, it can be concluded that the willow biomass provides raw material for sustainable energy production. However, heavy metals contained in the wood cause that the ash produced during wood combustion re-contaminates the environment. It can be used either as a primary fuel generated in the combustion process, or secondary one, i.e. biomethanol. Ash content obtained from a single ton of energy willow biomass is about 1% of the burnt biomass, while during combustion of low-grade coal it is as high as 20%. The use of energy willow as a heat source reduces the problem of ash storage and disposal. Due to the above mentioned characteristics the tested energy willow varieties can be used to remove heavy metals, toxic and other compounds from the soil by incorporating them into the biomass. Energy willow roots capture more than 80% of pollutants [15].

The use of energy willow is very beneficial from the point of view of environmental protection, the use of fallow land, management of degraded land and reclamation of contaminated sites. These advantages cause that this raw material will be a response to the future demand for fuel for the Polish agriculture, power engineering and business which makes its cultivation very promising [16].

To sum up, the development of energy willow cultivation may contribute to a significant reduction of the content of heavy metals in soils, obtaining a new and renewable energy source and creation of new jobs in the regions with particular risk of unemployment. In light of the above, empirical researches on the applicability of energy willow and its effect on the environment are of crucial importance.

REFERENCES

1. Ostrowski J., Gutkowska A., Model diagnostyczny typowania gruntów przydatnych do upraw roślin energetycznych, *Problemy Inżynierii Rolniczej*, 2008, 2, 145-152
2. Chołuj D., Podlaski S., Kompleksowa ocena biologicznej przydatności 7 gatunków roślin wykorzystywanych w uprawach energetycznych, *Studia i raporty IUNG-PIB*, 2008, 11, 81-100
3. Kuś J. et al., Produkcyjność wybranych gatunków roślin uprawianych na cele energetyczne w różnych siedliskach, *Studia i raporty IUNG-PIB*, 2008, 11, 67-80
4. Majtkowski W., Bioróżnorodność upraw energetycznych podstawą zrównoważonego rozwoju, *Problemy Inżynierii Rolniczej*, 2006, 2, 25-36
5. Majtkowski W., Rośliny energetyczne – przegląd, *Czysta Energia*, 2003, 10, 33-34
6. Szczukowski S., Tworkowski J., Stolarski M., Wierzba energetyczna, *Plantpress*, 2004
7. Dubas J., Wierzba energetyczna – uprawa i technologie przetwarzania, *Wyższa Szkoła Ekonomii i Administracji w Bytomiu*, 2004
8. Król K., Wierzba wiciowa – cenna roślina energetyczna, *Technika Rolnicza Ogrodnicza Leśna*, 2004, 2, 18-22
9. Kryściak J., Chapter in the book: Fotometria płomieniowa i spektrofotometria absorpcji, *Chemiczna analiza instrumentalna*, Wydawnictwo Lekarskie PZWL, 1999, 102-108
10. Szczepaniak W., Chapter in: Spektrometria atomowa, Metody instrumentalne w analizie chemicznej, Państwowe Wydawnictwo Naukowe, 2011, 143-168
11. Imbierowicz M., Zawadzka A., Chapter in: Rośliny energetyczne oraz technologie i urządzenia dla przetwórci biomasy, *Inwestowanie w energetykę*

odnawialną. Aspekty ekologiczne, technologie, finansowanie, benchmarking, Polska Akademia Nauk, 2010, 169-184

12. Harasimowicz-Herman G., Herman J., Uprawa wierzby krzewiastej na cele energetyczne alternatywą dla spalania słomy i zachowania żyzności gleby, *Wydawnictwo Uczelniane Uniwersytetu Technologiczno-Przyrodniczego w Bydgoszczy, 2007, 6-36*
13. Mitchell C. P., Stevens E. A., Watters M. P., Short-rotation forestry operations productivity and costs based on experience gained in the UK, *Forest Ecology and Management, 1999, 1-2, 123-136*
14. Kościk B., Rośliny energetyczne, Wydawnictwo Akademii Rolniczej w Lublinie, 2003
15. Zajączkowski K., Produkcyjne możliwości wybranych odmian topoli i wierzby w plantacjach o skróconym cyklu, *Maszynopis IBL, 2001*
16. Szczukowski S., Tworowski J., Wiwat M., Przyborski J., Wiklina (*Salix* sp.): uprawa i możliwości wykorzystania, *Wydawnictwo Uniwersytetu Warmińsko-Mazurskiego, 2002*

Detection of emulsion destabilisation processes on the basis of selected physicochemical parameters

*Alicja Kapuścińska, Izabela Nowak¹

¹Adam Mickiewicz University, Department of Chemistry, Poznan, POLAND
e-mail: kapuscinska.alicja@gmail.com

Keywords: *emulsion stability, flocculation, sedimentation, emulsion creaming, multiple light scattering*

ABSTRACT

Emulsion is a system of two immiscible liquids (a two-phase system) in which internal phase in the form of fine droplets is dispersed in the external phase [1]. Emulsions can be easily destabilised and this process can be initiated by Brownian motions or Ostwald phenomenon [2]. Emulsion instability can be related to changes in the size of the internal phase particles or their migration. Analysis of changes in the above parameters in time has been used for description of the instability of cosmetic formulations. The methods used for this purpose are particle size distribution determination and analysis of time changes in transmittance or light backscattering by coloured and colourless samples. Exemplary methods applied to increase the cosmetic emulsion stability include the introduction of electric charge, strengthening of the interface and addition of a properly selected emulsifier [3].

INTRODUCTION

The most popular cosmetic formulations on the market are emulsions. Their stability in time is a very important parameter as it affects the efficiency of the product and the safety of its use. Analysis of changes in parameters describing the emulsion brings information on the type of developing instability. Information about such changes are obtained by measurements of the particle size distribution.

Definition and types of emulsion

Emulsion is a system of two immiscible liquids (a two-phase system) in which fine droplets of one liquid (internal phase) are dispersed in the other liquid (external phase) [1]. According to composition, the emulsions can be divided into the oil-in-water type (O/W), water-in-oil type (W/O) and multiphase types. O/W is the emulsion in which oil is the internal phase dispersed in water. The use of O/W emulsions depends on the content of the dispersed phase, if the content of oil phase is between 20 and 30 % it can be used as base of light moisturising creams, lotions, facial masks, shampoos and deodorants. When the oil phase content is greater than 30 %, the emulsion can be used for the

production of universal creams, certain cold creams, milks and hair conditioners [4]. W/O is the emulsion in which water is dispersed in oil, usually the content of dispersed phase makes from 20 to 40 %. Such emulsions are used as the base of oily night creams, of creams for the skin around the eyes and for the skin cleansing milks [1,4]. The multiphase emulsion is the system in which the droplets of the internal phase dispersed in the external phase additionally contain even tinier droplets of the external phase, for instance O/W/O emulsion is composed of oil dispersed in water and additionally dispersed in oil, while W/O/W emulsion is water dispersed in oil and additionally dispersed in water [5]. The multiphase emulsions show a number of advantages over biphasic ones as they protect the reactive or unstable active ingredients against air and moisture and facilitate the permeability of the active ingredient into deeper layers of epithelium [1,3].

Types of emulsion instabilities

Kinetic stability of emulsions is not equivalent to their thermodynamic stability. The thermodynamically stable emulsions do not change in time and in certain conditions of pressure and temperature. The thermodynamic instability of emulsions leads to destabilisation and consequently to separation of phases making a given system [3,4]. According to the physicochemical mechanisms of instability, the instabilities can be divided into reversible and irreversible. The reversible instabilities can be removed by stirring the system [4] and they can be divided into creaming, sedimentation and flocculation of emulsion.

The creaming of emulsion is the process as a result of which particles of the dispersed phase accumulate on the surface of the system (the size of its particles is unchanged) . The instability of this type is most often met in O/W emulsions as the dispersed substance has lower density and thus its droplets are able to move towards the emulsion surface. To prevent this process the dispersed phase density and viscosity should be increased [6,7,8]. The sedimentation of emulsion is the process analogous to creaming but the dispersed phase particles (also of the unchanged size) move towards the bottom of the vessel in which the emulsion is contained and accumulate there. Sedimentation is a consequence of gravity and takes place in all types of emulsion. Similarly as creaming, the process of sedimentation can be to a certain degree controlled by the choice of density and viscosity of the dispersed phase and size and charge of the emulsion micelles [3,9]. The third type of reversible instability is flocculation that is aggregation of the dispersed phase droplets without joining in greater droplets not accompanied with movement towards the emulsion surface or the bottom of the vessel with emulsion [3, 10].

The instability of emulsion that cannot be removed by stirring of the system is called irreversible. The phenomenon characteristic of this type of

instability is coalescence which is most often a consequence of flocculation but in which the particles of dispersed phase join in greater droplets [3,11]. The final outcome of the processes of destabilisation is breaking up of the emulsion in which it is fully separated into the water phase and oil phase [3].

Causes of emulsion instability

The process of emulsion destabilisation is complex and depends first of all on the motion of particles of the dispersed phase. The most important physicochemical phenomena conducive to destabilisation include: linear motion of internal phase particles, mutual attraction of internal phase particles, Brown motions and Ostwald phenomenon [3].

Linear motion of internal phase particles

This phenomenon can be described by the Stokes law (assuming that the drops of dispersed phase are spherical) and is involved in the processes of creaming and sedimentation taking place in the emulsion system. The Stokes law defines the resistance that must be overcome by the spherical particle to take a linear motion (not turbulent) with a certain velocity, in a liquid or gas [3,12].

Mutual attraction of internal phase particles

This phenomenon is induced by the Van der Waals forces acting between electrically neutral particles or atoms. When the internal phase droplets are separated from each other, their charge is displaced in such a way that they become polarized. The oppositely polarised particles attract each other. When the droplets of internal phase get too close to each other, (inhomogeneous emulsion structure), they are repulsing each other which leads to flocculation. In order to minimize the influence of Van der Waals forces on the emulsion destabilisation, the droplets of internal phase must be kept at a certain distance [3, 13].

Oscillations of dispersed phase particles (Brownian motion)

Brownian motion is the name used to describe the random movements of particles dispersed in a liquid or gas as a result of collisions with the molecules or particles of the medium (liquid or gas). The Brownian motions weaken with increasing size of dispersed particles and decreasing temperature. They are unavoidable in a stable and homogeneous emulsion and weaken when the emulsion gets destabilised [14,15].

Ostwald ripening

As a result of this phenomenon the size of droplets of dispersed phase increases and eventually leads to a similar change as coalescence. However, the mechanism of this phenomenon is different. The energetically unstable particles of dispersed phase leave the smaller droplets and are adsorbed on the surface of greater ones which is energetically favoured [16]. Migration of the dispersed

phase particles can be indirect (with a few particles of the emulsifier) or direct (without emulsifier particles). The necessary condition for direct migration is partial solubility of dispersed particles in the dispersion medium. The destabilisation of emulsion caused by the Ostwald ripening or by Brownian motions can be minimized by effective homogenisation of the system [3, 17].

Stabilisation of emulsion

Introduction of an emulsifier into a system of two immiscible phases contributes to stabilisation of a dispersion system. The emulsifier considerably decreases the interfacial surface tension, however, it is impossible to reduce it to zero, so each emulsion will eventually tend to destabilisation. Formation of an emulsion system is related to increased energy, while it is known that all systems tend to reach the lowest energy. It is the fundamental reason for destabilisation of emulsions [3,4]. A few methods have been proposed to increase the emulsion stability: introduction of electric charge, strengthening of the interfacial surface and maximum prevention of mutual contact between particles of dispersed phase [18,19].

Introduction of electric charge

In this method, electric charge is introduced on the surface of the dispersed phase using the properly chosen emulsifier, most often from the group of anionic surfactants. The double electric layer formed around the drops of dispersed phase is responsible for mutual repulsion of the droplets, which hinders their flocculation and coalescence. This method is effective if the dispersion medium is a good conductor, so it is usually applied to stabilise O/W emulsions. On introduction of excessive amount of electrolytes, the emulsion can break down [3,20].

Strengthening of interfacial surface

Strengthening of the interfacial surface is realised by increasing packing of emulsifier particles at the surface of the droplets of dispersed phase. It is possible when emulating a system of two immiscible phases with the use of a mixture of emulsifiers. This method reduces the probability of coalescence as a result of flocculation of droplets of dispersed phase [3, 21]. At low concentrations of the emulsifiers, a monolayer of emulsifiers at the interface is formed. With increasing concentration of the emulsifiers, the layer growth into a lamellar liquid-crystal structure [22]. In O/W type emulsions, formation of such structures is facilitated by the presence of two emulsifiers, the main hydrophilic one and the auxiliary, hydrophobic one (the so-called co-emulsifier). To stabilise the emulsions containing an ionic emulsifier, a mixture of non-ionic emulsifiers characterised by different values of HLB parameter (HLB- hydrophilic-lipophilic balance) is used. Its use ensures better packing of a surfactant on the surface of the droplets of dispersed [3, 23]. The interface can be also

strengthened with the use of polymers. They are applied when a given emulsion is exposed to such destabilising factors as high temperature, high ionic-strength of the solution or continuous mechanical stress. The polymer adsorbed on the surface of droplets of dispersed phase is amphiphilic and makes a protecting layer. In comparison with the standard emulsifiers, polymers are better adsorbed at the interface and are more resistant to a high concentration of ions present in the system [3, 24, 25]. The interface can also be strengthened with the use of proteins. Proteins are biopolymers and similarly as the synthetic polymers their molecules are composed of a hydrophilic and a hydrophobic parts which interact with appropriate phase of the emulsion. Destruction of the higher order of protein structures weakens their stabilisation abilities. To improve the stabilisation of emulsion by the use of proteins, a small amount of polysaccharides can be added to the system [26, 27, 28, 29]. Another possibility of interface strengthening is the use of powders, insoluble in both phases of the emulsion. This method is effective when the powder particles (wetable by the dispersed phase and dispersion medium) are at the interface. The powders of greater hydrophilicity are applied to stabilise the O/W emulsions, while the powders of greater lipophilicity are used to stabilise W/O emulsions. The diameter of solid state particles used for stabilisation of emulsion should be much smaller than that of the particles of dispersed phase [3,30].

The effect of changes in physicochemical parameters of emulsion on its stability
Cosmetic emulsions are characterised by such parameters as viscosity, pH, structural homogeneity and particle size distribution of the dispersed phase. Changes in these parameters in time can initiate the process of emulsion destabilisation.

Methods of measurements of changes in the particle size distribution

Analysis of time changes in the particle size distribution of the dispersed phase permits detection of the process of emulsion destabilisation related to the these changes (flocculation, coalescence). Measurements of particle size distribution are performed on a Mastersizer 2000. The instrument has modular construction and is composed of a semi-automated attachment and the measuring setup. The stirrer in the attachment permits dispersion of substances made of particles of a wide range of sizes. The pump integrated with the stirrer facilitates the flow of the liquid to the measuring setup, the ultrasonic probe is used for breaking up the particle agglomerations. The first measurement is made before breaking up the agglomerates, while the second after breaking up the agglomerates. Comparison of the results brings information on the particle size distributions. The mechanism shifting the integrated stirrer, ultrasonic probe, and the head of the pump, facilitates the exchange of dispersed liquid and cleaning of the system. The part of the analyser responsible for the measurements is called

an optical unit. This unit comprises a single-objective optical analyser, with a He-Ne laser emitting red light beam of $\lambda = 633$ nm and a semiconductor laser source of blue light emitting $\lambda = 466$ nm, the use of two light sources extends the range of measured particle sizes. Besides the lasers, the measuring setup comprises the detectors of backscattered light. The instrument Mastersizer is used for analyses of liquid dispersions. The range of particle sizes that can be measured reaches from 0.02 to 2000 μm . The measurement is based on the phenomenon of laser diffraction and the Mie theory of scattering, describing elastic scattering of electromagnetic field on a homogeneous ball of arbitrary size and optical properties [31].

Measurements of Δ Back Scattering

Multiple Light Scattering, MLS, in which light beam scattered by a single particle is then many times scattered by neighbouring particles, is applied for analysis of stability of cosmetic formulations. The instrument which employs this phenomenon is called Turbiscan Lab Expert, it can work in the scanning mode and in a single position. In the scanning mode, the optical head scans the whole sample in vessels up to 55 cm in height, collecting the transmitted and back-scattered light at every 40 μm . Spectral transmittance is measured in analysis of transparent samples, while backscattering in analysis of opaque ones. Results are analysed with respect to a reference standard which is a suspension of monodispersed polymeric balls in a silicon oil. Measurements provide information on migration of particles in the emulsion studied. Measurements by Turbiscan Lab Expert permit detection of the processes of creaming, sedimentation and flocculation of emulsion and observation of the progress of these processes [32].

SUMMARY

Analysis of changes in the physicochemical parameters of the emulsion permits detection of processes of emulsion destabilisation, related to migration of dispersed phase particles and changes in their size. Stability of emulsions is vital for the safety of its use and preservation of desired skin care properties.

REFERENCES

- [1] Malinka W., Zarys chemii kosmetycznej, Volumed Wrocław, 1999, s. 147.
- [2] Morrison I., Emulsion Technology Dispersions in liquids: suspensions emulsions, and foams. ACS National Meeting, April 9 – 10, 2008, New Orleans.
- [3] Arct J., Pytkowska K., Emulsje kosmetyczne. *Wiadomości PTK*, 2000, 3, 2/3, 12-16.
- [4] Marzec A., *Chemia Kosmetyków*, wydanie III, Toruń 2009, 102-105

- [5] Becher, P., Emulsions, theory and practice, wyd. III.; Oxford University Press: New York 2001, 49- 54
- [6] Molski M., Chemia piękna. Warszawa, Wydawnictwo Naukowe PWN, 2010, 223-226.
- [7] Robins, M. M., Emulsions—creaming phenomena. *Current opinion in colloid & interface science*, 2000, 5(5), 265-272.
- [8] Chanamai, R., McClements, D. J., Dependence of creaming and rheology of monodisperse oil-in-water emulsions on droplet size and concentration. *Colloids and Surfaces A: Physicochemical and Engineering Aspects*, 2000, 172(1), 79-86.
- [9] Zhang, H., Cooper, A. I., Synthesis of monodisperse emulsion-templated polymer beads by oil-in-water-in-oil (O/W/O) sedimentation polymerization. *Chemistry of materials*, 2002, 14(10), 4017-4020.
- [10] Vingerhoeds, M. H., Blijdenstein, T. B., Zoet, F. D., van Aken, G. A., Emulsion flocculation induced by saliva and mucin. *Food Hydrocolloids*, 2005, 19(5), 915-922.
- [11] Danov, K. D., Denkov, N. D., Petsev, D. N., Ivanov, I. B., Borwankar, R., Coalescence dynamics of deformable Brownian emulsion droplets. *Langmuir*, 1993, 9(7), 1731-1740
- [12] Walser, R., Mark, A. E., van Gunsteren, W. F., On the validity of Stokes' law at the molecular level. *Chemical physics letters*, 1999, 303(5), 583-586.
- [13] Hamaker, H. C., The London—van der Waals attraction between spherical particles. *Physica*, 1937, 4(10), 1058-1072.
- [14] Vignati, E., Piazza, R., Lockhart, T. P., Pickering emulsions: interfacial tension, colloidal layer morphology, and trapped-particle motion. *Langmuir*, 2003, 19(17), 6650-6656.
- [15] Grebenkov, D. S., NMR survey of reflected Brownian motion. *Reviews of Modern Physics*, 2007, 79(3), 1077.
- [16] Kabalnov, A. S., Shchukin, E. D., Ostwald ripening theory: applications to fluorocarbon emulsion stability. *Advances in Colloid and Interface Science*, 1997, 38, 69-97.
- [17] Voorhees, P. W., Ostwald ripening of two-phase mixtures. *Annual Review of Materials Science*, 1992, 22(1), 197-215.
- [18] Kim, J. W., Lee, D., Shum, H. C., Weitz, D. A., Colloid surfactants for emulsion stabilization. *Advanced Materials*, 2008, 20(17), 3239-3243.
- [19] Levine, S., Bowen, B. D., Partridge, S. J., Stabilization of emulsions by fine particles I. Partitioning of particles between continuous phase and oil/water interface. *Colloids and Surfaces*, 1987, 38(2), 325-343.

- [20] Saleh, Navid, et al., Oil-in-water emulsions stabilized by highly charged polyelectrolyte-grafted silica nanoparticles. *Langmuir* 2005, 21, 22, 9873-9878.
- [21] Boyd, J. V., C. Parkinson, P. Sherman., Factors affecting emulsion stability, and the HLB concept. *Journal of Colloid and Interface Science*, 1972, 41, 2, 359-370.
- [22] Friberg, S., Per O.J., Ebba C., Surfactant association structure and emulsion stability. *Journal of Colloid and Interface Science* , 1976, 55, 3 614-623.
- [23] Gullapalli, Rampurna P., Bhogi B. Sheth, Influence of an optimized non ionic emulsifier blend on properties of oil-in-water emulsions. *European journal of pharmaceuticals and biopharmaceutics*, 1999, 48, 3, 233-238.
- [24] Schugens, Ch, Effect of the emulsion stability on the morphology and porosity of semicrystalline poly l-lactide microparticles prepared by w/o/w double emulsion-evaporation. *Journal of Controlled Release*, 1994, 32, 2, 161-176.
- [25] Williams, J. M., High internal phase water-in-oil emulsions: influence of surfactants and cosurfactants on emulsion stability and foam quality. *Langmuir* , 1991, 7,7, 1370-1377.
- [26] Grigoriev O. D., Miller R., Mono- and multilayer covered drops as carriers. *COICIS*, 2009, 14, 48-59.
- [27] Melzer, E., Kreuter, J., Daniels, R., Ethylcellulose: a new type of emulsion stabilizer. *European journal of pharmaceuticals and biopharmaceutics*, 2003, 56(1), 23-27.
- [28] Dickinson, E., Milk protein interfacial layers and the relationship to emulsion stability and rheology. *Colloids and Surfaces B: Biointerfaces*, 2001, 20, 3, 197-210.
- [29] Yang, Y., Tai-Shung C., Ngee P., Morphology, drug distribution, and in vitro release profiles of biodegradable polymeric microspheres containing protein fabricated by double-emulsion solvent extraction/evaporation method. *Biomaterials*, 2001, 22, 3, 231-241.
- [30] Levine, S., Sanford, E., Stabilisation of emulsion droplets by fine powders. *The Canadian Journal of Chemical Engineering*, 1985, 63(2), 258-268.
- [31] Kowas K., Rozpraszanie światła na pojedynczej cząstce. Rozdział III Badania aerozolu miejskiego. WUW, 2007.
- [32] Instrukcja Obsługi Aparatu Turbiscan Lab Expert [www.formulation.com].

Effect of acetic acid to ethylenic unsaturation molar ratio on the course of rapeseed oil epoxidation

*Kornelia Malarczyk, Eugeniusz Milchert

Faculty of Chemical Technology and Engineering, West Pomeranian University of Technology in Szczecin

e-mail: kornelia.malarczyk@zut.edu.pl

Key words: *epoxidation, epoxidation of rapeseed oil, effect of acetic acid*

ABSTRACT

In the present work rapeseed oil with iodine value of 102,8 (g I₂/100 g) was epoxidised using a peroxyacid generated *in situ* by the reaction of 30 wt% hydrogen peroxide and glacial acetic acid in the presence of an acidic ion exchange resin – Dowex 50Wx2. Process was carried out under the following conditions: temperature 348 K, stirring speed – 700 rpm, reaction time – 5 h, hydrogen peroxide to ethylenic unsaturation molar ratio – 1,5:1, ion exchange resin loading – 22 wt%. The effect of acetic acid to ethylenic unsaturation molar ratio on epoxy number and iodine number was studied. The fatty acids composition of the rapeseed oil used in this work was analyzed by gas chromatography.

INTRODUCTION

Fats and oils are primarily water-insoluble, hydrophobic substances in the plant and animal collection that are made up of one mole of glycerol and three moles of fatty acids and are commonly referred to as triacylglycerols [1]. The fatty acids are monocarboxylic acids which the hydrocarbon chain made of a different number of carbon atoms from 4 to more than 30. Natural fats contain mainly fatty acids with 16, 18 and 20 carbon atoms. The number of carbon atoms and the number of double bonds in the fatty acid are provided using the shortcuts, such as 18:0 means that the acid contains 18 carbon atoms, and it lacks the double bonds, and the shortcut 18:3 indicates acid with 18 carbon atoms and three bonds double [2].

Rapeseed oil is one of the most widely oils in the world. It is the third largest vegetable oil production in the world. Triacylglycerols constitute 98-99% of the content of rapeseed oil commercially available, the remaining portion forming a so called unsaponifiables, among them biologically active compounds, phenol compounds, sterols and tocopherols [3].

Vegetable oils are commonly available, cheap and, first of all renewable, products of natural origin. Of particular importance is their application in the

polymer industry, in which they are used for production and modification of polymers [4,5].

The reason for their universality of use for technological purposes is related to a possibility to change their chemical structure. One of the modification methods of fatty acid triglycerides (oils) is the epoxidation process by which epoxy groups are formed. Epoxidation of vegetable oils can be carried out by the conventional methods based on the use of carboxyl acids and hydrogen peroxide, by chemical-enzymatic methods, by the processes with employment of acidic ion-exchange resins and those with the use of high valency metals [5-8].

The use of the resins as the catalysts makes the process more friendly for the environment because of much easier separation of the catalyst and carboxylic acid. Usually formic acid or acetic acid are used to form the appropriate peroxyacids in the reaction with H_2O_2 . The catalysts are acidic ion-exchange resins, mainly Amberlite IR-120, Amberlite IR-122 and Amberlyst - 15. The process can be performed in the presence of a solvent [5,7-11].

In the present work rapeseed oil with iodine value of 102,8 (g I_2 /100 g) was epoxidised using a peroxyacid generated *in situ* by the reaction of 30 wt% hydrogen peroxide and glacial acetic acid in the presence of an acidic ion exchange resin – Dowex 50Wx2. The effect of acetic acid to ethylenic unsaturation molar ratio on epoxy number (EN) and iodine number (IN) was studied.

MATERIALS AND METHODS

Rapeseed oil was obtained from ZT „Kruszwica” S.A. (Poland) Glacial acetic acid (99,5%), 30wt% aqueous hydrogen peroxide solution and sodium carbonate were purchased from Chempur (Poland), while anhydrous magnesium from POCH Gliwice (Poland). Dowex 50Wx2 in acid form was purchased from Sigma Aldrich (Poland).

An acid composition of the rapeseed oil was analyzed by gas chromatography using an Thermoquest GC 8000^{Top} with a flame-ionization detector. The column was a 30 m × 0,32 mm × 0,5 μ m DB-Wax (J&W) capillary column with He as the carrier gas. Determination of fatty acids was performed according to standard PN-EN ISO 5508, in the form of methyl esters in samples, prepared according to standard PN-EN ISO 5509.

A reaction flask was charged with rapeseed oil, acetic acid and ion exchange resin. Subsequently, a 30 wt% hydrogen peroxide was added dropwise. After the process, the organic layer was neutralized with 4 wt% solution of Na_2CO_3 . The residuals of water were removed by means of anhydrous magnesium sulfate (VI). The degree of overreaction of rapeseed oil

to the epoxy compound was determined by means of the epoxy and iodine number.

The epoxy number [mol / 100g] was calculated in accordance with the applicable standard [EN ISO 3001], according to the equation:

$$LE = \frac{(V - V_o)c_{HClO_4} \times 100}{1000m}$$

where:

V - volume of chloric acid(VII) in acetic acid used for the titration of the studied sample [cm³],

V₀ - volume of chloric acid(VII) in acetic acid used for the titration of the blank test [cm³],

c_{HClO₄} - concentration of the solution of chloric acid(VII) in acetic acid, [mol/dm³],

m - mass of sample [g].

The iodine number [g/100g] was calculated according to standard [EN ISO 3961], according to the equation:

$$L_j = \frac{(V_1 - V_2) \times 0,1269 \times c_{Na_2S_2O_3} \times 100}{m}$$

where:

V₁ - volume of sodium thiosulphate(VI) used to titrate the blank test [cm³],

V₂ - volume of sodium thiosulphate(VI) used to titrate the sample proper [cm³],

c_{Na₂S₂O₃} - concentration of sodium thiosulphate(VI) [mol/dm³],

m - mass of the sample [g].

RESULTS

The fatty acid profile of the rapeseed oil used in this work is summarized in Table 1. There are three main types of fatty acids in a triglyceride: saturated (Cn:0), monounsaturated (Cn:1) and polyunsaturated with two or three double bonds (Cn:2,3).

Table 1 Fatty acid compositions (wt.%) of tested rapeseed oil

Fatty acid	A ^a B ^b	Acid content [wt.%]
Palmitic	16:0	4,38
Palmitoleic (9 cis)	16:1	0,11
Stearic	18:0	1,72
Oleic (9 cis)	18:1	64,38
Linoleic (9 cis, 12 cis)	18:2	18,56
Linolenic (9 cis, 12 cis, 15 cis)	18:3	7,76
Linolenic (6 cis, 9 cis, 12 cis)	18:3	0,26
Arachidic	20:0	0,57
Gadoleic	20:1	1,32
Erucic (13 cis)	22:1	0,44

^a Number of carbon atoms

^b Number of unsaturated bonds

The influence of the acetic acid to ethylenic unsaturation molar ratio on the epoxidation of rapeseed oil was investigated at seven different ratios: 0,2:1, 0,5:1, 0,8:1, 1,1:1, 1,4:1, 1,7:1, 2:1. Processes were carried out under the following conditions: temperature – 348 K, stirring speed – 700 rpm, reaction time – 5 h, hydrogen peroxide to ethylenic unsaturation molar ratio – 1,5:1, ion exchange resin loading – 22 wt%.

As can be seen from Fig. 1, an increase in the molar ratio of CH₃COOH/ethylenic unsaturation from 0,2 to 0,8 caused a decrease of the iodine number. With further increase in the molar ratio of CH₃COOH /ethylenic unsaturation iodine value persists at a constant level (1-2 g/100g). Fig. 2 shows the influence of the acetic acid to ethylenic unsaturation molar ratio on the epoxy number of the epoxidised oil. The value of the epoxy number increased with increasing molar ratio of CH₃COOH /ethylenic unsaturation from 0,2 to 0,5, but decreases above 0,5 molar ratio and remains at a constant level (about 0,235 mol/100g). Further increase in the molar ratio of CH₃COOH/ethylenic unsaturation above 1,4 causes decrease in the value of the epoxy number to 0,054 mol/100g at molar ratio equal to 2:1.

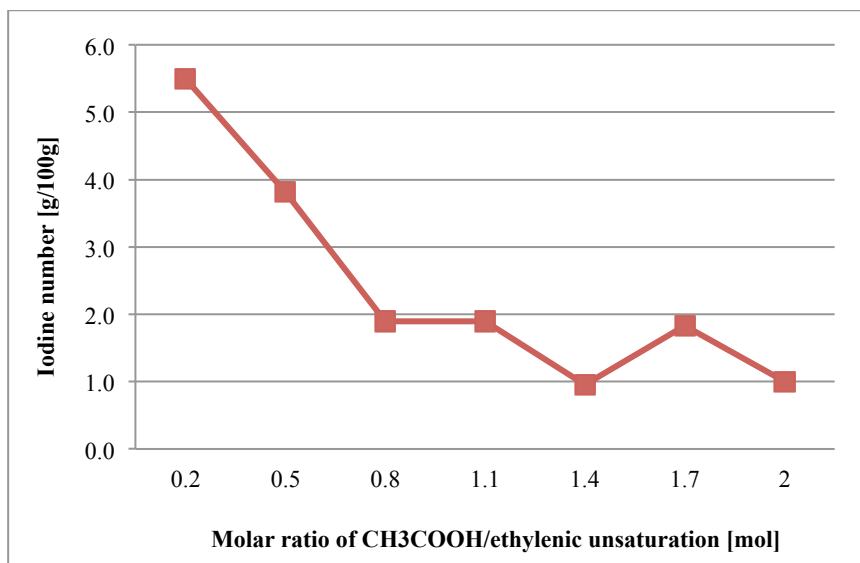


Fig. 1 Influence_of CH₃COOH/ethylenic unsaturation molar ratio on the iodine numbers of epoxidised rapeseed oil

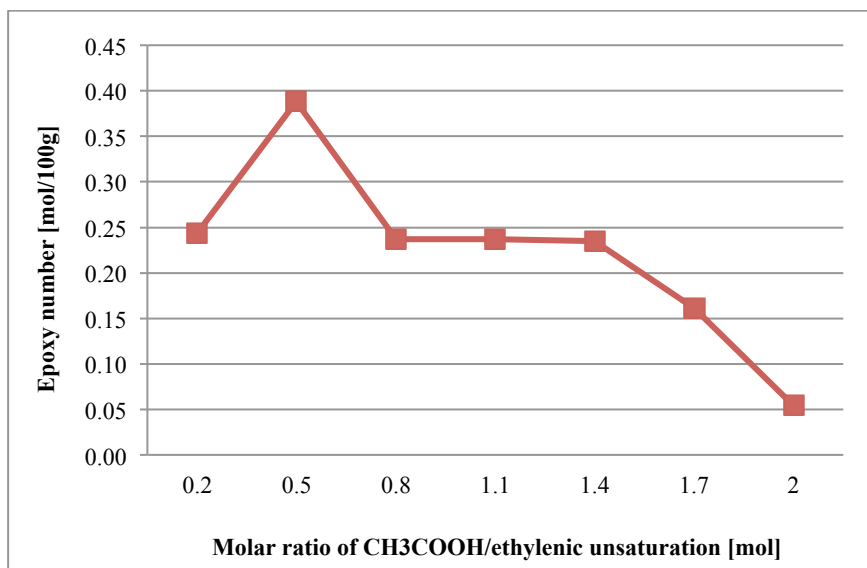


Fig. 2 Influence_of CH₃COOH /ethylenic unsaturation molar ratio on the epoxy numbers of epoxidised rapeseed oil

CONCLUSIONS

The best results of rapeseed oil epoxidation with regard to a high epoxy number at simultaneously low iodine number were achieved under molar ratio of acetic acid to ethylenic unsaturation: 0,5:1.

REFERENCES

1. Ma F., Hanna M. A., Biodiesel production: a review, *Bioresource Technology*, 1999, 70, 1, 1-15
DOI: 10.1016/S0960-8524(99)00025-5
2. Żak I., Szołtysek-Boldys I., Chapter in the book: Kwasy tłuszczowe i ikozanoidy, *Chemia medyczna*, Śląska Akademia Medyczna, 2001
3. Żbikowska A., Oleiste dobro narodowe, *Przegląd gastronomiczny*, 2010, 3, 10-11.
4. Monteavaro L. L., Da Silva E. O., Costa A. P. O., Samios D., Gerbase A. E., Petzhold C. L. Polyurethane networks from formiated soy polyols: synthesis and mechanical characterization, *Journal of the American Oil Chemists' Society*, 2005, 82, 5, 365-371
DOI: 10.1007/s11746-005-1079-0.
5. Malarczyk K., Milchert E., Kłós M., Vegetable oils epoxidation methods, *Dokonania Młodych Naukowców*, 2014, 3, 4, 114-116
6. Mungroo R., Pradhan N. C., Goud V. V., Dalai A. K. Epoxidation of Canola Oil with Hydrogen Peroxide Catalyzed by Acidic Ion Exchange Resin, *Journal of the American Oil Chemists' Society*, 2008, 85, 887-896
DOI: 10.1007/s11746-008-1277-z
7. Goud V. V., Patwardhan A. V., Dinda S., Pradhan N. C. Epoxidation of karanja (*Pongamia glabra*) oil catalysed by acidic ion exchange resin, *European Journal of Lipid Science and Technology*, 2007, 109, 575-584.
DOI: 10.1002/ejlt.200600298
8. Meshram P. D., Puri R. G., Patil H. V. Epoxidation of Wild Safflower (*Carthamus oxyacantha*) Oil with Peroxy acid in presence of strongly Acidic Cation Exchange Resin IR-122 as Catalyst, *International Journal of ChemTech Research*, 2011, 3, 3, 1152-1163.
9. Fiszer S., Szałajko U., Szeja W., Niemiec P. Epoksydowane oleje roślinne jako środki smarowe, *Przemysł Chemiczny*, 2003, 82, 8-9, 1016-1019.
10. Dinda S., Goud V. V., Patwardhan A. V., Pradhan N. C. Selective epoxidation of natural triglycerides using acidic ion exchange resin as catalyst, *Asia-Pacific Journal of Chemical Engineering*, 2011, 6, 870-878
DOI:10.1002/apj.466
11. Sinadinović-Fišer S., Janković M., Petrović Z. S. Kinetics of *in situ* Epoxidation of Soybean Oil in Bulk Catalyzed by Ion Exchange Resin, *Journal of the American Oil Chemists' Society*, 2001, 78, 7, 725-731
DOI: 10.1007/s11746-001-0333-9.

The epoxidation of limonene in toluene using hydrogen peroxide and over the Ti-MCM-41 catalyst

*Mariusz Wladyslaw Malko¹, Agnieszka Wróblewska¹

¹Institute of Organic Chemical Technology, Faculty of Chemical Technology and Engineering, West Pomeranian University of Technology, Szczecin, ul. Pulaskiego 10, 70-322 Szczecin, Poland

e-mail: mariuszmalko@gmail.com, agnieszka.wroblewska@zut.edu.pl

Keywords: *limonene epoxidation, 1,2-epoxylimonene, Ti-MCM-41, hydrogen peroxide*

ABSTRACT

R(+)-limonene is an unsaturated, cyclic and chiral terpene with the molecular formula of C₁₀H₁₆. The largest amount of R(+)-limonene is included in the peels of citrus fruits, which are the waste material from the fruit juice industry. In our studies we used a natural limonene extracted from the waste orange peels by the steam distillation and by the simple distillation. In the epoxidation of R(+)-limonene with hydrogen peroxide the Ti-MCM-41 catalyst was used. The influence of the following parameters was studied: the temperature and the reaction time. Studies were performed in toluene as the solvent.

INTRODUCTION

Limonene is a naturally occurring compound which belongs to the group of monoterpenes. It has one chiral center and thus, it can exist in the form of two enantiomers: R(+) and S(-). R(+)-limonene is a very popular compound in nature. It is the main component of essential oils obtained from the peels of citrus fruits which are the waste material from the orange juice industry. It is characterized by a fresh citrus scent. R(+)-limonene has different properties from S(-)-limonene. S(-)-limonene occurs in a small amounts in carrot roots, and in caraway. It is characterized by a pine aroma. Chemical structure of limonene molecule is similar to many containing oxygen derivatives such as: perillyl alcohol, carveol, carvone, and menthol. These compounds have a pleasant smell, and are very valuable intermediates in organic syntheses. Limonene can be used as a raw material in the synthesis of these containing oxygen derivatives. R-(+)-limonene is also present in drinks which are produced by large corporations like Coca-Cola Company, in fruit juices, ice creams and sweets [1]. Limonene is also used in air fresheners for the effective removing of the smoke smell. Moreover, it can be used in the manufacture of fabrics, for example limonene can be encapsulated in the structure of these fabrics and can play a role of fragrance

compound. Limonene can be formulated with surfactants to create environmentally friendly water cleaning preparations with low flammability, suitable for the treatment of the contaminated surfaces in many industrial environments (cleaning concrete, marine vessels, removing inks and adhesives) [2].

The very valuable utilization of R-(+)-limonene is the production of polymers which have special applications as the active biological polyesters. For example, R-(+)-limonene and 5-hydroxymethylfurfural are used as coatings for the window panes exhibiting a good permeability and stability to light. These coatings form an effective barrier to oxygen and water [3]. In the food industry are used polymers of R(+)-limonene and poly(lactic acid) or poly(hydroxybutyrate), and the obtained films are biodegradable and biocompatible in contact with food [4].

Ten years ago, the company Coates received the carbonate poly(limonene) during the copolymerization of carbon dioxide with limonene in the presence of zinc complex as a catalyst [5]. The obtained thermoplastic polymer had properties similar to polystyrene.

From a medical point of view, R-(+)-limonene is a very good solvent for cholesterol [6]. It is used in clinical removing gallstones. It also can neutralize stomach acid and promotes normal peristalsis. R-(+)-limonene is also active against certain types of cancer [7]. Limonene stopped the progression of breast cancer and colon cancer. The main problems connected with R(+)-limonene utilization are its allergenic properties. Under the influence of oxygen the formation of hydroperoxides irritating to the skin from limonene is observed [8]. Limonene is also used as a cleaner having superior antibacterial properties.

Very important from the point of view of organic processes is the obtaining of 1,2-epoxylimonene from R(+)-limonene in the epoxidation process. But the epoxidation of limonene to 1,2-limonene oxide is not an easy process because it requires the selection of a suitable catalyst and suitable reaction conditions to limit the amount by-products, for example: 1,2-epoxylimonene diol, carveol and carvone [9,10].

In the literature data there is a lot of information about the process of R(+)-limonene epoxidation using various catalysts. However, the main attention is directed to the utilization of the titanium silicate catalysts and hydrogen peroxide as the oxidizing agent in this process. Recent studies on the utilization of the titanium silicate catalysts in the epoxidation of limonene have shown that the most popular catalyst in this reaction is the Ti-MCM-41 catalyst [11,12].

Cagnoli et al. [13] studied the epoxidation of limonene at the temperature of 70°C, in a glass flask equipped with a reflux condenser, a thermometer and a magnetic stirrer. In the post-reaction mixtures were also

detected: carvone, carveol, diepoxy limonene and diols. During the studies it was found that the selectivity of transformation to organic compounds in relation to hydrogen peroxide consumed amounted to below 100%, due to the decomposition of hydrogen peroxide at the reaction conditions.

Berlin et al. [14] investigated the epoxidation of the unsaturated terpene (including limonene) over the Ti-MCM-41 catalyst. The epoxidation process was carried out in a glass reactor and at the temperature of 85°C. As the solvents acetonitrile and ethyl acetate were used. As the oxidizing agent an anhydrous t-butyl hydroperoxide was utilized. The molar ratio of oxidant/organic substrate was 1, and the amount of the catalyst in relation to organic substrate amounted to 30 wt%. In acetonitrile the conversion of limonene reached 62 mol%, and the selectivity towards the 1,2-epoxide was 79 mol%, while in ethyl acetate values of these functions amounted, respectively: 68 mol% and 62 mol%.

The epoxidation of R(+)-limonene was also performed with help of zincophosphates and zincochromates molecular sieves, in the presence of an ionic liquid and using the ion exchanger [15]. The epoxidation was carried out in the presence of hydrogen peroxide as the oxidant and butanol as the solvent. At the temperature of 60°C, the yield of 1,2-epoxy limonene reached 70%.

MATERIALS AND METHODS

For the process of limonene epoxidation as a raw material a natural limonene was used. It was obtained from the orange peels by the simple distillation. Its purity was tested by a gas chromatography method and it amounted to 99%. The next raw materials were: hydrogen peroxide (60 wt% water solution, Chempur), toluene (a.g., POCH Gliwice) and the obtained in our Institute the Ti-MCM-41 catalyst [16]. The conditions of the limonene epoxidation performing were as follows: the temperatures of 0°C, 40°C, 80°C and 120°C, the molar ratio of limonene/H₂O₂ = 1:1, toluene (solvent) concentration 80 wt%, the content of the Ti-MCM-41 catalyst 3 wt% and the intensity of stirring 500 rpm. The samples for the quantitative analyses were taken at the following reaction time: 0.25, 0.5, 1, 2, 3, 24 and 48h. The epoxidation was performed in the glass reactor with the capacity of 25 cm³ equipped with the magnetic stirrer and the condenser – Fig. 1

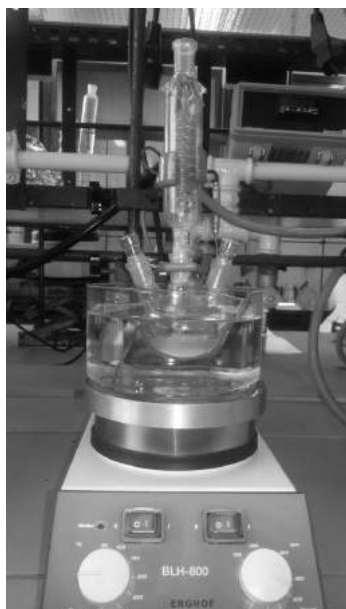


Fig 1 The apparatus for R(+)-limonene epoxidation with 60 wt% hydrogen peroxide

The post-reaction mixtures were analyzed by a gas chromatography and by iodometric titration (the determination of the unreacted hydrogen peroxide). In GC analyses the Focus apparatus equipped with the Restek RTX column (0.53 mm x 30m x 1.0 μ m film (polyethylene glycol 20,000 Da)) was used. After quantitative analyses the mass balance for each synthesis was calculated and main functions describing the process of limonene epoxidation (L) were determined: the selectivities of products (1,2-epoksyimonene, 1,2-epoksyimonene diol, carveol) in relation to limonene consumed – $S_{\text{product/L}}$, the conversion of limonene – C_L , the conversion of hydrogen peroxide – $C_{\text{H}_2\text{O}_2}$ and the selectivity of transformation to organic compounds in relation to hydrogen peroxide consumed – $S_{\text{H}_2\text{O}_2}$. These functions were calculated in the following way:

$$S_{\text{product/L}} = \frac{\text{amount of moles of product}}{\text{amount of moles of limonene consumed}} \cdot 100 \text{ [mol\%]}$$

$$C_L = \frac{\text{amount of moles of limonene consumed}}{\text{amount of moles of limonene introduced into reactor}} \cdot 100 \text{ [mol\%]}$$

$$S_{\text{H}_2\text{O}_2} = \frac{\text{amount of moles of formed organic compounds}}{\text{amount of moles of H}_2\text{O}_2 \text{ consumed}} \cdot 100 \text{ [mol\%]}$$

RESULTS AND DISCUSSION

The results of limonene epoxidation are presented in Tables 1-4, where: C_L - the conversion of limonene, $C_{\text{H}_2\text{O}_2}$ – the conversion of hydrogen peroxide $S_{\text{H}_2\text{O}_2}$ – the selectivity transformation to organic compounds in relation to hydrogen peroxide consumed.

The results showed that the process of limonene epoxidation is complicated and during this process various products can be obtained – Fig. 2.

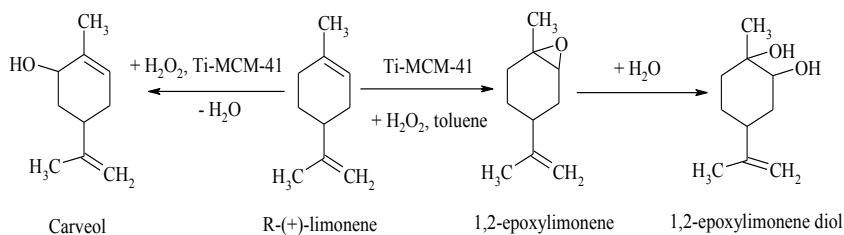


Fig. 2 The products of R(+)-limonene epoxidation

Table 1 The results of the epoxidation of limonene with hydrogen peroxide in the presence of Ti-MCM-41 at the temperature of 0°C

Number of synthesis		1	2	3	4	5	6	7
Temperature	[°C]	0						
Reaction time	[h]	0.25	0.5	1	2	3	24	48
S _{product/L} :								
1,2-epoxy limonene	[% mol]	0	0	0	0	0	0	0
1,2- epoxy limonene diol		15	11	10	11	10	10	8
Carveol		85	89	90	89	90	90	92
C _L		1	2	2	2	2	3	3
C _{H202}		84	89	88	97	97	97	97
S _{H202}		1	2	2	2	2	4	3

Table 2 The results of the epoxidation of limonene with hydrogen peroxide in the presence of Ti-MCM-41 at the temperature of 40°C

Number of synthesis		1	2	3	4	5	6	7
Temperature	[°C]	40						
Reaction time		0.25	0.50	1	2	3	24	48
S _{product/L} :								
1.2-epoxy limonene	[% mol]	0	0	0	0	0	0	0
1,2- epoxy limonene diol		3	0	28	26	30	34	36
Carveol		97	100	72	74	70	66	64
C _L		1	1	1	2	2	2	3
C _{H202}		95	94	93	94	93	93	93
S _{H202}		1	1	2	2	2	2	3

Table 3 The results of the epoxidation of limonene with hydrogen peroxide in the presence of Ti-MCM-41 at the temperature of 80°C

Number of synthesis		1	2	3	4	5	6	7
Temperature	[°C]	80						
Reaction time	[h]	0.25	0.5	1	2	3	24	48
$S_{\text{product/L}}$:								
1,2-epoxylimonene	[% mol]	0	4	5	4	6	10	13
1,2-epoxylimonen-diol		20	25	43	44	42	42	43
Carveol		80	71	52	52	52	48	44
C_L		3	4	4	5	5	6	6
C_{H202}		95	96	94	97	94	95	95
S_{H202}		4	4	4	5	5	6	6

Table 4 The results of the epoxidation of limonene with hydrogen peroxide in the presence of Ti-MCM-41 at the temperature of 120°C

Number of synthesis		1	2	3	4	5	6	7
Temperature	[°C]	120						
Reaction time	[h]	0.25	0.5	1	2	3	24	48
$S_{\text{product/L}}$:								
1,2-epoxylimonene	[% mol]	8	1	2	2	2	0	0
1,2-epoxylimonene diol		52	57	57	54	53	42	40
Carveol		40	42	41	44	44	58	60
K_L		5	4	5	5	5	6	7
K_{H202}		95	94	98	99	98	100	100
S_{H202}		5	4	4	5	5	5	4

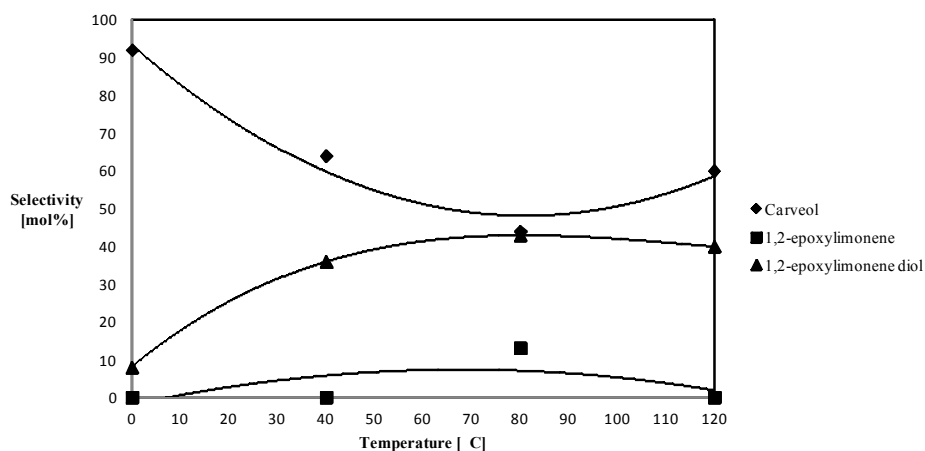
The studies for the lowest temperature (0°C) – Table 1, showed that only a small amount of limonene underwent conversion independent of the reaction time – about 1-3 mol%. At this temperature the conversion of hydrogen peroxide was high and amounted to 84 to 97 mol%. For this temperature the main product was carveol – product of cyclic allylic hydrogen abstraction (allylic oxidation) at the 6-position. It was formed with the selectivity of about 85-92 mol%.

During rising of the temperature of the epoxidation the conversion of limonene raised a little to 6-7 mol% (Tables 2-4). The conversion of hydrogen peroxide was still high and amounted to about 95-100 mol%. The raising of the temperature caused the second product of this process - 1,2-epoxylimonene diol

was the main product of the process. It is formed from 1,2-epoxylimonene as a result of hydration of the epoxide ring. For the temperature of 120°C (Table 4) the selectivity of this compound achieve the highest value of 57 mol% (for the reaction time 2 and 3h).

Fig. 3 The changes of the selectivity of transformation to 1,2-epoxylimonene, its diol and carveol depending on the temperature of limonene epoxidation process performing

The results presented on Fig 3. show that the increase of the temperature of the epoxidation causes decrease the selectivity of carveol and increase in



values of the selectivity of 1,2-epoxylimonene diol, which is obtained by hydration of 1,2-epoxylimonene. Thus, at lower temperatures mainly the allylic oxidation at the position 6 undergoes but at higher temperatures the epoxidation of the unsaturated bond takes place.

CONCLUSIONS

The studies showed that independent of the temperature of the epoxidation performing the Ti-MCM-41 catalyst was not very active catalyst in this process when toluene was used as the solvent. Probably, by choosing of the appropriate solvent the value of the main factions describing this process can be increased, but it needs further studies.

REFERENCES

1. U Ravid, M. Elkabetz, C. Zamir, K. Cohen, O.Larkov ,R. Aly, Authenticity assessment of natural fruit flavour compounds in foods and beverages by auto-HS–SPME stereoselective GC–MS, *Flavour Frag. J.*,2010, 25, 20-27
2. M.Uemura, G. Hata, T.Toda, F. S. Weine, Effectiveness of eucalyptol and d-limonene as gutta-percha solvents, *J. Endod.* 1997, 23, 12, 739–74

- 3.S. Chemat, V. Tomao and F. Chemat, Limonene as Green Solvent for Extraction of Natural Products, in *Green Solvents I: Properties and Applications in Chemistry*, ed. A. Mohammad and Inamuddin, Springer Science + Business Media, Dordrecht, 2012, 175–186.
4. A. T. Karlberg, K. Magnusson and U. Nilsson, Oxidized citrus oil (R-limonene): A frequent skin sensitizer in Europe, *Contact Dermatitis*, 1992, 5, 332–340.
5. E. Keinan, A. Alt, G. Amir, L. Bentur, H. Bibi and D. Shoseyov, Natural ozone scavenger prevents asthma in sensitized rats, *Bioorg.Med. Chem.*, 2005, 13, 557–562.
6. M. J. Cortez, H. G. Rowe, *Alternative Response Technologies: Progressing Learnings*, Interspill 2012, Houston, Texas, February 15, 2012.
- 7.H. Lazenby, "US Oil Sands' biosolvent extraction patent approved", *Mining Weekly*, 22 April 2014.
8. K. Faure, E. Bouju, P. Suchet and A. Berthod, Limonene in Arizona liquid systems used in countercurrent chromatography– I- Physico-chemical properties *Anal. Chem.*, 2013, 85, 4644–4650.
9. P. M. Arrieta, J. Lopez, A. Hernandez and E. Rayon, Bionanocomposite films based on plasticized PLA–PHB/cellulose nanocrystal blends *Eur. Polym. J.*, 2014, 50, 255–270.
10. C. M. Byrne, S. D. Allen, E. B. Lobkovsky and G. W. Coates, Alternating Copolymerization of Limonene Oxide and Carbon Dioxide *J. Am.Chem. Soc.*, 2004, 126, 11404–11405
11. M. Bahr, A. Bitto and R.Mulhaupt, Cyclic limonene dicarbonate as a new monomer for non-isocyanate oligo- and polyurethanes (NIPU) based upon terpenes *Green Chem.*, 2012, 14, 1447–1454.
12. B. Schäffner, F. Schäffner, S. P. Verevkin and A. Börner, Efficient hydrogenation of organic carbonates, carbamates and formates indicates alternative routes to methanol based on CO₂ and CO *Chem. Rev.*, 2010, 110, 4554–4581.
- 13.T. Sakakura and K. Kohno, The synthesis of organic carbonates from carbon dioxide. *Chem. Com.*, 2009, 1312–1330
14. Marino D., Gallegos N.G., Bengoa J.F., Alvarez A.M., Cagnoli M.V., Casuscelli S.G., Herrero E.R., Marchetti S.G.. Ti-MCM-41 catalysts prepared by post-synthesis methods limonene epoxidation with H₂O₂, *Catalysis Today* 2008,133-135: 632-638.
15. M. Santa A., Vergara G.C.J, Luz Amparo Palacio S., Adriana Echavarrí a I. Limonene epoxidation by molecular sieves zincophosphates and zincochromates. *Catalysis Today* 2008 133–135: 80-86

16. T. Blasco, A. Corma, M.T. Navarro, J.P. Pariente, Synthesis, Characterization, and Catalytic Activity of Ti-MCM-41 Structures, *Journal of Catalysis*, 1995, 156, 65-74.

Impact of loads and biofeedback to behavior of the center of gravity of the body

* Marek Andryszczyk¹, Sandra Śmigiel¹, Tomasz Topoliński¹

¹Faculty of Mechanical Engineering, University of Science and Technology, Bydgoszcz, POLAND

e-mail: andryszczyk.marek@gmail.com

***Keywords:** center of gravity, body balance, biofeedback, stabilography, balance platform.*

ABSTRACT

The balance of the body is the subject of research many scientists. To determine the center of human gravity and the changes of position are used the newer devices, which presents the length of delineated path and surface area. The purpose of the study was to demonstrate how the weight on back and return information about the changes the position of the center of gravity, affects the balance of the human body. In addition, as part of the research, attempted to determine the effect of factors, such as BMI, body posture and subjective of physical activity, for the maintain of the body balance.

INTRODUCTION

Liberty in standing position, which is characterized by a healthy person causes that the postural stability is considered as a matter of course, which does not require engagement and effort.

The complexity of the process of controlling the balance can be seen at the time of its deterioration, resulting a pathological changes or aging [1, 2]. The result of balance disorders is the postural instability, which in some cases can lead to the collapse [3].

The maintain postural stability covers many of issues such as: motor control, spatial orientation and impact on the body of various forces. In literature are two terms (used interchangeably): postural stability and body balance.

Balance control system, including many of the structures of the central nervous system, can be regarded as the controller with the three inputs, which will determine the spatial position of the center of gravity of the body balance. The correct orientation the body in space and maintain balance under physiological conditions, provide the signals coming from the vestibular system, ocular and deep sensory receptors, located in the muscles, joints and skin.

Balance of the body is a certain state of the postural system, which is characterized by the vertical orientation of the body, obtained by balancing the forces and moments acting on the person. The nervous system maintains the

balance of the body via controlled reflex muscle tension, called anti-gravity [4]. In this way, the balance relates to a system of motor control during the static conditions.

STABILOGRAPHY

Maintaining the balance of the body consists of static and dynamic balancing of destabilizing forces of gravity and inertia, via stimulating the appropriate muscle [5]. Stabilization of upright posture is based on minimizing the swing in such a way that the vertical projection of the center of mass of the body, was based on anatomical support, which is located in an area of the foot, adjacent to the substrate [5]. The study of balance of the body deals with the stabilography and also posturography.

The use of computer with measuring cards and specialized software, enabling control of research positions, archiving parameters and results are contributed to a significant broadening the scope of the study. Prior to the development of new techniques the scientific article were fragmentary and in most based on a narrow research material. The introduction of computer technology leads to complex describe the research material [2].

The study of stability via using the measuring platform consist at the time analysis of variability point of application of the resultant of ground reaction forces, during the attempt to maintain a balance in an upright position (fig. 1). Stability is the worse, when the frequency and extent of change in the point of application of the resultant of ground reaction forces of the substrate are higher. If the projection of the center of gravity on a support space exceeds the limit of stability comes to fall. The balance of the body occurs in the case of reaction of the with drawal of the limb, and an increase in the plane of the support [1, 5].

Until recently it was believed that stability limit it is the envelope of the foot - the boundary surface of the support [6]. The study carried out on students of the Faculty of Physical Education Academy of Physical Education in Wrocław showed, that even the most physically fit man never reached the hypothetical stability limit, defined by envelope feet. The actual border postural stability of the mechanical boundary (the outer edge of the foot) separates area called the margin of safety, which the size depends on the efficiency of the system to maintain a balance. They are also affected such factors as the: fear of falling and slope [7]. These assumptions reflect the figure 1 with the specified parameters: BS - boundary of stability, IBS - individual boundary of stability, SM - safety margin.

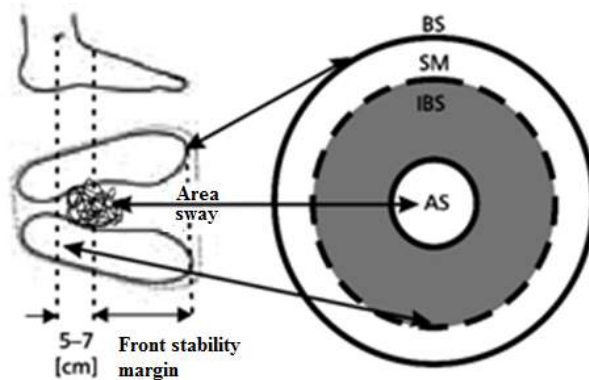


Fig. 1 Heuristic model for human stability [7]

Biofeedback

Biofeedback is a method provides human feedback about changes in physiological state and in the case of this article about changes the setting of center of gravity of the human body on the plane. The body's physiological changes are monitored by a computer system and transmitted via: the form of a visual on the computer screen. This functionality will provide the patient the opportunity to study and the ability to deliberate modifications in the system functions, which that are normally not consciously controlled. These systems have been used in medicine as a form of rehabilitation and sport in the range of optimization of body movements [2].

Taking into account the above phenomena, such as stabilography, biofeedback was formulated two overarching goals. The main aim of the authors was to determine the effect of weight on back and the biofeedback about the movements of the center of gravity to the balance of the body. Moreover, in the second part of the study attempt to determine the effect on the body's balance factors such as: BMI, features body posture and subjective evaluation of physical activity, demonstrated by the respondents.

MATERIAL

The study involved a group of students of the University of Technology and Life Sciences them. J.J. Śniadeckich in Bydgoszcz, diverse in terms of age (in the range of 19-24 years and mean age 20.5 years), gender, height and weight. Analyzed research group consisted of 32 people, including 14 women and 18 men.

Exclusion criteria from research were found the backache, neurodegenerative disease and physical disability.

METHODS

The study was conducted in three stages.

The I stage of the research included gathered information on the physical condition of the respondents. The study was conducted using a questionnaire, which included basic questions about:

- gender,
- declared type of physical activity,
- average weekly physical activity,
- vision correction occurring.

The II stage of the study included determined the weight, height and center of gravity, from the plane of the foot.

Measurements of body weight and growth has been using via using the electronic medical weight (RadWag). For the study, students should approach the clothes, taking a free standing position (the upper limbs abandoned along the trunk, the bare feet). The test weight is made to the nearest to 0.1 kg and grow to 0.5cm. The obtained data allowed for the calculation of BMI from the relationship:

$$BMI = \frac{wzrost}{(masa\ ciała)^2} \quad (1)$$

The distance the center of gravity r of the foot plane, here in after referred to as the height of center of gravity, was determined based on a horizontal platform (fig. 2), built for the execution of this study. The height of the center of gravity was determined using the relationship:

$$r = \frac{l * R}{Q} \quad (2)$$

where:

l – distance of the platform support weight from the center of rotation of the platform,

R – the force of the value indicated on the tared weighing platform,

Q – the burden of the mass of the people.

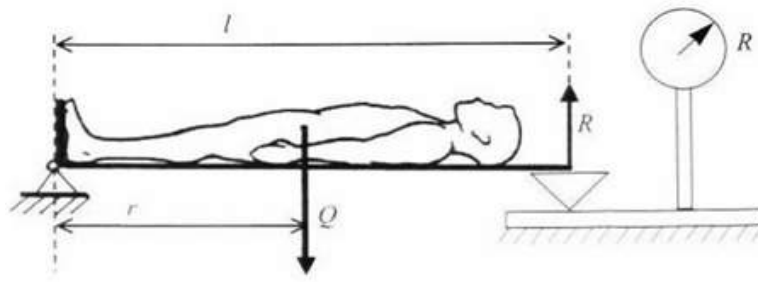


Fig. 2 Scheme platform for determination of the center of gravity

To determine the strength of R was used a portable, digital medical weight (RadWag). In this way it was possible to determine the height of center of gravity, according to the relation:

$$W = \frac{r}{wzrost} * 100\% \quad (3)$$

The III stage of the study was conducted using the specialized computer software, integrated with the stabilometric platform - ALFA (the Technomex company), which allows to determine the path length and surface area. These platform is equipped with strain gauges, which provide accurate results in the case of a static test [8].

For the study, students received a free standing position with feet parallel spaced in the middle of the stabilometric platform (the upper limbs abandoned along the trunk, the bare feet). In the context of this stage, performed 3 measurements for 30 seconds with no load on the eyes open (O.O.), eyes closed (O.Z.) and feedback (S.Z). Registrations balance of the body in the same sequence were also performed with the load occurring on the back (in the vicinity of the center of gravity of the test), constituting 10% of the examined person.

The result of each measurement parameters were as follows:

- the length of the path, which traveled the center of gravity,
- the surface area from stabilometric platform.

The results obtained are called the stabilometric parameters, which are used for later analysis.

Both of the above mentioned parameters are dependent on the imposed time registration. The length of the path is formed as the sum of all sections of the broken line, which is the trajectory of the center of gravity moves in the XY plane. The surface area is calculated as the area of polygonal shapes and irregular field is the sum of triangles, in which one vertex is stabilometric center point and the other vertices are two subsequent position of the center of gravity.

The final stage of the study was the statistical analysis of the data, performed using tools Statistica software 10 Site License. Statistical inference in view of the non-parametric distribution of the variables (shown Shapiro-Wilk test) was based on non-parametric tests.

Test comparing the dependent variables for the three variables was a test of Friedman, and made a test comparing two variables the test matched pairs Wilcoxon. For the independent variables, which are grouped by gender, index of BMI was used the U Manna Whitneya test. Comparison of the parameters for the three variables was applied using the ANOVA rang Kruskala-Wallis test. Correlation analysis was performed Spearman rank order test.

The verification of all analyzes was performed via used a level of significance coefficient $\alpha = 0.05$, which allowed for the variables considered statistically significant comparisons at $p < 0.05$.

RESULTS

Analysis the BMI parameter (table 1) shows the average value at 22.7 [kg/m²], and the standard deviation of 3.7 [kg/m²].

Table 1 Descriptive statistics BMI parameter for the study group

Anthropometric parameters							
	\bar{x}	SD	Min	Q1	Me	Q3	Maks
BMI	22,7	3,7	16,4	19,8	22,7	24,9	31,3

\bar{x} - medium; SD – standard deviation; Min – the minimum value; Q1 – the first quartile, Me – the median; Q3 – the third quartile; Maks – maximum value

Individual results indicate, that among the respondents there 3 people, which have underweight and 8 people, who suffer from overweight. In the remaining respondents have a normal index of BMI (table 2).

Table 2 The BMI parameter taking into account gender

Interpretation BMI parameter				
Gender		Underweight	Normal	Obesity
Women	N	2	10	2
	%	14,29%	71,43%	14,29%
Men	N	1	11	6
	%	5,56%	61,11%	33,33%

Analysis of responses of study group in the range of declared physical activity (table 3) shows that among the women is a higher percentage of people do not undertakes any physical activity, compared to a group of men.

Table 3 The type of declared physical activity

Type of physical activity	Gender			
	Women		Man	
Type of physical activity	N	%	N	%
Only athletics	1	7,14%	3	16,67%
Athletics in 75% and strength training 25%	4	28,57%	4	22,22%
Athletics in 50% and strength training 50%	3	21,43%	1	5,56%
Athletics in 25% and strength training 75%	1	7,14%	1	5,56%
Only strength training	0	0,00%	4	22,22%
Lack	5	35,71%	5	27,78%

In addition, among all respondents 25 people do not have any correction of the eye and the remaining 7 have a visual impairments (within the: 6 with myopia and 2 with foresight).

The answers of the respondents about the limb injuries in the last 5 years show s that in 8 on 32 people had a trauma, as result of example: fractures, sprains, dislocations.

The results of stabilographic research without load on back

The results obtained in the first stage of measurements without the weight on back are shown in table 4. For the study, students should approached with eyes closed respectively (O.Z.), eyes open (O.O.) and the visual feedback occurring motor (S.Z.).

The obtained values indicate that the average path length parameter decreased by 6,25 cm for the test with eyes open in relation to the trial with eyes closed, and 10,93 cm in trial with biofeedback in relation to the trial with eyes closed.

The similar results can be observed when comparing the results obtained for the surface area resulting via tracing the center of gravity. The difference in results between the sample with eyes closed and open was 0,73cm², and the difference for the test with biofeedback in relation to the trial with eyes closed 0,31cm².

Table 4 The results from stabilographic platform without load on back

The path length [cm]							
	\bar{x}	SD	Min	Q1	Me	Q3	Maks
O.Z.	30,43	21,62	8,40	19,40	25,15	35,15	118,00
O.O.	24,18	16,76	6,50	14,45	20,55	27,80	94,70
S.Z.	19,50	14,21	6,30	12,05	15,10	23,25	80,70
The surface area of the path [cm ²]							
O.Z.	2,51	4,01	0,30	0,75	1,35	2,90	21,90
O.O.	1,78	4,03	0,20	0,55	0,75	1,80	23,50
S.Z.	2,20	6,09	0,20	0,40	0,65	1,10	34,40

The statistical analysis of Friedman test (table 5) confirms statistically significant differences in the results between test carried out on the O.Z vs O.O. vs S.Z., both for the path length parameter and also for the results of surface area.

Performed comparative analysis of the algorithm Dunn showed statistically significant differences. The results are smaller between the values obtained from the sample S.Z. from the results of O.Z and O.O.

Table 5 Comparison parameter of the path length of respondents without load on back

Test Friedman P value < 0.0001		
Friedman statistic 33,81		
Dunn's Multiple Comparison Test	The difference of the sum of squares	Value p
O.Z. vs O.O.	17,00	ns
O.Z. vs S.Z.	46,00	<0,001
O.O. vs S.Z.	29,00	<0,001

For the analysis of surface area (table 6) was obtained results with significantly higher values for the OZ with respect to a O.O. and S.Z.

Table 6 Comparison parameter of the surface area of the respondents without load on back

Test Friedman P value < 0.0001		
Friedman statistic 21,98		
Dunn's Multiple Comparison Test	The difference of the sum of squares	Value p
O.Z. vs O.O.	23,00	<0.05
O.Z. vs S.Z.	35,50	<0,001
O.O. vs S.Z.	12,50	ns

The results of stabilographic research with load on back

The results obtained in the second stage of measurements with the weight on back are shown in table 7. For the study, students approached with the load on back, which amounted to 10% of their body weight. The results, as in the test without the load on back, showed that both the path length and also surface area reduces the size of the analyzed parameter for the trial O.O. and S.Z. compared to the results O.Z.

The difference in path length obtained for O.Z. with O.O. amounted to 8,15cm, and for S.Z. 8,86cm.

The differences obtained for the area of the O.Z. of O.O. amounted to 1,02cm² and for S.Z. 1,00cm².

Table 7 The results from stabilographic platform with load on back

The path length [cm]							
	\bar{x}	SD	Min	Q1	Me	Q3	Maks
O.Z.	33,00	14,58	13,40	22,40	28,55	44,40	81,30
O.O.	24,85	14,25	8,00	15,40	21,90	30,00	82,20
S.Z.	24,14	15,20	8,00	14,80	19,90	30,00	81,00
The surface area [cm ²]							
O.Z.	2,65	2,73	0,60	1,00	1,60	3,35	14,20
O.O.	1,63	2,39	0,30	0,60	1,00	2,00	13,80
S.Z.	1,65	1,83	0,30	0,55	0,80	2,30	8,70

The multiple statistical analysis carried out in the algorithm Dunn confirms the impact of visual control and biofeedback to reduce the results with respect to the parameters obtained during the trial of O.Z., both in the range of path length changes respondents, and also a parameter of surface area (table 8, 9).

Table 8 Comparison parameter of the path length of respondents without load on back

Test Friedman P value < 0.0001 Friedman statistic 33,77		
Dunn's Multiple Comparison Test	The difference of the sum of squares	Value p
O.Z. vs O.O.	35,50	<0,001
O.Z. vs S.Z.	42,50	<0,001
O.O. vs S.Z.	7,000	ns

Table 9 Comparison parameter of the surface area of the respondents with load on back

Test Friedman P value < 0.0001 Friedman statistic 21,71		
Dunn's Multiple Comparison Test	The difference of the sum of squares	Value p
O.Z. vs O.O.	33,00	<0,001
O.Z. vs S.Z.	28,50	<0,001
O.O. vs S.Z.	-4,500	ns

Comparison of the results in the case of without the applied load in relation to the load 10% on back, constitutes 10% weight respondents in three trials (OZ, OO, SZ)

In the second part of the statistical analysis were compared the values obtained for samples of stabilographic platform with eyes closed, eyes open and with the biofeedback, which was referred to two established conditions: without the applied load on the back and the load equivalent to 10% of body weight respondents.

Statistically significant differences were obtained for the path length in the two cases. First, when respondents had eyes closed, and the second, when was the biofeedback. In both cases, the load increasing effect on the analyzed values (table 10).

Table 10 Comparison of the results for the sample path length with no load vs. load occurring on the back

Test pair of sequence Wilcoxon			
No load vs. load	Median difference	Value T	Value p
O.Z.	-3,4	124,5	<0,01
O.O.	-1,35	222	ns
S.Z.	-4,8	56	<0,001

A similar relationship is also applied to compare the results of the area of the surface area path (table 11). Significant difference between the results obtained when the respondents had eyes closed and when was the biofeedback. In both cases, the larger the difference obtained at the load back (fig. 3, fig. 4).

Table 11 Comparison of the results for the surface are of the path for the test with no load vs. load occurring on the back

Test pair of sequence Wilcoxon			
No load vs. load	Median difference	Value T	Value p
O.Z.	-0,25	130,5	<0,1
O.O.	-0,25	142	ns
S.Z.	-0,15	134,5	<0,05

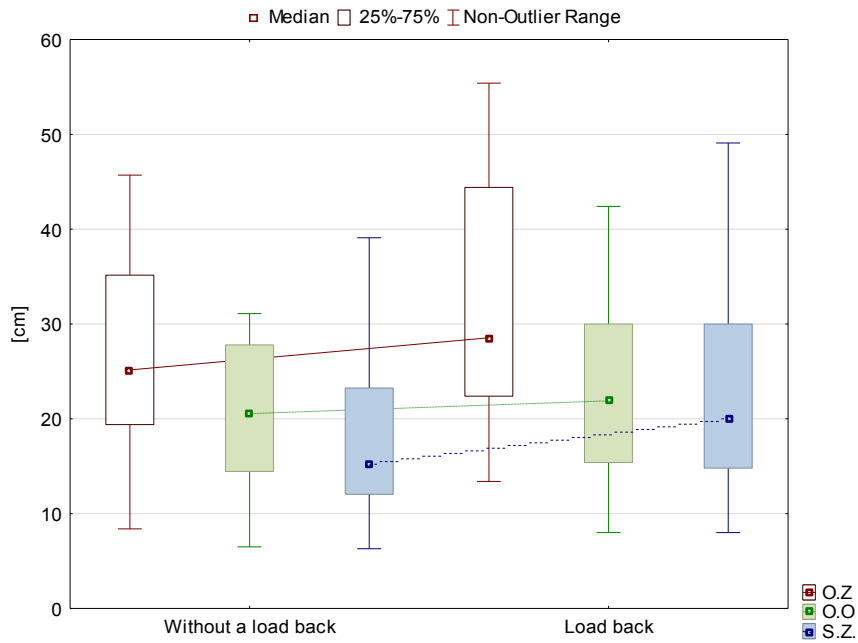


Fig. 3 Graphical representation of the distribution of the length of the path without a load and the load for the three tests: O.Z., O.O., S.Z

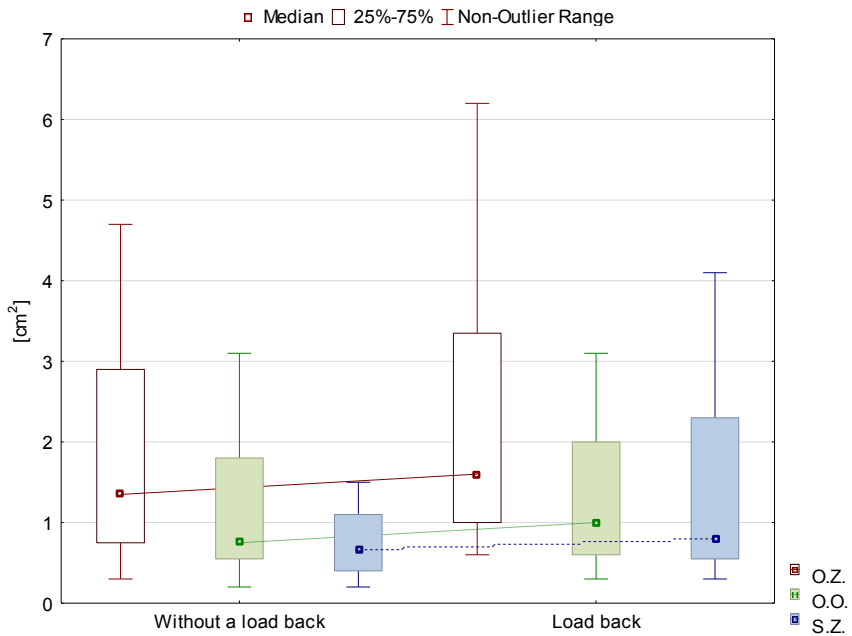


Fig. 4 Graphical representation of the distribution of the surface area of the path without a load and the load for the three tests: O.Z., O.O., S.Z

Correlations of parameters

Another parameter, which was analyzed to determine the relationship between the factor of the height on which the center of gravity in relation to the parameters of the path length and surface area for the sample: without load and load on the back, and also for the established conditions: O.Z., O.O. and S.Z.

In the conducted comparison demonstrated a statistically significant positive relationship between the average power of the center of gravity factor of the height and the length of the path, and also the area of the path for the test without load back, and in the case of the respondents when eyes were open, closed, and the biofeedback (table 12).

For a similar correlation with the load carried on the back of the assumed achieved a statistically significant association with poor strength only for the test with the eyes closed.

Table 12 The correlation coefficient of the center of gravity in relation to the parameters of the path length and surface area of the path in the samples wit O.Z., O.O. and S.Z. without a load and the load on the back

Spearman's rank order correlation.					
The relative height of the center of gravity.					
Simple		Path lenght		Surface area	
		R - Spearman	Value p	R - Spearman	Value p
Without load	O.Z.	0,519	0,002	0,526	0,002
	O.O.	0,356	0,046	0,303	0,092
	S.Z.	0,482	0,005	0,485	0,005
With load	O.Z.	0,363	0,041	0,352	0,049
	O.O.	0,301	0,100	0,280	0,127
	S.Z.	0,277	0,125	0,220	0,227

Additionally, in the range of analysis was performed a comparison of the coefficient of the center of gravity taking into account gender (table 13). The performed comparison via using the Test U Manna-Whitneya test for independent variables (table 14). The obtained results revealed a statistically significant difference between the groups. Factor of the center of gravity is higher for men than women, which may be due to greater shoulder girdle musculature in the case of the first group of people. Graphically representation shown in figure 5.

Table 13 Descriptive statistics height of center of gravity

Factor of the height of center of gravity							
Gender	\bar{x}	SD	Min	Q1	Me	Q3	Maks
Women	56%	1%	54%	55%	56%	57%	56%
Man	57%	1%	53%	56%	57%	59%	58%

Table 14 Comparison of the height of center of gravity between women and men

Test U Manna-Whitneya					
	The sum of the rang - Woman	The sum of the rang - Man	The average rang - Women	The average rang - Man	Value p
Factor of the center of gravity	157	371	11,2	20,6	0,004

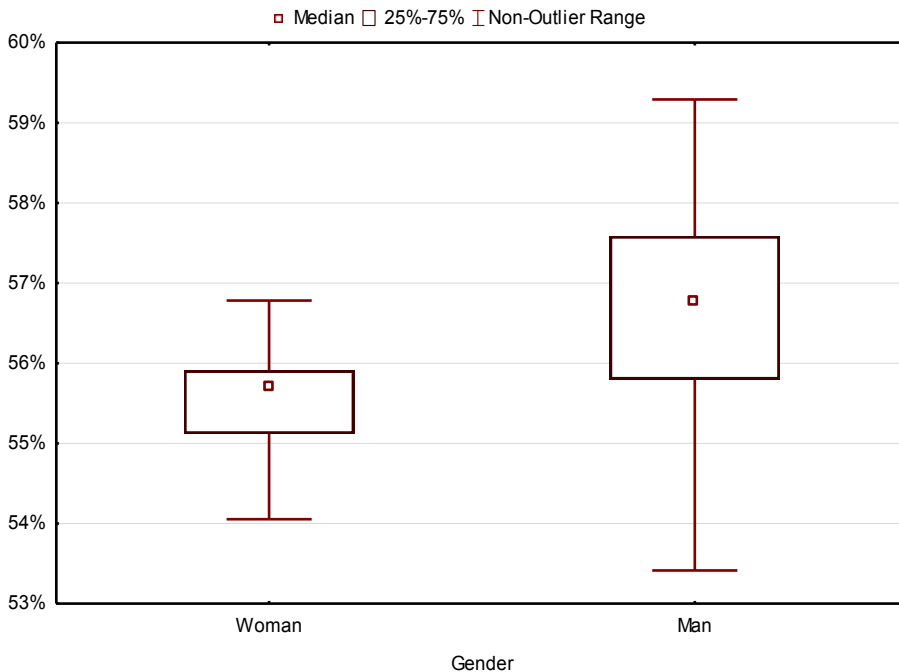


Fig. 5 Graphical representation of the distribution coefficient of the center of gravity

DISCUSSION

Increasing the length and surface area of path are related to the age of the respondents, neurodegenerative disease, and pre-postural muscle fatigue and force [1, 5, 6, 9, 10].

In this study, the results were consistent with results other researchers for young people, which not have any problems with obesity and neurodegenerative disease [3, 11].

In analyzing the parameters in the system with eyes closed, eyes open and eyes open biofeedback showed the statistically significant changes in both the case of without load and the load on the back (table 5, 6, 8, 9). These results confirm the relationship to improve stability and control the impact of vision on the parameters of length and surface area of path. A similar direction of change also occurs in the case of athletic and people with neurodegenerative disorders, confirming the positive impact of visual control and biofeedback to improve the results, which were demonstrated in this paper and are consistent with the current state of knowledge [2, 10].

Comparison of the results between the test without the load on the back, as well as their load showed statistically significant differences for samples with eyes closed and eyes open with biofeedback, and the absence of such a relationship has been achieved in the test with eyes open. Depending occurred can be explained via an increase load in postural muscles, which lead to increased tension and lack of full compensation aligned in each of group. The test results are in line with studies of other researchers [9, 12].

Further analysis showed a statistically significant difference in the height of the center of gravity between women and men. Dependence is due to the greater muscle mass in the men shoulder girdle in relation for women, and also less muscle and the less girdle in relation for women [13].

Analysis of the correlation coefficient of the center of gravity of the parameters for the length and surface area of path without load on the back showed the presence of statistically significant association with weak fit of the sample with O.Z., O.O. and S.Z. In the case of samples with load on the back these dependence are not observed in the sample with O.O. and S.Z. This can be explained by the deterioration of the ability to control the center of gravity especially in the case of the low coefficient of the center of gravity [9, 12].

In the analysis also was not obtained statistically significant differences between women and men in terms of length and surface area of the path for any of the three trials, and in the without load and with load on back.

Also failed to demonstrate a relation between physical activity and a form of physical activity in relation to analyzed parameters.

CONCLUSION

Conclusions on the basis of the study indicate that there is a statistically significant worsening of the body balance with load on the back. Conducted the statistical inference indicates that there was no statistically significant correlation between the results of body balance, and the parameter BMI and physical activity. It should also be noted that the gender does not affect to difference between the results with body balance, but there are differences in the height of the center of gravity. There is a relationship between the parameter coefficient the height of the center of gravity and stabilometric parameter in the case of respondents with absence of load on the back. This relationship is not evident in the case of load on the back.

REFERENCES

1. Blaszczyk, J.W., Hansen P.D., Lowe D.L.: Evaluation of the postural stability in man: movement and posture interaction, *Acta Neurobiologiae Experimentals* 1993, pp. 155-60
2. Meldrum D.: Effectiveness of conventional versus virtual reality based vestibular rehabilitation in the treatment of dizziness, gait and balance impairment in adults with unilateral peripheral vestibular loss: a randomised controlled trial, *BMC Ear Nose Throat Disord* 2012, pp. 3
3. Varela D.G., Carneiro J.A., Colafemina J.F.: Static postural balance study in patients with vestibular disorders using a three dimensional electromagnetic sensor system, *Brazilian Journal Otorhinolaryngology* 2012, vol. 78, no. 3, pp. 7-13
4. Strzecha M.: Człowiek zazwyczaj ma dwie nogi – ujęcie stabilograficzne, *NeuroCentrum* 2008, pp. 10
5. Blaszczyk J.W., Hansen P.D., Lowe D.L.: Postural sway and perception of the upright stance stability borders, *Perception* 1993, vol. 22, no. 11, pp. 1333-41
6. Blaszczyk J.W.: Effect of ageing and vision on limb load asymmetry during quiet stance, *Journal of Biomechanics* 2000, vol. 33, no. 10, pp. 1243-8
7. Błaszczuk J.W.: *Biomechanika kliniczna*, Warszawa Wydawnictwo Lekarskie PZWL 2004
8. Browne J., O'Hare N.: Development of a novel method for assessing balance: the quantitative posturography system, *Physiological Measurement* 2000, vol. 21, no. 4, pp. 525-34
9. Nam H.S.: The relationship between muscle fatigue and balance in the elderly, *Annals of Physical and Rehabilitation Medicine* 2013, vol. 37, no. 3, pp. 389-95
10. Ortiz-Gutierrez R.: A telerehabilitation program improves postural control in

- multiple sclerosis patients: a Spanish preliminary study, *International Journal Environmental Research and Public Health* 2013, vol. 10, no. 11, pp. 5697-710
11. Geib R.W.: Using computerized posturography to explore the connection between bmi and postural stability in long-term tai chi practitioners – *biomed, Biomedical Sciences Instrumental* 2011, vol. 47, pp. 288-93
 12. Wade C.: Walking on ballast impacts balance, *Ergonomics* 2014, vol. 57, no. 1, pp. 66-73
 13. Dorneles P.P., Pranke G.I., Mota C.B.: Comparison of postural balance between female and male adolescents, *Fisioterapia e Pesquisa* 2013, vol. 20, no. 3

Application of selected transition metals lignosulfonates as hydrogen peroxide electrochemical sensors and as electroplating baths

*Klaudia Śron, Grzegorz Milczarek,

Faculty of Chemical Technology Poznan University of Technology, Poznań,
POLAND

e-mail: klaudia.sron@put.poznan.pl

Keywords: lignosulfonates, sensors, hydrogen peroxide, electroplating

ABSTRACT

This research demonstrates the synthesis and application of Mn(II), Co(II), Cu(II) and Ni(II)-lignosulfonate complexes. The electrochemical properties of the resulting material deposited as a redox film were investigated by cyclic voltammetry. Mn(II) and Co(II)-lignosulfonate modified electrodes appeared to be effective electrocatalysts for the anodic oxidation of hydrogen peroxide. The second stage of the study includes the determination of optimal operating conditions of the non-toxic Cu(II)-lignosulfonate and Ni(II)-lignosulfonate baths for the plating of the corresponding metal layers.

INTRODUCTION

Lignosulfonates are byproducts of pulp and paper industry produced in quantities of millions metric tons per year. Lignosulfonates are obtainable as sodium, calcium or magnesium salts depending on the composition of chemical mixture used to digest wood in the paper making plant, which can be calcium, magnesium or sodium sulfite aqueous solutions. By the action of this salts the natural, insoluble lignin is changed into a water soluble lignosulfonate according to the reaction:

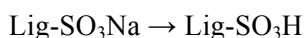


Lignosulfonate molecules are amphiphilic and contain hydrophobic groups, such as aromatic and aliphatic groups, but also contains many hydrophilic groups: sulfonic, carboxyl and phenolic hydroxyl. Their most important advantages are good solubility in aqueous solutions, their surfactant properties and complexing nature. Lignosulfonates are interesting from electrochemical point of view because they are negatively charged in a dissociated state, they have sulfonic groups which are the place of an ion exchange reaction between the hydrogen and the metal ion and they have quinone/hydroquinone redox couple [1-2] after initial electrooxidation. Due to the fact that lignosulfonates are a byproduct of paper production that are easily available, inexpensive material with interesting properties and also

environmentally friendly, it is worth to look for new possibilities of applying them in industry. In this report we demonstrate the preparation of selected transition metals lignosulfonates and the electrochemical properties of these complexes.

MATERIALS AND METHODS

Transition metals lignosulfonates were obtained by dissolving sodium lignosulfonates (LS-Na) technical powders in water, to a concentration of 50g/l. Next, the aqueous solution of sodium-lignosulfonates was passed slowly through a cationic ion-exchange bed where sodium ions are exchanged with hydrogen positively charged ions. This way we obtained an acidic form of lignosulfonates.



Then the eluate was used to obtain transition metal lignosulfonate complexes by reacting with an excess of freshly precipitated transition metal hydroxide. For this purpose, a portion of wet transition metal hydroxide was placed in solution of acidic form of lignosulfonate, and the overall volume of the reaction mixture was filled with water to twice the volume of the initial LS-Na solution. This ensured that the LS concentration in the final solution was 25mg/cm³. The dissolution process took place at room temperature (ca. 22°C) for 48 hours and for the whole time pH was controlled, until it reached a constant value. The unreacted hydroxide was removed by centrifuging. The final product was an aqueous solution of the respective transition metal lignosulfonate. In this way we obtained the following compounds: Mn(II)-lignosulfonate, Co(II)-lignosulfonate, Cu(II)-lignosulfonate and Ni(II)-lignosulfonate.



Finally the resulting solution was mixed with 1 M Na₂SO₄ to increase the ionic conductance.

The first stage of the electrochemical experiments that include the cyclic voltammetry, was performed in a conventional three-electrode cell powered by an Autolab electrochemical workstation (potentiostat/galvanostat,) controlled by a personal computer with NOVA software. The conventional three electrode system consisted of glassy carbon or gold disc electrode as a working electrode, platinum wire as a counter electrode and silver chloride electrode as reference electrode.

The second stage of the study included the determination of the optimal operating conditions of the Cu(II)-lignosulfonate and Ni(II)-lignosulfonate baths using electrolytic cell.

The Hull-cell is a type of electrolytic cell in a special trapezoidal container shape. This shape allows one to place the test panel on an angle of 29° to the anode. Consequently, the Hull-cell is a device that can be used to evaluate the plating characteristics on the cathode surface from a low-current to a high-current using a principle that the total current supplied from the anode to the cathode at a far distance regularly changes the current density. Accordingly, the Hull-cell pattern experiment can be used to observe the appearance of the deposited metal layer for a wide range of current densities [3].

RESULTS AND DISCUSSION

Before electrodeposition of lignosulfonate complexes or metals, the working electrodes (GC or Au electrodes) must be polished with alumina slurries of 1.0, 0.3, and 0.05 μm on a Buehler polishing cloth with distilled water as lubricant, rinsed with doubly distilled water, and sonicated in a water bath for 3 minutes. The electrodes was then electrochemically activated by cyclic voltammetry in a phosphate buffer (pH 7.4) between 0 and 1.2 V (15 scans at 100 mVs^{-1}).

Mn(II)-lignosulfonate and Co(II)-lignosulfonate were electrodeposited by anodic polymerisation on pre-activated glassy carbon electrode. After transferring the modified electrode to the appropriate electrolytes, the electrodes exhibited the electrochemical activity typical for manganese and cobalt at different oxidation states in neutral or basic electrolytes.

The redox activity of such modified electrode could be exploited for electrocatalytic applications. As demonstrated by obtained cyclic voltammetry plots (Fig. 1) the electrodeposited complex of Mn(II)-lignosulfonate exhibited reversible electrochemical transition due to a Mn(III)/Mn(II) and Mn(IV)/Mn(III) redox couples. The cyclic voltammetry curve of LS-Mn(II) modified electrode show four redox peaks (Fig. 1 – curve LS-Mn(II) without addition of H_2O_2). The first anodic peak at potential of 0,5 V is very broad, which can be attributed to the oxidation of manganese to Mn^{+3} . The second anodic peak at potential of 0,9 V can be attributed to the oxidation of Mn^{+3} to Mn^{+4} . The cathodic peak may be due to the reduction of MnO_2 to MnOOH at potential of 0,82 V, which is further reduced to Mn (II) at potential of 0,42 V. It also exhibited electrocatalytic activity leading to the oxidation of hydrogen peroxide in Na_2SO_4 solution. The figure 1 shows the curves obtained after successive additions of hydrogen peroxide A linear relationship was obtained in the concentration range of one milimole to five milimole.

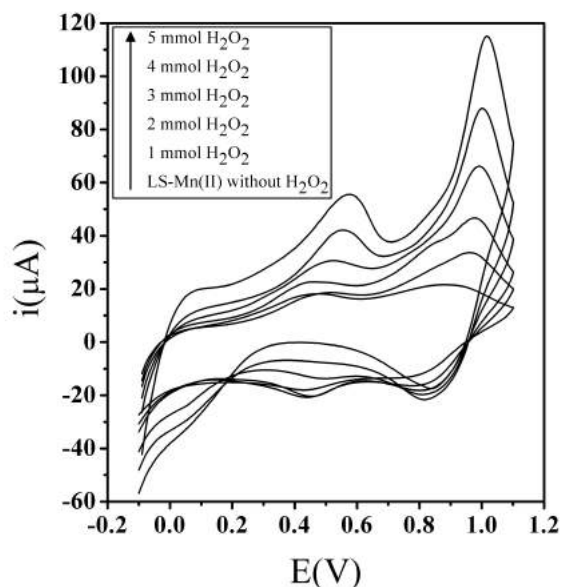


Fig. 1 Cyclic voltammograms of the stabilized (after 100 scans) LS-Mn(II) modified electrode in 0.1 M Na_2SO_4 for different H_2O_2 concentrations, at a 20 mV/s sweep rate. A voltammogram before H_2O_2 addition is also included for comparison.

Next the investigation of electrocatalytic oxidation of hydrogen peroxide was conducted with another method, more sensitive one, at constant potential. Chronoamperometry curves for the amperometric responses of LS-Mn(II) modified electrode to the successive addition of H_2O_2 in 0.1 M Na_2SO_4 solution at a constant potential of 0.65 V (versus Ag/AgCl) showed that the lowest concentration of hydrogen peroxide that modified electrode was able to determine was one micromole. A linear relationship was obtained in the concentration range of one micromole to one hundred twenty eight micromole. For comparison, the same test was carried out for unmodified electrode. We can observe sensibility increase for modified electrode. Similarly behaves the electrodeposited complex of Co(II)-lignosulfonate. We received a reversible redox couple of Co(II)/Co(III) and Co(III)/Co(IV), but at lower scan rate can be seen only one pair of peaks - Co(II)/Co(III). The anodic peak at potential of 0,33 V that comes from cobalt in an oxidation state of third and the cathodic peak from cobalt in an oxidation state of second at potential of 0,3 V. The electrocatalytic activity of such modified electrode leading to the oxidation of hydrogen peroxide but in alkaline solution (Fig. 2). The figure 2 shows the curves obtained after addition of hydrogen peroxide and for comparison curve for modified electrode without addition of hydrogen peroxide.

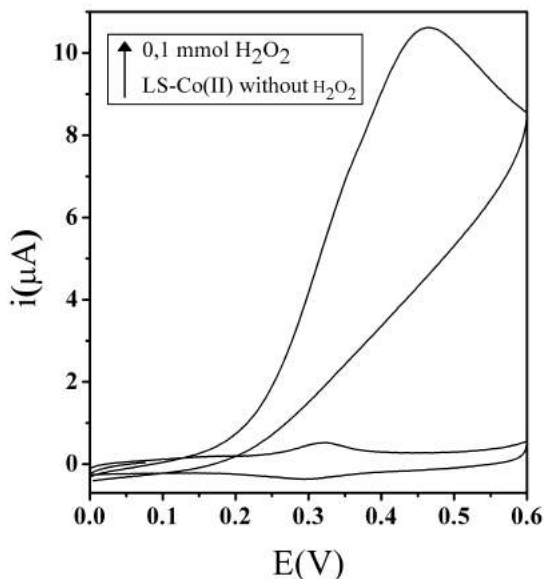


Fig. 2 Cyclic voltammograms of the stabilized (after 100 scans) LS-Co(II) modified electrode in 0.1 M NaOH for H₂O₂ concentrations, at a 20 mV/s sweep rate. A voltammogram before H₂O₂ addition is also included for comparison.

Chronoamperometry curves for the amperometric responses of LS-Co(II) modified electrode to the successive addition of H₂O₂ in 0.1 M NaOH solution at a constant potential of 0.35 V (versus Ag/AgCl) showed that the lowest concentration of hydrogen peroxide that modified electrode was able to determine was 0.5 micromole. A linear relationship was obtained in the concentration range of 0.5 micromole to 128 micromole. For comparison, the same test was carried out for unmodified electrode. We can observe sensibility increase for modified electrode.

Hydrogen peroxide (H₂O₂) is a commonly used strong oxidant and participates in a number of enzymatic reactions, and has an important role in many fields, such as food industry, pharmaceuticals, clinical control, industrial and environmental analysis. So the rapid, accurate and reliable detection of hydrogen peroxide is of great significance in these and many other fields. In the last years, many analytical methods for H₂O₂ detection have been developed including spectrometry, titration, fluorescence, chemiluminescence and chromatographic techniques. However, there are some disadvantages. They are usually expensive, time-consuming, and require professional personnel. Modified electrodes with the participation of the enzyme can accelerate the electron transfer between the electrode and H₂O₂ [5,6]. But the lack of stability and poor reproducibility, which originates from the intrinsic nature of enzymes,

i.e. easily damaged either thermally or chemically during biosensor fabrication and testing are the cause for searching a new non-enzymatic methods of H_2O_2 detection. The electrochemical method used in this research is characterized by high sensitivity, simple, accurate and fast detection, ease of operation and also low cost. Moreover Mn(II) lignosulfonate modified electrode appeared to be an effective electrocatalyst for the anodic oxidation of hydrogen peroxide in neutral electrolyte. Also Co(II) lignosulfonate modified electrode appeared to be an effective electrocatalyst for the anodic oxidation of hydrogen peroxide but in alkaline NaOH solution. Both of the modified electrodes can be used as electrochemical sensor of this compound but in another electrolyte.

Ni(II)- and Cu(II)-lignosulfonates were used to deposit bright layer of metals under cathodic conditions. But first the pre-activated electrodes was immersed in aqueous solution of M-LS (transition metal lignosulfonate) / Na_2SO_4 (in a conventional three-electrode cell) and the potential was scanned between the range that was selected on the basis of a series of preliminary experiments (for Cu(II)-lignosulfonates at potential range -0,2V to 1,0V and for Ni(II)-lignosulfonates at potential range 0,2 V to 0,7 V).

This way we obtained cyclic voltammetry graphs showing the potential at which the metal is deposited on an electrode surface and at which it gets dissolved. For LS-Cu(II) the anodic peak was at potential of 0.9 V. The anodic peak was due to the oxidation of Cu in an oxidation state of zero to Cu in an oxidation state of second. The cathodic peak was at potential of -0,1 and was due to the reduction of Cu in an oxidation state of second to Cu in an oxidation state of zero. Electrodeposition of nickel from solution occurs at potential of -0,3.

Copper electroplating from the Cu(II) lignosulfonate aqueous solution with addition of Na_2SO_4 and nickel electroplating from the Ni(II) lignosulfonate aqueous solution with addition of Na_2SO_4 and saccharin allowed to obtain a compact coating with a nice shine. Selected by the series of experiments, the optimum conditions for the deposition of nickel are: range of current density for electroplating 0,1 – 0,005 A/dm^2 , time – 20 min, mixing, addition of saccharin $3\text{g}/\text{dm}^3$ (the quantity of additive selected on the basis of literature data). The optimum conditions for the deposition of copper are: range of current density for electroplating 0,02 – 0,005 A/dm^2 , time – 7 min, mixing. The lower current density or to short work time makes it impossible to obtain compact layer. Operating at higher current densities has resulted in unacceptable edge burn, dendritic formation and break off, grain size and unacceptable values for surface roughness. Mixing allows using of higher current density, which is equivalent to an increase in the rate of deposition without the worrying about of deterioration of quality of the coating. It is possible to use a longer time of deposition if it

need to obtain a thicker coating. A shorter time (5 minutes for electrodeposition of copper) don't allow to obtain compact layer.

Research on the presented baths are still in progress. However, already at this stage it can be concluded that the non-toxic baths based on lignosulfonates can find applications. Constituents of former baths, such as cyanide, sulfuric acid or boric acid are strongly toxic. Finding a new alternative baths, allowing for the exclusion of these compounds significantly contributes to increase the ecological aspect of the electroplating processes. The compounds used in the project based on lignosulfonates, that are by-products of pulp and paper industry are also very inexpensive. Therefore they will reduce production costs.

REFERENCES

- [1] Milczarek G., Lignosulfonate-Modified Electrodes: Electrochemical Properties and Electrocatalysis of NADH Oxidation, *Langmuir*, 2009, 25 (17), 10345–10353
- [2] Ciszewski A., Śron K., Stepniak I., Milczarek G., Nickel (II) lignosulfonate as precursor for the deposition of nickelhydroxide nanoparticles on a glassy carbon electrode for oxidative electrocatalysis, *Electrochimica Acta*, 2014, 134, 355–362
- [3] Teeratananon M., Pruksathorn K., Damronglerd S., Dupuy F., Vergnes H., Fenouillet B., Duverneuil P., Experimental investigation of the current distribution in Mohler cell and Rotating Cylinder Hull cell, *ScienceAsia*, 2004, 30, 375-381
- [4] Gao P., Liu D., Facile synthesis of copper oxide nanostructures and their application in non-enzymatic hydrogen peroxide sensing, *Sensors and Actuators B: Chemical*, 2015, 208, 346–354
- [5] Yang S., Lia G., Wang G., Zhao J., Hu M., Qu L., A novel nonenzymatic H₂O₂ sensor based on cobalt hexacyanoferrate nanoparticles and graphene composite modified electrode, *Sensors and Actuators B: Chemical*, 2015, 208, 593–599

Influence of kind of sugars on selenium enrichment in baker's yeast

*Beata Szulc-Musioł¹, Barbara Dolińska¹, Florian Ryszka²

¹Department of Applied Pharmacy, School of Pharmacy and the Division of Laboratory Medicine, Medical University of Silesia, POLAND

²Pharmaceutical Research and Production Plant "Biochefa", Sosnowiec, POLAND

e-mail: szulc.beata@interia.pl

Keywords: *baker's yeast, selenium enrichment, incubation conditions*

ABSTRACT

Baker's yeast enriched by selenium can be used as a supplement of biologically available mineral in human and animal nutrition. The aim of the study was to influence of incubation condition on selenium enrichment in baker's yeast. Shake flask experiments were conducted to optimize the cultivation conditions. The cultures were incubated for 60 minutes in a shaker incubator and different carbon sources (glucose, sucrose, fructose, lactose, maltose) were used in the studies. The statistical analysis showed a significant ($p < 0.001$) effect of kind of sugar and selenium concentration in the yeast-culture medium upon selenium incorporation into the yeast cells. We also found that glucose is the best carbon source which facilitates the high selenium incorporation into yeast cells.

INTRODUCTION

Selenium is an essential trace element and a key component of several enzymes involved in antioxidant defense and metabolism [1-3]. Selenium supplementation may prevent various diseases and also alleviate other pathological conditions including oxidative stress and inflammation [4-9]. Supply of the selenium enriched food, especially, selenium enriched biomass with organic forms of this microelement is one efficient way to overcome selenium deficiency. Organic selenium complexes and seleno-amino acids are considered to be much more bioavailable and effective form of selenium than selenite and selenite selenium [10,11].

Baker's yeast is capable of accumulating large amounts of selenium under appropriate conditions and incorporating it into organic compounds. Selenomethionine was identified as the major selenium-containing compound in the protein fraction whole cells of the yeast [12].

Obtaining yeast biomass containing organic selenium is continuation of research on finding a method of dietary supplementation with selenium [13-17]. The aim of the study was to establish influence

of various carbon sources (glucose, sucrose, fructose, lactose, maltose) and selenium concentration in the yeast-culture medium upon selenium incorporation in the yeast cells.

MATERIALS AND METHODS

Chemicals

Fresh *Saccharomyces cerevisiae* baking yeast, light beige-colour and a solid consistency. The content of the dry mass was 33% (Lesaffre Bio-Corporation, Wołczyn, Poland). Anhydrous glucose, sucrose, fructose, lactose, maltose were purchased from Avantor Performance Materials Poland S.A. All the reagent were of analytical grade or higher purity. Milli-Q system (Millipore) system was used to obtain the water used in the experiment.

Experimental procedure

Crumbled yeast (15g of fresh, 5g of dry mass) was added to 50 ml of aqueous sugar solutions of concentrations of 2% and stirred up for 10 minutes, using a magnetic stirrer. Then, selenium solution in the form of sodium selenite was added, until the respective concentrations were 0.2, 0.4, and 0.6 mM. The whole mixture was again stirred up carefully, until a homogenous suspension was obtained. The yeast was grown for 60 minutes in a rotary shaker at 120 rpm, at the frequency of 120 cycles per minute and the temperature 30°C. Following the incubation the samples were harvested by centrifugation at 10,000g for 10min. The biomass obtained was twice suspended in 100 ml de-ionized water, stirred up for about 5 minutes, and then centrifuged again. The obtained wet sediment was initially dried at the temperature of 60°C for 2 hours. Next, the process of drying up was continued at 105°C, until the solid mass was obtained.

Selenium Assay Procedure

The samples were harvested by centrifugation at 10,000g for 10min. The biomass obtained was carefully washed several times to remove the extracellular selenium and dried at 105°C for 16h. The content of selenium in the yeast was determined by the fluorometric method according to Watkinson, as previously described [18]. Briefly, 500 mg of dried yeast sample was mineralized in 60% perchloric acid solution by means of repeated heating of samples for 15min at 100°C and for 30 min at 150°C. Proper mineralization occurred at 190°C after 1.5h. The excess perchloric acid was removed by heating the sample at 210°C for 45min. Selenium was measured with a spectrofluorometer LS-30 (Perkin-Elmer) as complex with 2,3-diaminonaphthalene. Excitation and emission wavelengths were 356 and 520

nm, respectively. The results were expressed in $\mu\text{g Se}^{+4}$ per one gram of the dry yeast biomass.

Statistical analysis

The achieved results were represented as the mean of five experiments (x). Standard deviation (SD) was calculated. The statistical significance of the differences between the means was analyzed using Kruskal-Wallis test. A level of $p \leq 0.05$ was adopted to indicate statistical significance.

Total process efficiency of the obtained yeast biomass was calculated according to the following formula:

$$\begin{aligned} \text{Total process efficiency [\%]} &= \frac{\text{content selenium in culture medium}[\mu\text{g}]}{\text{the amount of built – in selenium in } \left[\frac{\mu\text{g}}{\text{g}} \right] \text{ of dry biomass}} \\ &* 100\% \end{aligned}$$

RESULTS AND DISCUSSION

Baker's yeast are the source of the protein containing endogenous amino acids and enzymes, B vitamins and many other valuable biologically active compounds. Unfortunately, they are not a good source of minerals.

Saccharomyces cerevisiae show capability for binding the elements present in the environment often in the amounts considerably exceeding their physiological demand. Metal ions adsorbed on the cell's surface may next be a subject of intracellular bioaccumulation. This way yeasts produce metal-protein complexes called bioplexes.

Depending on the incubation conditions of baker's yeast it can accumulate copper, iron, manganese, selenium, chromium, zinc and iodine compounds [14-16,21-23]

In previous studies on yeast *Saccharomyces cerevisiae* it was demonstrated that sugar concentration in growth medium significantly influenced the biomass yield [14]. When using the lower sugar content (2%), the biomass was obtained with the efficiency of 93.5%. When the culture medium contained 4.7% sugar, the biomass yield was 25% lower than in the case of culture containing smaller amount of it.

The yeast content in the culture medium also significantly influences the biomass yield [14]. When the yeast content was amounting to 6% the yeast biomass efficiency was 90.73%. When the yeast content was higher i.e. 12%,

the biomass yield was 22% lower. Lower yeast and sugar content in the culture medium is also advantageous due to eliminating the problem of residue neutralization and easier drying process of the final product.

In the present work, yeast *Saccharomyces cerevisiae* was incubated in medium culture with different types of sugar (glucose, sucrose, fructose, lactose, maltose) and with inorganic form of selenium i.e. as sodium selenite at various selenium concentration (namely 0.1, 0.4, 0.6 mM selenium) at 30°C for 60 min.

Carbon source is the major nutrient which contributes to multiplication of yeast cells. Its application in the incubation medium of various sugars was to examine the effect of complexing agents on the process of selenium accumulation by living yeast.

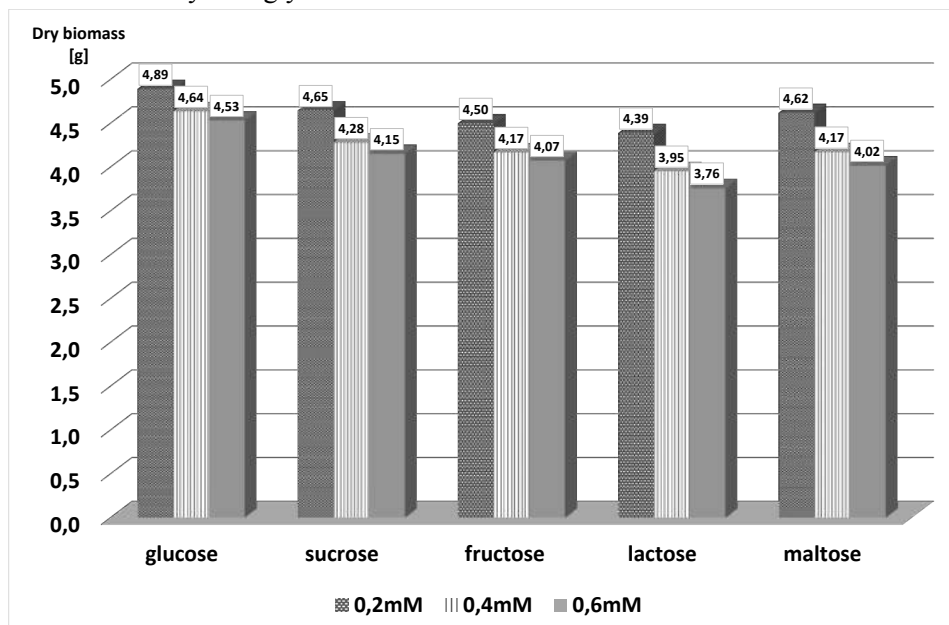


Fig. 1 Influence of kind of sugar and selenium concentration on yeast biomass production

Figure 1 presents influence of kind of sugar and selenium concentration on yeast biomass production. On the basis of the obtained results it could be concluded that the kind of sugar in the yeast growth medium have a significant ($p < 0.01$) influence on the yeast dry biomass yield. The dry biomass was obtained with varying yield from 75.08% to 97.80% (table 1).

Table 1 The influence of incubation conditions on the process of selenium-enriched yeast production

Variant	Selenium concentration [mM]	Kind of sugar	Biomass yield [%]	Total selenium accumulation [ug/g of dry biomass]	The amount of built-in selenium in [ug/g of dry biomass]	Selenium built-in [%]	Total content of selenium in the product [ug]	Total process efficiency [%]
1	0.2	Glucose	97,80	239,47	213,89	89,32	1045,92	66,20
2	0.2	Sucrose	92,90	141,45	120,96	85,51	561,86	35,56
3	0.2	Fructose	89,97	117,85	101,77	86,36	457,78	28,97
4	0.2	Lactose	87,73	47,60	38,24	80,34	167,75	10,62
5	0.2	Maltose	92,33	171,41	152,10	88,73	702,22	44,44
6	0.4	Glucose	92,56	310,22	291,83	94,07	1352,65	42,81
7	0.4	Sucrose	85,60	224,57	199,67	88,91	854,24	27,03
8	0.4	Fructose	83,32	211,47	181,45	85,80	756,05	23,93
9	0.4	Lactose	79,04	72,48	64,11	88,45	253,34	8,02
10	0.4	Maltose	83,40	261,23	238,14	91,16	993,06	31,43
11	0.6	Glucose	90,04	478,88	439,93	91,87	1993,61	42,06
12	0.6	Sucrose	82,68	362,58	322,86	89,05	1340,40	28,28
13	0.6	Fructose	81,48	341,40	302,64	88,65	1232,77	26,01
14	0.6	Lactose	75,08	209,24	176,76	84,48	664,33	14,02
15	0.6	Maltose	80,12	411,81	368,05	89,37	1478,94	31,20

The glucose carbon in the medium culture yields the highest yeast biomass which was significantly ($p < 0.05$) higher 5.0 to 23.1% compared with the other sources tested. Maximum yeast biomass (4.89 g) was obtained in variant 1, with the glucose concentration of 2%, the incubation temperature at 30°C and selenium concentration in medium of 0.2mM. Under these conditions the highest other sources tested. Maximum yeast biomass (4.89 g) was obtained in variant 1, with the glucose concentration of 2%, the incubation temperature at 30°C and selenium concentration in medium of 0.2mM. Under these conditions the highest total process efficiency, which amounted 66.2%. Numerous studies have confirmed that glucose is preferred in fermentation metabolism [11, 12].

Yields of biomass obtained from these culture mediums containing lactose were lower than amounts produced from mediums containing other sugars.

The carbon sources that supported yeast biomass production followed such order: glucose < sucrose < maltose < fructose < lactose, respectively. Decrease in yeast biomass was dose-dependent with increasing selenium concentration in culture medium.

The effect of incubation conditions upon the process of selenium incorporation into the *Saccharomyces Cerevisiae* yeast is shown in Table 1. In the process of intracellular accumulation depending on the culture conditions, selenium may be organically bound and/or reduced to elementary selenium which gives a reddish color to the yeast cells. Color of the yeast biomass grown in the media in all samples was drab which indicated that elemental selenium accumulated in the biomass was of low level.

The type of sugar and the concentration of selenium in the growth medium significantly influences ($p < 0.001$) the selenium content in baker's yeast cells. The greatest selenium contents in the dried bioplex (439.93ug / g dry weight) was obtained in variant 11 and is approx. 11.5 times more than the content of selenium in the variant 4. However, the highest total process efficiency (66.2%) was found in variant 1.

Cells did not absorb all ions present in the culture medium, even in the case of their low concentration. Accumulation of metal ions depends probably on intracellular transportation systems and on their chelating strength, by medium compounds and cellular substances [22].

Based on the obtained results it can be assumed that consumption of selenium by yeast probably occurs non-specific accumulation associated with the transport of selenium ions complexed with an assimilable substrate. This effect of complexing agents was particularly pronounced in the case of glucose and lactose.

CONCLUSION

In this study we optimized the culture medium for production of yeast enriched with high selenium content. Using different kind of sugars and selenium concentration in medium culture results in incorporation of selenium into the yeast cells in the range of 38.24–439.93 µg/g of dry biomass.

Concentration of selenium and kind of sugar in the medium culture play an important role in the process of selenium bioaccumulation.

We also found that glucose is a good and simple carbon source which facilitates high selenium incorporation into yeast cells.

REFERENCES

1. Papp L.V., Lu. J., Holmgren A., Khanna K.K., From selenium to selenoproteins: synthesis, identity, and their role in human health, *Antioxid. Redox Signal.*, 2007, 9, 7, 775-805 DOI: 10.1089/ars.2007.1528
2. Weekley C.M., Harris H.H., Which form is that? The importance of selenium speciation and metabolism in the prevention and treatment of disease, *Chem. Soc. Rev.*, 2013, 42, 23, 8870-8894 Doi: 10.1039/c3cs60272a. Epub 2013 Sep 13
3. Selenius M., Rundlof A.K., Olm E., Fernandes A.P., Bjornstedt M., Selenium and the selenoprotein thioredoxin reductase in the prevention, treatment and diagnostics of cancer, *Antioxid. Redox. Signal.*, 2010,12, 867–880 Doi: 10.1089/ars.2009.2884
4. Björnstedt M, Fernandes A.P., Selenium in the prevention of human cancers, *EPMA J.* 2010, 1, 3, 389-395 Doi: 10.1007/s13167-010-0033-2. Epub 2010 Jun 29
5. Sinha R., Sinha I., Facompre N., Russell S., Somiari R.I., Richie J.P. Jr, El-Bayoumy K., Selenium-responsive proteins in the sera of selenium-enriched yeast-supplemented healthy African American and Caucasian men, *Cancer Epidemiol. Biomarkers Prev.*, 2010, 9, 9, 2332-2340 Doi: 10.1158/1055-9965.EPI-10-0253. Epub 2010 Jul 19
6. Ravn-Haren G., Bügel S., Krath B.N., Hoac T., Stagsted J., Jørgensen K., Bresson J.R., Larsen E.H., Dragsted L.O., A short-term intervention trial with selenate, selenium-enriched yeast and selenium-enriched milk: effects on oxidative defence regulation, *Br. J. Nutr.*, 2008, 99, 4, 883-892 Doi: 10.1017/S0007114507825153
7. Bjelakovic G., Nikolova D., Simonetti R.G., Gluud C., Antioxidant supplements for preventing gastrointestinal cancers, *Cochrane Database Syst. Rev.*, 2008, 16, 3, CD004183 Doi: 10.1002/14651858.CD004183.pub3.
8. Boosalis M.G., The role selenium in chronic disease, *Nutr. Clin. Pract.*, 2008, 23,2, 152-160 Doi: 10.1177/0884533608314532.

9. Facompre N., El-Bayoumy K., Potential stages for prostate cancer prevention with selenium: implications for cancer survivors, *Cancer Res.*, 2009, 69, 7, 2699-26703 DOI: 10.1158/0008-5472.CAN-08-4359
10. Fairweather-Tait S.J., Collings R., Hurst R., Selenium bioavailability: current knowledge and future research requirements, *Am. J. Clin. Nutr.*, 2010, 91, 5, 1484-1491 Doi: 10.3945/ajcn.2010.28674J. Epub 2010 Mar 3.
11. Suhajda A., Hegóczy J., Janzó B., Pais I., Vereczkey G., Preparation of selenium yeasts. Preparation of selenium-enriched *Saccharomyces cerevisiae*, *Trace Elem. Med. Biol.*, 2000, 14,1, 43-47
12. Ponce de León C.A., Bayón M.M., Paquin C., Caruso J.A., Selenium incorporation into *Saccharomyces cerevisiae* cells: a study of different incorporation methods, *J. Appl. Microbiol.*, 2002, 92,4, 602-610
13. Dobrzański Z., Dolińska B., Górecka H., Bodak E., Ryszka F., The chemical composition of dietary yeast enriched with selenium, chromium, and zinc, *Folia Vet.*, 2002, 46, 2, 36-37
14. Dobrzański Z., Ryszka F., Górecka H., Dolińska B., Opaliński S., The dietary yeast enriched with the bioelements waste-free technology production, *Pol.J.Chem.Technol.*, 2004, 6, 4, 10-14
15. Dolińska B., Ryszka F., Dobrzański Z., Optimization of processes of incubation of yeasts *Saccharomyces cerevisiae* enriched with microelements, *Chemistry and biochemistry in the agricultural production, environment protection, human and animal health, Prague : Czech-Pol. Trade, 2006*
16. Ryszka F., Dobrzański Z., Dolińska B., Optimization of the process of selenium, chromium and zinc incorporation into yeast *Saccharomyces cerevisiae*, *Chemical products in agriculture and environment, Prague : Czech-Pol Trade, 2002*
17. Szulc-Musioł B., Danch A., Selenium incorporation into the *Saccharomyces cerevisiae* cells: waste -free technology production, *Pierwiastki, środowisko i życie człowieka, 2009, 324-329*
18. Danch A., Drózdź M., Uproszczona metoda fluorymetrycznego oznaczania selenu w materiale biologicznym, *Diagn. Lab.*, 1996, 32, 529-534
19. Dolińska B., Chojnacka K., Dobrzański Z., Górecki H., Ryszka F., Wzbogacenie drożdży *Saccharomyces cerevisiae* w miedź, żelazo i mangan, Enrichment of copper, iron and manganese in *Saccharomyces cerevisiae* yeast, *Przemysł Chemiczny, 2009, 88, , 162-166*
20. Ryszka F., Dolińska B., Zieliński M., Chyra D., Dobrzański Z., Permeation of iodide from iodine-enriched yeast through porcine intestine, *Acta Biochim. Pol.*, 2013, 60, 4, 737-739 on-line at: www.actabp.pl
21. Dolińska B., Zieliński M., Opaliński S., Korczyński M., Dobrzański Z., Ryszka F., Optimization of the conditions of iodine incorporation to *Saccharomyces cerevisiae* yeast, *Przemysł Chemiczny, 2011, 90, 5, 731-736*

22. Tuszyński T., Pasternakiewicz A., Bioaccumulation of metal ions by yeast cells of *Saccharomyces cerevisiae*, *Pol. J. Food Nutr. Sci.* 2000, 9(50), 31-39

Using hydrogen to recycle neodymium magnets

*Mateusz Szymanski¹, Bartosz Michalski¹, Marcin Leonowicz¹, Zbigniew Miazga²

¹Faculty of Materials Science and Engineering, Warsaw University of Technology, Warsaw, POLAND

²P.P.H.U. POLBLUME Zbigniew Miazga, Piaseczno, POLAND

e-mail: m.szymanski@inmat.pw.edu.pl

Keywords: HDDR, recycling, magnets

ABSTRACT

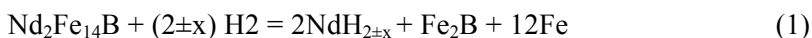
To deal with an increasing demand for raw materials a prospective procedure of recycling scrap Nd-Fe-B magnets was investigated. Hydrogen Decrepitation (HD) and the HDDR (Hydrogenation, Disproportionation, Desorption and Recombination) were applied to magnets in order to remove nickel coating and improve magnetic properties, respectively. Chemical composition (MS), microstructure (SEM), phase constitution (XRD) and magnetic properties (VSM) were analyzed to investigate processing progress. Coercive powder with $(BH)_{\max}$ around 60 kJ/m^3 was produced as a result of hydrogen treatment. A new bonded magnet was fabricated using nylon resin.

INTRODUCTION

Unusual technological development and increasing demand for raw materials are observed in last decades. Electronic equipment is widely used in both industrial and domestic appliances. Increasing amount of electronic waste becomes a potential source of resources. High-tech instruments contain valuable materials, like noble metals and rare earth elements, which are very desired [1]. Access to the rare earth deposits might be an important issue for countries, which want to develop high-tech industry. The Rare Earth Elements have been recognized by the US and Europe as a critical ones [2], which means they are very important for the industry. The waste of electrical and electronic equipment could be an important source of that metals. Particularly, Nd-Fe-B magnets are considered to be valuable for recovery, because their chemical composition is based on the rare earth elements [3]. Magnets are widely used in hard disc drives and other devices. Moreover, a need for high-energy permanent magnets is boosted by development of green energy technologies, such as wind turbines or electric cars [4].

MATERIALS AND METHODS

Neodymium magnets from different hard disc drives were studied. Chemical composition of 3 randomly chosen magnets is presented in Fig. 1. Hydrogen Decreptation (HD) was applied in order to obtain powder from magnets. Then, magnets were subjected to HDDR (Hydrogenation, Disproportionation, Desorption and Recombination), which is based on reaction Eq. (1):



This transformation occurs reversibly in the temperature range of 700-900°C under hydrogen pressure. During first stage the $\text{Nd}_2\text{Fe}_{14}\text{B}$ phase absorbs hydrogen and disproportionates into neodymium hydride, iron boride and iron. In the second stage hydrogen is evacuated from the processing chamber. Accumulated hydrogen is desorbed from the material and the recombination starts. All the three compounds ($\text{NdH}_{2\pm x}$, Fe_2B and Fe) react with each other to form the $\text{Nd}_2\text{Fe}_{14}\text{B}$ phase again. However, the recombined $\text{Nd}_2\text{Fe}_{14}\text{B}$ phase has much more smaller grain, then it had before the HDDR. In the end, powder is bonded with polymer to obtain new magnet.

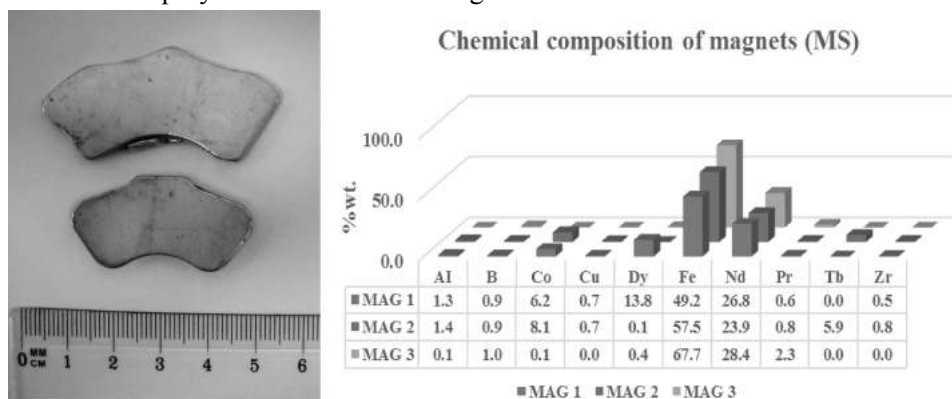


Fig. 1 Magnets – appearance and chemical composition.

RESULTS AND DISCUSSION

Powder obtained after HD and its size distribution are presented in Fig. 2. It was possible to separate nickel coating out of magnets. One could see wide distribution of particles size. Moreover, high amount of large particles can be observed. This is mostly correlated with residuals of Ni coating. However, it was also possible to distinguish large volumes of magnets, which did not undergoes decreptation and remained untouched. It is probably due to conditions of hydrogen treatment – diffusion of hydrogen might be harder in corners of magnets.

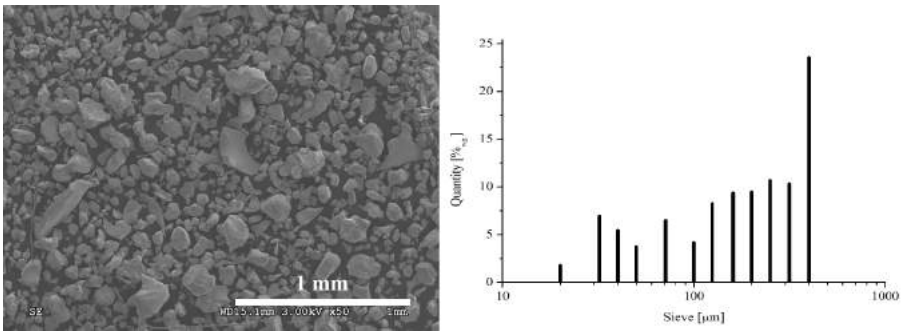


Fig. 2 Powder obtained after HD and its size distribution.

Subsequently, material was subjected to HDDR process. Structure transformation might be notice in fig. 3. One could see lamellar microstructure which is a mixture of $\text{NdH}_{2\pm x}$, Fe_2B and Fe. This results are very similar to [5]. During recombination stage submicron grains of $\text{Nd}_2\text{Fe}_{14}\text{B}$ phase was recovered (Fig. 4a), but with much more smaller grain then in initial state (Fig. 4b).

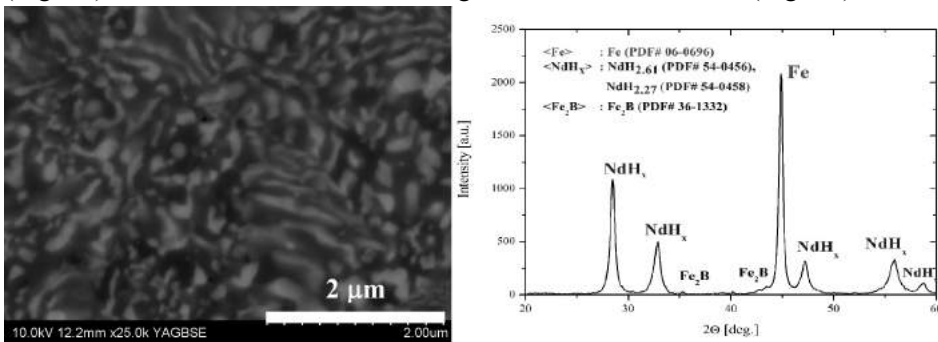


Fig. 3 Disproportionated structure obtained in bulk piece of material.

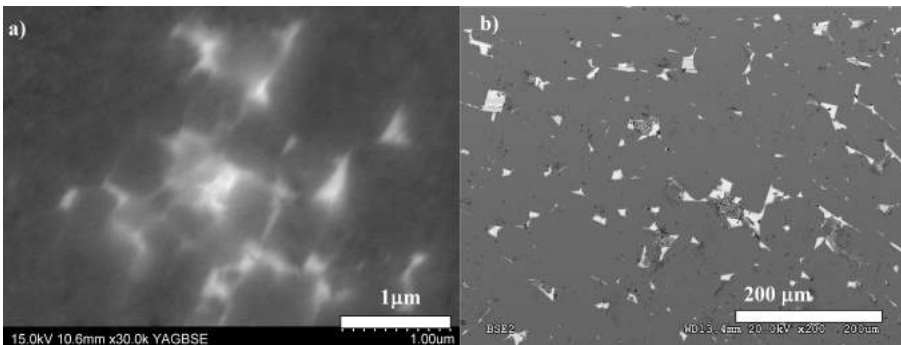


Fig. 4 Recombined structure with submicron grains – a, initial microstructure of model alloy – b. Both structures obtained in bulk piece of material.

Magnetic properties of powder after the HDDR are shown in Fig. 5. Almost 60 kJ/m^3 of maximum energy product $(BH)_{\max}$ was achieved. These results are comparable, but slightly lower than studies presented in [6]. It is due to different chemical composition of processed magnets and modifications of hydrogen treatment. On the other hand, obtained product has similar properties as commercial bonded magnets [7], which indicates, that it is potentially possible to use this powder for manufacturing of new magnets. For this reason a new resin bonded magnet was fabricated using nylon resin (Fig. 6).

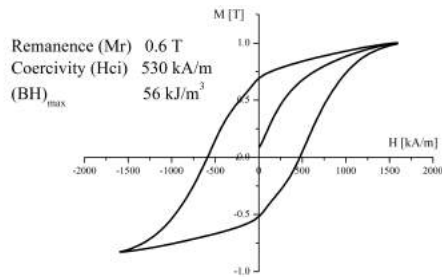


Fig. 5 Hysteresis loop for recombined powder.

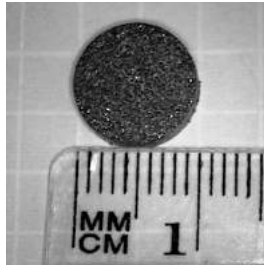


Fig. 6 Recycled resin bonded magnet.

ACKNOWLEDGEMENTS

The research was supported by the The National Centre for Research and Development within agreement no. INNOTECH-K2/IN2/18/181960/NCBR/13.

REFERENCES

- [1] Schluep M., Hagelueken Ch., Kuehr R., Magalini F., Maurer C., Meskers Ch., Mueller E., Wang F., Recycling From E-Waste To Resources - United Nations Environment Programme, *Oktoberdruck AG Berlin*, 2009.
- [2] http://ec.europa.eu/enterprise/policies/raw-materials/files/docs/crm-report-on-critical-raw-materials_en.pdf (access 30.01.2015).
- [3] <http://erean.eu/wordpress/additives-in-ndfeb-magnets> (access 30.01.2015)

- [4] Binnemans K., Jones P.T., Blanpain B., Gerven T.V., Yang Y., Walton A., Buchert M., Recycling of Rare Earths: a Critical Review, *Journal of Cleaner Production*, 2013, 51, 1-22 DOI 10.1016/j.jclepro.2012.12.037
- [5] Gutfleisch O., Controlling the properties of high energy density permanent magnetic materials by different processing routes, *Journal of Physics D: Applied Physics*, 2000, 33, 17, R157 DOI:10.1088/0022-3727/33/17/201
- [6] Sheridan R.S., Williams A.J., Harris I.R., Walton A., *Journal of Magnetism and Magnetic Materials*, 2014, 350, 114 DOI:10.1016/j.jmmm.2013.09.042
- [7] <http://www.magnesy.pl/magnesy-neodymowe-wiazane> (access 27.01.2015)

Influence of direct crystallization process on the bioactivity of silicate-phosphate glasses from $\text{KCaPO}_4\text{-SiO}_2$ system

*Aleksandra Wajda, Katarzyna Bułat, Maciej Sitarz

Akademia Górniczo-Hutnicza im. Stanisława Staszica w Krakowie,

Wydział Inżynierii Materiałowej i Ceramiki,

Al. Mickiewicza 30, 30-059 Kraków

*e-mail: olawajda@agh.edu.pl

Keywords: *silicate-phosphate glasses, direct crystallization, bioactivity, glass-crystalline materials*

ABSTRACT

Silicate-phosphate glasses from $\text{KCaPO}_4\text{-SiO}_2$ system are bioactive materials, which are capable of forming direct bonds with living tissue. An ideal biomaterial should be also biomechanically compatible with tissue. Application of glasses as biomaterials is limited mainly due to their very low strength and chemical stability. One of the best ways to improve the mechanical properties of the glasses is to change their chemical composition (for example, the introduction of Al^{3+} or B^{3+} ions) or to carry out their partial devitrification that allows to obtain glass-crystalline materials. This process needs to be highly controlled, because the appearance and growth of the crystalline phase may result in loss of the bioactivity. In order to fully control the direct crystallization process properly, it is necessary to know the structure and microstructure of the glassy precursor.

The subject of this paper are silicate-phosphate glasses from $\text{KCaPO}_4\text{-SiO}_2$ and $\text{KCaPO}_4\text{-SiO}_2\text{-AlPO}_4$ systems. Microscopic investigation showed that liquation takes place in all the studied glasses and it is thought that the boundaries of separated phases may be a barrier limiting the growth of crystalline phases. It has been found that aluminium has a homogenising effect on the texture of silico – phosphate glasses and causes the inversion of the composition of the matrix and the inclusions. The parameters for direct crystallization process were adjusted on the basis of thermal measurements (DTA) performed on selected glasses. XRD method was used to study the structure of obtained glass-crystalline materials. In order to verify their bioactivity, the in vitro tests were done in simulated body fluid and the samples were analyzed on a scanning electron microscope (SEM+EDX) and Raman spectroscopy.

Obtained results suggest that a properly controlled devitrification of the tested bioglasses may lead to the production of bioactive glass-crystalline materials.

INTRODUCION

Bioactive glasses have been used in medicine for 40 years as bones and teeth roots implants. Unlike metals, carbons, polymers or oxides, which are biologically inert, bioactive glasses have a capability to modify their surface by creating a biologically active films of hydroxyapatite (Hap). Such Hap films can form natural connection between living bone tissues and implants [1-6]. The use of bioactive glass in implants production allows to take advantage of specific properties of the glassy state (e.g. ability to obtain practically any shape, ability to control properties by adequate choice of chemical composition, possibility to apply various processing methods as well as isotropic properties). The main disadvantages of these materials are their minimal mechanical strength, fragility and low chemical stability that limit its practical applications for implants exposed to high mechanical loads. Increase of mechanical strength and reduction of glasses solubility can be achieved by the introduction of Al^{3+} in to their structure, however it can inhibit bone bonding on bioactive glasses [7, 8]. Another way to improve the toughness of glasses is to carry out their partial devitrification (direct crystallization) to obtain glass-crystalline materials. Such materials combine advantages of glassy and crystalline states (higher mechanical strength than glassy precursors, isotropic properties). However, uncontrolled crystallization and unrestricted growth of crystalline phase can lead to the loss of the glass bioactivity and may convert bioactive glass into inert material [9]. Hence, it is necessary to know structure, texture and thermal properties of the glassy precursor in order to have full control over this process [10, 11].

EXPERIMENTAL

3K from the $KCaPO_4-SiO_2$ system and 3AlK from the $KCaPO_4-SiO_2-AlPO_4$ were chosen to be researched. Table 1 presents compositions of the selected glasses. The glasses were obtained by sol-gel method in order to ensure the highest possible homogeneity. TEOS (SiO_2), H_3PO_4 (P_2O_5), K_2HPO_4 (K_2O), $Ca(NO_3)_2 \cdot 4H_2O$ (CaO), $Al(NO_3)_3 \cdot 9H_2O$ (Al_2O_3) were used to introduce particular oxides. All of obtained gels were dried at room temperature for 30 days and then the temperature was increased to $60^\circ C$ (7days). The dried gels were melted in platinum crucible at $1700^\circ C$ and rapidly cooled. The gels were heated with $5^\circ C$ heating speed till $1700^\circ C$ and then stabilized in the same temperature for 2 hours.

Obtained glasses have not been transparent. This may indicate that liquation phenomenon has taken place or the materials have not been completely amorphous.

The X-ray measurements were carried out using a X'Pert Pro Philips with a step of 0.01° and collecting time 5s.

In order to analyse the glasses thermal stability differential scanning calorimetry (DSC) measurements were performed on Netzch STA 449 F1 Jupiter, operating in the heat flux DSC mode. The samples were heated in platinum crucibles at a rate of 10°C/min up to 1100°C, in dry nitrogen atmosphere.

The gradient method was used to perform the direct crystallization process. The samples were heated in a gradient furnace for 2h at the temperature determined on the basis of DSC analysis. Obtained samples were analysed once again by XRD method to define their crystallinity.

The glasses and heated materials were soaked in a simulated body fluid (SBF) at 37°C for 30 days (SBF was changed every 5 days).

The morphology and composition of the samples were investigated with scanning electron microscope (SEM) NOVA NANO SEM 200 with a microprobe analyzer LINK ISIS (Oxford Instrument).

Modification of the surface of the soaked glasses were also investigated using Raman Spectroscopy using Horriba Yvon Jobin LabRAM HR micro-Raman spectrometer equipped with a CCD detector. Excitation wavelength of 532 nm was used and beam intensity was about 15 mW and acquisition time was set at 2300 s.

Table 1. Composition of obtained glasses [% mol.].

Series K	KCaPO ₄ -SiO ₂ system	Series AIK	KCaPO ₄ -SiO ₂ - AlPO ₄ system
3K	70% SiO ₂ · 30% KCaPO ₄	3AIK	70% SiO ₂ · 25% KCaPO ₄ · 5% AlPO ₄

RESULTS AND DISCUSSION

As it was already stated the glasses have not been transparent so, to confirm the amorphous nature of the samples, XRD (X-ray Diffraction) was carried out. Absence of any reflections in the X-ray diffraction patterns is the evidence of amorphous state (Fig. 1).

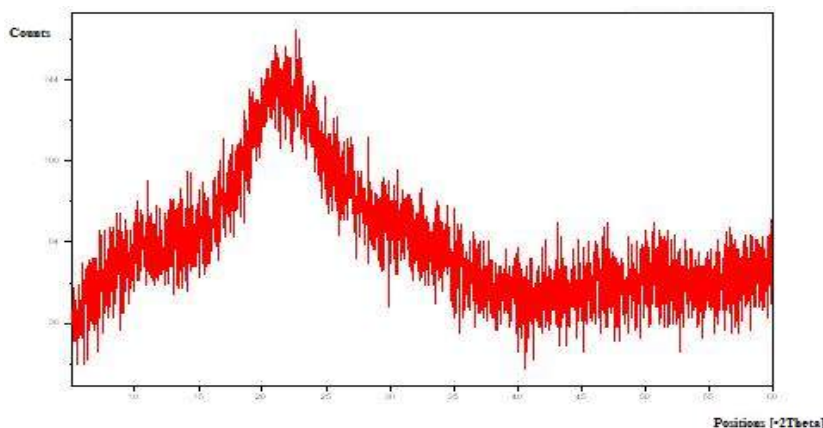


Fig. 1 XRD of the glass sample.

Our previous work [12] proves that in 3K and 3AlK glasses liquation phenomenon (phase separation) takes place – glassy spherical droplets (inclusions) in glassy matrix. The glass from $\text{KCaPO}_4\text{-SiO}_2$ has small statistically distributed inclusions but addition of Al^{3+} causes structure homogenization. The inclusions are bigger and it is smaller amount of them to compare with the 3K sample.

In the 3K glass the inclusions are mainly silico-calcium phase, while the matrix is enriched in potassium, calcium and phosphorus. The glass from $\text{KCaPO}_4\text{-SiO}_2\text{-AlPO}_4$ system has completely changed composition in the matrix and inclusions. The matrix is pure alumino-silicate phase and inclusions are silico-phosphate phase. In comparison to the glass without Al ions, the matrix and inclusion phase composition of the sample with Al ions is inverted [12].

Figure 2 presents SEM image, EDX spectra and Raman spectra of the glasses thermostating in SBF. It can be determined that both of them are bioactive. On their surface one can observe characteristic “shell” with chemical composition suggesting that it may be a layer of hydroxyapatite phase. This can be confirmed by the Raman spectra, as there are visible characteristic band for Hap [13].

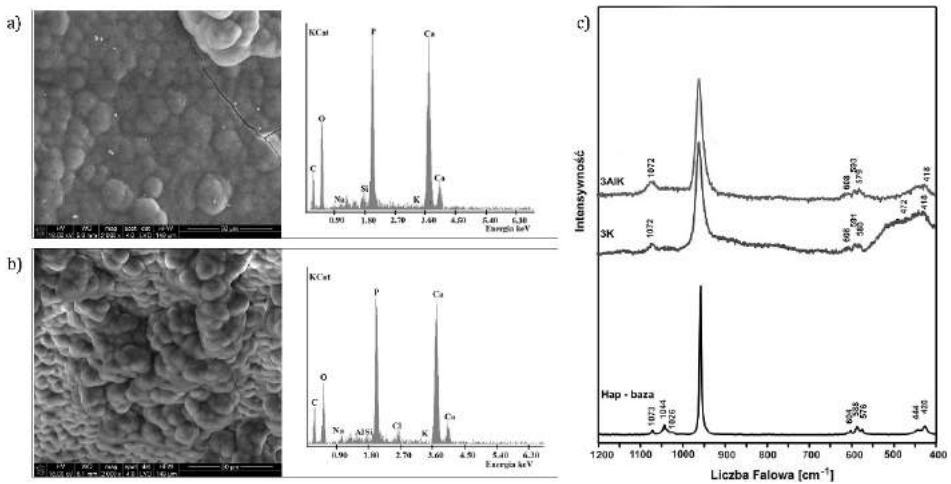


Fig. 2 SEM microphotographs and EDX spectra of the glasses after termostating in SBF: a) 3K, b) 3AlK, c) Raman spectroscopy spectra of the termostated glasses.

To design direct crystallization process it is necessary to examine the characteristic temperatures for the glassy state. Due to this fact DSC was made. Figure 3 presents DSC curves of 3K and 3AlK glasses. The crystallization process of 3K glass runs in two stages. This is evidenced by two separated exothermal peaks at 1033°C and 1059°C. Probably the matrix and inclusion crystallize separately. The DCS curve of 3AlK glass has only one peak. In this case crystallization runs in one stage. This may be due to homogenizing effect of Al^{3+} on the glass structure [14].

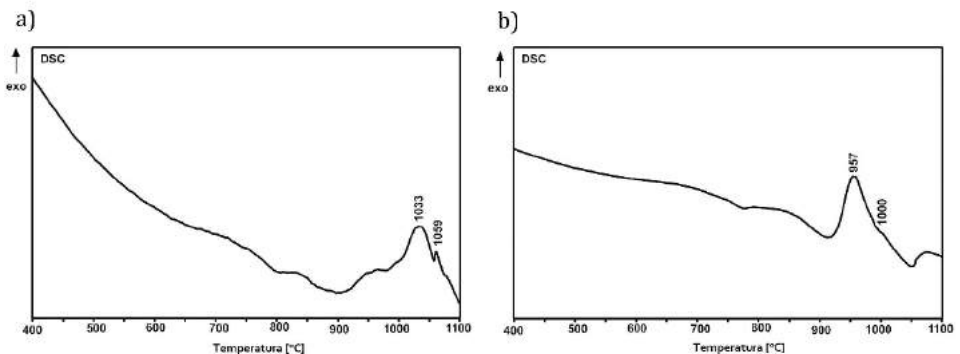


Fig. 3 DSC of the glasses: a) 3K, b)3AlK

The direct crystallization was conducted in gradient furnace. Pieces of glass were placed in heating tube for 2h. The next step was to determine the temperature distribution. For this purpose the temperature was read at every 1cm points along the axis of the furnace.

After heating to identify the type of crystallizing phases, obtained materials were analyzed by XRD methods. Figure 4 a) presents X-ray pictures of 3K glass heated between 831-1062°C. Till 890°C only amorphous phase was achieved, but between 932-977°C it was possible to obtain glass-crystalline material and in the higher temperature materials were crystalline. The crystalline phase was identified as calcium phosphates, wollastonite and crystallobalite.

Materials from 3AlK groups were heated till 950°C. The glass-crystalline materials managed to get in the range of temperature 750-940°C. The crystallizing phase was only calcium phosphate.

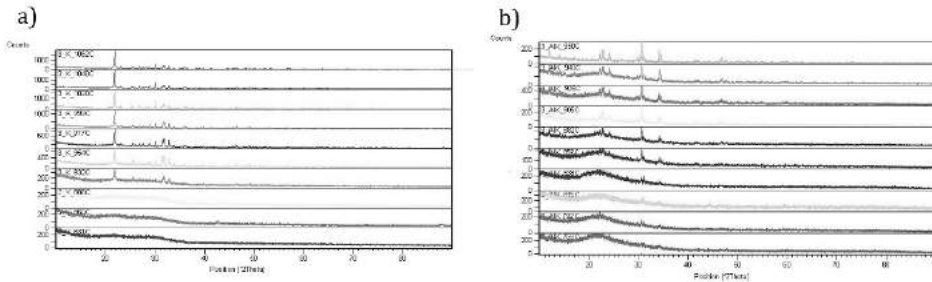


Fig. 4 XRD of the glasses after annealing at indicated temperatures: a) 3K, b) 3AlK

All heated materials in gradient furnace were tested for bioactivity in SBF. Based on the analysis of SEM, EDX and Raman spectroscopy, the influence of the process of crystallization on the bioactivity was researched.

The glass-crystalline and crystalline materials from 3K groups, like their glassy precursor, have thick calcium phosphate "shell" on the surface (Fig. 5a and 6a). Despite the full crystallization, the 3K material remained bioactive. All Raman spectra for this samples are similar to Hap spectrum (Fig. 5c and 6c).

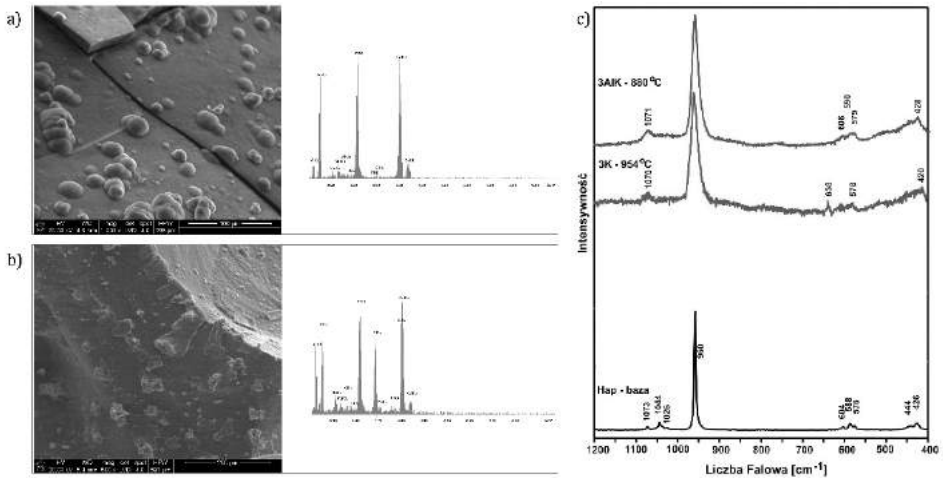


Fig. 5 SEM microphotographs and EDX spectra of the glass-crystalline materials after termostating in SBF: a) 3K, b) 3AIK, c) Raman spectroscopy spectra of the termostated materials.

Another situation can be observed among materials from 3AIK group. In this case, glass-crystalline material is also covered by layer of hydroxyapatite but it is discontinuous (Fig. 5b). The crystallized material lost its bioactivity and became totally inert. No traces of hydroxyapatite phase were detected on the surface (Fig. 6b). The microscopic observation found confirmation in Raman spectroscopy (absence band $1073\ 1044\text{cm}^{-1}$) (Fig. 5c and 6c).

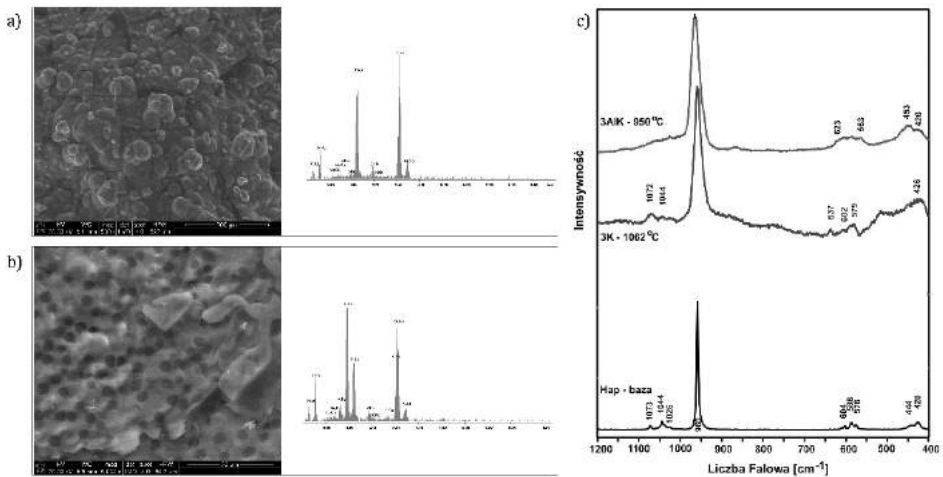


Fig. 6 SEM microphotographs and EDX spectra of the crystalline materials after termostating in SBF: a) 3K, b) 3AIK, c) Raman spectroscopy spectra of the termostated materials.

CONCLUSION

- Microscopic investigation proved that liquation phenomenon takes place in all prepared glasses. Presence of aluminum has a homogenizing influence on the texture of the glasses.
- EDX analysis indicated that chemical composition of inclusions and matrix is different. Addition of Al^{3+} to the 3K glass caused chemical composition inversion of the matrix and inclusions.
- The 3K and 3AlK glasses are characterized by the high level of bioactivity.
- Partial crystallization of 3K and 3AlK glasses does not cause loss of bioactivity.
- Crystalline materials from 3K group did not lose bioactive properties, unlike the 3AlK glass, which after devitrification changed into biologically inert material.
- Properly executed direct crystallization process allows to obtain glass-crystalline material without loss of bioactivity.

REFERENCES

- [1] L.L. Hench, R.J. Splinter, T.K. Greenlee, W.C. Allen: Bonding mechanisms at the interface of ceramic prosthetic materials, *J. Biomed. Res. Symp.*, 2, (1971), 117
- [2] G. Piotrowski, L.L. Hench, W.C. Allen: Mechanical studies of the bone bioglass interfacial bond, *J. Biomed. Res.*, 9, (1975), 47
- [3] L.L. Hench, H.A. Paschall: Direct chemical bond of bioactive glass-ceramic materials to bone and muscle, *J. Biomed. Res. Symp.*, 4, (1973), 25
- [4] R.D. Rawlings: Bioactive glasses and glass-ceramics, *Clinical Mater.* 14, (1993), 155
- [5] P. Li, I. Kangasniemi, K. Groot, T. Kokubo, A.U. Yli-Urpo: Apatite crystallization from metastable calcium phosphate solution on sol-gel-prepared silica, *J. Non-Cryst. Solids*, 168, (1994), 281
- [6] J.M. Oliveira, R.N. Correia, M.H. Fernandes, *Biomaterials* 23 (2002) 371
- [7] U. Gross, V. Strunz, *J. Biomem. Res.* 19 (1985) 251
- [8] O.H. Andersson, K.H. Kralsson, K. Kagasniemi, A. Yli-Urpo, *Glasstech. Ber* 61 (1988) 300.
- [9] P. Li, F. Zang, T.J. Kokubo, The effect of residual glassy phase in a bioactive glass-ceramic on the formation of its surface apatite layer in vitro, *Mater. Sci. Mater. Med.*, 1992;3:452-6
- [10] W. Cao, L.L. Hench, *Ceram. Int.* 22 (1996) 493
- [11] W. Bonfield, M. Wang, K.E. Tanner, *Acta Mater.* 46 (1998) 2509

- [12] M.Sitarz: Structure and texture of glasses belonging to $\text{KCaPO}_4\text{-SiO}_2$ and $\text{KCaPO}_4\text{-SiO}_2\text{-AlPO}_4$ system, Phys. Chem. Glasses Part B 06/2010
- [13] M.Sitarz, K.Bułat, D.Suka: Influence of modifiers and glass-forming ions on the bioactivity of glasses from $\text{NaCaPO}_4\text{-SiO}_2$, Phys. Chem. Glasses Part B 03/2011; 52(3):115
- [14] M. Handke, M. Sitarz, M. Rokita, E.W. Galuskin, J. Mol. Struct. 651-653 (2003) 39

Ti-MWW catalyst – the titanium silicate catalyst with the MWW topology

*Marika Walasek, Agnieszka Wróblewska, Ewa Drewnowska, Alicja Gawarecka

Institute of Organic Chemical Technology, Faculty of Chemical Technology and Engineering, West Pomeranian University of Technology, Szczecin, Pułaskiego 10, 70-322 Szczecin, Poland

e-mail address: marika.walasek@gmail.com, agnieszka.wroblewska@zut.edu.pl

Keywords: *Ti-MWW material, titanium silicate catalysts*

ABSTRACT

The zeolite material described as the Ti-MWW was obtained on the basis of the modified method, which was first described by Tatsumi et al. The preparation of this material was carried out in several steps. This method included: synthesis of the Ti-MWW gel, crystallization the obtained gel in the autoclave, washing the obtained solid with deionized water to pH 8.5-9, drying, activation with nitric acid and calcination. The analysis of the obtained Ti-MWW material was performed using the following instrumental methods: UV-vis spectroscopy, infrared spectroscopy (IR) and scanning electron microscopy (SEM). The possible ways of the transformation of the material with MWW topology to the new materials with the possible catalytic activity were also described (ITQ-2, MCM-36 and YNU-1).

INTRODUCTION

One of the most important discoveries of the last decade in the field of heterogeneous catalysis was performing the synthesis of the titanium silicalite TS-1 catalyst. This material belongs to the group of microporous materials. It has MFI topology and can be described as the structurally analogous to the ZSM-5 aluminosilicate. In its structure there are two subsystems: one sine and one simple. The structure of TS-1 is characterized by a three-dimensional channel system with relatively small pore size (0.53 x 0.56 nm) and by the channels inputs which are limited by ten edges [1].

The first synthesis of TS-1 was carried out in 1983 by Tamarasso et al. This method based on the hydrothermal synthesis [2]. This discovery revolutionized the heterogeneous catalysis due to the high selectivity of this catalyst in oxidation processes and its environmental friendly properties. But this catalyst can not be used in transformations of molecules with the size larger than 0.6 nm. In later years, many researchers have sought for new materials, which would be more suitable for reactions with bulky molecules. The challenge for

researches was the obtaining of new materials with larger pore size and description of the appropriate method of their synthesis.

The MWW structure is a framework type code name specified by International Zeolite Association. It belongs to group of materials, which is called MCM-22. The name of this group refers to a company, that synthesized it first (Mobile Composition of Matter) with sequence number twenty-two. Therefore, MWW abbreviation comes from this type of materials and means **M**CM-**t**Wenty-**t**Wo [3].

It is built from lamellar precursor undergoing dihydroxylation upon calcination between the layered sheets. This structure has two separate pore systems: 10-membered ring pore systems, which form sinusoidal channels and 12-membered ring supercages. Both systems are accessed by windows with the diameters of $4.0 \times 5.5 \text{ \AA}$ (Figure 1). The sinusoidal channels are suitable for adsorption and diffusion processes. The unique porosity creates an open reaction spaces [4]. Due to its construction, Ti-MWW can be used in petrochemical, fine chemical production and in the oxidation (especially – epoxidation) and hydroxylation processes as the active catalyst [5-6].

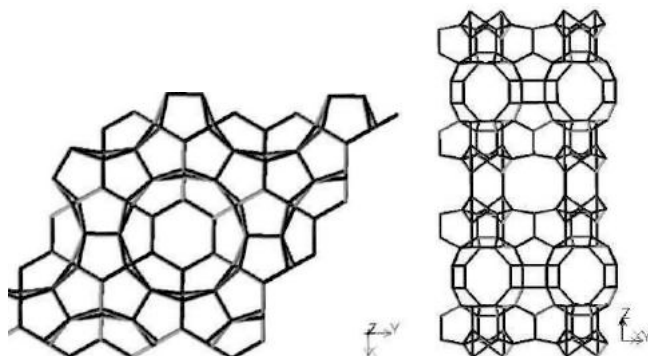


Fig. 1 Topology of the MWW structure

There are several new titanium silicate catalysts, whose structure is based on the MWW-type lamellar precursor. Corma et al. described the method which relies on the isolating of the crystalline sheets from MWW-type material and grafting titanocene onto their surface. The so-prepared material is denoted as the Ti/ITQ-2 [7]. Another MWW-related materials are Ti-YNU-1 and Ti-MCM-36. In the preparation of the first one catalyst, a borosilicate MWW as the precursor is required. In order to remove boron atoms from the structure, the post-synthetic acid treatments had to be used [8]. Furthermore, Ti-containing MCM-36 can be prepared from the Ti-MCM-22 precursor via surfactant swelling followed by polymeric silica pillaring [9]. All of the mentioned, new materials are excellent catalysts for the oxidation processes, and are

characterized by high conversions of raw materials and high selectivities of the desired products.

The aim of this work was the synthesis of Ti-MWW catalyst and its characteristic by various instrumental methods. Moreover, the presentation of the different ways of this catalyst modification in order to obtain the newest titanium silicate catalysts is shown in this work.

MATERIALS AND METHODS

Preparation of the Ti-MWW catalyst

The Ti-MWW catalyst was synthesized by the modified method of Wu et al. [10] (Figure 2).

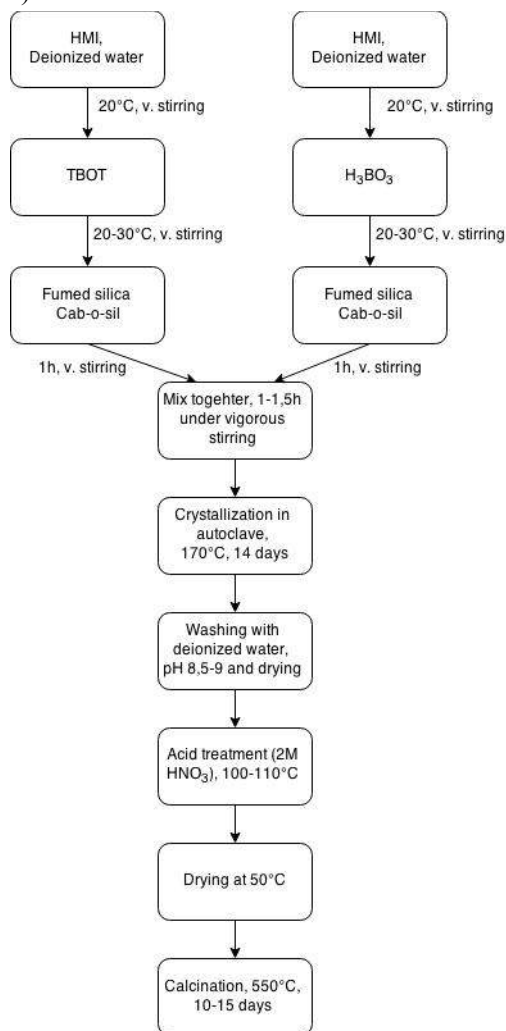


Fig. 2 The method of the synthesis of the titanium silicate Ti-MWW catalyst

Figure 2 presents method of the preparation of the Ti-MWW catalyst. For the synthesis of this catalyst the following raw materials were applied:

hexamethyleneimine (HMI, >98%, Merck), which was a template; tetrabutyl titanate (TBOT, 95%, Fluka) as a source of titanium; boric acid (H_3BO_3 , 99,5% Chempur) and fumed silica (Cab-o-sil M5, Biesterfeld) as a silica source.

The first step in the synthesis of the Ti-MWW material was the obtaining of a Ti-MWW gel. For its obtaining, two homogeneous solutions containing deionized water and HMI were prepared. To one from the solutions, TBOT and to the second - boric acid were added gradually. Both of the solutions were stirred vigorously for about 20 minutes. After this time, the appropriate amount of fumed silica was added. A further stirring for about an hour allowed to make two dense, homogeneous gels. This two gels were mixed together and stirred for 1-1.5 hour. The next step was crystallization of the resulting gel in the autoclave with PTFE insert (the capacity of 500cm^3). The crystallization was performed for 14 days in the temperature of 175°C , and with a stirring rate of 200-250 rpm. The resulting material was filtered off and washed with deionized water to a pH 8.5-9. The solid product was then dried in the temperature of 50°C for 4 days. The reconstituted MWW zeolite was treated with 2M nitric acid to remove boron atoms from the structure. This treatment was carried out in the temperature of $100\text{-}110^\circ\text{C}$ for several hours. The product was then dried at the temperature of 50°C . After cooling, the last procedure was the calcination of the zeolite crystals in the temperature of 550°C for about 10-15 hours, in order to remove residues of the organic compounds in the structure.

Characterization of the obtained sample of the Ti-MWW catalyst

The obtained sample the Ti-MWW catalyst was instrumentally tested in order to obtain its characteristic. For the preparation of this characteristic the following methods were used: SEM (scanning electron microscopy), UV-vis (ultraviolet–visible spectroscopy) and IR (infrared spectroscopy).

SEM method helps to determine a shape and a size of the catalyst crystals. The micrographs of the obtained Ti-MWW material were presented in Figure 3. The images show the catalyst crystals as thin plates with hexagonal morphology. One plate was estimated at about $1,5\mu\text{m}$ length and $0,15\mu\text{m}$ thickness. For the studies by this method JOEL JSM-6100 instrument was used.

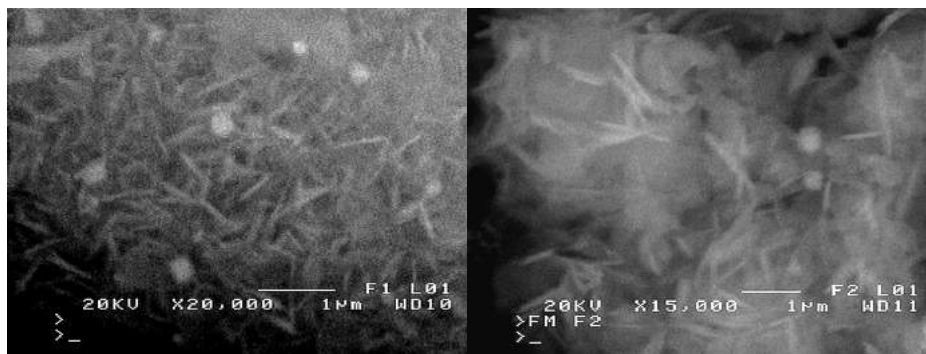


Fig. 3 SEM micrographs of the obtained Ti-MWW catalyst

The UV-vis spectroscopy was used to verify the presence of various Ti-species in the crystalline structure of the obtained catalyst. These studies were made on SPECORD M40 type V-530. The 260 nm band, which is visible in Figure 4, confirms that Ti atoms were incorporated into the framework sites within the sheets (Ti-species in the form of T^{4+} ions). The bands above 330 nm confirm the presence of a slight amount of the anatase phase in this material. The presence of TiO_2 (anatase) are not desirable in the framework of catalyst, because these species are not active sites and may cause ineffective decomposition of the oxidant [10].

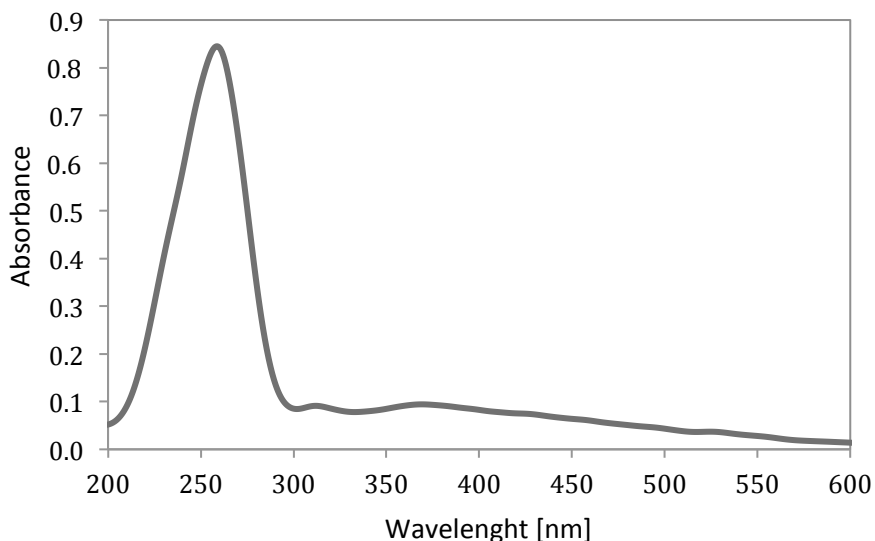


Fig. 4 UV-vis spectra of the obtained Ti-MWW catalyst

The third method used for analyzing the sample of the obtained catalyst was infrared spectroscopy – Figure 5. The studies by this method were made on Shimadzu FTIR-8100 spectrometer using the KBr pellet technique - the catalyst

concentration in the pill was 0.45wt%. This method helps to confirm the presence of titanium atoms in tetrahedral structure (Ti^{4+} ions). If the Ti is included to the structure of SiO_2 the presence of a characteristic band in the range of $950\text{-}960\text{ cm}^{-1}$ in the IR spectrum of the Ti-MWW catalyst is observed. This band is assigned to the vibration of Si-O-Ti, and alternatively attributed to titanyl groups ($\text{Ti}=\text{O}$) and silanol groups ($\text{Si}-\text{OH}$). The absorption band 1040 cm^{-1} is characteristic for Si-O-Ti group and also confirms the incorporation of titanium atoms into the structure. Bands at 3450 cm^{-1} and 930 cm^{-1} are associated with the presence of a hydroxyl group ($-\text{OH}$) and boron atoms, respectively. IR spectrum shows also two strong Si-O-B stretching bands (around 1400 cm^{-1} and 940 cm^{-1}). Also the Si-O-Si stretching vibration band at $1000\text{-}1300\text{ cm}^{-1}$ was observed.

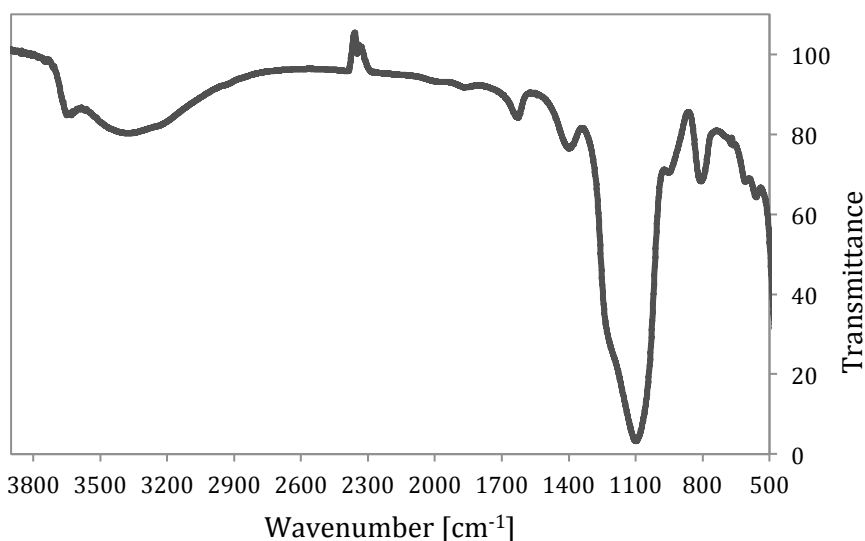


Fig. 5 IR spectra of obtained Ti-MWW catalyst

The ways of the obtaining of new titanium containing zeolites on the basis of MWW zeolite

The MWW lamellar precursor can be converted into silica pillared material, denoted as the MCM-36. Mesopores of this material has diameters of 3-3.5 nm and sinusoidal, 10-membered ring channels. Because of its structure, it can create a large surface area, thus MCM-36 can be excellent acid catalyst for the bulky molecules, which are present in reactions such as gasoil cracking, alkylation of iso-parafins, aromatics or epoxidation. Method of its preparation can be presented as follows: the swollen MCM-22 precursor is pillaring with titanasilicate forming via hydrolysis of an interlayer mixture of TEOS and TBOT [11-12]. Furthermore, MCM-36 also can be delaminated into ITQ-2. The ITQ material has extremely high surface area, as well as MCM-36. It is

characterized by very thin silica sheets (2,5 nm height). It is made by forcing the swelling precursor using ultrasounds [7]. On the other hand, ITQ-2 can be prepared by delaminating the precursor of the pure siliceous MWW polymorph (ITQ-1). The external surface of this catalyst is formed by the array of cups, which are arranged hexagonally and have dimensions of 0.7 x 0.7 nm. The structure is completed by a double 6-ring window and has 10-membered ring (10 MR) channel system [13]. However, ITQ-2 can be formed into a titanosilicate analogue (Ti/ITQ-2), which can be obtained by grafting titanocene onto its surface.

The synthesis of Ti-YNU-1 based on several steps. This method includes adjusting the titanium content in the synthesis gel of MWW-type lamellar precursor, and then washing the product with acid under refluxing conditions. This catalyst has larger pore diameters than Ti-MWW (about 6.7 Å) and therefore, it has more expanded interlayer space. Ti-YNU-1 has similar properties to 12-MR zeolites and has relatively high activity and selectivity in reactions with bulky cycloalkenes with H₂O₂ as an oxidant [14].

CONCLUSIONS

The used instrumental methods confirmed the obtaining of the Ti-MWW material. The literature data showed that the broad studies on the synthesis of the Ti-MWW catalyst can be utilized for the obtaining new catalysts which structure based on the MWW structure. To these catalysts belong: Ti-YNU-1, ITQ-2 and MCM-36. They are potential clean catalysts for the epoxidation, because of their high activity and selectivity in oxidation processes. These materials can successfully substitute other catalysts, which require stricter reaction conditions. Thus the studies on the better and more simply methods of the Ti-MWW material obtaining are very important.

REFERENCES

1. Wróblewska A., Epoksydacja związków allilowych nadtlenkiem wodoru w obecności katalizatorów tytanowo-silikalitowych. *Prace Naukowe Politechniki Szczecińskiej*. Instytut Technologii Chemicznej Organicznej. Szczecin, 2008, 13-19.
2. Taramasso M., Notaff B., U.S. Patent, 4 410 501, 1983.
3. Baur W. H., Fischer R. X., Springer Materials Website: http://materials.springer.com/lb/docs/sm_lbs_978-3-540-45870-8_22, Accessed: 8-04-2015.
4. International Zeolite Association Website: http://izasc.ethz.ch/fmi/xsl/IZA-SC/ftc_fw.xsl?-db=Atlas_main&-lay=fw&-max=25&STC=MWW&-find. Accessed: 28-01-2015.

5. Degan T. F., The implications of the fundamentals of shape selectivity for the development of catalysts for the petroleum and petrochemical industries. *J. Catal.* 216, 2003, 32–46.
6. Wróblewska A., Fajdek A., Milchert E., Grzmil B., The Ti-MWW catalyst – its characteristic and catalytic properties in the epoxidation of allyl alcohol by hydrogen peroxide. *Pol. J. Chem. Technol.* 12, 1, 2010, 29-34.
7. Corma A., Fornes V., Pergher S.B., Maesen T.M.L., Buglass J.G., Delaminated zeolite precursors as selective acidic catalysts. *Nature*. 1998. 353-356. DOI:10.1038/24592.
8. Moliner M., Corma A., Synthesis of Expanded Titanosilicate MWW-Related Materials from a Pure Silica Precursor. *Chem. Mater.* 2012, 24, 4371–4375.
9. Kim S., Seo G., Ahn W., Synthesis and characterization of B- and Ti-MCM-36. *Stud. Sur. Scien. Catal.* 165, 2007, 139–142.
10. Wu P., Tatsumi T., Komatsu T., Yashima T., A novel titanosilicate with MWW structure. I. Hydrothermal synthesis, elimination of extraframework titanium, and characterizations. *J. Phys. Chem. B*, 2001, 105, 15, 2897-2905. DOI:10:1021/jp002816s.
11. He Y.J., Nivarthi G.S., Eder F., Seshan K., Lercher J.A., Synthesis, characterization and catalytic activity of the pillared molecular sieve MCM-36. *Micropor. Mesopor. Mater.* 25, 1998, 207-224.
12. Jin F., Chen S., Jang L., Lee J., Cheng S., New Ti-incorporated MCM-36 as an efficient epoxidation catalyst prepared by pillaring MCM-22 layers with titanosilicate. *J. Catal.* 319, 2014, 247-257.
13. Corma A., Díaz U., Fornés V., Jordá J.L., Domine M., Rey F., Ti/ITQ-2, a new material highly active and selective for the epoxidation of olefins with organic hydroperoxides. *Chem. Commun.*, 1999, 779–780.
14. Fan W., Wu P., Namba S., Tatsumi T., Synthesis and catalytic properties of a new titanosilicate molecular sieve with the structure analogous to MWW-type lamellar precursor. *J. Catal.* 243, 2006, 183-191.

Abstracts

Thermo-Optical Parameters of Amorphous a-C:N:H Layers

*E. Baraniak¹, J. Jaglarz², K. Marszalek¹ and K. Tkacz-Śmiech¹

¹AGH University of Science and Technology, al. A. Mickiewicza 30, 30-059 Kraków, Poland

²Cracow Technical University, Podchorążych 1, 30-084 Kraków, Poland
e-mail: ewa.baraniakk@gmail.com

Key words: *a-C:N:H layers, PACVD, ellipsometry, thermo-optical parameters*

Good properties and high stability of carbon layers make their use growing. The carbon nitride layers have an advantage over amorphous carbon because of good adhesion to the substrate. Such effect is achieved thanks to nitrogen admixture which relaxes the structure and reduces internal stresses. The utility parameters of carbon nitride layers depend on their chemical composition, i.e. C, N and possibly H content, and atomic structure.

Amorphous a-C:N:H layers, deposited on monocrystalline silicon Si (001) by PACVD (13,56 MHz), were subjected to ellipsometric studies. The measurements were performed in a broad spectrum, 300÷1700 nm, at heating from the room temperature to 300 °C and at the reheating after earlier cooling the sample. The layer model was fitted to the recorded dispersion dependencies of ellipsometric angles, $\psi(\lambda)$ and $\Delta(\lambda)$. Hence, the dispersion of refractive and extinction indices, optical gap and thicknesses of the layer at various temperatures were determined.

The results show that all these parameters are essentially different for the unheated layer and the layer heated to 300°C, as well as for the same layer cooled down the room temperature. The re-heating hardly changes the layer parameters. All observed changes occur during first heating, at the temperatures 250÷270°C. Starting from the temperature 250°C the layer thickness decreases to 50% of the initial value. Simultaneously, the thermo-optical parameters, dn/dT and dk/dT , show abrupt changes from negative to positive values. On the basis of the obtained results a conclusion has been formulated that at the temperature 250÷300 °C a partial graphitization of the structure of a-C:N:H layer takes place. The structure transformation is irreversible. It is demonstrated mainly by the changes of the optical gap, from 2,45 eV (for the unheated sample), characteristic for the layers with small fraction of C-sp² phase (about 20%) to 0,7 eV (for the sample at 300°C and after cooling down), typical for the layers with prevailing C-sp² phase (50÷70%).

Such conclusion has been additionally confirmed by the changes in Raman spectrum, in which an increase of the intensity of G band, at about 1620 cm⁻¹ with respect to the intensity of D band at 1360 cm⁻¹, from $I_D/I_G \sim 0,8$ to $I_D/I_G \sim 0,45$ has been found.

Elimination of pollutants by adsorption onto activated carbon prepared from pistachio nut shells

*Aleksandra Bazan, Piotr Nowicki, Robert Pietrzak

Faculty of Chemistry, Adam Mickiewicz University in Poznań, Poznan, POLAND

e-mail: aleksandra.bazan@amu.edu.pl

Keywords: *pistachio shell, activated carbons, direct/physical activation, adsorption from liquid phase*

Activated carbons are microcrystalline materials which show a well-developed surface area and porous structure, so they can be used for removal of pollutants from liquid and gas phase. Thanks to their unique sorption properties, activated carbons have been used in many areas of industry. Wider and wider range of their application cause increasing demands for these materials and stimulate the search for new precursors. The most interesting materials (among those previously proposed in literature data) are all kinds of post-agricultural waste materials.

Therefore, the aim of this study was to check the usefulness of pistachio nut shells as precursors of low cost activated carbons as well as characterization their sorption properties toward organic and inorganic pollutants from liquid phase.

The starting material was dried and sieved to the grain size of 2,5-4,0 mm. Then it was subjected to two different treatments: (1) direct activation with CO₂ at 750 and 800°C for 1 hour, (2) pyrolysis of the precursor at 500 and 700°C followed by activation with CO₂ at 900°C, for 1 hour.

The activated carbons obtained were characterized by elementary analysis, textural studies, determination of pH and the number of surface oxygen groups. The sorption properties of the materials prepared were characterized by iodine, methylene blue, methyl red, crystalline violet and malachite green removal at room temperature.

The results presented have shown that pistachio nut shells can be successfully used as cheap and renewable precursor of activated carbons. The results obtained have also proved that through appropriate choice of activation procedure, it is possible to obtain adsorbents characterized by very good sorption properties toward iodine as well as organic dyes.

Acknowledgements

Financial support received from Polish Ministry of Higher Education and Science (Project Iuventus Plus No. IP2012 004072) is gratefully acknowledged.

Gold nanoparticles in catalysis

*Magdalena Blicharska¹, Sylwia Żołądek¹, Anna Dobrzeńska¹, Paweł Kulesza¹

¹Department of Chemistry, Warsaw University, Warsaw, POLAND

e-mail: mblicharska@chem.uw.edu.pl

Keywords: *catalysis, glucose, gold nanoparticles, sensors.*

Colloidal Au catalysts are active under mild conditions at ambient temperature or less, have rich inorganic and organic chemistry, possess distinct physical and chemical attributes, and this makes them unique.

Gold nanoparticles (AuNPs) have already been used in this form in a range of applications, including the biomedical, cosmetics and bactericides. Another aspect of nanoparticulate Au that is particularly exciting is its use in catalysis.

Au is readily prepared on the nanoscale. We investigate the phosphomolybdate-modified gold nanoparticles (PMo₁₂-AuNPs) which were prepared following the procedure reported by Żołądek et al. We use this method because the gold nanoparticles are catalytically active, its occurs in a water solution and polyoxometallate (PMo₁₂) is concurrently a stabilizing and a reduction agent. We used the gold nanoparticles (PMo₁₂-AuNPs) to prepare new hybrid materials additionally consisting of different carbon materials, conducting polymers or enzymes. The electrocatalytic activity of modified electrodes with this hybrid materials towards glucose oxidation, oxygen and hydrogen peroxide reduction was examined using common electroanalytical methods such as: cyclic voltammetry, chronoamperometry and rotating disk electrode. All of the catalytic systems were subjected physical characterization, like Scanning Electron Microscopy (SEM) and Transmission Electron Microscopy (TEM) to verify their nanostructure morphology.

We demonstrate new hybrid materials to act as the active catalysts toward different electrocatalytic processes. The mild conditions under which Au catalysts are active make them attractive for sensor applications. We prepare and characterize glucose sensors which can be used for monitoring the glucose metabolism of cancer cells.

Preparation and application new hybrid materials

*Magdalena Blicharska¹, Sylwia Żołądek¹, Anna Dobrzeniecka¹, Paweł Kulesza¹

¹Department of Chemistry, Warsaw University, Warsaw, POLAND

e-mail: mblicharska@chem.uw.edu.pl

Keywords: *catalysis, glucose, gold nanoparticles, sensors.*

Recently, interest in the catalytic properties of gold has increased rapidly. In particular, gold nanoparticles have been studied extensively for the design and fabrication of catalysts. Gold nanoparticles possess distinct physical and chemical attributes that make them excellent material for the fabrication of novel chemical and biological sensors. They are also used as catalysts which are applied in the fuel cells and glucose powered-devices.

The goal of our studies is the examination of electrocatalytic activity of new hybrid materials consisting of polyoxometallate (phosphododecamolybdates-PMo₁₂)- modified gold nanoparticles (AuNPs-PMo₁₂), prepared according to procedure described by Żołądek et al. for active bioanode and biocathode applications. We insert of AuNPs-PMo₁₂ on different carbon materials: carbon nanotubes, Norit and graphene. This carbon support we modified in order to improve the catalytic properties of hybrid materials. We used different methods of modification of activated carbons (introduction of appropriate functional groups on the surfaces of these carbons or introduction of heteroatoms by incorporated ferric and cobalt catalytic centers, which are coordinated with nitrogen). We use electroanalytical methods such as: cyclic voltammetry, chronoamperometry and rotating disk electrode to verify their stability and catalytic activity. To verify the structure morphology we use optical method like Scanning Electron Microscopy (SEM) and Transmission Electron Microscopy (TEM).

We demonstrate new hybrid materials to act as the active catalysts toward different electrocatalytic processes. A simple method of preparation, low cost, stability and high catalytic activity make them attractive for fuel cells and sensor applications.

Potentiometric response of solid contact ion selective electrodes (SC-ISE's) using carbon black supporting platinum nanoparticles

*Leszek Cabaj, Magdalena Pięk, Robert Piech, Beata Paczosa-Bator.

¹Faculty of Materials Science and Ceramics, AGH-UST University of Science and Technology, Cracow, POLAND

e-mail: lcabaj@agh.edu.pl

Keywords: *SC-ISEs, nanoparticles, platinum, carbon black.*

Potentiometric sensors having many advantages such as compact size, simple design, small amount of sample needed to analysis etc. can be used in different applications, starting from analyses of body fluids and blood, through many biological samples and ending even on geological samples.

Recent researches have shown that the fresh approach to the design of potentiometric sensors is needed. In the literature it can be found, that using many different materials (in example conducting polymers - CP) to modify the design of potentiometric sensors have great influence of their parameters. Nowadays whole world is focused on the nanoscale, nanomaterials and miniaturization. Several works have shown that in the potentiometric sensors field, nanomaterials such as platinum nanoparticles, graphene, carbon nanotubes or three-dimensionally ordered macroporous carbon can be also used with great success giving a chance to design a sensor with decent parameters, being capable to be easily miniaturized at any time. Sensors with mentioned nanomaterials presented better parameters in comparison with one modified with conducting polymers.

In this work potentiometric responses of the potassium and nitrate solid contact electrode using carbon black supporting platinum nanoparticles (CBNPTs) as an intermediate layer between glassy carbon and ion selective membrane is shown.

Addition of CBNPTs composite in the intermediate layer of sensors both for cation and anion selective electrodes have resulted in improvement of sensors parameters such as long term potential stability repeatability and the reproductibility. Nernstian response of these developed electrodes was good for potassium ions as well as for nitrate ions.

Electrochemical properties of solid contact ion selective electrodes modified with several nanomaterials

*Leszek Cabaj, Magdalena Pięk, Robert Piech, Władysław W. Kubiak, Beata Paczosa-Bator,

¹Faculty of Materials Science and Ceramics, AGH-UST University of Science and Technology, Cracow, POLAND

e-mail: lcabaj@agh.edu.pl

Keywords: *SC-ISEs, chronopotentiometry, EIS, nanomaterials.*

Since the first coated wire electrode (CWE) presented in 1979r by Catrall solid contact ion selective electrodes (SC-ISEs) have changed significantly. CWE electrode presents short-term stability due to unsettled interface between metal conductor and directly covering it ion selective membrane (ISM).

Several researches have been done to find optimal material for an intermediate layer between these two conductors with different ways of conducting. With great success conducting polymers (CP) have been used in potentiometric sensors in that place, and recent works have shown that also nanomaterials such as platinum nanoparticles, carbon nanotubes and other carbon-based materials can be usefull.

Electrochemical impedance spectroscopy (EIS) is a powerful method of investigation of developed potentiometric sensors. Thanks to this measurement we can check the bulk membrane resistances or the interfacial processes inuded by the currents.

Current-reversal chronopotentiometry can give us information about several parameters of potentiometric sensors. It can provide an information about potential stability of the developed electrode, or allows to evaluate electric capacity of the solid contact. Furthermore measurement is pretty fast and very accurate.

In this work results of EIS and current-reversal chronopotentiometry measurements of SC-ISEs containing in their design as an intermediate layer carbon black, platinum nanoparticles or carbon black supporting platinum nanoparticles is shown. It can be seen that there are some differences in behavior when two materials are combined and used as a solid contact in comparison with electrodes using these two materials separately.

Synthesis, microstructural studies and second-order optical nonlinearity of rare earth doped orthorhombic $\text{Bi}_2\text{ZnB}_2\text{O}_7$

*Maciej Chrunik¹, Jan Kroupa²

¹Institute of Applied Physics, Military University of Technology, Warsaw, POLAND

²Institute of Physics of the Academy of Sciences of the Czech Republic, Prague, CZECH REPUBLIC

e-mail: mchrunik@wat.edu.pl

Keywords: borates, second harmonic generation, sol-gel, nanoparticles, SEM

Current work is devoted to Pechini synthesis of orthorhombic $\text{Bi}_2\text{ZnB}_2\text{O}_7$ (BZBO) and its second-order nonlinear optical (NLO) features. The recent studies on this borate crystal showed this material besides SHG possesses excellent third-order NLO effects (THG). In case of efficient doping with RE^{3+} ions (Nd^{3+} , Pr^{3+} , Tb^{3+} , etc.) and effective SHG conversion it results as potential material for self-frequency doubling devices. It may be applied also as material for laser-operated devices. Apart from that it has interesting vibrational properties for μ -Raman investigations and photoluminescent features. In this study we present results of SHG measurements for BZBO: RE^{3+} powders obtained by means of modified Pechini synthesis. Applied technology is time-shorter comparing to solid-state reaction and results in very fine powder samples of pure BZBO: RE^{3+} , what was confirmed by XRD. The microstructure of obtained powders was examined using SEM.

Modification of material's surface properties by direct laser interference lithography

*Krzysztof Czyż¹⁾, Jan Marczak¹⁾, Antoni Rycyk¹⁾, Antoni Sarzyński¹⁾, Marek Strzelec¹⁾, Roman Major²⁾, Aldona Mzyk²⁾

¹⁾Institute of Optoelectronics, Military University of Technology, Warsaw, Poland

²⁾Institute of Metallurgy and Materials Engineering, Polish Academy of Sciences, Krakow, Poland

e-mail: kczyz@wat.edu.pl

Keywords: *direct laser interference lithography, laser micromachining, titanium alloys, bioengineering.*

Periodic structures are used in various fields of science and technology. Surfaces with a modified top structure are used for example in biomedical engineering, tribology and optoelectronics. The surface-formed materials (metals, semiconductors, dielectrics), due to a change in topography and in microstructure, may change their properties. One of the recent, simplest, single step techniques of creating change in topography and microstructure is the direct interference lithography method (DLIL). It is based on irradiating the surface of the materials with an interference pattern by means of a high-energy pulse laser.

The proposed article is divided into three main chapters. The first one shows brief mathematical introduction to DLIL based on a classical interference theory. The second chapter describes original construction of a dual-channel DLIL laser system. It consists of a stable and unstable (“p-branch”) Nd:YAG generator with Q-modulation and a dual channel amplification stage in Mach-Zehnder’s interferometer configuration with tunable energy and beams angles. Finally, authors present examples of practical applications of DLIL technique.

The most interesting results are connected with structuring of diamond like carbon (DLC) coatings, metals and polymers. For example, 1D and 2D profiles created on the surface of thin DLC layers on a silicone substrate are currently researched as scaffolds for the growth of biological cells. The initial results indicate improvement and strengthening the mutual interaction between the cells and the surface, and their traction, growth and direction of orientation. Laser structuring of the modern Ti13Nb13Zr alloy allowed also improvement of its wettability and further adhesion of hydroxyapatite layers for bone implants.

Summarizing, we have simulated and created periodical and hierarchical surface structures with different periods and shapes. Our motivation is to promote the idea of direct laser interference lithography as an advanced, cheap and effective manufacturing method with many existing and future applications.

Synthesis of periodic mesoporous organosilicas modified with Nb

*Paulina Dębek, Agata Wawrzyńczak, Izabela Nowak

Adam Mickiewicz University in Poznań, Faculty of Chemistry, Poznań,

POLAND

e-mail: paula612@poczta.onet.pl

Keywords: *periodic mesoporous organosilicas, niobium, synthesis and modification procedures*

Periodic mesoporous organosilicas (PMO's) are materials of strong scientific and commercial interest because they combine inorganic and organic properties. So far PMO-related studies were focused mainly on the incorporation of various organic groups in order to design materials for adsorption applications and only limited number of materials was premeditated for catalytic purposes. However, modifications with heteroatoms will alter chemical and physical properties of these materials due to large difference in the valence, coordination number, atomic weight and electronegativity between silicon and metallic elements. Thus, our study were targeted towards the design and synthesis of new inorganic-organic hybrid materials with a potential application as catalysts in the hydrodeoxygenation reactions.

Syntheses of siliceous materials with 2D (MCM-41) and 3D (SBA-15) hexagonal pore ordering were performed via typical hydrothermal method, using standard chemicals and procedures. In the case of SBA-15 material tetraethyl orthosilicate (TEOS) and triblock copolymer (Pluronic P123) were used as a Si source and structure-directing agent, respectively, whereas TEOS and ionic surfactant (CTABr) were applied during the synthesis of MCM-41. Different parameters of synthesis were adopted in order to obtain samples with diverse textural parameters. Template removal was based on the extraction procedure with HCl/EtOH solution. 3-(triethoxysilyl)propylamine or (triethoxysilyl)aniline were incorporated during synthesis to functionalize the mesoporous supports. Niobium was incorporated into the siliceous matrix using “one-pot” and impregnation techniques with ammonium tris(oxalate) complex of niobium(V) $[(\text{NH}_4)_3\text{NbO}(\text{C}_2\text{O}_4)_3(\text{H}_2\text{O})]$ as a metal source.

A comprehensive characterization of all products was performed by the means of N_2 sorption measurements, FT-IR, ICP-OES, XPS, TEM/SEM, XRD and elemental analysis. These techniques proved the mesoporosity and ordered structure of the obtained samples as well as the template removal and incorporation of niobium atoms.

National Science Centre is kindly acknowledged for the financial support (project no: DEC-2013/10/M/ST5/00652)

The utilization of the TS-1 catalyst in the epoxidation of diallyl ether

*Ewa Drewnowska¹, Agnieszka Wróblewska¹, Alicja Gawarecka¹, Marika Walasek¹

¹Institute of Organic Chemical Technology, West Pomeranian University of Technology, Szczecin, POLAND

e-mail: ewa.sokalska@zut.edu.pl

Keywords: epoxidation, TS-1 catalyst, diallyl ether, allyl-glycidyl ether

The microporous TS-1 catalyst was obtained first by Taramasso et al. in 1983. The precursor of this catalyst is a ZSM-5 zeolite. The TS-1 catalyst is characterized by a three-dimensional system of channels (linear-zigzag) and has the MFI structure. The size of the crystals of the TS-1 catalyst amounts to 0.1-1.0 μm and the size of the elliptical channels reached of 0.53 x 0.56 nm. The dimensions of the channels are sufficient for the absorption of the particles having a diameter of up to 6Å. Due to the small pore size this material can only be used for the epoxidation of unsaturated compounds with small molecules. Until now this catalyst has been used for the selective oxidation of olefins, alkanes, alcohols and phenols using hydrogen peroxide and at relatively mild conditions.

In this work the TS-1 catalyst was used for epoxidation of diallyl ether (DAE). These studies showed that the epoxidation leads mainly to the formation of allyl-glycidyl ether, a compound having a lot of applications in organic syntheses and in industry. Allyl-glycidyl ether is a valuable compound used for the obtaining of epoxy resins, epoxy adhesives, powder paints, epoxy coatings and many other interesting products. It is also used for the preparation of polynitrites which are applied as the explosive materials, cryptands which are used in medicine as the receptors for the selective binding of cations and anions and also as the antitumor agents. Moreover, the process of diallyl ether epoxidation also causes formation of a large group of by-products, such as: allyl alcohol, glycidol, 3-allyloxy-1,2-propanediol, glycerol and diglycidyl ether. These compounds have also a lot of applications in organic syntheses and in perfume, cosmetics and polymer production.

The studies showed that for the following parameters: the temperature of 70°C, the molar ratio of DAE/H₂O₂ = 2:1, solvent (methanol) concentration of 70 wt%, the amount of the TS-1 catalyst 4 wt%, the reaction time 3 h, the intensity of stirring 500 rpm, it is possible to obtain allyl-glycidyl ether with the selectivity of 78 mol%, at the conversion of diallyl ether of 8.8 mol%.

Optimization of amino acid-zinc carriers

*Renata Dyja¹, Barbara Dolińska^{1,2}, Florian Ryszka²

¹Department of Applied Pharmacy and Drug Technology, Medical University of Silesia, Sosnowiec, POLAND

²Pharmaceutical Research and Product Plant "Biochefa", Sosnowiec, POLAND

e-mail: rdyja@sum.edu.pl

Keywords: *suspensions, sustained release formulation, co-precipitation, zinc chloride*

Layered zinc chloride basic salts and layered zinc hydroxides have received increasing attention as materials for the construction of sustained release drug formulations. This paper describes a study on the co-precipitation of amino acid (histidine, tryptophan, tyrosine) and zinc chloride solution by sodium hydroxide solution.

The aim of that study was to optimize obtained amino acid-Zn(II) suspensions. The main focus was to obtain an optimum amino acid-Zn(II) precipitation yield. Amino acids were employed as model drug substances. The methodology included the preparation of suspensions with different Zn(II):amino acid molar ratios (15:1, 3:1, 1.5:1 or 0.75:1) and pH values (6.5-10.5). Briefly, 0.75 ml aliquot of the stock ZnCl₂ solution was mixed with His, Trp or Tyr solution of specific concentrations (0.001 M, 0.005 M, 0.01 M or 0.02 M in 0.015 M HCl) and then 0.75 – 1.45 ml of 0.2 M NaOH was added. The suspensions were stirred using a magnetic stirrer for 25 min and then were left at room temperature for 1 h. The suspensions were then centrifuged. Amino acid concentration was determined in the supernatant by spectrophotometric method. Zn(II) concentration was determined in the supernatant by complexometric titration using 0,05 M EDTA solution.

The relationship between pH and the amount of amino acid and Zn(II) bound in the dispersed phase was established by means of regression equations. The optimal pH values (pH_{opt}) and optimal Zn(II):amino acid molar ratio values for amino acid binding in the dispersed phase was determined for each amino acid. The values of pH_{opt} were higher than amino acid pI by 1.4-2.8 units. The values of the optimal Zn(II):amino acid molar ratios were: Zn(II):His_{opt} 1.51, Zn(II):Trp 0.85 and Zn(II):Tyr_{opt} 2.38.

The high correlation between used Zn(II):amino acid molar ratio and Zn(II):amino acid molar ratio in the dispersed phase supported zinc precipitation as zinc hydroxide or zinc hydroxide chloride. The values of pH_{opt} may indicate amino acid intercalation into zinc layered hydroxide chloride.

Dissolution profiles of optimized amino acid-zinc carriers

*Renata Dyja¹, Barbara Dolińska^{1,2}, Florian Ryszka²

¹Department of Applied Pharmacy and Drug Technology, Medical University of Silesia, Sosnowiec, POLAND

²Pharmaceutical Research and Product Plant "Biochefa", Sosnowiec, POLAND

e-mail: rdyja@sum.edu.pl

Keywords: *suspensions, sustained release formulation, co-precipitation, zinc chloride*

In recent years, there has been extensive research on sustained release drug carriers based on the layered zinc chloride basic salts or layered zinc hydroxides. In our previous work, we have reported intercalation of histidine, tryptophan and tyrosine into zinc compounds. This paper describes a study on the release of amino acid (histidine, tryptophan or tyrosine) from these model suspensions obtained by co-precipitation method.

The methodology included the preparation of suspensions with different Zn(II):amino acid molar ratios (15:1, 3:1, 1.5:1 or 0.75:1) with optimal for amino acid precipitation yield pH value (pH_{opt}) (His $\text{pH}_{\text{opt}}= 9.3-9.9$, Trp $\text{pH}_{\text{opt}}= 7.3-7.9$, Tyr $\text{pH}_{\text{opt}}= 7.5-8.5$). Amino acids were employed as model drug substances. Briefly, 0,75 ml aliquot of the stock ZnCl_2 solution was mixed with His, Trp or Tyr solution of specific concentrations (0.001 M, 0.005 M, 0.01 M or 0.02 M in 0.015 M HCl) and then 0.2 M NaOH was added. The suspensions were stirred using a magnetic stirrer for 25 min and then they were left at room temperature for 1 h. Then, the suspensions were centrifuged. The resulted pellets were re-suspended in 10 ml 0.9% NaCl solution. The suspensions were stirred using a magnetic stirrer for 30 min and then were subjected to centrifugation. The amount of dissolved amino acid was determined. Resulted pellets were re-suspended in 10 ml of fresh dissolution medium. That steps were repeated during 5 hours. The amount of amino acid was determined by spectrophotometric method.

The dissolution profiles of amino acid were analyzed on the basis of zero order kinetic, first order kinetic and Korsmeyer-Peppas equation. The values of $t_{1/2}$ were $t_{1/2}=2,1-3,4$ h (His), $t_{1/2}=0.7-2.1$ h (Trp) and $t_{1/2}= 0.4-0.5$ h (Tyr). The release of the His and Trp from the suspensions with higher supporting dose (1.5:1 and 0.75:1 Zn(II) amino acid molar ratios) followed the mechanism of zero order kinetic. The supporting dose determined the release profile of the amino acid. Basis on the knowledge of the amount of amino acid bound in the dispersed phase, the prediction and modeling of the release amino acid profiles is possible.

Natural stabilizers increasing survival of *Lactobacillus rhamnosus* during spray drying process

*Alicja Fedorowicz¹, Artur Bartkowiak², Wioletta Krawczyńska²
Center of Bioimmobilisation and Innovative Packaging Materials,
West Pomeranian University of Technology, Szczecin, POLAND
e-mail: alicja.fedorowicz@zut.edu.pl

Keywords: spray drying, *Lactobacillus rhamnosus*, survival

For successful delivery in foods, probiotics must survive food processing and storage conditions during product maturation and shelf life. A large number of food products contain probiotic bacteria such as *Lactobacillus rhamnosus*. Spray drying is a well-known technology in the food industry. Spray drying produces dry granulated powders from a slurry solution, by atomizing the wet product in a chamber. Spray drying is one of many methods of microencapsulation. Microencapsulation is defined as a technology for packaging solids, liquids or gaseous materials in miniature, sealed capsules. Microencapsulation by spray drying is a valuable technique to encapsulate probiotic bacteria, which produces small, uniformly coated microspheres containing viable cells. However, high cell mortality, is often observed during spray drying, as bacterial cultures are exposed to a number of stresses, such as dehydration, heat, and osmotic stress, etc. The addition of protectants to the media before drying is used to improve bacterial survival.

Lactobacillus rhamnosus was purchased from Leibnitz Institute DSMZ-German Collection of Microorganisms and Cell Cultures. 1.0 ml of the inoculum was inoculated into 50ml of MRS broth (Biocorp, Poland) and incubated at 37°C. Starch Capsul HS (National Starch & Chemical Limited, United Kingdom) was used as typical materials to encapsulate bacteria cells at a concentration of 20% (w/v), 17,5% or 15%, with 2,5% and 5% protective agents (natural stabilizers) added, respectively. For spray-drying, a mini spray-drier Büchi B-290 (Büchi, Switzerland) was used. The air inlet temperatures were 130, 150 and 180°C. Serial dilutions were prepared from the initial suspension and pour plated on MRS agar (Merck KgaA, Germany), in triplicate. Plates were incubated at 37°C for 48h and the number of colonies were counted.

The addition of natural stabilizers to the starch solution improved survival rate of *Lactobacillus rhamnosus* and reduced air outlet temperature during spray drying process (compared to the starch solution Capsul HS). The percent of cell viability after spray drying varied according to numerous factors, including the type and concentration of the protective agent, air inlet and outlet temperature.

Visible-light photochemical degradation of 2,4-dichlorophenol in aqueous solutions by singlet oxygen

*M. Foszpańczyk¹, D. Gryglik², M. Gmurek¹, S. Ledakowicz¹

¹Faculty of Process and Environmental Engineering,

²Faculty of Civil Engineering, Architecture and Environmental Engineering,

Lodz University of Technology, Wolczanska 213, 90-924 Lodz, Poland.

e-mail: mfozpanczyk@gmail.com

Keywords: 2,4-dichlorophenol, photosensitizers, photosensitized oxidation, kinetics, photodegradation

Chlorophenols (CPs) are compounds characterized by a dangerous impact on the environment due to its high toxicity. CPs are often formed in technological processes as well as chlorine disinfection, chlorination of phenol, can be formed environmental transformation from herbicides. It is well known that CPs have very low taste and odor thresholds. Existing methods to remove organic compounds are not able to remove these difficult degradable organic compounds. An alternative process may be photosensitized oxidation process, particularly using molecular oxygen. An interesting option appears to be the photooxidation of phenolic compounds by singlet oxygen due to its advantage of use oxygen from air and solar radiation.

The results of an investigation of photodegradation of the of 2,4-dichlorophenole (2,4-DCP) under photosensitized oxidation with visible light in aerated aqueous solutions are *presented herein*. The study was conducted in a semi-continuous system in flat reactors (0.06×0.10 m) of the volume 0.01dm³. Five reactors were symmetrically positioned around the xenon lamp (Osram 100W, $E_0 = 324 \text{ mEinstein s}^{-1} \text{ dm}^{-3}$), simulating solar radiation. The reaction mixture was agitated by gentle air or oxygen stream. Rose Bengal and derivatives of porphine and phthalocyanine were used as sensitizers.

pKa and possibility of the of 2,4-DCP decomposition via photolysis was checked. The influence of various parameters such as: sensitizers type, pH of the reaction solution, oxygen content on the photosensitized oxidation was examined. The major role of singlet oxygen in 2,4-DCP degradation was proved by the experiments performed in the presence of hydroxyl radicals scavengers and singlet oxygen quenchers. On the basis of experimental data reaction rate constants of photosensitized oxidation reaction of 2,4-DCP at two pH were determined.

Degradation of 2,4-DCP in the aqueous solution by photosensitized oxidation in homogeneous aqueous solution under visible-light irradiation is effective. The efficiency of the 2,4-DCP photodegradation strongly depends on the initial photosensitizer concentration, light intensity as well as oxygen content in reaction mixture.

Acknowledgement

This research was supported by the National Science Centre (NCN) in Poland within research project 2012/07/B/ST8/03787.

Synthesis and applications of the TS-1 catalyst

*A. Gawarecka, A. Wróblewska, E. Drewnowska, M. Walasek

Institute of Organic Chemical Technology, Faculty of Chemical Technology and Engineering, West Pomeranian University of Technology, Szczecin, Pułaskiego 10, 70-322 Szczecin, Poland

e-mail: alicja.gawarecka@zut.edu.pl

Keywords: *TS-1, limonene epoxidation*

The titanium silicalite TS-1 catalyst is a synthetic, porous and crystalline material with the structure which is described in the atlas of the crystalline structures as the MFI. It is characterized by three-dimensional channels system which is denoted as a linear-zigzag. The diameter of the pores of TS-1 amounts to 0.53 x 0.56 nm and the ring openings of channels have 10-edges. The crystals of this catalyst can have the size from 0.1 to 1.0 μm , depending on the crystallization conditions. The TS-1 crystallizes in orthorhombic crystal system. The nature of this catalyst is hydrophobic. This character causes that the TS-1 catalyst is an active catalyst in oxidation of alkanes and alkenes with the water solutions of hydrogen peroxide. Moreover, the TS-1 catalyst can be used in hydroxylation phenol to hydroquinone and pyrocatechol and in ammoxidation reactions.

The method of the preparation of this catalyst starts from mixture which includes the source of Si and the source of Ti. The template in this synthesis is tetrapropylammonium hydroxide. The resulting mixture is vigorously stirred and heated for several hours. The obtained gel is then crystallized in the autoclave with the PTFE insert for 7-10 days in the temperature of 165-175°C. The obtained, white material is filtered, dried and calcined at the temperature of 550°C.

The studies on the epoxidation of limonene over the TS-1 catalyst were performed. As a solvent in these studies acetonitrile was used. Limonene, acetonitrile and catalyst were put in a glass flask with the capacity of 50 cm^3 and then were heated. Next, at the appropriate temperature the 30 wt% hydrogen peroxide was added. The reaction was carried out in the temperatures of 50-70°C for several different times. Samples were analyzed with help of the GC method. The formation of the main product - limonene 1,2-oxide was observed.

The studies showed that the TS-1 catalyst can be effectively used in the process of limonene epoxidation. It is a very important process because the epoxide product of this reaction (limonene 1,2-oxide) has a lot of applications in perfume, cosmetic, drug and polymer industry.

The release studies of undecylenoyl phenylalanine through cellulose based membranes

*Aleksandra Głowska¹, Anna Olejnik¹, Izabela Nowak¹

¹Adam Mickiewicz University in Poznan, Faculty of Chemistry, Poznan, POLAND

e-mail: ola.glowka@gmail.com

Keywords: *release, amino acid derivative, porous membrane, active substance, undecylenoyl phenylalanine*

The release tests of active compounds from semisolid dosage forms are significant factor in estimating the efficiency of the active ingredients. This research permits to assess a product's quality and activity after introducing any changes in composition, in apparatus or in the production process. *In vitro* release studies are also useful in the design and development of the novel formulations. During this analysis the active compound, which is added to the semisolid, has to be released from the formulation through the porous membrane to the receptor fluid. The tremendous progress in science has created a great variety of innovative and highly sophisticated active compounds. One of them are amino acids derivatives such as undecylenoyl phenylalanine, which consists of amino acids and lipid residue. This compound is applied in cosmetics as skin-lightening agent to prevent skin cells from producing melanin pigmentation.

The aim of this study was to monitor the release kinetics of phenylalanine-fatty acid derivative, undecylenoyl phenylalanine, from hydrogels and emulsions through cellulose membranes. The release studies of undecylenoyl phenylalanine were performed with the use of an USP Apparatus 2 (Agilent Technologies DS 708) connected with spectrophotometer UV-Vis. The application of UV-Vis spectroscopy enables to estimate the release kinetics of active ingredient.

The obtained results showed that the thickness and pore size of the membrane have the influence on the release rate of undecylenoyl phenylalanine. Depending on the applied membrane the kinetics of the active compound release from hydrogels can be described by the Korsmeyer-Peppas model or by the Higuchi model. Additionally, it was proved that the rheological properties of semisolid formulations strongly determine the release rate of active compound. The higher viscosity of the semisolid the slower permeation through the membrane. Therefore, hydrogels presented the fastest release rate of undecylenoyl phenylalanine.

Thermocatalytic polyolefin processing system in pure synthetic oil distiller

* Łukasz Grabowski¹, Marta Wołosiewicz-Głąb²

¹AGH Faculty of Mining and Geoengineering, Department of Economics and Management in Industry

²AGH Faculty of Mining and Geoengineering, Department of Environmental Engineering and Mineral Processing

e-mail: lukgrabo@agh.edu.pl

Keywords: *polyolefins, plastics, synthetic oil, distiller, alternative fuel*

Polyolefins (polyethylene PE and polypropylene PP) are a major group of synthetic plastics. Due to the distinctive uniform chemical composition and high availability, they are interesting raw material for further processing and, consequently, to reduce the amount of waste.

The paper presents and characterized polyolefins. The treatment and management of this type of waste have been shown. Describes the process of obtaining a pure synthetic oil in distilleries. The possibilities to use thermocatalytic polyolefin processing system.

Outlines the prospects for using this type of technology. Their analysis was carried out taking into account the various stages of the recovery process, economics and environmental impact.

The industrial heritage in nowadays Polish cities.

*master of science of architecture Joanna Gruszczyńska

Warsaw University of Technology, Faculty of Architecture, Koszykowa55
Warsaw, Poland

e-mail: j.byszewska@gmail.com

Keywords: *Industrial areas, heritage, identity*

Year 2015 is announce the European Industrial and Technical Heritage Year. Considering that, it is good time to discuss this topic. The aim of the article is explore the impact of industrial buildings and structures for an image of urban areas. Every big Polish city, including cities like Warsaw, Krakow had been became the industrial centers by the end of the twentieth century. Most of the industrial area are now located in cities centers. Unfortunately most of them have become isolated, forgotten and unwanted areas.

Analyses of selected phenomenon's about city and industrial objects in Poland, the research was based on case studies. The first stage of the work was an overview of the literature about the history, the analysis of terms heritage, identity, city and industrial building. Then, make a review of selected examples of adaptation of the industrial building. Materials was collected in both the source text and iconography, site visits.

The research analysis issues of the definition of the term 'city', which is currently not clear, because of its complexity. The city is diversified, unique and variable system – an organism difficult to control. Nowadays city is rapidly developing and constantly changing. One of the basic function of the city is to provide a sense of security and the identity to its inhabitants. The progress of urbanization and globalization sparked fear that this values and cultural significance might be blurred. Modern city too often is build in a way which ignores ties to its history. It was forgotten that once industrial buildings were creating focal points of the city life and society's culture and that contributed to dereliction of industrial areas. It is important to remember that the cultural landscapes are integral part of our society, which reveals our relationship with the land over time. Another related issue is to try to preserve the buildings and attitude to reuse (search for a suitable method).

There are examples showing that if we traced or uncover the history and values that constitute the city image and use them in present development, it will be beneficial long term and on many levels. The analysis of society and understanding of an area lead to gaining knowledge of the place that people wish to live in, to identify the social perception of the place. It is important to realize that the whole city is our heritage. Furthermore, it is increasingly acknowledged that the values connected with culture and heritage are highly significant for inhabitance's lives and need to be identified and highlighted.

Visible light driven photocatalytic elimination of organic- and microbial pollutions by rutile-phase titanium dioxides

T. Gyulavári¹, *G. Veréb¹, Zs. Pap¹, K. Mogyorósi¹, L. Manczinger², A. Dombi¹, K. Hernádi¹

¹Research Group of Environmental Chemistry, Institute of Chemistry, Faculty of Sciences and Informatics, University of Szeged, Szeged, HUNGARY

²Department of Microbiology, Faculty of Sciences and Informatics, University of Szeged, Szeged, HUNGARY

e-mail: verebg@chem.u-szeged.hu

Keywords: rutile, TiO_2 , *E. coli*, phenol, peroxy-group

The characteristic properties and the resulted photocatalytic efficiencies of rutile-phase titanium dioxides were investigated in the present study. A series of rutile with different primary particle sizes (~5-300 nm) were produced by sol-gel method followed by calcination. Another series of rutile were prepared by the addition of various amounts of hydrogen peroxide. Commercial Aldrich rutile was also investigated.

The photocatalysts were characterized by XRD, DRS, TEM, XPS, IR and N_2 adsorption. Their photocatalytic efficiencies were determined via the decomposition of phenol, and in the inactivation of *E. coli* bacteria under visible light irradiation.

The DRS spectra indicated that the light absorption was shifted into the visible region with the increase of the calcination temperature, which may explain the significantly increased surface-normalized photocatalytic performance. On the basis of the recent results, in the case of rutile-phase titanium dioxide, the presence of Ti^{3+} and low-binding-energy oxygen (which indicates defects) was detrimental for the photocatalytic performance under visible light irradiation. However the appearance of Ti-O-O-Ti groups on the surface of rutile (at 687 cm^{-1} in the IR spectra) resulted in higher photocatalytic efficiency.

Acknowledgement: This research was supported by the European Union and the State of Hungary, co-financed by the European Social Fund in the framework of TÁMOP 4.2.4. A/2-11-1-2012-0001 'National Excellence Program'. This work was partially co-financed by the Swiss Contribution (SH/7/2/20).

Synthesis and mesomorphic properties of 2,3-difluoro-4,4''-dialkyl- and 2,2',3,3'-tetrafluoro-4,4''-dialkyl-p-terphenyl's homologous series

Przemyslaw Kula¹, *Piotr Harmata¹

¹Institute of Chemistry, Faculty of Advanced Technologies and Chemistry, Military University of Technology, Warsaw, POLAND

e-mail: pharmata@wat.edu.pl

Keywords: *terphenyl, nematic, smectic, fluorinated liquid crystal, vertical alignment nematic (VAN)*

Liquid crystalline (LC) materials proved to be the key feature in display industry. Dynamic development of this branch of industry requires constant improvement of the chemical and physical properties of LC materials. Display devices can be based on different switching mode, depending on the desired application. In the case of vertical alignment (VA) mode the required properties of LC materials most importantly are a broad temperature range of the nematic (N) phase and negative dielectric anisotropy. Low viscosity, medium birefringence, low rotational viscosity, high thermostability and photostability are also necessary.

The aim of this research was to synthesize compounds which could be used in mixtures fulfilling the above mentioned requirements. One way to achieve the negative dielectric anisotropy is to introduce polar groups in the lateral position of a LC compound. In our work we used fluorine substitute. We synthesized three homologous series of laterally fluoro-substituted terphenyl derivatives, 4''-alkyl-4-butyl-2,3-difluoro-p-terphenyls (series 1), 4''-alkyl-4-pentyl-2,3-difluoro-p-terphenyls (series 2) and 4''-alkyl-4-propyl-2,2',3,3'-tetrafluoro-p-terphenyls (series 3). We determined the influence of the position and number of fluorosubstitutes as well as the length of terminal chain on the properties of synthesized compounds. We measured mesomorphic properties, phase transition temperatures and enthalpies and we compared them with the similar trifluoro- and chlorodifluoro- substituted analogues. Selected compounds were used as dopants in LC mixtures for devices working in VA mode and they improved their properties as expected. In addition we optimized synthesis methods for receiving the above mentioned compounds.

The synthesized compounds have negative dielectric anisotropy, especially for Series 3, what is associated with the presence of four laterally substituted fluorine atoms. We noticed that with the extension of the chain length in Series 1 and 2 the smectic A and C phases are observed. We also observed that addition of lateral fluorine substitutes causes the disappearance of smectic phases. Synthesized products gave high yields and purity above 99,5%.

The influence of lateral substitutes on birefringence value of compounds based on molecular cores – tolanes and bistolanes

Przemyslaw Kula¹, *Piotr Harmata¹

¹Institute of Chemistry, Faculty of Advanced Technologies and Chemistry, Military University of Technology, Warsaw, POLAND

e-mail: pharmata@wat.edu.pl

Keywords: *birefringence, molecular core, liquid crystal, order parameter*

Creation of more sophisticated electro-optical devices was only possible with the simultaneous development of new liquid crystalline (LC) materials, which addressed the exact needs, depending on a device. Recently, one of desired parameters is high birefringence value of compounds with nematic phase. This is especially important for application in other than visible spectral regions such as infrared, THz or GHz.

The synthesis of highly birefringent nematics (HBN) depends on the proper design of molecular core and its functionalization by a good choice of lateral and terminal substitutes. It is important to note that the substitutes often deteriorate the value of birefringence, but are necessary to obtain LC characteristics.

The aim of our work was to determine the influence of lateral substitutes such as fluorine, chlorine, methyl and ethyl group on the birefringence value of compounds and to compare them with the values we could predict based on DFT numerical algorithm calculations. We based our research on the most commonly used molecular cores – tolanes and bistolanes. Because the compounds we received did not have any mesomorphic properties, we determined their birefringence by extrapolation from mixtures which show LC properties. In order to extrapolate the birefringence, we have prepared several mixtures of synthesized compounds with amounts of 5 to 15 molar %. To measure the birefringence we used two independent methods. First was Abbe refractometer and the second one was Metricon prism coupler.

For shorter cores (tolane series) the results we obtained were not what we expected. Contrary to our expectation, we observed much lower extrapolated birefringence values. For longer cores (bistolane series) the results are close to what we expected. In order to explain the results of tolane series we determined order parameters, which has shown that molecules in the LC matrix were not ordered. This implies that there must be a given value of length do breath ratio of molecule which provides sufficient ordering in LC matrix.

In vivo studies of cosmetic formulations with β -carotene

*Joanna Igielska-Kalwat, Izabela Nowak

Adam Mickiewicz University in Poznan, Faculty of Chemistry, Poland

e-mail: ji11602@amu.edu.pl

Keywords: *In vivo studies, emulsions, volunteers, instrumental testing, β -carotene*

Cosmetic producers have to guarantee the safety and stability of their products. The current legal regulations are based on the European Union Directive (1223/2009) as of 30 Nov. 2009. The main aims of the directive **are strengthened safety requirements for cosmetic products**. A new cosmetic product is subjected to thorough investigations prior to placing it on the market. The new cosmetic formulation should be studied not only with respect to its safety but also with respect to its effectiveness declared by the producer. The studies are performed *in vivo*, by the contact or epidermal patch tests on the human skin.

The *in vivo* studies are performed on healthy selected volunteers. Prior to each test the participants are dermatologically examined. Their type of skin and state of skin are determined. Additionally the information on substances showing allergic response to and other information is collected, e.g. on the past or present skin diseases and the treatment applied and on general state of health. Each volunteer is asked to sign a formal consent to participate in the tests and the person conducting the study is obliged to give details on the study and possible side effects. Each person taking part in the test is given a formal written instruction of the cosmetic use and the questionnaire to be filled when using it. The information from the questionnaire is used for possible further improvement of a given product.

The volunteers apply the tested product twice a day, in the morning and in the evening. The formulation with β -carotene was rubbed on the forearm of one hand, whereas placebo (without an active substance) on the other hand. The test lasted six weeks. During the test the volunteers were not allowed to use any other cosmetic products than the one tested. During the application of the cream with β -carotene any lesions were observed. All volunteers participating in the study did not notice any irritation of the skin during usage. The formulations with β -carotene improve moisturizing and elasticity and reduce transepidermal water loss from the skin.

Manufacturing and characteristics of Al₂O₃-Al functionally graded materials for brake disc application

*Justyna Jakubowska¹, Agata Strojny-Nędzka², Krzysztof Naplocha³, Michał Basista¹, Katarzyna Pietrzak^{1,2}

¹Institute of Fundamental Technological Research Polish Academy of Sciences, Warsaw, POLAND

²Institute of Electronic Materials Technology, Warsaw, POLAND

³Wrocław University of Technology Wrocław, POLAND

e-mail: jjakubow@ippt.pan.pl

Keywords: *FGM, brake disc, interpenetrating phase composite, squeeze casting, tape casting*

FGMs (functionally graded materials) are special type of composite materials usually made of ceramics and metals which accommodate a gradual transition of properties of different materials from one side to the other. They are used to reduce thermal residual stresses in the phase materials. The brake discs can reach high temperatures while operating, so heat should be quickly dissipated away from the braking system. This is ensured by aluminum alloy AlSi12 which is a heat conducting material in the investigated FGM.

Porous ceramic preforms were produced by tape casting method. To produce preforms rice starch was used in ceramic suspensions, which was burned out leaving porosity. Alumina preforms without gradient and one graded preform were infiltrated with AlSi12 alloy. The samples were characterized by electron and optical microscopy. Vickers hardness, thermal diffusivity and thermal conductivity were also measured. The obtained results were compared with the reference values of gray cast iron.

The obtained FGM shows superior properties e.g.:

- thermal conductivity is up to two times higher than the reference material (gray cast iron),
- hardness is considerably higher than that of gray cast iron.

Replacement of gray cast iron with the FGM will reduce thermal stresses and the brake disc mass. Processing of next samples of the FGM is in progress; relevant material properties will be tested (e.g. abrasive wear, friction coefficient, fracture toughness).

Assessment of pollutant content in energy willow growing in Puczniew village

Alicja Zawadzka, *Monika Janas

Faculty of Process and Environmental Engineering, Lodz University of Technology, 93-005 Lodz, Wolczanska 215, POLAND

e-mail: monika.janas90@gmail.com

Keywords: *energy willow, heavy metals, calorific value, heat of combustion*

At present we witness a progressive urbanization of the increasing range of area. As a result, the industry is growing and communication routes extend. Their development is accompanied by an increase in the emission of heavy metals that persists in the air and are deposited in the soil, polluting the environment.

The aim of this study is to assess the content of pollutants in energy willow growing in Puczniew. The analysis was carried out in reference to the usefulness of this type of wood from an experimental plantation as an ecological source of energy generated in the combustion process. For this purpose, the heat of combustion, calorific value and contents of selected heavy metals in energy willow were specified. The last parameter is important because of environmental protection to treat this kind of fuel as a renewable and ecological source of energy. The chemical composition of ash from biomass combustion, especially the content of heavy metals, determines a possibility of its use as a fertilizer.

In order to determine the environmental impact, the results were compared with limit values of these metals in the soil or in the ground, specified in the Regulation of the Minister of Environment of 9 September 2002 on the soil quality standards (Dz. U. 02.165.1359 of 4 October 2002). As a result it was found that the wood of osier grown for energy in the field contained unacceptable amounts of heavy metals. The presence of these elements in the ash from combustion of willow will be an obstacle to its agricultural use.

Based on the results and analysis it can be concluded that willow biomass as fuel provides an ecological and renewable raw material enabling sustainable energy production. It can be used both as a primary fuel – generated in the combustion process, or secondary one – biomethanol. Due to the above mentioned features confirmed by the tests, the species of energy willow can be used for removal of heavy metals, toxic and other compounds from the soil by embedding them in its biomass.

The use of willow is very beneficial from the point of view of environmental protection, the use of fallow land, management of degraded land and reclamation of contaminated sites. These advantages make this raw material a response to future demand for fuel for the Polish agriculture, energy and business, which makes its cultivation very promising.

Nanoporous titanium dioxide layer as substrate for enhanced osteoblast-like cells growth

*Magdalena Jarosz¹, Anna Pawlik¹, Danuta Jarocho², Marcin Majka², Grzegorz D. Sulka¹, Marian Jaskuła¹

¹ Department of Physical Chemistry & Electrochemistry, Jagiellonian University, Ingardena 3, 30-060 Krakow, Poland

² Department of Transplantation, Collegium Medicum of the Jagiellonian University, Wielicka 265, 30-663 Kraków

e-mail: jarosz@chemia.uj.edu.pl

Keywords: *titanium dioxide; anodization; osteoblast-like cells;*

Recently, the most widely used materials for bone-implants are titanium and its alloys. It is due to their good biocompatibility, high strength to weight ratio and excellent corrosion resistance. However, there are some downsides to those materials, such as their inertness and long-term osseointegration via the natural oxide (TiO₂) existing on Ti surface. Therefore, nanoporous materials on Ti surfaces become a novel solution for bone implants. One of such materials are nanoporous anodic titanium oxide (ATO) layers on Ti formed by electrochemical anodization. The main advantage of such materials is a direct growth of TiO₂ on Ti surface, using a simple and cost-effective method of anodic oxidation, and a possibility to modify the surface with antibacterial and anti-inflammatory medicines.

ATO films on Ti foil were prepared via a three-step anodization in an ethylene glycol based solution containing F⁻ ions. ATO layers were then annealed to obtain different polymorphic structures. Modifications of TiO₂ layers with Ag nanoparticles were performed and two different drugs were loaded. Samples were then used for cells culturing and microbial examinations. ATO films were enriched with antibacterial and anti-inflammatory medicines. Furthermore, the drug release profiles showed an extended release of compounds loaded inside the pores. Osteoblast-like cells exhibited preferential growth on the anatase phase. Additionally, anatase phase enriched with gentamicin inhibits the bacterial growth on TiO₂ surfaces.

All in all, nanoporous ATO on Ti may be a promising substrate for the osteoblast-like cell growth and a new potential implant material.

Acknowledgements

Magdalena Jarosz acknowledges the financial support from the project Interdisciplinary PhD Studies “Molecular sciences for medicine” (co-financed by the European Social Fund within the Human Capital Operational Programme).

Novel silver multielectrode sensor for stripping analysis

*Katarzyna Jedlińska, Bogusław Baś

AGH University of Science and Technology, Faculty of Material Science and Ceramics, Mickiewicza 30, 30-059 Kraków, Poland

e-mail: kat.jedlinska@gmail.com

Keywords: *Silver electrode, Stripping voltammetry, Lead, Mercury-free electroanalysis*

Solid-state I electrodes which are made of a noble metals or a carbon materials, for many years have been object of particular interest to electrochemists because of their numerous interesting properties. However, the problems associated with the preparation and renovation of their surface, significantly limit the possibilities of a direct application in the electroanalysis. Moreover a large area of the solid-state electrodes causes expansion of the double layer which results in a decrease of current signal over time.

This work describes a novel type of renovated sensor consist of six silver microelectrodes symmetrically arranged on the lateral surface of the guidewire formed of chemically stable resins. In the prototype version of this sensor microelectrodes were made of pure silver wire (99.999%) with a diameter of 0.5 mm.

Three segments of this wire were attached to a silver rod with a diameter of 1.6 mm, which was properly drilled and then this construction was covered by a resin Translux 180. Then the excess resin was mechanically removed and the surface of the resin and the silver part of the sensor was ground by emery papers of decreasing roughness and was finally polished with 0.05 μm Al_2O_3 powder. The last stage of the preparation of the electrode was through rinsing with a distilled water stream. The electrode is being electrochemically refreshed between measurements.

The usefulness for electrochemical measurements of the sensor was tested for the determination of trace Pb(II) by using a differential pulse anodic stripping voltammetry (DP ASV) in natural water samples. The analysis was performed without the removal of oxygen in the classical three-electrode quartz cell, with sensor described above as a working electrode, Ag/AgCl/3M KCl as a reference electrode and a Pt wire as a counter electrode. To obtain the best measurement conditions three parameters were optimized: pulse amplitude (dE) step potential (E_s) and pulse time as well as composition of the supporting electrolyte. Satisfactory results were obtained in the determination of Pb(II) in the range from 1 to 20 $\mu\text{g}\cdot\text{L}^{-1}$ with an accumulation time of 120 s.

The present study showed that the proposed sensor can be successfully applied for determination of Pb(II) in water samples.

Application of microfibrillar cellulose (mfc) obtained from agro-food byproducts for improved barrier and mechanical properties of paper

*Marek Jotko, Beata Kudawska

West Pomeranian University of Technology Szczecin, Faculty of Food Sciences and Fisheries, Center of Bioimmobilisation and Innovative Packing Materials

Janickiego 35, 71- 270 Szczecin, Poland,

e-mail: marek.jotko@zut.edu.pl

Keywords: *microfibrillar cellulose, byproducts, barrier properties, mechanical properties*

A large amount of research has been done in recent years to help us understand the unique features of microfibrillar cellulose (MFC). Their large surface area in a compact size and high capacity for gel formation are the main reasons for special interest in MFC in the subject of research in materials technology.

Barrier properties of MFC are particularly interesting because they can solve the problems of the weakness of traditional packaging made from paper and open a new way to pack entirely from renewable sources.

MFC may be used as a coating on paper or paperboard, because of the chemical homogeneity of the substrate gel and the possibility of having it dispersed in water. In comparison to the other coating systems its advantages are high flexibility, no need of usage any adhesive substance and low manufacturing costs.

By-products can be processed in the eco-friendly method with the use of enzymatic treatment and mechanical processing. Thus obtained product will be used for paper coatings to achieve unique properties such as increased oxygen and water vapor barrier and improved mechanical resistance to puncture and bursting.

Even though our community is not so concerned about the lack of biodegradable packages in the market right now, it is important that investments in research of biodegradable packaging materials have been increased. We need to be more aware of the importance of this type of packaging. It seems necessary to carry out extensive research, which will eventually lead to the implementation of the resulting ideas.

Assessing the applicability of 2H-1-benzopyran-2-one derivatives as a fluorescent molecular sensor for on-line monitoring photopolymerization processes.

*Iwona Kamińska, Magdalena Czarna, Joanna Ortyl

Faculty of Chemical Engineering and Technology, Department of Biotechnology and Physical Chemistry Cracow University of Technology, Cracow, POLAND

e-mail: i.kaminska@chemia.pk.edu.pl

Keywords: *fluorescent probe, coumarin, photopolymerization, free radical polymerization, photo-differential scanning calorimetry*

Acrylate monomers are crucial components in the formulation of coatings, inks, and adhesives. They are polymerized by UV light in the presence of appropriate photoinitiator and react fast, which is very important in rapid cure technologies. Quality of the polymeric product depends largely on the process conditions, therefore, photopolymerization reactions require monitoring changes in a polymerizing composition. Fluorescent probe-based monitoring, which is highly sensitive and precise, is modern method of monitoring photopolymerization processes.

In the FPT method (Fluorescent Probe Technology) fluorescent compound, dissolve in a polymerizing system, is used as molecular sensor of changes occurring in its surroundings. Monitoring on-line of progress photopolymerization reaction using by FPT technique provide valuable information about the reaction kinetics. Addition of a fluorescent probe to the reacting composition, even at such a small concentration as 0.01 - 0.5% by weight, allow to monitor changes in the reaction environment at each stage of polymer network formation.

The behavior in polymerizable media of 2H-1-benzopyran-2-one derivatives has been studied. The performance of 3-carboxy-coumarin derivatives in the role of fluorescent probes for monitoring progress of free-radical photopolymerization of a series of multifunctional acrylic monomers by the FPT method is reported. The response of the probe's emission to changes in its environment during polymerization was determined. Photo-differential scanning calorimetry (photo-DSC) was used to investigate the cure kinetics for the UV-initiated radical photo-polymerization of acrylate compositions.

Acknowledgments

Research financed within the project LIDER (LIDER/014/471/L-4/12/NCBR/2013) by The National Centre for Research and Development (NCBiR).

Analysis of the stability of cosmetic emulsion containing jasmonates using the multiple light scattering phenomenon

*Alicja Kapuścińska¹, Anna Olejnik¹, Izabela Nowak¹

¹ Adam Mickiewicz University in Poznan, Faculty of Chemistry, Applied Chemistry Laboratory, Poznan, POLAND

e-mail: ak75416@st.amu.edu.pl

Keywords: *jasmonates, emulsion stability, multiple light scattering.*

Multiple light scattering (MLS) phenomenon is used inter alia in the analysis of the stability of the emulsion. Apparatus that uses MLS phenomenon is Turbiscan Lab Expert, where the source of light is electroluminescence diode emitting photons (near infrared light source with a wavelength of 880nm) into the sample. These photons, after being scattered many times by the particles (or droplets) in the dispersion emerge from the sample and are detected by the 2 detectors of the Turbiscan reading head. One of detectors collects backscattered light, whereas the another one collects transmitted light. The phenomenon of light transmission is used for transparent samples, while light backscattering is preferred for opaque samples.

Presented technique allows to monitor particle size changes versus time, local particle concentrations change versus time as well as measure particle mean diameters or concentration changes while the sample is destabilizing. Therefore, different types of emulsion destabilization can be detected. Additionally, the emulsion instability associated with the migration of the dispersed phase particles without changing their size (emulsion sedimentation and creaming) as well as instability related to changes in the particle size of the internal phase emulsion (coalescence and flocculation) can be distinguished.

Three types of emulsion (heat process o/w emulsion prepared in the traditional heat process, cold process o/w emulsion prepared with the addition of auto emulsifier and heat process w/o emulsion) containing jasmonates, plant hormones that accelerate the regeneration of the skin and accelerate the desquamation, were prepared. For a period of 100 days with the use of Turbiscan, changes in the samples have been studied. The effect of jasmonates on cosmetic emulsion stability (with respect to the stability of a cosmetic base) as well as the influence of emulsion storage conditions (temperature 25 vs. 5°C) was examined. With reference to the findings, jasmonates have little effect on the emulsion stability compared with the cosmetic base, so they can be active ingredients of cosmetics. Moreover, refrigerated products display higher stability as against to those stored at room temperature.

The use of diffusion phenomena in the theoretical model of active substances transdermal transport

*Alicja Kapuścińska¹, Izabela Nowak¹

¹ Adam Mickiewicz University in Poznan, Faculty of Chemistry, Applied Chemistry Laboratory, Poznan, POLAND

e-mail: ak75416@st.amu.edu.pl

Keywords: *diffusion kinetics, transdermal transport, active cosmetic substance*

The active substance is called a cosmetic substance which has a physical or physico-chemical effect on the skin. The efficacy of such substance is dependent on many factors such as size of the particles, chemical characteristics and condition of the skin. Molecules of smaller size and lipophilic nature easily penetrate the skin barrier, as compared to larger hydrophobic particles. The effectiveness of the active substance depends also to a cosmetic base, wherein the substance is located. The lower the viscosity of the cosmetic base is, the greater percentage of active substance release is observed.

In the most cases, the transport of active ingredients into the skin is based on the phenomenon of diffusion. Analysis of the kinetics of this phenomenon, in suitable laboratory conditions for the active substance enables the creation of a theoretical model of substance diffusion through the skin barrier. For this purpose, the diffusion apparatus Agilent Technologies 708-DS s used.

During the measurement the extraction chamber containing tested active substance in cosmetic formula, protected from moving with special membrane imitating the skin barrier, is placed into a vessel. Each vessel should be filled with an acceptor liquid, called also a medium. When measuring the contents of the vessel, it is mixed with paddles.

Medium properties have a significant impact on the results of the substance release. An important parameter of the medium is its pH value. When selecting the medium, its similarity to the physiological conditions of the skin has to be considered. Depending on the solubility of the active substance,, aqueous solutions (substances soluble in water) or aqueous alcoholic (sparingly soluble substances in water) are used. Usually, the dissolution apparatus is connected to a UV-Vis spectrophotometer. The UV-Vis detector allows the analysis of the released substance amount during the absorbance changes of the medium as a function of time. There is the limit for the use of this method for substances that do exhibit the ability to absorb radiation at the wavelength range characteristic for used detector.

The crystallization pathway and photocatalytic activity of Bi₂WO₆ microflowers

*Zsolt Kása¹, Kata Saszet², Zsolt Pap^{1, 2, 3}, Gábor Kovács^{2, 3}, András Dombi¹, Klára Hernádi¹, Lucian Baia³, Virginia Danciu²

¹Research Group of Environmental Chemistry, University of Szeged, Szeged, HUNGARY

²Faculty of Chemistry and Chemical Engineering, University of Babeş-Bolyai, Cluj-Napoca, ROMANIA

³Faculty of Physics, University of Babeş-Bolyai, Cluj-Napoca, ROMANIA

e-mail: chemkasa@gmail.com

Keywords: hydrothermal synthesis, bismuth tungstate, visible light driven photocatalysis

Nowadays semiconductor photocatalysis is getting high attention due to its wide applications in solar energy conversion and degradation of organic pollutants. Bismuth-tungstate (Bi₂WO₆) is attracted a great deal of attention as a new photocatalyst with a potential of excellent photocatalytic performance under visible light irradiation.

In this study, Bi₂WO₆ photocatalysts with different morphologies were synthesized by a one step hydrothermal method. The resulted 3D structures (e.g. “flowers”) (d≈2 µm) were constructed from individual nanoplates (d≈50 nm). The synthesis procedure involved acetic acid, surfactants (Triton X-100) and thiourea. These shaping reagents’ effects were also investigated in-detail. The crystallization was performed using the well-known hydrothermal pathway.

The crystal growth was investigated in the frame of the hydrothermal treatment parameters, taking under the loupe especially the duration of the hydrothermal treatment. The obtained microcrystals were analyzed using scanning electron microscopy (SEM), X-Ray diffraction (XRD), Raman and infrared (IR) spectroscopy, while the optical features were followed by diffuse reflectance spectrometry (DRS). A supplementary calcination was also applied to increase the crystallinity grade of the obtained photocatalysts. At 400 °C the individual nanoplates were sintered while at 1000 °C the 3D structure vanished.

The above mentioned morphological changes influenced significantly influenced the photocatalytic activity, which was evaluated successfully for the degradation of Rhodamine B (RhB) under visible light irradiation.

The main objective was to correlate the photocatalytic performance and morphological features (3D flowers→microplates→sintering of the microplates) of the Bi₂WO₆ particles.

The financial support was provided by the Campus Hungary Programme (TÁMOP-4.2.4.A/2-11/1-2012-0001) and the Swiss Contribution (SH/7/2/20).

Sawdust pellets from coniferous species as precursors of carbonaceous adsorbents

*Justyna Kazmierczak-Razna, Barbara Gralak-Podemska, Piotr Nowicki, Robert Pietrzak

Faculty of Chemistry, Adam Mickiewicz University in Poznań, Poznan, POLAND

e-mail: justykaz@amu.edu.pl

Keywords: *microwave radiation, sawdust pellets, adsorbents, toxic gases removal, activation*

Activated carbons can be produced from various precursors containing carbon in organic bonds. Taking this into regard and in view of high cost of fossil coals as well as economical and ecological aspects, recently much attention has been paid to the use of waste products of plant origin as precursors of carbon. So far the suitability of corn cobs, cherry or plum stones, coconut or walnut shells as precursors has been checked.

The aim of this work was to obtain a series of activated carbons from pine tree sawdust with the use of microwave radiation as well as examination of their physico-chemical properties and sorption capacity towards gas phase pollution. Different preparation parameters were examined in order to evaluate the influence of activation conditions on the adsorption properties of the final product.

At the beginning the precursor was subjected to pyrolysis in a microwave oven (Phoenix, CEM). This process was carried out under a stream of nitrogen with a flow rate of 0.170 L/min. The sample was heated from room temperature to the final pyrolysis temperature of 400 and 500°C. In the final pyrolysis temperature, sample was kept for 60 min and then cooled down. The products of pyrolysis were next subjected to physical activation which was carried out at two temperatures 600 and 700°C under a stream of carbon dioxide with a flow rate of 0.250 L/min, for 30 min. Some part of the precursor was also subjected to direct activation with CO₂, which was performed in the same conditions as physical activation.

The activated carbons obtained were characterised by elementary analysis, surface area measurements (BET) and estimation of the number of surface oxygen groups by the Boehm method. The sorption properties of the materials obtained were characterised by nitrogen dioxide and hydrogen sulfide adsorption in dry and wet conditions.

The results obtained in our study have proved that a proper selection of the pyrolysis and activation procedure for sawdust allows to produce activated carbons with high NO₂ adsorption ability, reaching to 86 mg NO₂/g_{ads}.

Extraction methods of ranitidine isolation from natural water

*Ilona Kiszkiel

Institute of Chemistry, University of Bialystok, Bialystok, POLAND

e-mail: i.kiszkiel@uwb.edu.pl

Keywords: *H₂ receptor antagonists, extraction techniques, surface water analysis*

Pharmaceutically active compounds are widely used and are released into the environment as a result of unsuitable utilization from households and hospital wastes. The emerging of pharmaceutical residues in natural water harmfully influences for human health and aquatic organisms. Therefore, monitoring environmental contamination by these compounds is necessary. The different groups of pharmaceuticals are frequently found in wastewater and surface water samples including histamine H₂ receptor antagonists. These pharmaceuticals, especially ranitidine, are usually used for treatment of duodenal and gastric ulcers. Ranitidine is hydrophilic compound and exhibits the basic chemical properties. This compound is metabolized to their N-oxide and S-oxide and is excreted in 70% in unchanged forms. The discussed histamine H₂ receptor antagonists were found in natural water at the very low level concentration (in the order of magnitude of ng L⁻¹ up to the µg L⁻¹). Additionally, the similar components in structures of these pharmaceuticals introduce difficulties during their selective determination. Therefore, analysts are forced to develop extraction methods for effective isolation of these compounds.

The performed studies describes elaborated procedures for selective ranitidine isolation following by different extraction techniques. In this purpose, solid phase extraction and micellar extraction methods were elaborated. In the first isolation method, ranitidine is adsorbed on the Oasis HLB column, while in micellar extraction, the studied analyte is solubilized in the hydrophobic core of the micelles of surfactants (Triton X-114 and sodium dodecylsulfate). The extracts were determined by spectrophotometric and high performance liquid chromatography methods with ultraviolet detection system (HPLC-UV). The obtained results indicate that the elaborated methods allow for effective isolation of ranitidine and their separation from other H₂ receptor antagonists. These methods are characterized by wide range of linearity. Additionally, the ultrasound assisted extraction of ranitidine and single drop microextraction of this drug have given possibility for detection of studied analyte at the low level concentrations. The elaborated methods will be applied for determination of ranitidine in the river water wastewater samples.

Influence of the reaction time on the epoxidation of linseed oil with performic acid

*Marlena Kłos¹, Eugeniusz Milchert, Kornelia Malarczyk

¹Faculty of Organic Chemical Technology, Institute of Organic Chemical Technology, West Pomeranian University of Technology in Szczecin, Szczecin, POLAND

e-mail: marlena.klos@zut.edu.pl

Keywords: *epoxidation, linseed oil, peracetic acid*

The epoxidation of double bonds in linseed oil using peracids forms an epoxy groups. Linseed oils have traditionally been used as drying oils in the manufacture of paints and varnishes. Linseed oil is triglycerides consisting of a mixture of saturated, oleic, linoleic and linolenic fatty acid. Linseed oil can be used for preparing novel plasticizers, elastomers, polyols used in the production of polyurethanes, novel or modified lubricating agents, modifiers of epoxy resin properties and others.

The epoxidation study was conducted in the following manner. The required amount of linseed oil was placed in a glass reactor capacity 250 mL, equipped with turbine agitator, reflux condenser, dropping funnel and thermometer. The reactor was located in a thermostated oil bath. During stirring, the reactor was charged with a known amount of formic acid and the catalyst (H₂SO₄), and then a 30 wt% aqueous hydrogen peroxide was slowly added. The reaction was further continued for a 2, 4, 6, 8 and 10 hours. After a defined time of process duration, a sample was collected for analysis, the content was cooled to the ambient temperature, a separated organic layer was neutralized by a 5 wt% solution of sodium carbonate to obtain the pH=7, the organic layer was rinsed with distilled water and dried over anhydrous MgSO₄. The course of process was controlled by determination of the epoxy and iodine number.

The most favorable time of epoxidation of linseed oil with performic acid, formed "in situ" in the reaction of formic acid with a 30 wt% hydrogen peroxide in the presence of sulphuric acid(VI) is 10 hours. At this time the epoxy number was achieved EN=0.45 mol/100g and the iodine number IN=0.11 mol/100g.

Rheological properties of liquid surface layer in selected commercial instant coffee

*Joanna Kmiecik, Janusz Dobrychłop

Faculty of Chemical Technology, Poznan University of Technology, Poznan, POLAND

e-mail: joanna.j.kmiecik@doctorate.put.poznan.pl

Keywords: *interfacial shear rheology, instant coffee, foam*

Interfacial rheology is important for food dispersions since the structural and mechanical properties of food emulsifiers at fluid interfaces influence the production, stability and texture of the product. Interfacial rheology technology provides information on the behavior and interaction of molecules at interfaces, which is important for the application and processing of many materials of the general type, for example beverages and foods. The shear rheology of interfacial layers at gas/liquid or liquid/liquid phase boundaries is relevant in a wide range of technical applications, especially in colloidal systems which comprise large interfaces, such as foams and emulsions.

The aim of the study was to compare the interfacial rheology properties of instant coffee samples. The taste qualities of instant coffees are mainly determined by such factors as the amount and stability of foam emerging on the surface. Stability of the foam is related to the rheological properties of the liquid, from which the bubble's walls are made.

Interfacial rheological measurements were determined applying rotational rheometer Physica MCR 501 by Anton Paar (Graz, Austria) equipped with Interfacial Rheology System (IRS). IRS has bicone geometry with diameter 68.243mm, penetration depth 2.214mm, angle 4.997° and truncation 46 µm. In this paper a comparison of the interfacial rheological properties of three different instant coffees (Jacobs Krönung, Tchibo Gold Crema, Douwe Egberts Crema Silk) is presented.

On the basis of these results, it was found that the tested coffees are Newtonian fluids while the interface area has viscoelastic properties. There were also observed a relationship between the stability of the foam of the coffees and viscoelastic properties of the interface.

Application of UV spectrophotometry in the quality control of galactooligosaccharides production

Sára Koncz¹, Ferenc Firtha², *Zoltán Kovács¹

¹Department of Food Engineering, Corvinus University of Budapest, Hungary

²Department of Physics and Control, Corvinus University of Budapest, Hungary

e-mail: zoltan.kovacs5@uni-corvinus.hu

Keywords: *galactooligosaccharides, online monitoring, UV spectrophotometry, partial least square regression, prebiotics, chemical analytics, chemometrics*

Galactooligosaccharides (GOS), hence they have a positive effect on the microbial composition of the gut, are considered as prebiotics. From lactose as substrate, GOS are produced by enzymatic synthesis with β -galactosidases. In the industrial practice of GOS production, batch reactors are widely used. In order to make the process more effective and to reduce costs, other configurations, like enzyme membrane reactors or immobilized enzyme reactors operating in continuous fashion, can be considered. The implementation of such processes requires the online monitoring of the quality of the product stream.

The enzymatic reaction results in a saccharide mixture consisting of non-reacting lactose, GOS of various degree of polymerization, and glucose as by-product. The standard chemical analysis of such multi-component products involves High Performance Liquid Chromatography (HPLC). Although HPLC is reliable and accurate, it is generally considered as a time-consuming, expensive, and offline method.

This research deals with the development of an online technique that allows the real-time monitoring of carbohydrate composition during the production of GOS. For that purpose, we considered ultraviolet-visible (UV) spectrophotometry combined with partial least squares regression (PLSR). UV spectrophotometry is known as a fast and inexpensive quantitative method which enables continuous sampling. PLSR is a bilinear technique that extracts the most relevant information as a mathematical model of linear combinations of the spectral bands to predict a property of interest (chemical, physical or sensory attributes) of different samples.

More than eighty samples, containing various amounts of mono-, di-, and oligosaccharides, were generated in our lab by using an enzyme membrane reactor. UV spectral data of the samples were used together with the respective concentration data quantified by HPLC, in order to develop a PLSR model. The proposed model predicts the carbohydrate composition well. Our results show that UV spectral data combined with PLSR data processing can be used in quality control of continuous GOS production.

Synthesis of silica-templated three-dimensional graphene xerogels

*Izabela Kondratowicz, Kamila Żelechowska, Wojciech Sadowski

Faculty of Applied Physics and Mathematics, Gdańsk University of Technology,
Gdańsk, POLAND

e-mail: ikondratowicz@mif.pg.gda.pl

Keywords: *porous carbons, graphene xerogel, graphene oxide, silica particles,*

Porous carbonaceous materials are of great scientific and industrial interest due to their low cost, good electrical conductivity and high surface area. Most porous carbons require the uniform pore size distribution as well as the specific pore diameters in order to adsorb different molecules. Therefore many approaches were applied to template the carbon scaffold and among them the use of silica particles is by far the most widespread. Moreover the possibility to assemble graphene sheets- one-atom thick layer of graphite- into a three-dimensional structure gives a new promising material called graphene xerogel (GX) which exhibits better electrical and mechanical properties.

In our work we control the architecture of graphene xerogels by the use of silica particles of different sizes (50, 150 and 300 nm). Graphene xerogel is prepared via chemical oxidation of graphite. As-obtained graphene oxide (GO) is then mixed with silica spheres and subsequently reduced hydrothermally in order to obtain a three dimensional material. The spheres are then etched using the HF solution. To the best of our knowledge there is no previous studies relating the pore size distribution of the silica-templated graphene xerogels with their specific surface area. The materials were characterized by FTIR spectroscopy and SEM microscopy. BET surface area was determined by recording nitrogen adsorption/desorption isotherms.

The results show that the use of silica spheres of different sizes enables to create pores that are either accumulated on a surface or in a bulk of the xerogel depending on the sequence of the reaction. Firstly, we studied the mass ratio of GO to SiO₂ (10:1 and 1:1) that needs to be satisfied to ensure the homogeneous coverage of the reduced graphene oxide sheets on the silica surface. We also examined a use of a surfactant that helped to stabilize the graphene oxide-silica suspension and thus to create the 3D structure.

Our study reveals the new material with the well-ordered inner structure that can be used as a complete electrode in many different devices such as lithium-ion batteries, fuel or biofuel cells and biosensors.

Preparation of abrasion resistant ceramic – intermetallics composites using sintering method with the exothermic reaction

*Mateusz Kopec

Military University of Technology, Faculty of Advanced Technology and Chemistry

Kaliskiego 2, 00-908 Warsaw, Poland

e-mail: mateusz.kopec1990@gmail.com

Keywords: *cermets composites, reaction synthesis, powder metallurgy*

The paper contains the preliminary attempts to produce a ceramic – intermetallics composites by sintering powders of iron, aluminum and mullite using the self-propagating high-temperature synthesis SHS combined with the phenomenon of liquid metal infiltration of a porous ceramic. The experiment involved four powder mixtures of iron, aluminum and mullite, involving different oxide phase. In order to consolidate the powder mixtures were used sided die pressing treatment, and then sintered in a vacuum molding involving the SHS reaction. On the basis of differential thermal analysis, DTA, defined agglomerates obtained homogenization temperature , which then underwent at 600°C for up to 200h. In order to verify the applied technological parameters and their influence on the properties of the manufactured material, samples were subjected to structure observation (SEM), the chemical composition analysis (EDS), phase analysis (XRD), the compression test and measurement of microhardness, Young modulus and fracture toughness. The resulting material properties are compared using CES with previously used, conventional construction materials.

Graphene oxide coating used to modified method of interference-wedge in the study of optical parameters in the nematic liquid crystal.

*Krystian Kowiorski¹, Jerzy Kędzierski¹, Ludwika Lipińska², Maciej Chronik¹,

¹Department of Advanced Technologies and Chemistry, Military University of Technology, Warsaw, POLAND

²Institute of Electronic Materials Technology, Warsaw, POLAND
e-mail: kkowiorski@wat.edu.pl

Keywords: *birefringence, graphene, liquid crystals, refractive indexes, nematics*

In this paper we present the modified method of interference wedge that can be applied to determine the refractive indices for ordinary (n_o) and extraordinary beam (n_e) in nematic liquid crystals (NLC), as well as their anisotropy (Δn). It is believed that described method does not have any limits within measured values of the n_o and n_e refractive indexes. In this study the graphene oxide coating was used as the ordering layer. This kind of coating possesses similar properties comparing to polyimide. However, the as-prepared surface structure does not need to be rubbed in additional process. Scanning Electron Microscope (SEM) technique was used to allow us to image the topography of glass (without and covered with ordering layer) used to make the wedges.

***Tert*-butanol as radical scavenger material for investigation of heterogeneous photocatalysis and other advanced oxidation processes**

*Zsuzsanna Kozmér^{1,3}, Liliána Póta¹, Tünde Alapi^{1,2}, Erzsébet Takács³, László Wojnárovits³, András Dombi¹

¹Research Group of Environmental Chemistry, University of Szeged, Szeged, HUNGARY

²Department of Inorganic and Analytical Chemistry, University of Szeged, Szeged, HUNGARY

³Department of Radiation Chemistry, Centre of Energy Research, Hungarian Academy of Sciences, Budapest, HUNGARY

e-mail: kozmerzs@chem.u-szeged.hu

Keywords: *phenol, vacuum ultraviolet photolysis, radiolysis, O₂*

Advanced oxidation processes, for example the heterogeneous photocatalysis (*H*) based on TiO₂, the vacuum ultraviolet photolysis (*V*) and the gamma radiolysis (*R*) are promising alternatives for water purifying. Using these methods the destruction of the target compounds takes place through reactions with reactive species ([•]OH, H[•], e⁻, h⁺, HO₂[•]/O₂^{•-}). For the optimization of the degradation pathways accurate knowledge of the mechanisms is needed, for example the role of the less reactive radicals. Our study aimed to investigate the effects of *tert*-butanol as radical scavenger material on the radical set during *H*, *V* and *R* on the example a simple model compound, phenol.

In the experiments 250 mL 1.0×10⁻⁴ mol L⁻¹ aqueous phenol solutions or suspensions (1.0 g L⁻¹ TiO₂) were irradiated with UV_{365 nm}, VUV_{172 nm} or γ photons during *H*, *V* and *R*, respectively. The samples contained 0.500 mol L⁻¹ *tert*-butanol to transform mainly [•]OH to the carbon-centred radicals of low reactivity. The solutions were bubbled with N₂ or O₂ gas before and throughout the irradiation. The degradation rate of phenol was followed using high performance liquid chromatography with UV detection.

In O₂-free solutions, the radical scavenger material increased the degradation rate of phenol in the case of *H* and *V*, however decreased it during *R*. On the contrary, in O₂-saturated solutions the degradation rate of phenol decreased for all methods in the presence of *tert*-butanol.

The most significant effect of *tert*-butanol was obtained during *R* and it has the most slightly effect during *V*.

Research on optimally balanced bioelements rate in *in vitro* cultured mushroom

*Agata Krakowska¹, Bożena Muszyńska², Witold Reczyński¹, Bogusław Baś¹, Małgorzata Wolska¹

¹AGH University of Science and Technology, Faculty of Materials Science and Ceramics, St. A. Mickiewicza 30, 30-059 Cracow

²Jagiellonian University Collegium Medicum, Department of Pharmaceutical Botany, St. Medyczna 9, 30-688 Cracow

e-mail: asmalec@agh.edu.pl

Keywords: *elements, in vitro cultures, analysis, AAS*

Bioelements are significant for proper functioning of the human body. These elements deficiency, as a result of unbalanced diet, may lead to numerous disorders, so enrichment of food products with bioelements is reasonable. Characteristic feature of higher fungal mycelium is its readiness to absorb and accumulate minerals from the environment. For the research in the project species of *Agaricus bisporus* (J.E. Lange) Imbach was selected, due to its health-promoting qualities (antimutagenic activity, radiation protective features) and popularity among consumers. The potential use of mycelium as medium for bio-elements accumulation is due to the fact that it is of natural origin, contradictory to synthetic pharmaceutical products. The main aim of the study was to obtain fruiting bodies of *Agaricus bisporus* enriched with certain bioelements.

The material subjected to examination consisted of fruiting bodies of mushrooms derived from *in vitro* culture. A desired ratio of the individual elements concentrations was obtained by chemical modification of composition of the media and monitoring of *in vitro* culture at the stage of culture. The culture media were enriched with copper, zinc, magnesium and iron.

Mycelia obtained from *in vitro* cultures were lyophilized and then subjected to microwave digestion. Optimal conditions of *in vitro* cultures in terms of chemical composition and pH of the media and environmental factors were determined by monitoring biomass yield. After quantitative determination of microelements by atomic absorption spectrometry the rate of accumulation in *in vitro* cultures was determined.

For the obtained results, chemometric analysis of PCA and CA was carried out. The results of metals determination the fruiting bodies of *Agaricus bisporus* are as follows Zn: 450.5 - 4462.0 µg/g, Mg: 323.5 - 10550.0 µg/g, Cu: 117.0 - 4489.0 µg/g, Fe: 622.5 - 16127.0 µg/g.

Analyzed *Agaricus bisporus* fruiting bodies are characterized by high content of Mg and Fe. Mycelia from *in vitro* cultures of *Agaricus bisporus* may comprise matrix that allows monitoring of microelements accumulation. Based on our analysis of similarity (CA), it was observed that the various elements are characterized by being very similar volatility. For a given cluster, clear positive correlation between elements' concentrations variability was observed.

ANALYSIS OF SELECTED MICRO AND MACRO ELEMENTS IN *IN VITRO* CULTURE of *Bacopa monnieri*

*Agata Krakowska¹, Maciej Łojewski², Bożena Muszyńska², Witold Reczyński¹,
Małgorzata Wolska¹

¹AGH University of Science and Technology, Faculty of Materials Science
and Ceramics, al. A. Mickiewicza 30, 30-059 Cracow

²Jagiellonian University Collegium Medicum, Department of Pharmaceutical
Botany, ul. Medyczna 9, 30-688 Cracow

e-mail: asmalec@agh.edu.pl

Keywords: *Bacopa monnieri*, AAS, serotonin, anthranilic acid

Bacopa monnieri (L.) Pennell (water hyssop), known locally in India as Brahmi or Jalamimba, is one of the most interesting and important plants in the traditional Hindu system of medicine. The richness of this plant due to the content of important physiologically-active compounds such as triterpenoid saponins, alkaloids, herpestine and steroid compounds. It also exhibits antidepressant, antioxidant, antibacterial and antitumor effects. The aim of the presented work was to create composition of *in vitro* medium which guarantees the optimal increase of biomass, optimal concentration of the chosen organic compounds which lead to maximal accumulation of the selected physiologically active elements.

To obtain samples with expected amount of the chosen elements, culture media composition was modified. *In vitro* culture medium was enriched with serotonin, anthranilic acid and magnesium respectively, in various combinations of concentrations. Finally collected plant material was lyophilized and wet digested. In the prepared material concentrations of the selected macro- and microelements were determined by means of AAS method.

The concentrations of microelements in culture *in vitro* of *B. monnieri* enriched with serotonin are Zn: 131.1 -189.3 µg/g; Mg: 665.9 - 2104 µg/g; Cu: 0.8371 – 2.560 µg/g; Fe: 74.07 - 233.9 µg/g; Ca: 954.3 - 1640 µg/g; Na: 552.1 – 1502 µg/g; with anthranilic acid: Zn: 54.75 -154.5 µg/g; Mg: 20560 - 57410 µg/g; Cu: 0.7455 – 3.706 µg/g; Fe: 63.17 - 194.1 µg/g; Ca: 968.7 - 3025 µg/g; Na: 279.2 – 702.4 µg/g.

Obtained biomass from *in vitro* culture of *Bacopa monnieri* is material rich in physiologically active elements important for humans. Plant material is the source of physiologically active bioelements. An increase has been observed of content of Mg in *in vitro* culture enriched with anthranilic acid. Substantial increase of the essential microelements concentrations in the collected plant material was the result of properly selected composition of *in vitro* culture medium.

Cellulose acetate membranes for dyes removal from liquid phase

*Joanna Krason, Robert Pietrzak

Faculty of Chemistry, Adam Mickiewicz University in Poznań, Poznan,
POLAND

e-mail: asia.krason@amu.edu.pl

Keywords: *polymer membranes, dyes removal, separation*

Membrane filtration is one of the popular method used in environmental protection. It is used to remove different pollutions from liquid phase such as heavy metal ions, organic compounds or dyes. Membranes can be produced from different polymers such cellulose acetate, polyethersulfone or polysulfone. During the membrane synthesis we can add pore generating agent (e.g. polyvinylpyrrolidone) to obtain more efficiency membrane. Phase inversion is the method that allows to obtain a porous polymer membranes. This method consists of immersing the mixture of polymers and solvent in a coagulation bath (with deionized water) after evaporating solvent, As a result of this process we can obtain flat sheet porous membrane.

Dyes are commonly used in various industry branches such as paper, cosmetic, textile, pharmaceutical and many others. It is known they are cancerogenic, mutagenic and cause many diseases both for people and animals. There are many ways to remove these pollutants from water, e.g. using activated carbons, ordered mesoporous materials or membrane filtrations.

The purpose of this work was to obtain cellulose acetate membranes with polivinylpyrrolidone and to characterize their sorption properties of dyes from liquid phase.

The experiments were performed using compressed nitrogen gas and dyes solutions. Final concentrations of testing solutions after experiments were analyzed using an UV-Vis spectrophotometer (Varian Cary 100 Bio).

Furthermore, we determined porosity, equilibrium water content, contact angle, content of surface oxygen groups, water flux and membrane resistances.

Cyclodextrin production from different types of starch - kinetic characteristics

*Beata Kudawska, Marek Jotko

West Pomeranian University of Technology Szczecin, Faculty of Food Sciences and Fisheries, Center of Bioimmobilisation and Innovative Packing Materials Janickiego 35, 71- 270 Szczecin, Poland,

e-mail: beata.kudawska@zut.edu.pl

Keywords: *cyclodextrin, starch, kinetic*

Cyclodextrins (CDs) are water soluble cyclic oligosaccharides built up from D-glucopyranose units linked by α -1,4-glycosidic bonds. They have multiple applications in analytical chemistry, agriculture, pharmaceutical and the nutrition field. They are also used in food and packaging industry for flavor protection and delivery.

Three well known, industrially produced cyclodextrins (α , β and γ) are formed by six, seven and eight glucopyranose units, respectively. Structure of the CD molecule resembles hollow truncated cone with a special internal cavity. Because of this hydrophobic cavity they can easily create molecular host/guest-type inclusion complexes with different substances. The cavity provides a special microenvironment for nonpolar molecules but the outer surface is hydrophilic what makes CDs water-soluble. The formation of inclusion complexes is one of the most fascinating properties of cyclodextrins.

Cyclodextrins can be produced by enzymatic bioconversion of starch using cyclodextrin glucanotransferase enzyme (CGTase). In this study the kinetic characteristics of cyclodextrin production by a CGTase produced by genetically modified *Bacillus licheniformis* was investigated. As the substrates for enzyme action corn, waxy corn and potato starch were examined. This study provided the necessary information that may be useful to find the most suitable conditions for production of cyclodextrin with the high yield and productivity.

Transition Metal Oxides influence on phosphate and borate glasses structure

*Tomasz Lewandowski¹, Leszek Wicikowski¹, Marta Przesniak-Welenc¹, Leon Murawski¹

¹Faculty of Solid State Physics, Gdansk University of Technology, ul. Gabriela Narutowicza 11/12 80-233 Gdansk, POLAND

email: tlewandowski@mif.pg.gda.pl

Keywords: transition metal, FTIR, glass materials, DSC

Due to many potential luminescence and optical applications, phosphate and borate glasses are one of the most often studied amorphous materials. In recent years these glasses, doped with transition metal oxides (TMO), gained much attention due to their tunable structural and thermal properties. Many authors reported systems based on phosphate, silicate, borate glasses that contained high amount of transition metal atoms such as Fe, Mn, Zn, V that greatly influenced materials properties such as density, viscosity, thermal stability or fracture resistance. Review of structural characterization papers of such systems is presented.

Binary MnO-P₂O₅ and MnO-B₂O₃ systems are introduced. In this work xMnO-(100-x)P₂O₅ and xMnO-(100-x)B₂O₃ (where x = 40, 50 and 60 mol%) glasses have been synthesized and compared. To melt the obtained mixtures conventional melt-quenching technique has been used in both cases. Amorphous material has been obtained in case of both systems.

Infrared spectroscopy studies (FTIR) shown some structural modifications in function of MnO content. It is proposed that MnO causes degradation of structural units of both phosphate and borate glasses. FTIR spectra show some evidence of such process including bands from Q₀ species in case of phosphate glass and diborate groups in case of borate glass systems. However no direct evidence for Mn-O bonds in glass structures has been found. Additional DSC studies presented different effect on T_g and melting temperature in case of considered systems. Further, TMO affects differently the thermal stability of considered glasses. In examined compositional range MnO is found to decrease thermal stability in case of phosphate glass and increase it in case of borate glass. Structure and thermal properties changes induced by MnO have been observed. Thermal properties change may be connected with structural modifications caused by transition metal oxide. Additionally, at that high MnO concentration level new continuous network of this oxide could be created what might influenced properties of obtained glass samples.

Energetic properties of a new salt of TNBI

Rafał Lewczuk¹, Mateusz Szala¹

¹Military University of Technology, Department of Explosives
ul. gen. S. Kaliskiego 2, 00-908 Warsaw, Poland

e-mail: rlewczuk@wat.edu.pl

Keywords: *TNBI; energetic salts; high-nitrogen compounds*

High-energetic salts of explosives which can form ionic compounds could have more advantages than classic explosives. Cations and anions with high nitrogen content cause improvement in density, standard enthalpy of formation and oxygen balance. During decompositions of these compounds large amount of gaseous products are formed. For that reasons the salts could be introduced to many civilian and military applications.

An example of such material is a semicarbazidium salt of 4,4',5,5'-tetrinitro-2,2'-biimidazole (TNBI). The salt can be easily prepared from widely available substrates. After filtration and drying, it shows no signs of hygroscopicity and decomposes at 187°C. The structure of newly obtained compound was confirmed with NMR spectroscopy. Thermal properties were investigated with DTA/TG analysis. We also determined standard enthalpy of formation. Detonation parameters were calculated with CHEETAH code for density determined for pressed sample. Detonation ability and velocity of detonation was measured experimentally.

Effect of the electrode roughness on the electrode reaction

*A. Ładocha, W.W Kubiak

AGH University of Science and Technology for them. of Stanisław Staszic
in Cracow,

Faculty of Materials Science and Ceramics the Ave. A. Mickiewicz 30,
30-059 Cracow

e-mail: agnieszkaladocha@gmail.com

Keywords: *electrode, roughness, voltammetric*

The substrate for voltammetric disc electrode are the most often precious metals (platinum, gold) or carbon material (glassy carbon). They are used mostly for measurements in oxidation mode or very often as a substrate for the chemical. The later is to obtain specific functionality of the electrode. The surface of unmodified electrode is prepared by mechanical polishing followed sometimes by chemical or electrochemical cleaning/conditioning process. The aim of these operations is to achieve a smooth surface similar to the ideal surface of mercury electrode.

Surface roughness is quantified by the deviations in the normal direction of a real surface from its ideal form. To define roughness quantitatively the number of parameters R is applied. The most suitable for characterizing electrode roughness is R_z defined as average difference between the highest peak and lowest valley on the measured distance.

In the literature, there are no systematic studies showing the effect of roughness on the electrochemical as well as on the measured voltammetric curves. The results of measurements obtained by cyclic voltammetry for several selected substances. Measurements were performed on the working disk glassy carbon electrode with varying degrees of surface roughness obtained by polishing, grinding and scratching surface. In many cases, controlled surface roughness enhances the reversibility of the electrode reaction.

Comparison of coffee beans and grounds as additives for *Macrolepiota konradii* biomass production

*Łukasz Łopusiewicz, Sławomir Lisiecki

Center of Bioimmobilisation and Innovative Packaging Materials, West Pomeranian University of Technology in Szczecin, POLAND

e-mail: lukasz.lopusiewicz@zut.edu.pl

Keywords: *Macrolepiota konradii*, biomass, coffee beans, coffee grounds

Macrolepiota konradii is fungus belongs to family *Agaricaceae*. To produce high quantity of active compounds huge amount of biomass is required. For this reason search for growth stimulators should be carried.

The aim of this research was comparison of coffee beans and grounds as additives for *M. konradii* biomass production.

The fungus grown in medium supplemented by 0,1%, 0,5%, 1%, 4% of milled coffee beans or grounds respectively. Control sample was pure medium. Incubation time was 10 days at 25 °C in a rotary shaker 150 rpm in triplicates. After incubation period cultures were filtered and biomass was dried 24 hours at 70°C. Obtained residues were weighted.

In comparison to the control sample concentrations 0,1%, 0,5%, 1% and 4% of coffee grounds caused respectively 2,99%, 19,7%, 58,2% and 68,6% loss of dry biomass. Milled coffee beans had positive as well as negative influence on a biomass amount depending on concentration. Dry biomass ratio in samples supplemented with 0,1% and 0,5% was higher respectively on 4,43% and 1,97%. Increased concentrations caused decreasing of biomass amount, 1% and 4% of milled coffee beans caused 2,84% and 79,1% loss of dry biomass amount, respectively.

Coffee grounds have definite negative influence and could not be use as additives for *M. konradii* biomass production. Small concentrations (up to 0,5%) of milled coffee beans could be good additives for *M. konradii* biomass production.

Effect of acetic acid to ethylenic unsaturation molar ratio on the course of rapeseed oil epoxidation

*Kornelia Malarczyk, Eugeniusz Milchert

Faculty of Chemical Technology and Engineering, West Pomeranian University of Technology in Szczecin, POLAND

e-mail: kornelia.malarczyk@zut.edu.pl

Keywords: *epoxidation, rapeseed oil, ion exchange resin*

Vegetable oils epoxidation is a method of chemical modification. Introduction of epoxy groups into the carbon-carbon double bonds leads to new compounds with valuable performance qualities. Epoxidized oils and their derivatives find numerous applications in many branches of industry. They are used, among others, as additives for lubricating oils, resin modifiers. Moreover, they enhance flexibility and durability of thermoplastics, are used in the production of polyurethane foams, paints, varnishes, paper and many other products.

In the present work rapeseed oil (RO) with iodine value of 102,8 (g I₂/100 g) was epoxidised using a peroxy acid generated *in situ* by the reaction of 30 wt% hydrogen peroxide and glacial acetic acid in the presence of an acidic ion exchange resin - Dowex 50Wx2. Process was carried out under the following conditions: temperature 348 K, stirring speed – 700 rpm, reaction time – 5 hours, hydrogen peroxide to ethylenic unsaturation molar ratio – 1,5/1, ion exchange resin loading – 22 wt%. The effect of acetic acid to ethylenic unsaturation molar ratio on epoxy number (EN) and iodine number (IN) was studied.

A reaction flask was charged with rapeseed oil, acetic acid (FA) and ion exchange resin. Subsequently, a 30 wt% hydrogen peroxide was added dropwise. After the process, the ion exchange resin was filtered, the organic layer was neutralized with 4 wt% solution of Na₂CO₃. The residual water was removed by means of anhydrous magnesium sulfate (VI). The degree of overreaction of RO to the epoxy compound was determined by means of the epoxy and iodine number.

The study shows that an increase in the molar ratio of CH₃COOH/ethylenic unsaturation from 0,2 to 2 caused a decrease of the iodine number. The value of the epoxy number decreases with increasing from 0,5 to 2 molar ratio of CH₃COOH/ethylenic unsaturation.

The best results of rapeseed oil epoxidation with regard to a high epoxy number at simultaneously low iodine number were achieved under molar ratio of acetic acid to ethylenic unsaturation 0,5/1.

The epoxidation of R(+)-limonene in the presence of toluene using hydrogen peroxide and over the Ti-MCM-41 catalyst

*Mariusz Władysław Malko, Agnieszka Wróblewska

Institute of Organic Chemical Technology, Faculty of Chemical Technology and Engineering, West Pomeranian University of Technology, Szczecin, Pułaskiego 10, 70-322 Szczecin, Poland

e-mail: mariuszmalko@gmail.com

Keywords: *R(+)-limonene, epoxidation, carveol, limonene 1,2-oxide, limonene 1,2-oxidediol*

R(+)-limonene is an unsaturated, cyclic and chiral terpene with the molecular formula of C₁₀H₁₆. R(+)-limonene has a pleasant smell of oranges and it is not toxic and not carcinogenic compound, but it triggers an allergy in 3% of the population. Limonene is the main constituent of essential oils present in the peels of citrus fruits. It is obtained by a steam distillation of the waste citrus peels (the purity of R(+)-limonene obtained in this method achieves of 98%). Its annual production is estimated at 110-165 million pounds.

The epoxidation of R(+)-limonene over the titanium silicalite catalysts allows to obtain a lot of valuable derivatives of R(+)-limonene. In our studies we used a natural limonene extracted from waste orange peels by the steam distillation and by the simple distillation. In the epoxidation of R(+)-limonene with hydrogen peroxide the Ti-MCM-41 catalyst was used. The influence of the following parameters was studied: the temperature and the reaction time. The post-reaction mixtures were analyzed by a gas chromatography and by iodometric titration (the determination of the unreacted hydrogen peroxide).

The epoxidation of R(+)-limonene over the Ti-MCM-41 catalyst by hydrogen peroxide and in toluene as the solvent showed very interesting results. During epoxidation the following products were obtained: limonene 1,2-oxide, its diol and carveol. At the temperatures of 0°C and 40°C the total amount of limonene 1,2-oxide underwent hydration to the appropriate diol. At the temperatures of 80°C and 120°C a part of limonene 1,2-oxide did not react with water molecules and this epoxide compound was detected in the post-reaction mixtures. Independent of the temperature of the epoxidation performing carveol was the main product of this process: the selectivity of this compound was from 50 mol% to 96 mol%.

The epoxidation of R(+)-limonene over the Ti-MCM-41 catalyst by hydrogen peroxide and in toluene as the solvent is a good method for the obtaining of the oxygenated derivatives of R(+)-limonene – compounds with a lot of applications in perfume, cosmetics, drugs and polymer production.

Adsorption of L-histidine onto mesoporous carbons functionalized with carboxylic groups

*Michał Marciniak, Joanna Goscińska, Robert Pietrzak

Faculty of Chemistry, Adam Mickiewicz University in Poznań, Poznań, POLAND

e-mail: michalmarc@amu.edu.pl

Keywords: *mesoporous carbon, adsorption, L-histidine, amino acid*

Amino acids are simple molecules that are the building blocks of proteins and possessing both carboxyl and amino groups whose adsorption behavior could be adequately used toward the understanding of the adsorption of enzymes on solid adsorbents. They are used as supplements to improve the quality of proteins in food technology. On the other hand, the controlled adsorption of amino acid is crucial in the field of biotechnology, where well-ordered amino acid layers may lead to new generation of reactor beds for catalysis and disease diagnostics. From this view point, the adsorption behavior of amino acids on the surfaces of materials such as hydroxyapatite, zirconium phosphate modified silica, silica-gels, activated carbon and zeolite has been investigated. However, these materials are found to be unsuitable for the amino acid adsorption due to their low pore volume and hidden pores which limit their adsorption capacity. The promising adsorbents of amino acids are mesoporous carbon materials, because of the hydrophobic nature of their surfaces, high surface area, and good thermal stability.

The aim of our study was the application of mesoporous carbons functionalized with carboxylic groups in the L-histidine adsorption process. Mesoporous carbons were synthesized by soft-template method with triblock copolymer Pluronic F127 as the soft-template matrix and resorcinol together with formaldehyde as carbon precursors. The materials were treated with the mild oxidant of a 1 M ammonium persulfate solution ((NH₄)₂S₂O₈ - APS) prepared in 2 M H₂SO₄. The carbon materials obtained were characterized by XRD, low-temperature nitrogen adsorption, FTIR, TEM and SEM. The content of the surface oxygen functional groups, both acidic and basic, was determined according to Boehm method. We correlated the surface properties with ability of mesoporous carbons functionalized with carboxylic groups to adsorb of amino acid.

The results show that textural properties of carbon obtained can be conveniently tuned by using different oxidation conditions, including concentration, temperature, and duration. The surface area and porosity deteriorate considerably compared to the pristine carbon after the oxidation treatment, and the micropores/small mesopores are the major contribution to the deterioration. All mesoporous carbons functionalized with carboxylic groups are promising adsorbents of L-histidine with high capacities and excellent binding capabilities.

Knowledge and model-based framework for nanofiltration modelling

*Agata Marecka, Piotr Tomasz Mitkowski

Faculty of Chemical Technology, Institute of Chemical Technology and Engineering, Department of Chemical Engineering and Equipment, Poznan University of Technology, Poznan, POLAND

e-mail: agata.j.marecka@doctorate.put.poznan.pl

Keywords: *nanofiltration modelling, mathematical modelling, process simulation*

Nanofiltration (NF) classified as a pressure-driven membrane process is among one of the newer separation techniques for aqueous and organic solutions. It is impossible to unequivocally determine what type of membrane, which process configuration and parameters should be used for given solute-solvent system in order to obtain the most effective separation. Every case has to be considered separately, even for very experience researcher. The most popular solution to this problem is to perform series of trial-and-error experiments. This is a labour-consuming and cost-intensive way of looking the optimal solution, which sometimes brings unexpected results. Another way is to apply mathematical model-based modelling supported by computer simulations and verify with experiments. Authors are convinced, that thanks to the mathematical models, it is possible to find out whether the separation needs can be achieved with NF. Such identifications are possible through development of a model-based and knowledge-based framework. Mathematical models can define feed-membrane-permeate relationship and therefore could provide guidelines for process development.

This contribution will presents a review of the most popular mathematical models used for NF modelling (Kedem-Katchalsky, Zeman-Wales, Log-Normal, Solution-Diffusion, Maxwell-Stefan, etc.) which have to be familiar for modeller. It is important that the framework not only consist of model equations but also provides information which model can be applied to certain case and which parameters need to regressed (or optimized). Additionally, summary of models equations clarify the number of variables and parameters which is a great assistance in computer-aided simulations for engineering-oriented design. The framework is supported with two case studies. The first case study refers to Kedem-Katchalsky model describing solute transport through membrane in NF separation of fumaric acid aqueous solution, carried out in tubular module. Whereas second case deals with recovery of diammonium fumarate from aqueous solution in NF. Both cases were simulated with use of gPROMS software.

Investigation of surface leakage current for HgCdTe barrier infrared detectors

*Olga Markowska¹, Małgorzata Kopytko²

¹Scientific Club of Physics, Faculty of Material Engineering, Institute of Applied Physics, Military University of Technology, Warsaw, POLAND

²Institute of Applied Physics, Military University of Technology, Warsaw, POLAND

e-mail: o.k.markowska@gmail.com

Keywords: *infrared photodetectors, HgCdTe, barrier detectors, surface leakage current, wet-chemical etching*

The work presents processing steps proposed for HgCdTe p⁺BpnN⁺ barrier detectors based nBn-design detectors for the mid-wave infrared (MWIR) spectral region. The traditional mesa definition etch process induces undesirable changes in HgCdTe surface properties. In narrow bandgap materials these surface changes could deteriorate a device performance. Uncontrolled band bending (dangling bonds) occurred on the slopes of the active layer increase of the recombination velocity causing surface leakage current. Adequate passivation is essential to minimize the effects from the surface states by saturating them.

Test structures with a round mesa geometry with different diameters from 100 to 500 μm were defined by a standard optical photolithography and wet chemical etched with Br:HBr (1:100) solution to the N⁺ bottom contact layer. The bulk leakage (J_{bulk}) and surface leakage (J_{surf}) components of the dark current in HgCdTe p⁺BpnN⁺ barrier detectors were investigated for unpassivated devices. The experimental value of J_{bulk} was found at the level of 8.1 mA/cm² and J_{surf} of 0.155 mA/cm at -0.2 V bias and a temperature of 300 K. For devices with large diameters (above 400 μm), the bulk component consists of about 40% of the total dark current. In the case of detectors with small diameters, the dark current is dominated by the surface leakage current. For a detector with a diameter of 100 μm, the bulk current consists only of 10% of the total dark current. Therefore, additional passivation processes are required following the mesa definition process to eliminate dangling bonds as much as possible.

The effect of construction and operating conditions of medical inhaler on atomization process

*Magdalena Matuszak

Faculty of Chemical Technology, Poznan University of Technology, Poznan, POLAND

e-mail: magdalena.p.markuszezwska@doctorate.put.poznan.pl

Keywords: *atomization, drug delivery, pneumatic and ultrasonic inhaler, drop size histogram*

Aerosol therapy is a modern drugs delivery method in order to treat a different diseases of the lungs and respiratory system. The medical inhalers are one of the oldest and the most commonly used devices in medicine to inhalation drugs. There are many types of inhalers, but the most widely used are: a pneumatic, ultrasonic and vibrating mesh inhalers. The effectiveness of the aerosol therapy depends on a large number of factors, including the construction of the device, operating conditions of device and properties of the sprayed liquid or suspension (for instance density, viscosity, surface tension, hygroscopicity, shape and morphology). Therefore, the physical processes associated with the drug delivery to the respiratory tract require further analysis in order to achieve high efficiency in inhalation.

The study has been concerned with the determination of an effect of construction and operating conditions of medical inhaler on drop diameters and drops size histograms.

Inhaled drugs with different chemical composition were sprayed in the pneumatic inhaler (MedelJet Family) and ultrasonic inhaler (delivered by Medisana). In the paper the results of experimental studies on atomization obtained by use the microscopic method with MultiScanBase and Image-Pro Plus programs, have been presented. The coated-slide technique has been applied.

The experimental results showed that the differences in the design of the inhalers lead to the significant changes in the drop size histograms. It has been shown that the drop sizes are dependent on design of device. Drop size histograms based on number of drops showed that the ultrasonic inhaler generated more drops with smaller diameter than the pneumatic inhaler one. It has been shown that the temperature of atomized liquid may have evident effects on the drop diameters and drop size distributions produced by medical inhalers.

The results obtained allow a better understanding of the atomization process, moreover they are important in the pharmaceutical spray formulations to change and/or improve the characteristics of the spray.

Chiral terphenylates – perspective materials for fast switching modes

*Katarzyna Milewska

Institute of Chemistry, Faculty of Advanced Technologies and Chemistry,
Military University of Technology, Warsaw, POLAND

e-mail: milewskasia@gmail.com

Keywords: *liquid crystals, chirality, antiferroelectric, terphenylates, electroclinic effect.*

An electric field applied to a chiral, non-tilted smectic liquid crystals may induce an inclination of molecules in the plane normal to the electric field. The electrooptic switching with such a characteristic is called an electroclinic effect. From a practical point of view the electroclinic effect allows for electrooptic switching which is a factor of 10-100 faster than the surface stabilized ferroelectric liquid crystal, depending on the material and operating temperature. Recently we have developed new chiral materials from the terphenyl family, which occurred to be potentially useful for such application.

Continuing our interest of orthoconic liquid crystals a new series of chiral 2',3' – difluoro p-terphenylates have been synthesized. These mesogens having chiral chain and partially fluorinated alkoxy chain show ferroelectric and antiferroelectric phases in broad temperature ranges: Cr 44.9 SmC_A* 68.5 Sm_A* 74.0 Iso for R_F=C₃F₇ and n = 3, and Cr 42.1 SmC_A* 60.2 SmC* 83.0 Sm_A* 91.3 Iso for R_F – C₃F₇ and n = 4. The influence of the length of an alkyl bridge between the fluorinated part and rigid core on mesomorphic properties, especially on ferroelectric and antiferroelectric phase stability, as well as on basic physical properties will be given. The strong even-odd effect on antiferroelectric phase stability has been observed. Synthetic details to all of the innovative steps will be presented.

Investigation of a single mesogens at temperatures where SmA* phase is present brought significant improvement of tilt angles induced by the electric field. Along with high tilt angles obtained in this material we observed also submicrosecond electrooptic switching. The objective of this presentation is to raise a discussion in order to find out the real nature of this behavior.

New high tilted antiferroelectric liquid crystals for multimedia LCD's

*Katarzyna Milewska, Roman Dąbrowski

Institute of Chemistry, Faculty of Advanced Technologies and Chemistry,
Military University of Technology, Warsaw, POLAND

e-mail: milewskasia@gmail.com

Keywords: *Liquid crystals, chiral compounds, esters, antiferroelectric, orthoconic*

Liquid crystal displays (LCDs) have been used around for about 40 years, and since that time their use has been increasing in various areas of life, with the progress of science. Right at the beginning they were used for the production of simple seven-segment number displays for calculators and watches. Today they are used in higher resolution matrix displays for flat panel TVs, computers, projectors, cameras, smart phones etc. To improve the quality and expand potential application of these equipments, we investigated orthoconic antiferroelectric liquid crystals (OAFLCs). This class of materials is different from regular antiferroelectric liquid crystals (AFLCs) because they have extremely high molecular tilt angle, reaching 45° and their tilt direction alternates from layer to layer by 90° . That means that the excellent ideally perfect dark state is generated and consequently very high-contrast is produced.

Continuing the search of OAFLCs with improved electrooptical properties we have prepared novel chiral (*S*)-(+)-4'-(1-methylalkoxycarbonyl)-biphenyl 4-(ω -(2,2,3,3,4,4,4-heptafluorobutoxy)alkoxybenzoates and (*S*)-(+)-4'-(1-methylalkoxycarbonyl)biphen-4-yl 4-(ω -(2,2,3,3,4,4,4-heptafluorobutoxy)-alkoxy-2-fluoro-benzoates. Their mesogenic and optical properties will be presented. The mesophase sequences of the compound and their phase transition temperatures were determined by polarizing optical microscopy and differential scanning calorimetry (DSC). The helical pitch was estimated with selective reflection method.

Synthesized compounds are attractive to formulation of new multicomponent mixtures with broad temperature ranges of orthoconic antiferroelectric phases with direct transition SmC_A^* -Iso. Those liquid crystalline materials are supposed to be useful, especially for high frame rate video and other applications, using a simple passive control techniques, which by the application of mode "color sequential" can generate increased image resolution compared to a standard display.

Effects of formic acid and sodium formate on the $\cdot\text{OH}$ -initiated transformation of phenol

*Máté Náfrádi¹, Zsuzsanna Kozmér¹, Tünde Alapi^{1,2}, András Dombi¹

¹Research Group of Environmental Chemistry, University of Szeged, Szeged, HUNGARY

²Department of Inorganic and Analytical Chemistry, University of Szeged, Szeged, HUNGARY

e-mail: 7nmate7@gmail.com

Keywords: vacuum ultraviolet photolysis, radical transfer materials, N_2O

The advanced oxidation processes (AOPs) are an important, still investigated methods for the degradation of organic contaminants. The transformation of the contaminants takes place in reactions with different reactive radicals, mainly $\cdot\text{OH}$ of most high reactivity. One such AOP is the vacuum ultraviolet (VUV) photolysis, which is able to form $\cdot\text{OH}$ from water ($\text{H}_2\text{O} + h\nu \rightarrow \cdot\text{OH} + \cdot\text{H}$) initiated by high-energy VUV photons (<200 nm). Radical transfer materials compete with the target molecule for the radicals, result in different reactive species.

For the optimization of the water purifying technologies using AOPs, the accurate knowledge of the chemical mechanisms are needed. This study aimed to investigate the effect of two radical transfer materials, such as formic acid and sodium formate in various concentrations on the VUV photolysis of phenol in presence of dinitrogen oxide (N_2O) (as a radical transfer material: $\cdot\text{H}$ to $\cdot\text{OH}$).

In our experiments 10^{-4} mol L^{-1} aqueous solutions of phenol were irradiated by a VUV lamp, with the addition of radical transfer materials: N_2O bubbling and formic acid or sodium formate in different concentrations. The degradation of phenol was followed using HPLC-UV.

N_2O was used to transform the $\cdot\text{H}$ to $\cdot\text{OH}$, thus the radical set includes mainly $\cdot\text{OH}$. Therefore the degradation rate of phenol was significantly higher in the presence of N_2O than in absence it.

The formic acid and the sodium formate react with $\cdot\text{OH}$, result in carbon-centred radicals of low reactivity. These materials reduce the degradation rate of phenol because of the concentration of $\cdot\text{OH}$ decrease significantly. Effects of these radical transfer materials depend on their concentration, in low concentration it is negligible, while in high concentration they hinder significantly, or even block the degradation of phenol.

Pollutant emission from biomass combustion

*Grzegorz Wielgosiński¹, Patrycja Łechtańska¹, Olga Namiecińska¹

¹Faculty of Process and Environmental Engineering, Lodz University of Technology, Lodz, POLAND

e-mail: grzegorz.wielgosinski@p.lodz.pl

Keywords: *biomass, pollution emission factors, hard coal*

Biomass is regarded as an ecological fuel where the combustion results in lower pollution of the environment than it is the case in terms of classical mineral fuels. Hence, it was resolved to assess the real situation. Four samples of biomass were subjected to investigations, i.e. rape straw, oak bark, wood pellet, energetic willow and, for comparison, the fine hard coal samples. The aim of the study was to determine and compare the pollution emission factors (in reference to the mass of fuel) - carbon monoxide (CO), nitrogen oxide (NO) and sums of hydrocarbons (counted as total organic carbon TOC) generated in the process of biomass samples combustion and to compare them with the results obtained for coal as well as to determine the effect of the conditions of the process (the temperature and the air flow) on the value of the emission factor. The investigations were carried out in a laboratory chamber furnace electrically heated at five different temperatures (in the range of 700-1100°C and at three different air flow rates). In all tests one could observe the excess of the air in relation to its stoichiometric quantity. As a result of the investigations which were carried out it was found that in many cases the determined emission indicators for biomass combustion are higher than for hard coal.

COD reduction in landfill leachate treatment by photo electro-Fenton process – an overview

*Ramin Nikpour¹, Maciej Szwał¹, Wojciech Piątkiewicz¹, Michał Zalewski¹

¹Faculty of Chemical and Process Engineering, Warsaw University of Technology, Warsaw, POLAND

e-mail: r.nikpour@ichip.pw.edu.pl

Keywords: *Electrochemical Advanced Oxidation Processes, Photo Electro - Fenton, COD removal, Free Radical Technology, landfill leachate*

Nowadays, human activities produce large quantities of waste and sewage and therefore is causing some environmental risks towards public health and ecosystems.

Landfill leachate treatment is one of the important issue among the waste management systems, because untreated landfill leachate can contaminates both surface and groundwater sources.

Advanced oxidation processes such as Electro-Fenton and Photo Electro-Fenton processes are alternative promising methods than other biological and classic physicochemical methods and have been applied effectively in leachate treatments. These advanced methods cause the production a large amount of free radicals such as “hydroxyl” ($\bullet\text{OH}$) which can remove both organic and oxidizable inorganic components due to their ability to change in the chemical structure of the pollutants.

This study is an overview about chemical oxygen demand reduction from leachate by using the continuous photo Electro-Fenton method given the increasing importance of its application. This reaction is a catalytic reaction that iron ion from a ferrous salt is its catalyst and simultaneously, hydrogen peroxide is added to leachate. Main advantages of these technology such as environmental friendly and good economic situation are reviewed. And also some influencing factors and parameters in this process including reaction time, electrical current density and voltage, size and distance between the electrodes particularly their materials, the optimum pH, initial concentration of ferrous ion, H_2O_2 to Fe(II) molar ratio and etc. will be investigated by using the other authors reports and their available experimental results. Also applying the electrodes made of suitable materials such as graphite cathode and titanium with platinum coating anode is discussed in this work.

Reflection on the perspective in the future is providing an improved mathematical model that can explain better the operating conditions of this process. In this path, is needed suitable experimental results, so an installation of photo electro-Fenton system will prepare and will report new desired results in the next related works in future.

The use of electrochemical impedance spectroscopy to study the semiconducting properties of oxide layers on titanium alloys in a simulated body fluid

*Patrycja Osak, Bożena Łosiewicz, Tomasz Gorczyka

Institute of Materials Science, Silesian Interdisciplinary Centre for Education and Research, University of Silesia, Chorzów, POLAND

e-mail: posak@us.edu.pl

Keywords: *electrochemical impedance spectroscopy, Mott-Schottky analysis, oxide layer, semiconductivity, titanium alloys*

Titanium and its alloys are materials widely used in medicine most often in orthopedic and orthodontics. Particularly popular are NiTi alloys showing shape memory effect. NiTi shape-memory alloys belong to a group of intelligent materials characterized by such properties as one- and two-way shape memory effect and pseudoelasticity. NiTi alloys with a composition close to equiatomic show very good mechanical properties and high biocompatibility. NiTi implant alloys have a high corrosion resistance due to the spontaneous formation on the surface of oxide layer acting in protector function. Such a thin passive film consists essentially of titanium dioxide. Corrosion in the biological milieu presents the basic science background to understand the nature of corrosion processes associated with medical devices and the metallic biomaterials from which they are made.

In this study, the semiconducting properties of the spontaneous oxide layer on NiTi shape-memory alloy in the biological milieu has been studied using the following measurements: (i) open-circuit potential versus time of exposure, (ii) a complementary method of electrochemical impedance spectroscopy (EIS), and (iii) potentiodynamic polarization. Electrochemical studies were conducted in Ringer's solution. The electrolyte was modified to simulate inflammation. A comparative study has also been carried out in a solution of neutral pH. In order to determine the effect of the type of electrolyte used on the conductivity of the naturally formed TiO₂ layer on the NiTi substrate, the Mott-Schottky analysis has been applied. Independently on the type of the electrolyte used, a normal n-type semiconducting Mott-Schottky behavior was observed for TiO₂ layer on NiTi shape-memory alloy. Difference in the determined density of electric charge carriers has been observed and discussed.

Multi-electrode potentiometric sensor

*Magdalena Pięk, Leszek Cabaj, Robert Piech, Beata Paczosa-Bator

Faculty of Material Science and Ceramics, AGH University of Science and Technology, Cracow, POLAND

e-mail: mras@agh.edu.pl

Keywords: *multi-electrode sensor, potentiometry, carbon black, sensor platform*

An ion-selective electrodes produce a potential that is related to the activity of one kind of an ions in the presence of others. Thus, they can be used as analytical tools for direct measurement ion content in complex samples in clinical and environmental analysis and in the process control. The elimination of the internal solution with conventional ion-selective electrodes significantly simplify their construction and contributed to their miniaturization. In order to improve analytical parameters of electrodes without inner solution, intermediate layers between ion selective membrane and electric conductor were used. The application of e.g. conducting polymers, ionic liquid, carbon nanotubes or graphene greatly affect the sensitivity, selectivity, response time and long term potential stability of sensors.

In our study we propose to use carbon black as an intermediate layer in potentiometric multi-electrode system consisting of four electrodes with built-in silver chloride reference electrode. Electrodes placed in one body were coated by potassium, sodium, chloride and nitrate selective membrane. The analytical parameters of sensor platform were evaluated by the determining appropriate ions. These modified sensors have shown great improve in parameters in comparison to non-modified sensors (without an intermediate carbon black layer) especially in long term potential stability. Furthermore, the response time was very short, even at a low concentration of determined ions. The subsequent advantage was absence of water layer between ion-selective membrane and conductor thanks to hydrophobic characters of carbon. The potentiometric sensor platform was used for estimation of sodium, potassium, chloride and nitrate concentration in different water samples.

This new multi-electrode system allowed to obtain information about concentration of many ions in analyzed sample at the same time. Such a device greatly shortens the time and lower the costs of analysis.

All-solid-state nitrate-selective potentiometric electrode with carbon black

*Magdalena Pięk, Leszek Cabaj, Robert Piech, Beata Paczosa-Bator

Faculty of Material Science and Ceramics, AGH University of Science and Technology, Cracow, POLAND

e-mail: mras@agh.edu.pl

Keywords: ion selective electrode, nitrate sensor, carbon black

Conventional ion selective electrodes consist on a selective membrane, an internal solution and an electrode. However this construction has some disadvantages and the application of such electrodes in practice is limited. Ion selective electrodes with a solid contact (used instead of internal solution) have significant advantages over the conventional electrodes, e.g. they are maintenance-free and able to work in any position. Materials that have been used in sensors as a layer between ion-selective membrane and the electric conductor are conductive polymers, platinum nanoparticles, carbon nanotubes, fullerene and graphene. The use of mentioned carbon nanomaterials seems to be the best solution because of their properties, but it is restricted due to the cost of production. Nevertheless there is one more carbon nanomaterial, in addition, is relatively cheap – carbon black.

Carbon black (CB) also can be successfully used as an active ion-to-electron transducer layer in solid-state ion-selective electrodes. The carbon black exhibit many excellent properties such as high conductivity, large surface area, high hydrophobicity and low production cost. Considering the mentioned qualities it becomes obvious that the carbon black is the most advantageous material for the fabrication of the solid-state selective electrodes.

The potentiometric properties of all-solid-state nitrate selective electrodes based on polymer-CB composites containing different types of nanosized carbon black were investigated. To evaluate analytical features of sensors the potentiometry and chronopotentiometry measurements were performed. The use of a carbon black interlayer is shown to significantly improve the potentiometric response. The electrodes display a close-to-Nernstian slope in the range from 10^{-1} to 10^{-6} M, highly stable potentials and low membrane resistance. However, different analytical parameters were found depending on the type of the carbon black used.

Characteristics of metallic structured catalysts for catalytic combustion of biogas

*Ewelina Piwowarczyk¹, Damian K. Chlebda², Magdalena Chrzan¹, Roman J. Jędrzejczyk^{2,3}, Przemysław J. Jodłowski⁴, Joanna Łojewska²

¹ Faculty of Process and Environmental Engineering, Technical University of Lodz, Wólczańska 213, 90-924 Łódź, Poland

² Faculty of Chemistry, Jagiellonian University, Ingardena 3, 30-060 Kraków, Poland

³ Malopolska Centre of Biotechnology, Gronostajowa 7A, 30-387 Kraków, Poland

⁴ Faculty of Chemical Engineering and Technology, Cracow University of Technology, Warszawska 24, 31-155 Kraków, Poland

e-mail: ewelina.piwowarczykk@gmail.com

Keywords: *catalysts, metal oxides, methane combustion, structured catalysts*

New method for the production of heat and energy with minimal influence on environment has attracted great interest of researchers as well as energetic industry. The current technological achievements allow flammable biogas to be used as energy source to produce energy at local level. One of the possibilities of energy production is to combust biogas in catalytic biogas turbines. However, some hazardous gases such as methane, carbon monoxide, VOCs and NO_xs may be present in the effluent gases. According to the safety regulations, the effluent gases has to be purified to the desired level. From many possible routes of the gas exhaust abatement, the catalytic methods are the most effective from the economical and chemical point of view. Although, the catalytic systems for the gas clean-up has been developed almost 30 years ago they still suffers many drawbacks such as high price, big installation size and weak heat and mass transport parameters. These inconveniences can be removed by applying non-precious catalysts based on structured supports. The catalyst preparation is based on the usage of porous media, eg. Al₂O₃, or zeolites. In the following step, support is impregnated with a precursor of the catalytic phase. The preparation stage is the key step during the catalyst development.

In this study the series of the metal oxides catalysts based non-noble metals is prepared. The catalysts composition was determined by using X-ray Fluorescence and UV-Vis spectroscopic methods. The catalyst activity during the methane combustion was determined by using plug flow reactor Catlab. The composition of the effluent gas (N₂, CO, CO₂, O₂, H₂O), was analyzed with a quadropole mass spectrometer (QMS).

Acknowledgments

The Project was financed by the National Science Center Poland based on the decision No. 2013/09/B/ST8/00171.

Synthesis and physicochemical properties of amine modified carbon xerogels

*Magdalena Ptaszkowska, Joanna Goscińska, Robert Pietrzak

Faculty of Chemistry, Adam Mickiewicz University in Poznań, Poznań, POLAND

e-mail: magdalena.ptaszowska@amu.edu.pl

Keywords: *carbon xerogels, functionalization with amine groups, synthesis, physicochemical properties*

Carbon gels are materials of controllable pore size, high porosity and well developed surface area. They can be also shaped in various forms for practical applications (such as monoliths, thin films or pellets). The textural and structural properties of carbon xerogels can be controlled according to the synthesis and processing conditions (e.g., pH of preparation, drying conditions and carbonization temperature). The main advantage of these materials is the possibility for tailoring their properties to fit specific applications. For this reason, they are used in adsorption, catalysis and energy storage.

The main purpose of the study was to synthesize a few series of amine modified carbon xerogels and to determine their physicochemical properties.

Carbon xerogels were prepared by polycondensation of resorcinol with formaldehyde at different pH values. The gelation step was allowed to proceed at 85°C for 3 days. After this period gels were crushed and dried in an oven during 4 days at 60, 80, 100 and 120°C. In the next step, samples were carbonized under nitrogen flow (100 ml/min.) at different temperatures: 500, 700 and 900°C in a tubular furnace. All materials obtained were modified with various amines. Structure and surface properties of amine modified carbon xerogels were characterized in detail by low-temperature nitrogen sorption, XRD, FTIR, SEM and TEM. The content of the surface oxygen functional groups, both acidic and basic, was determined according to Boehm method.

The results show that amine groups strongly determine structural, textural as well as acid-base properties of the carbon xerogels. The functionalization of the carbonaceous supports with organic groups leads to decreasing the surface area and pore volume. These phenomena are probably caused by pore blocking being a result of amines and carbon matrix interaction.

High nitrogen salts of azotetrazole

*Judyta Rećko, Stanisław Cudziło

Institute of Chemistry, Military University of Technology, Warsaw, POLAND

e-mail: jrecko@wat.edu.pl

Keywords: *explosives, azotetrazole salts, high nitrogen materials*

Azotetrazole is a modern high energy compound, which unfortunately has high sensitivity to mechanical stimuli and chemical instability. Its reactivity is a result of the presence of two acidic protons. The substitution of these protons by cations with high nitrogen content, for example guanidine cation, leads to formation of compounds without azotetrazole defects, that could be used in military technology. Their advantages are: relatively low sensitivity, high enthalpy of formation and high volume of products of explosion.

This paper describes the methods of synthesis and study of the characteristics of high nitrogen azotetrazole salts. To obtain all compounds were used cheap and easily available materials. After purification and drying samples, the structure of products was confirmed by the techniques of nuclear magnetic resonance spectroscopy. To determine the physical properties was used method of thermal analysis DTA/TG. Finally there were experimentally determined basic energetic and explosive characteristics of studied materials.

Application of core-shell mesoporous silica nanospheres modified with titanium dioxide in cement mortars for self-cleaning and bactericidal purposes

*Paweł Sikora^{1,2}, Krzysztof Cendrowski³, Agata Markowska-Szczupak³ Elżbieta Horszczaruk², Ewa Mijowska³

¹Faculty of Civil Engineering, Warsaw University of Technology, Warsaw, POLAND

²Faculty of Civil Engineering and Architecture, West Pomeranian University of Technology, Szczecin, POLAND

³Faculty of Chemical Engineering, West Pomeranian University of Technology, Szczecin, POLAND

e-mail: pawel.sikora@zut.edu.pl

Keywords: *photocatalysis, nanosilica, titanium dioxide, self-cleaning, bactericidal*

In recent decades, sustainable engineering and environmental issues became a major concern on a global scale. The increased emission of gasses in large urban centres made way for previously small scale pollution related problems.

Therefore, there is a growing concern drawing the attention of governments, industry, and researchers towards various methods of developing photocatalytic mortars, capable of reducing the pollutant concentration in indoor air and contribute to a more sustainable construction.

Due to their different properties, both nanosilica and titanium dioxide are often applied separately into the cementitious composites. Nanomaterials demand high water quantities (as a result of high surface area) and this causes major problems concerning the proper and uniform dispersion of the nanomaterial in the cement matrix.

The presented study is focused on the potential application of the silica/titania core-shell structure (so far not applied in the cement-based composites) in order to obtain self-cleaning and bactericidal properties while improving the rheological and mechanical properties.

Compared to the commercially available titanium dioxide Aeroxide® P25, the tested structures proposed by the authors showed improved compressive strength and did not negatively affect the consistency of the cement mortar. Moreover, the structure of the core-shell mesoporous silica nanospheres that was modified with titanium dioxide proved to be more photocatalytically efficient (compared to P25) and exhibited good bactericidal properties (*E. coli* K12).

Acknowledgments: The authors are grateful for the financial support of the National Science Center Poland within the PRELUDIUM Programme (2011/03/N/ST5/04696).

The influence of nanosilica on the mechanical properties of polymer-cement composites (PCC)

*Paweł Sikora^{1,2}, Paweł Łukowski¹, Krzysztof Cendrowski³, Elżbieta Horszczaruk², Ewa Mijowska³

¹Faculty of Civil Engineering, Warsaw University of Technology, Warsaw, POLAND

²Faculty of Civil Engineering and Architecture, West Pomeranian University of Technology, Szczecin, POLAND

³Faculty of Chemical Engineering, West Pomeranian University of Technology, Szczecin, POLAND

e-mail: pawel.sikora@zut.edu.pl

Keywords: *nanosilica, polymer-cement composites, compressive strength, nanomaterials*

Concrete is the single most widely used material in the world. Its primary ingredient, cement, is also the most costly and environmentally unfriendly component in concrete mix. Cement industry is one of two primary industrial producers of carbon dioxide (CO₂), creating up to 5% of worldwide man-made emissions of this gas. Therefore, additives and admixtures (such as polymers and nanomaterials) are arousing the interest of researchers in order to reduce the quantity of cement and obtain the same qualities of concrete.

The material which has received considerable attention in the last few years due to its unique properties is nanosilica. It is estimated that 1 kg of nanosilica can effectively replace 4 kg of cement which leads to reduction of cement production. In modern concrete construction and repair works the role of polymers is increasing day by day. The incorporation of polymers greatly improves strength, adhesion, resilience, impermeability, chemical resistance and durability properties of mortars and concrete. Although the number of publications devoted to the influence of nanosilica on the properties of cementitious composites raised over the course of the last decade, the field of polymer-cement composites (PCC) has remained under-studied. Therefore, this paper will deal with the potential application and the influence on the mechanical properties of PCC.

Studies have shown that nanosilica particles (100 nm and 250 nm diameter) positively affected the physical and mechanical properties of polymer-cement composites. Moreover, scanning electron microscope (SEM) analysis showed that nanosilica improved the microstructure of cement matrix.

Structural analysis and photocatalytic activity of titania photocatalysts immobilized onto ceramic paper support

*Gergő Simon¹, Tünde Alapi^{1,2}, Klára Magyar³, Klára Hernádi¹, Gábor Kovács^{3,4}, Zsolt Pap^{1,3,4}, Virginia Danciu⁴, András Dombi¹, Lucian Baia³

¹Research Group of Environmental Chemistry, University of Szeged, Szeged, HUNGARY

²Faculty of Inorganic and Analytical Chemistry, University of Szeged, Szeged, HUNGARY

³Faculty of Physics, Babeş-Bolyai University, Cluj-Napoca, ROMANIA

⁴Faculty of Chemistry and Chemical Engineering, Babeş-Bolyai University, Cluj-Napoca, ROMANIA

e-mail: gsimon@chem.u-szeged.hu

Keywords: *titania, ceramic paper, immobilization, pesticides' removal*

Environmental organic pollutants, originated from agriculture, chemical and pharmaceutical industries have become a major concern. Advanced oxidation processes are promising methods for the removal of such contaminants from water. One of the methods applicable is heterogeneous photocatalysis, which is based on the generation of reactive radicals using metal oxide semiconductors. Titania is used widely due to its beneficial properties, but its application for large scale water treatment is problematic in form of suspensions due to the need to separate the photocatalyst particles after the water treatment process. The immobilization of the nanoparticles could be an inovative solution to this problem, if sufficient information is available regarding the properties and usability (change in activity, wearing of the surface) of these materials.

During this study commercially available titania (Aeroxide P25) was immobilized onto the surface of ceramic paper carrier in different concentrations (covering ratios), using a method developed by our research group, in which the ceramic paper is impregnated by tetraethyl titanate, and then the titania is sprayed onto the surface from an alcohol based suspension.

Afterwards, the produced photocatalytic surfaces were studied using diffuse reflectance spectroscopy (DRS), infrared- and Raman-spectroscopy, x-ray diffractometry (XRD) and scanning electron microscopy (SEM) coupled with energy-dispersive x-ray analysis (EDAX).

The results show that the immobilization process was successful, and that the amount of titania deposited, influences the properties of the surfaces produced, including activity, pollutant adsorption, nanoparticle distribution and optical peculiarities (particle agglomeration issues).

Biodegradable polymer composites with nanoparticles of silver and natural fibers to the elements of rehabilitation equipment in veterinary medicine

*Natalia Sitek, Stanisław Kuciel

Faculty of Mechanical Department, Cracow University of Technology, Cracow, POLAND

e-mail: natalia.sitek@vp.pl

Keywords: *veterinary application, biocomposites, nanoparticles of silver and natural fibers*

This publication considers biodegradable polymer biocomposites with nanoparticles of silver and natural fibers which can be used in rehabilitation equipment in veterinary medicine. The main point of work is to help to develop better materials which can be used in medical equipment. Materials should be durable, antibacterial, humidity-proof and easy-cleaned at the same time.

The theoretical part of the work describes rehabilitation equipment division in veterinary, especially for dogs, but this equipment can be used for treatment various kind of domestic animals. The main classes of rehabilitation equipment described here are orthosis, braces, stabilizers, collars and special orthopedic shoes. In this section information about the properties and use of nanoparticles of silver, with biodegradable composites and natural fillers is also included. Experiments were carried out on polylactide and its biocomposites. Among the experiments distinguish bending test, tensile test and impact strength. It was showed absorbency of physiological saline and the analysis of the surface was done.

The results confirmed the possibility of producing biodegradable polylactide composites based on natural particles modified with the addition of nano-silver antibacterial. The main issue is to remove moisture from the particles of natural fibers, which would improve the strength of the composites in addition to the observed increase in their rigidity. Standardized particles of walnut - used as an ingredient in cosmetic peels and known for their antibacterial properties, seem to be better than cellulose microparticle preparation of such composites. On the other hand, the cellulose particle size of several microns are mixed with attractive filler nanoparticles as both the carrier and by the possibility of producing elements of the 3D printing method. Biodegradable composites which has got antiseptic properties can be used for the fabrication of folding stabilizers snap like Lego (sizes 3-4), and decicated to the animals such as dogs, cats and guinea pigs for minor injuries which require immobilization of the limb for a period of several weeks.

The relation between Kirkendall porosity and Matano plane position in binary system Fe-Pd

*Wojciech Skibiński¹, Bartek Wierzbą²

¹Faculty of Materials Science and Ceramics, AGH University of Technology, al. Mickiewicza 30, 30-059 Kraków, POLAND

²Faculty of Mechanical Engineering and Aeronautics, Rzeszow University of Technology, al. Powstańców Warszawy 12, 35-959 Rzeszów, POLAND

e-mail: wskibi@agh.edu.pl

Keywords: *diffusion, Kirkendall porosity, Matano plane, Kirkendall plane*

In this paper the position of the Matano and Kirkendall planes versus place of the Kirkendall porosity (Frenkel effect) in binary Fe-Pd system is discussed. The complete understanding of Kirkendall porosity related to initial contact interface of diffusion couple (Matano plane) is still lacking. Kirkendall porosity (Frenkel effect) often occurs in elements working at high temperatures due to diffusion process causes the damage of the element (ex. microelectronic device damage caused by the voids creation). Better understanding of this process can help to develop new materials and to prevent the failure of the working element.

The diffusion couple technique was employed to investigations. Several experiments in binary Fe-Pd system were conducted. Pure foils (thickness 1 mm) of palladium (99.9%) and iron (99.9%) provided by Sigma Aldrich were used as starting materials. Inert markers of ThO₂ were placed at the initial contact interface of diffusion couple to indicate the Kirkendall plane.

After the experiment and standard metallographic preparations samples were examined with SEM. Experimental concentration profile was measured with EDX and compared with calculations. The diffusion processes were calculated using generalized Darken method. This method was described in our earlier works. Intrinsic diffusion coefficients used in calculations were approximated using Generalized Boltzmann-Matano method for multicomponent systems.

The relation between Matano plane and the place of the Kirkendall porosity in binary Fe-Pd system is presented and discussed.

Verification of ciders origin based on voltammetric signals

*Wanda Sordoń, Małgorzata Jakubowska

Department of Analytical Chemistry, Faculty of Material Science and Ceramics,
AGH University of Science and Technology, Krakow, POLAND

e-mail: wsordon@agh.edu.pl

Keywords: *voltammetric electronic tongue, multivariate analysis, cider*

The main human sense that allows for the detection and determining quality of food products is the sense of taste. By the brain analysis of signals, that are caused by chemical reactions between substances contained in food products and specific taste receptors cells, a human being is able to determine the flavor.

The significant development in technology of sensors, methods of chemical analysis, measurement processes with the use of multivariate analysis has given a great possibility for the discrimination and identification of food samples. It has led to digitizing of human taste sense known as the conception of Electronic Tongue (ET). An array of chemical sensors in ET plays the role of taste receptors. The response (potentiometric, voltammetric, optical or enzymatic) of sensor array is analyzed with the usage of chemometric techniques. The role of them is to recognize, categorize and particularly classify the investigated objects.

The conception of voltammetric electronic tongue was applied to distinguish Polish ciders. Differential pulse voltammetry was used in this investigation. The sensor was the glassy carbon electrode being also a working electrode. The voltammograms were registered for every cider at the range of positive potential values (300-1000 mV) in the electrolyte of Britton-Robinson buffer (pH=2.2). Some samples were studied in the consecutive days from the opening. The responses were processed with the usage of continuous wavelet transform and specially defined mother wavelet. In the multivariate analysis, preliminary data mining was performed using clustering methods and principal components analysis. Their main purpose of this stage was recognition of the set structure, identification of groups of objects with similar characteristics or disclosure of the samples significantly different from the others. Classification was realized using various algorithms. Typical strategies were used to optimize and validate models, to confirm the ability of the correct classification.

Freeze-dried microcapsule in bioconversion reaction of whey

*Magdalena Stobińska, Artur Bartkowiak

Center of Bioimmobilisation and Innovative Packing Materials, West Pomeranian University of Technology, Szczecin, POLAND

e-mail: mstobinska@zut.edu.p

Keywords: *immobilization, lactase, freeze-drying*

Enzyme have a wide range of biotechnological, pharmaceutical and bioconversion applications. The enzyme lactase (β -galactosidase - EC.3.2.1.23) belongs to the family of hydrolases and the group of sugar converting enzymes. The hydrolysis of lactose from whey with lactase is a well-know process used in the dairy industrial scale. The presence of lactose in food products is limited because of low sweetener power, low solubility and laxative effect after ingestion in high concentration.

Enzyme lactase was immobilized in calcium alginate beads and freeze-dried. In experiment was compared activity of lactase immobilized in alginate beads before and after freeze-drying. The aim of this study was efficiency of using liquid-core microcapsules as a novel methodology of microencapsulation using a novel co-extrusion technique. Liquid core solution of enzyme and shell materials sodium alginate was pumped through concentric nozzle, with the core material flowing in the central nozzle, and the shell material flowing through the outer nozzle.

Microencapsulated lactase within the alginate beads allows to be separated from the reaction solution and can be used potentially many times which leads to reduction of cost and formation of bioconversion solution without enzyme. In the same time it was found that immobilized enzymes exhibit greater activity and stability during the bioconversion process and after during long-term storage. The obtained results confirm that novel alginate core/shell microcapsules with lactase in liquid-core could contribute to the development of new continuous processes.

In this study we report on the use of freeze-drying as a relatively simple method for increasing the strength and longevity of denitrifying alginate beads with enzyme lactase.

Influence of incubation condition on selenium enrichment in baker's yeast

*Beata Szulc-Musioł¹, Barbara Dolińska¹, Florian Ryszka²

¹ Department of Applied Pharmacy, School of Pharmacy and the Division of Laboratory Medicine, Medical University of Silesia, POLAND

²Pharmaceutical Research and Production Plant "Biochefa", Sosnowiec, POLAND

e-mail: szulc.beata@interia.pl

Keywords: baker's yeast, selenium enrichment, incubation conditions

Selenium is an essential trace element and a key component of several enzymes involved in antioxidant defence and metabolism. Selenium supplementation may prevent various diseases and also alleviate other pathological conditions including oxidative stress and inflammation. Supply of the selenium enriched food, especially, selenium enriched biomass with organic forms of this microelement is one efficient way to overcome selenium deficiency. Organic selenium complexes and seleno-aminoacids are considered to be much more bioavailable and effective form of selenium than selenite and selenite selenium.

Baker's yeast (*Saccharomyces cerevisiae*) is capable of accumulating large amounts of selenium under appropriate conditions and incorporating it into organic compounds. Selenomethionine was identified as the major selenium-containing compound in the protein fraction as well as in whole cells of this yeast. *Saccharomyces cerevisiae* is only yeast strain that has been used by manufacturers for production of Se-enriched yeast.

The present study is a continuation of the research conducted by our Department on microelement incorporation into baker's yeast cells. The aim of this work was to influence of incubation condition on selenium enrichment in baker's yeast. Shake flask experiments were conducted to optimize the cultivation conditions. The cultures were incubated for 24h in a shaker incubator and different carbon sources (glucose, sucrose, fructose, lactose, maltose) were used in the studies. The statistical analysis showed a significant ($p < 0.05$) effect of selenium concentration in the yeast-culture medium upon selenium incorporation into the yeast cells. We also found that glucose is the best carbon source which facilitates the high selenium incorporation into yeast cells.

Using hydrogen to recycle neodymium magnets

*Mateusz Szymanski¹, Bartosz Michalski¹, Marcin Leonowicz¹, Zbigniew Miazga²

¹Faculty of Materials Science and Engineering, Warsaw University of Technology, Warsaw, POLAND

²P.P.H.U. POLBLUME Zbigniew Miazga, Piaseczno, POLAND

e-mail: m.szymanski@inmat.pw.edu.pl

Keywords: HDDR, recycling, magnets

Extremely tremendous technological development, observed in last decades, results in rapidly increasing demand for raw materials. A need for high-energy permanent magnets is boosted by development of green energy technologies, such as wind turbines or electric cars. The Rare Earth Elements were recognized by the US and Europe as a critical ones, which means they are very important for the industry. The waste of electrical and electronic equipment could be an important source of that metals. Nd-Fe-B magnets, widely used in hard disc drives and other devices, are considered to be valuable for recovery, due to their chemical composition based mostly on critical elements (Nd, Dy, Pr). According to literature data, hydrogen methods HD (hydrogen decrepitation) and HDDR (hydrogenation, disproportionation, desorption, recombination) were tested as a part of prospective procedure of recycling scrap neodymium magnets from hard disc drives, into new resin bonded magnets. Chemical composition (MS), microstructure (SEM), phase constitution (XRD) and magnetic properties (VSM) were studied. Apart from scrap magnets, model Nd-Fe-B alloy was examined. Results from the experiments show, that the HD process is good enough to separate nickel coating from the scrap magnets. The HD works even at room temperature, however elevated temperature is more effective. This method also pulverizes magnet, which is necessary for further processing. During the HDDR, microstructure and phase constitution were observed. Disproportionated structure (mixture of $\text{NdH}_{2,3}$, Fe_2B and Fe grains) was achieved in proper stage. Then, during recombination stage, initial phase structure was recovered, but with much more smaller grain. Coercive material was produced as a result of hydrogen treatment. Finally, a new bonded magnet was fabricated using nylon resin. Therefore, the whole procedure can be considered as a recycling technique. Unfortunately, scrap magnets can differ in composition, which has an influence on absorption/desorption characteristic during hydrogen treatment and, subsequently, properties. Thus, hydrogen treatment should be adjusted to average composition of the scrap magnets.

Impact of loads and biofeedback to behavior of the center of gravity of the body

*Sandra Śmigiel¹, Marek Andryszczyk¹

¹Faculty of Mechanical Engineering, University of Science and Technology, Bydgoszcz, POLAND

e-mail: sandra.smigiel@gmail.com

Keywords: *center of gravity, body balance, biofeedback, stabilography, balance platform.*

The balance of the body is the subject of research many scientists, both in the population of children, adolescents, as well as the elderly. From a biomechanical point of view the normal of human motion develops for the whole of this life. The ability to maintain of the body balance in a vertical position consists to minimize the sway of the body (so-called: rocking attitude), so that the vertical projection of the center of mass of the body (ie. the center of gravity) was in the anatomical stability of boundaries defined by the surface area of the base of the foot. The stability of this attitude is conditioned by the work of the sensory systems, such as: vestibular, proprioceptive, tactile, which responsible for the development of basic human senses.

To determine the center of human gravity and the changes of its position are used the newer devices, which presents not only the change of deflection, but also the speed of deflection, the length of delineated path and surface area.

The purpose of the study was to demonstrate how the weight on back and return information (so-called biofeedback) about the changes the position of the center of gravity, affects the balance of the human body.

In addition, as part of the research, attempted to determine the effect of factors, such as BMI, body posture and subjective of physical activity, for the maintain of the body balance.

The study was performed on a group of young people aged 20 to 24 years. To determine the balance of the human body was used the stabilometric platform – ALFA-Technomex, and the main analyzed parameters are: the length of the path and the surface area, that creates by changing position of the center of gravity. The results were statistically analyzed via using the packet of STATISTICA 10.

The results confirmed the positive influence of biofeedback, both in the case of the length of delineated path and surface area. There were no significant the statistically differences in improving results in the control group, which had no biofeedback.

Preliminary results shows that the gender, BMI, body posture, physical activity and the weight on back, have no affect on the improvement of body balance.

Application of selected transition metals lignosulfonates as hydrogen peroxide electrochemical sensors and as electroplating baths

*Klaudia Śron, Grzegorz Milczarek,

Faculty of Chemical Technology Poznan University of Technology, Poznań,
POLAND

e-mail: klaudia.sron@put.poznan.pl

Keywords: *lignosulfonates, sensors, hydrogen peroxide, electroplating*

Lignosulfonates are byproducts of pulp and paper industry produced in quantities of millions metric tons per year. Lignosulfonates are interesting in electrochemical point of view because they are negatively charged in a dissociated state, they have sulfonic groups which are the place of an ion exchange reaction between the hydrogen and the metal ion and they have quinone/hydroquinone redox couple. And precisely due to the fact that lignosulfonates are a byproduct of paper production that is easily available, inexpensive material with interesting properties and also environmentally friendly, it is worth to look for new possibilities of applying them in industry. In this report we demonstrate the preparation of selected transition metals lignosulfonates and the electrochemical properties of these complexes.

Transition metals lignosulfonates were obtained by dissolving the excess of freshly precipitated transition metal hydroxide in lignosulfonic acid. Lignosulfonic acid in turn was obtained by ion exchanging of softwood sodium lignosulfonate on an ion exchanging column with acidic resin (Dowex®). Mn(II)-lignosulfonate and Co(II)-lignosulfonate were electrodeposited by anodic polymerisation on pre-activated glassy carbon electrode.

After transferring the modified electrode to the appropriate electrolytes, the electrodes exhibited the electrochemical activity typical for manganese and cobalt at different oxidation states in neutral or basic electrolytes. The redox activity of such modified electrode could be exploited for electrocatalytic applications. As demonstrated by obtained cyclic voltammetry plots the electrodeposited complex of Mn(II)-lignosulfonate exhibited reversible electrochemical transition due to a Mn(III)/Mn(II) and Mn(IV)/Mn(III) redox couples and electrocatalytic activity leading to the oxidation of hydrogen peroxide in Na₂SO₄ solution. Similarly behaves the electrodeposited complex of Co(II)-lignosulfonate. We received two reversible redox couples of Co(III)/Co(II) and Co(IV)/Co(III) and electrocatalytic activity leading to the oxidation of hydrogen peroxide but in alkaline solution.

Ionic liquids as interdisciplinary materials

*Urszula Świerczek, Joanna Feder-Kubis

Faculty of Chemistry, Wrocław University of Technology, Wrocław, POLAND

e-mail: urszula.swierczek@pwr.edu.pl

Keywords: *organic salts, biological activity, separation, organic synthesis, nanomaterials*

In the past years Ionic Liquids (ILs) have aroused scientists interest. Attractive and unique chemical and physical properties, such as: extremely low vapor pressure, incombustibility, thermal and chemical stability, flexibility in molecular design and high ionic conductivity have concerned scientific and industrial considerable attention. ILs are known as “multipurpose liquids” and have already found usage in almost every field of chemistry (e.g. separation/extraction, catalysis, synthesis, electrochemistry). Today ILs as novel materials enjoy a plethora of applications.

Ionic liquids belong to organic salts. As commonly accepted concept, ionic liquids are organic salts, composed of distinct cations and anions, whose melting point is below 100 °C.

The number of new ionic liquids is still growing. Because of unusual properties, they have become promising alternatives to many toxic solvents. Ionic liquids have been touted as “green solvents”. ILs are used as selective catalysts in chemical and enzymatic reactions. Extremely important is the fact that these salts facilitate product recovery and they might be recycled and/or biodegradable. Ionic liquids found application in several processes: separation, extraction, gas absorption and synthesis of nanoparticles.

ILs show much higher biological activity than other antibacterial and antifungal substances. They can be applied as effective disinfectants, antiseptics and biocides. Furthermore, recent studies show that ionic liquids might be successfully used in anti-cancer therapy. Ionic liquids as electrolytes can be used in batteries, fuel cells, photovoltaics, and electrodeposition. They are good candidates for a number of energy related applications.

Ionic liquids offer a unique suite of properties, therefore they are so attractive compounds for scientist and industry. In many cases ILs are more eco-friendly alternative. These salts can easily compete with other materials.

The biotechnological potential of ionic liquids

*Urszula Świerczek, Joanna Feder-Kubis

Faculty of Chemistry, Wrocław University of Technology, Wrocław, POLAND

e-mail: urszula.swierczek@pwr.edu.pl

Keywords: *organic salts, biotransformation, biocatalysis, biofuel, biodegradation*

For thousands of years, biotechnology has been an important part of human life. In the beginning, we have used this technology without understanding: how does it work? Today, thanks to science, biotechnology can help us in medicine, agriculture and in almost every branch of industry (as an example: chemical, petrochemical, food industry).

Biotechnology promises great benefits for producers and consumers. The growing demand for high quality bio-products (such as: enzymes, antibodies, drugs) show that this technology is necessary and should be developed.

Examples of ionic liquid use in biotechnological processes are described in a significant part of literature. These compounds are considered to be an alternative to unfriendly organic solvents for biocatalysis and biotransformations. Ionic Liquids (ILs) are defined as organic salts with melting point below 100°C, but sometimes they remain liquid in room temperature (RTILs - Room Temperature Ionic Liquids). Due to possibility to fine-tune physicochemical and biological properties they are known as “designer solvents”. The advantages of ILs are low vapor pressure, nonflammability, biocompatibility, high conversion rates, biodegradation, solubility of many of organic and inorganic substances etc. Therefore, these salts might be excellent enzymatic reaction media, in terms of enhanced activity, stability or selectivity of proteins.

In recent years, ionic liquids have been widely used in processes: biodiesel or biomass production, synthesis of enormous number of useful intermediates and active pharmaceutical ingredients. Furthermore, ILs can be applied in sewage treatment plant as co-solvent in enzyme-based purification of water.

Ionic liquids are often related to as the “green compounds”. They can go well with enzymes in many biotechnological processes. These low-melting salts are more eco-friendly media for biocatalysis and biotransformations than other organic substitutes. Ionic liquids tend to be a perfect solution for biotechnology.

Biocompatible coatings for stainless steel surfaces

*Paulina Trzaskowska, Tomasz Ciach

Faculty of Chemical and Process Engineering, Warsaw University of Technology, Warsaw, POLAND

e-mail: p.trzaskowska@ichip.pw.edu.pl

Keywords: *coatings for medical devices, stainless steel*

Stainless steel (SS) 316L is often used for medical applications, e.g. for fabrication of stents or artificial valves. These life-saving devices are commonly applied, however they have long-term influence on tissues of a patient. This means that after a particular time the removal or replacement of them is unavoidable. Coating the surface of steel with biocompatible polymer layer is expected to minimize harmful effects and prolong the lifetime of a steel device.

As a base material, discs made of SS 316L were used. Coatings were obtained from biocompatible polymers solutions, such as poly(ethylene glycol) dimethacrylate - PEGDMA (Sigma). The coatings were introduced on SS surface with the use of electrochemical methods (e.g. electropolymerization). Only aqueous solutions of polymers were applied. As a power source, DC current supply was used.

Through a set of experiments, the procedure of SS coating with a biocompatible film was elaborated. It was possible to obtain smooth, homogenous and durable layers on SS surface, which was determined with several analytical techniques (e.g. SEM, FTIR-ATR). As laboratory tests on mouse fibroblasts (L929) revealed, covering SS with polymer layers actually led to decrease of SS toxicity.

It has been proven that the electrochemical method of SS surface coating could be possibly used to prevent some unwanted effects that SS cause after some time from implantation. Thanks to the absence of organic solvents and application of DC supplier the proposed method is innovative and shows a potential to be scaled-up.

Portable system for detection of biological threats.

*Maciej Trzaskowski, Tomasz Ciach

Faculty of Chemical and Process Engineering, Warsaw University of Technology, Warsaw, POLAND

e-mail: m.trzaskowski@ichip.pw.edu.pl

Keywords: *surface plasmon resonance, portable analytical devices, biological warfare*

Surface plasmon resonance phenomenon (SPR) is becoming one of the mostly used in detection of interactions between analyte and immobilized biomolecule. The main reason is that it enables fast, accurate and marker-free analysis. Therefore the detection process is possible to become fully automatic. Since the advanced miniature SPR chips are already developed, SPR technique has a potential to be implemented in devices that could be used for on-site examination of environmental samples.

In the presented work we developed an automatic sample analysis system for detection and identification of microorganisms considered as possible biological threats. It is based on TI Spreeta 2000 chips. These chips are miniature sized and include all the components necessary for performance of a detection experiment. We modify the chips with the use of specific antibodies and amine coupling technique in order to obtain affinity to chosen species of bacteria. The device includes fluidic system with dedicated pump and valve for collection of samples. The electronic part of the device acquires signals from multiple Spreeta chips that can be sent to a computer, where they can be analyzed with the use of specially designed software. Our device can also perform automatic procedure of sample analysis including data analysis and is able to send result of an experiment.

First tests of a prototype device have been conducted. It was proven that it can detect hazardous microorganisms such as *B. Anthracis*, *V. Cholerae* and many more. Further experiments will test possibility of detecting several species of microorganisms simultaneously.

Influence of direct crystallization process on the bioactivity of silicate-phosphate glasses from $\text{KCaPO}_4\text{-SiO}_2$ system

*Aleksandra Wajda, Katarzyna Bułat, Maciej Sitarz

Akademia Górniczo-Hutnicza im. Stanisława Staszica w Krakowie,

Wydział Inżynierii Materiałowej i Ceramiki,

Al. Mickiewicza 30, 30-059 Kraków

e-mail: olawajda@agh.edu.pl

Keywords: *silicate-phosphate glasses, direct crystallization, bioactivity, glass-crystalline materials*

Silicate-phosphate glasses from $\text{KCaPO}_4\text{-SiO}_2$ system are bioactive materials, which are capable of forming direct bonds with living tissue. An ideal biomaterial should be also biomechanically compatible with tissue. Application of glasses as biomaterials is limited mainly due to their very low strength and chemical stability. One of the best ways to improve the mechanical properties of the glasses is to change their chemical composition (for example, the introduction of Al^{3+} or B^{3+} ions) or to carry out their partial devitrification that allows to obtain glass-crystalline materials. This process needs to be highly controlled, because the appearance and growth of the crystalline phase may result in loss of the bioactivity. In order to fully control the direct crystallization process properly, it is necessary to know the structure and microstructure of the glassy precursor.

The subject of this paper were silicate-phosphate glasses from $\text{KCaPO}_4\text{-SiO}_2$ and $\text{KCaPO}_4\text{-SiO}_2\text{-AlPO}_4$ systems. Microscopic investigation showed that liquation takes place in all the studied glasses and it is thought that the boundaries of separated phases may be a barrier limiting the growth of crystalline phases. It has been found that aluminium has a homogenising effect on the texture of silico – phosphate glasses and causes the inversion of the composition of the matrix and the inclusions. The parameters for direct crystallization process were adjusted on the basis of thermal measurements (DTA) performed on selected glasses. XRD method was used to study the structure of obtained glass-crystalline materials. In order to verify their bioactivity, the in vitro tests were done in simulated body fluid and the samples were analyzed on a scanning electron microscope (SEM+EDX) and Raman spectroscopy.

Obtained results suggest that a properly controlled devitrification of the tested bioglasses may lead to the production of bioactive glass-crystalline materials.

Luminescence properties of Eu^{3+} and Tb^{3+} doped silica-based xerogels

*Michalina Walas¹, Barbara Kościelska¹, Wojciech Sadowski¹, Andrzej M. Klonkowski¹, Marcin Łapiński¹, Wiesław Wiczak², Irena Bylińska²

¹Faculty of Applied Physics and Mathematics, Solid State Department, Gdansk University of Technology, Gabriela Narutowicza 11/12, 80-233 Gdansk, POLAND

²Faculty of Chemistry, Gdansk University, Wita Stwosza 63, 80-308 Gdansk, POLAND

e-mail: mwalas@mif.pg.gda.pl

Keywords: luminescence, lanthanide ions, LED, energy transfer, sol-gel

Luminescent SiO_2 xerogels and SiO_2 xerogels containing SrF_2 nanocrystals doped with Eu^{3+} and Tb^{3+} were prepared using sol-gel method and then heat treatment was performed. The lanthanide ions luminescence properties were investigated as a function of heat treatment temperature and additionally host matrix influence has been observed due to entrapping luminescent ions into the crystalline phase.

Luminescent spectra of Eu^{3+} and Tb^{3+} doped samples were obtained using fluorescent spectroscopy technique. These spectra showed excitation and emission peaks characteristic to Eu^{3+} and Tb^{3+} $4f - 4f$ transitions: $^5D_0 \rightarrow ^7F_J$ ($J=0, 1, 2, 3, 4$) and $^5D_4 \rightarrow ^7F_J$ ($J=5, 6$), respectively. Thus, the sample doped with Eu^{3+} ions emits in reddish-orange wavelength range while sample doped with Tb^{3+} ions emits in bluish-green, green and greenish-yellow range. Moreover, when xerogel sample co-doped with both Eu^{3+} and Tb^{3+} was irradiated by 378nm wavelength light, the energy transfer (*ET*) between Tb^{3+} and Eu^{3+} ions has been observed.

X-ray diffraction (*XRD*) pattern of SiO_2 matrix confirmed lack of long range order. Patterns of $\text{SiO}_2\text{-SrF}_2\text{:Eu}^{3+}$ and $\text{SiO}_2\text{-SrF}_2\text{:Tb}^{3+}$ showed peaks corresponding to crystalline SrF_2 phase. The size of crystallites in these samples was estimated based on Scherrer's equation. Obtained results indicate nanosize of these crystallites. Images obtained with Scanning Electron Microscopy (*SEM*) have shown agglomerates of spherical particles and presence of pores confirming amorphous character of SiO_2 matrix. Fourier Transform Infrared Spectroscopy (*FTIR*) spectra showed bands related to Si-O vibrations and also vibrations associated with the OH bonds, confirming presence of some residual water in samples.

Thus, $\text{SiO}_2\text{-SrF}_2$ system doped with Eu^{3+} and Tb^{3+} could be a potential candidate for LEDs applications. Additionally, review of other matrices for LEDs applications doped with lanthanide ions is presented.

Novel titanium-silicate catalysts with the MWW topology

*Marika Walasek, Agnieszka Wróblewska, Ewa Drewnowska, Alicja Gawarecka

Institute of Organic Chemical Technology, Faculty of Chemical Technology and Engineering, West Pomeranian University of Technology, Szczecin, Pułaskiego 10,

70-322 Szczecin, Poland

e-mail: marika.walasek@gmail.com

Keywords: *materials with the structure of MWW, titanium-silicate*

Porous materials can be divided into three groups taking into account the size of the pores: microporous materials (pores diameter less than 2 nm), mesoporous (pores diameter 2-50 nm) and macroporous materials (pores diameter more than 50 nm). Zeolites can replace environmentally unfriendly acid catalysts. These materials indirectly contribute to reducing the amount of wastes, by-products and energy consumption. It allows to design a new, low-cost technologies. Due to the catalytic properties they found broad applications in many sectors of chemical industry, for example: in the refining and petrochemical industry, and in the syntheses of other compounds. These materials also exhibit good adsorption capacities. Nowadays, the aim of the researchers is the obtaining of such zeolites, which will have better features and applications. Thus, a lot of research has been conducted about creating a new structures or modifying existing ones.

The MWW material belongs to the zeolite material group. Its structure – MWW, has two separate pore systems: 10-membered ring pore systems, which form sinusoidal channels and 12-membered ring supercages. Both systems are accessed by windows with the diameters of 4.0 x 5.5 Å. The sinusoidal channels are suitable for adsorption and diffusion processes. The unique porosity creates an open reaction spaces.

The MWW structure is a framework type code name specified by International Zeolite Association. A crystalline zeolite with MWW structure is called as the MCM-22. This structure is obtained in few steps from boric acid as a crystallization-supporting agent and hexamethyleneimine or piperidine as a structure directing agent. The synthesis takes several days (including hydrothermal treatment in an autoclave) and after this step, the obtained material is filtrated and dried. After drying, the treatment with nitric or sulfuric acid is carried out in order to remove the atoms, which are not built into the silicate structure. The obtained solid product is next calcinated at the temperatures of 540-600°C.

There are several titanium-silicate catalysts, whose construction based on MWW topology. As the examples Ti-YNU-1, Ti-MCM-36 and Ti-ITQ-2 can be given. These materials can be prepared by various modification of the MWW precursor. They are excellent catalysts for oxidation processes, characterized by high conversions of raw materials and high selectivities to the desired products.

Construction and application of bismuth bulk electrode for adsorptive stripping determination of cobalt(II)

*Krystian Węgiel, Bogusław Baś

Faculty of Material Science and Ceramics, AGH University of Science and Technology, Kraków, POLAND

e-mail: krystweg@agh.edu.pl

Keywords: *Bismuth bulk electrode, Stripping voltammetry, Cobalt, Mercury-free electroanalysis*

Working electrode is an important element of every voltammetric measurement system. Metrology and utility sensors parameters determine accuracy of the measurements, application flexibility and opportunities for standardization. However, according to the EU Directive, mercury measuring devices can not be traded. Hence, the search for alternative electrode materials is in line with the actual trend in modern electrochemistry development.

Various types of coal or noble metals (Au, Pt, Ag etc.) and their alloys or modifications with plated differential films are proposed as potentially the best electrode materials. In our work, we present a new renewable bismuth bulk annular band electrode (RBiABE), which central element is a ring made of unmodified metallic bismuth, mounted on a stainless steel and embedded in resin. Working with the solid-state electrodes requires mechanical or electrochemical treatment, therefore, also outer cell activation was used in order to remove reaction products of the surface electrode at a potential of -2.0 V for a few seconds. This construct allows to precise control time contact of the sensor with the solution and between successive measurements.

The application of the RBiABE to determination of cobalt traces by differential pulse adsorptive stripping voltammetry (DP AdSV) is presented in this work. The procedure is based on the preconcentration of the cobalt-dimethylglyoxime (Co-DMG) complex at testing electrode held at -0.70 V (versus Ag/AgCl/3 M KCl) in a supporting electrolyte consisting of 0.1 mol L⁻¹ ammonia buffer (pH=8.2) and 50 μmol L⁻¹ dimethylglyoxime. The reduction current of complex Co-DMG is catalytically enhanced by the presence of 0.4 mol L⁻¹ nitrite. The peak current is proportional to the concentration of cobalt over the range from 1·10⁻⁹ to 70·10⁻⁹ mol L⁻¹, with detection limit 3·10⁻¹⁰ mol L⁻¹ and accumulation time of 30 s. Finally, the RBiABE was applied to the determination of cobalt in certified reference material and river water samples with satisfying results.

Phosphorothioate analogs of uridine nucleotides in wound healing

*Edyta Węglowska, Edyta Gendaszewska-Darmach

Faculty of Biotechnology and Food Science, Lodz University of Technology,
Lodz, POLAND

e-mail: edyta.laska@edu.p.lodz.pl

Keywords: *wound healing, angiogenesis, nucleotides*

Wound healing is a complex and dynamic process which requires coordination of many cellular processes such as fagocytosis, chemotaxis, angiogenesis, proliferation and migration. Proper wound healing is essential for tissue reconstruction after injury. Angiogenesis connected with formation of new blood vessels plays a key role in wound healing process and protein growth factors are significant molecules involved in this process. Particularly, VEGF (*Vascular Endothelial Growth Factor*) released by fibroblasts and keratinocytes promotes endothelial cells to create new blood vessels in wound environment.

The aim of our studies was to enhance wound healing process by the use of nucleotides and their phosphorothioate analogs. Experiments were performed with cells naturally occurring in skin and involved in skin wound healing. *Firstly we examined the effect of nucleotides on proliferation (CyQUANT® Direct Cell Proliferation) and viability (PrestoBlue™ Cell Viability) of human endothelial cells, fibroblasts and keratinocytes. We have also investigated the influence of these compounds on production of VEGF (Human VEGF ELISA) by fibroblasts.*

According to our results uridine nucleotides and their phosphorothioate analogs affect proliferation and viability of HaCaT keratinocytes. Less effect was observed in the case of HUVEC endothelial cells and HDFa fibroblasts. Tested nucleotides also stimulated the release of VEGF from fibroblasts.

Naturally occurring uridine nucleotides are agonists of transmembrane G-protein coupled receptors. We postulate that phosphorothioate analogs of uridine nucleotides may also bind to these receptors and in this way affect cellular processes. Moreover, phosphorothioate analogs are more stable than native nucleotides being better inducers of angiogenesis compared to their unmodified counterparts.

The analysis of discharge coefficient for atomization of the liquid of different viscosity

Sylwia Włodarczak

Faculty of Chemical Technology, Poznan University of Technology, Poznan, POLAND

e-mail: sylwia.a.wlodarczak@doctorate.put.poznan.pl

Keywords: *construction of atomizer, discharge coefficient, liquid viscosity, pressure-swirl atomizer*

Pressure-swirl atomizers are found in a wide range of engineering applications, for example engine or industrial turbines. These atomizers demonstrate good atomization characteristics and relative geometrical simplicity. The discharge coefficient (C_D) is the main parameter, which characterizes pressure-swirl atomizers. The values of C_D depend on pressure drops generated in the nozzle. This parameter is influenced by: the Reynolds number, the ratio of length to diameter of outlet, injection pressure, ambient pressure and cavitation. The discharge coefficient allows to determine the character of liquid flows through the atomizer. It takes different values depending on the range of flow (laminar, transitional and turbulent).

The experimental studies were directed on analysis relationship of discharge coefficient on liquid flow rate, profile of outlet pressure-swirl atomizer and liquid viscosity. Experimental tests were performed for single-phase flow using pressure-swirl atomizer with different profiles of outlet. The atomizer with cylindrical, conical and profiled outlet has been tested. The cylindrical outlets characterized by varying ratio of length l_0 to diameter d_0 . The test fluids used in experimental study were water and aqueous solution of glycerol different concentration. The test liquids were atomized in temperature $T = 20^\circ\text{C}$. The liquid was atomized at a flow rate of the liquid calculated in a cross-section of the outlet below the values $w_c = 15$ [m/s]. The liquid with a specific flow rate flowed from rotameters to the nozzle, where the atomization followed. The pressure drop was observed during outflow of liquid from the nozzle, which value was read from the digital pressure gauge.

The relationship between the discharge coefficient and the Reynolds number has been shown. When the Reynolds number is small, the value of the flow rate increases linearly. During the turbulent flow, the flow rate stabilized and reached a constant level. Based on these studies, it was found that the discharge coefficient has different values which depend on the shape of the outlet.

Solution blow spinning of polyurethane nanofibers

*Michał Wojasiński, Małgorzata Bieniak, Tomasz Ciach

Faculty of Chemical and Process Engineering, Warsaw University of Technology, Warsaw, POLAND

e-mail: m.wojasinski@ichip.pw.edu.pl

Keywords: *solution blow spinning, nanofibers, polyurethane, rheology*

Nanofibrous non-woven finds an application in wide range of industries: from textiles, through filtration materials to biomedical applications. The most popular, but non-efficient, technologies for nanofibers formation are self-assembly, drawing and electrospinning. We propose, previously reported in literature, solution blow spinning technique for efficient nanofibers production. We described adjustment the process parameters suitable for control of the final product properties.

We used 6, 8, and 10% solutions of polyurethane (Elastollan 1185A, BASF, Germany) in tetrahydrofuran to prepare nanofibers in solution blow spinning (SBS). The rheological analysis of the polymer solutions was performed on rotational viscometer Rheotest 2.1 (VEB MLW, Germany). SBS system relies on application of concentric nozzles system to stretch the polymer solution jet in air stream to form nanofibers. Nanofibers were collected on rotating drum, with different distance between nozzles system and collector, and different rotational speed. For nanofibers characterization: diameter distribution, average diameter, and fibers alignment we used scanning electron microscope (SEM, PhenomTM, Phenom World) images. Porosity of the materials was determined by gravimetric analysis. Wettability measurements for materials were performed on DSA100 goniometer (Krüss, Germany), and meta-stable Cassie-Baxter equation was applied to calculate wettability of the single fiber.

We present best-fitted surfaces for average nanofiber diameter in function of polymer solution concentration and air pressure applied to the nozzles system. Materials consist nanofibers with diameters from about 100nm to 600nm. Porosity of the analyzed samples increases from about 80% to 95% with increasing distance between nozzles system and collector. Preferred orientation of the nanofibers in the materials is visible for samples obtained with rotational speed of 11000rpm. Wettability measurements suggest hydrophobic character of the material, when single fiber exhibits hydrophilic properties.

We presented the thorough investigation of the solution blow spinning process for formation of polyurethane nanofibers. Based on presented results, it is possible to design polyurethane nanofibrous materials for specific applications by tailoring product properties by adjusting process parameters.

Chemical engineer vs biology – a case study about toxicity of ZnO based nanomaterials

*Anna Wojewódzka¹, Małgorzata Wolska-Pietkiewicz¹, Katarzyna Tokarska¹, Katarzyna Wójcik², Janusz Lewiński^{1,2}

¹Faculty of Chemistry, Warsaw University of Technology, Noakowskiego 3, 00-664 Warsaw, POLAND

²Institute of Physical Chemistry, Polish Academy of Sciences, Kasprzaka 44/52, 01-224 Warsaw, POLAND

e-mail: aniawojew@interia.pl

Keywords: quantum dot, zinc oxide, cellular imaging, cytotoxicity, MTT assay.

Nowadays, luminescent semiconductor nanocrystals like zinc oxide nanoparticles (ZnO NPs) are promising candidates for novel labeling agents in cellular imaging. Therefore, considerable effort has been placed on identifying and verification the potential toxicity of ZnO NPs towards cells.

The goal of the presented work is the design and synthesis of luminescent organic-inorganic water-soluble functional materials based on semiconducting ZnO nanoparticles as systems ready for potential biological applications. The presented results include the synthesis of organometallic precursor, its controlled transformation into ZnO NPs as well as characterization of basic physicochemical properties of described systems, *i.e.* size, morphology and optical properties. Another integral part of this work was the investigation of the stability of ZnO NPs and their water-solubilization. Then the selected systems were tested in viability test (MTT) using different cell lines. After determining the safe range of concentrations we used prepared ZnO NPs like fluorescent agent in bioimaging.

Finally, the obtained results show that ZnO NPs might be a very good alternative for commercially available Cd-based nanomaterials because of their relatively low cytotoxicity.



Fig. 1 Viability of A549 cells depending on the concentration of ZnO NPs (after 24 h).

Application of Yttria-stabilized Zirconia materials for heavy metals removal

*M. Wolska, A. Smalec, E. Niewiara, W.W. Kubiak,

AGH University of Science and Technology, Faculty of Materials Science and Ceramics, A. Mickiewicza 30, 30-059 Kraków, Poland

e-mail: wolska.malgorzata@op.pl

Keywords: *heavy metals, YSZ nanopowders, rare earth elements, voltammetry*

The determination of heavy metals such as cadmium and lead is important because they may be toxic through biomagnification, or to investigate their geochemistry. The most dangerous form of occupational exposure to cadmium is inhalation of fine dust and fumes, or ingestion of highly soluble cadmium compounds. Cadmium is also an environmental hazard. Human exposures to environmental cadmium are primarily the result of fossil fuel combustion, phosphate fertilizers, natural sources, iron and steel production, cement production and related activities, nonferrous metals production, and municipal solid waste incineration. Lead is a highly poisonous metal (whether inhaled or swallowed), affecting almost every organ and system in the body. The main target for lead toxicity is the nervous system, both in adults and children. Long-term exposure of adults can result in decreased performance in some tests that measure functions of the nervous system.[98] Long-term exposure to lead or its salts (especially soluble salts or the strong oxidant PbO₂) can cause nephropathy, and colic-like abdominal pains.

The presented work is aimed at the development of effective method of heavy metals such as cadmium and lead removal from the sample water solution (pH 2-8) with the use of Yttria-stabilized Zirconia nanomaterials as adsorbents. Zirconium and yttrium nano-powders doped with rare earth elements (Gd, Sm, Nd) were synthesized and tested. Nano-powders were applied either directly to the measuring system or prior to the measurements to the sample solution (and then centrifuged). The quantitative measurements applied for determination of heavy metals removal effectiveness were made using stripping voltammetry measurements.

Research were performed using the three electrodes: working electrode CGMDE, reference electrode Ag/AgCl and auxiliary electrode Pt, electrolyte was deoxidised before each measurement. The nano-powders were added to 10ml of solutions containing 50 ppb Pb and Cd. Then it was blended (5min.) and centrifuged. (pH 2-8).

All nano-powders were helpful in elimination of cadmium and lead from water and the highest sorption was found solutions with zirconium and yttrium nano-powders doped with neodymium. The above materials worked well for remove of heavy metals and humic acids from solutions.

Innovative screening device for high-sensitive chemical vapors detection

*Anna Zalewska¹

¹Military Institute of Chemistry and Radiometry, Warsaw, POLAND

e-mail: a.zalewska@wichir.waw.pl

Keywords: *Differential ion mobility spectrometry, DMS, chemical warfare agents, explosives*

In Military Institute of Chemistry and Radiometry was made portable contamination signaling device (PRS-1) used for detection and identification wide range of chemical substances. PRS-1 was constructed based on the differential ion mobility spectrometry (DMS). DMS belongs to the group of methods based on an ion mobility effect and it can be used in screening mobile devices for high-sensitive detection of chemical warfare agents, explosives and drugs. Detection possibilities of apparatus using the DMS method are based on the occurrence of different mobility of ions (K) in the alternating electric field.

Our device is designed for the detection of chemical warfare agents, and initial testing of the detection explosives yielded positive results and form the basis for the concept of further research. Innovative solutions applied to the device PRS-1 cause that its technical parameters are very high – one of the best in the world. Its high detection parameters allow for take a chance to select biomarkers in exhaled air. Based on the collected spectra will be determined the differences in position and amplitude of received signals, what can be used to find correlation between the occurrence of pathogenic changes and particular volatile organic compound (VOC) to define biomarkers. Obtained results will provide a basis for further research to develop applications leading to early diagnosis of asymptomatic diseases.

In summary it can be concluded that the DMS method allow for detection of chemical vapors up to ppb-ppt level using ion mobility determinate on the experimental way (K) for different voltages of the electric field (E).

Nickel aluminate spinel (NiAl_2O_4) in $\text{Al}_2\text{O}_3/\text{NiO}$ and $\text{Al}_2\text{O}_3/\text{Ni}$ system

*Justyna Zygmuntowicz¹, Aleksandra Miazga¹, Katarzyna Konopka¹

¹Faculty of Materials Science and Engineering, Warsaw University of Technology, Warsaw, POLAND

e-mail: justyna.zygmuntowicz@inmat.pw.edu.pl

Keywords: $\text{Al}_2\text{O}_3/\text{NiAl}_2\text{O}_4$ composite, spinel phase, stereological analysis

This work presents composites from $\text{Al}_2\text{O}_3/\text{NiO}$ and $\text{Al}_2\text{O}_3/\text{Ni}$ system. The uniaxially pressing at 100 MPa and sintering at 1400°C/1h in air atmosphere was applied for the purpose of producing these materials. This atmosphere has allowed the emergence of spinel phase NiAl_2O_4 . The final product of applied process was $\text{Al}_2\text{O}_3/\text{NiAl}_2\text{O}_4$ composites. The results of microstructure, physical properties are discussed.

In the experiment, the following powders were used: $\alpha\text{-Al}_2\text{O}_3$ TM-DAR Company (Japan) with averaged particle size of 133 ± 30 nm and density 3.96g/cm^3 , and NiO powder produced by Alfa Aesar Company of average particle size $5\ \mu\text{m}$ and density $8.9\ \text{g/cm}^3$, as well as Ni powder produced by Sigma Aldrich of average particle size $8.5\ \mu\text{m}$ and density 8.9g/cm^3 .

The physical properties of the composites were measured by Archimedes method in water. X-ray diffraction (XRD) was used to identify the phase present un the samples. Microstructure observation of the longitudinal sections and cross-section of samples were using scanning electron microscope. Quantitative description of the microstructure of the composites was made on the basis of SEM images of randomly selected areas on the cross-section using computer image analysis equipped into the program Micrometer.

The X-ray phase analysis and SEM observations of composites confirmed the presence of two phases Al_2O_3 and NiAl_2O_4 in whole volume of each samples. All tested samples were characterized by homogeneous distribution of NiAl_2O_4 phase in the whole volume of the material. In each samples, it was observed that the spinel phase is characterized by two forms. The full oval shape of spinel phase and the spinel phase areas with characteristic voids, which given then the shape of 'doughnuts' were observed. In $\text{Al}_2\text{O}_3/\text{Ni}$ system is no evident influence of Ni initial powder on the spinel phase formation and morphology. On the other hand in the case of $\text{Al}_2\text{O}_3/\text{NiO}$ system it has been observed that with increase of NiO volume, the volume of fraction spinel phase in composites. Additionally, the spinel forming retards the densification of the composites.

This work was supported by Faculty of Material Science and Engineering Warsaw University of Technology (statute work).

Index

A

Alapi T. 399, 416, 427,
Andryszczyk M. 305, 434,

B

Baia L. 390, 427,
Baraniak E. 360,
Bartkowiak A. 372, 431,
Basista M. 382,
Baś B. 385, 400, 443,
Bazan A. 361,
Bieniak M. 446,
Blicharska M. 25, 362, 363,
Bułat K. 343, 440,
Bylińska I. 180, 441,

C

Cabaj L. 364, 365, 420, 421,
Cendrowski K. 425, 426,
Chlebda D. K. 422,
Chrunik M. 366, 398,
Chrzan M. 422,
Ciach T. 163, 438, 439, 446,
Cudziło S. 424,
Czarna M. 387,
Czyż K. 367,

D

Danciu V. 390, 427,
Dąbrowski R. 415,
Dębek P. 368,
Dobrzaniecka A. 25, 362, 363,
Dobrychłop J. 394,
Dolińska B. 220, 329, 370, 371,
432,
Dombi A. 378, 390, 399, 416,
427,
Drewnowska E. 45, 207, 352, 369,
374, 442,
Dyja R. 220, 370, 371,

F

Feder-Kubis J. 151, 436, 437,
Fedorowicz A. 372,

Firtha F. 70, 395,
Foszpańczyk M. 373,

G

Gawarecka A. 207, 229, 352, 369,
374, 442,
Gendaszewska-Darmach E. 444,
Główka A. 241, 375,
Gmurek M. 373,
Goryczka T. 419,
Gościańska J. 410, 423,
Grabowski Ł. 59, 376,
Gralak-Podemska B. 391,
Gruszczyńska J. 250, 377,
Grylik D. 373,
Gyulavári T. 378,

H

Harmata P. 379, 380,
Hernádi K. 378, 390, 427,
Horszczaruk E. 425, 426,

I

Igielska-Kalwat J. 264, 381,

J

Jaglarz J. 360,
Jakubowska J. 382,
Jakubowska M. 430,
Janas M. 272, 383,
Jarocho D. 384,
Jarosz M. 384,
Jaskuła M. 384,
Jedlińska K. 385,
Jędrzejczyk R. J. 422,
Jodłowski P. J. 422,
Jotko M. 386, 403,

K

Kamińska I. 387,
Kapuścińska A. 281, 388, 389
Kása Z. 390,
Kazmierczak-Razna J. 391,
Kędziński J. 398,
Kiszkiel I. 392,
Kłonkowski A. M. 180, 441,

Kłos M. 393,
Kmieciak J. 394,
Koncz S. 70, 395,
Kondratowicz I. 79, 396,
Konopka K. 450,
Kopeć M. 397,
Kopytko M. 412,
Kościelska B. 180, 441,
Kovács G. 390, 427,
Kovács Z. 70, 395,
Kowiorski K. 398,
Kozmér Z. 399, 416,
Krakowska A. 400, 401,
Krason J. 402,
Krawczyńska W. 372,
Kroupa J. 366,
Kubiak W. W. 365, 406, 448,
Kuciel S. 428,
Kudawska B. 386, 403,
Kula P. 379, 380,
Kulesza P. 25, 362, 363,

L

Ledakowicz S. 373,
Leonowicz M. 338, 433,
Lewandowski T. 97, 180, 404,
Lewczuk R. 405,
Lewiński J. 447,
Lipińska L. 398,
Lisiecki S. 407,

Ł

Ładocha A. 406,
Łapiński M. 180, 441,
Łechtańska P. 417,
Łojewska J. 422,
Łojewski M. 401,
Łopusiewicz Ł. 407,
Łosiewicz B. 419,
Łukowski P. 426,

M

Magyari K. 427,
Majka M. 384,
Major R. 367,
Malarczyk K. 113, 289, 393, 408,
Malko M. W. 123, 294, 409,

Manczinger L. 378,
Marciniak M. 410,
Marczak J. 367,
Marecka A. 411,
Markowska O. 412,
Markowska-Szczupak A. 425,
Marszałek K. 361,
Matuszak M. 413,
Miazga Z. 338, 433, 450,
Michalski B. 338, 433,
Mijowska E. 425, 426,
Milchert E. 113, 289, 393, 408,
Milczarek G. 322, 435,
Milewska K. 414, 415,
Mitkowski P. T. 411,
Mogyorósi K. 378,
Murawski L. 404,
Muszyńska B. 400, 401,
Mzyk A. 367,

N

Namiecińska O. 417,
Naplocha K. 382,
Náfrádi M. 416,
Niewiara E. 448,
Nikpour R. 134, 418,
Nowak I. 241, 264, 281, 368,
375, 381, 388, 389
Nowicki P. 361, 391,

O

Olejnik A. 241, 375, 388,
Ortyl J. 387,
Osak P. 419,

P

Paczosa-Bator B. 364, 365, 420, 421,
Pap Z. 378, 390, 427,
Pawlik A. 384,
Piątkiewicz W. 134, 418,
Piech R. 364, 365, 420, 421,
Pietrzak K. 382,
Pietrzak R. 361, 391, 402, 410, 423,
Pięk M. 364, 365, 420, 421,
Piwowarczyk E. 422,
Póta L. 399,
Prześniak-Welenc M. 97, 404,

Ptaszkowska M. 423,

R

Reczyński W. 400, 401,
Rećko J. 424,
Rycyk A. 367,
Ryszka F. 220, 329, 370, 371, 432,

S

Sadowski W. 79, 180, 396, 441,
Sarzyński A. 367,
Saszet K. 390,
Sikora P. 425, 426,
Simon G. 427,
Sitarz M. 343, 440,
Sitek N. 428,
Skibiński W. 429,
Smalec A. 448,
Sordoń W. 430,
Stobińska M. 431,
Strojny-Nędza A. 382,
Strzelec M. 367,
Sulka G. D. 384,
Szala M. 405,
Szulc-Musioł B. 329, 432,
Szwast M. 134, 418,
Szymański M. 338, 433,

Ś

Śmigiel S. 305, 434,
Śron K. 322, 435,
Świerczek U. 151, 436, 437,

T

Takács E. 399,
Tkacz-Śmiech K. 360,
Tokarska K. 447,
Topoliński T. 305,

Trzaskowska P. 163, 438,
Trzaskowski M. 171, 439,

V

Veréb G. 378,

W

Wajda A. 343, 440,
Walas M. 180, 441,
Walasek M. 123, 207, 352, 369,
374, 442,
Wawrzyńczak A. 368,
Węgiel K. 443,
Węglowska E. 444,
Wicikowski L. 97, 404,
Wiczek W. 180, 441,
Wielgosiński G. 417,
Wierzba B. 429,
Włodarczyk S. 445,
Wojasiński M. 446,
Wojewódzka A. 447,
Wojnárovits L. 399,
Wolska M. 400, 401, 448,
Wolska-Pietkiewicz M. 447,
Wołosiewicz-Głąb 59, 376,
Wójcik K. 447,
Wróblewska A. 45, 123, 207, 229,
294, 352, 369, 374, 409, 442,

Z

Zalewska A. 194, 449,
Zalewski M. 134, 418,
Zawadzka A. 272, 383,
Zygmuntowicz J. 450,

Ż

Żelechowska K. 79, 396,
Żołądek S. 25, 362, 363,